APPROVED FOR RELEASE: 2007/02/08: CIA-RDP82-00850R000200100009-9

ON

BY

3 JULY 1980 I. I. KLYUKIN AND I. I. BOGOLEPOV

APPROVED FOR RELEASE: 2007/02/08: CIA-RDP82-00850R000200100009-9

APPROVED FOR RELEASE: 2007/02/08: CIA-RDP82-00850R000200100009-9

FOR OFFICIAL USE ONLY

JPRS L/9179

3 July 1980

Translation

MANUAL ON SHIP ACOUSTICS

By

I.I. Klyukin and I.I. Bogolepov

FBIS FOREIGN BROADCAST INFORMATION SERVICE

FOR OFFICIAL USE ONLY

APPROVED FOR RELEASE: 2007/02/08: CIA-RDP82-00850R000200100009-9

APPROVED FOR RELEASE: 2007/02/08: CIA-RDP82-00850R000200100009-9

JPRS L/9179

3 July 1980

MANUAL ON SHIP ACOUSTICS

Leningrad SPRAVOCHNIK PO SUDOVOY AKUSTIKE [Manual on Ship Acoustics] in Russian 1978 signed to press 26 Oct 78 pp 2-91, 94-103, 160-480

[Excerpts from book edited by Doctor of Engineering Sciences, Professor I.I. Klyukin and Candidate of Engineering Sciences I.I. Bogolepov, Izdatel'stvo Sudostroyeniye, 6,600 copies]

CONTENTS

Foreword 1
Basic Definitions 3

Chapter 1. Acoustic Vibrations and Waves (A. A. Kleshchev, I. I. Klyukin, A. S. Nikiforov) 5
1.1. Basic Acoustic Field Equations 5
1.2. Plane, Spherical and Cylindrical Waves in Gases and Fluids 7
1.3. Wave Propagation in Elastic and Viscous Media 14
1.4. Elastic Waves in Rods, Plates and Cylindrical Shells 22
1.5. Mechanical Strength of Rods, Plates and Hull Structures. Acoustic Irradiation of Plates and Shells 34
1.6. Electromechanical and Electroacoustic Analogies 42
1.7. Electrical, Mechanical and Acoustic n-Poles 48
Bibliography 51

Chapter 2. Principles of Measurement Acoustics (A. Ye. Kolesnikov) 56
2.1. Input and Metering Circuits. Calibration of Acoustic- and Vibration Meters 56
2.2. Measurement of Noise and Vibration 67
2.3. Spectral and Correlation Analysis 70
2.4. Measurement of Vibration Power Radiated by Machinery 78
2.5. Similitude and Dimensional Techniques in Marine Acoustics 84
2.6. Determination of Reliability and Precision of Acoustic Measurements 86
2.7. Application of Electronic Digital Computers for Acoustic Measurements 90
Bibliography 94

APPROVED FOR RELEASE: 2007/02/08: CIA-RDP82-00850R000200100009-9

APPROVED FOR RELEASE: 2007/02/08: CIA-RDP82-00850R000200100009-9

Chapter 3. General Characteristics of Machinery as Vibration and Noise Sources (V. I. Popkov, V. K. Il'kov) 97
3.1. Induced Mechanical Vibrations 97
3.2. Mechanical Radiation of Vibration Energy 108
Bibliography 119

4.2. Standardization of Noise and Vibration on Ships 121
4.3. Monitoring of Ship Noise and Vibration 127
Bibliography 130

Chapter 6. Reduction of Noise of Steam Turbine and Gas Turbine Power Plants (V. I. Zinchenko) 133
6.1. Basic Sources of Noise of STP and GTP 133
6.2. Gas Turbine Engine Noise. Turbocompressor Noise Reduction 135
6.3. Elimination of Gas Dynamic Free Vibrations in Exhaust Pipes 141
6.4. Gas Turbine Engine Intake and Exhaust Mufflers and Their Calculation 145
6.5. Reducer Noise and Ways to Reduce It 157
6.6. Ship Pipe Valve Noise and Ways to Reduce It 163
Bibliography 176

Chapter 7. Reduction of Noise of Ventilation and Air Conditioning Systems (N. F. Yegorov, Yu. I. Petrov, G. A. Khoroshev) 179
7.1. Noise Sources in Ventilation and Air Conditioning System 179
7.2. Reduction of Turbulence Noise and Nonuniform Flow Noise of Blowers 186
7.3. Acoustic Calculation of Ventilation and Air Conditioning Systems 202
7.4. Ways to Reduce Noise of Ventilation and Air Conditioning Systems 214
7.5. Noise Mufflers of Ship Ventilation and Air Conditioning Systems 217
Bibliography 222

Chapter 8. Noise Reduction of Ship Hydraulic Systems, Compressors and Electrical Machinery (N. I. Duan, M. A. Fedorovich) 224
8.1. Causes of Noise in Ship Hydraulic Systems 224
8.2. Hydrodynamic and Mechanical Noise Sources in Pumps 231
8.3. Ways to Reduce Pump Noise 234
8.4. Noise and Vibration of Reciprocating Compressors 238
8.5. Basic Noise Sources of Electrical Machinery 241
8.6. Reduction of Noise of Electrical Machinery 251
Bibliography 259

Chapter 9. Reduction of Noise of Operating Engines and Other Systems (L. S. Boroditskiy) 261
9.1. Engine Noise in Ship Rooms 261
9.2. Methods of Reducing Screw and Other Engine Noise 269
9.3. Noise Interference on Bridge and Ways to Reduce It 272
Bibliography 286

APPROVED FOR RELEASE: 2007/02/08: CIA-RDP82-00850R000200100009-9

APPROVED FOR RELEASE: 2007/02/08: CIA-RDP82-00850R000200100009-9

Chapter 10. Acoustic Insulation on Ships (I. I. Bogolepov, E. I. Avferonok, K. I. Mal'tsev) 289
10.1. Importance of Acoustic Insulation on Ships 289
10.2. Basic Principles of Acoustic Insulation 289
10.3. Acoustic Insulation of Single-Wall Structures 294
10.4. Acoustic Insulation of Double-Wall Structures 300
10.5. Planning of Acoustic Insulation of Ship 306
10.6. Soundproofing Shields and Booths 319
10.7. Acoustic Insulation of Ship Machinery 325
10.8. Materials for Marine Acoustic Insulation and Soundproofing Structures 334
10.9. Measurement of Acoustic Insulation 336
10.10. Personal Acoustic Insulation Gear 341
Bibliography 343

Chapter 11. Soundproofing of Ships (K. A. Velizhanina, I. V. Lebedeva) 346
11.1. Application of Soundproofing Structures 346
11.2. Wave Parameters. Porous Panel. Resonant Sound Absorbers 350
11.3. Laminated Soundproofing Structures. Space Absorbers. Membrane Acoustic Absorbers 355
11.4. Soundproofing Structures with Oblique and Diffusive Incidence 361
11.5. Acoustic Absorption in High Acoustic Pressure Levels 363
11.6. Measurement of Acoustic Absorption 366
Bibliography 371

Chapter 12. Vibration Damping of Marine Machinery (I. I. Klyukin, N. G. Belyakovskiy, B. P. Polonskiy, V. I. Popkov) 373
12.1. Purpose and Classification of Vibration-Damping Shock-Absorbing Structures and Fasteners 373
12.2. Calculation of Effectiveness of Vibration-Damping Mounts Using Electromechanical Analogies, Matrix Procedures and Orthogonal Polynomials 395
12.3. Energy Analysis of Effectiveness of Shock-Absorbing Mounts 408
12.4. Marine Shock Absorbers 415
12.5. Calculation of Shock-Absorbing Mounts of Marine Machinery 424
12.6. Vibration Damping of Nonbearing Connections of Machinery 428
12.7. Measurement of Vibration Damping of Shock-Absorbing Mounts 434
Bibliography 436

Chapter 13. Vibration Damping of Ship Hull Structures (L. S. Nikiforov, V. T. Lyapunov) 438
13.1. Basic Principles and Laws of Vibration Damping for Bending Waves 438
13.2. Vibration Damping of Vibration-Impeding Masses and Stiffening Ribs 441

APPROVED FOR RELEASE: 2007/02/08: CIA-RDP82-00850R000200100009-9

APPROVED FOR RELEASE: 2007/02/08: CIA-RDP82-00850R000200100009-9

13.3. Vibration Damping of Plate Joints 445
13.4. Vibration Damping of Periodic Barriers 448
13.5. Influence of Features of Ship Structures on Vibration Damping of Barrier 449
13.6. Vibration Damping as Function of Vibration Absorption 452
13.7. Efficiency Analysis of Ship Vibration-Damping Techniques 453
13.8. Personal Vibration Safety Gear 455
13.9. Measurement of Vibration Damping 458
Bibliography 464

Chapter 14. Vibration Absorption on Ships (A. S. Nikiforov, I. I. Klyukin) 465
14.1. Absorption of Vibration Energy in Deformable Media and Structures 465
14.2. Hard Vibration-Absorbing Coatings 468
14.3. Soft Vibration-Absorbing Coatings 472
14.4. Reinforced Vibration-Absorbing Coatings 474
14.5. Vibration-Absorbing Construction Materials 476
14.6. Bulk Vibration Absorbers and Bituminous Damping Materials 478
14.7. Local Vibration Absorbers 482
14.8. Where to Install Vibration Absorbers in Ship Structures 491
14.9. Analysis of Effectiveness of Vibration Absorption Techniques in Ship Structures 493
14.10. Measurement of Vibration Absorption 495
Bibliography 498

Chapter 15. Forecasting of Acoustic Situation and Combined Application of Noise Control Techniques on Ships (V. M. Spiridonov) 500
15.1. General Description of Problem 500
15.2. Forecasting of Noise Level on Ship in Design Stage 502
15.3. Basic Relations and General Calculation Procedure 504
15.4. Requirements on Programming of Calculation of Anticipated Noise Level with Computer 513
15.5. Graphoanalytical Calculation of Anticipated Noise Level 518
15.6. Features of Combined Application of Noise Control Techniques 530
Bibliography 539

APPROVED FOR RELEASE: 2007/02/08: CIA-RDP82-00850R000200100009-9

APPROVED FOR RELEASE: 2007/02/08: CIA-RDP82-00850R000200100009-9

PUBLICATION DATA

English title	: MANUAL ON SHIP ACOUSTICS
Russian title	: SPRAVOCHNIK PO SUDOVOY AKUSTIKE
Author (s)	:
Editor (s)	: I. I. Klyukin, I. I. Bogolepov
Publishing House	: Sudostroyeniye
Place of Publication	: Leningrad
Date of Publication	: 1978
Signed to press	: 26 Oct 78
Copies	: 6600
COPYRIGHT	: Izdatel'stvo "Sudostroyeniye", 1978

APPROVED FOR RELEASE: 2007/02/08: CIA-RDP82-00850R000200100009-9

APPROVED FOR RELEASE: 2007/02/08: CIA-RDP82-00850R000200100009-9

ANNOTATION

[Text] The results of scientific studies and developments on ship acoustics are generalized in this manual. Sources of ship noises are examined. Basic data, methods and information necessary for the design, manufacture and testing of systems for noise and acoustic vibration abatement at the source, on propagation paths and in ship rooms are presented. Problems of acoustic insulation, sound absorption, vibration insulation and vibration damping and of the combined application of noise abatement systems are examined in detail.

Advanced Soviet experience in acoustical developments, undertaken for the purpose of improving the inhabitability of ships and of work conditions on them, and the results of foreign practice are reflected.

The manual is intended for scientific researchers at institutions, planning-design offices and factories. It will be beneficial to students and post-graduate students.

APPROVED FOR RELEASE: 2007/02/08: CIA-RDP82-00850R000200100009-9

APPROVED FOR RELEASE: 2007/02/08: CIA-RDP82-00850R000200100009-9

FOREWORD

Modern machinery and mechanisms produce strong noises. The relentless increase of their power is accompanied by a further increase of noise. At the same time requirements on living conditions on ships are becoming increasingly more rigid. Therefore noise abatement has taken on special scientific and practical importance in recent years.

In view of the importance of marine acoustics problems Sudostroyeniye has published in the last decade a number of books on that subject. Noteworthy, in particular, are the following publications: "Rasprostraneniye i Poglo-shcheniye Zvukovoy Vibratsii na Sudakh" [Propagation and Absorption of Acoustic Vibrations on Ships], 1968 (authors A. S. Nikiforov, S. V. Budrin); "Akusticheskiye Izmereniya v Sudostroyenii" [Acoustic Measurements in Ship-building], 2nd edition, 1968 (authors I. I. Klyukin, A. Ye. Kolesnikov); "Zvukoizolyatsiya na Sudakh" [Acoustic Insulation on Ships], 1970 (authors I. I. Bogolepov, E. I. Avferonok); "Bor'ba s Shumom i Zvukovoy Vibratsiyey na Sudakh" [Noise and Acoustic Vibration Abatement on Ships], 2nd edition, 1971 (author I. I. Klyukin); "Shum Sudovykh Sistem Ventilyatsii i Kon-ditsionirovaniya Vozdukha" [Noise of Ship Ventilation and Air Conditioning Systems], 1974 (authors N. F. Yegorov, Yu. I. Petrov, G. A. Khoroshev); "Vibroakusticheskaya Diagnostika i Snizheniye Vibroaktivnosti Sudovykh Mekhanizmov" [Vibroacoustic Diagnostics and Reduction of Vibration Activity of Ship Machinery], 1974 (author V. I. Popkov); "Snizheniye Strukturnogo Shuma v Sudovykh Pomeshcheniyakh" [Reduction of Structural Noise in Ship Rooms], 1974 (authors L. S. Boroditskiy, V. M. Spiridonov); "Vibroizo-lyatsiya v Sudovykh Konstruktsiyakh" [Vibration Insulation in Ship Con-structions], 1975 (authors V. T. Lyapunov, A. S. Nikiforov) and certain others.

The time has come to summarize the experience that has been compiled in the field of marine acoustics, in a comprehensive manual, covering its various aspects. This manual, which serves this purpose to a certain extent, in addition to data from the above-cited and other books on acoustics, includes information from scientific and trade periodicals that have appeared in recent years in the USSR and abroad.

APPROVED FOR RELEASE: 2007/02/08: CIA-RDP82-00850R000200100009-9

APPROVED FOR RELEASE: 2007/02/08: CIA-RDP82-00850R000200100009-9

The authors deemed it appropriate not to restrict the contents of the manual to reference information; the book also includes materials of a methodological nature. Calculation data are given, as a rule, in the International Units System. In some cases the SGS [Centimeter-gram-second] and MKSS [Meter-kilogram-second-candle] systems are used.

This book is the first manual on ship acoustics. Readers are invited to send inquiries and comments to the following address: 191065, Leningrad, ul. Gogolya, 8, izdatel'stvo "Sudostroyeniye."

APPROVED FOR RELEASE: 2007/02/08: CIA-RDP82-00850R000200100009-9

APPROVED FOR RELEASE: 2007/02/08: CIA-RDP82-00850R000200100009-9

BASIC DEFINITIONS

A -- acoustic absorption
a -- length
B -- bending rigidity of beam
b -- width
C -- longitudinal or linear rigidity
c -- speed of sound in medium
c_b -- bending wave velocity
c_{lo} -- longitudinal wave velocity
c_{sh} -- shear wave velocity
D -- bending rigidity of plate; diameter
d -- thickness
E -- energy; Young's modulus
F -- force
f -- frequency
f_{cr} -- critical frequency of plate
G -- shear modulus; flow rate
g -- acceleration of gravity
h -- height; thickness
I -- acoustic intensity; moment of inertia; electric current
i -- imaginary unit; electric current
J -- moment of inertia
k -- wave number
L -- acoustic pressure level
L_N -- acoustic power level
l -- linear dimension
M -- momentum; mass
m -- mass per unit area or length
N -- acoustic power
n -- rotation frequency
p -- acoustic pressure
Q -- generalized force; Q-factor; productivity
R -- sound insulation; radiation resistance
R_a -- active component of acoustic impedance
r -- radius, distance

APPROVED FOR RELEASE: 2007/02/08: CIA-RDP82-00850R000200100009-9

APPROVED FOR RELEASE: 2007/02/08: CIA-RDP82-00850R000200100009-9

S -- area
T -- period; reverberation time; absolute temperature
t -- time; temperature; thickness
U -- voltage
V -- volume
v -- velocity
W -- specific acoustic impedance; moment of resistance
w -- acoustic energy density
X_a -- reactive part of acoustic impedance
x, $\dot{x}$, $\ddot{x}$ -- displacement, velocity and acceleration in x coordinate for waves in solids
y, $\dot{y}$, $\ddot{y}$ -- displacement, velocity and acceleration in y coordinate for waves in solids
Z_a -- acoustic impedance
Z_m -- total mechanical impedance
α -- absorption coefficient; attenuation coefficient (constant)
β -- reflection coefficient; wave number (phase constant)
δ -- elastic deformation; thickness
ΔL -- acoustic pressure drop
η -- loss coefficient
θ, ϑ -- angle of incidence
λ -- acoustic wavelength; Lame's first constant
μ -- Lame's second constant
ξ, $\dot{\xi}$, $\ddot{\xi}$ -- displacement, velocity and acceleration
ρ -- density of medium
σ -- Poisson's ratio
ϕ -- ratio of vibration frequency of plate to critical frequency; velocity potential; angle
ω -- circular frequency

When symbols given in this list are used in the text of the book for other definitions additional explanation is given. Symbols not contained in the list are also explained.

APPROVED FOR RELEASE: 2007/02/08: CIA-RDP82-00850R000200100009-9

APPROVED FOR RELEASE: 2007/02/08: CIA-RDP82-00850R000200100009-9

CHAPTER 1. ACOUSTIC VIBRATIONS AND WAVES

1.1. Basic Acoustic Field Equations

Elastic and fluid media (including gases), examined in marine acoustics, are considered to be continuous. This means physically that the length of a wave propagating in such a medium vastly exceeds the size of the molecules, and the period of vibrations vastly exceeds their free flight time between collisions. A medium (elastic or fluid) is perfect when internal friction and thermal conductivity are ignored. Only a longitudinal acoustic wave exists in a perfect fluid, and the particles of such a medium in a plane acoustic wave are displaced in the direction of propagation of the wave. The displacement of particles involves a change of pressure (normal pressure) p and density ρ, which are transferred by the wave. An acoustic wave has five parameters: pressure p, density ρ and three components of velocity vector $\vec{v}$. The adiabatic equation of state of a medium establishes the relationship between pressure p_Σ and density ρ_Σ [3, 10]:

$$p_\Sigma = \Phi(\rho_\Sigma). \tag{1.1.1}$$

Euler's nonlinear vectorial motion equation includes the following: velocity of particles v, pressure p_Σ and density ρ_Σ:

$$\frac{\partial \vec{v}}{\partial t} = -\frac{1}{\rho_\Sigma} \operatorname{grad} p_\Sigma. \tag{1.1.2}$$

The continuity equation derives from the requirement that a medium exhibit continuity and is determined by the law of conservation of mass:

$$\nabla(\rho_\Sigma \vec{v}) = -\frac{\partial \rho_\Sigma}{\partial t}, \tag{1.1.3}$$

where ∇ is Hamilton's vector operator.

Marine acoustics specialists are usually interested in small amplitudes of vibrations of particles. This enables them to linearize the equations derived above.

APPROVED FOR RELEASE: 2007/02/08: CIA-RDP82-00850R000200100009-9

APPROVED FOR RELEASE: 2007/02/08: CIA-RDP82-00850R000200100009-9

The linear equation of state acquires the form [15]

$$p = \left(\frac{\partial p_\Sigma}{\partial \rho_0}\right)_{s=\text{const}} \cdot \rho, \tag{1.1.4}$$

where s is entropy; p, ρ are the deviations of the pressure and density in an acoustic wave from equilibrium p_0, ρ_0, and here $p \ll p_0$, $\rho \ll \rho_0$.

Since acoustic vibrations and waves are adiabatic processes, a constraint is placed on entropy:

$$\frac{\partial s}{\partial t} = 0. \tag{1.1.5}$$

In view of the fact that velocity $\vec{v}$ in an acoustic wave is small, convective acceleration in Euler's equation (1.1.2) is negligible in comparison with the local acceleration and the linear equation of motion acquires the form

$$\frac{\partial \vec{v}}{\partial t} + \frac{\nabla p}{\rho_0} = 0. \tag{1.1.6}$$

Linearization of the continuity equation (in consideration of the inequality $\rho \ll \rho_0$, which is equivalent to $v \ll c$, where c is the acoustic wave propagation velocity) leads to the equation

$$\frac{\partial \rho}{\partial t} + \rho_0 \nabla \vec{v} = 0. \tag{1.1.7}$$

Variable density ρ in an acoustic wave in continuity equation (1.1.7) is replaced with p with the aid of equation of state (1.1.4):

$$\frac{\partial p}{\partial t} + \rho_0 \left(\frac{\partial p_\Sigma}{\partial \rho_0}\right)_{s=\text{const}} \nabla \vec{v} = 0. \tag{1.1.8}$$

We introduce velocity potential ϕ in accordance with $\vec{v}$ = grad ϕ; this can always be done for a perfect fluid, since the motion of its particles is eddy-free.

Linear equation of motion (1.1.6) establishes the relationship between acoustic pressure p and velocity potential ϕ [37]:

$$p = -\rho_0 \frac{\partial \varphi}{\partial t}. \tag{1.1.9}$$

It follows from equation (1.1.9) that in a harmonic acoustic wave of frequency ω pressure p differs from the velocity potential by the constant factor

$$p = -i\omega\rho_0\varphi. \tag{1.1.10}$$

APPROVED FOR RELEASE: 2007/02/08: CIA-RDP82-00850R000200100009-9

APPROVED FOR RELEASE: 2007/02/08: CIA-RDP82-00850R000200100009-9

Substituting (1.1.9) into equation (1.1.8), we derive a second-order differential equation, called the wave equation:

$$\Delta\varphi = \frac{1}{c^2}\frac{\partial^2\varphi}{\partial t^2}, \qquad (1.1.11)$$

where $c = \sqrt{\left(\frac{\partial p_\Sigma}{\partial \rho_0}\right)_{s=\text{const}}}$ is the acoustic wave velocity; Δ is Laplace's scalar operator, which in Cartesian coordinates x, y, z acquires the form

$$\Delta = \frac{\partial}{\partial x^2} + \frac{\partial}{\partial y^2} + \frac{\partial}{\partial z^2}.$$

If an acoustic wave is characterized by a harmonic dependence on time exp ($i\omega t$), then it is possible to convert from the wave equation, which velocity potential ϕ, acoustic pressure p, particle velocity components $\vec{v}$ and density ρ satisfy, to the Helmholtz equation for the same acoustic field variables:

$$\Delta\Phi + k^2\Phi = 0, \qquad (1.1.12)$$

where Φ is any of the above-listed acoustic wave parameters; $k = 2\pi/\lambda$ is the wave number; λ is the acoustic wavelength in a fluid.

In orthogonal curvilinear coordinates x_1, x_2, x_3 equation (1.1.12) acquires the form [21]

$$\sum_{m=1}^{3}\frac{1}{h_1h_2h_3}\frac{\partial}{\partial x_m}\left[\frac{h_1h_2h_3}{h_m^2}\frac{\partial\Phi}{\partial x_m}\right] + k^2\Phi = 0, \qquad (1.1.13)$$

where h_1, h_2, h_3 are scale factors.

The solution of second-order differential equation (1.1.13) in partial derivatives, which explains the dependence of function Φ on the coordinates, can be found by the classic variable separation method.

1.2. Plane, Spherical and Cylindrical Waves in Gases and Fluids

General Premises. The wave equation for a plane wave can be derived from general wave equation (1.1.11), on the assumption that there is no dependence on the y and z coordinates [3, 10]:

$$c^2\frac{\partial^2\Phi}{\partial x^2} = \frac{\partial^2\Phi}{\partial t^2}. \qquad (1.2.1)$$

APPROVED FOR RELEASE: 2007/02/08: CIA-RDP82-00850R000200100009-9

APPROVED FOR RELEASE: 2007/02/08: CIA-RDP82-00850R000200100009-9

Particle velocity $\vec{v}$ in a plane wave is perpendicular to the leading edge of the wave, i.e., coincides with wave propagation direction x, since the velocity components on the y and z axes vanish: $\frac{\partial\Phi}{\partial y} = \frac{\partial\Phi}{\partial z} = 0$.

The solution of equation (1.2.1), derived by d'Alembert, is [33]

$$\Phi(x, t) = \Phi_1(ct - x) + \Phi_2(ct + x), \tag{1.2.2}$$

where Φ_1 and Φ_2 are arbitrary functions.

Acoustic velocity $c = \sqrt{\left(\frac{\partial p_\Sigma}{\partial \rho_0}\right)_{s=\text{const}}}$ in a fluid may be expressed through the adiabatic compressibility modulus κ_{ad}:

[ад=ad]

$$c = \sqrt{\left(\frac{\partial p_\Sigma}{\partial \rho_0}\right)_{s=\text{const}}} = \sqrt{\frac{\varkappa_{\text{ад}}}{\rho_0}}. \tag{1.2.3}$$

For gases (in consideration of Poisson's adiabatic law) the acoustic velocity may be found from the expression

$$c = \sqrt{\frac{\gamma p_0}{\rho_0}}\left(\frac{\rho}{\rho_0}\right)^{\frac{\gamma-1}{2}} \approx \sqrt{\frac{\gamma p_0}{\rho_0}}\left(1 + \frac{\gamma-1}{2\rho_0 c^2}p + \cdots\right), \tag{1.2.4}$$

where p_0 is constant gas pressure; $\gamma = c_p/c_v$ is the specific heat ratio.

The values that the acoustic velocity acquires in certain fluids are listed in Table 1.1.

Pressure p in a plane wave is related to particle velocity $\dot{\xi} = V_x$ by the equation

$$p = \rho_0 c\dot{\xi}. \tag{1.2.5}$$

Thus, the pressure in a plane wave is proportional to the velocity of the particles and is in the identical phase with it. Proportionality factor $\rho_0 c$ is called the wave resistance of a medium; its values for certain fluids are given in Table 1.1.

Pressure p in a plane harmonic wave of frequency ω is written as

$$p = p_0 \exp[-i(\omega t - \vec{k}\vec{r})], \tag{1.2.6}$$

where $\vec{k}$ is the wave vector $\vec{k} = k\vec{n}_0$; $\vec{n}_0$ is the unit vector of wave normal

APPROVED FOR RELEASE: 2007/02/08: CIA-RDP82-00850R000200100009-9

APPROVED FOR RELEASE: 2007/02/08: CIA-RDP82-00850R000200100009-9

Table 1.1. Acoustic Velocities in Certain Fluids

1) Среда	ρ_0, кг/м³	c, м/с	$\rho_0 c$, кг/(м²·с)
2) Воздух, 0°C и 760 мм рт. ст.	1,29	333	433
3) Водород, 0°C и 760 мм рт. ст.	0,09	1260	113
4) Вода дистиллированная, 0°C	999	1430	$1429 \cdot 10^3$
5) Вода морская, 10°C	1 030	1500	$1545 \cdot 10^3$
6) Ртуть	13 600	1460	$1986 \cdot 10^4$
7) Спирт этиловый	790	1180	$932 \cdot 10^2$

Key: 1. Medium
2. Air, 0°C and 760 mm Hg
3. Hydrogen, 0°C and 760 mm Hg
4. Distilled water, 0°C
5. Sea water, 10°C
6. Mercury
7. Ethyl alcohol

[кг=kg; c=s]

$\vec{n}$, perpendicular to the leading edge of the wave; $\vec{r}$ is the radius vector of the point of observation; p_0 is a constant.

To write wave equation (1.1.11) in spherical coordinates r, θ, ϕ (r is distance, θ is the polar angle and ϕ is the azimuthal angle), we may use the expression for the Laplacian in an arbitrary orthogonal curvilinear coordinate system:

$$\sum_{m=1}^{3} \frac{1}{h_1 h_2 h_3} \frac{\partial}{\partial x_m} \left[\frac{h_1 h_2 h_3}{h_m^2} \frac{\partial \Phi}{\partial x_m} \right] = \frac{1}{c^2} \frac{\partial^2 \Phi}{\partial t^2}. \qquad (1.2.7)$$

In this spherical coordinate system $h_1 = h_r = 1$; $h_2 = h_\theta = r$; $h_3 = h_\phi = r \sin\theta$; wave equation (1.2.7) acquires the form

$$\frac{\partial^2 \Phi}{\partial r^2} + \frac{2}{r} \frac{\partial \Phi}{\partial r} + \frac{1}{r^2 \sin\theta} \frac{\partial}{\partial \theta} \left(\sin\theta \frac{\partial \Phi}{\partial \theta} \right) + \frac{1}{r^2 \sin\theta} \frac{\partial^2 \Phi}{\partial \varphi^2} = \frac{1}{c^2} \frac{\partial^2 \Phi}{dt^2}. \qquad (1.2.8)$$

When the dependence on time is harmonic the right hand side will contain, instead of $\frac{1}{c^2} \frac{\partial^2 \Phi}{dt^2}$, the term $k^2\Phi$, and equation (1.2.8) becomes the scalar Helmholtz equation

$$\Delta\Phi + k^2\Phi = 0. \qquad (1.2.9)$$

Solving equation (1.2.9) by separating the variables, we find the partial solution $\Phi_m(r, \theta, \phi)$ of Helmholtz equation in spherical coordinates:

APPROVED FOR RELEASE: 2007/02/08: CIA-RDP82-00850R000200100009-9

APPROVED FOR RELEASE: 2007/02/08: CIA-RDP82-00850R000200100009-9

$$\Phi_{mn}(r, \theta, \varphi, t) = (A_m \cos m\varphi + B_m \sin m\varphi)[D_{mn}P_n^m(\cos\theta) + \\ + C_{mn}Q_n^m(\cos\theta)][E_n j_n(kr) + F_n n_n(kr)]e^{-i\omega t}, \quad (1.2.10)$$

where A_m, B_m, D_{mn}, C_{mn}, E_n, F_n are arbitrary constants; $P_n^m(\cos\theta)$ and $Q_n^m(\cos\theta)$ are conjugate first- and second-kind Legendre functions, respectively; $j_n(kr)$ and $n_n(kr)$ are spherical Bessel and Neumann functions [20].

The simplest kind of spreading spherical wave is produced when sound is emitted by a uniformly pulsating ball, i.e., by a ball that expands and contracts in such a way that the amplitudes of the vibrations do not depend on θ and ϕ (spherically symmetric waves). Wave equation (1.2.8) in this case acquires the form

$$\frac{1}{r^2}\frac{\partial}{\partial r}\left(r^2\frac{\partial\Phi}{\partial r}\right) = \frac{1}{c^2}\frac{\partial^2\Phi}{dt^2}. \quad (1.2.11)$$

The general solution of this equation, which is finite everywhere except at the point r = 0, is

$$\Phi(r, t) = \frac{1}{r}f_1(r - ct) + \frac{1}{r}f_2(r + ct).$$

If this motion is harmonic the partial solution of Helmholtz equation (1.2.9) for acoustic field potential Φ of this pulsating ball is

$$\Phi_0 = E[j_0(kr) \pm in_0(kr)]e^{-i\omega t} = \\ = Eh_0^{(1),(2)}(kr)e^{-i\omega t}, \quad (1.2.12)$$

where $h_0^{(1),(2)}(kr)$ are spherical first- and second-kind Hankel functions.

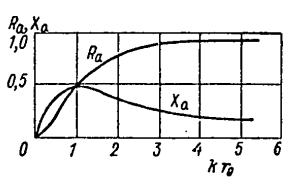

Figure 1.1. Normal active R_a and reactive X_a components of specific acoustic pressure of pulsating sphere.

If there is no dispersion the spherical waves will not change form during propagation, but their amplitude decreases by virtue of the factor 1/r.

A pulsating ball of small radius in comparison with the wavelength of the radiated sound, is called a point source. Pressure p in the acoustic wave generated by a harmonic point source with space velocity $q = q_0e^{-i\omega t}$ at great distances from the source, is expressed as follows:

APPROVED FOR RELEASE: 2007/02/08: CIA-RDP82-00850R000200100009-9

APPROVED FOR RELEASE: 2007/02/08: CIA-RDP82-00850R000200100009-9

$$p \approx -i\omega\left(\frac{\rho_0}{4\pi r}\right)q_0 e^{ik(r-ct)}. \qquad (1.2.13)$$

Specific acoustic impedance z of a pulsating sphere is determined as the ratio of acoustic pressure p on the radiating surface ($r = r_0$) to its vibration speed $\dot{\xi}$:

$$z = \rho_0 c\,(R_a + iX_a) = \rho_0 c\left[\frac{(kr_0)^2}{1+(kr_0)^2} - i\,\frac{kr_0}{1+(kr_0)^2}\right]. \qquad (1.2.14)$$

The dependences of R_a and X_a on $kr_0 = \frac{2\pi r_0}{\lambda}$ are plotted in Figure 1.1.

Particle velocity $\dot{\xi}$ in a spherically symmetric wave is aligned with the radius vector and does not depend on angles θ and ϕ:

$$\dot{\xi} = \pm\frac{p}{\rho_0 c} + \frac{1}{\rho_0 r}\int_{-\infty}^{t} p\,dt \qquad (1.2.15)$$

(the plus sign of the first term in the right hand side pertains to a converging wave).

The simplest directional radiator is an acoustic dipole, which may be a small (in comparison with the radiated wavelength) ball of radius r_0. The center of the ball vibrates (oscillates) along the axis at velocity $\dot{\xi} = \dot{\xi}_0 e^{-i\omega t}$. The pressure developed by this kind of source is determined by the expression [20, 30]:

$$p = A_1 p_1(\cos\theta)\,h_1^{(1)}(kr)\,e^{-i\omega t},$$

where A_1 is a constant, which depends on the velocity of points on the surface of the ball.

Assuming that the radius of the ball is small in comparison with the radiated wavelength ($kr_0 \ll 1$), the pressure developed by it is

$$p = i\rho_0\omega 2 r_0^3 \dot{\xi}_0 \frac{ikr-1}{4\pi r^2} e^{ikr}\cos\theta e^{-i\omega t}. \qquad (1.2.16)$$

It follows from (1.2.16) that the field intensity of a dipole is determined by the function $\cos\theta$ and is figure-8 shaped.

Specific acoustic impedance z of an oscillating sphere is

$$z = \frac{\rho_0 c}{3}(R_1 + iX_1) = \frac{1}{3}\rho_0 c\,\frac{k^4 r_0^4}{4+k^4 r_0^4} + i\,\frac{1}{3}\rho_0 c k r_0\,\frac{2+k^2 r_0^2}{4+k^4 r_0^4}.$$

APPROVED FOR RELEASE: 2007/02/08: CIA-RDP82-00850R000200100009-9

APPROVED FOR RELEASE: 2007/02/08: CIA-RDP82-00850R000200100009-9

The active impedances R_a (of a pulsating sphere) and R_1 (of an oscillating sphere) are compared in Figure 1.2.

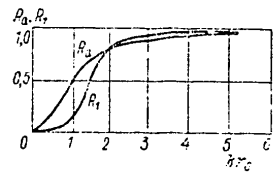

Figure 1.2. Normal radiation resistances of pulsating R_a and oscillating R_1 spheres.

In cylindrical coordinate system r, z, ϕ, assuming in equation (1.2.7) that $x_1 = r$, $x_2 = z$, $x_3 = \phi$, $h_1 = h_r = 1$, $h_2 = h_z = 1$, $h_3 = h_\phi = r$, we derive the wave equation in the form

$$\frac{1}{r}\frac{\partial}{\partial r}\left(r\frac{\partial\Phi}{\partial r}\right)+\frac{1}{r^2}\frac{\partial^2\Phi}{\partial\varphi^2}+\frac{\partial^2\Phi}{\partial z^2}=\frac{1}{c^2}\frac{\partial^2\Phi}{\partial t^2}. \qquad (1.2.17)$$

For a time function of the form $\exp(-i\omega t)$ the right hand side of the equation will contain the term $k^2\Phi$, and equation (1.2.17) changes to Helmholtz scalar equation, partial solution $\Phi_m(r, z, \phi, t)$ of which is expressed as

$$\Phi_m(r, z, \varphi, t)=\left(Ae^{ik_z z}+Be^{ik_z z}\right)\left[C_m I_m(k_r r)+\right.$$
$$\left.+D_m N_m(k_r r)\right]\left(E_m e^{im\varphi}+F_m e^{-im\varphi}\right)e^{-i\omega t}, \qquad (1.2.18)$$

where A, B, C_m, D_m, E_m, F_m are arbitrary constants; k_z is a separation constant; $k_r^2 = k^2 - k_z^2$; I_m and N_m are cylindrical Bessel and Neumann functions, respectively.

If a wave process does not depend on z, then $k_z = 0$ and $k_r = k$. The general solution of the Helmholtz equation (there is no function of z) for waves propagating from the center (r = 0) is written in the form

$$\Phi(r, \varphi, t)=e^{-i\omega t}\sum_{m=0}^{\infty}C_m H_m^{(1)}(kr)\cos(m\varphi-\varphi_m), \qquad (1.2.19)$$

where $H_m^{(1)}(kr)$ are cylindrical first-kind Hankel functions.

A radially symmetric (depending on t and r) cylindrical wave is radiated by a pulsating cylinder with radius r_0. In expression (1.2.19) for the velocity potential only the first term of the series remains (m = 0):

$$\Phi(r, t)=C_0 H_0^{(1)}(kr)e^{-i\omega t}. \qquad (1.2.20)$$

The radial vibration velocity is

APPROVED FOR RELEASE: 2007/02/08: CIA-RDP82-00850R000200100009-9

APPROVED FOR RELEASE: 2007/02/08: CIA-RDP82-00850R000200100009-9

$$v_r = k\frac{\partial\Phi}{\partial(kr)} = C_0 k\frac{\partial[H_0^1(kr)]}{\partial(kr)}e^{-i\omega t}. \tag{1.2.21}$$

For long waves ($kr_0 \ll 1$) specific acoustic resistance z to a pulsating cylinder is

$$z \approx \frac{\pi\rho_0 c}{2}kr_0 + i\rho_0 ckr_0 \ln\left(\frac{1}{kr_0}\right). \tag{1.2.22}$$

The pressure in a cylindrical wave at a great distance from the source changes as $r^{-1/2}$, and the specific acoustic resistance in a cylindrical wave far from the source is $\rho_0 c$, just as in a plane wave.

Energy Density w_1, Power N and Intensity of Sound (Power Flux Density) I in Acoustic Wave. Acoustic energy density w_1 is the specific (per unit volume of a medium) energy of an acoustic wave.

The instantaneous value of w_1 in a traveling wave is

$$w_1 = \frac{1}{2}\rho_0\dot{\xi}^2 + \frac{1}{2}\frac{1}{\rho_0 c^2}p^2. \tag{1.2.23}$$

In a traveling plane wave $p = \rho_0 c\dot{\xi}$ and the instantaneous energy density w_1 is

$$w_1 = \frac{1}{\rho_0 c^2}p^2 = \rho_0\dot{\xi}^2. \tag{1.2.24}$$

The mean energy density $\overline{w}_1$ (in time and space) in a traveling plane harmonic wave [$p = P_0 \cos(\omega t - kx)$] is

$$\overline{w}_1 = \frac{1}{2}\frac{1}{\rho_0 c^2}P_0^2 = \frac{1}{2}\rho_0\dot{\xi}_0^2, \tag{1.2.25}$$

where $\dot{\xi}_0$ is the amplitude of the vibration velocity.

Sound intensity (power flux density vector) $\vec{I}$, which determines the magnitude and direction of acoustic flux through a unit area per unit time, is

$$\vec{I} = p\vec{v}. \tag{1.2.26}$$

In a traveling plane acoustic wave the modulus of $\vec{I}$ is

$$I = p\dot{\xi} = \frac{1}{\rho_0 c}p^2 = \rho_0 c\dot{\xi}^2 = w_1 c. \tag{1.2.27}$$

In a harmonic spherically symmetric wave, generated by a pulsating sphere $\left(p = P_0\frac{e^{ikr}}{r}\right)$, the intensity is ($kr \gg 1$):

APPROVED FOR RELEASE: 2007/02/08: CIA-RDP82-00850R000200100009-9

APPROVED FOR RELEASE: 2007/02/08: CIA-RDP82-00850R000200100009-9

$$I = \frac{P_0^2}{\rho_0 c r^2}\left[\cos^2(\omega t - kr) + \frac{1}{kr}\sin(\omega t - kr)\cos(\omega t - kr)\right]. \tag{1.2.28}$$

The mean intensity is

$$\bar{I} = \frac{1}{2}\frac{P_0^2}{\rho_0 c r^2}. \tag{1.2.29}$$

The total mean power $\bar{N}$, radiated by a monopole (pulsating sphere), is

$$\bar{N} = S\bar{I} = 4\pi r^2 \bar{I} = \frac{2\pi P_0^2}{\rho_0 c}. \tag{1.2.30}$$

The mean power of a dipole, formed by a small sphere with radius r_0 ($kr_0 \ll 1$), is

$$\bar{N} = \frac{1}{6}\pi r_0 \rho_0 c (kr_0)^4 \dot{\xi}_0^2, \tag{1.2.31}$$

where $\dot{\xi}_0$ is the oscillation velocity of the sphere.

The mean intensity (power flux density) $\bar{I}$ of an oscillating sphere of small radius r_0 is given by the formula

$$\bar{I} = \frac{1}{2}\rho_0 c k^4 r_0^6 \cos^2\theta \frac{\dot{\xi}^2}{r^2}. \tag{1.2.32}$$

1.3. Wave Propagation in Elastic and Viscous Media

In a perfectly elastic body deformation and tension vanish simultaneously when external forces are removed, and the body returns to its original undeformed condition. The deformed condition of a body is characterized by the deformation tensor -- a symmetric second-rank tensor [13, 19]:

$$\begin{bmatrix} \varepsilon_x & \gamma_{xy} & \gamma_{xz} \\ \gamma_{yx} & \varepsilon_y & \gamma_{yz} \\ \gamma_{zx} & \gamma_{zy} & \varepsilon_z \end{bmatrix}, \tag{1.3.1}$$

where ε_x, γ_{xy}, ε_y, γ_{xz}, ε_z, γ_{yz}, γ_{yx}, γ_{zx}, γ_{zy} are the components of the deformation tensor.

In linear approximation the deformation tensor components are

$$\begin{gathered} \varepsilon_x = \frac{\partial U}{\partial x}; \quad \varepsilon_y = \frac{\partial V}{\partial y}; \quad \varepsilon_z = \frac{\partial W}{\partial z}; \quad \gamma_{xy} = \gamma_{yx} = \frac{1}{2}\left(\frac{\partial U}{\partial y} + \frac{\partial V}{\partial x}\right); \\ \gamma_{xz} = \gamma_{zx} = \frac{1}{2}\left(\frac{\partial U}{\partial z} + \frac{\partial W}{\partial x}\right); \quad \gamma_{yz} = \gamma_{zy} = \frac{1}{2}\left(\frac{\partial V}{\partial z} + \frac{\partial W}{\partial y}\right), \end{gathered} \tag{1.3.2}$$

APPROVED FOR RELEASE: 2007/02/08: CIA-RDP82-00850R000200100009-9

APPROVED FOR RELEASE: 2007/02/08: CIA-RDP82-00850R000200100009-9

where dU, dV, dW are components of vector $\vec{dU}$ (on the x, y, z axes, respectively), which determines the change of distance between two points of a body as a result of the application of forces.

In the case of small deformations deformation components ε_x, ε_y, ε_z coincide with the relative elongation along the corresponding coordinate axis, and components γ_{ik} are virtually equal to the change of the angle (relative displacement) between two infinitesimal small segments, which prior to deformation intersected at a right angle.

The return of a body from a deformed state to the original state when external forces are relieved is the result of the action of internal stresses that appear in the deformed elastic body. To explain this concept in a perfectly elastic body, existing in equilibrium under the action of external loads, we isolate an elementary surface ds, described by the external normal $\vec{n}$ (Figure 1.3). We reduce the forces on elementary surface ds to the main force vector $d\vec{T}_n$ and main momentum $\vec{dM}_n$. We now may introduce the concept of force stress t_n

$$t_n = \frac{dT_n}{ds}$$

and momentum stress m_n

$$m_n = \frac{dM_n}{ds}.$$

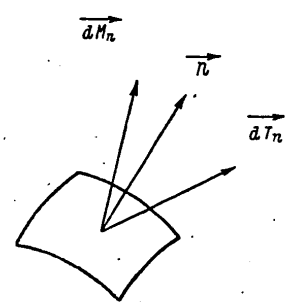

Figure 1.3. Forces and moments on elementary surface of elastic body.

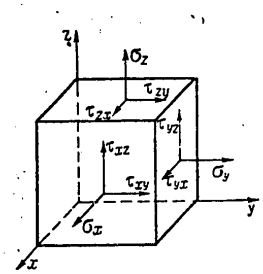

Figure 1.4. Components of stress tensor.

Since momentum stress is a value of the first order of smallness in comparison with force stress, we may ignore it and examine only the force stress t_n.

APPROVED FOR RELEASE: 2007/02/08: CIA-RDP82-00850R000200100009-9

APPROVED FOR RELEASE: 2007/02/08: CIA-RDP82-00850R000200100009-9

To determine the stress at a given point on any surface it is sufficient to know the stresses in three mutually perpendicular planes, passing through a given point. Three such planes and the stresses acting upon them, normal and tangential, are illustrated in Cartesian coordinates in Figure 1.4. The nine resulting stresses are written in the form of a quadratic table [35]:

$$\begin{bmatrix} \sigma_x & \tau_{xy} & \tau_{xz} \\ \tau_{yx} & \sigma_y & \tau_{yz} \\ \tau_{zx} & \tau_{zy} & \sigma_z \end{bmatrix}, \tag{1.3.3}$$

which is called a stress tensor, and its component elements are called stress tensor components. A stress tensor, like a deformation tensor, is a symmetric second-rank tensor. The equation of motion of an elastic medium (in projections onto the Cartesian coordinate axes) is[1]

$$\left.\begin{aligned} \frac{\partial\sigma_x}{\partial x} + \frac{\partial\tau_{yx}}{\partial y} + \frac{\partial\tau_{zx}}{\partial z} &= \rho\frac{\partial^2 u}{\partial t^2}; \\ \frac{\partial\tau_{xy}}{\partial x} + \frac{\partial\sigma_y}{\partial y} + \frac{\partial\tau_{zy}}{\partial z} &= \rho\frac{\partial^2 v}{\partial t^2}; \\ \frac{\partial\tau_{xz}}{\partial x} + \frac{\partial\tau_{yz}}{\partial y} + \frac{\partial\sigma_z}{\partial z} &= \rho\frac{\partial^2 w}{\partial t^2}, \end{aligned}\right\} \tag{1.3.4}$$

where u, v, w are components of displacement vector $\vec{u}$ of the points of a medium on the x, y, z axes.

When motion equation (1.3.4) was written the static forces of gravity were discarded as being insignificant in the dynamic mode. System (1.3.4) of three equations contains nine unknowns: six independent stress tensor components and three displacement vector components. The six missing equations are given by Hooke's generalized law, which establishes the relationship between stresses and deformations in an elastic body with small deformations. In accordance with this law each of the six stress tensor components at any point of a body is a linear function of six deformation tensor components:

$$\sigma_{ik} = c_{iklm}\gamma_{lm}, \tag{1.3.5}$$

where $c_{iklm} = \left(\frac{\partial\sigma_{ik}}{\partial\gamma_{lm}}\right)_{\gamma_{lm}=0}$ is Young's modulus.

If the deformations are assumed to be functions of stresses we obtain:

$$\gamma_{ik} = s_{iklm}\sigma_{lm}, \tag{1.3.6}$$

where s_{iklm} is the deformation coefficient, or the flexibility constant.

[1]Here and hereinafter ρ is the equilibrium density.

APPROVED FOR RELEASE: 2007/02/08: CIA-RDP82-00850R000200100009-9

APPROVED FOR RELEASE: 2007/02/08: CIA-RDP82-00850R000200100009-9

The combination of the values $c_{ikl m}$ constitutes a symmetric fourth-rank tensor, i.e., tensor of Young's moduli, or tensor of elastic constants. In the general case an arbitrary three-dimensional fourth-rank tensor has 81 independent constants. The symmetry of the deformation and stress tensors and the assumption that thermal effects are negligible reduce the number of independent tensor components of Young's moduli to 21. But then, this number of independent Young's moduli is characteristic of just materials that exhibit spatial symmetry (for instance, crystals of a triclinic system). The number of Young's moduli decreases for a solid body with symmetric elastic properties.

The elastic properties of an isotropic medium are identical in all directions that pass through a given point. Such a medium has two independent Young's moduli λ and μ, called Lame coefficients.

The second Lame coefficient μ coincides with the shear modulus. Other moduli of elastic media and bounded solids are expressed through λ and μ:

hydrostatic compression modulus, or compressibility modulus

$$K = \lambda + \frac{2}{3}\mu;$$

Young's modulus E for a rod

$$E = \frac{\mu(3\lambda + 2\mu)}{\lambda + \mu};$$

Poisson's ratio σ, equal to the ratio of transverse compression to longitudinal compression in a thin cylindrical rod under stress

$$\sigma = \frac{\lambda}{2(\lambda + \mu)}.$$

The elastic wave velocities and other characteristics of materials used in shipbuilding are given in Table 1.2.

Generalized Hooke's law (1.3.5) for an elastic medium makes it possible to exclude stresses from equations of motion (1.3.4); as a result these equations will contain one variable -- displacement vector $\vec{u}(u, v, w)$ of the points of an elastic medium.

In the case of an isotropic elastic medium the equation of motion acquires the form [22]

$$(\lambda + \mu)\,\mathrm{grad}\,\mathrm{div}\,\vec{u} + \mu\Delta\vec{u} = \rho\frac{\partial^2\vec{u}}{\partial t^2}. \qquad (1.3.7)$$

Equation (1.3.7) is called Lame's equation of motion. Two equations can be derived from Lame's equation: the first -- the scalar wave equation for expansion $\vartheta = \varepsilon_x + \varepsilon_y + \varepsilon_z$

APPROVED FOR RELEASE: 2007/02/08: CIA-RDP82-00850R000200100009-9

APPROVED FOR RELEASE: 2007/02/08: CIA-RDP82-00850R000200100009-9

$$\rho \frac{\partial^2 \vartheta}{\partial t^2} = (\lambda + 2\mu) \Delta \vartheta, \tag{1.3.8}$$

the second -- the vector wave equation for an eddy of the displacement vector $\vec{\omega} = \mathrm{rot}\, \vec{u}$

$$\rho \frac{\partial^2 \vec{\omega}}{\partial t^2} = \mu \Delta \vec{\omega}. \tag{1.3.9}$$

Table 1.2. Elastic Wave Velocities and Other Characteristics of Certain Shipbuilding Materials

1) Материал	2) Модуль Юнга $E \cdot 10^9$, Н/м²	3) Модуль сдвига $G \cdot 10^{10}$, Н/м²	4) Плотность $\rho \cdot 10^3$ кг/м³	5) Коэффициент Пуассона σ	6) Коэффициент внутренних потерь $\eta \cdot 10^{-4}$	7) Скорость продольной волны $c_п \cdot 10^3$, м/с	8) Скорость поперечной волны $c_с \cdot 10^3$, м/с	9) Скорость продольной волны в стержне $c_{п,ст} \cdot 10^3$, м/с	10) Скорость продольной волны в пластине $c_{п,пл} \cdot 10^3$, м/с
11) Сталь	210	8,14	7,8	0,29	1	5,94	3,22	5,2	5,4
12) Алюминиевые сплавы	72	2,77	2,8	0,3	5	5,87	3,14	5,1	5,3
13) Стеклопластик	21	0,955	1,7	0,1	130	3,55	2,36	3,5	3,54
14) Фанера	3,4	—	0,8	—	130	—	—	—	—
15) Плиты древесно-волокнистые	3	—	1	0,17	200	—	—	—	—

Key: 1. Material
2. Young's modulus
3. Shear modulus
4. Density
5. Poisson's ratio
6. Internal loss coefficient
7. Longitudinal wave velocity
8. Transverse wave velocity
9. Longitudinal wave velocity in rod
10. Longitudinal wave velocity in plate
11. Steel
12. Aluminum alloys
13. Glass fiber-reinforced plastic
14. Plywood
15. Wood fiber panels

[Н=N; кг=kg; с=s; п=lo; ст=r; пл=pl]

Displacement vector $\vec{u}$, according to Helmholtz theorem, is

$$\vec{u} = \mathrm{grad}\Phi + \mathrm{rot}\vec{A}, \tag{1.3.10}$$

where Φ is the scalar potential, which describes motion produced by sources of bulk displacements; $\vec{A}$ is the vector potential, which describes motion produced by eddies.

It turns out here that the scalar potential satisfies equation (1.3.8) [34, 41]:

APPROVED FOR RELEASE: 2007/02/08: CIA-RDP82-00850R000200100009-9

APPROVED FOR RELEASE: 2007/02/08: CIA-RDP82-00850R000200100009-9

$$\rho \frac{\partial^2 \Phi}{\partial t^2} = (\lambda + 2\mu) \Delta \Phi, \tag{1.3.11}$$

and vector potential $\vec{A}$ satisfies equation (1.3.9):

$$\rho \frac{\partial^2 \vec{A}}{\partial t^2} = \mu \Delta \vec{A}. \tag{1.3.12}$$

Volume expansion ϑ propagates in an isotropic medium at velocity

[п=lo]

$$c_п = \sqrt{\frac{\lambda + 2\mu}{\rho}}, \tag{1.3.13}$$

and an eddy propagates at velocity

$$c_c = \sqrt{\frac{\mu}{\rho}}. \tag{1.3.14}$$

When an expansion wave (free of eddies) propagates in a medium deformations of expansion (compression) and displacement occur, and when an eddy wave (distortion wave) propagates particles of the medium rotate and deformation of displacement occurs. An eddyless plane wave in a boundless elastic isotropic medium changes to a longitudinal wave, since displacement vector $\vec{u}$ in it is aimed in the direction of wave normal $\vec{n}$, i.e., in the direction of propagation. A plane distortion wave is a transverse wave with a displacement vector perpendicular to the wave normal, i.e., parallel to the wave front.

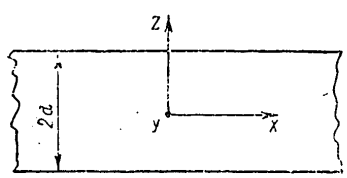

Figure 1.5. Elastic layer.

The velocities of longitudinal and transverse waves c_{lo} and c_{sh} in certain elastic media are given in Table 1.2.

During an analysis of harmonic processes in solids Lame's equation (1.3.8) reduces to two Helmholtz equations -- scalar and vector for the scalar (Φ) and vector ($\vec{A}$) potentials [see (1.3.10)], respectively:

$$(\Delta + k^2) \Phi = 0; \tag{1.3.15}$$

$$(\Delta + k^2) \vec{A} = 0. \tag{1.3.16}$$

The mathematical tool of the theory of elasticity and motion of a viscous fluid is identical, and therefore it is helpful to examine the problem of the propagation of sound in a viscous fluid. Viscous (tangential) forces occur between layers of fluid, moving at different velocities, and they try to equalize these velocities, i.e., prevent relative motion of the layers. In contrast to perfect fluid, the stress tensor of which contains only

APPROVED FOR RELEASE: 2007/02/08: CIA-RDP82-00850R000200100009-9

APPROVED FOR RELEASE: 2007/02/08: CIA-RDP82-00850R000200100009-9

diagonal members -- normal stresses (pressures), there are also tangential stresses in a viscous fluid, which are proportional to the deformation velocities.

Potential ϕ of a plane acoustic wave in a viscous medium obeys the equation [14]

$$\frac{1}{c^2}\frac{\partial^2\varphi}{\partial t^2}=\frac{\partial^2\varphi}{\partial x^2}+\frac{4}{3}\frac{\nu}{c^2}\frac{\partial^3\varphi}{\partial t\partial x^2}, \tag{1.3.17}$$

where ν is the kinematic viscosity coefficient.

Equation (1.3.17) is satisfied by the attenuating acoustic waves

$$\varphi=-\varphi_m e^{i(\omega t-k_\mu x)}e^{\alpha_m x},$$

where ϕ_m is the amplitude of the acoustic potential; α_m is the attenuation coefficient; $k_\mu = \omega/c_\mu$ is the wave number for a viscous medium; c_μ is the speed of sound in a viscous medium.

The coefficient α_m and wave number k_μ are related by the equation system

$$\left.\begin{aligned} 2\alpha_m k_\mu &= \frac{\frac{4}{3}\omega^3\nu}{c^4+\frac{16}{9}\omega^2\nu^2};\\ k_\mu^2-\alpha_m^2 &= \frac{c^2\omega^2}{c^4+\frac{16}{9}\omega^2\nu^2}.\end{aligned}\right\} \tag{1.3.18}$$

Up until now we have been examining boundless solids -- elastic media. In a semi-infinite medium surface waves, first analyzed by Rayleigh and thus called Rayleigh waves [4], can occur along its single stress-free boundary.

In a solid plate (layer) with free boundaries (Figure 1.5) Lamb waves can propagate, and these waves exhibit displacement both in the direction of wave propagation, and perpendicular to the plane of the plate.

Lamb's zero waveforms, which exist in an elastic layer at any frequency, are important for marine acoustics. They are a symmetric zero wave, called longitudinal, and antisymmetric zero wave, called bending.

Reciprocity Principle. Reciprocity is one of the most fundamental principles for linear vibrating systems. It connects the properties of acoustic fields and, in particular, permits the sources and receivers of oscillations to be interchanged, which is important for the solution of some problems [2].

Let Φ and Ψ be the velocity potentials. The wave equations for them are written in the form (1.1.13):

APPROVED FOR RELEASE: 2007/02/08: CIA-RDP82-00850R000200100009-9

APPROVED FOR RELEASE: 2007/02/08: CIA-RDP82-00850R000200100009-9

$$\Delta\Phi + k^2\Phi = 0; \quad \Delta\Psi + k^2\Psi = 0, \tag{1.3.19}$$

whence

$$\Delta\Phi\Psi - \Phi\Delta\Psi = 0. \tag{1.3.20}$$

We restrict the analysis to the case of plane waves. Then

$$\Delta\Phi = \frac{\partial^2\Phi}{\partial x^2}; \quad \Delta\Psi = \frac{\partial^2\Psi}{\partial x^2}.$$

Also considering the relationship between potentials and vibration pressures and velocities in harmonic processes for two points in space (the subscripts 1 and 2)

$$p_1 = i\omega\rho\Phi; \quad \dot{\xi}_1 = -\frac{\partial\Phi}{\partial x}; \; p_2 = i\omega\rho\Psi; \quad \dot{\xi}_2 = -\frac{\partial\Psi}{\partial x},$$

we obtain from (1.3.20)

$$p_1\dot{\xi}_2 = p_2\dot{\xi}_1. \tag{1.3.21}$$

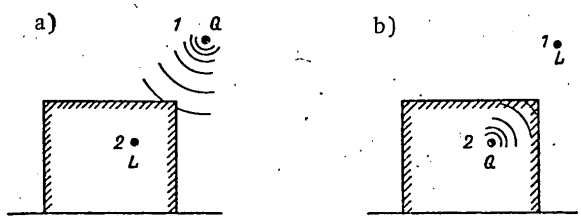

Figure 1.6. Illustration of application of reciprocity principle to sound-insulating systems.

It follows from equation (1.3.21) that interchanging the radiator and receiver while staying in the radiating mode does not alter the acoustic pressure on the receiver.

Integrating vibrating surface S in terms of area (which in this case is equal to the area of the wave front), we obtain

$$\int_S p_1\dot{\xi}_2\,ds = \int_S p_2\dot{\xi}_1\,ds. \tag{1.3.22}$$

An equation of the type (1.3.21) can be applied to the case of mechanical systems. We obtain

$$F_1\ddot{y}_2 = F_2\ddot{y}_1, \tag{1.3.23}$$

APPROVED FOR RELEASE: 2007/02/08: CIA-RDP82-00850R000200100009-9

APPROVED FOR RELEASE: 2007/02/08: CIA-RDP82-00850R000200100009-9

or for a harmonic process

$$F_1\dot{y}_2 = F_2\dot{y}_1. \qquad (1.3.24)$$

In the last equations F_1 and F_2 are the oscillating forces of two sources; $\ddot{y}_1$ and $\ddot{y}_2$ are the oscillating accelerations; $\dot{y}_1$ and $\dot{y}_2$ are the oscillation velocities (they, of course, may be replaced with oscillation displacements).

The reciprocity principle is also valid for inhomogeneous and absorbing media, and for cases when a wave experiences reflections and refractions when propagating from one point to another.

Example. A source with productivity Q operates at point 1 in the engine room. The sound level at point 2, located in the sound-insulated control booth, is L (Figure 1.6a). The level will be the same at point 1 when source Q is moved to point 2 (Figure 1.6b).

1.4. Elastic Waves in Rods, Plates and Cylindrical Shells[1]

Elastic Wavelength [42]. The main characteristic of elastic waves is their wave number k, related to wavelength λ by the equation $k = 2\pi/\lambda$.

Since $k = \omega/c$ (c is the wave propagation velocity), elastic wavelength is $\lambda = c/f$.

Longitudinal Waves in Rod. A rod is traditionally called an elongate elastic body, the length of which is substantially greater than the cross section. The cross sections of a rod with longitudinal waves shift in the direction of its axis (Figure 1.7). The longitudinal wave propagation velocity along the rod is

[п=lo; ст=r]

$$c_{\text{п. ст}} = \sqrt{\frac{E}{\rho}}, \qquad (1.4.1)$$

where E and ρ are Young's modulus and the density of the rod material.

In the cross sections of a rod with longitudinal waves with amplitude x there are also transverse displacements of its ends with amplitudes y and z. The ratio of these values for a rod of rectangular cross section is

$$\frac{y}{x} = \sigma\frac{k_{\text{п. ст}}a}{2}; \quad \frac{z}{x} = \sigma\frac{k_{\text{п. ст}}b}{2}, \qquad (1.4.2)$$

where a and b are the cross section dimensions of the rod; $k_{\text{lo.r}}$ is the wave number of longitudinal waves in a rod; σ is Poisson's ratio.

[1]S. V. Budrin contributed to this section.

APPROVED FOR RELEASE: 2007/02/08: CIA-RDP82-00850R000200100009-9

APPROVED FOR RELEASE: 2007/02/08: CIA-RDP82-00850R000200100009-9

The energy density of longitudinal waves (i.e., the amount of energy, averaged for a period, present in a segment of unit length of the rod) is

$$w_{\text{п. ст}} = \frac{1}{2} m_{\text{ст}} \omega^2 x_0^2, \qquad (1.4.3)$$

where m_r is the linear mass of the rod; x_0 is the amplitude of the displacement of the rod cross section.

The energy flux in a rod, i.e., the amount of energy passing through a cross section of the rod per unit time, is determined by the expression

$$\Pi_{\text{п. ст}} = \frac{1}{2} m_{\text{ст}} c_{\text{п. ст}} \omega^2 x_0^2 = w_{\text{п. ст}} c_{\text{п. ст}}. \qquad (1.4.4)$$

The values of $c_{\text{lo. r}}$ are given in Table 1.2 for certain materials that are used in shipbuilding.

The frequencies at which free longitudinal waves occur in a rod of length l, are

$$f_i = \frac{\pi}{2l} c_{\text{п. ст}} \quad (i = 1, 2, 3, \ldots). \qquad (1.4.5)$$

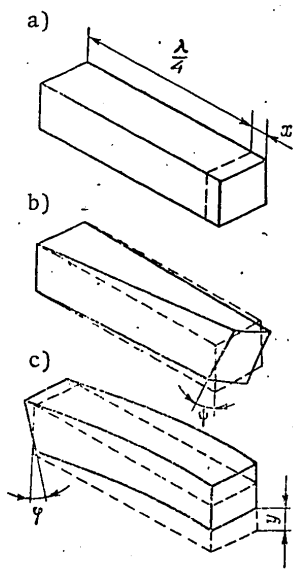

Figure 1.7. Nature of deformation of rod with longitudinal (a), torsional (b) and bending (c) vibrations.

Formula (1.4.5) is valid both for the free and for the fastened ends of a rod.

The number of frequencies of free longitudinal vibrations in a rod of length l that fall within frequency band Δf (the density of natural frequencies) is determined by the expression

$$N(\Delta f) = \frac{2l}{c_{\text{п. ст}}} \Delta f. \qquad (1.4.6)$$

Torsional Waves in Rod [26]. In the case of torsional vibrations the cross sections of a rod rotate around the center of gravity. The torsional wave propagation velocity in a rod of circular or annular cross section is

$$c'_{\text{к. ст}} = \sqrt{\frac{G}{\rho}}, \qquad (1.4.7)$$

where G is the shear modulus of the rod material (see Table 1.2).

APPROVED FOR RELEASE: 2007/02/08: CIA-RDP82-00850R000200100009-9

APPROVED FOR RELEASE: 2007/02/08: CIA-RDP82-00850R000200100009-9

The torsional wave propagation velocity in rods with a different cross section differs from $c'_{t.r}$, described by formula (1.4.7). Thus, for a rectangular cross section with sides a and b

[k=t; ct=r]

$$c''_{\text{к. ст}} = \chi c'_{\text{к.ст}}. \tag{1.4.8}$$

The dependence of coefficient χ on the ratio of sides a and b of the cross section of a rectangular rod are given below:

a/b	1	1,5	2	3	6
χ	0,92	0,85	0,74	0,56	0,32

As can be seen, a torsional wave propagates in a rod of noncircular or annular cross section at a lower velocity. When a/b > 6

$$c''_{\text{к. ст}} \approx \frac{2b}{a} c'_{\text{к. ст}}. \tag{1.4.9}$$

Expressions (1.4.8) and (1.4.9) are valid if the condition $k_{w.b}a < 1$, where $k_{w.b}$ is the wave number of the bending vibrations, determined by formula (1.4.28), in a plate of thickness d, is satisfied.

In the general case

$$c_{\text{к. ст}} = \sqrt{\frac{C}{\rho I_p}}, \tag{1.4.10}$$

where C is the rigidity of a rod in torsion; I_p is the polar moment of inertia of the rod cross section.

In particular, for a circular or annular cross section $C = I_p G$ and (1.4.10) changes to (1.4.7). The energy density of torsional vibrations in a rod is

$$w_{\text{к. ст}} = \frac{1}{2} \rho I_p \psi_0^2, \tag{1.4.11}$$

where ψ_0 is the amplitude of the rotation angle of the rod cross section.

For an annular cross section

$$I_p = \frac{\pi}{2}(r^4 - r_1^4), \tag{1.4.12}$$

where r and r_1 are the outside and inside radii of the cross section, respectively.

When $r_1 = 0$ expression (1.4.12) describes I_p for a circular cross section. For a rectangular rod cross section

$$I_p = \frac{ab}{12}(a^2 + b^2). \tag{1.4.13}$$

APPROVED FOR RELEASE: 2007/02/08: CIA-RDP82-00850R000200100009-9

APPROVED FOR RELEASE: 2007/02/08: CIA-RDP82-00850R000200100009-9

The energy flux in a rod with torsional vibrations is

$$\Pi_{\text{к. ст}} = \omega_{\text{к. ст}} c_{\text{к. ст}}. \tag{1.4.14}$$

Bending Waves in Rod. In the case of bending vibrations the cross sections of a rod experience transverse displacements and rotate around the axis passing through the neutral plane (the neutral plane does not experience deformations of strain when a rod is bent) [17]. The rotation angle ϕ of the rod cross section with a harmonic process is connected to its transverse displacement y by the relation $|\phi| = k_{b.r}|y|$, where $k_{b.r}$ is the wave number of the bending vibrations of the rod

[и=b]

$$k_{\text{и. ст}} = \frac{\omega}{c_{\text{и. ст}}}; \tag{1.4.15}$$

where $c_{b.r}$ is the speed at which the phase of deformations moves along a rod with bending vibrations, called the phase velocity, which is

$$c_{\text{и. ст}} = \sqrt{\omega c_{\text{п. ст}} r_{\text{ст}}}, \tag{1.4.16}$$

where r_r is the radius of inertia of the rod cross section. For a rectangular rod

$$r_{\text{ст}} = \frac{a}{\sqrt{12}}, \tag{1.4.17}$$

where a is the dimension of the cross section in direction y; for rods with circular and annular cross sections, respectively,

$$r_{\text{ст}} = \frac{r}{2}; \quad r_{\text{ст}} = \frac{\sqrt{r^2 - r_1^2}}{2}. \tag{1.4.18}$$

It follows from expression (1.4.16) that the phase velocity of bending waves in a rod depends on the frequency, i.e., there is dispersion of velocity.

Expression (1.4.16) is valid when the condition $c_{b.r}f^{-1} < 6a$ is satisfied.

Bending vibrations in a rod are characterized by the existence of so-called inhomogeneous bending waves along with traveling waves. They occur near inhomogeneities in a rod (for example, changes of cross section), or near points of application of external forces. The change of amplitude of inhomogeneous waves along a rod is described by an exponent that diminishes with distance from the origin of the waves in accordance with the expression

$$y_1(x) = y_{01} e^{\pm k_{\text{и. ст}} x}, \tag{1.4.19}$$

where y_{01} is the amplitude of an inhomogeneous wave at the origin.

The expression B = EI expresses the bending rigidity of a rod. Here I is the moment of inertia of the rod cross section ($I = r_r^2 s$). The density and energy flux in a rod with bending vibrations are, respectively,

APPROVED FOR RELEASE: 2007/02/08: CIA-RDP82-00850R000200100009-9

APPROVED FOR RELEASE: 2007/02/08: CIA-RDP82-00850R000200100009-9

[и=b; ст=r]

$$w_{\text{и. ст}} = \frac{1}{2} m_{\text{ст}} \omega_1^2 y_0^2; \quad \Pi_{\text{и. ст}} = 2w_{\text{и. ст}} c_{\text{и. ст}}, \tag{1.4.20}$$

where y_0 is the amplitude of transverse displacement of the cross section of the rod.

The frequencies of free bending vibrations of a rod of finite length depend on how its ends are fastened (boundary conditions). When the ends rest on hinges, for instance,

$$f_i = \frac{\pi r_{\text{и. ст}} c_{\text{и. ст}}}{2l^2} i^2 \qquad (i = 1, 2, 3, \ldots), \tag{1.4.21}$$

and for free or pinched ends

$$f_i \approx \frac{\pi r_{\text{и. ст}} c_{\text{и. ст}}}{2l^2} (i + 0{,}5) \qquad (i = 1, 2, 3, \ldots). \tag{1.4.22}$$

The density of natural frequencies of a rod of length l for the above-described boundary conditions is

$$N(\Delta f) = \frac{l \Delta f}{c_{\text{и. ст}}}. \tag{1.4.23}$$

Longitudinal Waves in Plate. Longitudinal vibrations of a plate are accompanied by a displacement of its cross sections with amplitude in the plane of the plate in the direction of the wave. The longitudinal wave propagation velocity for a plate is

[п=lo; пл=pl]

$$c_{\text{п. пл}} = \sqrt{\frac{E}{\rho(1 - \sigma^2)}}. \tag{1.4.24}$$

As can be seen, a longitudinal wave propagates faster in a plate than in a rod. For $\sigma = 0.3$, which is characteristic of metals, $c_{\text{lo.pl}} = 1.05 c_{\text{lo.r}}$. The energy density of longitudinal waves in a plate (the amount of energy present in the part of a plate with unit area, the mass of which is m_{pl}) is

$$w_{\text{и. ст}} = \frac{1}{2} m_{\text{пл}} \omega^2 x_0^2. \tag{1.4.25}$$

The energy flux of longitudinal vibrations in a plate (the amount of energy passing through a section of the cross section of a plate of unit length per unit time) is

$$\pi_{\text{и. ст}} = w_{\text{и. ст}} c_{\text{и. пл}}. \tag{1.4.26}$$

Shear Waves in Plate. The cross sections of a plate with shear waves move with amplitude y_0 in the plane of the plate in a direction perpendicular to the wave. The shear wave propagation velocity is

[c=sh]

$$c_{\text{с. пл}} = \sqrt{\frac{G}{\rho}}. \tag{1.4.27}$$

APPROVED FOR RELEASE: 2007/02/08: CIA-RDP82-00850R000200100009-9

APPROVED FOR RELEASE: 2007/02/08: CIA-RDP82-00850R000200100009-9

and corresponds to the transverse wave velocity in an infinite elastic medium. The density and energy flux of shear waves in a plate can be calculated using expressions (1.4.25) and (1.4.26), respectively, after replacing in them $c_{lo.pl}$ with $c_{sh.pl}$ and x_0 with y_0.

Bending Waves in Plate. The cross sections of a plate with bending vibrations complete transverse displacements with amplitude y_0 and rotate with angular amplitude ϕ_0. These values, just as in the case of bending waves in a rod, are connected by the relation $|\phi_0| = k_{b.pl}|y_0|$; here $k_{b.pl}$ is the wave number of bending waves in a plate:

$$k_{\text{и. пл}} = \frac{\omega}{c_{\text{и. пл}}}, \tag{1.4.28}$$

where $c_{b.pl}$ is the phase velocity of bending waves, described by the expression

$$c_{\text{и. пл}} = \sqrt{\omega c_{\text{и. пл}} r_{\text{пл}}}; \tag{1.4.29}$$

r_{pl} is the radius of inertia of the plate cross section

$$r_{\text{пл}} = \sqrt{\frac{I_{\text{пл}}}{d}} = \frac{d}{3{,}45}. \tag{1.4.30}$$

The expression

$$B_{\text{пл}} = \frac{EI}{1-\sigma^2} \tag{1.4.31}$$

is called the bending rigidity of a plate. For metal plates with thickness d the phase velocity $c_{b.pl}$, m/s, can be expressed approximately by the formula

$$c_{\text{и. пл}} = 10^2\sqrt{df}, \tag{1.4.32}$$

where d is in meters and f in Hz.

Expressions (1.4.29) and (1.4.32) are valid when $c_{b.pl}f^{-1} < 6d$.

The energy density and flux in a plate with bending vibrations are expressed, respectively, as

$$w_{\text{и. пл}} = \frac{1}{2} m_{\text{пл}}\omega^2 y_0^2; \quad \Pi_{\text{и. пл}} = 2w_{\text{и. пл}} c_{\text{и. пл}}. \tag{1.4.33}$$

In plates of finite dimensions bending vibrations can occur on certain frequencies, called natural frequencies. For instance, for a rectangular plate with dimensions $l_1 \times l_2$ and with hinged edges, these frequencies are

APPROVED FOR RELEASE: 2007/02/08: CIA-RDP82-00850R000200100009-9

APPROVED FOR RELEASE: 2007/02/08: CIA-RDP82-00850R000200100009-9

$$f_{nm} = \frac{\pi r_{пл} c_{п.\,пл}}{2} \left(\frac{n^2}{l_1^2} + \frac{m^2}{l_2^2} \right)^{\frac{1}{2}}, \tag{1.4.34}$$

where n, m are arbitrary integers.

The first natural frequency of bending vibrations of a plate is determined by (1.4.34) for n = m = 1. The density of natural frequencies of bending vibrations of a plate is

$$N(\Delta f) \approx \frac{l_1 l_2 \Delta f}{2 r_{пл} c_{п.\,пл}} = \frac{s_{пл} k^2_{и.\,пл} \Delta f}{4\pi f}. \tag{1.4.35}$$

The first three forms of free bending vibrations of a rectangular plate with hinged edges are illustrated in Figure 1.8. These waveforms for a plate are described by the function

$$\xi_{nm}(x, y) = A_{nm} \psi_{nm}(x, y) = A_{nm} \sin k_n x \cdot \sin k_m y, \tag{1.4.36}$$

where A_{nm} is the amplitude of vibrations; k_n, k_m are the projections of the wave number of bending vibrations of a plate $k_{b.nm}$ onto the x and y axes, equal to

$$k_n = \frac{\pi}{l_1} n, \quad k_m = \frac{\pi}{l_2} m. \tag{1.4.37}$$

The dependence of mode amplitude on mode number is expressed by the formula

$$A_{nm} = \frac{4F_0}{m_{пл} S_{пл} [\omega^2_{nm}(1 + j\eta) - w^2]}, \tag{1.4.38}$$

where ω is the frequency of a driving force with amplitude F_0; η is the loss coefficient of the vibration energy in a plate.

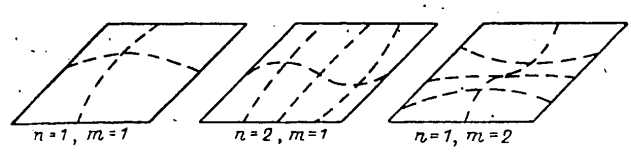

Figure 1.8. Waveforms of first three modes of bending vibrations of rectangular plate with hinged edges.

Amplitude A_{nm} is plotted in Figure 1.9 as a function of the mode number for different loss coefficients. As can be seen, the modes whose natural frequencies coincide with or are close to frequency ω of the driving force, have the greatest amplitudes.

APPROVED FOR RELEASE: 2007/02/08: CIA-RDP82-00850R000200100009-9

APPROVED FOR RELEASE: 2007/02/08: CIA-RDP82-00850R000200100009-9

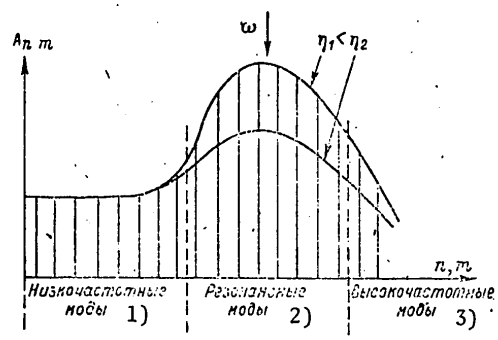

Figure 1.9. Amplitude of bending vibration modes of finite plate as function of mode number.
Key: 1. Low-frequency modes 3. High-frequency modes
2. Resonance modes

A vector diagram of the n, m mode is shown in Figure 1.10, where the coordinate axes are aligned with the edges of a rectangular plate.

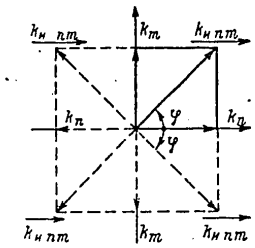

Figure 1.10. Vector diagram for n, m-th mode of bending vibrations of rectangular plate. [и=b]

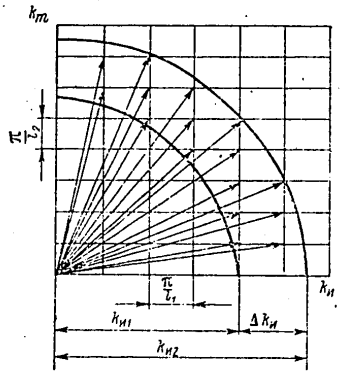

Figure 1.11. Vector diagram for modes of bending vibrations of rectangular plate with hinged edges.

If simplified vector diagrams of several modes (the top right quadrant in Figure 1.10) are superimposed on each other the result is a picture similar to the one in Figure 1.11. That figure shows the vectors of three modes, frequencies ω_{nm} of which fall in frequency band $\Delta\omega$, bounded by frequencies corresponding to the wave numbers

APPROVED FOR RELEASE: 2007/02/08: CIA-RDP82-00850R000200100009-9

APPROVED FOR RELEASE: 2007/02/08: CIA-RDP82-00850R000200100009-9

[и=b]

$$k_{и2} - k_{и1} = \Delta k_и. \tag{1.4.39}$$

Before a diffuse bending wave field can exist, according to experience, at least five modes must be excited simultaneously. The corresponding frequency condition is

[п=lo; пл=pl]

$$f > \frac{10\, c_{п.\,пл} d}{\sqrt{12(1-\sigma^2)}\, s_{пл} \beta_0}, \tag{1.4.40}$$

where β_0 is a numerical coefficient that depends on bandwidth $\Delta\omega$, in which the natural frequencies of the excited resonance modes fall. For a one-third octave band $\beta_0 = 0.232$, for a one-half octave $\beta_0 = 0.345$, and for one octave $\beta_0 = 0.707$.

In a diffuse vibration field the directions of the vectors of individual modes are distributed fairly uniformly in terms of angle ϕ. The angle between adjacent vectors is

$$\Delta\varphi = \frac{2\pi^2 c_{п.\,пл} d}{\sqrt{12(1-\sigma^2)}\, \Delta\omega s_{пл}}. \tag{1.4.41}$$

Reflection and Propagation of Elastic Waves in Plates. When a plane bending wave strikes the corner of two connected plates at incidence angle ϕ_{b1} relative to the normal to the hinge line, reflected waves and longitudinal and shear waves that pass through the plate, occur in addition to reflected waves and bending waves that pass through the plates. The angles of reflection and transmission of these waves are connected to angle ϕ_{b1} by the following relations [35]:

[c=sh]

$$\frac{c_{и.\,пл\,1}}{\sin\varphi_{и1}} = \frac{c_{и.\,пл\,2}}{\sin\varphi_{и2}} = \frac{c_{п.\,пл\,1}}{\sin\varphi_{п1}} = \frac{c_{п.\,пл\,2}}{\sin\varphi_{п2}} = \frac{c_{с.\,пл1}}{\sin\varphi_{с1}} = \frac{c_{с\,пл\,2}}{\sin\varphi_{с2}}, \tag{1.4.42}$$

where ϕ_{b2} is the angle of transmission of a bending wave; ϕ_{lo1}, ϕ_{lo2} are the angle of reflection and angle of transmission of a longitudinal wave; ϕ_{sh1}, ϕ_{sh2} are the angle of reflection and angle of transmission of a shear wave.

Elastic Waves in Cylindrical Shells. The theory of thin cylindrical shells, for which $r_{mid} >> d$, where r_{mid} is the radius of the middle surface of a cylindrical shell, and d is the wall thickness of the shell (Figure 1.12), is traditionally used in practice. The error of such an analysis is proportional to the ratio d/r_{mid}.

The dimensionless frequency

[cp=mid]

$$\nu = \omega r_{ср}/c_{п.\,пл} \tag{1.4.43}$$

APPROVED FOR RELEASE: 2007/02/08: CIA-RDP82-00850R000200100009-9

APPROVED FOR RELEASE: 2007/02/08: CIA-RDP82-00850R000200100009-9

is usually introduced for analyzing vibrations of shells. The so-called annular resonance frequency corresponds to dimensionless frequency $\nu = 1$.

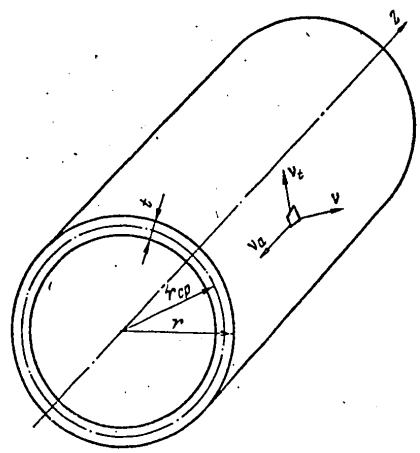

Figure 1.12. Cylindrical shell geometry.
[cp=mid]

If an endless thin cylindrical shell with radius r_{mid} and thickness d is excited by a pressure distribution, oscillating with frequency ω, and the time-independent part of which is

$$p = p_0 \cos n\varphi e^{ikz}, \tag{1.4.44}$$

where ϕ is the azimuth angle, the vibrations of a cylindrical shell may be expressed as follows:

$$\left.\begin{aligned} &\alpha v + n v_t + \sigma k r_{cp} v_a = i\nu^2 p_0/\omega\rho d; \\ &n v + \left[n^2 - \nu^2 + \frac{1}{2}(1-\sigma) k^2 r_{cp}^2\right] v_t + \frac{1}{2}(1+\sigma) n k r_{cp} v_a = 0; \\ &\sigma k r_{cp} v + \frac{1}{2}(1+\sigma) n k r + \left[k^2 r_{cp}^2 + \frac{1}{2}(1-\sigma) n^2 - \nu^2\right] v_a = 0, \end{aligned}\right\} \tag{1.4.45}$$

where v is the radial component of the amplitude of the vibration velocity of the shell; v_t is the tangential component of the amplitude of the vibration velocity; v_a is the axial component of the vibration velocity; n is one-half the number of mode (waveform) nodes of the vibration of a shell in the circumferential direction; k is the wave number of elastic vibrations of a shell along its axis (the z axis); σ is Poisson's ratio for the shell material; ρ is its density.

APPROVED FOR RELEASE: 2007/02/08: CIA-RDP82-00850R000200100009-9

APPROVED FOR RELEASE: 2007/02/08: CIA-RDP82-00850R000200100009-9

The difference in the analyses of shell vibrations, done by different authors, consists in the expression for coefficient α. If only membrane stresses in a shell are considered (the bending rigidity of a shell is assumed to be zero), then

$$\alpha = 1 - \nu^2. \tag{1.4.46}$$

When bending stresses are analyzed

$$\alpha = 1 - \nu^2 + \left(n^2 + k^2 r_{cp}^2\right)^2 d^2 / 12 r_{cp}^2. \tag{1.4.47}$$

The last expression yields fairly accurate results, except for the case when the values of n are small. In this case it is better to use an expression derived in the literature [46]:

$$\alpha = 1 - \nu^2 + \left\{\left(n^2 + k^2 r_{cp}^2\right)^2 - \frac{1}{2}\left[n^2(4-\sigma) - 2 - \sigma\right](1-\sigma)^{-1}\right\} \frac{d^2}{12 r_{cp}^2}. \tag{1.4.48}$$

The resonance frequencies of a finite cylindrical shell of length l, resting on its edges, are determined by the expression

$$\nu_{nm}^2 = (1-\sigma^2)\left(\frac{m\pi r_{cp}}{l}\right)^4 \left[\left(\frac{m\pi r_{cp}}{l}\right)^2 + n^2\right]^{-2} + \left\{\left[\left(\frac{m\pi r_{cp}}{l}\right)^2 + n^2\right]^2 - \right.$$
$$\left. - \frac{1}{2}\left[n^2(4-\sigma) - 2 - \sigma\right](1-\sigma)^{-1}\right\} \frac{d^2}{12 r_{cp}^2}, \tag{1.4.49}$$

where m is one-half the number of nodes of the waveform of the vibrations of a shell in the axial direction. It is easier to use the approximate expression

$$\nu_{nm} = \frac{\gamma_1^2}{n^2 + \gamma_1^2} + \beta\left(n^2 + \gamma_1^2\right), \text{ where } \gamma_1 = \frac{m\pi r_{cp}}{l}; \quad \beta = \frac{d}{r\sqrt{12}}. \tag{1.4.50}$$

This expression is perfectly acceptable, except for the case $\gamma_1^2 \approx (n^2 + \gamma_1^2)\beta$. A dramatic difference in the behavior of a cylindrical shell and plate is illustrated in Figure 1.13 by the isolines of frequencies ν, plotted in the plane of the numbers m and n. The isoline of $\nu_{n,m}$ for a rectangular plate is a quarter circle, as follows from formula (1.4.34). The region in Figure 1.13 that is bounded by the curve

$$n = \sqrt[4]{(1-\sigma^2)} \cdot \sqrt{\frac{\nu}{2\beta}(\sqrt{2} - \nu)}, \tag{1.4.51}$$

in which the behavioral features of a cylindrical shell are manifested, is shaded. In the rest of the region of the values of m-n the behavior of a cylindrical shell is similar to that of a plate. Shell behavior is usually assumed to be similar to plate behavior on frequencies above $\nu = 1$, i.e., above the annular frequency.

APPROVED FOR RELEASE: 2007/02/08: CIA-RDP82-00850R000200100009-9

APPROVED FOR RELEASE: 2007/02/08: CIA-RDP82-00850R000200100009-9

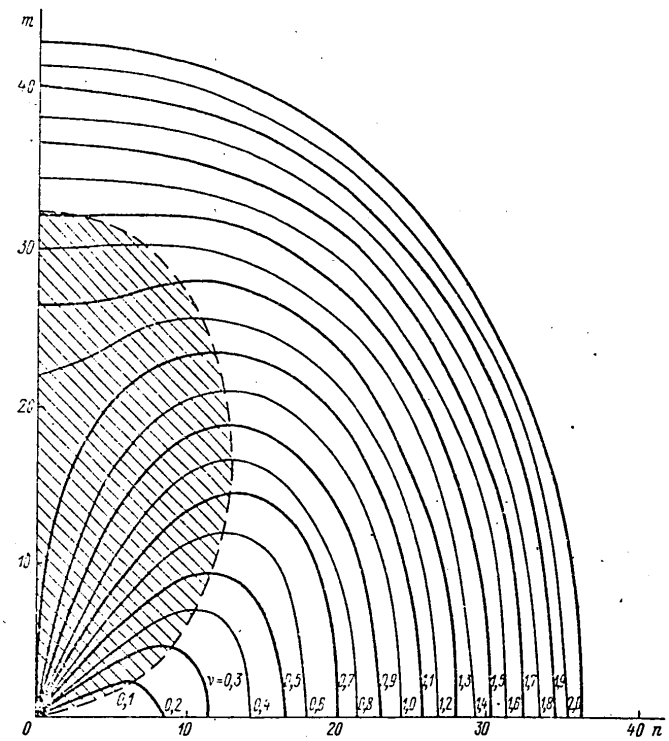

Figure 1.13. Isolines of dimensionless frequency ν for cylindrical shell.

The approximate expression for the total number of resonance frequencies of a shell of finite size, the values of which are lower than a certain frequency, is

$$N(\nu)=\begin{cases}\sum\limits_{m=1}^{m_{\text{кр}}}(n_m^+-n_m^-) & \text{for } \nu<1;\\ \sum\limits_{m_1}^{m_{\text{кр}}}n_m^+-\sum\limits_{m=1}^{m_0}n_m^-+\frac{m_0}{2} & \text{for } 1\leqslant\nu<\sqrt{2};\\ \sum\limits_{m=1}^{m_0}n_m^++\frac{m_0}{2} & \text{for } \nu\geqslant\sqrt{2},\end{cases}\qquad(1.4.52)$$

APPROVED FOR RELEASE: 2007/02/08: CIA-RDP82-00850R000200100009-9

APPROVED FOR RELEASE: 2007/02/08: CIA-RDP82-00850R000200100009-9

where

$$m_0 = \frac{\sqrt[4]{\nu^2 - 1}}{\gamma\sqrt{\beta}}; \quad m_{\text{кр}} = \frac{\nu}{\gamma\sqrt{2\beta}};$$

[kp=cr]

$$n^{\pm} = \frac{1}{\sqrt[4]{2\beta^2}} \left\{\left[\nu^2 \pm \left(\nu^4 - 4\beta^2\gamma^4 m^4\right)^{1/2}\right]^{1/2} - \sqrt{2\beta^2}\,\gamma^2 m^2\right\}^{1/2},$$

and the density of resonance frequencies for $\nu \gg 1$ is

[п=lo; пл=pl]

$$\frac{\Delta N}{\Delta \nu} = \frac{l}{4r\beta} = \frac{\sqrt{3}\,l}{2dc_{\text{п. пл}}}. \tag{1.4.53}$$

In the range $\nu < 1$ and $\nu \approx 1$ the analogous expressions acquire the form

$$\frac{\partial N(\nu)}{\partial \nu} = \frac{\sqrt{\nu}}{4\gamma\beta}\left(1 - \frac{\nu_{\text{кр}}}{\nu}\right)\left[2 + \frac{1 + \nu_{\text{кр}}/\nu}{\sqrt{2(1-\nu)}}\right] \tag{1.4.54}$$

for $\nu_{cr} < \nu \leq 0.95$;

$$\frac{\partial N(\nu)}{\partial \nu} = \frac{\pi}{4\gamma\beta}\sqrt[3]{\frac{\nu}{\sqrt{\nu^2 - 1}}} \tag{1.4.55}$$

for $\nu_{cr} \geq 1.05$, where $\nu_{cr} = \gamma\sqrt{2\beta}$.

In the range $0.95 < \nu < 1.05$ the density of frequencies has to be computed with expressions (1.4.52) and (1.4.53).

1.5. Mechanical Strength of Rods, Plates and Hull Structures. Acoustic Irradiation of Plates and Shells[1]

Mechanical Strength of Rods, Plates and Hull Structures. The velocity of a structure at an analyzed point when a unit of force is applied to the structure is defined as mechanical strength. Mechanical strength is called input if the point of application of a force coincides with the point where velocity is measured, and it is called transiert otherwise. In the general case, when a structure is excited at several points, its velocity at any point is determined both by the input, and by the transient strengths of the structure. The mechanical strength of a structure is represented formally as a quadratic matrix, which connects the column matrix of the forces that excite the structure[2] and the row matrix of the same order, which describes reciprocating and angular velocities at all points of excitation [28]:

[1]This section was written by V. S. Konevalov and V. A. Svyatenko.

[2]Since three components of forces and three components of moments can act upon each point of excitation, matrix order is determined by the number of excitation points, multiplied by six.

APPROVED FOR RELEASE: 2007/02/08: CIA-RDP82-00850R000200100009-9

APPROVED FOR RELEASE: 2007/02/08: CIA-RDP82-00850R000200100009-9

$$[F] = [Z][V]. \tag{1.5.1}$$

In practice matrix [Z] is usually replaced with the inverse conductance matrix $[Y] = [Z]^{-1}$.

The frequency characteristics of mechanical strengths of structures are used for determining their resonance properties and for detuning the resonance frequencies from the fundamental frequencies of perturbing forces [28]. The frequency characteristic of the mechanical strength of complex structures, with resonance valleys and antiresonance peaks, is estimated on the basis of the characteristic mechanical strength [35]. The characteristic strength of a structure corresponds to the mechanical strength of an analogous structure, but with infinite dimensions or with a high internal loss coefficient, which eliminates wave reflection from boundaries. The characteristic strengths of structures in relation to various perturbing forces, such as a rod [26], a homogeneous plate [24, 25, 26], a homogeneous shell [18], orthotropic plate [43], and a ribbed plate [48], are now known. These strengths are presented in Table 1.3.

Acoustic Irradiation of Plates and Shells. The radiation of sound by ship structures is attributed to vibrations, which are usually defined as bending vibrations of structures (plates or shells). The practical problem is to determine acoustical pressure p in a medium, or to determine acoustical power N radiated by a structure.

The radiating capacity of a structure is characterized by radiation resistance R, which is related to the radiated acoustical power and mean square vibration velocity $\langle \dot{x}^2 \rangle$ of a plate, in terms of time and area, by the equation [42, 49]

$$N = R\langle \dot{x}^2 \rangle, \tag{1.5.2}$$

or by the radiation loss coefficient

[и=b]

$$\eta_{и} = \frac{R}{\omega m S_{и}}, \tag{1.5.3}$$

where m is mass per unit area; S_b is the area of the surface of a plate or shell.

The emissivity of structures is estimated variously, depending on critical frequency f_{cr}, on which the bending wavelength in a structure and acoustical wavelength in the medium are

[kp=cr]

$$f_{кр} = \frac{c^2}{2\pi}\sqrt{\frac{m}{B}}, \tag{1.5.4}$$

where m is the mass of a structure per unit area; B is cylindritical rigidity; c is the speed of sound in the medium.

APPROVED FOR RELEASE: 2007/02/08: CIA-RDP82-00850R000200100009-9

APPROVED FOR RELEASE: 2007/02/08: CIA-RDP82-00850R000200100009-9

Table 1.3. Strength of Structures in Relation to Perturbing Forces

Vibrating system	Type of perturbing force	Input mechanical strength
1	2	3
Uniform endless rod	Longitudinal force	$Z_p = 2\rho s c_п = \omega\rho s \lambda_п/\pi$
	Transverse force	$Z_F = 2\rho s c_и (1+j) = \omega\rho s \frac{\lambda_и (1+j)}{\pi}$
	Bending moment	$Z_м = 2\rho s c_и (1-j)/k_и^2 \approx 0{,}12\rho s \sqrt{c_п^3 h^3}(1-j)/\sqrt{j}$
	Torsional moment	$Z_к = 2\rho J_p c_к = \omega\rho J_p \lambda_к/\pi$
Homogeneous semi-infinite rod	Longitudinal force	$Z_p = \rho s c_п = \omega\rho s \lambda_п/2\pi$
	Transverse force	$Z_F = 0{,}5\rho s c_и (1+j) = \omega\rho s \lambda_и (1+j)/4\pi$
	Bending moment	$Z_м = 0{,}5\rho s c_и (1-j)/k_и^2 \approx 0{,}03\rho s \sqrt{c_п^3 h^3}(1-j)/\sqrt{f}$
	Torsional moment	$Z_к = \rho J_p C_к = \omega\rho J_p \lambda_к/2\pi$
Homogeneous infinite plates	Force in plane of plate	$Z_p = j8\pi G h/\omega = j\omega\rho\pi\left(\frac{\sqrt{2}}{\pi}\lambda_c\right)^2 h$
	Transverse force	$Z_F = 8\sqrt{B\rho h} \approx 2{,}3 c_п \rho h^2 = \omega\rho h \lambda_и^2/5$
	Bending moment	$Z_м = 16B/\omega\left[1 - \frac{4}{\pi} j \ln(0{,}9 k_и a)\right]$
	Torsional moment	$Z_к = j8\pi h a^2 G/\omega$
Orthotropic plate	Transverse force	$Z_F = 8\sqrt{m}\sqrt[4]{B_1 B_2}$

[и=b; п=lo; ст=r; пл=pl; c=sh; k=t]

APPROVED FOR RELEASE: 2007/02/08: CIA-RDP82-00850R000200100009-9

APPROVED FOR RELEASE: 2007/02/08: CIA-RDP82-00850R000200100009-9

Table 1.3 (Continued)

Vibrating system	Type of perturbing force	Input mechanical strength
1	2	3
Homogeneous semi-nite plate with free edge	Transverse force on edge Bending moment parallel to edge	$Z_F = 2{,}3\sqrt{B\rho h} \approx c_{\text{п}}\rho h^2 = \omega\rho h\lambda_{\text{и}}^2/11{,}5$ $Z_{\text{м}} = 5{,}3B/\omega\,[1 - 1{,}46j\ln(0{,}9k_{\text{п}}a)]$
Homogeneous cylindrical shell	Transverse force	$Z_c = 4\sqrt{2}\sqrt{mB}\sqrt{\frac{\omega_k}{\omega}}(1-j),\ \omega < \omega_k$ $Z_c = 8\sqrt{mB},\ \omega > \omega_k$
Infinite plate with rigid circular disk	Transverse force in center of disk	$Z_F = j\omega M - 12{,}6\sqrt{mB}\,jK_{\text{и}}a\left[\frac{K_0(K_{\text{и}}a)}{K_1(K_{\text{и}}a)} - \frac{H_0^{(2)}(k_{\text{и}}a)}{H_1^{(2)}(k_{\text{и}}a)}\right]^{-1}$
Reinforcing rib fastened to plate	Transverse force exerted on rib	$Z_F^{-1} = \frac{\omega}{4K_{\text{и. ст}}^3 B_{\text{в}}}\left\{1 - j + \frac{j}{k_{\text{и. ст}}L}\times\right.$ $\left.\times\frac{4}{\pi}\left[1 + \frac{3-r^2}{2r^3\sqrt{1-r^2}}\arccos r + \frac{3+r^2}{2r^3\sqrt{1-r^2}}\operatorname{arcsh} r\right]\right\},$ $r = \frac{K_{\text{и. ст}}}{K_{\text{и. пл}}},\quad L = \frac{B_{\text{ст}}}{B_{\text{пл}}}.$

Comment. Definitions: ρ, h, m -- density of material, thickness of plate and mass of plate per unit area; s -- cross section area; a, M -- radius and mass of rigid disk; J_p -- polar radius of inertia of cross section relative to center of gravity; f, ω, ω_R -- frequency, circular and annular frequencies; k -- wave number; c -- wave velocity; λ -- wavelength; B, B_1, B_2 -- bending rigidity, bending rigidities in orthotropic plate; r -- ratio of wave numbers of bending waves in rod and in plate attached to it; L -- ratio of bending rigidities of rod and of plate attached; $H_0^{(2)}$, $H_1^{(2)}$, K_0, K_1 -- cylindrical Hankel and MacDonald functions. Subscripts: r, pl refer, respectively, to rod and plate; lo, sh, b, t -- longitudinal, shear, bending and torsional vibrations. Imaginary unit denoted as j.

APPROVED FOR RELEASE: 2007/02/08: CIA-RDP82-00850R000200100009-9

APPROVED FOR RELEASE: 2007/02/08: CIA-RDP82-00850R000200100009-9

On frequencies above the critical frequency the bending wave velocity exceeds the speed of sound in a medium, and on frequencies below critical it is less, and the vibration waveforms are traditionally called acoustically fast and acoustically slow modes, respectively.

Radiation as a Physical Process. When acoustically slow modes propagate in an infinite plate radiation does not occur. The reason is that the distance between the vibration node lines in a plate is shorter than one-half the wavelength in the medium. In this case the medium behaves as an incompressible medium and the medium only flows along the surface of the plate between adjacent sections, which move in antiphase (Figure 1.14).

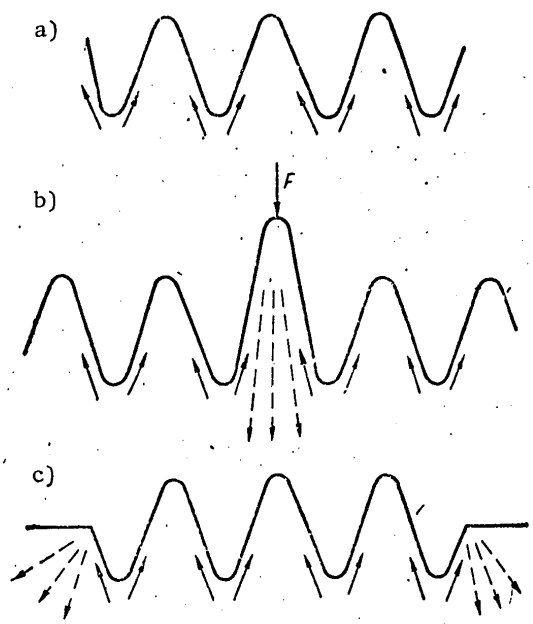

Figure 1.14. Diagram of interaction of bending-vibrating plate and medium: a -- infinite plate with free bending wave; b -- infinite plate driven by point force; c -- finite plate in rigid screen. Solid arrows indicate flow of medium, dash arrows indicate acoustical radiation.

When acoustically fast modes are generated the distance between the vibration node lines in a plate is greater than one-half the wavelength in the medium. In this case the medium exhibits properties of elasticity. Compression of the medium occurs between adjacent in-phase vibrating sections of the plate, and consequently the entire surface effectively radiates sound.

APPROVED FOR RELEASE: 2007/02/08: CIA-RDP82-00850R000200100009-9

APPROVED FOR RELEASE: 2007/02/08: CIA-RDP82-00850R000200100009-9

The radiation resistance of an infinite plate per unit area, on which a free bending wave propagates, is

[kp=cr]

$$R = \begin{cases} 0 & f < f_{\text{кр}}, \\ \dfrac{\rho c}{\sqrt{1-\varphi^{-1}}} & f > f_{\text{кр}}, \end{cases} \qquad (1.5.5)$$

where $\phi = f/f_{cr}$.

If the vibration waveform of a plate is such that both projections of the bending wavelength onto the coordinate axes, aligned with the edges of the plate, are longer than the wavelength in the medium, the radiation of all sections of the plate, vibrating in antiphase, is canceled out, with the exception of quarter-wave sections at the corners of the plate (piston modes). If one of the projections of the bending wavelength onto the coordinate axes is longer, and the other shorter than the wavelength in the medium, the radiation of the quarter-wave strips along the edges of the plate is not canceled out (band modes, Figure 1.15).

Radiation of Infinite Plate Excited by Point Forces. When a plate is excited by a point force the modulus of the amplitude of the acoustical pressure in the far wave zone ($kR_0 > 1$) will be

$$|p| = \frac{kF}{2\pi r_0} \cdot \frac{\cos\vartheta}{\left[1 + \left(\frac{\omega m}{\rho c}\right)^2 \cos^2\vartheta\,(1 - \varphi^2 \sin^4\vartheta)^2\right]^{1/2}}, \qquad (1.5.6)$$

where r_0 is the distance between the point of application of the force and the point of observation; ϑ is the angle between the line to the point of observation and the line perpendicular to the plate.

On frequencies below critical the cofactor $(1 - \phi^2 \sin^4 \vartheta)$ in the denominator is approximately one.

On low frequencies in a medium with a high wave resistance radiation is dipole in nature and the modulus of the acoustical pressure amplitude is

$$|p| = \frac{kF\cos\vartheta}{2\pi r_0}. \qquad (1.5.7)$$

Radiation in a medium with low wave resistance (air) is nondirectional, and the acoustic pressure is determined by the formula

$$|p| = \frac{k\rho c F}{2\pi\omega m r_0}. \qquad (1.5.8)$$

The acoustic power radiated by a plate is:

on frequencies $f < f_{cr}$

APPROVED FOR RELEASE: 2007/02/08: CIA-RDP82-00850R000200100009-9

APPROVED FOR RELEASE: 2007/02/08: CIA-RDP82-00850R000200100009-9

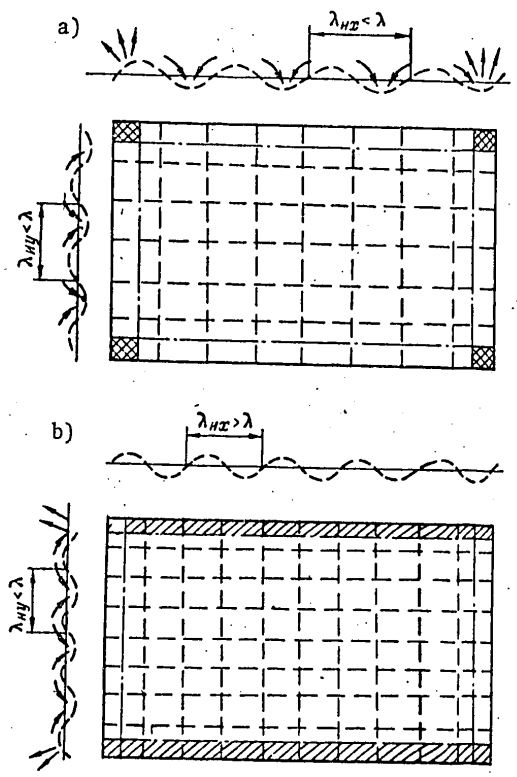

Figure 1.15. Diagram of vibration waveforms of plate (radiating portions cross-hatched): a -- for piston modes; b -- for strip modes. [и=b]

$$N = \frac{\rho c k^2 F^2}{4\pi (\omega m)^2} \left(1 - \frac{\rho c}{\omega m} \operatorname{arctg} \frac{\omega m}{\rho c}\right); \qquad (1.5.9)$$

on frequencies $f > f_{cr}$

$$N = \frac{F^2}{16\sqrt{mB}} \frac{\dfrac{\rho c}{\omega m \sqrt{1-\varphi^{-1}}}}{\eta + \dfrac{\rho c}{\omega m \sqrt{1-\varphi^{-1}}}}. \qquad (1.5.10)$$

On frequencies close to critical the acoustic power can be determined by numerical integration [6].

When a plate is driven by linear force F_1 the acoustic pressure amplitude modulus acquires the form

APPROVED FOR RELEASE: 2007/02/08: CIA-RDP82-00850R000200100009-9

APPROVED FOR RELEASE: 2007/02/08: CIA-RDP82-00850R000200100009-9

$$|p_1| = \left(\frac{k}{2\pi r_0}\right)^{1/2} \frac{F_1 \cos\vartheta}{\left[1 + \left(\frac{\omega m}{\rho c}\right)^2 \cos^2\vartheta\,(1 - \varphi^2 \sin^4\vartheta)^2\right]^{1/2}}, \qquad (1.5.11)$$

and the acoustic power radiated by the plate on frequencies $f < f_{cr}$ is

$$N_1 = \frac{k\rho c F_1^2}{4(\omega m)^2}\left[1 - \frac{1}{\sqrt{1 + \left(\frac{\omega m}{\rho c}\right)^2}}\right]. \qquad (1.5.12)$$

The subscript 1 in expressions (1.5.11) and (1.5.12) signifies that the acoustic power and driving force are expressed in terms of unit length.

The acoustic power radiated by a plate driven by a point moment M on frequencies $f < f_{cr}$ is

$$N = \frac{\rho c k^4 M^2}{12\pi(\omega m)^2}\left\{1 + \frac{3}{2}\left(\frac{\rho c}{\omega m}\right)^2 - \frac{3}{2}\frac{\rho c}{\omega m}\left[1 + \left(\frac{\rho c}{\omega m}\right)^2\right] \operatorname{arctg}\frac{\omega m}{\rho c}\right\}. \qquad (1.5.13)$$

Radiation of Finite Plate. Expressions for the radiation resistance of single vibration waveforms of a plate are presented in the literature [48], but they are rarely used in practice. If the linear dimensions of a structure are shorter than the wavelength in the medium and the frequency is higher than the first resonance frequency of the vibrations of a plate, the radiation resistance of a hinged plate will be

[kp=cr]

$$R = \frac{4\rho c^3}{\pi^4 f_{\text{кр}}^2 \sqrt{\varphi}}. \qquad (1.5.14)$$

If the linear dimensions of a structure are longer than the wavelength in the medium, then on frequencies $f < f_{cr}$

$$R = \frac{\rho c^3}{f_{\text{кр}}^2} q_1(\varphi) + \frac{\rho c^2 P}{f_{\text{кр}}} q_2(\varphi), \qquad (1.5.15)$$

where P is the perimeter of a plate,

$$q_1(\varphi) = \begin{cases} \dfrac{4(1-2\varphi)}{\pi^4\sqrt{\varphi}\sqrt{1-\varphi}} & f < \dfrac{1}{2} f_{\text{кр}}, \\ 0 & f > \dfrac{1}{2} f_{\text{кр}}; \end{cases} \quad q_2(\varphi) = \frac{2\sqrt{\varphi} + (1-\varphi)\ln\dfrac{1+\sqrt{\varphi}}{1-\sqrt{\varphi}}}{4\pi^2(1-\varphi)^{3/2}}. \qquad (1.5.16)$$

For different boundary conditions the expression $q_2(\phi)$ will acquire the form

$$q_2(\varphi) = \frac{2\sqrt{\varphi} + 2(1-\varphi)\ln\dfrac{1+\sqrt{\varphi}}{1-\sqrt{\varphi}} + (1-\varphi)\arcsin\dfrac{2\sqrt{\varphi}}{1+\varphi}}{4\pi^2(1-\varphi)^{3/2}} - \qquad (1.5.17)$$

APPROVED FOR RELEASE: 2007/02/08: CIA-RDP82-00850R000200100009-9

APPROVED FOR RELEASE: 2007/02/08: CIA-RDP82-00850R000200100009-9

for a pinched plate;

$$q_2(\varphi) = \frac{2\sqrt{\varphi} - 2(1-\varphi)\ln\frac{1+\sqrt{\varphi}}{1-\sqrt{\varphi}} + (1-\varphi)\arcsin\frac{2\sqrt{\varphi}}{1+\varphi}}{4\pi^2(1-\varphi)^{3/2}} \tag{1.5.18}$$

for a free plate;

[и=b]

$$q_2(\varphi) = \frac{2\sqrt{\varphi} - 2\frac{(1-\varphi)(1-\gamma^2)}{1+2\gamma+2\gamma^2}\ln\frac{1+\sqrt{\varphi}}{1-\sqrt{\varphi}} + \frac{(1-\gamma)(1-2\gamma)}{1+2\gamma+2\gamma^2}\arcsin\frac{2\sqrt{\varphi}}{1+\varphi}}{4\pi^2(1-\varphi)^{3/2}}, \tag{1.5.19}$$

$$\gamma = \frac{m_0}{m} k_и -$$

for a plate, around whose contour is fastened a rib with linear mass m_0; k_b is the wave number for the bending wave in a plate.

On frequencies $f > f_{cr}$ the boundary conditions have no effect on the emissivity of plates, and the radiation resistance is

$$R = \frac{\rho c S}{\sqrt{1-\varphi^{-1}}}. \tag{1.5.20}$$

When the force that drives the structure is known the acoustic power radiated by resonance vibration waveforms can be determined from the expression

$$N = \frac{F^2}{16\sqrt{mB}}\frac{\eta_и}{\eta + \eta_и}. \tag{1.5.21}$$

Mounting hardware exerts a negligible influence, in the first approximation, on the radiating capacity of ship structures. This problem is solved in various approximations in the literature [7, 32].

Radiation of Cylindrical Shell. The problem of the radiation of a cylindrical shell is much more complicated than the problem of the radiation of flat plates; a computer must be used to find the exact solution of this problem. However, in the case when the conditions $f > f_a$ and $f_{cr} >> f_a$ are satisfied, where $f_a = c/\pi d$, which is called the annular frequency, the radiation resistance of a cylindrical shell is equal numerically to the radiation resistance of an equivalent plate of equal size. This subject is examined in greater detail in the literature [45].

1.6. Electromechanical and Electroacoustic Analogies

Table of Analogies. By using differential equations of the identical order and form for vibrations in media with the same elastic constant (acoustic processes), for mechanical (reciprocating and rotating) vibrations and

APPROVED FOR RELEASE: 2007/02/08: CIA-RDP82-00850R000200100009-9

APPROVED FOR RELEASE: 2007/02/08: CIA-RDP82-00850R000200100009-9

electrical oscillations it is possible to establish analogies both between the parameters of all these processes, and between the parameters and impedances of vibrating systems [12, 27, 31, 35, 39, 40, 47].

The convenient and elegant techniques that have been developed in electrical engineering for analyzing vibration processes and systems provide an opportunity to conduct a similar analysis in mechanical and acoustic systems [47].

The most important analogies of the parameters of vibration processes and the parameters of systems themselves and of their impedances are presented in Table 1.4. The electrical equivalent diagrams for determining the required parameters are drawn on the basis of the analogies presented in the table.

Comparison of Equivalent Diagrams. A few rules and suggestions that are helpful in the comparison of equivalent diagrams are presented below.

1. Elasticity (spring, pad) transmits all of a vibrating force, and therefore an element or a combination of elements placed upon it should be included in a diagram as a parallel system (then the voltages on them and on the elasticity analog will be identical). Mass transmits all of a vibration velocity, and therefore an element or a set of elements that comes after it should be series-connected in the diagram (then the currents in them and in the mass analog will be identical).

2. The velocity of a spring is equal to the difference of the velocities of its ends, and therefore the currents in the analogs of mass and of a spring that comes after it can be equal only at zero velocity, i.e., when the far end of the spring is rigidly attached. The force of mass is equal to the difference of the forces acting upon its front and rear faces.

3. The part of a circuit with a mass or elasticity analog is shortened when the mass or elasticity is equal to zero, and it is broken when the mass or elasticity is infinite.

4. A friction element in an equivalent diagram is series-connected to the elasticity analog, since the total force transferred by an elastic pad is equal to the sum of the forces transmitted by elasticity and friction.

Example 1. A mass is placed on an elastic pad (frictionless), which is placed on another mass (Figure 1.16a). A vibrating force acts upon the first mass.

The equivalent diagram is shown in Figure 1.16b. The first mass is series-connected to a circuit consisting of two different elements, because the force (electric voltage) on the circuit is equal to the difference of forces -- original and lost on the mass. The last two elements are

APPROVED FOR RELEASE: 2007/02/08: CIA-RDP82-00850R000200100009-9

APPROVED FOR RELEASE: 2007/02/08: CIA-RDP82-00850R000200100009-9

Table 1.4. Mechanical, Electrical and Acoustic Analogies (→ -- Sign of Analogy)

Mechanical parameters (for reciprocating and rotation vibrations)	Electrical parameters	Acoustic parameters
Parameters of vibration processes		
Vibration force F Vibration moment M }	← Voltage → (emf) U	Acoustic pressure p
Vibration velocity (for one of coordinates) $\dot{x}$ Same for rotation vibrations $\dot{\phi}$ }	← Current i, I →	Volume vibration velocity v, vibration velocity $\dot{\xi}$
Vibration displacement x Same for rotation vibrations ϕ }	← Charge q →	Volume vibration displacement ξ_v, vibration displacement ξ
Parameters and impedances of systems		
Mass m, M Mass moment of inertia I }	← Inductance → L	Acoustic mass m_a
Inertial impedance $i\omega m$, $i\omega M$ Same for rotation vibrations $i\omega I$ }	← Inductive impedance → $i\omega L$	Inertial acoustic impedance $im_a\omega$
Flexibility (pliability) C_m Same for rotation vibrations D_t	← Capacitance → C_e	Acoustic pliability C_a
Elasticity (rigidity) $C = C = \frac{1}{C_M} = \frac{1}{C_M}$ Same for rotation vibrations $D = 1/D_m$	← $\frac{1}{C_e}$ →	Acoustic rigidity $C = 1/C_a$
Deformation resistance $C/j\omega$ Same for rotation vibration $D/j\omega$	← Capacitive impedance → $1/i\omega C_e$	Acoustic reactance $C_a/j\omega$

APPROVED FOR RELEASE: 2007/02/08: CIA-RDP82-00850R000200100009-9

APPROVED FOR RELEASE: 2007/02/08: CIA-RDP82-00850R000200100009-9

Table 1.4 (Continued)

Mechanical parameters (for reciprocating and rotation vibrations)	Electrical parameters	Acoustic parameters
Friction resistance R	Ohmic ← impedance → R_e	Active acoustic impedance R_a
Total mechanical strength Z_m	← Total electrical impedance → Z_e	Total acoustic impedance Z_a

parallel-connected, since elasticity transfers all the vibration force to the second mass, i.e., the electrical voltages on these elements should be identical.

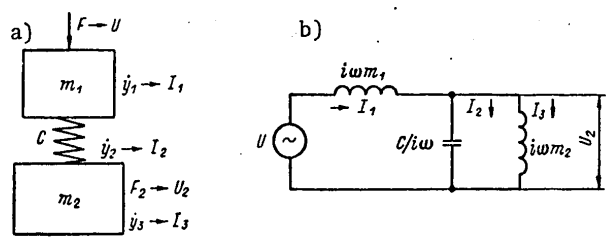

Figure 1.16. Construction of equivalent electrical circuit for two-mass mechanical system with intermediate elasticity.

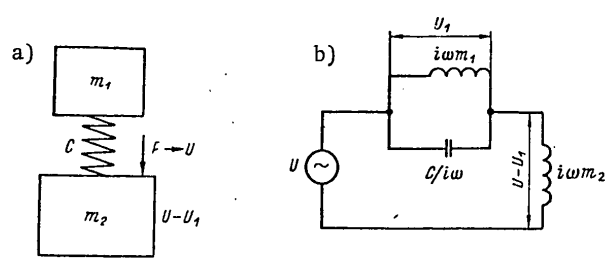

Figure 1.17. Same as Figure 1.16, but force applied to bottom mass.

All the limit transitions confirm the validity of the diagram. When m_2 = = 0, for instance, elasticity exerts no "backwater effect"; nor does it

APPROVED FOR RELEASE: 2007/02/08: CIA-RDP82-00850R000200100009-9

APPROVED FOR RELEASE: 2007/02/08: CIA-RDP82-00850R000200100009-9

exert any action in the circuit, since the right hand branch is shorted. When c = 0 the left hand branch is shorted and only the first mass counteracts the force.

Example 2. The force is transferred to the second mass (Figure 1.17a). The two top elements now function in the antivibrator mode. In the equivalent diagram (Figure 1.17b) these elements are parallel-connected, since the elasticity transfers all the force acting upon it to the top mass.

Example 3. The equivalent electrical diagram is transformed inversely to a mechanical system.

In light of what we have said above both systems shown in Figure 1.18a, b are electrically equivalent, since the currents in all the elements of the circuit are identical. However, if the same arrangement of elements as in the top circuit (Figure 1.18a) is used in the construction of the mechanical diagram, and a vibrating force is applied to the elastic element, the identical vibration displacement of the masses and elasticity cannot be achieved. By rearranging the elements as is shown in Figure 1.18b it is possible to arrive at the desired mechanical system.

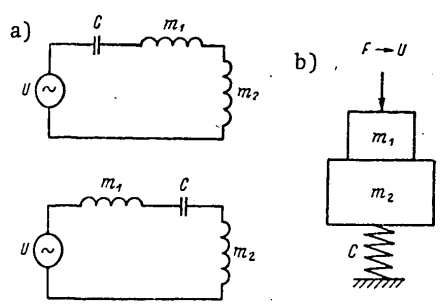

Figure 1.18. Equivalent electrical diagram with series-connected elements converted to corresponding mechanical system.

Consider now a circuit in which all three elements are parallel-connected, i.e., the voltages on them are identical. Here the identical force must be applied to all three elements. It is easy to see by the lower left circuit in Figure 1.19a that force must be applied to the spring. The desired effect is achieved, in particular, by using a rigid equal-arm lever with hinges (Figure 1.19b).

The electromechanical analogy procedure can also be used for analyzing such systems as, for example, elastic sound-insulating couplings on the shafts of machinery. When torsional vibrations occur in the elastic elements of

APPROVED FOR RELEASE: 2007/02/08: CIA-RDP82-00850R000200100009-9

APPROVED FOR RELEASE: 2007/02/08: CIA-RDP82-00850R000200100009-9

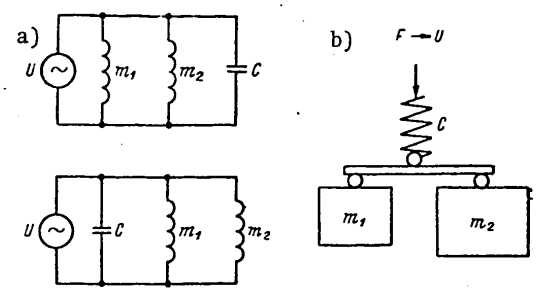

Figure 1.19. Same as Figure 1.18 with parallel-connected elements in electric circuit.

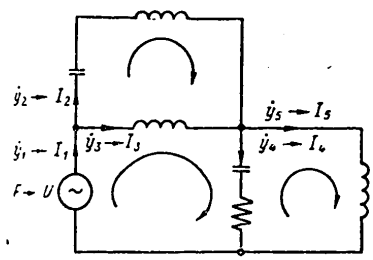

Figure 1.20. Analysis of equivalent electric circuits by loop current method.

the coupling, depending on its design, torsional or shear vibrations occur, which are described by second-order differential equations.

Analysis of Equivalent Diagrams. It is helpful to use Kirchhoff's loop current method for analyzing branched equivalent circuits. To do this the currents in the loops are numbered and their possible voltages are indicated. For the loops with a voltage source the sum of the voltage drops on all the elements of each loop should be equal to the voltage applied, and for the other loops it should be zero (Figure 1.20; for more details see [38]). The resulting equation system gives all the currents, and on their basis the voltage drops (equivalent to mechanical forces) in every part of the circuit (see Chapter 12).

It has been noted [35] that the second system of analogies, in which the current is equivalent to force, can be useful in complicated circuits, when the first system of analogies leads to nonplanar electrical circuits.

Application of Graph Theory to Analysis of Complex Mechanical Systems. Graph theory [5] can be used for analyzing complex branched mechanical systems, for example three-stage and group (unit) vibration-insulating

APPROVED FOR RELEASE: 2007/02/08: CIA-RDP82-00850R000200100009-9

APPROVED FOR RELEASE: 2007/02/08: CIA-RDP82-00850R000200100009-9

damping systems. Graph theory was first used for calculating electromechanical converters by G. Mason [23] and V. A. Fedorovich.

1.7. Electrical, Mechanical and Acoustic n-Poles

Simple and Compound Quadrupoles. An extremely convenient formalized mathematical tool -- the theory of quadrupoles, which describes oscillation processes in individual electrical elements and circuits [1, 38], is often used in electrical engineering. Quadrupole theory is valid for systems that are described by second-order differential equations. In consideration of electromechanical and electroacoustic analogies, quadrupole theory can be applied to longitudinal waves in mechanical and acoustic systems, in this case conventionally called mechanical (or acoustic) quadrupoles [11, 12, 28, 50].

There are only six known kinds of equation systems of a quadrupole, of which two are in the so-called A, B, C, D form, and four are solved in terms of input and transient impedances or conductances of a system [8, 29]. The A, B, C, D equations are suitable for analyzing the passage of vibrations through mechanical systems with distributed constants (elastic pads, models of mechanisms and foundations), for which the acoustic impedance of the material and geometric dimensions are known, and through acoustic systems with distributed constants (Figure 1.21a).

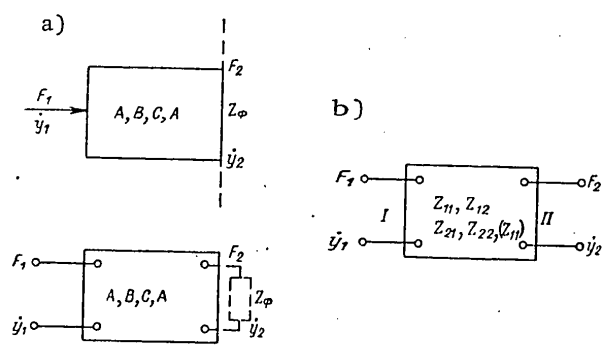

Figure 1.21. Homogeneous symmetric mechanical link with distributed constants (for longitudinal waves) and equivalent electric quadrupole in A, B, C, A form (a); asymmetric or symmetric link with given input and transient impedances of equivalent quadrupole (no load resistance) (b).

For systems (for instance shock absorbers), for which the mechanical impedances or conductances are known as the result of testing or calculation (Figure 1.21b), it is better to use the quadrupole equations that contain these parameters.

APPROVED FOR RELEASE: 2007/02/08: CIA-RDP82-00850R000200100009-9

APPROVED FOR RELEASE: 2007/02/08: CIA-RDP82-00850R000200100009-9

The matrix equation that connects the parameters of an input longitudinal wave with the analogous parameters at the output of a passive symmetric (homogeneous) mechanical system with distributed constants (see Figure 1.21a), is (for harmonic waves)

$$\begin{bmatrix} F_1 \\ \dot{y}_1 \end{bmatrix} = \begin{bmatrix} A & B \\ C & A \end{bmatrix} \begin{bmatrix} F_2 \\ \dot{y}_2 \end{bmatrix}. \tag{1.7.1}$$

Equation (1.7.1) is equivalent to the system of two algebraic equations

$$\begin{aligned} F_1 &= AF_2 + B\dot{y}_2, \\ \dot{y}_1 &= CF_2 + A\dot{y}_2. \end{aligned} \tag{1.7.2}$$

The terms of the summary transition matrix (with the Σ symbol), in consideration of the continuity of vibration forces and vibration displacements, can be found by multiplying the component matrices (Figure 1.22):

$$M_\Sigma = \begin{bmatrix} A_\Sigma & B_\Sigma \\ C_\Sigma & D_\Sigma \end{bmatrix} = \prod_{i=1}^{n} \begin{bmatrix} A_i & B_i \\ C_i & A_i \end{bmatrix}. \tag{1.7.3}$$

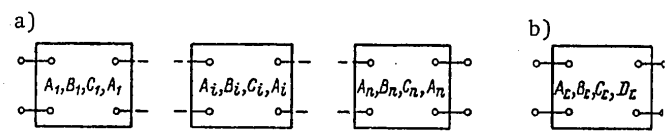

Figure 1.22. Chain-connected mechanical homogeneous (symmetric) quadrupoles (a) and equivalent asymmetric quadrupole (b).

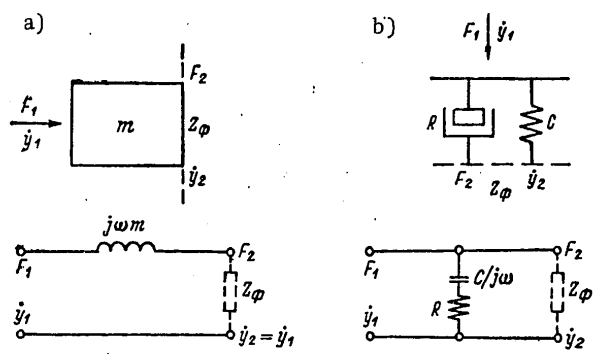

Figure 1.23. Mechanical elements of mass (a) and of elasticity with friction (b) and corresponding quadrupoles.

APPROVED FOR RELEASE: 2007/02/08: CIA-RDP82-00850R000200100009-9

APPROVED FOR RELEASE: 2007/02/08: CIA-RDP82-00850R000200100009-9

Thus, a compound quadrupole, equivalent to several chain-connected different homogeneous (symmetric) quadrupoles, is asymmetric, i.e., the terms of the left diagonal are not equal to each other (Figure 1.22b).

The quadrupole equations in which the parameters of the transition matrices are expressed as input and transient impedances (see Figure 1.21b) are suitable for inhomogeneous links in a system. The matrix equation

$$\begin{bmatrix} F_1 \\ F_2 \end{bmatrix} = \begin{bmatrix} Z_{11} & Z_{12} \\ Z_{21} & Z_{22} \end{bmatrix} \begin{bmatrix} \dot{y}_1 \\ \dot{y}_2 \end{bmatrix} \tag{1.7.4}$$

is very often used. It is equivalent to a system of two algebraic equations:

$$\begin{aligned} F_1 &= Z_{11}\dot{y}_1 + Z_{12}\dot{y}_2, \\ F_2 &= Z_{21}\dot{y}_1 + Z_{22}\dot{y}_2. \end{aligned} \tag{1.7.5}$$

In equations (1.7.4) and (1.7.5) $Z_{11} = F_1/\dot{y}_{10}$ is the input impedance at input I with output II open; $Z_{21} = F_2/\dot{y}_{10}$ is the transient impedance from input I to output II with output II open; $Z_{12} = F_2/\dot{y}_{10}$ is the transient impedance from output II to input I with input I open; $Z_{22} = F_1/\dot{y}_{20}$ is the input impedance from output II with input I open; for a symmetric vibrating system (which, incidentally, is quite rare in this class of equations) $Z_{22} = Z_{11}$.

If the conditions of the problem stipulate that the input parameters of a process not be expressed through the output parameters, but rather the output through the input, then the equation for any chain structure must include the inverse matrix of M_Σ [see (1.7.3)]:

$$\begin{bmatrix} F_2 \\ \dot{y}_2 \end{bmatrix} = [M_\Sigma]^{-1} \begin{bmatrix} F_1 \\ \dot{y}_1 \end{bmatrix} = \frac{1}{A_\Sigma D_\Sigma - B_\Sigma C_\Sigma} \begin{bmatrix} D_\Sigma & -B_\Sigma \\ -C_\Sigma & A_\Sigma \end{bmatrix} \begin{bmatrix} F_1 \\ \dot{y}_1 \end{bmatrix} \tag{1.7.6}$$

(for $A_\Sigma D_\Sigma - B_\Sigma C_\Sigma \neq 0$).

If the system completes two independent vibrations simultaneously, each of which is characterized by a second-order differential equation (for example, longitudinal and torsional vibrations or longitudinal vibrations and shear vibrations), then the general matrix equation of the vibrations of the system may be represented as

[пр=lo;
kp=t]

$$\begin{bmatrix} M_1 \\ F_1 \\ \dot{y}_1 \\ \dot{\varphi}_1 \end{bmatrix} = \begin{bmatrix} A_{\Sigma\,кр} & 0 & 0 & B_{\Sigma\,кр} \\ 0 & A_{\Sigma\,пр} & B_{\Sigma\,пр} & 0 \\ 0 & C_{\Sigma\,пр} & D_{\Sigma\,пр} & 0 \\ C_{\Sigma\,кр} & 0 & 0 & D_{\Sigma\,кр} \end{bmatrix} \begin{bmatrix} M_2 \\ F_2 \\ \dot{y}_2 \\ \dot{\varphi}_2 \end{bmatrix}, \tag{1.7.7}$$

APPROVED FOR RELEASE: 2007/02/08: CIA-RDP82-00850R000200100009-9

APPROVED FOR RELEASE: 2007/02/08: CIA-RDP82-00850R000200100009-9

where the subscripts "lo" and "t" indicate the kind of vibration (longitudinal or torsional); M_1 and M_2 are the torsional moments at the input and output of the system; $\dot{\phi}_1$ and $\dot{\phi}_2$ are the corresponding vibration velocities.

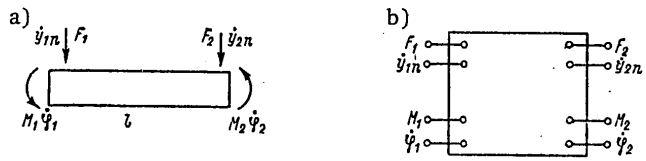

Figure 1.24. Mechanical system with bending vibrations (a) and corresponding eight-terminal network (b).

Elements with Bunched Constants in Four-Terminal and Two-Terminal Networks. For relatively low vibration frequencies, when the elastic wavelength of a given form is substantially shorter than the dimensions of the element, the dimensions are represented as a point mass, elasticity and friction. For point mass m (Figure 1.23a) the equation is

$$\begin{bmatrix} F_1 \\ \dot{y}_1 \end{bmatrix} = \begin{bmatrix} 1 & i\omega m \\ 0 & 1 \end{bmatrix} \begin{bmatrix} F_2 \\ \dot{y}_2 \end{bmatrix}, \tag{1.7.8}$$

where ω is circular frequency.

For a combination of elements of elasticity C and friction R (elastic pad with losses on low frequencies, Figure 1.23b) the equation will be

$$\begin{bmatrix} F_1 \\ \dot{y}_1 \end{bmatrix} = \begin{bmatrix} 1 & 0 \\ \dfrac{1}{\dfrac{C}{i\omega} + R} & 1 \end{bmatrix} \begin{bmatrix} F_2 \\ \dot{y}_2 \end{bmatrix}. \tag{1.7.9}$$

Eight-Terminal Networks. A straight rod (and plate), completing plane bending vibrations (Figure 1.24a), is described by a fourth-order differential equation and accordingly is represented by the equivalent eight-terminal network (Figure 1.24b), at the input and output of which figure, in addition to vibrating forces of velocities for transverse deformations, vibration moments and velocities of rotation vibrations. The parameters of the transition matrices for it (quadratic fourth-order matrices) are given in the literature [9, 42].

BIBLIOGRAPHY

1. Ango, A., "Matematika dlya Elektro- i Radioinzhenerov" [Mathematics for Electrical and Radio Engineers], Moscow, Nauka, 1964.

APPROVED FOR RELEASE: 2007/02/08: CIA-RDP82-00850R000200100009-9

APPROVED FOR RELEASE: 2007/02/08: CIA-RDP82-00850R000200100009-9

2. Belousov, Yu. I., and A. V. Rimskiy-Korsakov, "Reciprocity Principle in Acoustics and Its Application for Calculating Acoustic Fields of Vibrating Objects. A Survey," AKUSTICHESKIY ZHURNAL [Acoustics Journal], 1975, Vol 21, No 2, pp 161-173.

3. Brekhovskikh, L. M., "Volny v Sloistykh Sredakh" [Waves in Lamellar Media], 2nd edition, Moscow, Nauka, 1973.

4. Viktorov, I. A., "Fizicheskiye Osnovy Primeneniya Ul'trazvukovykh Voln Releya i Lemba v Tekhnike" [Physical Principles of Application of Ultrasonic Rayleigh and Lamb Waves in Technology], Moscow, Nauka, 1966.

5. Gerlikh, A. Yu. and I. I. Klyukin, "Application of Graph Theory for Analyzing Efficiency of Multistage and Unit Vibration Insulation Systems of Mechanisms," TRUDY LKI [Proceedings of Leningrad Shipbuilding Institute], 1974, No 91, pp 13-18.

6. Gutin, L. Ya., "Acoustic Radiation of Infinite Plate Driven by Normal Point Force," AKUSTICHESKIY ZHURNAL, 1964, Vol 10, No 4, pp 431-434.

7. Yevseyev, V. N., "Acoustic Radiation of Infinite Plate with Periodic Inhomogeneities," AKUSTICHESKIY ZHURNAL, 1973, Vol 19, No 3, pp 345-351.

8. Zelinger, Dzh., "Osnovy Matrichnogo Analiza i Sinteza" [Fundamentals of Matrix Analysis and Synthesis], Moscow, Sovetskoye radio, 1970.

9. Ivovich, V. A., "Perekhodnyye Matritsy v Dinamike Uprugikh Sistem" [Transition Matrices in Elastic Systems Dynamics], Moscow, Mashinostroyeniye, 1969.

10. Isakovich, M. A., "Obshchaya Akustika" [General Acoustics], Moscow, Nauka, 1973.

11. Klyukin, I. I., "On Theory of Sound-Insulating Pads," ZHURNAL TEKHNICHESKOY FIZIKI [Journal of Engineering Physics], 1950, Vol 20, No 5, pp 579-589.

12. Klyukin, I. I., "Bor'ba s Shumom i Zvukovoy Vibratsiyey na Sudakh" [Control of Noise and Acoustic Vibrations on Ships], 2nd edition, Leningrad, Sudostroyeniye, 1971.

13. Kol'skiy, G., "Volny Napryazheniy v Tverdykh Telakh" [Stress Waves in Solids], Moscow, IL, 1956.

14. Lamb, G., "Gidrodinamika" [Hydrodynamics], Moscow, Gostekhizdat, 1947.

APPROVED FOR RELEASE: 2007/02/08: CIA-RDP82-00850R000200100009-9

APPROVED FOR RELEASE: 2007/02/08: CIA-RDP82-00850R000200100009-9

15. Landau, L. D. and Ye. M. Lifshits, "Mekhanika Sploshnykh Sred" [Mechanics of Continua], Moscow, GITTL, 1953.

16. Lyamshev, L. M., "On Reciprocity Principle in Acoustics," DOKLADY AN SSSR [Reports of the USSR Academy of Sciences], 1959, Vol 125, No 6, pp 1231-1234.

17. Lyapunov, V. T. and A. S. Nikiforov, "Vibroizolyatsiya v Sudovykh Konstruktsiyakh" [Vibration Insulation in Ship Structures], Leningrad, Sudostroyeniye, 1975.

18. Lyapunov, V. T. and T. D. Rozhinova, "Characteristic Impedance of Cylindrical Shell in Relation to Point Force," AKUSTICHESKIY ZHURNAL, 1970, Vol 16, No 1, pp 156-157.

19. Meyz, Dzh., "Teoriya i Zadachi Mekhaniki Sploshnykh Sred" [Theory and Problems of Continuum Mechanics], Moscow, Mir, 1974.

20. Morz, F., "Kolebaniya i Zvuk" [Oscillations and Sound], Moscow-Leningrad, GITTL, 1949.

21. Morz, F. and G. Feshbakh, "Metody Teoreticheskoy Fiziki" [Methods of Theoretical Physics], Vol 1, Moscow, IL, 1958.

22. Morz, F. and G. Feshbakh, "Metody Teoreticheskoy Fiziki," Vol 2, Moscow, IL, 1960.

23. Meyson, S. and G. Tsimmerman, "Elektronnyye Tsepi, Signaly i Sistemy" [Electronic Circuits, Signals and Systems], Moscow, IL, 1963.

24. Nikiforov, A. S., "Impedance of Infinite Plate in Relation to Torsion Moment," AKUSTICHESKIY ZHURNAL, 1971, Vol 17, No 3, pp 484-485.

25. Nikiforov, A. S., "Impedance of Infinite Plate in Relation to Force Acting in Its Plane," AKUSTICHESKIY ZHURNAL, 1968, Vol 14, No 2, pp 297-298.

26. Nikiforov, A. S. and S. V. Budrin, "Rasprostraneniye i Pogloshcheniye Zvukovykh Vibratsiy na Sudakh" [Propagation and Absorption of Acoustic Vibrations on Ships], Leningrad, Sudostroyeniye, 1968.

27. Olson, G., "Dinamicheskiye Analogii" [Dynamic Analogies], Moscow, IL, 1947.

28. Popkov, V. I., "Vibroakusticheskaya Diagnostika i Snizheniye Vibroaktivnosti Sudovykh Mekhanizmov" [Vibroacoustic Diagnosis and Reduction of Vibration Activity of Ship Mechanisms], Leningrad, Sudostroyeniye, 1974.

APPROVED FOR RELEASE: 2007/02/08: CIA-RDP82-00850R000200100009-9

APPROVED FOR RELEASE: 2007/02/08: CIA-RDP82-00850R000200100009-9

29. Reza, F. and S. Sili, "Sovremennyy Analiz Elektricheskikh Tsepey" [Modern Analysis of Electric Circuits], Moscow, Energiya, 1964.

30. Rzhevkin, S. N., "Kurs Lektsiy po Teorii Zvuka" [Course of Lectures on Acoustics Theory], Izd-vo MGU, 1960.

31. Rimskiy-Korsakov, A. V., "Elektroakustika" [Electroacoustics], Moscow, Svyaz', 1973.

32. Romanov, V. N., "On Acoustic Radiation of Infinite Plate with Rigidity Ribs," AKUSTICHESKIY ZHURNAL, 1972, Vol 18, No 4, pp 602-607.

33. Skuchik, Ye., "Osnovy Akustiki" [Fundamentals of Acoustics], Vols 1 and 2, Moscow, IL, 1958-1959.

34. Skuchik, Ye., "Osnovy Akustiki," Vol 1, 2, Moscow, Mir, 1976.

35. Skuchik, Ye., "Prostyye i Slozhnyye Kolebatel'nyye Sistemy" [Simple and Compound Oscillating Systems], Moscow, Mir, 1971.

36. Stashkevich, A. P., "Akustika Morya" [Marine Acoustics], Leningrad, Sudostroyeniye, 1966.

37. Strett, Dzh. V. (Lord Rayleigh), "Teoriya Zvuka" [The Theory of Sound], Vol 1, Moscow-Leningrad, GITTL, 1955.

38. Tolstov, Yu. G., "Teoriya Lineynykh Elektricheskikh Tsepey" [Theory of Linear Electrical Circuits], Moscow, Vysshaya shkola, 1978.

39. Furduyev, V. V., "Elektroakustika" [Electroacoustics], Moscow-Leningrad, OGIZ, 1948.

40. Kharkevich, A. A., "Izbrannyye Trudy" [Selected Works], Vol 1, Moscow, Nauka, 1973.

41. Shenderov, Ye. L., "Volnovyye Zadachi Gidroakustiki" [Wave Problems in Hydroacoustics], Leningrad, Sudostroyeniye, 1972.

42. Cremer, L. and M. Heckl, "Korperschall-physikalische Grundlagen und technische Anwendungen," Berlin, Springer Verlag, 1967.

43. Heckl, M., "Untersuchungen an Ortotropen Platten," ACUSTICA, 1960, Vol 10, No 2, pp 109-115.

44. Heckl, M., "Vibrations of Point-Driven Cylindrical Shells," J. ACOUST. SOC. AMERICA, 1962, Vol 34, No 10, pp 1553-1557.

45. Junger, M. and D. Feit, "Sound, Structures and Their Interaction," Cambridge, Mass., MIT Press, 1972.

APPROVED FOR RELEASE: 2007/02/08: CIA-RDP82-00850R000200100009-9

APPROVED FOR RELEASE: 2007/02/08: CIA-RDP82-00850R000200100009-9

46. Kennard, E., "The New Approach to Shell Theory," J. OF APP. MECHANICS, 1953, Vol 20, No 1, pp 33-40.

47. Kurtze, G., "Physik und Technik der Larmebekampfung," Karlsruhe, 1964.

48. Lamb, G., "Input Impedance of a Beam Coupled to a Plate," J. ACOUST. SOC. AMERICA, 1961, Vol 33, No 5, pp 628-632.

49. Maidanik, G., "Response of Ribbed Panels to Reverberant Acoustic Fields," J. ACOUST. SOC. AMERICA, 1962, Vol 34, No 6, pp 809-826.

50. Snowdon, J. C., "Mechanical Four-Pole Parameters and Their Application," J. SOUND VIB., 1971, Vol 15, No 4, pp 307-324.

APPROVED FOR RELEASE: 2007/02/08: CIA-RDP82-00850R000200100009-9

APPROVED FOR RELEASE: 2007/02/08: CIA-RDP82-00850R000200100009-9

CHAPTER 2. PRINCIPLES OF MEASUREMENT ACOUSTICS

2.1. Input and Metering Circuits. Calibration of Acoustic- and Vibration Meters

Metering circuits are used for measuring the characteristics of acoustic and vibration fields. These circuits include the following basic units: electroacoustic converter -- a sound or vibration receiver, amplifiers, filters, voltage dividers, displays and recording instruments.

In laboratory research a metering circuit includes an input circuit, which turns on a generator that produces electric oscillations of a given kind, a power amplifier and an electroacoustic converter -- a source of sound or vibration. A block diagram of a typical acoustic channel for laboratory studies is shown in Figure 2.1. A measurement space should satisfy a number of requirements, determined by the purpose of investigations, frequency range and utilized equipment. Electronic units of audio channels (amplifiers, generators, indicators and recording machines) are selected in consideration of the frequency band and purpose of the investigation; they satisfy typical requirements, imposed on radio electronic test instruments. In most cases industrial instruments are used if their parameters meet requirements.

An acoustic metering channel must be calibrated (for instance, sensitivity and concentration factor are determined). Calibration is done comparatively rarely. Calibration is done several times for the purpose of checking the performance of a channel during the measurement process. This procedure determines how well the condition of a channel corresponds to its rated parameters.

Through and two-step calibration procedures are used for metering channels. In through calibration a known acoustic parameter, for instance p, is supplied to the receiver part, the readings of dividers N_1 and indicators N_2 of the channel are recorded and correction factor Δ, which must be added to their readings after measurement, is determined:

$$\Delta = p - N_1 - N_2, \qquad (2.1.1)$$

APPROVED FOR RELEASE: 2007/02/08: CIA-RDP82-00850R000200100009-9

APPROVED FOR RELEASE: 2007/02/08: CIA-RDP82-00850R000200100009-9

where all the values are given in decibels (relative to an arbitrary level).

Measured pressure p_x is determined by the expression

$$p_x = N_1' + N_2' + \Delta, \qquad (2.1.2)$$

where N_1' and N_2' are readings of the dividers and indicators of the channels during measurement; p_x is read in decibels relative to the same zero level.

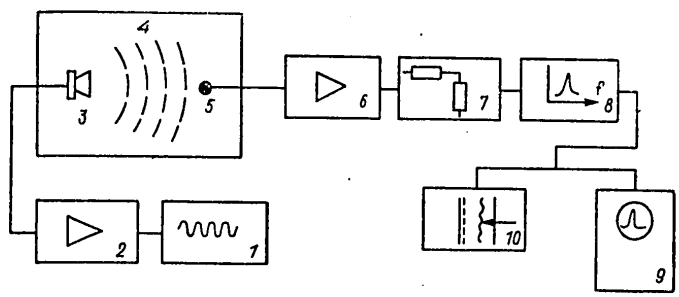

Figure 2.1. Schematic diagram of typical acoustic channel for laboratory research: 1 -- oscillator; 2 -- power amplifier; 3 -- electroacoustic transducer; 4 -- test room; 5 -- electroacoustic receiver; 6 -- amplifier; 7 -- voltage divider; 8 -- filter; 9 -- oscillograph; 10 -- recorder.

In two-step calibration the sensitivity of the electroacoustic receiver is determined separately and the electronic part of the metering channel is calibrated. Acoustic pressure p_x during measurements in this case is determined by the formula

$$p_x = N_1' + N_2' - M + u - N_1 - N_2, \qquad (2.1.3)$$

where u is electrical voltage, V (in decibels during calibration of the electronic part of the channel); M is receiver sensitivity, dB; N_1', N_2', N_1, N_2 are the same as in formulas (2.1.1) and (2.1.2).

The analogous expressions can be formulated for the calibration of vibration metering channels.

During the assembly of audio metering channels from individual devices it is essential to consider the following requirements: the input impedance of each successive instrument must be substantially greater than the output

APPROVED FOR RELEASE: 2007/02/08: CIA-RDP82-00850R000200100009-9

APPROVED FOR RELEASE: 2007/02/08: CIA-RDP82-00850R000200100009-9

impedance of the one before it; the capacitance of connecting wires and cables must be taken into consideration when connecting the instruments up. Electrical calibration must be done for the entire channel to ensure that all of the components have a linear response.

Methods used for calibrating electroacoustic converters are: calibration on the basis of the reciprocity principle; electrostatic calibration; electrodynamic and piezocompensation calibration; vibrating liquid column calibration. In addition, calibration by comparison with a reference converter is used extensively.

Calibration Based on Reciprocity Principle. In accordance with the reciprocity principle the sensitivity of a linear two-way electroacoustic converter in the receive and radiate modes is related as

$$M = TH,$$

where M is the sensitivity of the electroacoustic converter in the receive mode (the ratio of the output voltage of the converter to the acoustic pressure acting upon the instrument); T is the sensitivity of the electroacoustic converter in the radiate mode (the ratio of the acoustic pressure at a given distance to the electric current that drives the converter); H is the reciprocity coefficient (parameter).

The reciprocity coefficient is determined by the conditions of radiation and reception and by the nature of the generated acoustic field. When spherical, cylindrical and plane waves are radiated and received the reciprocity coefficients are, respectively,

$$H = \frac{2r\lambda}{\rho c}; \quad H = \frac{2L\sqrt{r\lambda}}{\rho c}; \quad H = \frac{2S}{\rho c}, \tag{2.1.4}$$

where r is the distance to the receiver; λ is the acoustic wavelength in the medium; ρ, c are the density and speed of sound in the medium; L is converter length; S is converter area.

Using three converters is the most common calibration technique. In addition to a test converter it is necessary to have a two-way converter and an auxiliary audio source. Calibration is done in three steps (Figure 2.2). Step one: the auxiliary source radiates and voltage u_1 at the output of the tested audio receiver is measured. Step two: a two-way converter, operating in the receive mode, is set up in place of the instrument to be tested. The operating mode of the auxiliary audio source is not changed. Voltage u_2 at the output of the two-way converter is measured. Step three: the two-way converter is set up in place of the source, is driven by current i and generates acoustic pressure, which acts upon the tested receiver.

APPROVED FOR RELEASE: 2007/02/08: CIA-RDP82-00850R000200100009-9

APPROVED FOR RELEASE: 2007/02/08: CIA-RDP82-00850R000200100009-9

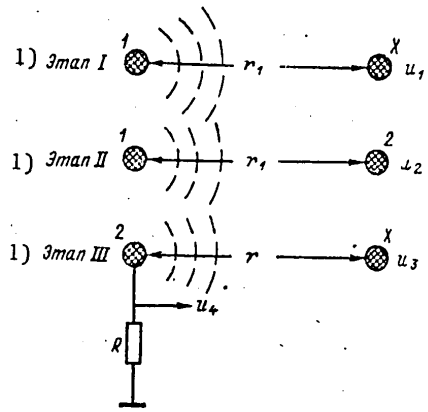

Figure 2.2. Calibration of audio receivers with three converters based on reciprocity principle: 1 -- auxiliary source; 2 -- two-way converter; R -- small active impedance; u_1-u_4 -- measured voltages; X (here and hereinafter) -- tested receiver.
Key: 1. Stage

Small resistor R is usually connected in series with the two-way converter. Voltage u_4 on that resistor (proportional to current i) and voltage u_3 at the output of the tested receiver are measured.

Sensitivity M, in V/Pa, is determined by the formula

$$M = \sqrt{\frac{u_1 u_3}{u_2 u_4} RH} \; . \qquad (2.1.5)$$

If during calibration with voltage dividers the same signal appears on the indicator, then sensitivity M, in dB, is determined from readings of k_1-k_4 on the scales of the dividers:

$$M = \frac{1}{2}(k_1 - k_2 + k_3 - k_4 + R + H) \qquad (2.1.6)$$

(here all values are expressed in decibels relative to units of the International Units System, and scale values k_1-k_4 are expressed in terms of an arbitrary unit).

This procedure can also be used for calibrating directional converters if they are aimed at the sound source in all calibration steps. The metering channel must be kept linear in all calibration steps. Distance must correspond to the inequality $r > D^2/\lambda$, where D is the size of the converters.

APPROVED FOR RELEASE: 2007/02/08: CIA-RDP82-00850R000200100009-9

APPROVED FOR RELEASE: 2007/02/08: CIA-RDP82-00850R000200100009-9

Test conditions should correspond to a boundless medium. Therefore calibration is often done in the pulse mode; calibration can also be done in a slightly deadened room, the dimensions of which do not exceed the calibration distance by a factor of more than 20.

When complicated types of converters are used at short distances the correctness of a selected distance must be determined on the basis of the dependence of 1/p on r; segment Δr, cut on the r axis by the extension of this function, is the correction factor.

To avoid repeated setups during the calibration process the converters are arranged so that progression from one step to the next can be done with an electric switch. A sample schematic diagram of a pulse metering channel for calibrating converters set up "in line" is shown in Figure 2.3.

To switch from the first position to the second (i.e., to switch to the second calibration step) an electric motor is turned on, which rotates the radiator by 180°. If the radiator has a symmetric electric-plane characteristic or is nondirectional the radiator need not be rotated. The three-converter method is used on frequencies from hundreds of hertz to hundreds of kilohertz.

Self-calibration of reversible converters is based on the following principle. The converter receives the signals it radiated after they bounce off a reflector (reflecting surface), located at distance r/2. The dimensions of the converters D, reflector R_e and r are connected by the relations

[∃=e]

$$r > 6\lambda; \quad \frac{2D^2}{\lambda} < r < \frac{R_э^2}{\lambda}. \qquad (2.1.7)$$

The surface of water may be used as a reflector.

Calibration is done in the pulse mode. Measures must be taken to prevent blocking of the amplifier when a driving pulse reaches it. During calibration voltage u_x of the signal reflected from the reflector, and voltage u_1 proportional to the driving current, are measured. Converter sensitivity is

$$M = \sqrt{\frac{u_x}{u_1} RH}. \qquad (2.1.8)$$

This procedure is used for high frequencies.

Reciprocity calibration on low frequencies is done in small booths (the calibration of microphones by this method is regulated by standards in many countries). The booth must be substantially smaller than the acoustic wavelength in the medium, and the booth walls must be rigid. Then the reciprocity coefficient is $H = kV/\rho c$, where k is the wave number for the medium; V is booth volume. A booth is a miniature setup, to two sides of which are

APPROVED FOR RELEASE: 2007/02/08: CIA-RDP82-00850R000200100009-9

APPROVED FOR RELEASE: 2007/02/08: CIA-RDP82-00850R000200100009-9

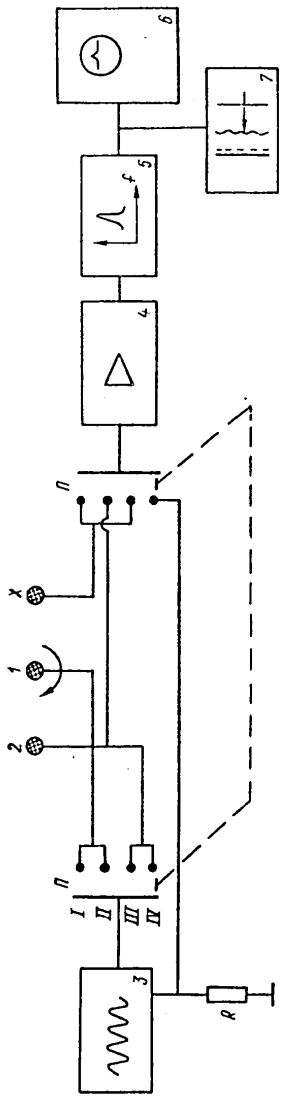

Figure 2.3. Calibration of converters by reciprocity procedure in one setup: 1 -- auxiliary source; 2 -- two-way converter; 3 -- electric oscillator; 4 -- amplifier; 5 -- filters; 6 -- oscillograph; 7 -- recording instrument; П -- four-way switch; R -- small active resistor; I-IV -- stages.

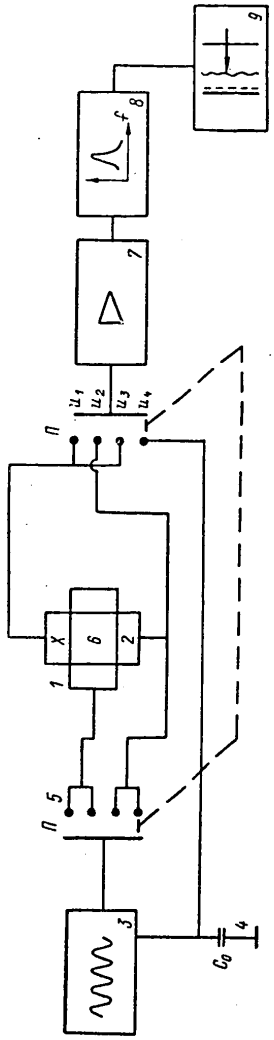

Figure 2.4. Calibration of microphones in small booth: 1 -- piezoceramic radiator; 2 -- two-way converter; 3 -- electric oscillator; 4 -- electric capacitor; 5 -- switch; 6 -- measurement space; 7 -- amplifier; 8 -- filters; 9 -- recorder.

APPROVED FOR RELEASE: 2007/02/08: CIA-RDP82-00850R000200100009-9

APPROVED FOR RELEASE: 2007/02/08: CIA-RDP82-00850R000200100009-9

connected radiators and microphones, which are replaced in accordance with the above-described procedure.

A booth made of a piezoceramic ring, the walls of which function as an auxiliary acoustic source (Figure 2.4), is used in order to convert from multiple setups to electric switches. Large capacitor C_0 is series-connected to the reversible converter instead of a resistor. Sensitivity is determined by the formula

$$M = \sqrt{\frac{u_1 u_3}{u_2 u_4} \frac{V}{C_0 \rho c^2}}. \qquad (2.1.9)$$

The frequency band for this method is about 100-5,000 Hz.

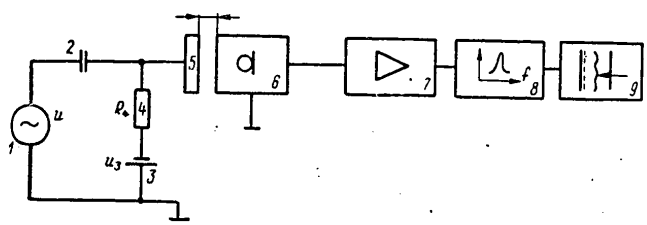

Figure 2.5. Electrostatic calibration of capacitive microphones: 1 -- AC voltage generator; 2 -- coupling capacitor; 3 -- DC source; 4 -- filter resistor; 5 -- extra electrode; 6 -- capacitive microphone; 7 -- amplifier; 8 -- filters; 9 -- recorder.

Calibration of piezoconverters-hydrophones by measurement of their electrical resistance in water R_r and in air R_a is a modification of the reciprocity method. This procedure minimizes the measurement space and is especially suitable for nondirectional receivers. On frequencies below the mechanical resonance, during measurement on an AC bridge, sensitivity is determined by the formula [17]

[c=r; в=a]

$$M = \left[\frac{4\pi c\gamma (R_c - R_в)}{\rho\omega^2}\right]^{1/2}, \qquad (2.1.10)$$

where γ is the concentration coefficient of the hydrophone; ω is angular frequency.

Sensitivity, in V/Pa, for nondirectional hydrophones in water is

$$M = \frac{0,7}{f} \sqrt{R_c - R_в}. \qquad (2.1.11)$$

APPROVED FOR RELEASE: 2007/02/08: CIA-RDP82-00850R000200100009-9

APPROVED FOR RELEASE: 2007/02/08: CIA-RDP82-00850R000200100009-9

An industrial instrument, or Q-factor meter, may be used for such measurements [16]. The precision of the procedure is 1 dB and the frequency range is 4-30 kHz.

Electrostatic Calibration. This method is used for calibrating flat membrane microphones in air (Figure 2.5). An electric potential in the form of DC and AC voltages, with the DC voltage substantially higher than the AC voltage, is applied to the gap between the sensitive element of the microphone and the auxiliary electrode. Under the influence of the electric field electrostatic forces act upon the membrane of a receiver, and the pressure p of these forces, in Pa, is

$$p = \frac{8{,}85 u_0 u \cdot 10^{-12}}{d^2}, \qquad (2.1.12)$$

where u_0 is DC voltage, in V; u is the amplitude of AC voltage, in V; d is the gap.

The electrode is perforated to eliminate the influence of the elasticity of water in the gap; in this case a correction factor is added to the value of d according to formula (2.1.12).

The frequency range is 5-10,000 Hz. Precision is 1 dB.

Electrodynamic Compensation Calibration [3]. The pressure, developed in a small chamber in which is placed an instrument that senses acoustic pressure in water, or a hydrophone, is compensated by the electrodynamic force that drives a membrane, mounted in one of the walls of the chamber. At the time of compensation, which is achieved by selecting the proper amplitude and phase of the driving current, the membrane does not vibrate, and this fact is shown by an optical indicator. The constant of the chamber is determined by calibrating the chamber to a known static pressure p_{st}. The sensitivity of the tested hydrophone is determined by the formula

[ct=st]

$$M = \frac{u_x I_0}{I_x p_{ст}}, \qquad (2.1.13)$$

where I_0 is the static pressure compensation current; I_x is the acoustic pressure compensation current.

The frequency range is 0.1-1,000 Hz. When laser systems are used high precision can be achieved in the monitoring of the compensation time. We note that it is not necessary to perform compensation during measurements; it is sufficient to use compensation for determining the constant of the chamber and to drive the electrodynamic converter with a given current during calibration. The precision of the method is ±1/2 dB.

Piezocompensation Calibration. A small chamber is made of two elastically coupled piezoelectric cylinders, the ends of which are capped (Figure 2.6). An auxiliary radiator is inserted in one of the end caps. The hydrophone to be tested is placed in the chamber.

APPROVED FOR RELEASE: 2007/02/08: CIA-RDP82-00850R000200100009-9

APPROVED FOR RELEASE: 2007/02/08: CIA-RDP82-00850R000200100009-9

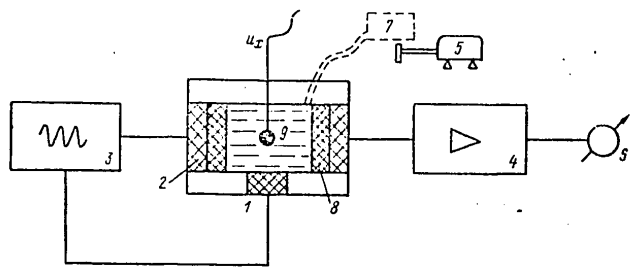

Figure 2.6. Piezocompensation calibration of hydrophones: 1 -- radiator; 2 -- null member; 3 -- electric oscillator; 4 -- amplifier; 5 -- cam drive; 6 -- volt meter; 7 -- reservoir; 8 -- null indicator; 9 -- tested hydrophone.

According to the literature [9] the calibration procedure consists in the following. Some pressure on a given frequency is produced with radiator 1 in the chamber. Voltage u_x at the input of the test receiver is measured, and then the pressure is compensated by changing the amplitude and phase of the drive voltage of one of the cylinders (null member 2). The compensation time is determined by the weakest signal picked up by the second cylindrical converter (null indicator 3).

The sensitivity of the procedure is determined by the formula

$$M = \frac{u_x}{u_k M_0}, \qquad (2.1.14)$$

where M_0 is the constant of the setup, determined by compensating pressure p_0 in the chamber, developed by a variable column of liquid on low frequencies [3].

The frequency band for which the described method is suitable is 1 to 3,000 Hz. In this band M_0 does not depend on frequency.

The calibration procedure can be simplified substantially by virtue of the fact that p_0 is directly proportional to the drive voltage of the null member. Therefore calibration in the working frequency band can be done by maintaining voltage u_k on the null member constant and by measuring the voltage u_x on the hydrophone output. Sensitivity is also determined by formula (2.1.14), and constant M_0, as before, should be determined by compensating the pressure developed by a variable column of liquid. Precision is ±0.3 dB.

A piezocompensation chamber, consisting of two piezocylinders, can also be used for calibrating hydrophones by the reciprocity principle (three

APPROVED FOR RELEASE: 2007/02/08: CIA-RDP82-00850R000200100009-9

APPROVED FOR RELEASE: 2007/02/08: CIA-RDP82-00850R000200100009-9

converters in a small chamber). The null member here is an extra source, and the null indicator is a reversible converter. The following voltages are measured: u_1, u_3 -- of the tested receiver, u_2 -- of the reversible converter and u_4, which is proportional to the drive current of the null indicator. Sensitivity is determined by the formula

$$M = \left(\frac{u_1 u_3 RH}{u_2 u_4}\right)^{1/2}. \qquad (2.1.15)$$

Here $H = \omega C_0$, where C_0 is the total flexibility of the measurement space, characteristic of a given setup. Its value is determined by calibrating the instrument with a column of liquid or with a water-air resonator [15].

Calibration with Variable Column of Liquid over Hydrophone. This method is used on frequencies not higher than 2-3 Hz. The hydrostatic pressure can be changed by vertically shifting the hydrophone in a vessel of water or by changing the water level over the stationary hydrophone. The dash line in Figure 2.6 explains how the second method is done. The cavity of the test chamber is connected to an open vessel, which completes vertical motions through a cam drive. The sensitivity of the hydrophone being calibrated is determined by the formula

$$M = \frac{u_x}{\rho g h}, \qquad (2.1.16)$$

where ρ is the density of water; g is the acceleration of gravity; h is the amplitude of the vertical displacement of the water level.

The frequency range is fractions of a hertz to 1 Hz. The error is about 1 dB.

Relative Calibration of Acoustic Pressure Receivers. This method is based on comparison of the readings of a reference and test receivers when acted upon by a given acoustic field. There are the comparison method, whereby the source radiation acts simultaneously upon the reference and tested receivers, and the substitution method, whereby the receivers are placed one after another at the same point of the field. The second method is more accurate if the source is kept in the same excitation mode and the same electronic meter is used. The use of a rotating system that places the receivers in the same place in the field (Figure 2.7) speeds up the comparison procedure. In relative calibration of acoustic radiators equal conditions of electrical excitation are created and the pressures developed by the radiator are compared with an auxiliary test instrument.

Calibration of Vibration Receivers. The basic method is calibration on vibration stands, in which vibrations of a given frequency are generated on a massive (in comparison with the receiver to be calibrated) vibration bench. The parameter of vibration (displacement, vibration velocity,

APPROVED FOR RELEASE: 2007/02/08: CIA-RDP82-00850R000200100009-9

APPROVED FOR RELEASE: 2007/02/08: CIA-RDP82-00850R000200100009-9

vibration acceleration) is usually determined by the contactless method, i.e., optically or capacitively, with the aid of eddy currents, the Mossbauer effect, etc. Relative calibration by comparison of the signals from a reference and test receivers, reacting to the vibrations from the same vibration source, is used extensively.

Stationary systems for calibrating acceleration receivers on frequencies of 0.1 Hz to 20,000 Hz are being manufactured. The most precise methods of determining vibration levels are procedures that use interference laser setups, by strobe interference, by counting the number of times the interference bands disappear, etc. They provide a displacement measurement error of about 0.1 micron. When working on vibration stands it is very important to keep the vibrations linear and to prevent spurious vibrations of the vibration bench.

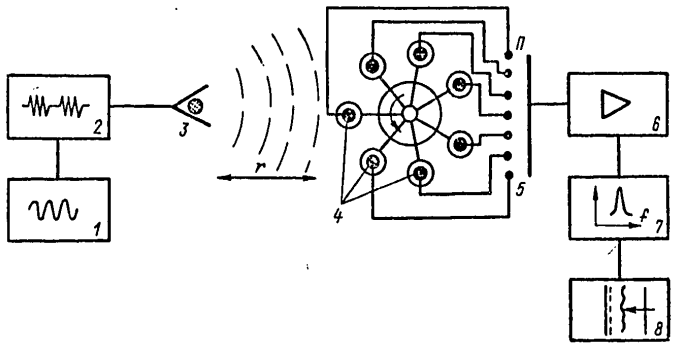

Figure 2.7. Relative calibration of audio receivers: 1 -- electric oscillator; 2 -- pulse generator; 3 -- radiator; 4 -- receivers; 5 -- switch; 6 -- amplifier; 7 -- filters; 8 -- recorder.

Automated portable vibration stands provide constant vibration accelerations of the vibration bench in the working frequency range. This is accomplished by using electromechanical feedback with the aid of a reference vibration receiver, set up symmetrically with respect to the one being tested on the opposite side of the vibration bench [7].

When calibrating by comparing the readings of the reference and tested vibration receivers it is important to maintain the excitation mode constant and to keep external conditions (temperature, pressure and nature of fastening) consistent with the mode of calibration of the reference receiver. The best results are obtained when the receivers are fastened alternately to the same point on a structure. The use of one meter, switched to the reference and tested receivers, improves the accuracy of the comparison if the outputs of the receivers are correctly matched to the

APPROVED FOR RELEASE: 2007/02/08: CIA-RDP82-00850R000200100009-9

APPROVED FOR RELEASE: 2007/02/08: CIA-RDP82-00850R000200100009-9

amplifier input. The effect of transverse vibrations is checked by fastening the receiver at a right angle to the direction of the basic vibrations.

Reciprocity calibration of vibration receivers [14] is comparatively rarely utilized in connection with the high level of electrical induction from the driving generator. However, calibration on frequencies higher than 30-35 kHz can be done only by this method.

2.2. Measurement of Noise and Vibration

Quantitative measurement of noises and vibrations requires the selection of the proper audio receivers (microphones, hydrophones, vibration receivers), meters, measurement facilities (when possible), proper setup and determination of the number of measurement points and the corresponding methodological evaluation of the results obtained.

Meters that receive acoustic pressure in air -- microphones -- should meet rigid (in comparison with their popular household counterparts) requirements on performance stability in time and under various external conditions, and on the dynamic and working frequency ranges. Electrostatic microphones, with high and uniform sensitivity in a wide frequency range, are used for the measurements. The sensitivity of the microphones, their directivity and intrinsic noise level should be taken into consideration during measurements.

A noise meter, an instrument with an amplifier with a given frequency characteristic and an indicator, in addition to a microphone, is used for measuring noise in air. Modern noise meters are capable of using different frequency characteristics (A, B, C), regulated by IEC [International Electrotechnical Commission], of octave analysis and of transmitting information to recording and analyzing systems. The requirements on the characteristics of noise meters are set forth in international recommendations of IEC.

Piezoceramic watertight spherical and cylindrical receivers, and disk receivers on high ultrasonic frequencies, are used as measuring hydrophones during measurements in water. Systems that measure vibration displacement, vibration velocity and vibration acceleration are used for analyzing the parameters of a vibration process.

Displacement is measured with a microscope and capacitive receivers, and vibration velocity is measured with inductive receivers -- velocity meters [11]. The piezoelectric vibration acceleration receivers (accelerometers), which utilize lead zirconate-titanate piezoceramic (TsTS-19, TsTS-23) and other compounds, are the most popular [8]. The working band of these receivers is 1 Hz to tens of kilohertz. Accelerometers with integrated circuits can measure vibration velocity and displacement. High stability and sensitivity, compactness, light weight, wide working temperature range,

APPROVED FOR RELEASE: 2007/02/08: CIA-RDP82-00850R000200100009-9

APPROVED FOR RELEASE: 2007/02/08: CIA-RDP82-00850R000200100009-9

the ability to function in liquids and gases are typical features of piezoceramic vibration receivers.

The characteristics of modern microphones and vibration receivers are presented in Table 2.1 [13].

Table 2.1. Characteristics of Modern Microphones and Vibration Receivers

1) Тип и марка прибора	2) Диапазон рабочих частот, Гц	3) Чувствительность	4) Динамический диапазон, дБ	5) Размеры микрофонного капсюля, мм	6) Реакция на изменение температур, дБ на 1°	7) Масса, г	8) Страна-изготовитель
9) Микрофоны:							
4131	20—18 000	50 мВ/Па	15—148	25,2	0,2	—	Дания
4134	10—40 000	13 мВ/Па	28—160	12,6	0,1	—	Дания 10)
4136	5—100 000	2,8 мВ/Па	60—174	6,3	0,1	—	Дания
4138	5—140 000	0,1 мВ/Па	65—184	3,17	0,1	—	Дания
МК 6	20—40 000	10 мВ/Па	40—154	15	0,1	—	СССР 11)
ИМК 6М	20—20 000	—	50—154	17	0,1	—	СССР
12) Виброприемники:							
4332	0—6 000	50 мВ/g	—	—	0,1	30	Дания
4335	0—8 000	19 мВ/g	—	—	0,1	13	Дания 10)
4336	0—25 000	4 мВ/g	—	—	0,1	2	Дания
4339	0—10 000	10 мВ/g *	—	—	—	—	Дания
Д-11	2—10 000	40 мВ/g	—	—	—	—	СССР 11)

13) * Подбирается строго постоянной.

Key:
1. Type and brand of instrument
2. Working frequency range, Hz
3. Sensitivity
4. Dynamic range, dB
5. Microphone capsule dimensions, mm
6. Temperature reaction, dB/1°
7. Weight, g
8. Manufacturer
9. Microphones
10. Denmark
11. USSR
12. Vibration receivers
13. *Set strictly constant

[мВ=mV; Па=Pa; ИМК=IMK; Д=D]

Acoustic parameters are usually measured on logarithmic scale -- in decibels, because of the difficulty of using linear scales in a wide range of change of noise: from the audibility threshold of $2 \cdot 10^{-5}$ to the discomfort threshold of 10^6 Pa, i.e., a factor of 10^{11}.

The decibel scale for sound intensity I and pressure p is determined by the expression

[дб=db]

$$N_{дб} = 10 \lg \frac{I}{I_0} = 20 \lg \frac{p}{p_0}, \qquad (2.2.1)$$

APPROVED FOR RELEASE: 2007/02/08: CIA-RDP82-00850R000200100009-9

APPROVED FOR RELEASE: 2007/02/08: CIA-RDP82-00850R000200100009-9

where N is the noise level in terms of intensity and pressure; I_0, p_0 are the zero (or threshold) levels of the examined values.

The international threshold intensity in air is $I = 10^{-12}$ W•m^2. The acoustic pressure threshold is $p_0 = 2 \cdot 10^{-5}$ Pa; threshold p_0 is used in water. The acoustic pressure level is routinely expressed in decibels, and it is not stipulated, but understood that the zero level is $p_0 = 2 \cdot 10^{-5}$ Pa.

Vibrations are also measured in decibels relative to the acceleration threshold (acceleration of gravity) $g = 9.80665$ m/s^2. The sensitivity of accelerometers is expressed as $M = u/g$ and is measured in decibels in terms of 1 mV/g. The zero vibration velocity threshold is sometimes $\dot{\xi} = 5 \cdot 10^{-8}$ m/s, and the vibration acceleration threshold is $\ddot{\xi} = 3 \cdot 10^{-2}$ m/s^2.

Arbitrary zero levels, usually equal to a unit of measurement, are often used for calculations. For example, $\ddot{\xi} = 1$ m/s^2, $\dot{\xi}_0 = 1$ m/s, $p_0 = 1$ Pa. There are many advantages in representing results in decibels, but non-standard zero levels that are used must be indicated.

Measurement of noises produced by different sources requires that several conditions be satisfied in regard to the measurement space, number and location of measurement points. The most precise measurements can be made in specially equipped sound chambers, the interior of which is lined with sound-absorbing coverings (usually wedges), and measures are taken during the construction of the building to prevent the infiltration of exterior noises. The quality of sound chambers is usually expressed as the acoustic ratio at the test point -- the ratio of the total energy of reflected signals to the energy of the incident signal. For satisfactory measurements this ratio should be smaller than 0.1 (then the error introduced by reflections will be less than 5%). Sound chambers are also evaluated in terms of the nature of change of a signal as the distance between the receiver and the source increases: deviation from the ratio 1/r should not exceed 0.5 dB.

In cases when the requirements of boundless space cannot be satisfied the acoustic energy density is measured in a room, in which a noise source is installed. Reverberation chambers with surfaces that reflect the incident sound serve well for this purpose.

The procedure for measuring noise generated by electrical machinery is regulated by GOST 11270-66. There are also several international recommendations of IEC-ISO on various aspects of atmospheric noise measurement: R-1996, R-1680, R-495, R-392; R-357, R-354, etc. [37] (these recommendations are called "ISO Standards" since 1972).

To obtain reliable results the noises of machinery on ships should be measured at several points around a machine at a distance of about 1 m from the hull, and the results are averaged [24].

APPROVED FOR RELEASE: 2007/02/08: CIA-RDP82-00850R000200100009-9

APPROVED FOR RELEASE: 2007/02/08: CIA-RDP82-00850R000200100009-9

During acoustic vibration measurements the quality of the results depends on how the vibration receivers are fastened and on how much influence it exerts on the source of vibrations. The best results are obtained when the vibration receivers are firmly fastened to the vibrating surface. The vibration receiver may be assumed to exert no influence on the vibrations of a surface if its mass is negligible in comparison with the linear mass of the vibrating surface per unit length. Therefore low mass receivers, from 20 to 3 g, are used [7].

2.3. Spectral and Correlation Analysis

Virtually all modern acoustic analyzers are electronic instruments, i.e., they work with electrical signals that are proportional to the acoustical values that are measured. When all the elements of the metering channel (electroacoustic converters, amplifiers, indicators) are linear acoustic signals may be replaced with electric signals, and acoustic values can be assigned to the results.

The determination of the amplitudes and frequencies (or frequency bands) of vibrations that are contained in a measured signal is called spectral analysis. Analysis consists in the experimental determination with frequency selective elements -- filters for individual components of a compound signal under analysis. The types of analysis are sequential, when the spectrum of a signal is found by sequentially changing the frequency properties of the filters while "watching" the entire analyzed band (Figure 2.8a), and simultaneous analysis, when a signal is fed to a bank of parallel-connected filters, so that the analyzed frequency components appear at their outputs all at the same time (Figure 2.8b). The performance of each filter in simultaneous analysis is similar to the performance of the filter in the corresponding position during sequential analysis.

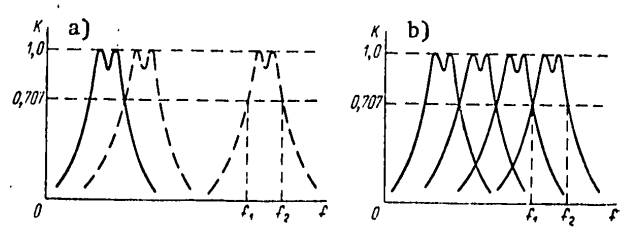

Figure 2.8. Position of filter passbands in sequential and simultaneous spectral analysis.

The only practical difference between sequential and simultaneous analysis is the fact that the number of filters in the second case is limited and the seams between the filters are analyzed with less precision, and therefore the results of simultaneous analysis are not quite as good as in the case of sequential analysis.

APPROVED FOR RELEASE: 2007/02/08: CIA-RDP82-00850R000200100009-9

APPROVED FOR RELEASE: 2007/02/08: CIA-RDP82-00850R000200100009-9

The main element of spectral analysis is the filter, which is characterized by the passband, transadmittance in the pass and opaque bands, and transconductance. Passband Δf of a filter is determined by the difference of the top and bottom frequencies, on which the transadmittance of the filter (the ratio of the output voltage to the input voltage) decreases by 3 dB. Transadmittance may vary within 3 dB in the passband.

The transconductance of a filter is usually evaluated by attenuation outside of the passband for a given frequency error. In one-third octave analysis with more than 20 dB attenuation on the middle frequency of the adjacent filter, the error related to the reception of signals from the no-pass band does not exceed 2 dB. The requirements on the attenuation outside of the passband are considerably more rigid (more than 60 dB for a three-octave frequency difference) in the case of analysis of a wide passband.

The analyzing capabilities of a channel as a whole are characterized by resolution, dynamic range and analysis time.

Resolution expresses the capability of the analyzer to distinguish two side-by-side frequency components of an analyzed signal and is expressed as interval ΔF between the frequencies of two sinusoidal signals with different amplitudes, separated with a valley in the frequency characteristic, equal to 50% of the maximum (Figure 2.9). The smaller ΔF the higher the resolution.

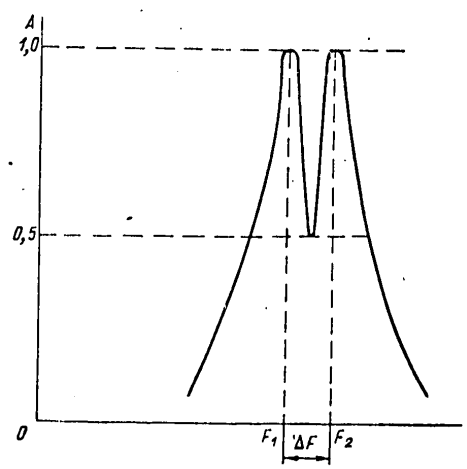

Figure 2.9. Determination of resolution of analyzer.

Resolution depends on the properties of the filter and on analysis conditions. In simultaneous analysis it is related to the passband and

APPROVED FOR RELEASE: 2007/02/08: CIA-RDP82-00850R000200100009-9

APPROVED FOR RELEASE: 2007/02/08: CIA-RDP82-00850R000200100009-9

transconductance of the filters, and in sequential analysis it is also related to the speed of analysis. For an LCR circuit resolution is $4\Delta f$, and for a bandpass filter it is approximately $3\Delta f$.

Analysis time is determined by the transient time of each filter, which is turned on during analysis for only a certain length of time. Transient time Δt_t is related to passband Δf by the ratio $\Delta t_t \Delta f = A$, where the coefficient A is determined by measurement conditions and by the characteristic of the filter. For an LCR circuit A = 1 for the time it takes the signal to build up to 0.95 of steady state.

Filters with a bell-shaped frequency characteristic, for example weak-coupled LCR circuits [2], have the shortest transient time.

Signal analysis is done with the passband held constant in the entire frequency range (Δf = const), or with the relative passband $\Delta f/f_0$ = const kept constant, where f_0 is the middle frequency of the filter.

In simultaneous analysis $\Delta f/f_0$ = const low-pass filters have the longest transient time.

In sequential analysis the speed of analysis must be selected correctly. The dynamic frequency characteristic of a filter with a continuously changing middle frequency differs from static because the peak of the curve falls and shifts toward a change of frequency, and the passband gets wider (the characteristic becomes asymmetric). This is due to the influence of inertial elements of the filter and of the interaction of its induced and natural vibrations. To obtain undistorted results the rate of change of frequency v to which the filter is tuned in sequential analysis must be determined by the expression

$$v \leqslant \mu_0 (\Delta f)^2, \tag{2.3.1}$$

where μ_0 is a constant, which depends on the requirements imposed on the analysis and on filter characteristics [27].

When filter characteristics are not know an analysis is general in nature; to determine v, in Hz/s, one may use the approximate expression

$$v = (0{,}25 \div 1{,}0)(\Delta f)^2. \tag{2.3.2}$$

The total time of sequential analysis is determined by the quotient of the bandwidth of the analyzer, divided by the analysis speed. The analysis time is many times longer than of simultaneous analysis.

The dynamic range of an analyzer -- the ratio of the peaks of the individual components that can be distinguished by the instrument in its working

APPROVED FOR RELEASE: 2007/02/08: CIA-RDP82-00850R000200100009-9

APPROVED FOR RELEASE: 2007/02/08: CIA-RDP82-00850R000200100009-9

frequency band, to the valleys -- characterizes the uncorrectable error of analysis (for a given instrument), caused by deviation of the frequency characteristics of perfect filters from real ones in the no-pass band. For successful analysis the dynamic range of the signal should be narrower than the dynamic range of the analyzer.

Spectral analysis of random processes discloses the characteristics of stable averages, and therefore the values obtained must be averaged appropriately in time, which is called integration. Signal integration time Δt is determined on the basis of the acceptable relative mean square error δ of the results of analysis of a random process:

$$\delta = (A_1/\Delta t \Delta f)^2, \qquad (2.3.3)$$

where A_1 is a coefficient that is determined by the type of filter, detection and integration methods; A_1 = 0.04-0.1.

Calculation of the time of analysis of random processes shows that the time spent on such analysis is considerably longer than the time spent on the analysis of deterministic signals. When commercial instruments with a comparatively wide passband (octave, third-octave) are used for spectral analysis of random processes larger errors are acceptable, if features of the averaging of a random signal are ignored.

When selecting the instruments and conditions for conducting an analysis it is important to consider the nature of the spectrum of the signal to be analyzed, the purpose of the studies and the acceptable time of analysis. For finding noise sources the analysis should have a constant passband, which, however, should not be too narrow, since industrial noise sources inevitably fluctuate during operation. Analysis with a constant relative passband is better for noise abatement or sound insulation, since rather wide frequency ranges are usually sound-insulated.

One way to reduce the analysis time is to transpose the signals during recording on magnetic tape. Then the signal is recorded at a slower tape transport speed and is played back at a higher speed; the band of the reproduced signal is wider and the analysis time is shorter. Low-frequency signals are also easier to transpose because the spectrum of the signal, transferred to a higher frequency range, can be analyzed with commercial instruments, designed for the medium- and high-frequency ranges [20]. Noteworthy among the spectrum analyzers for transposition analysis are the 7001, 7003 and 7004 magnetic recording meters, manufactured by the (Bryul' and K"yer) firm.

The basic technical specifications of industrial analyzers and spectrometers are listed in Table 2.2.

Correlation analysis determines the strength of the relationship between random phenomena on the basis of probability analysis of processes that

APPROVED FOR RELEASE: 2007/02/08: CIA-RDP82-00850R000200100009-9

APPROVED FOR RELEASE: 2007/02/08: CIA-RDP82-00850R000200100009-9

are taking place. A mathematical measure of the relation of processes is the correlation function, which expresses the probability relation of samples of processes, separated by an interval of time.

Correlation analysis consists in the experimental determination of the dependence of correlation functions on the time delay of one of the parameters of an analyzed process.

The cross-correlation function of two processes x(t) and y(t) is written as

$$\varphi_{xy}(\tau) = \lim_{T\to\infty} \frac{1}{T} \int_0^T x(t)\, y(t \pm \tau)\, dt = \overline{x(t)\, y(t \pm \tau)}, \qquad (2.3.4)$$

where τ is the time delay of one function in relation to another; the superscore over the product indicates averaging in time.

The autocorrelation function, which determines the probability relation of one process at different moments of time, is written as

$$\varphi_{xx}(\tau) = \lim_{T\to\infty} \int_0^T x(t)\, x(t \pm \tau)\, dt. \qquad (2.3.5)$$

The practical importance of T is determined by the tolerable error and the type of instrument used.

Correlation functions are connected by Fourier transforms to the energy spectrum of the processes:

$$\varphi_{xy}(\tau) = \frac{1}{\pi} \int_0^\infty G(\omega) \cos \omega\tau\, d\omega \quad \text{и} \quad G(\omega) = 2 \int_0^\infty \varphi_{xy}(\tau) \cos \omega\tau\, d\tau, \qquad (2.3.6)$$

where $G(\omega)$ is the relative energy spectrum of the analyzed processes.

Hence it follows that correlation analysis methods cannot give any more information than spectral analysis. But correlation methods in some cases make it possible to simplify, speed up or facilitate an analysis.

Normal values -- cross-correlation coefficient $R_{xy}(\tau)$ and autocorrelation $R(\tau)$ -- are used for eliminating the influence of the numerical characteristics of processes on the analysis:

$$R_{xy} = (\tau) = \frac{\overline{x(t)\, y(t \pm (\tau)}}{\sqrt{\overline{x^2(t)}\, \overline{y^2(t)}}}; \qquad R(\tau) = \frac{\overline{y(t)\, x(t \pm \tau)}}{\overline{x^2(t)}}. \qquad (2.3.7)$$

APPROVED FOR RELEASE: 2007/02/08: CIA-RDP82-00850R000200100009-9

APPROVED FOR RELEASE: 2007/02/08: CIA-RDP82-00850R000200100009-9

Table 2.2. Technical Specifications of Analyzers and Spectrometers

1) Тип и марка прибора	2) Диапазон рабочих частот	3) Входное сопротивление	4) Динамический диапазон, дБ	5) Полоса анализа	6) Страна-изготовитель
7) Спектрометр 3347	25—20 000 Гц (8) (30 фильтров)	1 МОм	50	9) 1/3 октавы и октава	10) Дания
11) Анализатор 2107	2—4 000 Гц (12) (6 диапазонов)	1 МОм	40	13) От 6 до 30%	Дания
7) Спектрометр 2113	95—40 000 Гц (14) (33 фильтра)	1 МОм	40	9) 1/3 октавы и октава	Дания
11) Анализатор С4-48	10 Гц — 20 кГц	10 кОм	70	5—150 Гц	17) СССР
11) Анализатор С4к-26	10 Гц — 60 кГц	50 кОм	60	5, 30, 150 Гц	СССР
11) Анализатор 64к-34	20 Гц — 200 кГц	50 кОм	60	5, 10, 150, 300 Гц	СССР
11) Анализатор 64-53	20 Гц — 400 кГц	600 кОм	60	0, 6, 2, 6, 20, 60, 200, 600 Гц	СССР
15) Анализатор спектра низкочастотный Р-80	1,5 — 22 400 Гц (14) (33 фильтра)		40	1/3 октавы 16)	18) ГДР

Key:
1. Type and make of instrument
2. Working frequency range
3. Input impedance
4. Dynamic range, dB
5. Analysis band
6. Manufacturer
7. Spectrometer
8. (30 filters)
9. 1/3 octave and one octave
10. Denmark
11. Analyzer
12. (6 bands)
13. From 6 to 30%
14. (33 filters)
15. Low-frequency spectrum analyzer R-80
16. 1/3 octave
17. USSR
18. GDR

[Гц=Hz; МОм=MΩ; кОм=kΩ]

APPROVED FOR RELEASE: 2007/02/08: CIA-RDP82-00850R000200100009-9

APPROVED FOR RELEASE: 2007/02/08: CIA-RDP82-00850R000200100009-9

If processes are independent their normal cross-correlation function is zero. However, even mutually related processes, under certain conditions, have correlation coefficients that are equal to zero.

The cross-correlation and autocorrelation coefficients change from +1 to -1. Equality to one means that there is a linear relationship between processes: $x(t) = ny(t)$, where n is a numerical coefficient. The autocorrelation function for $\tau = 0$ is equal to the mean square of the function, i.e., it expresses the power of an analyzed process. The autocorrelation coefficient for $\tau = 0$ is equal to unity.

The correlation functions of different signals used for analysis are characterized by the coherence (or correlation) interval, i.e., the time delay between phenomena, after which they may be assumed to be independent. The time delay, after which the envelope of the autocorrelation function cannot exceed a prescribed value (usually 0.1) after a further increase of the time delay, is used in practice as the correlation interval.

The autocorrelation function of periodic processes is also periodic, and the correlation interval is infinite.

The correlation interval is inversely proportional to the signal bandwidth. Signals with the shortest correlation interval (for example, random signals with a bell-shaped spectrum) are of special importance in correlation analysis.

The typical correlation analyzer [22] contains two amplifier and filter channels, a variable time delay unit in one of the channels, a multiplier and an integrating unit. Because it is so difficult to perform multiplication in modern correlation analyzers a system is used for estimating the probability that analyzed signals, after being amplitude-limited, will have the same sign. The delay of these instruments can be assigned by digital components -- shift registers, controlled by a clock pulse generator, which makes it much easier to set the delay [23]. Correlation analyzers, combined with relative spectrum analyzers, are also important [1].

Let us examine the application of correlation analysis by way of example of the determination of the acoustic ratio in a room, i.e., the ratio of the energy of all reflected signals to the energy of the incident signal at the point of reception. A schematic diagram of a setup for measuring is shown in Figure 2.10. When a noise signal is radiated one of the channels of the correlator picks up the signal radiated in the room, received with a microphone and amplified in the electronic channel, and the other channel, equipped with a variable time delay, receives the signal directly from the noise generator. The signal received by the microphone is produced not only by the direct sound from the radiator, but also by reverberations from the walls, floor and ceiling of the room. The path of the sound from the radiator to the receiver is shorter than the path of any reflected signal. Therefore the parameters of the analyzer and the characteristics of the

APPROVED FOR RELEASE: 2007/02/08: CIA-RDP82-00850R000200100009-9

APPROVED FOR RELEASE: 2007/02/08: CIA-RDP82-00850R000200100009-9

signal are selected such that coherence interval τ_0 of the signal (which here expresses the length of a coherent parcel in space $l = 2\tau_0 c$) will be shorter than the time difference of the propagation of the sound via the direct path from the radiator to the receiver l_1, and via the shortest path from the reflector l_2:

$$\tau_0 < \frac{l_1 - l_2}{c}.$$

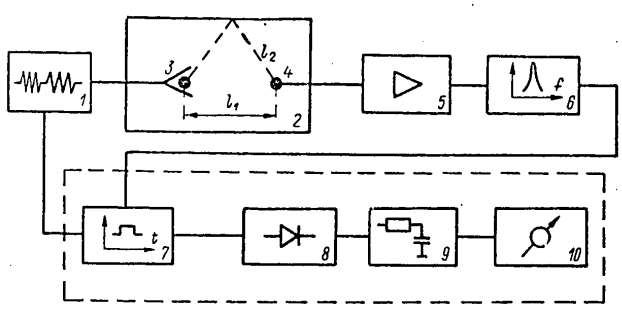

Figure 2.10. Schematic diagram of setup for measuring acoustic ratio in room by correlation method: 1 -- noise band generator; 2 -- room to be tested; 3 -- radiator; 4 -- receiver; 5 -- amplifier; 6 -- filters; 7 -- delay; 8 -- multiplier; 9 -- integrator; 10 -- indicator.

The acoustic ratio R is given by the formula

$$R = \frac{1}{R^2(\tau_1)} - 1, \qquad (2.3.8)$$

where $\tau_1 = l_1/c$ is the delay corresponding to the direct path.

Correlation analyzers are used extensively for detecting periodic signals in random interference.

The correlation procedure measures sound insulation, sound absorption and reflections, and because of its high sensitivity it is especially suitable for rooms with poor sound insulation and with a high noise level.

Correlation analysis determines the contribution of each operating machine to the total acoustic or vibration field without having to turn the machinery off.

Correlation analysis is good for determining the acoustic propagation velocity in a material on the basis of data on the correlation function as

APPROVED FOR RELEASE: 2007/02/08: CIA-RDP82-00850R000200100009-9

APPROVED FOR RELEASE: 2007/02/08: CIA-RDP82-00850R000200100009-9

a function of the delay. Longitudinal waves, bending waves and Rayleigh and Lamb waves, propagating at different velocities, can be identified. To do this the reference wavelength should be selected in accordance with the coherence interval of the utilized signals and the expected difference in propagation velocities.

2.4. Measurement of Vibration Power Radiated by Machinery[1]

The vibration processes of most mechanisms are stationary random processes. Vibration power N, radiated by such mechanisms into bearing and nonbearing connections is the scalar product of force pressure P(s, t), averaged in time, from the machine and the vibration velocity of the plane of contact q(s, t):

$$N = \lim_{t_1 - t_2 = \Delta t \to \infty} \frac{1}{\Delta t} \int_{t_1}^{t_2} \int_{s} p(s, t)\, q(s, t)\,. \tag{2.4.1}$$

A machine and its shock absorber and foundation may be viewed as a single system with a certain number of flat contact surfaces. In this case N is the sum of vibration powers N_i^n, radiated through individual plane contact surfaces with bearing and nonbearing connections by individual components of the generalized forces coming from the machine. Spectral density $N_i^n(\omega)$ of the vibration energy flux is

[эф=ef]

$$N_i^n(\omega) = Q_{i\,\text{эф}}^n(\omega)\, q_{i\,\text{эф}}^n(\omega) \cos\alpha, \tag{2.4.2}$$

where $Q_{i\ ef}^n(\omega)$ and $q_{i\ ef}^n(\omega)$ are the effective spectral components of the force from the machine and the vibration velocity of the n-th part in the i-th direction; α is the phase shift between force and velocity.

In the frequency band $\Delta\omega$

$$N_i^n(\Delta\omega) = Q_{i\,\text{эф}}^n(\Delta\omega)\, q_{i\,\text{эф}}^n(\Delta\omega)\, \mathrm{Re}\,\mathrm{R}n, \tag{2.4.3}$$

where ReRn is the real part of the correlation coefficient between Q_i^n and q_i^n in frequency band $\Delta\omega$.

In the first approximation

[аф=af]

$$N_i^n(\Delta\omega) = [q_{i\,\text{эф}}^n(\Delta\omega)]^2\, \mathrm{Re}\, Z_{ii\,\text{аф}}^{nn}(\Delta\omega), \tag{2.4.4}$$

[1]This section was written by V. I. Popkov.

APPROVED FOR RELEASE: 2007/02/08: CIA-RDP82-00850R000200100009-9

APPROVED FOR RELEASE: 2007/02/08: CIA-RDP82-00850R000200100009-9

where $\mathrm{Re}Z^{nn}_{ii\ af}(\Delta\omega)$ is the real part of the impedance of the shock absorber-foundation system in the frequency band.

The vibration power of a machine can be determined experimentally by two methods: direct -- as the scalar product, averaged in time, of force Q^n_i and corresponding velocity q^n_i, and indirect -- on the basis of the vibration velocities of the machine and mechanical impedances of bearing and non-bearing couplings.

Vibration power, radiated by forces normal to bearing surfaces, is measured directly.

A schematic diagram of an instrument that measures vibration power directly is shown in Figure 2.11. The Soviet IKM-69 meter is built on this design. The meter performs synchronous and cophasal analysis of signals, proportional to force and velocity, multiplies the signals in the passband of the analyzer and averages the product in time. The zero levels for determining (in dB) force, velocity and power are $2\cdot10^{-9}$ N; $7\cdot10^{-6}$ cm•s and 10^{-16} W.

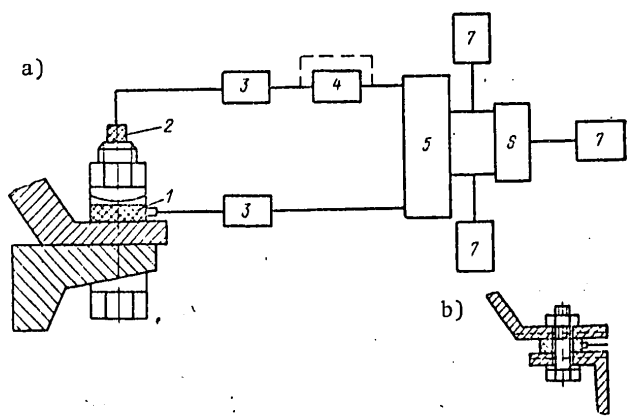

Figure 2.11. Schematic diagram of vibration power meter: a -- diagram; b -- position of dynamic pickup under machine; 1 -- dynamic pickup; 2 -- acceleration pickup; 3 -- amplifiers; 4 -- integrator; 5 -- dual-channel analyzer; 6 -- multiplier; 7 -- recorders.

The dynamic pickup is installed in the bolt connection and serves as an element, through which force is transmitted from the machine to bearing and nonbearing couplings. This sensor can be installed between the foot and foundation (Figure 2.11b), or between the foot and nut (Figure 2.11a). In

APPROVED FOR RELEASE: 2007/02/08: CIA-RDP82-00850R000200100009-9

APPROVED FOR RELEASE: 2007/02/08: CIA-RDP82-00850R000200100009-9

the former case 70 to 90% of the force acting on the foundation is picked up, and in the latter case approximately one-tenth [26].

Vibration powers radiated as a result of excitation of any vibration components -- linear and rotation, can be determined indirectly. The impedances of the bearing and nonbearing couplings in relation to forces and moments are measured by methods that will be explained below.

Signals from the sensors are fed to preamplifiers and then to a common meter amplifier. The phase characteristics of the sensors should differ by 180°, and the gains of the preamplifiers $k_{\ddot{q}1}$ and $k_{\ddot{q}2}$ are set so that the equality

$$\xi_{\ddot{q}1} k_{\ddot{q}1} = \xi_{\ddot{q}2} k_{\ddot{q}1} \tag{2.4.5}$$

is satisfied.

Sensitivity to torsional vibrations is

$$\chi_{\ddot{\varphi}} = k_{\ddot{q}1} \chi_{\ddot{q}1} l.$$

Measurement of Mechanical Impedance. The exact mechanical impedance in relation to force Z_F is determined as the combined ratio of force F, applied to a linear system, to the velocity component of the point of application of that force $\dot{q}_F$:

$$Z_F = \frac{F}{\dot{q}_F}. \tag{2.4.6}$$

A diagram of a system that measures mechanical impedance is shown in Figure 2.12. An electrical signal from audio frequency generator 1 passes through compression unit 2 and power amplifier 3 to vibrator 8. The frequency of the signal is gradually changed, and the voltage is controlled by the compression unit so that the velocity level of the generated vibrations is maintained constant in the entire frequency band. In this case the applied force is proportional to the modulus of the impedance of all the examined structures, and the frequency characteristic of the effective force, recorded on the tape of recording instrument 17, corresponds to the frequency characteristic of the modulus of impedance. The product of the signals of force u_F and velocity $u_{\dot{q}}$ in consideration of the cosine of phase shift α between them is proportional to the real part $\mathrm{Re}Z_F$ of the impedance, and the same product in consideration of the sine of the phase shift is the imaginary part $\mathrm{Im}Z_F$. A signal of acceleration is converted by integrating amplifier 15 to a signal that is proportional to the vibration velocity, and $u_F u_{\dot{q}}$ and $\cos\alpha$ are multiplied by electronic multiplier 16.

For measuring mechanical pliancy M (the inverse of mechanical impedance) compressor unit 6 maintains the force constant, and the frequency

APPROVED FOR RELEASE: 2007/02/08: CIA-RDP82-00850R000200100009-9

APPROVED FOR RELEASE: 2007/02/08: CIA-RDP82-00850R000200100009-9

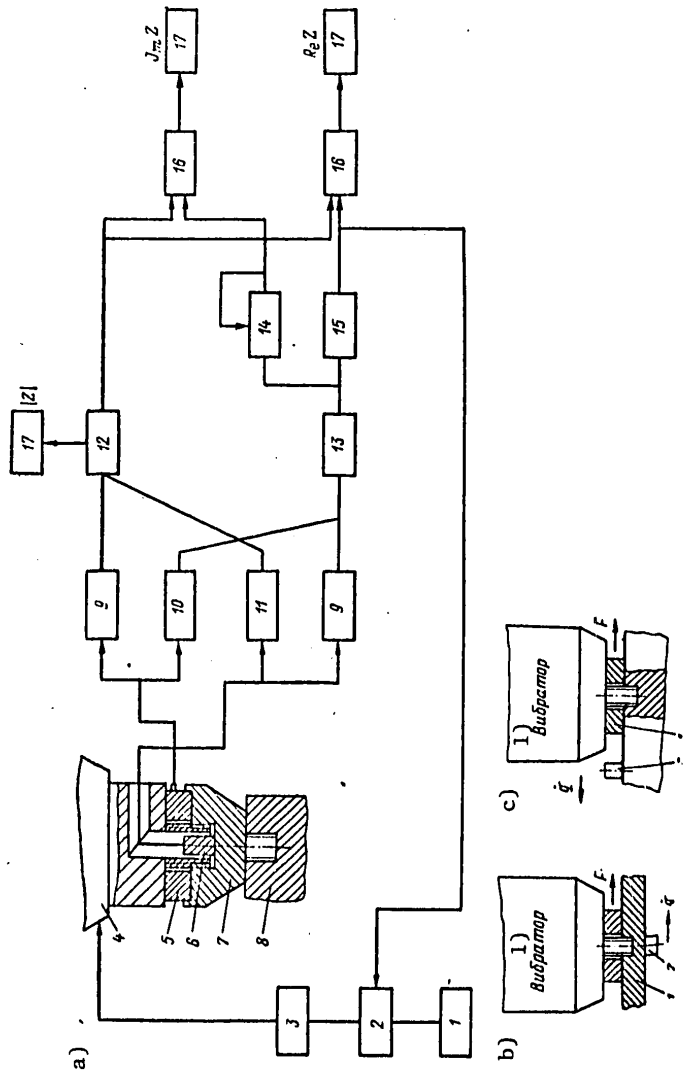

Figure 2.12. Schematic diagram of mechanical impedance meter: a -- measurement with combined pickup; b -- measurement with force and acceleration pickups, acceleration pickup under force pickup; c -- likewise, acceleration pickup some distance from force pickup.
Key: 1. Vibrator

APPROVED FOR RELEASE: 2007/02/08: CIA-RDP82-00850R000200100009-9

APPROVED FOR RELEASE: 2007/02/08: CIA-RDP82-00850R000200100009-9

characteristic of the velocity of the generated vibrations is recorded on tape as the modulus $|M_F|$.

A block diagram of channels for measuring impedances and pliancies with an instrument built by the Bryul' and K"yer firm [7] is shown in Figure 2.13.

A combined sensor -- impedance head, which generates force and acceleration signals, or instruments made up of dynamic and acceleration pickups, are used for measuring force and velocity. Rigid requirements are imposed on the design of combined pickups and instruments and on how they are attached to test products, because of the wide ranges of frequencies and mechanical impedances.

The basic factors that influence the precision with which Z_f and M_f are measured are:

the mass of the transition part (adapter) between the dynamic pickup and analyzed structure;

the rigidity of the adapter and of the fastener that holds the pickup to the analyzed structures;

the strain sensitivity of the acceleration pickup.

The mass of the adapter restricts the lower limit of the dynamic impedance measurement range, particularly on high frequencies, since the dynamic pickup also measures the force spent to overcome the inertia of the adapter.

The rigidities of the adapter and contact and the strain sensitivity of the acceleration pickup restrict the upper limit of the dynamic impedance measurement range.

The search for designs of combined sensors and instruments is aimed at correcting the above-mentioned factors. Possible designs of force and acceleration pickups and of combined pickups are illustrated in Figure 2.14 [26, 38]. The errors introduced by the adapter can be corrected by correcting the signals from the force and acceleration pickups with the aid of electronic instruments [26].

The mechanical impedance of structures in relation to moment Z_m is determined by the ratio of combined bending moment M, applied to a harmonically vibrating structure, to rotation velocity component $\dot{\phi}$. Bending moment can be applied to an analyzed system with the aid of a cantilever T- or L-beam.

An instrument that determines impedance in relation to moment is shown in Figure 2.14. Transverse force is applied to the free end of the beam. A bending moment appears at the point where the beam is fastened. A segment

APPROVED FOR RELEASE: 2007/02/08: CIA-RDP82-00850R000200100009-9

APPROVED FOR RELEASE: 2007/02/08: CIA-RDP82-00850R000200100009-9

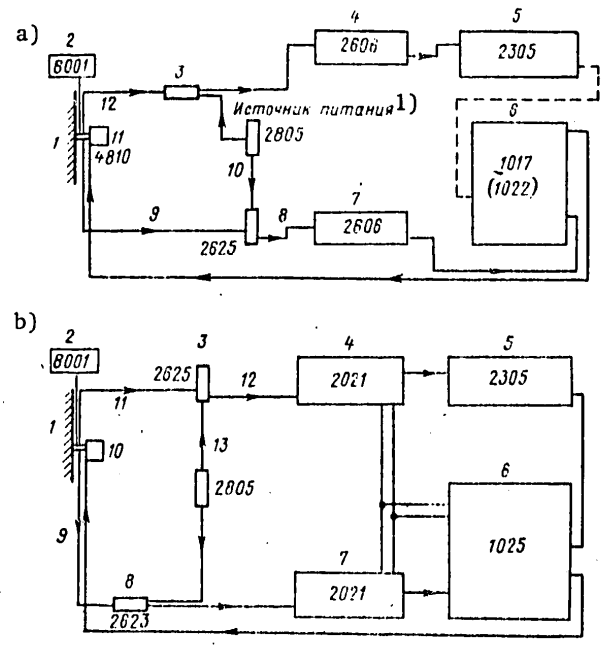

Figure 2.13. Schematic diagram of impedance meter channel of Bryul-K"yer instruments; a -- excited by pure tone; 1 -- vibrating product to be analyzed; 2 -- impedance head; 3 -- 2623 preamplifier; 4, 7 -- meter amplifier; 5 -- level recorder; 6 -- signal generator; 8 -- velocity signal; 9 -- acceleration signal; 10 -- preamplifier integrator; 11 -- vibrator; 12 -- force signal; b -- frequency-selective meter: 1 -- vibrating product to be analyzed; 2 -- impedance head; 3 -- preamplifier integrator; 4, 7 -- heterodyne tracking filter; 5 -- level recorder; 6 -- signal generator; 8 -- preamplifier; 9 -- force signal; 10 -- vibration stand; 11 -- acceleration signal; 12 -- velocity signal; 13 -- power source.
Key: 1. Power source

of the beam that is short in comparison with the total length is assumed to experience pure bending, and the longitudinal deformation of the boundary layer is proportional to the moment acting upon its cross section. To measure M it is sufficient to determine the deformation of the boundary layer of the beam near its root section. Deformation pickups are cemented to both ends of the beam in the plane of application of the moment and are electrically counter-wired to each other to eliminate the influence of shear deformation and of the longitudinal wave on their readings.

APPROVED FOR RELEASE: 2007/02/08: CIA-RDP82-00850R000200100009-9

APPROVED FOR RELEASE: 2007/02/08: CIA-RDP82-00850R000200100009-9

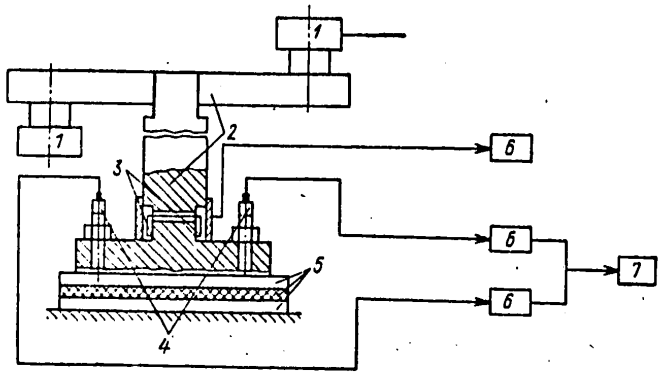

Figure 2.14. Determination of impedances in relation to moment: 1 -- vibrators; 2 -- beam; 3 -- deformation pick-ups; 4 -- rotary vibration pickup; 5 -- product to be analyzed; 6 -- preamplifiers; 7 -- meter amplifier.

2.5. Similitude and Dimensional Techniques in Marine Acoustics

Phenomena are called similar if the numerical values of parameters that characterize the process in one system of objects can be found by multiplying the values of parameters corresponding to them in another system by constant dimensionless factors. Similitude is used for establishing suitable conditions for analyzing certain processes, a full-scale evaluation of which is difficult, expensive or unreliable. A substitution of this kind is called modeling.

Geometric, physical and mathematical modeling are employed. Geometric modeling is used for demonstrating or showing the principle of operation, general character of a process or kind of acoustic field. Physical modeling is intended for determining the numerical values of parameters that describe the behavior of a process in full scale, by measuring the corresponding parameters in a model. Mathematical models are based on a mathematical description of phenomena and on the numerical solution of equations that describe their real behavior.

Before phenomena and processes can be similar in physical modeling both the basic equations that describe a process must be solved, and several boundary conditions that make processes identical and unique in reality and in the model, must be satisfied. The ratios of the corresponding values that characterize similar processes at the corresponding points and moments of time are called similitude constants. In physical modeling these abstract numbers are called modeling scales. The dimensionless sets of parameters that have the identical values in similar phenomena are called similitude criteria. Such criteria for vibrations of an isotropic solid, for example, are

APPROVED FOR RELEASE: 2007/02/08: CIA-RDP82-00850R000200100009-9

APPROVED FOR RELEASE: 2007/02/08: CIA-RDP82-00850R000200100009-9

$$\frac{cl}{t} = \text{idem}; \quad \frac{p}{\rho E_f \delta} = \text{idem}; \quad G = \text{idem}, \tag{2.5.1}$$

where c, l, t, p, ρ, δ are the dimensions of velocity, length, time, pressure, density and volume of expansion, and E_f, G are Young's modulus and shear modulus.

If the equations that describe investigated phenomena are not known, but the physical values that describe them are known, the similitude criteria can be found on the basis of dimensional analysis.

Some of the modeling scales can be selected arbitrarily for experimental convenience, and the others are determined through the similitude criteria and requirements of uniqueness.

The physical modeling of processes with geometric similitude intact (i.e., the dimensions of the model can be reduced or increased in comparison with the original) is of greatest importance in acoustic research. The scales for certain parameters (for example, length and acceleration) are assigned for convenience; all other parameters are determined in accordance with the similitude criteria and on the basis of dimensional analysis. Dissipative losses due to internal friction are analyzed on the basis of the combined representation of the Young's and shear moduli; the similitude conditions are unchanged if the Young's moduli do not depend on the amplitude and frequency of vibrations.

Dissipative losses in gases due to heat transfer, viscosity and molecular absorption are not simulated.

The modeling scale for linear dimensions M_L should be equal to time scale M_T and inversely proportional to frequency scale M_f, i.e., $M_L = M_T = 1/M_f$, for physical modeling using the same materials in real life and in the model (i.e., the constants ρ, E_f, G are maintained identical). The propagation velocity of longitudinal and transverse waves remains unchanged in the model. Bending wave propagation velocity also remains constant, in spite of a change of size, since a decrease of thickness is compensated by an increase of frequency. In this kind of modeling an arbitrary ratio of the scale of deformations to the scale of linear dimensions may be used. For example, the velocity scale in reality and in a model with the same acceleration should be M_L, and the displacement modeling scale is M_L^2.

The choice of numerical values of the main modeling scales depends on the specific purposes of the analyses. The linear scales for geometrically similar reality and model are determined by the feasibility of imparting to the model all the features of the original and by convenience of measurement on the model. The linear scale usually varies from 1:5 to 1:200. Too

APPROVED FOR RELEASE: 2007/02/08: CIA-RDP82-00850R000200100009-9

APPROVED FOR RELEASE: 2007/02/08: CIA-RDP82-00850R000200100009-9

large a modeling scale will not produce the desired scientific and economic effect -- the models turn out too expensive and unwieldy, even if they are quite exact. Too small a scale does not correctly reproduce reality, and measurements on a small model produce gross errors.

The biggest problems in the modeling of acoustic processes in shipbuilding are related to dissipative losses, since modeling is valid only if the losses are identical on the frequencies of the model and the original.

The correct setup of measurements under conditions of smaller linear dimensions and higher frequency requires the selection of instruments and techniques that correspond to the model frequency band: the audio and vibration receivers must be substantially smaller than the shortest acoustic wavelengths. They must not exert any influence on the manner in which an acoustic process takes place through their dissipative and sound-damping properties.

Electrical modeling of many acoustic processes, on the basis of the generality of the differential equations that describe acoustic propagation through structures and the flow of current in complicated electrical circuits, is also used successfully [13].

2.6. Determination of Reliability and Precision of Acoustic Measurements[1]

Before obtaining quantitative data for any acoustic measurements it is important to make sure of the reliability of the expected result and to estimate the anticipated precision. Otherwise gross errors may occur, and a collection of random variables that bear no relationship to the process being analyzed, measured or tested, may be accepted as a valid result.

A reliability check gives assurance that the metering channel receives precisely the acoustic parameters being analyzed, and not different types of interference (electrical induction, noises from a neighboring facility, etc.). Noteworthy among the various check methods is the procedure whereby the useful signal source is turned off, its power is attenuated with insulating screens and the distance between the radiator and receiver is changed. When the measurements are reliable the output signal of the receiving channel changes exactly in accordance with a change of the acoustic value.

A reliability evaluation must also include the characteristics of interference, i.e., readings of the metering channel in the absence of the signal to be analyzed.

The reliability of acoustic measurements also depends on the measurement procedure, which must correspond to the nature of the parameter to be

[1] I. I. Bogolepov contributed to the writing of this section.

APPROVED FOR RELEASE: 2007/02/08: CIA-RDP82-00850R000200100009-9

APPROVED FOR RELEASE: 2007/02/08: CIA-RDP82-00850R000200100009-9

measured. For instance, measurements of a fluctuating variable require some averaging in time; measurements of noise from a moving source with a stationary receiver require the selection of the correct measurement time and, if need be, consideration of the Doppler effect, etc.

Visual monitoring of a measured value by oscillograph is also very important, because it often helps to evaluate the nature of interference, which may be of both acoustic and electrical origin.

Measurement precision is determined in all cases by specific conditions.

Measurement precision is characterized by error ΔR, which expresses the difference between the true value R_0 and the measured value R of the parameter being measured:

$$\Delta R = R_0 - R. \tag{2.6.1}$$

The acoustic measurement errors of the typical acoustic channel can be represented as follows.

The general expressions for a measured acoustic pressure or vibration acceleration are of the form

$$p = \frac{u}{Mk(f)s(f)}, \quad \ddot{\xi} = \frac{u_1}{M_1 k_1(f) s_1(f)}, \tag{2.6.2}$$

where u, u_1 are readings on the scales of the voltage dividers and indicator; M, M_1 are the sensitivities of the receivers; k(f), $k_1(f)$ are the summary transadmittance of the metering channel; s(f), $s_1(f)$ are functions that characterize the influence of measurement conditions on the results (for instance, the influence of surrounding surfaces, how the vibration receivers are fastened, etc.).

The measurement error of u, u_1 on the scales of the instruments is determined by the class of the instruments and by how well they correspond to the nature of the measured signals (particularly during the recording of brief and fluctuating signals). The divider calibration error can be substantial. Therefore it is better to avoid switching the dividers during the measurement process. However, the error can be reduced to an acceptable level, if need be, by means of electrical calibration of the channel.

The error introduced by the instability of the transadmittance of the channel for k(f) and $k_1(f)$ depends on the quality of the power sources and on the character of heat transfer between the instruments and the environment. The measurement instruments must be turned on in advance for warmup for at least 30 min before the beginning of measurements to assure the proper thermal balance.

APPROVED FOR RELEASE: 2007/02/08: CIA-RDP82-00850R000200100009-9

APPROVED FOR RELEASE: 2007/02/08: CIA-RDP82-00850R000200100009-9

The calibration error (in terms of M and M_1) is usually specified in the technical documentation of the receiver along with calibration conditions -- temperature, pressure, orientation, etc. If calibration conditions do not correspond to measurement conditions appreciable errors can occur, since the sensitivity of many receivers depends on temperature, orientation, etc.

Errors attributed to the influence of measurement conditions, expressed in terms of s(t) and $s_1(t)$, are often the most serious, since they include the influence of diffraction and wave guide phenomena, reflections from the enclosure of the measurement space, the fastening of the receiver, etc.

The correct choice of distance r between the sound source and the measurement point is very important for high measurement precision; it is desirable that the measurements be done in the zone where the electric plane characteristic of the source is formed; $r > 2D^2/\lambda$, where D is the size of the radiator.

Acoustic measurement errors consist of the sum of systematic errors and random errors of the measured value.

Systematic errors are usually known before measurements begin. They are determined by standard procedures and are taken into account by incorporating the appropriate correction factors in the measurement results. It is desirable to use an acoustic reference to eliminate systematic errors [4]. To do this it is helpful to reduce the measurements to relative measurements, taken with one channel, when working out the measurement procedure.

Errors caused by random factors cannot be ascertained before measurements, even in individual measurements. They can be taken into consideration only by statistical processing of repeated measurements, and the larger the series of measurements the more complete the information about random errors.

Random error ΔR with a normal distribution and probability 2Φ(t) are connected by the relation

$$B(|\Delta R| < t\sigma_0) = 2\Phi(t), \qquad (2.6.3)$$

where σ_0 is the mean square deviation; $\Phi(t) = \frac{1}{\sqrt{2\pi}}\int_0^t e^{-\frac{v^2}{2}}dv$ is a Laplace function.

If R is measured n times and the result is averaged

$$R = \frac{1}{n}\sum_{i=1}^{n} R_i, \qquad (2.6.4)$$

APPROVED FOR RELEASE: 2007/02/08: CIA-RDP82-00850R000200100009-9

APPROVED FOR RELEASE: 2007/02/08: CIA-RDP82-00850R000200100009-9

then

$$B\left(|\Delta R|_n < t\frac{\sigma_0}{\sqrt{n}}\right) = 2\Phi(t). \tag{2.6.5}$$

To calculate the random error by formulas (2.6.3) and (2.6.5) it is necessary to know σ_0 -- the mean square deviation of the measured value.

The mean square deviation of random variable S, based on data of n samples, is

$$S = \sqrt{\frac{1}{n-1}\sum_{i=1}^{n}(R_i - R)^2}. \tag{2.6.6}$$

If the samples are taken from a normal group, then nS^2/σ_0^2 has a χ^2-distribution with k = n - 1 degrees of freedom. Here σ_0 is the desired mean square deviation.

The probability of the χ^2-distribution is calculated by the formula

$$B(\chi^2 > \chi_q^2) = \psi(\chi_q^2), \tag{2.6.7}$$

where

$$\psi(\chi_g^2) = \int_{\chi_g^2}^{\infty} \frac{1}{\Gamma\left(\frac{k}{2}\right)2^{k/2}} x^{k/2-1}e^{-x/2}dx;$$

$$\Gamma\left(\frac{k}{2}\right) = \int_0^{\infty} e^{-t}x^{k/2-1}dt.$$

Let us estimate σ_0 with the aid of the distribution probability

$$B\left(\sigma_0 < \frac{S\sqrt{n}}{\chi_g}\right) = \psi(x_g^2). \tag{2.6.8}$$

We use with probability $\psi(\chi_g^2)$, close to unity, the largest of the possible values of σ_0 as the desired mean square deviation (top estimate):

$$\tilde{\sigma}_0 = \frac{S\sqrt{n}}{\chi_g}. \tag{2.6.9}$$

If there are k > 30 degrees of freedom formula (2.6.8) may be simplified:

$$B\left(\sigma_0 < \frac{S\sqrt{2n}}{\sqrt{2k-1}-t}\right) \approx 0{,}5 + \Phi(t). \tag{2.6.10}$$

APPROVED FOR RELEASE: 2007/02/08: CIA-RDP82-00850R000200100009-9

APPROVED FOR RELEASE: 2007/02/08: CIA-RDP82-00850R000200100009-9

APPROVED FOR RELEASE: 2007/02/08: CIA-RDP82-00850R000200100009-9

APPROVED FOR RELEASE: 2007/02/08: CIA-RDP82-00850R000200100009-9

Consequently we obtain with a given probability, close to unity, the top estimate of the mean square deviation:

$$\tilde{\sigma}_0 = \frac{S\sqrt{2n}}{\sqrt{2n-3-t}}. \qquad (2.6.11)$$

Formulas (2.6.9) and (2.6.11) are the calculation relations for determining σ_0.

If the assumed probability is close to unity we obtain, by substituting $\tilde{\sigma}_0$ into formulas (2.6.3) and (2.6.5), the following calculation relations:

$$B(|\Delta R| < t\sigma_0) \approx 2\Phi(t); \qquad (2.6.12)$$

$$B\left(|\Delta R|_n < \frac{\tilde{\sigma}}{\sqrt{n}} \approx 2\Phi(t)\right), \qquad (2.6.13)$$

where

$$|\Delta R|_n = \left|R_0 - \frac{1}{n}\sum_{i=1}^{n} R_i\right|.$$

The approximately equal sign in formulas (2.6.12) and (2.6.13) appears in connection with the fact that not the true mean square deviation σ_0, but its top estimate $\tilde{\sigma}_0$, with a probability close to unity (0.99, for example), enters in formulas (2.6.3) and (2.6.5).

The limiting random measurement error, with a probability of about $2\Phi(t) = 0.9973$, is determined by the following formulas:

$$\Delta R = 3\tilde{\sigma}_0, \qquad (2.6.14)$$

$$\Delta R_N = \frac{3\sigma_0}{\sqrt{n}}. \qquad (2.6.15)$$

Sometimes it is worthwhile to perform statistical processing of the results of full-scale acoustic measurements in a range of small samples and confidence intervals [5].

2.7. Application of Electronic Digital Computers for Acoustic Measurements

Modern acoustic research requires that many measurements be taken at many points of a test subject under various conditions and in different operating modes. The required measurement operations are so voluminous that they cannot realistically be done manually. The entire research process must be automated, and this can be done with the large arsenal of computer technology -- electronic digital computers, which substantially improve precision, reliability and speed of data processing in all stages of experiments.

APPROVED FOR RELEASE: 2007/02/08: CIA-RDP82-00850R000200100009-9

APPROVED FOR RELEASE: 2007/02/08: CIA-RDP82-00850R000200100009-9

Modern computers are indistinguishable from acoustic instruments in terms of size and input power and do not require special operating conditions. However, problems of interface between computers and acoustic metering systems remain largely unsolved. The reason is the complexity of acoustic signals, their wide frequency range (from hertz to tens of megahertz), wide dynamic range (120-170 dB) and the varying character of signal elements that carry useful information.

For input into a computer signals must be of digital, and not of analog form. The existing analog-digital converters (ADC) cannot completely digitize compound acoustic signals. Additional conversion of analog signals must be accomplished so that the converted signals can be fed into a computer without changing the information that needs to be measured. Systems that transpose signals into a lower frequency range by means of magnetic recording and playback at different speeds (for instance, with the types 7001-7004 meter tape recorders, the "Siluet" video recording and processing machine [25], etc.).

Signals are often recorded in coded form on magnetic tape, perforated tape and punch cards and are then fed into a computer for calculation operations.

A digital computer completely automates the measurement process, including tuning, calibration of the instruments, recording and analysis of the results. Subjective readings are replaced with objective measurements and precision is improved. Processing time (for grouping and analysis) of the results is sharply reduced, which makes it possible to increase the volume of information to be processed by eliminating random errors and by reducing systematic errors (for instance by using a small step it is possible to refine the curve of a function).

The new opportunities opened by electronic digital computers for experimental research include the following:

real-time processing of results during the course of an experiment and forecasting of future data and planning of the future course of an experiment;

statistical processing of data during the course of an experiment and determination of distribution laws, histograms, etc;

metrologic evaluation of results with the exclusion of doubtful data by the signal-interference criterion and by the tolerable deviation from a series of measurements;

control of acoustic metering processes on the basis of an original program and of information obtained during the course of an experiment.

Examples of the last, most promising trend are: generation of a prescribed acoustic field in space by controlling the radiating, scattering and

APPROVED FOR RELEASE: 2007/02/08: CIA-RDP82-00850R000200100009-9

APPROVED FOR RELEASE: 2007/02/08: CIA-RDP82-00850R000200100009-9

absorbing elements; optimization of a measurement process by means of automatic selection of a parameter that indicates how analyzed processes are taking place (generation level, frequency measurement step, necessary number of repetition cycles) for achieving a prescribed precision, reliability and dependability of the results at the minimum time cost; automatic recognition and synthesis of acoustic specimens in application to random (sounds, speed, noises of the sea) and regular (diffraction, interference) acoustic processes.

Problems that stand in the way of the practical application of electronic digital computers in acoustics are connected with the development of interface systems for acoustic data input into the computer, the need for qualified service, maintenance and modernization of computers and time outlays for debugging programs.

Modern computer technology is characterized by the application of complexes of analog and digital systems that combine enormous capabilities in terms of the averaging of continuous processes, inherent to analog systems, with the flexibility and speed of digital technology, which provides an opportunity to build potent, easily tuned information metering systems [15].

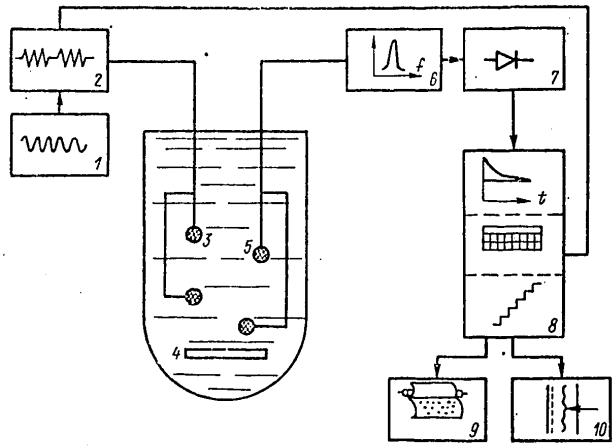

Figure 2.15. Schematic diagram of system for reverberation measurements with "Dnepr" electronic digital computer: 1 -- master oscillator; 2 -- pulse generator; 3 -- radiators; 4 -- specimen; 5 -- receiver; 6 -- filters; 7 -- video detector; 8 -- "Dnepr" computer; 9 -- digital printer; 10 -- level recorder.

Computers are being used extensively for the spectral and correlation analysis of compound signals. The 3347 spectrum analyzer [6] is a parallel-action spectrometer, connected to a small, but potent digital

APPROVED FOR RELEASE: 2007/02/08: CIA-RDP82-00850R000200100009-9

APPROVED FOR RELEASE: 2007/02/08: CIA-RDP82-00850R000200100009-9

computer, which performs all the necessary data processing. Programs have been developed for this system for measuring noise, for calculating loudness and for spatial averaging.

A multichannel analog machine for measuring vibroacoustic parameters, intended for preprocessing of data prior to input into the computer, was developed under B. D. Tartakovskiy's supervision [18].

Yu. M. Yelokhin and A. Ye. Kolesnikov developed a system for measuring the characteristics of the trailing edge of a signal in a reverberating chamber with the aid of the "Dnepr" computer (Figure 2.15) [10].

The driving signal, in the form of a long pulse, is generated by an analog system, but the amplitude of the pulse is set by a digital computer on the basis of the highest level that is acceptable for linear operation. The envelope of the trailing edge, which is subjected to quantization, is fed into a digital computer. The computer determines the working part, or the signal is much stronger than the interference, and then, by the least squares procedure, finds the exponent that characterizes the curve of the trailing edge. The measurement operation is repeated many times, and statistical characteristics are determined. The computer automatically establishes the number of necessary measurements n for achieving a given mean square error ε:

[cp=me]

$$n = \left(\frac{\beta_{cp}}{s}\frac{t_m}{\varepsilon}\right)^{1/2}, \qquad (2.7.1)$$

where β_{me} is the mean exponent for 10 measurements; s is the mean square deviation of β_{me}; t_m is Student's coefficient.

Several measurement cycles are completed within a selected band for finding the desired mean exponent in terms of frequency, and the result is averaged and printed out as a function of frequency. The loss coefficients of structures, the absorption coefficient of materials, etc., can be found with the aid of the described system.

Computer optimization of an experiment consists in the correct choice of measured data by the signal-noise test, restriction of the number of measurements within the prescribed accuracy (since redundant information greatly increases measurement time) and culling out of the most time-consuming processing algorithms. Automation of the frequency step (or other arguments) consists in the analysis and forecasting of the increment of a measured function as a function of frequency. For example, a digital computer estimates three consecutive previously plotted functions, predicts the next value on the basis of Legendre extrapolation polynomials and, in consideration of prescribed precision, determines the increment of the argument, i.e., of frequency. The application of this principle shows that the density of measurement points near the extremum is substantially higher than on other frequencies [10, 18].

APPROVED FOR RELEASE: 2007/02/08: CIA-RDP82-00850R000200100009-9

APPROVED FOR RELEASE: 2007/02/08: CIA-RDP82-00850R000200100009-9

BIBLIOGRAPHY

1. "Aviatsionnaya Akustika" [Aviation Acoustics], edited by A. G. Munin and V. Ye. Kvitka, Moscow, Mashinostroyeniye, 1973.

2. Blinova, L. P., A. Ye. Kolesnikov and L. B. Langans, "Akusticheskiye Izmereniya" [Acoustic Measurements], Moscow, Izd-vo standartov, 1971.

3. Bobber, R., "Gidroakusticheskiye Izmereniya" [Hydroacoustic Measurements], Moscow, Mir, 1974.

4. Bogolepov, I. I., "Standard of Sound Insulation," in the book "Voprosy Sudostroyeniya" [Problems of Shipbuilding], No 5, Leningrad, 1974, pp 17-19.

5. Bogolepov, I. I. and V. F. Okhrimenko, "Statistical Processing of Full-Scale Acoustic Measurement Results," in the book "Voprosy Sudostroyeniya," No 5, Leningrad, 1974, pp 24-28.

6. Brokh, E., "Primeneniye Apparatury Firmy Bryul' i K"yer dlya Izmereniy Akusticheskogo Shuma" [Application of Bryul' and K"yer Instruments for Measuring Acoustic Noise], Copenhagen, Izd-vo Bryul' i K"yer, 1971.

7. Brokh, E., "Izmereniye Mekhanicheskikh Kolebaniy i Udarov" [Measurement of Mechanical Vibrations and Impacts], Copenhagen, Izd-vo Bryul' i K"yer, 1973.

8. Glozman, I. A., "P'yezokeramika" [Piezoceramics], Moscow, Energiya, 1972.

9. Golenkov, A. N. and L. Ye. Pavlov, "Absolute Calibration of Metering Hydrophones in Audio Frequency Range," IZMERITEL'NAYA TEKHNIKA [Measurement Technology], 1967, No 5, pp 123-128.

10. Yelokhin, Yu. M. and A. Ye. Kolesnikov, "Application of Digital Computer for Calibrating Audio Receivers by Reciprocity Principle," "Sb. Dokladov VII Vsesoyuznoy Akusticheskoy Konferentsii" [Collected Reports of Seventh All-Union Acoustics Conference], Leningrad, Izd-vo LKI, 1973, pp 208-213.

11. Iorish, Yu. Ya., "Vibrometriya" [Vibrometry], Moscow, Mashgiz, 1963.

12. Klyukin, I. I., "Bor'ba s Shumom i Vibratsiyey na Sudakh" [Control of Noises and Vibrations on Ships], 2nd edition, Leningrad, Sudostroyeniye, 1971.

13. Klyukin, I. I. and A. Ye. Kolesnikov "Akusticheskiye Izmereniya v Sudostroyenii" [Acoustic Measurements in Shipbuilding], 2nd edition, Leningrad, Sudostroyeniye, 1968.

APPROVED FOR RELEASE: 2007/02/08: CIA-RDP82-00850R000200100009-9

APPROVED FOR RELEASE: 2007/02/08: CIA-RDP82-00850R000200100009-9

14. Kolesnikov, A. Ye., "Calibration of Vibration Receivers by Reciprocity Principle," IZMERITEL'NAYA TEKHNIKA, 1962, No 11, pp 53-56.

15. Kolesnikov, A. Ye., "Application of Electronic Computer Technology in Acoustic Measurements," "Sb. Dokladov VII Vsesoyuznoy Akusticheskoy Konferentsii," Leningrad, Izd-vo LKI, 1972, pp 25-31.

16. Kolesnikov, A. Ye. and Ye. S. Sokolova, "Calibration of Converters by Measuring Their Electric Impedance," in the book: "Izvestiya LETI" [News of Leningrad Electrotechnical Institute imeni V. I. Ul'yanov (Lenin)], 1970, No 89, pp 175-182.

17. Kolesnikov, A. Ye., "Determination of Audio Receiver Sensitivity," IZMERITEL'NAYA TEKHNIKA, 1971, No 8, pp 71-73.

18. Lyubashevskiy, G. S. and E. D. Tartakovskiy, "Control of Vibroacoustic Measurements by Digital Computer," AKUSTICHESKIY ZHURNAL [Acoustics Journal], 1970, Vol 16, No 3, pp 476-478.

19. Lyubashevskiy, G. S., B. D. Tartakovskiy and V. E. Frishberg, "System for Automated Measurements of Real Noises and Vibrations," in the book: "Kiberneticheskaya Diagnostika Mekhanicheskikh Sistem po Vibro-akusticheskim Protsessam" [Cybernetic Diagnosis of Mechanical Systems by Vibroacoustic Processes], Kaunas, Izd-vo KPI, 1972, pp 6-9.

20. Martynov, V. A. and Yu. I. Selikhov, "Panoramnyye Priyemniki i Analizatory Spektra" [Panorama Receivers and Signal Analyzers], Moscow, Sovetskoye radio, 1964.

21. Myasnikov, L. L., Ye. N. Myasnikova and Ya. I. Shchuchinskiy, "Novyye Metody Izmereniy v Podvodnoy Akustike i Radiotekhnike" [New Measurement Techniques in Submarine Acoustics and Electronics], Leningrad, Sudostroyeniye, 1974.

22. Novikov, A. K., "Korrelyatsionnyye Izmereniya v Korabel'noy Akustike" [Correlation Measurements in Ship Acoustics], Leningrad, Sudostroyeniye, 1971.

23. Novikov, A. K. and V. M. Strelkova, "Analog-Digital Correlator for Acoustic Measurements," "Sb. Dokladov VII Vsesoyuznoy Akusticheskoy Konferentsii," Leningrad, Izd. LKI, 1973, pp 44-46.

24. Osipov, G. L., D. Z. Lopashov, et al, "Izmereniye Shuma Mashin i Oborudovaniya" [Measurement of Noise of Machines and Equipment], Moscow, Izd-vo standartov, 1968.

APPROVED FOR RELEASE: 2007/02/08: CIA-RDP82-00850R000200100009-9

APPROVED FOR RELEASE: 2007/02/08: CIA-RDP82-00850R000200100009-9

25. Petrenko, A. I., "Preobrazovaniye Grafikov v Elektricheskiye Signaly" [Conversion of Graphs to Electrical Signals], Kiev, Gostekhizdat USSR, 1964.

26. Popkov, V. I., "Vibroakusticheskaya Diagnostiki i Snizheniye Vibroaktivnosti Sudovykh Mekhanizmov" [Vibroacoustic Diagnosis and Reduction of Vibration Activity of Ship Machinery], Leningrad, Sudostroyeniye, 1974.

27. Turbovich, I. T., "On Dynamic Frequency Characteristics," RADIOTEKHNIKA [Radio Engineering], 1957, No 11, pp 94-97.

28. "Ukazateli Rekomendatsiy Mezhdunarodnoy Organizatsii po Standartizatsii (ISO)" [Indices of Recommendations of International Standardization Organization (ISO)], Moscow, Izd-vo standartov, 1974.

29. Kelvin, R. L. and J. C. Snowdon, "Driving Point Impedance of Cantilever Beams," JASA, 47, No 1, pt. 2, 1970, pp 220-228.

APPROVED FOR RELEASE: 2007/02/08: CIA-RDP82-00850R000200100009-9

APPROVED FOR RELEASE: 2007/02/08: CIA-RDP82-00850R000200100009-9

CHAPTER 3. GENERAL CHARACTERISTICS OF MACHINERY AS VIBRATION AND NOISE SOURCES

3.1. Induced Mechanical Vibrations

The great diversity of dynamic forces that occur in operating assemblies of machines and mechanisms, which produce vibrations and audible noise, can be classified into three groups of forces in relation to their physical nature.

The first group includes forces of mechanical origin -- produced by residual disbalances of rotors, by machining defects of rotating parts (journals of rotors, half-couplings, etc.), of bearings and their parts, by the asymmetric rigidities of rotors in the principal bending planes, by technological and operational defects in drive lines (acentricity, bending and sagging of shafts, dynamic misalignments), by perturbations from impacts of parts in piston and crank mechanisms, etc.

The second group includes forces of electromagnetic origin, produced by magnetic fields that are basically variable in time and in space. In addition to the main working magnetic field, fields from an unevenly saturated magnetic conductor, asymmetric power voltage, asymmetric magnetic circuit, etc., occur in electrical machinery.

The third group includes forces of aerodynamic and hydrodynamic origin in pumps, turbines, compressors and blowers.

One of the basic tasks of the designers and planners of quiet machinery is to establish the nature of the power action in mechanisms, the relationship between vibration forces and the energy parameters of the mechanism, kinematics of the motion of elements in working assemblies. However, the physics of the formation of noises and vibrations is extremely complicated. The exact theoretical relations among the energy and vibroacoustic parameters have not yet been established, and calculation procedures for determining forces that act in the vicinity of working assemblies have not been found for most mechanisms and processes. Therefore a sufficiently formal theory of the vibration activity of machines and mechanisms, with

APPROVED FOR RELEASE: 2007/02/08: CIA-RDP82-00850R000200100009-9

APPROVED FOR RELEASE: 2007/02/08: CIA-RDP82-00850R000200100009-9

which it would be possible to work with actually determined (experimentally or theoretically) parameters that are general for different classes of mechanisms, needs to be formulated.

A linear harmonic vibration process in the parts of a mechanism is examined below. The mechanism, shock absorbers (vibration-damping structures) and foundation are assumed to be linear discrete mechanical systems with a finite number of contact points. The spatial position of contact points is determined by six coordinates: three reciprocating displacements of the center and three rotary displacements around the axes passing through the center. The component of the displacement of the n-th contact point on frequency ω is denoted through $q_i^n(\omega)$, where i = 1, 2, 3, 4, 5, 6 are the numbers of the coordinates. Generalized forces $Q_i^n(\omega)$ correspond to the generalized coordinates.

The source action in a mechanism is assumed to be equivalent to the action of harmonic force ${}^sQ_r(\omega)$, directed along vector r and applied at point "s." The vibration generated in the region of application of the force propagates through the structures of the mechanism, bearing and nonbearing connections. In the vicinity of the n-th contact point between the mechanism and bearing and nonbearing connections is produced in the i-th direction the vibration velocity

[и=s]
$$\dot{q}_i^n(\omega) = {}^uQ_r(\omega)\,{}^uM_{ri}^n(\omega), \tag{3.1.1}$$

where ${}^sM_{ri}^n(\omega)$ is the transient pliancy of the mechanism-bearing and nonbearing connections system between the point of application of the force and the n-th point of contact between the mechanism and connections, which is a function of the characteristics of the structures of a mechanism itself and of the impedances of bearing and nonbearing couplings.

The vibration velocity of a free mechanism (installed on zero impedance bearing surfaces) is

$$\dot{q}_{i0}^n(\omega) = {}^uQ_r(\omega)\,{}^uM_{ri0}^n(\omega).$$

In the case of a single-point contact between the mechanism and bearing surfaces and unidirectional vibrations n = 1 equation (3.1.1) acquires the form

$$\dot{q}_i(\omega) = {}^uQ_r(\omega)\,{}^uM'_{ri0}(\omega) + Q'_i(\omega)\,M''_{ii0}(\omega), \tag{3.1.2}$$

where $M''_{ii0}(\omega)$ is the point pliancy of the structures of the free mechanism at the point of contact with the bearing surface; $Q'_i(\omega)$ is the force of interaction between the mechanism and bearing surface

APPROVED FOR RELEASE: 2007/02/08: CIA-RDP82-00850R000200100009-9

APPROVED FOR RELEASE: 2007/02/08: CIA-RDP82-00850R000200100009-9

[aф=af]

$$Q_i'(\omega) = \dot{q}_i(\omega) \cdot Z''_{ii\ af\phi}(\omega),$$

where $Z''_{ii\ af}(\omega)$ is the point impedance of the bearing (of the shock absorber-foundation system in particular). When there is a finite number of contact points, in consideration of the six components of vibration,

$$\dot{q}_i^n(\omega) = {}^{H}M_{ri0}^n(\omega)\,{}^{H}Q_r(\omega) + \sum_{k=1}^{m}\sum_{j=1}^{6} Q_j^k(\omega)\, M_{ji0}^{kn}(\omega), \qquad (3.1.3)$$

where m is the number of points of contact between the mechanism and bearing and nonbearing connections; $M_{ji0}^{kn}(\omega)$ is the pliancy of the structures of the free mechanism between the contact surfaces with the subscripts k and n. Force $Q_j^k(\omega)$ is determined by the expression

$$Q_j^k(\omega) = -\sum_{p=1}^{m}\sum_{\nu=1}^{6} \dot{q}_\nu^p(\omega) \cdot Z_{\nu j\ a\phi}^{pk}(\omega), \qquad (3.1.4)$$

where

$$Z_{\nu j\ a\phi}^{pk}(\omega) = \left.\frac{Q_j^k(\omega)}{\dot{q}_{\nu a}^p(\omega)}\right|_{\substack{\dot{q}_{ia}^n(\omega) = 0,\ n \neq p \\ \dot{q}_{ia}^p(\omega) \neq 0,\ i \neq \nu}}$$

is the transient mechanical impedance of the shock absorber-foundation system with the corresponding boundary conditions.

In consideration of equation (3.1.4) $\dot{q}_i^n(\omega)$ can be determined from the equation system

$$\dot{q}_i^n(\omega) + \sum_{k=1}^{m}\sum_{j=1}^{6} M_{ji0}^{kn} \cdot \sum_{p=1}^{m}\sum_{\nu=1}^{6} \dot{q}_\nu^p(\omega) \cdot Z_{\nu i\ a\phi}^{pk}(\omega) = {}^{H}Q_r(\omega)\,{}^{H}M_{ri0}^n(\omega). \qquad (3.1.5)$$

Pliancies ${}^{S}M_{ri0}^n(\omega)$ and $M_{ji0}^{kn}(\omega)$, characterizing the properties of the structures of a mechanism, can be determined experimentally [4]. When ${}^{S}M_{ri0}^n(\omega)$, $M_{ji0}^{kn}(\omega)$ and the impedances of bearing and nonbearing connections $Z_{\nu j\ af}^{pk}(\omega)$ are known the vibration of a mechanism is determined by 6m equations (3.1.5).

APPROVED FOR RELEASE: 2007/02/08: CIA-RDP82-00850R000200100009-9

APPROVED FOR RELEASE: 2007/02/08: CIA-RDP82-00850R000200100009-9

If in the working parts of a mechanism there are several forces $\{{}^{s}Q_{r}(\omega)\}$, $s = 1, 2, \ldots, m^{s}$ is the number of points of application of the forces; $r = 1, 2, \ldots, 6$, then equation system (3.1.5) is changed to the form

$$\dot{q}_i^n(\omega) + \sum_{k=1}^{m}\sum_{j=1}^{n} M_{ji0}^{kn}(\omega)\cdot\sum_{p=1}^{m}\sum_{\nu=1}^{6}\dot{q}_\nu^p(w)\,Z_{\nu i\,a\phi}^{pk}(\omega) = \sum_{\text{н}=1}^{m^{\text{н}}}\sum_{r=1}^{6}{}^{\text{н}}Q_r(\omega)\,{}^{\text{н}}M_{ri0}^n(\omega). \qquad (3.1.6)$$

When several vibration forces are at work the phase and amplitude relations among the forces must be known in order to compute the vibrations of the bearing surfaces of the mechanism and the transient pliancy of its structures [5].

The above relations among forces in the sources and vibration velocities of a mechanism may be represented in more compact matrix form. Set 6m of vibration velocities forms the vector (column matrix) of vibration velocity:

$$\bar{\dot{q}} = \begin{bmatrix} \dot{q}_1^1(\omega) \\ \dot{q}_2^1(\omega) \\ \vdots \\ \dot{q}_6^1(\omega) \\ \dot{q}_1^2(\omega) \\ \vdots \\ \dot{q}_6^m(\omega) \end{bmatrix}.$$

Vectors of forces ${}^{s}\bar{Q}$ and $\bar{Q}$ are formed in like manner.

The combination of pliancies that characterize the inertial rigidity properties of the structures of mechanisms, from the working parts to the bearing surfaces, forms the pliancy matrix

$${}^{\text{н}}\bar{M}_0 = \begin{bmatrix} {}^{1}\bar{M}_0^1 & {}^{1}\bar{M}_0^2 & \cdots & {}^{1}\bar{M}_0^m \\ {}^{2}\bar{M}_0^1 & {}^{2}\bar{M}_0^2 & \cdots & {}^{2}\bar{M}_0^m \\ \cdots & \cdots & \cdots & \cdots \\ {}^{m^{\text{н}}}\bar{M}_0^1 & {}^{m^{\text{н}}}\bar{M}_0^2 & \cdots & {}^{m^{\text{н}}}\bar{M}_0^m \end{bmatrix},$$

where ${}^{s}\bar{M}_0^n$ is a sixth-order quadratic matrix:

$${}^{\text{н}}\bar{M}_0^n = \begin{bmatrix} {}^{\text{н}}M_{110}^n(\omega) & {}^{\text{н}}M_{120}^n(\omega) & \cdots & {}^{\text{н}}M_{160}^n(\omega) \\ {}^{\text{н}}M_{210}^n(\omega) & {}^{\text{н}}M_{220}^n(\omega) & \cdots & {}^{\text{н}}M_{260}^n(\omega) \\ \cdots & \cdots & \cdots & \cdots \\ {}^{\text{н}}M_{610}^n(\omega) & {}^{\text{н}}M_{620}^n(\omega) & \cdots & {}^{\text{н}}M_{660}^n(\omega) \end{bmatrix},$$

APPROVED FOR RELEASE: 2007/02/08: CIA-RDP82-00850R000200100009-9

APPROVED FOR RELEASE: 2007/02/08: CIA-RDP82-00850R000200100009-9

which expresses the relations among the components of force, acting at point "s" of the source, and the vibration velocity at the n-th bearing (or nonbearing) point of the surface of the mechanism.

The pliancy matrix of the structures of a mechanism in the vicinity of bearing and nonbearing connections $\overline{M}_0$ and the matrix of impedances of bearing and nonbearing connections $\overline{Z}_{af}$ are constructed in like manner.

The matrix equation of the relation between source forces and vibration levels of a mechanism is

$$\overline{\dot{q}} + \overline{M}_0 \overline{Q} = {}^{n}\overline{M}_0{}^{n}\overline{Q}. \tag{3.1.7}$$

Considering that $\overline{Q} = \overline{Z}_{af}\overline{\dot{q}}$, we obtain

$$\overline{\dot{q}} = [\overline{E} + \overline{M}_0 \overline{Z}_{a\phi}]^{-1\,n}\overline{M}^{0\,n}\overline{Q}, \tag{3.1.8}$$

where $\overline{E}$ is the unit matrix.

Matrix equations (3.1.8), which describe the dynamics of a mechanism with a harmonic vibration process, are general relations for all classes of mechanisms, irrespective of the nature of the vibration forces and of design execution. Here all the characteristics of the dynamic properties of mechanisms and of the inertial rigidity properties of the structures of mechanisms and of bearing and nonbearing connections, entering in the equation, can be found experimentally [4].

When determining the effectiveness of vibration damping and the causes of resonance phenomena in the vicinity of points of contact between a mechanism and shock-absorbing elements, and when calculating the vibrations of mechanisms, moving from some bearing surfaces to others, there is no need to consider features of the interaction of the forces that arise in moving parts with the structures of a mechanism. It is important to determine how much the vibration of mechanisms changes when the applied forces and mechanical impedances of the structures of mechanisms remain constant, and only the characteristics of bearing and nonbearing connections are changed. Techniques that do not call for a knowledge of vibration forces in working parts and of transient pliancies between the source and bearing and nonbearing connections, may be used for solving questions of this kind. Specifically, the matrix of forces, reduced to the fasteners between a mechanism and bearing and nonbearing connections, may be introduced in the examination:

$$\overline{Q}_0 = \overline{M}_0^{-1\,n}\overline{M}_0{}^{n}\overline{Q}.$$

In consideration of this equation (3.1.7) acquires the form

$$\overline{\dot{q}} = \overline{M}_0 [\overline{Q}_0 - \overline{Q}] = \overline{M}_0 [\overline{Q}_0 - \overline{Z}_{a\phi}\overline{\dot{q}}], \tag{3.1.9}$$

APPROVED FOR RELEASE: 2007/02/08: CIA-RDP82-00850R000200100009-9

APPROVED FOR RELEASE: 2007/02/08: CIA-RDP82-00850R000200100009-9

whence the velocity matrix is written as

[aϕ=af] $$\bar{\dot{q}} = [\bar{E} + \bar{M}_0 Z_{a\phi}]^{-1} \bar{M}_0 \bar{Q}_0. \quad (3.1.10)$$

A vibration process may also be described in terms of mechanical impedances with the aid of the impedance matrix of a mechanism in the vicinity of contact points with bearing and nonbearing connections: $\bar{Z}_0 = \bar{M}_0^{-1}$. Equation (3.1.10) in this case is converted to

$$\bar{Q}_0 = \bar{Z}_0 \bar{\dot{q}} + \bar{Q} = [\bar{Z}_0 + \bar{Z}_{a\phi}] \bar{\dot{q}}. \quad (3.1.11)$$

This equation has the following physical meaning: vibration forces $\bar{Q}_0$, produced by a mechanism, are spent on overcoming impedance $\bar{Z}_0$ of a mechanism itself and impedance $\bar{Z}_{af}$ of bearing and nonbearing connections.

If the mechanism is in the so-called "free state" ($\bar{Z}_{af} = 0$) its bearing surface velocity is given by the formula

$$\bar{\dot{q}}_0 = \bar{Z}_0^{-1} \bar{Q}_0.$$

If the mechanism is installed on structures with infinite mechanical impedance (in practice it is sufficient to maintain $|\bar{Z}_{af}| >> |\bar{Z}_0|$), then forces $\bar{Q}$ are equal to forces $\bar{Q}_0$.

Thus, a mechanism as a vibration source may be described not only through perturbations in the vicinity of moving parts in combination with intrinsic input and transient impedances, or pliancies. The following parameters may also be used as characteristics:

1. Reduced forces $\bar{Q}_0$, which convey the physical meaning of forces exerted by a mechanism on bearing and nonbearing connections with infinite mechanical impedance, in combination with intrinsic pliancies $\bar{M}_0$ or impedances $\bar{Z}_0$ of structures of mechanisms in the vicinities of bearing and nonbearing connections.

2. Vibration velocity of bearing surfaces of a mechanism in the free state $\bar{\dot{q}}$ in combination with intrinsic pliancies $\bar{M}_0$ or impedances $\bar{Z}_0$ of a mechanism.

According to studies of the spectral characteristics of vibration processes, the vibration forces and vibration velocities in real mechanisms are characterized by a continuous spectrum, in addition to discrete components, particularly in the intermediate and high-frequency ranges. Analyses of the time and correlation characteristics of vibration processes necessitate

APPROVED FOR RELEASE: 2007/02/08: CIA-RDP82-00850R000200100009-9

APPROVED FOR RELEASE: 2007/02/08: CIA-RDP82-00850R000200100009-9

examination of random vibrations of mechanisms, and random vibrations are stationary in most cases.

To the forces that occur in the moving parts of mechanisms, as functions of time in the frequency range, correspond the energy spectral densities of a force, forming the corresponding vector (or column matrix):

[и=s]

$$\overline{S}\left({}^{\text{и}}Q, {}^{\text{и}}Q\right) = \begin{bmatrix} S\left({}^{\text{и}}Q_1^1, {}^{\text{и}}Q_1^1\right) \\ S\left({}^{\text{и}}Q_2^1, {}^{\text{и}}Q_2^1\right) \\ \cdots\cdots \\ S\left({}^{\text{и}}Q_6^1, {}^{\text{и}}Q_6^1\right) \\ S\left({}^{\text{и}}Q_1^2, {}^{\text{и}}Q_1^2\right) \\ \cdots\cdots \\ S\left({}^{\text{и}}Q_6^{m\text{и}}, {}^{\text{и}}Q_6^{m\text{и}}\right) \end{bmatrix},$$

where

$$S\left({}^{\text{и}}Q_r^n, {}^{\text{и}}Q_r^n\right) = \lim_{\Delta\omega\to 0} \lim_{T\to\infty} \frac{1}{\Delta\omega T} \int_0^T \left[{}^{\text{и}}Q_r^n(t, \omega, \Delta\omega)\right]^2 dt,$$

and ${}^{s}Q_r^n(t, \omega, \Delta\omega)$ are components of force ${}^{s}Q_r^n$ as functions of time and lying in the frequency range $\left[\omega - \frac{\Delta\omega}{2}, \omega + \frac{\Delta\omega}{2}\right]$.

Vectors of energy spectral densities $\vec{S}(Q, Q)$ of force and $\vec{S}(\dot{q}, \dot{q})$ of velocity are determined in like manner.

However, in order to construct the equations of the dynamics of a mechanism with a random stationary vibration process it is necessary to use more than just the energy spectral densities. If, during an examination of harmonic vibrations in linear systems, information is available, for example, on the phase relation between velocities (or forces) in the i-th and k-th and in the i-th and m-th points, then the phase relation between velocities (or forces) at the k-th and m-th points will be determined uniquely, i.e., the process will be completely described by the combined amplitudes of velocities and forces. In the case of a random stationary vibration process in linear systems it is necessary to know both the energy spectral densities of the forces and velocities, and the relative spectral densities of forces, the relative spectral densities of velocities and the relative spectral densities of forces and velocities. The matrix of the relative spectral densities of forces that occur in moving parts of mechanisms is

APPROVED FOR RELEASE: 2007/02/08: CIA-RDP82-00850R000200100009-9

APPROVED FOR RELEASE: 2007/02/08: CIA-RDP82-00850R000200100009-9

$$\overline{S}({}^{\text{н}}Q,\ {}^{\text{н}}Q) = \begin{bmatrix} S({}^{\text{н}}Q_1^1,\ {}^{\text{н}}Q_1^1) & S({}^{\text{н}}Q_1^1,\ {}^{\text{н}}Q_2^1) & \dots & S({}^{\text{н}}Q_1^1,\ {}^{\text{н}}Q_6^1) & \dots & S({}^{\text{н}}Q_1^1,\ {}^{\text{н}}Q_1^2) & \dots & S({}^{\text{н}}Q_1^1,\ {}^{\text{н}}Q_6^{m\text{н}}) \\ S({}^{\text{н}}Q_2^1,\ {}^{\text{н}}Q_1^1) & S({}^{\text{н}}Q_2^1,\ {}^{\text{н}}Q_2^1) & \dots & S({}^{\text{н}}Q_2^1,\ {}^{\text{н}}Q_6^1) & \dots & S({}^{\text{н}}Q_2^1,\ {}^{\text{н}}Q_1^2) & \dots & S({}^{\text{н}}Q_2^1,\ {}^{\text{н}}Q_6^{m\text{н}}) \\ \dots & \dots & \dots & \dots & \dots & \dots & \dots & \dots \\ S({}^{\text{н}}Q_6^1,\ {}^{\text{н}}Q_1^1) & S({}^{\text{н}}Q_6^1,\ {}^{\text{н}}Q_2^1) & \dots & S({}^{\text{н}}Q_6^1,\ {}^{\text{н}}Q_6^1) & \dots & S({}^{\text{н}}Q_6^1,\ {}^{\text{н}}Q_1^2) & \dots & S({}^{\text{н}}Q^1,\ {}^{\text{н}}Q_6^{m\text{н}}) \\ \dots & \dots & \dots & \dots & \dots & \dots & \dots & \dots \\ S({}^{\text{н}}Q_6^{m\text{н}},\ {}^{\text{н}}Q_1^1) & S({}^{\text{н}}Q_6^{m\text{н}},\ {}^{\text{н}}Q_2^1) & \dots & S({}^{\text{н}}Q_6^{m\text{н}},\ {}^{\text{н}}Q_6^1) & \dots & S({}^{\text{н}}Q_6^{m\text{н}},\ {}^{\text{н}}Q_1^2) & \dots & S({}^{\text{н}}Q_6^{m\text{н}},\ {}^{\text{н}}Q_6^{m\text{н}}) \end{bmatrix}.$$

Matrices of the relative spectral densities of velocities $\overline{S}(\dot{q},\ \dot{q})$ and of forces $\overline{S}(Q,\ Q)$, $\overline{S}({}^{S}Q,\ Q)$ are constructed in like fashion.

Equations analogous to (3.1.7) and (3.1.8) and characterizing random stationary vibrations of a mechanism are of the form

$$\overline{S}(\dot{q},\ \dot{q}) = {}^{\text{н}}\overline{M}_0\overline{S}({}^{\text{н}}Q,\ {}^{\text{н}}Q)\,{}^{\text{н}}\overline{M}_0^{*\prime} - {}^{\text{н}}\overline{M}_0\overline{S}({}^{\text{н}}Q,\ Q)\,\overline{M}_0^{*\prime} - \\ - \overline{M}_0\overline{S}(Q,\ {}^{\text{н}}Q)\,{}^{\text{н}}\overline{M}_0^{*\prime} + \overline{M}_0\overline{S}(Q,\ Q)\,\overline{M}_0^{*\prime}; \qquad (3.1.12)$$

$$\overline{S}(\dot{q},\ \dot{q}) = [\overline{E} + \overline{M}_0\overline{Z}_{\text{аф}}]^{-1}\,{}^{\text{н}}\overline{M}_0\overline{S}({}^{\text{н}}Q,\ {}^{\text{н}}Q)\,[\overline{E} + \overline{M}_0\overline{Z}_{\text{аф}}]^{-1*\prime}\,{}^{\text{н}}\overline{M}_0^{*}. \qquad (3.1.13)$$

Thus, if the inertial rigidity characteristics of a mechanism and of a bearing structure are known, then it is possible, on the basis of prescribed energy and relative spectral densities of forces in moving parts, to determine all parameters of a random stationary vibration process of a mechanism.

The combined mechanical impedances and pliancies, determined when a system is in the state of stationary sinusoidal vibrations, or through the spectral densities of force and kinematic processes in the case of stationary random vibrations, enter in the equations of vibrations of a mechanism. The structures of mechanisms on intermediate and high frequencies have about the same resonances and a larger number of points of contact with bearing and nonbearing connections. In this connection the use of the above equations for calculating induced vibration in the mechanisms can experience considerable technical and computational difficulties. The requirements on the points of measurement of the combined mechanical impedances and pliancies turn out to be exceedingly rigid.

The calculation is simplified when the mechanical impedances, determined as combined coefficients in the passband of the analyzing filter by the formulas

APPROVED FOR RELEASE: 2007/02/08: CIA-RDP82-00850R000200100009-9

APPROVED FOR RELEASE: 2007/02/08: CIA-RDP82-00850R000200100009-9

[∃ϕ=ef]

$$
\begin{aligned}
|Z_{ii}^{nn}(\Delta\omega)| &= \frac{Q_{i\,\exists\phi}^{n}(\Delta\omega)}{\dot{q}_{i\,\exists\phi}^{n}(\Delta\omega)},\\
\mathrm{Re}Z_{ii}^{nn}(\Delta\omega) &= \frac{Q_{i\,\exists\phi}^{n}(\Delta\omega)}{\dot{q}_{i\,\exists\phi}^{n}(\Delta\omega)}\mathrm{Re}R_{Q\dot{q}}(\Delta\omega),\\
\mathrm{Im}Z_{ii}^{nn}(\Delta\omega) &= \frac{Q_{i\,\exists\phi}^{n}(\Delta\omega)}{\dot{q}_{i\,\exists\phi}^{n}(\Delta\omega)}\mathrm{Im}R_{Q\dot{q}}(\Delta\omega),
\end{aligned}
\qquad (3.1.14)
$$

where Re $R_{Q\dot{q}}(\Delta\omega)$ and Im $R_{Q\dot{q}}(\Delta\omega)$ are the real and imaginary parts of the correlation coefficient between force $Q_i^n(\Delta\omega)$ and vibration velocity $\dot{q}_i^n(\Delta\omega)$ in frequency band $\Delta\omega$, are used in the equations presented above.

The impedance in the frequency band should be determined when the mechanism or bearing and nonbearing structures are acted upon by the forces of a stationary random process, analogous to the character of the vibration process of a moving mechanism in the examined frequency band.

By definition Re $Z(\Delta\omega)$ and Im $Z(\Delta\omega)$ are the coefficients of proportionality between the squared vibration velocity of a point on an analyzed mechanism or of a bearing and nonbearing structure, and the real and imaginary parts of the vibration power, radiated by the action of the forces on that part. However, the representation of impedance in the frequency band as a combined parameter and its utilization for calculating the vibrations of a mechanism are impossible without errors, due to the difference of the spectra of a real working mechanism and of a vibrator during artificial determination of impedance in the frequency band.

An analysis [4] shows that when the parameters of impedances or pliancies in an octave or narrower frequency band are used the relative errors are values of not higher than the second order of smallness. Thus, the combined impedances in the frequency band may be used with dependability in these cases.

Up until now mechanisms and connecting bearing and nonbearing couplings have been examined as discrete linear mechanical systems with a finite number of points of contact, characterized by six-component vectors of dynamic forces and vibration velocities. Vibration processes in such systems, harmonic and random stationary, are described by matrix equations with coefficients that represent a combination of input and transient mechanical impedances or pliancies. Here it does not matter much in what terms a description is presented. Impedance matrices are the inverse of pliancy matrices.

During the solution of some problems, for example calculation of the vibration energy flux radiated by a mechanism in flange contact with bearing surfaces, analysis of working processes in certain mechanisms, calculation of pipe vibrations due to oscillations of the medium, determination of the

APPROVED FOR RELEASE: 2007/02/08: CIA-RDP82-00850R000200100009-9

APPROVED FOR RELEASE: 2007/02/08: CIA-RDP82-00850R000200100009-9

radiation of atmospheric noise by mechanisms, etc., it is not possible to identify a finite number of points of interaction of the elements of a system. In these cases a vibration process cannot be described in the traditional form with a finite number of input and transient impedances or pliancies. However, it is possible in principle to construct a set of integral relations that describe the dynamics of a mechanism in this case.

As an example let us examine a harmonic vibration process. Let a force be exerted upon a linear mechanical system on frequency ω on surface Ω and be characterized by complex surface density p(S). According to Hilbert's theorem, no matter what the integrable function p(S) (and virtually all physically feasible kinds of actions are described by them), the solution for the reaction of a system, in particular the vibration velocity at a point, may be represented as

$$\dot{q}(S) = \int_{\Omega} M(S, S')\, p(S')\, dS', \tag{3.1.15}$$

where M(S, S') is a Green function for a specific boundary problem.

The physical sense of Green's function is the transient mechanical pliancy between point S and point S'.

If working processes in a mechanism, which cause vibrations and atmospheric noise, are such that the vibration forces are distributed on surface Ω_s with density $^s p(S)$, and the mechanism and bearing and nonbearing surfaces are in contact on area Ω_{af}, the dynamics of the mechanism is described by the following integral relations:

[и=s; аф=af]

$$\dot{q}_i(S) = \sum_{j=1}^{6} \int_{\Omega_и} {}^и M_{0ij}(S, S')\, {}^и P_j(S')\, dS' - \sum_{j=1}^{6} \int_{\Omega_{аф}} M_{0\,ij}(S, S')\, P_j(S')\, dS', \tag{3.1.16}$$

where $P_j(S')$ is the j-th component of the surface density of the reaction of the bearing and nonbearing connections.

Considering that

$$\dot{q}_i(S) = \sum_{j=1}^{6} \int_{\Omega_{аф}} M_{аф\,ij}(S, S')\, P_j(S')\, dS', \quad i=1,2,\ldots,6 \tag{3.1.17}$$

APPROVED FOR RELEASE: 2007/02/08: CIA-RDP82-00850R000200100009-9

APPROVED FOR RELEASE: 2007/02/08: CIA-RDP82-00850R000200100009-9

we obtain an integral equation system for determining $P_j(S')$ on the basis of known surface density ${}^{S}P_j(S')$:

$$\sum_{j=1}^{6} \int_{\Omega_{\text{аф}}} [M_{\text{аф}\, ij}(S, S') - M_{0ij}(S, S')] P_j(S')\, dS' = \sum_{j=1}^{6} \int_{\Omega_{\text{н}}} {}^{\text{н}}M_{0\, ij}(S, S')\, {}^{\text{н}}P_j(S')\, dS' \tag{3.1.18}$$

for i = 1, 2, ..., 6.

In the case when a mechanism is characterized by power density $P_0(S)$, reduced to a contact surface with bearing and nonbearing connections, the equations of vibrations of a mechanism acquire the form

$$\sum_{j=1}^{6} \int_{\Omega_{\text{аф}}} [M_{\text{аф}\, ij}(S, S') - M_{0ij}(S, S')] P_j(S')\, dS' = \sum_{j=1}^{6} \int_{\Omega_{\text{аф}}} M_{0ij}(S, S')\, P_0(S')\, dS'. \tag{3.1.19}$$

The solution of the problem of the vibrations of a mechanism in the case of forces that are distributed continuously over the surface encounters substantial difficulties and can be found basically by numerical methods. In many important special cases, however, an analysis of the relations of the input and transient pliancies of structures of a mechanism of a specific type in relation to different forces makes it possible to substantially simplify the general equations of the relationship between forces and levels of vibrations and to reduce them to a form that yields an analytical solution.

Approximate equations that reflect the physics of a vibration process point to the right direction in the design of quiet mechanisms.

The following simplifications are acceptable with sufficient accuracy for virtually all the nomenclature of marine machinery.

1. The relation between vibrations of the points of contact of a machine with bearing and nonbearing connections can be ignored on medium and high frequencies.

2. The centers of gravity and rigidity of vibration-damping elements (shock absorbers and branch pipes) are usually arranged on the same axis, normal to the area of contact to the mechanism and passing through that

APPROVED FOR RELEASE: 2007/02/08: CIA-RDP82-00850R000200100009-9

APPROVED FOR RELEASE: 2007/02/08: CIA-RDP82-00850R000200100009-9

area. The bearing plates of such shock absorbers and branch pipes, under the influence of forces from the mechanism, complete independent vibrations in the direction of the following coordinates: vertical and rotary around the vertical axis, and pair-connected vibrations in the horizontal-longitude and rotary around the horizontal-longitudinal axes and in the horizontal-transverse direction and rotary around the horizontal-transverse axis.

3. Moments of reaction that occur in the area where shock absorbers are fastened to a machine exert little influence on vertical vibration components of its bearing surface. The influence of the impedances of shock absorbers in relation to moments on the vibration of a mechanism, normal to bearing surfaces, may be ignored (by analogy with other linear components of vibration).

4. The relationship between unidirectional linear vibrations of various areas of contact of a mechanism with bearing and nonbearing connections may be ignored on frequencies above 2-3 kHz.

3.2. Mechanical Radiation of Vibration Energy

The operation of ship machinery is accompanied by the radiation into connected structures and into the environment of vibration energy. The vibration energy radiated into bearing and nonbearing connections is the basic parameter that characterizes the vibration activity of mechanisms. A mechanism can be precisely and uniquely evaluated as a vibration and noise source, and the number of points of connection, the directions of the vibrations, the power action and mechanical impedances of structures can be considered only on the basis of vibration energy. If the radiated vibration energy is known it is possible to find the sources of vibrations both in a mechanism, and in assembled units [5, 8]. The vibration power radiated by a mechanism is the integral of the scalar product of the vectors, forces, exerted by a mechanism on bearing and nonbearing connections, and the vibration velocities of the points of contact of a mechanism with these connections, averaged in time:

$$N = \sum_{n=1}^{m} \lim_{\Delta t \to \infty} \frac{1}{\Delta t} \int_{t_1}^{t_2} \left(\overline{Q}^n(t) \cdot \overline{\dot{q}}^n(t) \right) dt = \\ = \sum_{n=1}^{m} \sum_{i=1}^{6} \lim_{\Delta t \to \infty} \frac{1}{\Delta t} \int_{t_1}^{t_2} Q_i^n(t) \dot{q}_i^n(t)\, dt, \qquad (3.2.1)$$

where $\Delta t = t_2 - t_1$.

In other words, vibration power N, radiated by a mechanism into bearing and nonbearing connections, is equal to the sum of the powers radiated by the

APPROVED FOR RELEASE: 2007/02/08: CIA-RDP82-00850R000200100009-9

APPROVED FOR RELEASE: 2007/02/08: CIA-RDP82-00850R000200100009-9

components of the forces exerted by the mechanism through individual points of contact with bearing and nonbearing surfaces:

$$N = \sum_{n=1}^{m} \sum_{i=1}^{6} N_i^n, \tag{3.2.2}$$

The spectra of the vibrations of machinery, depending on the character of the working process, can contain discrete components and continuous parts. Vibrations of mechanical and electromagnetic origin in the frequency range of up to 1,000 Hz are usually discrete.

The vibration power radiated by a mechanism on a discrete component with frequency ω as a result of force $Q_i^n(\omega)$ cos ωt, is determined by the formula

[∋ϕ=ef]

$$N_i^n(\omega) = \frac{1}{T}\int_0^T Q_i^n(\omega, t)\,\dot{q}_i^n(\omega, t)\,dt = Q_{i\ni\phi}^n(\omega)\,\dot{q}_{i\ni\phi}^n\,\omega\cos\alpha_{Q\dot{q}}, \tag{3.2.3}$$

where $Q_{i\ ef}^n$ and $\dot{q}_{i\ ef}^n$ are the effective (mean square) values of force and velocity; $\alpha_{Q\dot{q}}$ is the angle of phase shift between active forces and vibration velocity.

If the combined amplitudes of force and velocity are defined as $Q_i^n(\omega)$ and $\dot{q}_i^n(\omega)$, respectively, then the expression for the radiated power may be written as

$$N_i^n(\omega) = \frac{1}{2}\,\mathrm{Re}\left(Q_i^n(\omega)\dot{q}_i^{n*}(\omega)\right), \tag{3.2.4}$$

where the asterisk denotes complex conjugation.

Formulas (3.2.3) and (3.2.4) are suitable for calculating the vibration power radiated on discrete components of the spectrum of ship machinery. However, vibrations of electrical and mechanical origin on frequencies above 1,000-3,000 Hz and hydrodynamic vibrations do not exhibit pronounced discrete components and may be viewed as random stationary processes. In this case the spectral density of the vibration power radiated on frequency ω is determined by the relative spectral density of active force and vibration velocity:

$$N_i^n(\omega) = \mathrm{Re}S\left(Q_i^n, \dot{q}_i^n\right) =$$

$$= \mathrm{Re}\lim_{\Delta\omega\to 0}\lim_{\Delta T\to\infty}\frac{1}{\Delta\omega T}\int_0^T Q_i^n(t, \omega, \Delta\omega)\cdot\dot{q}_i^n(t, \omega, \Delta\omega)\,dt. \tag{3.2.5}$$

APPROVED FOR RELEASE: 2007/02/08: CIA-RDP82-00850R000200100009-9

APPROVED FOR RELEASE: 2007/02/08: CIA-RDP82-00850R000200100009-9

In practice force and velocity are usually measured in the frequency bands, for instance, of 1/3- or 1/2-octave, from which the frequency characteristic of a process in the analyzed range is formed. Vibration power $N_i^n(\Delta\omega)$, radiated by a mechanism in frequency band $\Delta\omega$, is determined by the formula

[∃ϕ=ef]
$$N_i^n(\Delta\omega) = \int_{\omega-\frac{\Delta\omega}{2}}^{\omega+\frac{\Delta\omega}{2}} N_i^n(\omega)\,d\omega = Q_{i\exists\phi}^n(\Delta\omega)\cdot\dot{q}_{i\exists\phi}^n(\Delta\omega)\cdot \mathrm{Re}R_{Q\dot{q}}(\Delta\omega), \qquad (3.2.6)$$

where Re $R_{Q\dot{q}}(\Delta\omega)$ is the real part of the correlation coefficient between force and velocity in frequency band $\Delta\omega$:

$$R_{Q\dot{q}}(\Delta\omega) = \frac{\lim\limits_{\Delta t\to\infty}\frac{1}{\Delta t}\int\limits_{t_1}^{t_2} Q_i^n(\Delta\omega)\cdot\dot{q}_i^{n*}(\Delta\omega)\,dt}{Q_{i\exists\phi}^n(\Delta\omega)\cdot\dot{q}_{i\exists\phi}^n(\Delta\omega)}.$$

If the mechanism is in contact with bearing and nonbearing surfaces with area Ω_{af}, the radiated vibration power is

[∃ϕ=af]
$$N(\omega) = \mathrm{Re}\int\limits_{\Omega_{a\phi}} P_i(S,\omega)\,\dot{q}_i^*(S,\omega)\,dS, \qquad (3.2.7)$$

where $P_i(S, \omega)$ is the surface density of the force; $\dot{q}_i(S, \omega)$ is the vibration velocity at point S on frequency ω.

The values $N_i^n(\omega)$ and $N_i^n(\Delta\omega)$ will be positive if the energy flux goes from the mechanism into bearing and nonbearing connections. On some frequencies vibration energy can enter a mechanism from nearby vibration sources. There are also cases when vibration energy is radiated by a mechanism in one zone of contact with shock absorbers and re-enters the mechanism through other areas of contact. When the vibration energy flux goes into the mechanism the values $N_i^n(\omega)$ and $N_i^n(\Delta\omega)$ are negative.

Thus, if the forces and vibration velocities are known in each area of contact between a mechanism and bearing and nonbearing surfaces (or if the surface distribution of the forces and velocities is known), and if the phase and correlation relation between the forces and velocities are known, it is then possible, on the basis of equations (3.2.3), (3.2.5), (3.2.6) and (3.2.7), to determine the vibration power radiated by a mechanism. It can also be found on the basis of information about mechanical impedances or about the pliancies of bearing and nonbearing connections.

APPROVED FOR RELEASE: 2007/02/08: CIA-RDP82-00850R000200100009-9

APPROVED FOR RELEASE: 2007/02/08: CIA-RDP82-00850R000200100009-9

In the case of unidirectional harmonic vibrations of a mechanism and single-point contact with the shock absorber-foundation system, we obtain:

in terms of mechanical impedances

$$N_i^n(\omega) = [\dot{q}_{i\,\text{эф}}^n(\omega)]^2 \operatorname{Re} Z_{ii\,\text{аф}}^{nn}(\omega), \tag{3.2.8}$$

i.e., the vibration power radiated by a mechanism is a function of the square of the vibration velocity and the real part of the input mechanical impedance of the shock absorber-foundation system;

in terms of mechanical pliancies

$$N_i^n(\omega) = [Q_{i\,\text{эф}}^n(\omega)]^2 \operatorname{Re} M_{ii\,\text{аф}}^{nn}(\omega), \tag{3.2.9}$$

i.e., the vibration power radiated by a mechanism may be expressed through the square of the force and the real part of the input mechanical pliancy of the shock absorber-foundation system.

Likewise, for the vibration power radiated by a mechanism in the frequency band

$$N_i^n(\Delta\omega) = [\dot{q}_{i\,\text{эф}}^n(\Delta\omega)]^2 \cdot \operatorname{Re} Z_{ii\,\text{аф}}^{nn}(\Delta\omega), \tag{3.2.10}$$

$$N_i^n(\Delta\omega) = [Q_{i\,\text{эф}}^n(\Delta\omega)]^2 \cdot \operatorname{Re} M_{ii\,\text{аф}}^{nn}(\Delta\omega). \tag{3.2.11}$$

In the general case bearing and nonbearing connections of ship mechanisms are multipoint vibrating systems, in which the vibration velocity of each point is a function of all the forces exerted by the mechanism. In consideration of this dependence the expression for the radiated vibration power may be written as follows:

in terms of mechanical impedances

$$N_i^n(\omega) = \frac{1}{2}\sum_{n=1}^{m} |\dot{q}_i^n(\omega)|^2 \cdot \operatorname{Re} Z_{ii\,\text{аф}}^{nn}(\omega) + \sum_{n=1}^{m}\sum_{k=1}^{m}\sum_{j=1}^{6} \operatorname{Re}[Z_{ii\,\text{аф}}^{nk}(\omega)\cdot \dot{q}_i^n(\omega)\cdot \dot{q}_j^{k*}(\omega)]; \tag{3.2.12}$$

in terms of mechanical pliancies

$$N_i^k(\omega) = \frac{1}{2}\sum_{n=1}^{m} |Q_i^n(\omega)|^2 \operatorname{Re} M_{ii\,\text{аф}}^{nn}(\omega) +$$

APPROVED FOR RELEASE: 2007/02/08: CIA-RDP82-00850R000200100009-9

APPROVED FOR RELEASE: 2007/02/08: CIA-RDP82-00850R000200100009-9

$$+\sum_{n=1}^{m}\sum_{k=1}^{m}\sum_{j=1}^{6}\mathrm{Re}\left[M_{ij\,\text{аф}}^{nk}(\omega)\cdot Q_i^n(\omega)\cdot Q_j^{k*}(\omega)\right]. \qquad (3.2.13)$$

The second sums in the right hand sides of the equations are used for evaluating the influence of the connectedness of vibrations at various points and in different directions on the radiated vibration energy.

In the case when there is surface contact between a mechanism and bearing and nonbearing connections the vibration energy radiated by the mechanism can be determined only through mechanical pliancies:

$$N_i(\omega)=\sum_{j=1}^{6}\int_{\Omega_{\text{аф}}}\int_{\Omega_{\text{аф}}} M_{ij\,\text{аф}}(S,S'\omega)\,P_i(S,\omega)\,P_j^*(S',\omega)\,dS'\,dS. \qquad (3.2.14)$$

It follows from the above formulas that the vibration power radiated by a mechanism may be determined experimentally in two different ways: directly, as the scalar product, averaged in time, of force and the corresponding velocity, and indirectly -- on the basis of the vibration velocities of the mechanism and mechanical impedances of bearing and nonbearing connections.

The direct method is used for measuring the vibration power radiated by forces normal to bearing surfaces [6, 7].

The indirect method can be used, in principle, to determine all components of vibration power.

Vibration power should be assumed to be the basic parameter for analyzing the vibration activity of machinery. Vibration power contains information that tells the vibration levels and forces that a mechanism exerts upon bearing and nonbearing connections.

It is possible on the basis of radiated vibration power, first of all, to compare different types of machinery and mechanisms, utilizing different operating principles, and with different masses, sizes and installed in different places as sources of vibrations. Such a comparison cannot be made on the basis of vibration levels. In fact, the forces generated in different assemblies are spent to overcome mechanical impedances of structures of a mechanism itself and of connected bearing and nonbearing couplings. For large and heavy mechanisms and foundations even large forces produce near the mechanism a vibration that does not exceed the vibration of small mechanisms on pliant foundations [5].

Spectrograms of the vibration of an electric motor and ship reducer, and also of a diesel engine and gas turbine, are presented in Figure 3.1. As can be seen, the vibration of the reducer is about the same as the vibration of the electric motor. At the same time it is obvious that the reducer has substantially greater vibration activity. A comparison of the

APPROVED FOR RELEASE: 2007/02/08: CIA-RDP82-00850R000200100009-9

APPROVED FOR RELEASE: 2007/02/08: CIA-RDP82-00850R000200100009-9

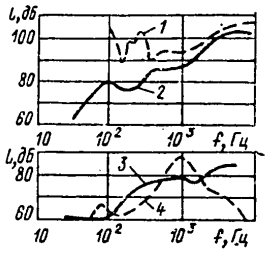

Figure 3.1. Spectrograms of vibration: 1 -- gas turbine; 2 -- diesel engine; 3 -- electric motor; 4 -- MTRA [main turbine reducer assembly]. [дБ=dB; Гц=Hz]

spectrograms of the radiated vibration powers (Figure 3.2) confirms this: the reducer radiates 2-3 times more vibration power.

A comparison of the vibration powers radiated by a diesel engine and gas turbine (Figure 3.3) shows that the gas turbine is preferable, in spite of the fact that the diesel engine produces lower levels of vibration.

It can be established, on the basis of the spectrum of vibration power radiated by a mechanism, what is the main source -- a moving part or a process.

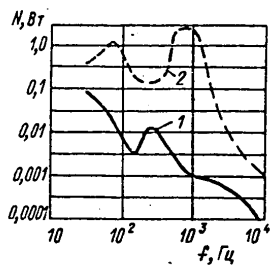

Figure 3.2. Spectrograms of radiated vibration power: 1 -- electric motor; 2 -- MTRA. [Вт=W]

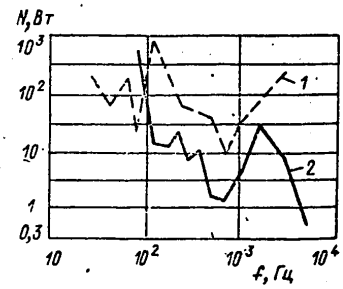

Figure 3.3. Spectrograms of radiated vibration power: 1 -- diesel; 2 -- gas turbine.

It is important, during the development of recommendations on the reduction of vibration activity of mechanisms, to determine what component must be reduced first. In connection with differences in the magnitude of linear and rotary vibrations, and also in the impedances of bearing structures in relation to forces of different directions, this can be solved only after the components of the vibration power radiated by a mechanism are separated. Measurement results show that in application to ship machinery there is no one kind of action on bearing surfaces that determines the radiation of energy. The component vibrations have different significance in each particular case, depending on the design features of the mechanism and on the system of forces acting upon moving assemblies.

The frequency characteristics of the ratio of vibration power N_3, radiated by a vibration component normal to bearing surfaces, to the total radiated

APPROVED FOR RELEASE: 2007/02/08: CIA-RDP82-00850R000200100009-9

APPROVED FOR RELEASE: 2007/02/08: CIA-RDP82-00850R000200100009-9

vibration power N_Σ, are plotted in Figure 3.4 for several ship machines. As can be seen, vibration power N_3 has different values (in fractions of the total radiated power). The vibration activity of a mechanism in relation to bearing and nonbearing connections can be compared only in terms of vibration power.

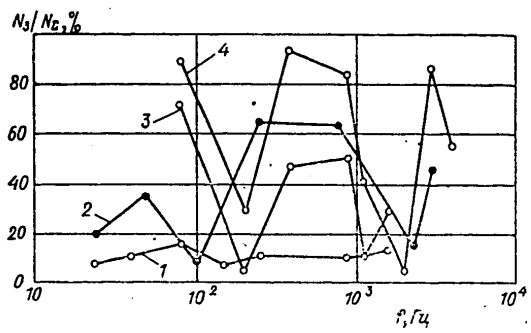

Figure 3.4. Frequency characteristics of ratio N_3/N_Σ: 1 -- diesel generator; 2 -- generator; 3 -- steam turbine; 4 -- reducer.

Information about radiated vibration powers can also be used for determining mechanisms -- the basic sources of vibration activity of assembled units. The influence of the causes of vibration not only on individual frequencies, but also in the frequency band, is an important feature of such diagnosis.

In some cases it is important to analyze the energy radiated by a shock-absorbing mechanism into foundation structures. Let us examine a harmonic vibration process in the mechanism-shock absorber-foundation system.

Each shock absorber can be represented as being a linear mechanical quadrupole with unidirectional vibrations. In the general case set n_0 of shock absorbers, with all six components of vibration taken into account, is a $24n_0$-pole. Vibration processes obviously should be described with the aid of matrix coefficients.

The relationship between vibration velocities $\overline{\dot{q}}$ in mechanism-shock absorber cross sections and $\overline{\dot{q}}_f$ in shock absorber-foundation cross sections, and also between the forces of interaction of the shock absorber and mechanism $\overline{Q}$ and foundation $\overline{Q}_f$, is given by the following matrix equations:

APPROVED FOR RELEASE: 2007/02/08: CIA-RDP82-00850R000200100009-9

APPROVED FOR RELEASE: 2007/02/08: CIA-RDP82-00850R000200100009-9

$$[\phi=f] \qquad \left.\begin{aligned} \bar{Q} &= \bar{Z}_{\text{ам}}\dot{\bar{q}} + \bar{Z}_{\text{амф}}\dot{\bar{q}}_{\phi}; \\ \bar{Q}_{\phi} &= \bar{Z}_{\text{амф}}\dot{\bar{q}} + \bar{Z}_{\text{аф}}\dot{\bar{q}}_{\phi}, \end{aligned}\right\} \tag{3.2.15}$$

where quasidiagonal matrices $\bar{Z}_{am}$, $\bar{Z}_{am.f}$, $\bar{Z}_{am.f}$, $\bar{Z}_{af}$ describe the mechanical impedance of the shock absorbers.

By combining these equations with equation (3.1.11), which describes the dynamic properties of a mechanism, and also considering that

$$\bar{Q}_{\phi} = -\bar{Z}_{\phi}\dot{\bar{q}}_{\phi}, \tag{3.2.16}$$

where $\bar{Z}_f$ is the matrix of mechanical impedances of the foundation, we obtain the following matrix equation system that completely describes the combined harmonic vibrations of the mechanism, shock absorber and foundation:

$$\left.\begin{aligned} \bar{Q}_{\text{о}} &= \bar{Z}_{\text{о}}\dot{\bar{q}} + \bar{Q}; \\ \bar{Q} &= \bar{Z}_{\text{ам}}\dot{\bar{q}} + \bar{Z}_{\text{амф}}\dot{\bar{q}}_{\phi}; \\ \bar{Q}_{\phi} &= \bar{Z}_{\text{афм}}\dot{\bar{q}} + \bar{Z}_{\text{аф}}\dot{\bar{q}}_{\phi}; \\ \bar{Q}_{\phi} &= -\bar{Z}_{\phi}\dot{\bar{q}}_{\phi}. \end{aligned}\right\} \tag{3.2.17}$$

The equations may also be written in dual form -- in terms of mechanical pliancies:

$$\left.\begin{aligned} \dot{\bar{q}} &= \bar{M}_{\text{о}}\bar{Q}_{\text{о}} + \bar{M}_{\text{о}}\bar{Q}; \\ \dot{\bar{q}} &= \bar{M}_{\text{ам}}\bar{Q} + \bar{M}_{\text{амф}}\bar{Q}_{\phi}; \\ \dot{\bar{q}}_{\phi} &= \bar{M}_{\text{амф}}\bar{Q} + \bar{M}_{\text{аф}}\bar{Q}_{\phi}; \\ \dot{\bar{q}}_{\phi} &= -\bar{M}_{\phi}\bar{Q}_{\phi}. \end{aligned}\right\} \tag{3.2.18}$$

The equations of the propagation of vibrations through nonbearing connections are of the analogous form if the impedances or pliancies of flexible parts in nonbearing connections are defined, respectively, as impedances $\bar{Z}_{am}$, $\bar{Z}_{amf}$, $\bar{Z}_{afm}$, $\bar{Z}_{af}$ or pliancies $\bar{M}_{am}$, $\bar{M}_{amf}$, $\bar{M}_{afm}$, $\bar{M}_{af}$.

From equations (3.2.17), after simple algebraic transformations, we obtain the equations of the balance of the vibration energy in the mechanism-shock absorber-foundation system [3]:

APPROVED FOR RELEASE: 2007/02/08: CIA-RDP82-00850R000200100009-9

APPROVED FOR RELEASE: 2007/02/08: CIA-RDP82-00850R000200100009-9

$$\left.\begin{aligned}
\tilde{N}_{м} &= \tilde{N}_{мм} + \tilde{N}_{аф};\\
\tilde{N}_{аф} &= \frac{1}{2}\,[\bar{Z}_{ам}\cdot\bar{\dot{q}}]\,\bar{\dot{q}}^{*\prime} + \frac{1}{2}\,[\bar{Z}_{амф}\cdot\bar{\dot{q}}_{ф}]\,\bar{\dot{q}}^{*\prime};\\
\tilde{N}_{ф} &= \frac{1}{2}\,[\bar{Z}_{афм}\cdot\bar{\dot{q}}]\,\bar{\dot{q}}^{*\prime} + \frac{1}{2}\,[\bar{Z}_{аф}\cdot\bar{\dot{q}}_{ф}]\,\bar{\dot{q}}^{*\prime}_{ф};\\
\tilde{N}_{ф} &= -\frac{1}{2}\,[\bar{Z}_{ф}\cdot\bar{\dot{q}}_{ф}]\,\bar{\dot{q}}^{*\prime}_{ф},
\end{aligned}\right\} \qquad (3.2.19)$$

where $\tilde{N}_m$ is the combined vibration power, developed by the source of power $\bar{Q}_0$; $\tilde{N}_{mm} = \frac{1}{2}\,[\bar{Z}_0\overline{\dot{q}\dot{q}}^{*\prime}]$ is the combined vibration power in the structures of the mechanism; $\tilde{N}_{af}$ is the combined vibration power at the input of the shock absorber-foundation system; $\tilde{N}_f$ is the combined vibration power at the input of the foundation.

Equations (3.2.19) give the vibration power radiated both into the foundation, and into the shock absorbers, on the basis of data on the impedances of the shock absorbers and vibration velocities of the mechanism and foundation alone.

In some cases, when the mechanical impedances of the shock absorbers are known in advance, this method is very convenient.

An important feature of equation system (3.2.19) is the fact that combined powers enter in it. The real part of combined power is equal to the absorbed (radiated) power, and the imaginary part to the power that is always present in the mechanism-shock absorber-foundation system and is manifested as potential and kinetic energies of the elements.

In each cross section there are six components of vibration power. Equations (3.2.19) derived above describe the energy balance both for each component separately, and for all of them taken together.

Using the concept of effective impedance and generalized effective force [2, 3], we can write equation system (3.2.19) in the following form:

[эф=ef; ф=f]

$$\left.\begin{aligned}
{}^0Q_{i0} &= {}^0Z_{i0}\langle\dot{q}_{i\,эф}\rangle + {}^0Q_i;\\
{}^0Q_i &= {}^0Z_{i\,ам}\langle\dot{q}_{iф}\rangle + {}^0Z_{i\,амф}\langle\dot{q}_{iф}\rangle;\\
{}^0Q_{iф} &= {}^0Z_{i\,афм}\langle\dot{q}_{i\,эф}\rangle + {}^0Z_{i\,аф}\langle\dot{q}_{iф}\rangle;\\
{}^0Q_{iф} &= -{}^0Z_{iф}\langle\dot{q}_{i\,эф}\rangle,
\end{aligned}\right\} \qquad (3.2.20)$$

where ${}^0Z_{i0}$ is the effective impedance of a mechanism

$$ {}^0Z_{i0} = \frac{\tilde{N}_{i\,мм}}{[\langle\dot{q}_{i\,эф}\rangle]^2} = \frac{[\bar{Z}_{ii\,0}\bar{\dot{q}}_i]_i\,\bar{\dot{q}}^{*\prime}_i}{\frac{1}{2}\,\bar{\dot{q}}_i\,\bar{\dot{q}}^{*\prime}_i}; \qquad (3.2.21)$$

APPROVED FOR RELEASE: 2007/02/08: CIA-RDP82-00850R000200100009-9

APPROVED FOR RELEASE: 2007/02/08: CIA-RDP82-00850R000200100009-9

$^0Z_{if}$ is the effective impedance of the foundation

$$^0Z_{i\text{ф}} = \frac{\tilde{N}_{i\text{ф}}}{[\langle \dot{q}_{i\text{ф эф}} \rangle]^2} = \frac{[\bar{Z}_{ii\text{ ф}} \bar{\dot{q}}_{i\text{ф}}]_i \bar{\dot{q}}^{*\prime}_{i\text{ф}}}{\frac{1}{m_\text{ф}} \bar{\dot{q}}_{i\text{ф}} \bar{\dot{q}}^{*\prime}_{i\text{ф}}}. \tag{3.2.22}$$

A vibration-damping structure (a set of shock absorbers, in particular) is characterized by four impedances for each direction:

$$^0Z_{i\text{ ам}} = \frac{[\bar{Z}_{\text{ам}} \bar{\dot{q}}]_i \bar{\dot{q}}^{*\prime}_i}{\frac{1}{m_\text{м}} \bar{\dot{q}}_i \bar{\dot{q}}^{*\prime}_i}; \quad ^0Z_{i\text{ амф}} = \frac{[\bar{Z}_{\text{амф}} \bar{\dot{q}}_\text{ф}]_i \bar{\dot{q}}^{*\prime}_i}{\frac{1}{m_\text{м}} \sqrt{(\bar{\dot{q}}_i \bar{\dot{q}}^{*\prime}_i)(\bar{\dot{q}}_{i\text{ф}} \bar{\dot{q}}^{*\prime}_{i\text{ф}})}};$$

$$^0Z_{i\text{ афм}} = \frac{[\bar{Z}_{\text{амф}} \bar{\dot{q}}] \bar{\dot{q}}^{*\prime}_{i\text{ф}}}{\frac{1}{m_\text{ф}} \sqrt{(\bar{\dot{q}}_{i\text{ф}} \bar{\dot{q}}^{*\prime}_{i\text{ф}})(\bar{\dot{q}}_i \bar{\dot{q}}^{*\prime}_i)}}; \quad ^0Z_{i\text{ аф}} = \frac{[\bar{Z}_{\text{аф}} \bar{\dot{q}}_\text{ф}]_i \bar{\dot{q}}^{*\prime}_{i\text{ф}}}{\frac{1}{m_\text{ф}} \bar{\dot{q}}_{i\text{ф}} \bar{\dot{q}}^{*\prime}_{i\text{ф}}}; \tag{3.2.23}$$

^0Q_i is the generalized effective force that the mechanism exerts on the shock-absorbing system

$$^0Q_i = \frac{\tilde{N}_{i\text{ аф}}}{\langle \dot{q}_{i\text{ эф}} \rangle} = \frac{\bar{Q}_i \bar{\dot{q}}^{*\prime}_i}{\sqrt{\frac{1}{m} \bar{\dot{q}}_i \bar{\dot{q}}^{*\prime}_i}}; \tag{3.2.24}$$

$^0Q_{if}$ is the generalized effective force of interaction of the shock-absorbing system and the foundation:

$$^0Q_{i\text{ф}} = \frac{\tilde{N}_{i\text{ф}}}{\langle \dot{q}_{i\text{ф эф}} \rangle} = \frac{\bar{Q}_{i\text{ф}} \bar{\dot{q}}^{*\prime}_{i\text{ф}}}{\sqrt{\frac{1}{m} \bar{\dot{q}}_{i\text{ф}} \bar{\dot{q}}^{*\prime}_{i\text{ф}}}}; \tag{3.2.25}$$

m_m is the number of contact surfaces between the mechanism and shock-absorbing system; m_f is the number of contact surfaces between the shock-absorbing system and the foundation (if, in particular, the vibration-damping system is a set of shock absorbers, then $m_m = m_f$).

Thus, instead of formulas for a multipoint active system, we obtain expressions that coincide with the equations of the vibrations of a system, in which the shock-absorbing structure is in contact with the machine itself and with the foundation at a single point. This simplification was the result of the introduction of generalized effective forces in the effective impedances, which characterize in concentrated fashion the driving force and the inertial-rigidity and damping properties of the elements of a system at different points and in different directions from the energy viewpoint. The physical meaning of effective impedance is the

APPROVED FOR RELEASE: 2007/02/08: CIA-RDP82-00850R000200100009-9

APPROVED FOR RELEASE: 2007/02/08: CIA-RDP82-00850R000200100009-9

proportionality coefficient between the combined energy in an examined element of a system and the square of the mean square (on the perimeter of the cross section) vibration velocity. The physical meaning of generalized effective force is the proportionality coefficient between the flux of vibration velocity, averaged in terms of the perimeter of the cross section.

In the important special practical case, when the vibration-damping system is a collection of m identical shock absorbers and completes linear vibrations that are weakly connected in different directions, expressions (3.2.20) for each direction are converted as follows:

$$\begin{gathered} {}^0Q_{i0} = {}^0Z_{i0}\langle \dot{q}_{i\,\text{эф}}\rangle + {}^0Q_i; \\ {}^0Q_i = mZ^{nn}_{ii\,\text{ам}}\langle \dot{q}_{i\,\text{эф}}\rangle + mZ^{nn}_{ii\,\text{амф}}R(\dot{q}_{i\text{ф}}, \dot{q}_i)\langle \dot{q}_{i\text{ф}\,\text{эф}}\rangle; \\ {}^0Q_{i\text{ф}} = mZ^{nn}_{ii\,\text{аф}\text{м}}R(\dot{q}_i, \dot{q}_{i\text{ф}})\langle \dot{q}_{i\,\text{эф}}\rangle + mZ^{nn}_{ii\,\text{аф}}\langle \dot{q}_{i\text{ф}\,\text{эф}}\rangle; \\ {}^0Q_{i\text{ф}} = -{}^0Z_{i\text{ф}}\langle \dot{q}_{i\text{ф}\,\text{эф}}\rangle, \end{gathered} \tag{3.2.26}$$

where $Z^{nn}_{ii\ am}$, $Z^{nn}_{ii\ amf}$, $Z^{nn}_{ii\ afm}$, $Z^{nn}_{ii\ af}$ are the input and transient mechanical impedances of the shock absorbers as quadrupoles; $R(\dot{q}_{if}, \dot{q}_i)$ is the spatial correlation coefficient of the vibration velocities at the input and output of the shock absorbers for unidirectional vibrations:

$$R(\dot{q}_{i\text{ф}}, \dot{q}_i) = e^{-i\arg\frac{{}^0Z_{i\text{ф}} + mZ^{nn}_{ii\,\text{аф}}}{mZ^{nn}_{ii\,\text{ам}}}}.$$

If a vibration process in a system is a stationary random process effective impedances and the spectral density of the generalized effective force acquire the form

$${}^0Z_i = \frac{S(\tilde{N}_i)}{[\langle S(\dot{q}_{i\,\text{эф}})\rangle]^2}, \tag{3.2.27}$$

$$S({}^0Q_i) = \frac{S(\tilde{N})}{\langle S(\dot{q}_{i\,\text{эф}})\rangle}, \tag{3.2.28}$$

where $S(\tilde{N}_i)$ is the spectral density of the vibration energy in any cross section; $\langle S(\dot{q}_{i\ ef})\rangle$ is the effective spectral density of vibration velocity, averaged by a quadratic law in terms of the perimeter of the cross section.

In the case of surface contact between elements of a system the effective impedances and the generalized effective force are determined (for unidirectional vibrations) by the equations:

APPROVED FOR RELEASE: 2007/02/08: CIA-RDP82-00850R000200100009-9

APPROVED FOR RELEASE: 2007/02/08: CIA-RDP82-00850R000200100009-9

$$^{0}Z_i = \frac{\int\limits_{\Omega}\int\limits_{\Omega} M_{ii}(s, s')\, P_i^*(s)\, P_i(s')\, ds\, ds'}{\frac{1}{S_\Omega}\int\limits_{\Omega}\int\limits_{\Omega} M_{ii}(s, s')\, P_i(s')\, ds' \int\limits_{\Omega} M^*(s, s')\, P^*(s')\, ds'\, ds}, \qquad (3.2.29)$$

$$^{0}Q_i = \frac{\int\limits_{\Omega}\int\limits_{\Omega} M_{ii}(s, s')\, P^*(s)\, P(s')\, ds\, ds'}{\sqrt{\frac{1}{S_\Omega}\int\limits_{\Omega}\int\limits_{\Omega} M_{ii}(s, s')\, P(s')\, ds' \int\limits_{\Omega} M_{ii}^*(s, s')\, P^*(s')\, ds'\, ds}}, \qquad (3.2.30)$$

where S_Ω is the area of the contact surface of the elements in the examined cross section.

Introducing the generalized effective forces and effective impedances not only greatly simplifies the equations that describe the vibrations of a complex active mechanical system, but also facilitates the experimental analyses of systems [3, 4].

Thus, a mechanism as a vibration source may also be characterized with the aid of energy parameters -- the generalized effective force $^{0}Q_{i0}$ and the effective impedance $^{0}Z_{i0}$. With information about the effective impedances of shock absorbers or other elastic elements in nonbearing connections it is possible on the basis of measurement data on the mean square velocities to determine the vibration energy flux radiated by the mechanism into both the vibration-damping system and foundation structures, i.e., to describe most completely a mechanism as a source of vibrations [2].

BIBLIOGRAPHY

1. Genkin, M. D. and V. V. Yablonskiy, "Vibration Energy Flux as Criterion of Vibration Activity of Mechanism," MASHINOVEDENIYE [Mechanical Engineering], 1965, No 5, pp 55-58.

2. Il'kov, V. K. and V. I. Popkov, "Utilization of Vibration Energy Parameter for Analyzing Design Efficiency of Complex Active Mechanical Systems," "Trudy VIII Vsesoyuznoy Akusticheskoy Konferentsii" [Proceedings of 8th All-Union Acoustics Conference], Moscow, Nauka, 1974, pp 158-161.

3. Il'kov, V. K. and V. I. Popkov, "Vibrations of Complex Active Mechanical Systems," in the book: "Akusticheskaya Dinamika Mashin i Konstruktsiy" [Acoustic Dynamics of Machines and Structures], Moscow, Nauka, 1973, pp 32-38.

APPROVED FOR RELEASE: 2007/02/08: CIA-RDP82-00850R000200100009-9

APPROVED FOR RELEASE: 2007/02/08: CIA-RDP82-00850R000200100009-9

4. Popkov, V. I., "Vibroakusticheskaya Diagnostika i Snizheniye Vibroaktivnosti Sudovykh Mekhanizmov" [Vibroacoustic Diagnosis and Vibration Reduction of Ship Machinery], Leningrad, Sudostroyeniye, 1974.

5. Popkov, V. I., "Vibroacoustic Diagnosis of Mechanical Units," in the book: "Akusticheskaya Dinamika Mashin i Konstruktsiy," Moscow, Nauka, 1978, pp 50-56.

6. Popkov, V. I., "Piezoelectric Converter for Measuring Dynamic Forces Exerted by Machine on Foundation," IZMERITEL'NAYA TEKHNIKA [Measurement Technology], 1967, No 9, pp 34-36.

7. Popkov, V. I., "Instrument for Measuring Vibration Power Radiated by Machines," METROLOGIYA [Metrology], 1971, No 11, pp 52-56.

8. Popkov, V. I., "Description of Mechanisms as Vibration Sources," IZVESTIYA LETI IM. V. I. UL'YANOVA (LENINA) [News of Leningrad Electrotechnical Institute imeni V. I. Ul'yanov (Lenin)], 1968, No 63, pp 276-287.

APPROVED FOR RELEASE: 2007/02/08: CIA-RDP82-00850R000200100009-9

APPROVED FOR RELEASE: 2007/02/08: CIA-RDP82-00850R000200100009-9

4.2. Standardization of Noise and Vibration on Ships[1]

General Premises. In accordance with Soviet legislation on labor, protection of the environment and health of citizens in all installations, including ships, healthful and safe conditions must be maintained for the people who service them during operation, and for the population and nature of the surrounding region.

Excessive noise is a form of harmful emissions (GOST 12.0.003-74). Not a single ship can be placed in operation and accepted for series production if the requirements on noise levels are not observed. Compliance with measures to prevent harmful noise is mandatory for all workers and service personnel, engaged in the development, construction and operation of ships. These measures must be reflected in plans, instructions and rules on their design, construction and operation.

The first standards on the limitation of noise on ships were drafted and introduced in 1962 [9]. The Noise Health Standards in Compartments of River Ships [11] and the Vibration Health Standards [12] were adopted as supplements to them.

The State Committee of Standards of the USSR Council of Ministers, in a resolution of 1 January 1977, placed into effect the pioneering standard on noise control in the system of labor safety standards -- GOST 12.1.003-76 "Noise. General Safety Requirements." It applies to all sectors of the national economy, and also to seagoing, lake and river ships. These standards establish a classification of noises, the characteristic standards of noise at work stations, noise safety measures, requirements on the noise characteristics of machinery and noise measurement procedures.

Classification of Noises. Noises are divided in terms of the character of their spectrum into wide-band with a continuous spectrum wider than one octave, and audio frequency, in whose spectrum are audible discrete tones. Audio noise, in accordance with the above standard, is characterized by the fact that when measured in third-octave bands the level in one band exceeds the level in the adjacent bands by not less than 10 dB. Noises are classified in relation to time characteristics as continual, the sound level of which in an 8-hour work day changes in time by not more than 5 dBA (during measurements on the "slow" time characteristic of the noise meter in accordance with GOST 17187-71), and intermittent, the sound level of which in an 8-hour work day changes in time by not less than 5 dBA (under the same measurement conditions).

Intermittent noises are divided into the following: fluctuating, the sound level of which changes continuously in time; sporadic, the sound level of which falls sharply to the background noise level, and the duration of

[1] I. I. Bogolepov contributed to this section.

APPROVED FOR RELEASE: 2007/02/08: CIA-RDP82-00850R000200100009-9

APPROVED FOR RELEASE: 2007/02/08: CIA-RDP82-00850R000200100009-9

intervals in which the sound level remains constant and exceeds the background level is 1 s and longer; pulse noises, consisting of one or several audio signals, each with a duration of less than 1 s (the sound levels in this case, measured with the "slow" and "pulse" characteristics of the noise meter turned on in accordance with GOST 17187-71, differ by not more than 10 dB).

Characteristics and Standards of Noise at Work Stations. The characteristics of continual noise at work stations are the acoustic pressure levels in the octave bands (in dB) with mean geometric frequencies of 63, 125, 250, 500, 1,000, 2,000, 4,000, 8,000 Hz, determined by the formula

$$L = 20 \lg \frac{p}{p_0},$$

where p is the mean square acoustic pressure, Pa; $p_0 - 2 \cdot 10^{-5}$ is the threshold level of the mean square acoustic pressure, Pa.

A wider frequency band may be used for standardization of noise characteristics.

For approximate evaluations (for example, during inspections by supervisory organizations, during an assessment of necessary noise abatement measures, etc.) it is permissible to use as the characteristic of continual noise at a work station the acoustic level L_a, in dBA, measured on the A scale of the noise meter (GOST 17187-71) and determined by the formula

$$L_a = 20 \lg \frac{p_a}{p_0},$$

where p_a is the mean square acoustic pressure in consideration of correction factor A of the noise meter, in Pa.

The permissible acoustic pressure levels in octave frequency bands, acoustic levels and equivalent acoustic levels in decibels at work stations are: for wide-band noise see Table 4.1; for audio frequency and pulse noises, measured with a noise meter on the "slow" characteristic -- 5 dB lower than the values indicated in Table 4.1; for noise produced by room air conditioners, blowers and hot air heaters -- 5 dB lower than the values indicated in Table 4.1, or than the actual levels in those rooms if the latter do not exceed the values in the table (the correction factor for audio frequency and pulse noises in this case need not be used). For work stations not covered by the table the permissible acoustic pressure levels in octave frequency bands, acoustic levels and equivalent sound levels in decibels are established by health standards [11] (Table 4.2).

Noise Safety Measures. During the design, construction and operation of seagoing, lake and river ships all necessary measures must be taken to reduce noises to which human beings are exposed to levels that do not exceed the acceptable levels. This is accomplished by technical means (by

APPROVED FOR RELEASE: 2007/02/08: CIA-RDP82-00850R000200100009-9

APPROVED FOR RELEASE: 2007/02/08: CIA-RDP82-00850R000200100009-9

Table 4.1. Permissible Noise Levels in Engine Room in Accordance with GOST 12.1.003-76

1) Рабочие места	2) Уровни звукового давления, дБ, в октавных полосах со среднегеометрическими частотами, Гц								3) Уровни звука (и эквивалентные уровни звука), дБА
	68	125	250	500	1000	2000	4000	8000	
4) Машинные отделения с постоянной вахтой морских, озерных и речных судов	99	92	86	83	80	78	76	74	85

Key: 1. Work stations
2. Acoustic pressure levels, dB, in octave bands with mean geometric frequencies, Hz
3. Acoustic level (and equivalent acoustic level), dBA
4. Continuously manned engine rooms of seagoing, lake and river ships

reducing the noise of machinery at the source, etc.), by acoustic construction measures, by using remote controlled noisy machinery, by using personal safety gear (GOST 15762-70) and organizational measures (proper work and rest schedule, reduction of time of exposure to excessive noise, clinical and other measures). Areas with a sound level higher than 85 dBA should be so designated by danger signs. The administration must equip workers in these zones with personal safety gear. Even a brief stay in zones with noise levels above 135 dB in any octave band is prohibited.

Requirements on Noise Characteristics of Machinery. The standards and technical requirements on machinery must specify the noise characteristics. The noise characteristic of a machine is the octave level of acoustic power (GOST 8.055-73), or indices specified by the standards for specific kinds of machinery. The noise characteristics of machinery must conform with the acceptable noise levels at work stations (in consideration of the basic purpose of a machine). If the characteristics do not comply with the most progressive world standards the optimum and technically acceptable noise characteristics must be achieved. The substantiation that such characteristics are achieved are the following: the results of noise measurements of machines; data on acoustic power levels of the most progressive similar machines, built in the CEMA countries and in the capitalist countries; analysis of utilized structural noise abatement techniques; analysis of measures to reduce noise at work stations.

APPROVED FOR RELEASE: 2007/02/08: CIA-RDP82-00850R000200100009-9

APPROVED FOR RELEASE: 2007/02/08: CIA-RDP82-00850R000200100009-9

Table 4.2. Health Standards on Ship Noise

Room	Standards			
	for seagoing ships (SN 416-62)		for river boats (SN 1404-76)	
	limiting spectrum index (LS)	permissible sound levels, dBA	limiting spectrum index (LS)	permissible sound levels, dBA
Engine room:				
permanently manned	80	85	80	85
periodically manned	90	95	90	95
unmanned	95	100	95	100
Power plant control center	65	70	65	70
Production rooms:				
in engine room	--	--	80	85
outside of engine room	--	--	65	70
Service rooms:				
for category (group) I ships	40	50	50	60
for category (group) II ships	40	50	55	65
for category (group) III ships	45	55	55	65
Quarters:				
state rooms of category (group) I ships	40	--	40	50
duty rooms of category (group) II ships	--	--	50	60
duty rooms of category (group) III ships without bunks	--	--	55	65
Medical rooms	40	50	40	50

Technical Standardization of Noise. The technical standardization of mechanical noise is the establishment of the maximum tolerable acoustic power levels, at which work station noise standards are satisfied. The noise level at work stations must be reduced by a combination of different methods of controlling noise at the source, construction-planning methods and organizational measures (see Chapter 13). Unlike health standardization, technical standardization of noise refers to machinery, and not to human beings, and is based on the judicious utilization of all the examined noise control techniques and measures. The judicious utilization of techniques is determined by the least economic cost necessary for implementing a system of acoustic measures. These costs are borne by a specific enterprise; we will call them first-kind costs. Second-kind costs are borne by the government. They are incurred when the required reduction of noise cannot be achieved and the noise levels at work stations exceed the standards. An excessive noise level that reduces labor productivity and is reflected in human health leads to a loss to some degree or another of

APPROVED FOR RELEASE: 2007/02/08: CIA-RDP82-00850R000200100009-9

APPROVED FOR RELEASE: 2007/02/08: CIA-RDP82-00850R000200100009-9

professional and overall performance, entails early retirement, etc. Second-kind costs characterize the extent of this damage and loss. The purpose of technical standardization, in particular, is to implement a system of noise control measures such that second-kind costs will be reduced as the result of first-kind costs [3].

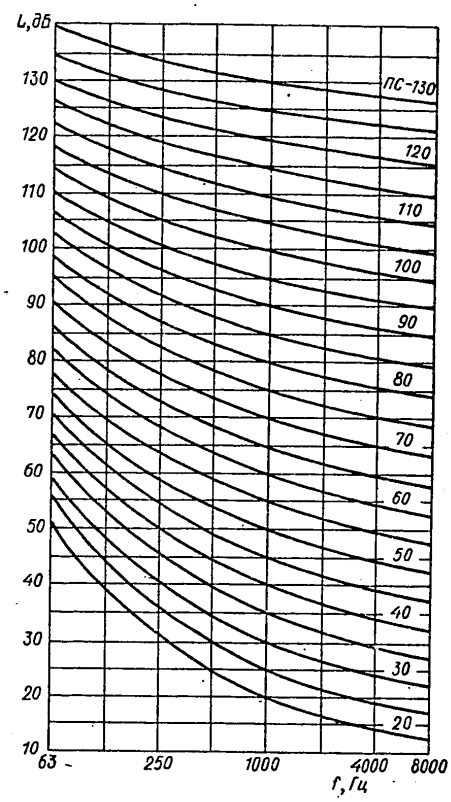

Figure 4.1. Family of standard spectra.
[дБ=dB; ПС=LS; Гц=Hz]

Health Standardization of Noise. Technical Committee No. 43 of the International Standardization Organization (ISO TC 43) recommended that noise be standardized in accordance with the requirement of the complete protection of hearing. In publication No. 235 (August 1961) of ISO TC 43 there is a family of standard spectra (Figure 4.1), which are suggested as limits during the drafting of recommendations to reduce noise at places inhabited by people at work and at leisure. The curves take into account the reduced sensitivity of the human ear on low frequencies and represent the

APPROVED FOR RELEASE: 2007/02/08: CIA-RDP82-00850R000200100009-9

APPROVED FOR RELEASE: 2007/02/08: CIA-RDP82-00850R000200100009-9

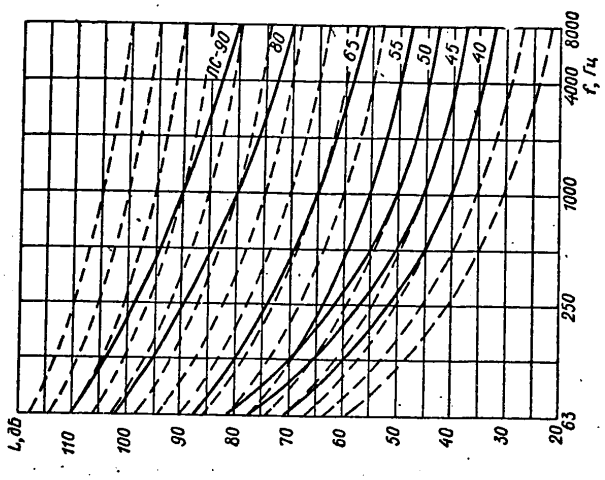

Figure 4.3. Family of limiting spectra, used for noise standardization.

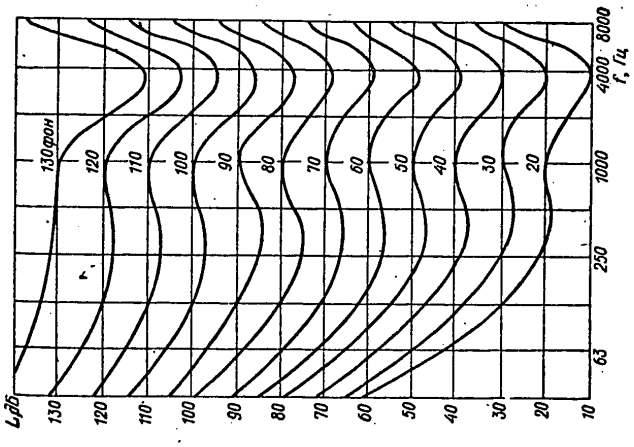

Figure 4.2. Loudness isolines.

APPROVED FOR RELEASE: 2007/02/08: CIA-RDP82-00850R000200100009-9

APPROVED FOR RELEASE: 2007/02/08: CIA-RDP82-00850R000200100009-9

rectified curves of different loudnesses (Figure 4.2). The numbers in the designations of the spectra characterize the acoustic pressure level in the octave with the middle frequency of 1,000 Hz. It is recommended that the acceptable noise level be evaluated on the basis of acoustic level measurement results (in dBA).

In accordance with ISO TC 43 recommendations a long (5 hours per day and longer) uninterrupted stay in noise exceeding LS 85 is injurious and unacceptable. Higher noise levels are permissible for a stay of less than 5 hours a day in continuous or intermittent wide-band noise.

The indices of the limiting spectra and the acceptable noise levels, established by the standards of SN [Construction norms] 416-62 and SN 1404-76 (Figure 4.3), are presented in Table 4.2.

Standardization of Vibration. Level $L_{\dot{\xi}}$, in dB, of the mean square vibration velocity $\dot{\xi}$ of a structure in octaves with mean geometric frequencies of 2, 4, 8, 16, 32 and 63 Hz, is used for standardizing and evaluating the acceptability of vibrations. It is determined by the formula

$$L_{\dot{\xi}} = 20 \lg \frac{\dot{\xi}}{\dot{\xi}_0},$$

where $\dot{\xi}_0 = 5 \cdot 10^{-8}$ m/s is the mean square vibration velocity at the threshold acoustic pressure in air of $2 \cdot 10^{-5}$ Pa on 1,000 Hz.

In the USSR the maximum tolerable vibrations in places occupied by the crew and passengers of seagoing, lake and river ships are established by the health standards [12]. The tolerable vibration levels are established in accordance with the purpose of a room, the time of exposure to vibrations and living conditions on a ship, and also in accordance with the class of ship in accordance with the classification presented in the health rules [13, 14].

4.3. Monitoring of Ship Noise and Vibration

Measurement Conditions. Measurements should be taken on a ship fully loaded or under ballast, at the rated speed and in the rated operating modes, in the absence of atmospheric precipitation, and in wave action and in wind not exceeding three points. The heading of the ship should be held as steady as possible. Windows, hatches and portholes should be closed. In addition, exterior noise should be measured in rated modes with the portholes in the engine room opened and hatches closed, with the main engines running at medium and low rpm. Exterior noise levels during the measurements should not be less than 10 dB lower in the entire spectrum than the noise level developed by the ship.

APPROVED FOR RELEASE: 2007/02/08: CIA-RDP82-00850R000200100009-9

APPROVED FOR RELEASE: 2007/02/08: CIA-RDP82-00850R000200100009-9

During measurements service, production, social rooms, state rooms and dispensaries must be completely furnished. The number of people in them should not exceed the established official limit. There should be no echoes from dams, mountains, cliffs, bridges or other engineering structures during measurements of exterior noise within a radius of 100-200 meters from the ship. The measurement results are recorded in a special log, which also should contain as complete as possible description of the test area, the condition of the ship and weather conditions (the width of the channel, the size of reflecting objects, wind velocity and precipitation, exterior acoustic noise levels, the amount of precipitation, speed and heading of the ship, power and running speed of the main and primary auxiliary engines).

Locations of Ship Noise Measurements. Measurements should be taken at at least one point in the center and at work and leisure locations in each state room, corridor, social and service room with an area of less than 15 m^2. In large rooms with an area above 15 m^2 as many measurement points are used as provides a sufficiently accurate arithmetic mean noise level, but at not less than one point for every 15 m^2. The distance between measurement points should not be shorter than 2 m, and the distance between measurement points and bulkheads should not be less than 0.5 m. In state rooms, where the measured noise level exceeds the approximate control level at least two measurements must be taken, one 0.25 m above bunk level, and the other at head level of a person sitting at a desk.

On the bridge measurements should be taken on the windward side, 1.5-1.65 m above the deck, and they must be repeated for all versions of wind direction relative to heading: in wind from the bow, from the stern and from each side. On the deck measurements should be taken at all places occupied by crew and passengers, especially around vents and funnels of engines, air conditioners and refrigerators, near hatches and portholes of the engine room and at other places where the noise level may be excessive.

During measurements of noise levels around engine intake and exhaust funnels, fans, air conditioners and the refrigerator room the microphone should be placed outside of the main flow at a distance of 1 m from the edge of the vent at 45° to its axis.

In permanently manned engine and production rooms measurements are taken at control centers of the main engines, auxiliary and engineering mechanisms, at permanent work stations and in soundproof control booths. For periodic and manned and routine service measurements are taken at a distance of 0.5 m from the main engines and from each of the auxiliary mechanisms that require periodic servicing, and also at points as far away as possible from the main and noisiest auxiliary engines, but not closer than 1 m to bulkheads.

Everywhere else, unless specifically stipulated, the microphone should be set up for measurements with its axis pointing upward at a height of

APPROVED FOR RELEASE: 2007/02/08: CIA-RDP82-00850R000200100009-9

APPROVED FOR RELEASE: 2007/02/08: CIA-RDP82-00850R000200100009-9

1.5-1.65 m above the deck (floor). At work stations where people sit (control center, desk) and in leisure areas (sofa, bed) the microphone is set up at a height of 1.2-1.3 m.

Vibrations in engine, production and service rooms are measured at work stations and sitting positions, if the main working posture is the sitting position. In state rooms, social and medical rooms measurements are taken selectively on the deck, chairs and cots (when fastened to bulkheads).

Test Equipment. The equipment for noise and vibration measurements consists of acoustic and vibration receivers, amplifiers and amplitude or level indicators. In necessary cases the amplifier should be connectable to external systems for recording, frequency analysis and conversion of external variable parameters of noise and vibration to mean square values. For measuring noise and vibration during testing of acoustic conditions of inhabitability measurements should be taken only with instruments that meet the technical requirements of the USSR State Standards.

For measurements of noise at outside stations, on open decks and in the vicinity of a ship the test equipment should include, in addition to acoustic instruments, instruments for measuring wind velocity (anemometers) and distances (range finders). The anemometer should be capable of measuring wind velocities in the 1-10 m/s range, and the range finder should be capable of measuring distances of 15-100 m with an error of not more than 5%.

All instruments used for test measurements should be certified by agencies of the Soviet government and, if need be, should be equipped with tables of correction factors based on calibration results.

Many companies are manufacturing instruments that record the equivalent acoustic level or daily "dose" of noise (for example, the 4424 instrument of the Bryül' and K"yer firm). The main requirement on the development of these instruments is that the tolerable noise exposure time should be cut in half when the noise level exceeds by 3 dBA the acceptable level for an 8-hour exposure. These instruments are capable of monitoring how the crew observes safety requirements during periodically manned and unmanned servicing of power plants.

Measurement Procedure. During tests the overall noise level, in dBA, the acoustic pressure levels in all octave bands of the standard frequency range and the equivalent acoustic level, in dBA, are measured.

If the noise level exceeds the health standards through the spectrum additional measures may be taken to determine the cause of this violation and to determine measures to prevent harm to people due to exposure to excessive noise.

APPROVED FOR RELEASE: 2007/02/08: CIA-RDP82-00850R000200100009-9

APPROVED FOR RELEASE: 2007/02/08: CIA-RDP82-00850R000200100009-9

During tests in the vicinity of a ship, on its open decks and in air streams from the ventilation and air conditioning systems at stream velocities of more than 2 m/s, the microphone should be protected with a wind shield.

Vibration measurement is done in accordance with GOST 13731-68: "Mechanical Vibrations. General Requirements on Conducting Measurements." Measurements must be taken at every point in the vertical position and selectively (in individual cases) in the horizontal longitudinal and horizontal transverse directions to the axis of the ship. The highest measured values must be used for comparison with standards. Vibration is measured at each point at least three times, the results are averaged arithmetically with corrections factored in for the sensitivity of the sensor and for the nonuniformity of the frequency characteristic of the vibration meter channel (based on their test results).

If a person stands on the floor or sits on a platform at a test point, and there are no elastic cushions between his body and the bearing structure, the sensor should be installed on that rigid structure. In cases when the human body and the vibrating surface are separated by some elastic element (for instance a seat cushion), some rigid element may be placed during tests between the seat cushion and the person. But in this event care must be taken to ensure that this device does not exert an appreciable influence on the vibration as it is transmitted through the seat to the body, or does not cause additional vibrations.

BIBLIOGRAPHY

1. Alekseyev, S. V., A. V. Kadyskiy and G. A. Suvorov, "Some Data on Noise Sickness and Its Treatment. Physical Factors of Industrial Environment and Their Influence on the Body," TRUDY LSGMI [Proceedings of Leningrad Sanitation and Hygiene Medical Institute], Leningrad, Meditsina, 1972, pp 83-86.

2. Andreyeva-Galanina, Ye. Ts., E. D. Drogichina and V. G. Artamonova, "Vibratsionnaya Bolezn'" [Vibration Sickness], Moscow, Meditsina, 1961.

3. Bogolepov, I. I., "Basic Reasons for Technical Standardization of Noise," in the collection: "Shumoglusheniye" [Noise Absorption], edited by I. I. Bogolepov and D. A. Matelenk, Moscow, VTsNIIOT VTsSPS, 1976.

4. Vozhzhova, A. I., "Functional Displacements in Analyzer Systems due to Exposure to Noise and Vibration with Different Parameters," "Materialy Nauchnykh Rabot po Voprosam Gigiyeny Vodnogo Transporta (za 1964-1965 gg.)" [Materials of Scientific Research on Health Aspects of Water Transport (1964-1965)], Moscow, Meditsina, 1966, pp 33-34.

APPROVED FOR RELEASE: 2007/02/08: CIA-RDP82-00850R000200100009-9

APPROVED FOR RELEASE: 2007/02/08: CIA-RDP82-00850R000200100009-9

5. Vozhzhova, A. I. and V. K. Zakharov, "Influence of Noise and Vibrations of Ship Parameters on Analyzer Functions. Standardization of Noise and Vibrations in Transportation," in the book: "Zashchita ot Shuma i Vibratsiy na Sovremennykh Sredstvakh Transporta" [Noise and Vibration Control in Modern Transportation], Leningrad, Meditsina, 1968, pp 83-101, 117-143.

6. "On Biological Effect of Infrasound. Brief Theses of Reports of All-Russian Conference on Subject 'Noise and Noise Sickness, Clinical Aspects'," N. I. Karpov, S. V. Alekseyev, A. V. Kadyskin, G. A. Suvorov, TRUDY LSGMI, Vol 98, Leningrad, 1973, pp 76-77.

7. Lyubomudrov, V. Ye., B. N. Onopko and L. Ya. Basamygina, "Vibratsionno-Shumovaya Bolezn'" [Vibration-Noise Sickness], Kiev, Zdorov'ya, 1968.

8. "Some Data on Influence of Infrasound on Peripheral Blood Circulation. Physical Factors of Industrial Environment and Their Influence on the Body," N. I. Karpov, S. V. Alekseyev, A. V. Kadyskin, G. A. Suvorov, TRUDY LSGMI, Vol 97, Leningrad, 1972, pp 76-78.

9. "Normy Dopustimykh Urovney Shuma na Morskikh, Rechnykh i Ozernykh Sudakh i Pravila po Preduprezhdeniyu Ikh Vrednogo Vozdeystviya" [Standards of Acceptable Noise Levels on Oceangoing, River and Lake Ships and Rules on Prevention of Harm], No. 416-62, Moscow, Izd-vo Minzdrava SSSR, 1963.

10. Rusinova, A. P., "Manifestation of Noise Sickness in Steel Cable Factory Workers. Brief Theses of Reports of All-Russian Conference on Subject 'Noise and Noise Sickness, Clinical Aspects'," TRUDY LSGMI, Vol 98, Leningrad, 1973, pp 134-136.

11. "Sanitarnyye Normy Shuma v Pomeshcheniyakh Sudov Rechnogo Flota" [Noise Health Standards in Rooms of River Fleet Ships], No. 1404-76, Moscow, Izd-vo Minzdrava SSSR, 1976.

12. "Sanitarnyye Normy Vibratsii na Morskikh, Rechnykh i Ozernykh Sudakh" [Vibration Health Standards on Oceangoing, River and Lake Ships], No. 1103-73, Moscow, Izd-vo Minzdrava SSSR, 1973.

13. "Sanitarnyye Pravila dlya Morskikh Sudov SSSR" [Health Rules for Soviet Oceangoing Ships], Moscow, Transport, 1973.

14. "Sanitarnyye Pravila dlya Rechnykh i Ozernykh Sudov SSSR" [Health Rules for Soviet River and Lake Ships], Transport, 1965.

15. "Noise Sickness," Ye. Ts. Andreyeva-Galanina, S. V. Alekseyev, A. V. Kadyskin, G. A. Suvorov, in the book: "Shum i Shumovaya Bolezn'" [Noise and Noise Sickness], Leningrad, Meditsina, 1972, pp 216-271.

APPROVED FOR RELEASE: 2007/02/08: CIA-RDP82-00850R000200100009-9

APPROVED FOR RELEASE: 2007/02/08: CIA-RDP82-00850R000200100009-9

16. "Acoustics. Measurement of Noise on Board Vessels," International Standard ISO 2923, 1975 (E). (ISO/TC43).

17. "Guide for the Evaluation of Human Exposure to Wholebody Vibration," ISO/DIS 2631, 1972 (ISO/TC 108).

18. Jansen, G., "Zur Entstehung vegetativen Functionsstorungen durch Larmeinwirkung," ARCHIV FUR GEVERBEPATHOLOGIE UND GEWERBEHIGIENE, 1957, Vol 3, No 17, pp 238-261.

19. Lehrmann, G., "Der Kampf gegen den Larm -- eine richtige Aufgabe der prophylaktischen Medizine," DEITCH MED. W. SCHR., 1957, 82, 14, 5, pp 465-470.

20. "Proposal for a Guide to the Measurement of Acoustical Noise and Evaluation of Its Effect on Man," Sc.-7, 10, 1969 (ISO/TC 43).

APPROVED FOR RELEASE: 2007/02/08: CIA-RDP82-00850R000200100009-9

APPROVED FOR RELEASE: 2007/02/08: CIA-RDP82-00850R000200100009-9

CHAPTER 6. REDUCTION OF NOISE OF STEAM TURBINE AND GAS TURBINE POWER PLANTS

6.1. Basic Sources of Noise of STP and GTP

Steam Turbine Power Plants. The basic sources of noise in a ship STP are: the main turbine reducer assembly (MTRA), consisting of the steam turbine and reducer; the steam generator (boiler) with the machinery that services it -- turbocompressors or boiler blowers; the steam pipes and control valves; auxiliary turbogenerators.

The steam turbine of an MTRA, in view of features of its working process and high heat and sound insulation, cannot be the predominant source of the noise of a power plant; the main source of noise is the MTRA -- the gear reducer.

The steam boiler is usually not a source of noise, but under certain conditions gas dynamic self-oscillation processes can occur in the boiler itself, and more often in its tail parts, which contains various kinds of tube heat exchangers, and these processes produce not only strong noise, but also can damage the unit. The noise of the boiler blower system is generated in the region of the boiler blowers and in their air intake systems.

Boilers with high air pressure, supplied for fuel combustion -- so-called blown boilers, or steam generators, have been adopted in modern marine power engineering. Gas turbine compressors, which are powerful noise sources, are used for compressing the air.

Steam pipes (gas pipes) with control valves, just like reducers, are the principal sources of noise of STP and GTP. Methods of controlling the noise of these sources pose a certain problem and will be examined below.

The main source of noise in auxiliary steam generators, just as in MTRA, is the gear reducer. However, if it is well made the noise level of the steam generator will not exceed 85-95 dBA. Reducer quality depends to a considerable extent on the size of the gears: the smaller the gears are the more precisely they can be manufactured and the lower the noise level of the reducer. Soviet industry is producing quiet reducers for

APPROVED FOR RELEASE: 2007/02/08: CIA-RDP82-00850R000200100009-9

APPROVED FOR RELEASE: 2007/02/08: CIA-RDP82-00850R000200100009-9

turbogenerators. The noise problem usually does not appear in reducerless turbogenerators, in which power is transmitted directly from the turbine to the generator, if they are properly assembled and the rotors are balanced.

Atomic power plants differ little in terms of noise from ordinary STP, with the exception of the fact that in them such sources of noise as the steam pipes and control valves play an important role.

Gas Turbine Plants. Unlike a steam turbine, a gas turbine engine (GTE) has the greatest influence on the noise level of MTRA. In view of specific design features and of the nature of working processes of GTE, the noise it produces can reach 110-120 dBA at a distance of 1 m, and this level is substantially higher than the acceptable standards. If necessary measures are not taken promptly abnormal working conditions can arise on a ship.

GTP noise, like STP noise, has high-frequency spectra, which explains its special hazard. The basic GTP noise sources, other than the gas turbine engine, are: the reducer of the MTRA, the air ducts with various types of control systems, and the exhaust system of the power plant.

Two types of gas turbine power plants are used on ships: "heavy" and "light" GTP. A heavy GTP is designed for a long service life and is very heavy and large. Light GTP are usually built on the basis of high performance aviation gas turbine engines, which have a shorter service life. Therefore they are replaced several times during the service life of a ship. Their chief distinction from the standpoint of noise is the fact that they are very compact. They have considerably smaller areas of sound-emitting surfaces and accordingly less acoustic power, radiated by the gas turbine engine housing.

The major noise sources in both types of gas turbine power plants are the air intake systems of the turbocompressors, the noise level of which reaches 140-150 dBA. This noise is reduced by installing a system of special mufflers, which should have an effectiveness of 60-75 dBA.

The exhaust noise of heavy marine gas turbine power plants is considerably lower due to the installation of various kinds of heat exchangers in the flues. If the discharge velocity of the exhaust gases does not exceed 25-35 m/s, the exhaust noise poses no danger and exhaust mufflers need not be installed. The acoustic level of small open exhaust ships with short exhaust pipes can reach 100-110 dBA. Therefore mufflers must be installed.

The development of extremely noisy gas dynamic self-oscillation processes in the heat exchangers of the exhaust system is a special case for a gas turbine power plant.

APPROVED FOR RELEASE: 2007/02/08: CIA-RDP82-00850R000200100009-9

APPROVED FOR RELEASE: 2007/02/08: CIA-RDP82-00850R000200100009-9

6.2. Gas Turbine Engine Noise. Turbocompressor Noise Reduction

Causes of Gas Turbine Engine Noise. The main source of GTE noise is the turbocompressor. Basically axial multistage compressors are used in marine gas turbine power plants. More than 95% of the acoustic power of GTP is radiated by the compressor air intake (L_N = 135-150 dBA). The compressor also plays a principal role in the spectrum of the noise emitted by the gas turbine engine housing, although the acoustic power of the housing is 20-30 dBA less than that of the intake.

The noise spectra of GTE have strong discrete (audio) components, which on high frequencies are produced by aerodynamic rotor-stator interaction of the blades in the compressor (so-called blade, or siren noise). Mechanical noise, related to rotor disbalance, misalignment of the shafts of the GTE and power untilizers, etc., or related to GTE manufacture and assembly deficiencies, can occur on low frequencies. Discrete components include fundamental frequencies, determined by the formulas

$$f_e = n/60 \text{ and } f_{b1} = nz_1/60 \qquad (6.2.1)$$

and their harmonics. (Here n is the rotor speed, in rpm; z_1 is the number of blades of the first stage of the compressor).

When the rotors are well balanced dynamically (disbalance does not exceed 2-6 g·cm) and are properly assembled the low-frequency discrete components of mechanical origin decrease substantially.

The high-frequency audio and continuous components of noise propagate into the intake and supercharger ducts of the compressor basically through the air stream. Perturbing forces are transmitted through the vibrating stator blades to the gas turbine engine housing and, as a result of aerodynamic interaction of the perturbed flow, to the walls of the compressor itself and of the supercharger and intake ducts. The compressor ducts of heavy gas turbine power plants play a special role in the emission of noise by the housing. The metal walls of the ducts do not isolate the high-frequency aerodynamic components of the stream very well due to matching resonance. Therefore they are very strong noise radiators.

The noise and vibration spectra of the supercharger duct of the low-pressure compressor (LPC) of the GTU-20 gas turbine power plant are shown in Figure 6.1. As can be seen by the curves, the noise and vibration spectra are extremely intense and perfectly identical. The analogous phenomena also occur in the intake duct all the way from the compressor to the muffler.

APPROVED FOR RELEASE: 2007/02/08: CIA-RDP82-00850R000200100009-9

APPROVED FOR RELEASE: 2007/02/08: CIA-RDP82-00850R000200100009-9

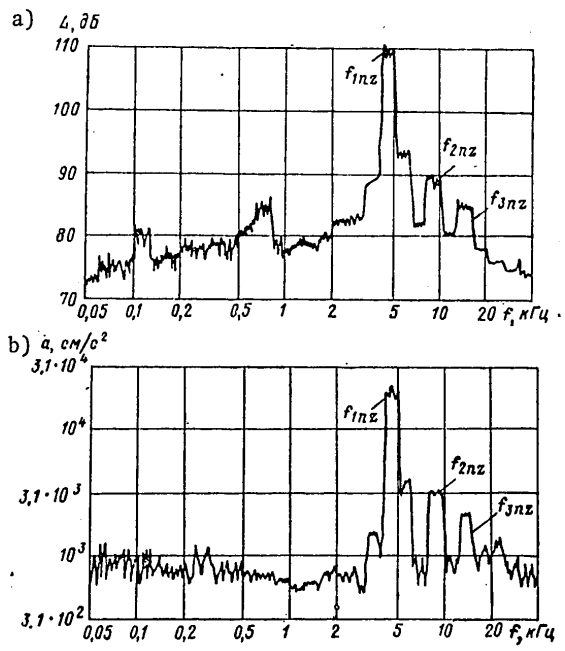

Figure 6.1. Noise (a) and vibration (b) of supercharger pipe of axial compressor of gas turbine power plant. [дБ=dB; c=s; кГц=kHz]

Calculation of Gas Turbine Engine Noise. The acoustic power level L_N, in dB, in the intake of the axial compressor can be calculated through the following formula, proposed by Ye. Ya. Yudin and S. N. Kuznetsov [14]:

[ад=ad]

$$L_N = 10\lg\frac{0,5}{N_0}\left(\frac{1-\eta_{ад}}{\eta_{ад}}\right)^2\frac{G_t^2 H_{ад}^2}{\rho c^3 D_2^2}; \qquad (6.2.2)$$

where η_{ad} is the adiabatic efficiency of the first compressor stage; G_t is the mass flow rate through the compressor, in kg/s; H_{ad} is the adiabatic head of the stage, in J/kg; D_2 is the diameter of the drive wheel of the first stage, in m; $N_0 = 10^{-12}$ W is the standard threshold value of acoustic power.

The theoretical relative noise spectrum of a compressor intake is given in Figure 6.2 for determining the spectrum of acoustic power levels. Dimensionless frequency $\overline{f} = 60\ f/n$, where f is the frequency of the third-octave band, in Hz, is plotted on the abscissa axis; n is the compressor rotation

APPROVED FOR RELEASE: 2007/02/08: CIA-RDP82-00850R000200100009-9

APPROVED FOR RELEASE: 2007/02/08: CIA-RDP82-00850R000200100009-9

in rpm. The spectrum in absolute levels is determined by subtracting from level L_N, calculated by formula (6.2.2), the relative levels ΔL in each third-octave band, indicated in the typical spectrum.

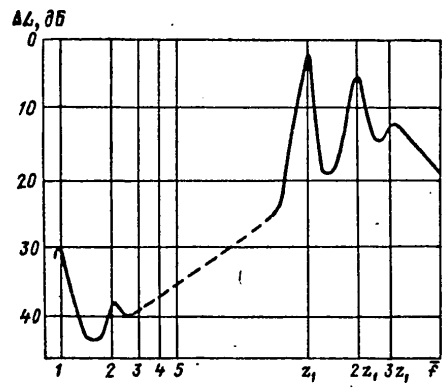

Figure 6.2. Typical spectrum of acoustic power of gas turbine power plant compressor intake. z -- number of blades of rotor stage.

The levels of the discrete component $\bar{f} = nz$ and of its harmonics, where z is the number of blades of the first rotor stage, are determined on frequencies f = z, 2z, 3z, ...

The spectra of the acoustic power levels L_N, in dB, in the intake and exhaust of gas turbine power plants can be estimated on the basis of empirical formulas and typical spectra of ASME [22]:

for intake noise

$$L_N = 127 + 10 \lg G_t + 3{,}5; \qquad (6.2.3)$$

for exhaust noise

$$L_N = 119 + 10 \lg G_t + 3{,}5. \qquad (6.2.4)$$

These expressions are most exact for a gas turbine engine with a specific air flow rate $G_t/N_e = 7.5 \cdot 10^{-3}$ kg/(s•kW), where N_e is the power of the GTE, in kW; G_t is the air flow rate, in kg/s. The spectrum is calculated on the basis of the relative spectra in the octave bands (Figure 6.3). The acoustic power level in any octave L_N can be calculated by subtracting from the total level L_N, calculated by formulas (6.2.3) and (6.2.4), the

APPROVED FOR RELEASE: 2007/02/08: CIA-RDP82-00850R000200100009-9

APPROVED FOR RELEASE: 2007/02/08: CIA-RDP82-00850R000200100009-9

corresponding values ΔL_{in} or ΔL_{suc}, determined by the graphs in Figure 6.3. The calculation data determine the levels without consideration of acoustic attenuation in the pipes and heat exchangers.

The acoustic power radiated by the uninsulated gas turbine power plant housing (intake and exhaust noises are ignored) can be calculated on the basis of the typical spectra of the United States standard [19] in Figure 6.4. The spectra are given as functions of gas flow rate G_t through the flow part (15-180 kg/s). This approximately corresponds to effective powers of 2, 6, 12 and 24 MW at normal atmospheric pressure and at an air temperature of 27°C.

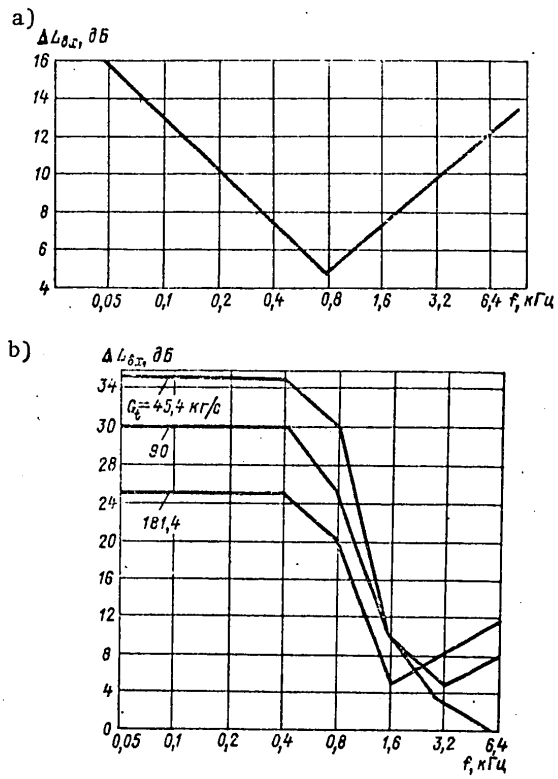

Figure 6.3. Correction curves for calculating acoustic power spectra of gas turbine power plant: a -- exhaust; b -- intake. [вх=in; дБ=dB; кГц=kHz; кг=kg; c=s]

APPROVED FOR RELEASE: 2007/02/08: CIA-RDP82-00850R000200100009-9

APPROVED FOR RELEASE: 2007/02/08: CIA-RDP82-00850R000200100009-9

From this point the acoustic pressure levels are calculated in accordance with GOST 8.055-73. To calculate the noise radiated by the housing it is necessary to consider the acoustic characteristics of the engine room, and to calculate the acoustic pressure levels in the intake and exhaust -- the attenuation in the flue and manifold chamber and the directivity of radiation at the discharge of the intake and exhaust pipes. Basic information on these problems is given in the literature [6]. The required effectiveness of exhaust systems -- in the intake and in the exhaust, and of the sound-insulating housing for gas turbine engines is determined by subtracting the acoustic pressure levels produced by the noise source and the acceptable standard for the examined work station.

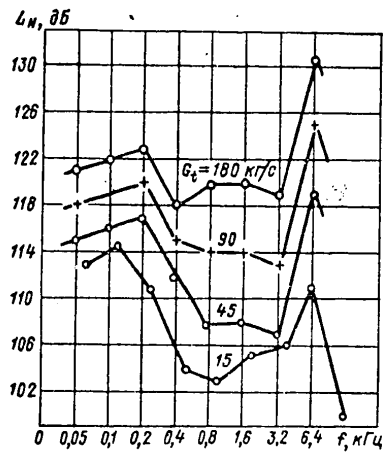

Figure 6.4. Typical spectra for calculating acoustic power of noise radiated by gas turbine power plant housing. [дБ=dB; кг=kg; с=s; кГц=kHz]

Methods of Reducing Noise at the Source. Seventy-five percent of the acoustic power of a multistage axial compressor is radiated by the first two stages. Therefore it is necessary from the outset to focus attention on these stages during the design of a quiet compressor.

The most effective way to reduce intake noise is to "block" the sound at the entrance into the flow part of the compressor. The reduction of noise as a function of flow velocity in the critical compressor intake cross section obeys the law

$$\Delta L = 10 \lg \frac{1}{1 - M}, \qquad (6.2.5)$$

where M is the Mach number.

APPROVED FOR RELEASE: 2007/02/08: CIA-RDP82-00850R000200100009-9

APPROVED FOR RELEASE: 2007/02/08: CIA-RDP82-00850R000200100009-9

When the flow velocity is close to the speed of sound, i.e., when $M \approx 1$, acoustic energy is not transferred into the intake pipe, and all the vibration energy is carried away by the flow. Here the acoustic power in the supercharger pipe is doubled and increases by only 3 dB. For M = 0.9-1.0 noise is reduced by 30-35 dB (in practice a system begins to operate at $M \geqslant 0.6$-0.7).

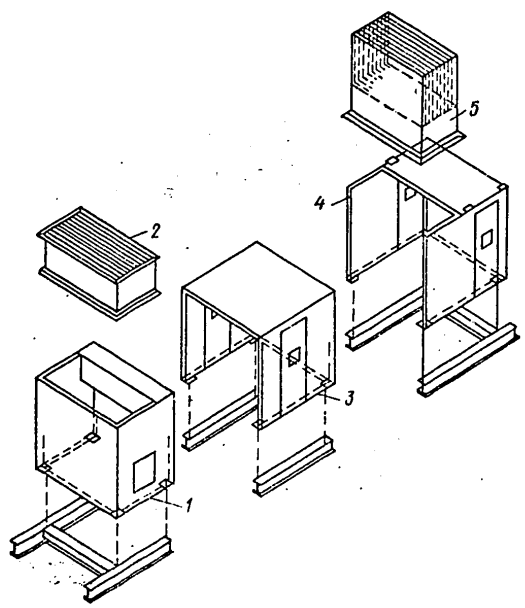

Figure 6.5. Sectional sound-insulating housing with mufflers.

The reduction of noise due to the increase of axial clearances can be evaluated through the formula

$$\Delta L_a = 20 \lg \bar{\delta}/\bar{\delta}_a, \qquad (6.2.6)$$

where $\bar{\delta}_a$ is the initial dimensionless axial clearance.

When $\bar{\delta}/\bar{\delta}_a = 2.0$ it is possible to achieve a 4-6 dB noise reduction. The axial clearance can reach the distance of two rotor blade chords.

It is recommended that the optimum ratio of rotor and stator blade numbers be used for reducing noise. By optimizing this ratio it is possible to reduce the noise level by 3-5 dB. By angling the blades at approximately

APPROVED FOR RELEASE: 2007/02/08: CIA-RDP82-00850R000200100009-9

APPROVED FOR RELEASE: 2007/02/08: CIA-RDP82-00850R000200100009-9

10° compressor noise can be reduced by 3-4 dB. The blade pitch has comparatively little effect on compressor noise; a change of pitch by 5° produces a 1-2 dB change of the acoustic level. Deviation of the mean attack angle by 1° from optimum in the maximum thrust mode increases noise by 1 dB. Blade thickness has virtually no effect on compressor noise [13].

Gas turbine engine noise can be reduced by using a sound-insulating enclosure and the corresponding intake and exhaust mufflers.

Requirements on Gas Turbine Engine Sound-Insulating Housing. The purpose of a sound-insulating housing is to reduce audible noise emitted by the gas turbine power plant housing. One-piece enclosures may be used for small GTP; sectional frame or frameless housings that provide access to the GTE for service without dismantling the housing, are usually employed for heavy marine gas turbine power plants.

It is extremely important to install intake and exhaust mufflers in the immediate vicinity of the gas turbine engine, or even inside of the housing itself. This precludes complicated and expensive measures for sound insulation of pipes.

A moduluar box type of housing, in which there are access doors for servicing the gas turbine power plant, is recommended for more ready access to the engine. An example of this type of housing is illustrated in Figure 6.5. It consists of three removable sections. Exhaust muffler 5 and intake muffler 2 are inserted in turbine section 4 and compressor section 1, respectively. Power turbine section 4 and middle section 3 have access doors. Profiled elastic gaskets, which should meet the requirements of high oil-, gasoline- and heat resistance, should be used for sealing hatches, covers and doors. This type of housing provides a noise reduction on 500 Hz of 15-25 dB. The noise reduction on low frequencies, for example on the gas turbine engine rotation frequency (80-150 Hz) is 5-8 dB.

6.3. Elimination of Gas Dynamic Free Vibrations in Exhaust Pipes

Gas Dynamic Free Vibrations as Physical Process. Under certain conditions the gas flow in two heat exchangers, installed in the exhaust ducts of gas turbine power plants and in the tail parts of steam boilers, become unstable in relation to natural vibrations of gas exchange. This leads to free vibrations, which are maintained by the kinetic energy of the gas flow. This is often manifested externally as destructive vibration of the heat exchanger and loud noise in the engine room and at the discharge of the exhaust pipe (Figure 6.6).

Before the initial natural vibrations can occur there must be strong pressure pulsations in the flow around the exchanger bundles, and therefore the frequency of flow separation processes should be close to the frequency of free vibrations in the flue. The frequency of free vibrations in the flue is

APPROVED FOR RELEASE: 2007/02/08: CIA-RDP82-00850R000200100009-9

APPROVED FOR RELEASE: 2007/02/08: CIA-RDP82-00850R000200100009-9

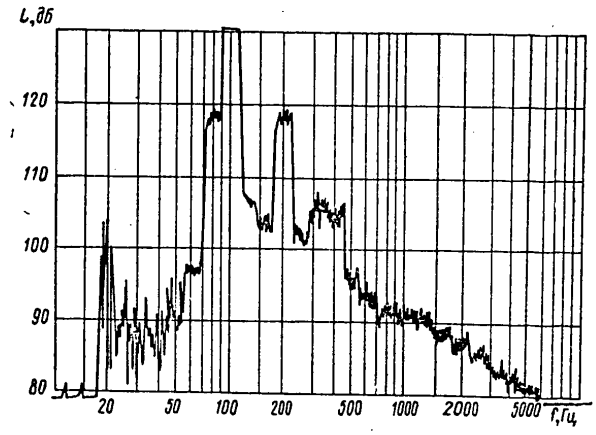

Figure 6.6. Noise spectrum at smokestack discharge (r = = 1 m, <45°) with gas dynamic free vibrations in gas flue of utilizer steam generator. [дБ=dB; Гц=Hz]

$$\Omega_i = \frac{c}{2l} i = \frac{20{,}1\sqrt{T}}{2l}, \qquad (6.3.1)$$

where l is the cross section of the flue perpendicular to the pipes and flow; i is the mode of vibrations; T is the absolute temperature of the gas. gases.

Circulation $\Delta\Gamma$ around the cylinder occurs when eddy separation takes place. According to N. Ye. Zhukovskiy's theorem, force impulse

$$\Delta P = \rho v \Delta\Gamma$$

acts upon the medium from the body in this case.

Since in eddy separation on different sides of the cylinder circulation acquires opposite signs, positive and negative impulses alternate. These periodic pulses radiate acoustic waves.

The eddy frequency is determined by the formula

[п=b]

$$\omega = 2\pi \mathrm{St} \frac{\bar{v}}{d_п}, \qquad (6.3.2)$$

where $\bar{v}$ is the average flow velocity; d_b is the characteristic geometric dimension of the bundle, which in the ensuing analysis will be set equal to pipe diameter d.

APPROVED FOR RELEASE: 2007/02/08: CIA-RDP82-00850R000200100009-9

APPROVED FOR RELEASE: 2007/02/08: CIA-RDP82-00850R000200100009-9

The value $\bar{v}$ is estimated in consideration of the blocking of the flow by the pipes and by the constriction of the flow by turns:

[Г=f]
$$\bar{v} = \frac{\psi s_{\text{г}}}{s_{\text{г}} - s_{\text{т}}} v_{\infty} = \frac{\psi s_{\text{г}}/s_{\text{т}}}{s_{\text{г}}/s_{\text{т}} - 1} v_{\infty}, \qquad (6.3.3)$$

where ψ is the coefficient of constriction of the flow by a turn; s_f is the cross section area of the flue, perpendicular to the gas flow; s_t is the cross section area of the flue, blocked by the tubes; v_∞ is the gas velocity in front of the bundle.

For a strong free vibration process the frequencies of eddy separation ω^* and of natural vibrations in the flue are identical, i.e., $\omega^* = \Omega_i$. Then, based on equations (6.3.1) and (6.3.2), we may write the following expression for the free vibration process in the flue:

$$\frac{\omega^*}{\Omega_i} = 0{,}1 \frac{\mathrm{St}^* \bar{v}}{i \sqrt{T}} \mu = 1, \qquad (6.3.4)$$

where $\mu = l/d$ is a geometric parameter; St* is the effective Strouhal number under conditions of induced separation, which is different from the Strouhal number for free eddy turbulence.

The number St* can be determined on the basis of the generalized characteristics of gas dynamic vibrations, determined by TsNIIMF [Central Scientific Research Institute of the Maritime Fleet] experimentally [6] (Figure 6.7) for different heat exchangers of steam-gas and gas turbine installations. The sawtooth curve represents abrupt changes of the values of St*, computed on the basis of the experimental data by formula (6.3.2). An abrupt change of St* occurs at the instant of transition to a different frequency of natural vibrations in the flue.

A change of St* occurs in a narrow range of values, which may be assumed approximately to be 0.2-0.1. This greatly facilitates the calculation of heat exchangers in terms of resistance to gas dynamic pulsations. The maximum value St* = 0.2 corresponds to the beginning of a free vibration process, and the minimum value St* = 0.1 corresponds to the time of destruction of the free vibration process or of its conversion to frequency Ω_{i+1}.

Calculation of Position of Stabilizing Baffles. The easiest way to eliminate vibrations is to install baffles in the flue along the flow in cross sections parallel to the bundles. On the basis of formula (6.3.4) we may write the expression for the excitation of vibrations:

$$1 \leqslant i \frac{10 \sqrt{T}}{\bar{v}\mu} \leqslant 2. \qquad (6.3.5)$$

APPROVED FOR RELEASE: 2007/02/08: CIA-RDP82-00850R000200100009-9

APPROVED FOR RELEASE: 2007/02/08: CIA-RDP82-00850R000200100009-9

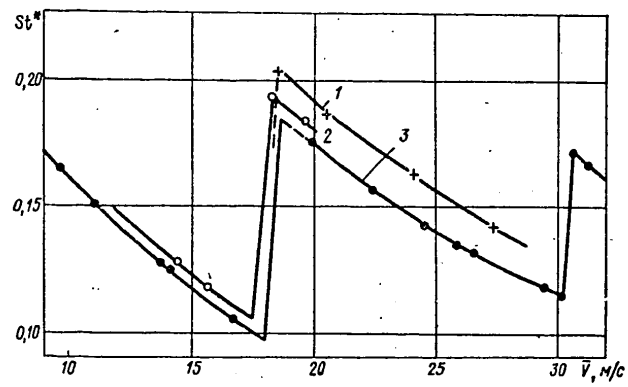

Figure 6.7. Changes of St*: 1 -- for No. 1 economizer of PGU-1; 2 -- for No. 3 economizer of PGU-2; 3 -- for KVKA 6/5 steam generator of GTU-20 gas turbine power plant. [c=s]

This formula is used for evaluating the possibility of the occurrence of vibrations in the flue. Vibrations can occur if the values of the middle part of the inequality for some i = 1, 2, 3, ..., etc., fall within the range of 1-2. The parameters T and $\bar{v}$ are taken on the basis of thermal calculation data or on the basis of measurements. If the calculation shows the existence of vibrations the geometric parameter μ should be changed in order to eliminate them.

There are minimum and maximum values of μ, for which vibrations cannot occur:

$$\mu_{max} = \frac{100\sqrt{T}}{\bar{v}} \quad \text{and} \quad \mu_{min} = \frac{50\sqrt{T}}{\bar{v}}. \tag{6.3.6}$$

The value of parameter μ must be selected so as to satisfy the condition

$$\mu_{min} \leqslant \mu \leqslant \mu_{max}. \tag{6.3.7}$$

When baffles are installed the calculation is done by the inequality

$$l \leqslant \frac{50\sqrt{T}\,d}{\bar{v}}. \tag{6.3.8}$$

The minimum critical value l_{min} is calculated by the formula

$$l_{min} = \frac{50\sqrt{T}\,d}{\bar{v}}. \tag{6.3.9}$$

APPROVED FOR RELEASE: 2007/02/08: CIA-RDP82-00850R000200100009-9

APPROVED FOR RELEASE: 2007/02/08: CIA-RDP82-00850R000200100009-9

Vibrations of any form will be impossible if $l < l_{min}$.

Sheet steel baffles 1-3 mm thick are installed across the entire width of the heat exchanger, parallel to the tubes. To eliminate pulsations it is sufficient to place baffles just behind the bundles. The types of fasteners are selected structurally such that the baffle will not bear any load, other than its own weight, under normal conditions. Number k of baffles is determined by the condition $k = l/l_{min} - 1$, where the fraction is rounded off to the next larger integer.

Stabilizing baffles, designed in accordance with the calculation presented above, usually completely eliminate the possibility of gas dynamic free vibrations in flues in all calculated operating modes of a power plant.

6.4. Gas Turbine Engine Intake and Exhaust Mufflers and Their Calculation[1]

Designs of Mufflers and Requirements on Them. The designs of mufflers used for the turbocompressors of diesel engines are examined in Chapter 5. A typical design of a plate-type muffler is illustrated in Figure 6.8. The muffler consists of a package of 800 mm long corrugated steel plates, faced with a 16 mm thick porolon film. The air space between the plates is 50 mm. Efficiency on the compressor blade frequency is 29 dB, aerodynamic drag is 330 Pa at a mass air flow rate of 34.6 kg/s and channel flow velocity of 24 m/s. Flat plates, which are easier to manufacture, are more often used for gas turbine power plant mufflers. The optimum air space, thickness and acoustic properties of the material are determined by calculation.

Mufflers with air gaps of not more than 20-60 mm and with baffle plates of the same thickness may be used for the intake; mufflers with thick (100-200 mm) baffle plates and with correspondingly larger (100-250 mm) air spaces, should be used for the gas turbine power plant exhaust due to lower frequency noise. Mufflers with a 50% blockage of the cross section are often used; in this case the thickness of the plates is equal to the air gap. The mufflers should be installed in the immediate vicinity of the source.

The required efficiency of the intake muffler of a gas turbine power plant should be very high: 60-75 dB. Therefore it is necessary sometimes to install a second muffler in addition to the main one, or to coat the inside of the air duct with a sound-absorbing material (SAM). The extra muffler may be installed in the air intake chamber (see Figure 6.8); it is calculated for the frequency spectrum that comes out of the main muffler.

The materials indicated in Table 6.1 are used for sound absorption. Refractory materials with a melting point not lower than 600°C are used for the exhaust. The SAM is coated with glass fiber or with several layers of

[1]This section was written by N. V. Pogrebnyak with V. I. Zinchenko's assistance.

APPROVED FOR RELEASE: 2007/02/08: CIA-RDP82-00850R000200100009-9

APPROVED FOR RELEASE: 2007/02/08: CIA-RDP82-00850R000200100009-9

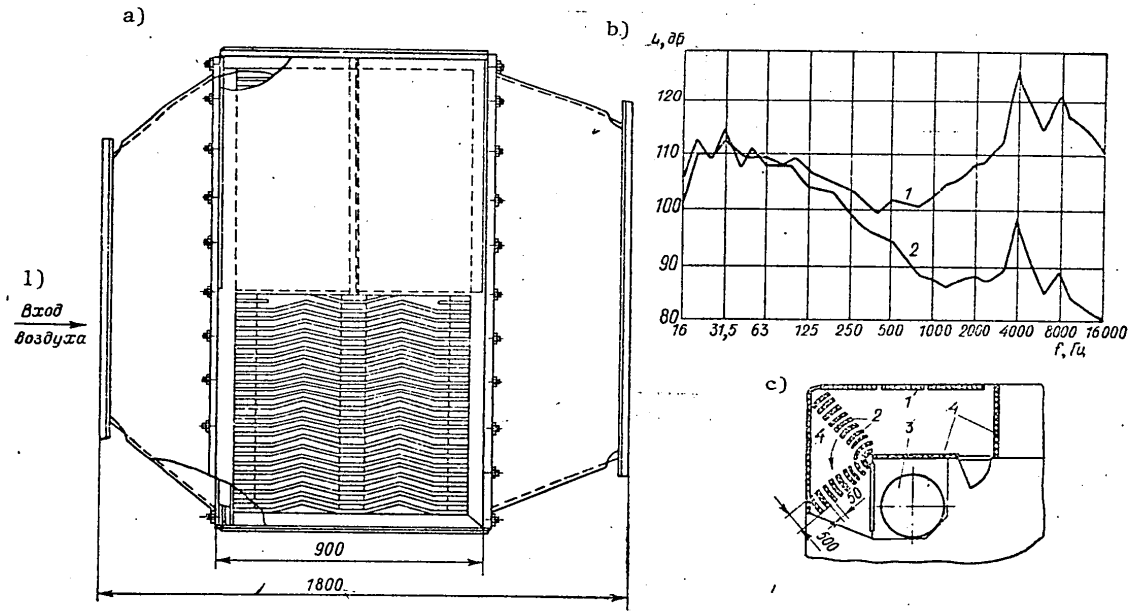

Figure 6.8. Gas turbine power plant intake muffler (a); its acoustic effect (b) (1 -- without muffler; 2 -- with muffler); diagram of air intake chamber with muffler of gas turbine ship "Parizhskaya kommuna" (c). 1 -- adiabatic louvers; 2 -- muffler; 3 -- TKND water intake pipe; 4 -- soundproofing hood.
Key: 1. Air intake

APPROVED FOR RELEASE: 2007/02/08: CIA-RDP82-00850R000200100009-9

APPROVED FOR RELEASE: 2007/02/08: CIA-RDP82-00850R000200100009-9

glass fiber cloth to prevent blowout; at flow velocities above 50 m/s the SAM is covered with 5-10 mm thick steel wool or with matted wire; all of this is covered with galvanized wire screen and perforated sheet metal. Uncovered coarse felt or elastic polyurethane foam (porolor) may be used in the intake at air velocities of 15-25 m/s.

Mufflers must have the minimum aerodynamic drag: a drag of 500-600 Pa leads to a 0.5-1.0% power loss of a gas turbine power plant. The following drags for the intake and exhaust channels of GTP, in Pa [19], are considered to be acceptable:

Intake along with muffler	1,000
Exhaust along with muffler (without heat exchangers)	1,000
Muffler at intake	500
Muffler at exhaust	500
Intake filter	130
Utilizer boiler	1,500-3,000
Regenerator	1,000-6,000

The aerodynamic drag ΔH, in Pa, of a muffler can be calculated by the formula

[c=d; в=a]

$$\Delta H = 4{,}9\frac{\xi_c a \rho \bar{v}^2}{d_в g}, \qquad (6.4.1)$$

where ξ_d is the drag taken from nomograms [7]. For baffle plate mufflers one may use ξ_d = 0.04-0.06 in consideration of losses in the diffuser and confuser; a is the length of the calculated channel, in m; d_a is the air gap between the plates, in mm; ρ is the density of air, in kg/m^3; $\bar{v}$ is the velocity of air, averaged through the cross section of the channel, in m/s.

The dimensions of a muffler are determined by the length of the active part, found from acoustic calculation, and by the cross section necessary for the passage of air. Air velocity $\bar{v}$ should fall within the range $\bar{v}$ = = 15-35 m/s. The necessary total area for the passage of gases is

$$S = \frac{G}{\rho \bar{v}}, \qquad (6.4.2)$$

where G is the mass air flow rate of the gases.

The necessary number of channels is

$$n = \frac{S}{d_в b}, \qquad (6.4.3)$$

where d_a is taken on the basis of acoustic calculation; b is baffle plate width (taken from design considerations).

APPROVED FOR RELEASE: 2007/02/08: CIA-RDP82-00850R000200100009-9

APPROVED FOR RELEASE: 2007/02/08: CIA-RDP82-00850R000200100009-9

Table 6.1. Acoustic Parameters of Certain SAM Used in Active Mufflers

Kind of SAM	Parameter*		Frequency, Hz							
			250	315	400	500	630	800	1000	1250
PPU-ET Poroplast polyurethane (porolon), ρ = = 40 kg/m^3	$\gamma_1=\beta+j\alpha$	β	0,12	0,14	0,16	0,19	0,22	0,27	0,3	0,34
		α	0,15	0,18	0,24	0,29	0,36	0,44	0,52	0,62
	$W_1=W_R+jW_j$	W_R	4,60	4,50	4,40	4,30	4,10	3,90	3,70	3,40
		W_j	—0,90	—0,80	—0,70	—0,60	—0,50	—0,40	—0,30	—0,20
Brand VT-4S heat-sound insulating material, ρ = = 50 kg/m^3	$\gamma_1=\beta+j\alpha$	β	0,060	0,060	0,061	0,062	0,070	0,080	0,081	0,100
		α	0,065	0,080	0,100	0,120	0,140	0,180	0,220	0,260
	$W_1=W_R+jW_j$	W_R	1,80	1,52	1,40	1,37	1,32	1,30	1,25	1,20
		W_j	—0,90	—0,70	—0,50	—0,40	—0,32	—0,30	—0,30	—0,20
Ultrasuperfine basaltic fiber lap, ρ = 20-25 kg/m^3	$\gamma_1=\beta+j\alpha$	β	0,08	0,09	0,10	0,11	0,15	0,20	0,25	0,30
		α	0,300	0,330	0,370	0,410	0,450	0,500	0,520	0,550
	$W_1=W_R+jW_j$	W_R	3,40	3,17	2,94	2,70	2,47	2,26	2,07	1,87
		W_j	—1,70	—1,50	—1,32	—1,20	—1,09	—1,00	—0,90	—0,81
Ultrasuperfine glass fiber lap, ρ = 8-10 kg/m^3	$\gamma_1=\beta+j\alpha$	β	0,060	0,075	0,080	0,090	0,110	0,130	0,140	0,190
		α	0,100	0,150	0,190	0,220	0,260	0,300	0,330	0,360
	$W_1=W_R+jW_j$	W_R	2,00	1,90	1,80	1,70	1,60	1,56	1,52	1,50
		W_j	—0,90	—0,77	—0,65	—0,55	—0,45	—0,35	—0,26	—0,20
Brand ATM-1 heat-sound insulating material, ρ = = 10 kg/m^3	$\gamma_1=\beta+j\alpha$	β	0,032	0,048	0,060	0,080	0,100	0,120	0,142	0,161
		α	0,060	0,090	0,135	0,180	0,210	0,260	0,320	0,380
	$W_1=W_R+jW_j$	W_R	2,40	2,20	1,85	1,80	1,75	1,70	1,62	1,60
		W_j	—1,00	—0,7	—0,55	—0,48	—0,40	—0,38	—0,35	—0,31

*The letter j denotes imaginary unit.

APPROVED FOR RELEASE: 2007/02/08: CIA-RDP82-00850R000200100009-9

APPROVED FOR RELEASE: 2007/02/08: CIA-RDP82-00850R000200100009-9

Table 6.1 (continued)

Kind of SAM	Parameter		Frequency, Hz							
			1600	2000	2500	3150	4000	5000	6300	8000
PPU-ET Poroplast polyurethane (porolon), ρ = 40 kg/m^3	$\gamma_1=\beta+j\alpha$	β	0,36	0,37	0,39	0,40	0,42	0,45	0,48	0,42
		α	0,74	0,86	0,95	0,98	1,03	1,00	1,00	1,03
	$W_1=W_R+jW_j$	W_R	3,30	3,00	2,80	2,70	2,60	2,50	2,45	2,60
		W_j	—0,20	—0,20	—0,20	—0,20	—0,20	—0,20	—0,20	—0,20
Brand VT-4S heat-sound insulation, ρ = 50 kg/m^3	$\gamma_1=\beta+j\alpha$	β	0,120	0,140	0,170	0,170	0,170	0,170	0,170	0,170
		α	0,340	0,410	0,480	0,540	0,600	0,680	0,720	0,740
	$W_1=W_R+jW_j$	W_R	1,19	1,13	1,10	1,08	1,05	1,01	1,01	1,10
		W_j	—0,16	—0,12	—0,11	—0,11	—0,11	—0,11	—0,11	—0,11
'Ultrasuperfine basaltic fiber lap, ρ = 20-25 kg/m^3	$\gamma_1=\beta+j\alpha$	β	0,35	0,41	0,47	0,52	0,57	0,59	0,61	0,63
		α	0,570	0,610	0,640	0,690	0,720	0,780	0,800	0,830
	$W_1=W_R+jW_j$	W_R	1,67	1,5	1,85	1,21	1,11	1,04	1,01	1,05
		W_j	—0,74	—0,65	—0,61	—0,57	—0,54	—0,53	—0,52	—0,50
Ultrasuperfine glass fiber lap, ρ = 8-10 kg/m^3	$\gamma_1=\beta+j\alpha$	β	0,210	0,240	0,280	0,310	0,340	0,380	0,410	0,450
		α	0,370	0,415	0,440	0,460	0,480	0,505	0,520	0,540
	$W_1=W_R+jW_j$	W_R	1,47	1,45	1,45	1,44	1,44	1,44	1,44	1,44
		W_j	—0,15	—0,10	—0,08	—0,06	—0,05	—0,04	—0,04	—0,04
Brand ATM-1 heat-sound insulation, ρ = 10 kg/m^3	$\gamma_1=\beta+j\alpha$	β	0,180	0,198	0,205	0,210	0,220	0,220	0,220	0,220
		α	0,440	0,510	0,600	0,690	0,740	0,800	0,820	0,840
	$W_1=W_R+jW_j$	W_R	1,58	1,50	1,50	1,50	1,50	1,50	1,50	1,50
		W_j	0,30	—0,29	—0,27	—0,25	—0,25	—0,25	—0,25	—0,25

APPROVED FOR RELEASE: 2007/02/08: CIA-RDP82-00850R000200100009-9

APPROVED FOR RELEASE: 2007/02/08: CIA-RDP82-00850R000200100009-9

Then the cross section of a muffler in consideration of obstruction by the baffle plates is

[п=p; в=a]

$$S_{п} = n(d_{п} + 2d_{1} + d_{п})b, \tag{6.4.4}$$

where d_p is plate thickness; d_1 is the thickness of the muffler wall liner.

Acoustic Calculation of Muffler. There are several ways to calculate the attenuation of acoustic waves as they slide along the absorbing walls of an acoustic wave guide. They are based on the principles of energy theory, wave impedance theory and theory of lamellar inhomogeneous wave guides.

According to energy theory attenuation ΔL, in dB/m, is determined by the familiar expression

$$\Delta L = 2{,}2\alpha^* \frac{l}{d_{п}}. \tag{6.4.5}$$

The empirical attenuation coefficient α*, which depends on the acoustic properties of the liner, and on the design of the channel, is introduced in formula (6.4.5). This method is used for approximate calculations. Calculation by formula (6.4.5) is inconvenient because it is first necessary to estimate the values of L* experimentally for an examined muffler design. The values of L* for certain materials are presented in Table 6.2 in application to baffle plate mufflers.

Helmholtz equation is based on wave impedance theory (see Chapter 1):

$$\Delta\Phi + k^2\Phi = 0. \tag{6.4.6}$$

The liner is characterized only by normal surface impedance

$$Z_a = \frac{p}{\dot{y}}, \tag{6.4.7}$$

i.e., there is assumed to be in the material itself only the normal component of vibration velocity. The solution of equation (6.4.6) in consideration of boundary conditions (6.4.7) and of the quality of the normal vibration velocity to zero along the axis of the channel, leads to the equation

$$\frac{j\omega\rho \operatorname{ctg}\sqrt{\Gamma^2 + k^2}\, d_0}{\sqrt{\Gamma^2 + k^2}} = z_a, \tag{6.4.8}$$

where d_0 is one-half the air space between the plates, and the real part of propagation constant Γ determines the acoustic attenuation per unit length of the channel:

$$\Delta L = 20 \lg e \operatorname{Re} \Gamma.$$

APPROVED FOR RELEASE: 2007/02/08: CIA-RDP82-00850R000200100009-9

APPROVED FOR RELEASE: 2007/02/08: CIA-RDP82-00850R000200100009-9

Table 6.2. Experimental Attenuation Coefficients α* for Different Baffle Plate Mufflers

1) Толщина материала d_1, мм	2) Воздушный зазор d, мм	3) Значения α* при частоте в третьоктавных полосах f, Гц									
		500	630	800	1000	1250	1600	2000	2500	3150	4000
1	2	3	4	5	6	7	8	9	10	11	12
4) Материал ВТ-4С											
13	15	0,11	0,12	0,12	0,14	0,15	0,18	0,19	0,21	0,24	0,27
	30	0,18	0,19	0,21	0,22	0,23	0,24	0,26	0,29	0,33	0,38
	60	0,33	0,34	0,34	0,37	0,40	0,44	0,46	0,52	0,59	0,66
26	15	0,15	0,16	0,17	0,18	0,20	0,22	0,24	0,25	0,28	0,29
	30	0,20	0,22	0,23	0,25	0,27	0,29	0,30	0,33	0,37	0,41
	45	0,29	0,30	0,32	0,33	0,38	0,41	0,42	0,46	0,52	0,56
39	20	0,17	0,18	0,18	0,19	0,21	0,23	0,24	0,27	0,30	0,34
	35	0,28	0,29	0,30	0,31	0,34	0,39	0,41	0,44	0,46	0,54
	45	0,31	0,33	0,35	0,38	0,41	0,46	0,50	0,53	0,62	0,70
5) Поролон											
10	25	0,08	0,12	0,12	0,13	0,21	0,26	0,37	0,70	1,03	1,36
	45	0,12	0,14	0,16	0,18	0,21	0,32	0,47	0,82	1,45	2,36
	60	0,11	0,14	0,18	0,24	0,27	0,31	0,54	1,02	2,06	1,37
20	20	0,23	0,30	0,39	0,59	0,84	0,74	0,84	0,60	0,76	0,76
	30	0,27	0,35	0,50	0,68	1,06	0,90	1,03	0,75	0,87	0,84
	40	0,32	0,42	0,61	0,80	1,28	1,05	1,20	0,88	0,98	0,82
	55	0,30	0,36	0,59	0,74	1,30	1,12	1,22	0,99	0,96	0,89
30	20	0,21	0,27	0,36	0,49	0,88	0,66	0,77	0,72	0,67	0,64
	35	0,36	0,48	0,66	0,92	1,18	0,92	1,00	1,00	1,05	1,06
	60	0,40	0,60	0,92	1,32	1,47	1,05	1,00	1,26	1,47	1,42
6) Войлок											
13	25	0,27	0,31	0,35	0,44	0,59	0,70	0,78	0,85	0,89	0,92
	30	0,27	0,30	0,35	0,46	0,61	0,71	0,80	0,85	0,87	0,94
	40	0,25	0,31	0,36	0,52	0,65	0,76	0,82	0,88	0,91	1,00
	50	0,20	0,27	0,36	0,48	0,66	0,78	0,85	0,91	1,00	1,06
	70	0,19	0,32	0,42	0,56	0,70	0,83	0,92	0,99	1,12	1,27
26	30	0,44	0,57	0,57	0,52	0,59	0,64	0,71	0,76	0,82	0,89
	40	0,54	0,77	0,71	0,71	0,80	0,88	0,88	0,90	0,96	1,15
	65	0,66	0,90	0,93	0,90	0,90	0,90	0,88	0,90	0,97	1,08
39	25	0,37	0,49	0,60	0,62	0,60	0,65	0,72	0,76	0,82	0,87
	35	0,54	0,70	0,73	0,72	0,73	0,82	0,88	0,93	0,98	1,05
	70	0,79	1,21	0,92	0,59	0,62	0,66	0,85	0,98	1,05	1,15

Key: 1. Thickness of material d_1, mm
2. Air space d, mm
3. Values of α* on frequency in third octave bands f, Hz
4. VT-4S material
5. Porolon
6. Felt

APPROVED FOR RELEASE: 2007/02/08: CIA-RDP82-00850R000200100009-9

APPROVED FOR RELEASE: 2007/02/08: CIA-RDP82-00850R000200100009-9

The solution of equation (6.4.8) is simplified when the widely used nomograms, constructed by Morse, in dimensionless parameters, are used; this calculation method is often called the Morse procedure [2]. The calculation procedure consists in the following:

1. Determine the impedance phase angle

$$\Phi = \operatorname{arctg}\frac{X_a}{R_a}, \quad \text{where} \quad X_a = \operatorname{Im} Z_a;\ R_a = \operatorname{Re} Z_a.$$

2. Compute wave parameter h

$$h = \frac{1}{\sqrt{X_a^2 + R_a^2}} \cdot \frac{d_0}{\lambda}.$$

3. Using Morse's nomograms (Figure 6.9) for known Φ and h, determine distribution parameter μ.

4. For known μ compute $\operatorname{Re}\Gamma = \sqrt{\mu^2 - k^2}$.

5. Compute the acoustic effect $\Delta L = 20 \lg h \cdot \operatorname{Re}\Gamma$.

For rather rigid walls with small absorption the approximate solution of equation (6.4.8) may be used, which for the main mode is expressed by a formula that coincides with formula (6.4.5).

The value of the liner impedance ($Z = W_1 \operatorname{cth}\gamma_1 d_1$) necessary for the calculation can be calculated through the acoustic parameters, which are presented in Table 6.1 for certain sound-absorbing materials. Wave impedance theory does not take into account the acoustic conductivity of materials. Therefore it is suitable only for dense materials with low acoustic conductivity (of the felt type). For soft materials (VT-4, ultrafine glass fiber, etc.) calculation based on Morse nomograms for mufflers with a small air space yields inaccurate results. The errors increase as the air space gets narrower and the liner thinner [5].

In lamellar inhomogeneous wave guide theory the air layer and sound-absorbing material layer have their own wave impedances W and propagation constant γ, i.e., a wave guide with rigid walls, filled with a lamellar inhomogeneous material (a layer of liner and a layer of air) is examined.

On the basis of Helmholtz equation are derived:

for air

$$\Delta\Phi_0 - \gamma_0^2\Phi_0 = 0;$$

APPROVED FOR RELEASE: 2007/02/08: CIA-RDP82-00850R000200100009-9

APPROVED FOR RELEASE: 2007/02/08: CIA-RDP82-00850R000200100009-9

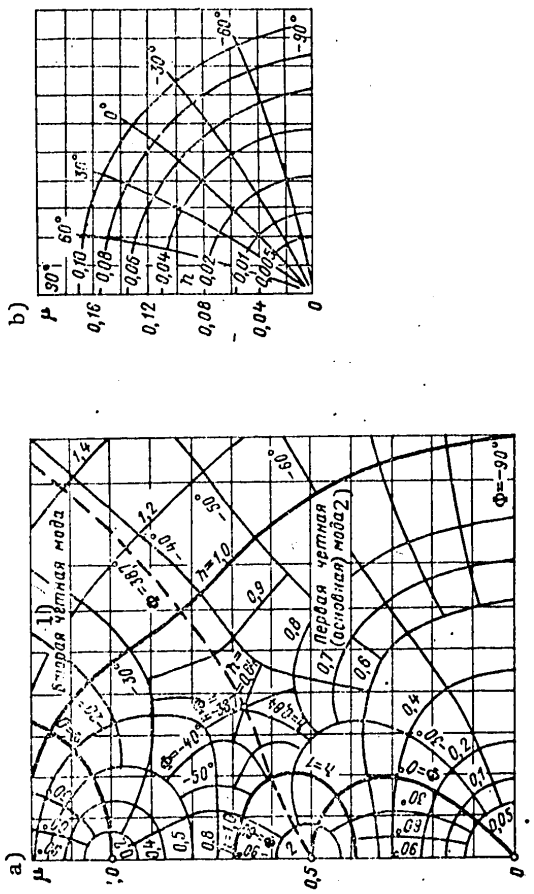

Figure 6.9. Distribution parameter μ as function of Φ (a) and of h (b).
Key: 1. Second even mode 2. First even (main) mode

APPROVED FOR RELEASE: 2007/02/08: CIA-RDP82-00850R000200100009-9

APPROVED FOR RELEASE: 2007/02/08: CIA-RDP82-00850R000200100009-9

for the liner

$$\Delta\Phi_1 - \gamma_1^2\Phi_1 = 0, \tag{6.4.9}$$

where γ_0 is the propagation constant for air; γ_1 is the propagation constant for the material.

On the basis of this theory the equation relative to unknown propagation constant Γ in the channel is written as follows:

$$\frac{\sqrt{\Gamma^2-\gamma_0^2}\,\mathrm{tg}\,\sqrt{\Gamma^2-\gamma_0^2}\,d_0}{W_0\gamma_0} + \frac{\sqrt{\Gamma^2-\gamma_1^2}\,\mathrm{tg}\,\sqrt{\Gamma^2-\gamma_1^2}\,d_1}{W_1\gamma_1} = 0, \tag{6.4.10}$$

where W_0 is the wave impedance of air; W_1 is the wave impedance of the material.

For $|\Gamma| \ll |\gamma_1|$ equation (6.4.10) changes to equation (6.4.8). In other words, lamellar inhomogeneous wave guide theory better describes processes associated with the propagation of acoustic waves in lined channels and produces better results during calculation of mufflers. Experimental results and the results of calculation by formulas (6.4.8) and (6.4.10) of the attenuation in a channel, lined with porolon with d_1 = 20 mm, are plotted in Figure 6.10.

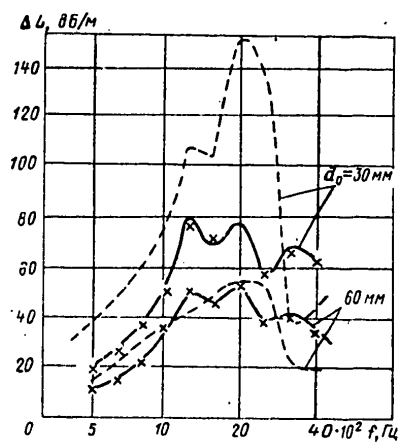

Figure 6.10. Comparison of methods of calculating attenuation in lined channel: —— by formula (6.4.10); --- by formula (6.4.8); × -- experimental data. [дБ=dB; Гц=Hz]

Calculation by formula (6.4.10) is suitable for virtually all materials and designs of baffle plate mufflers. To do the calculations it is necessary

APPROVED FOR RELEASE: 2007/02/08: CIA-RDP82-00850R000200100009-9

APPROVED FOR RELEASE: 2007/02/08: CIA-RDP82-00850R000200100009-9

to have data on the acoustic parameters W_1 and γ_1 of the materials. Some of these data are presented in Table 6.1. Calculation by equation (6.4.10) is rather complicated and is done by computer [5].

By applying residue theory to expansion into prime fractions of the terms of (6.4.10) it is possible to substantially simplify the mathematical tools for calculating acoustic attenuation in channels.

The desired propagation constant Γ is then determined as

$$\Gamma = \sqrt{\frac{s_0^2}{d_0^2} - \gamma_0^2}, \tag{6.4.11}$$

where

$$s_0^2 = \frac{B + \sqrt{B^2 - 4AC}}{2A};$$

$$A = G\varepsilon^2;\ B = \beta_1 + \beta_0\varepsilon^2 + G\,\Delta\gamma d_1^2;\ C = \beta_0\,\Delta\gamma d_1^2;\ \varepsilon^2 = \left(\frac{d_1}{d_0}\right)^2;$$

$$G = -\frac{1}{3}(\beta_0 + \beta_1);\ \Delta\gamma = \gamma_0^2 - \gamma_1^2;\ \beta_0 = d_0 W_0 \gamma_0;\ \beta_1 = d_1 W_1 \gamma_1.$$

When the thickness of the sound-absorbing material is equal to one-half the air space $d_0 = d_1$ formulas (6.4.11) are simplified:

$$s_0^2 = -E + \sqrt{E^2 - D}, \tag{6.4.12}$$

where

$$E = \frac{d_0^2\,\Delta\gamma - 3}{2};\ D = -\frac{3d_0^2 W_0\gamma_0\,\Delta\gamma}{W_0\gamma_0 + W_1\gamma_1}.$$

The acoustic attenuation in a channel, in dB/m, is

$$\Delta L = 868{,}6\,\mathrm{Re}\,\Gamma.$$

An analysis of the two last theories of attenuation of sound in channels suggests that mufflers with greater acoustic attenuation should be used if the same conditions exist in them as in a wave impedance channel. The sound-absorbing material layer is divided into individual cells by metal baffle plates, perpendicular to the wave guide axis (cell dimensions should be smaller than wavelength). Experimental results (Figure 6.11) show that there is considerable improvement of attenuation in the 2-5 kHz range. As air space d_0 and cell length l increase the maximum attenuation is shifted toward lower frequencies, decreasing in absolute value. By varying cell size it is possible to regulate the frequency characteristic of mufflers. When a cellular liner is used it becomes possible to make small baffle plate mufflers with a high acoustic effect.

APPROVED FOR RELEASE: 2007/02/08: CIA-RDP82-00850R000200100009-9

APPROVED FOR RELEASE: 2007/02/08: CIA-RDP82-00850R000200100009-9

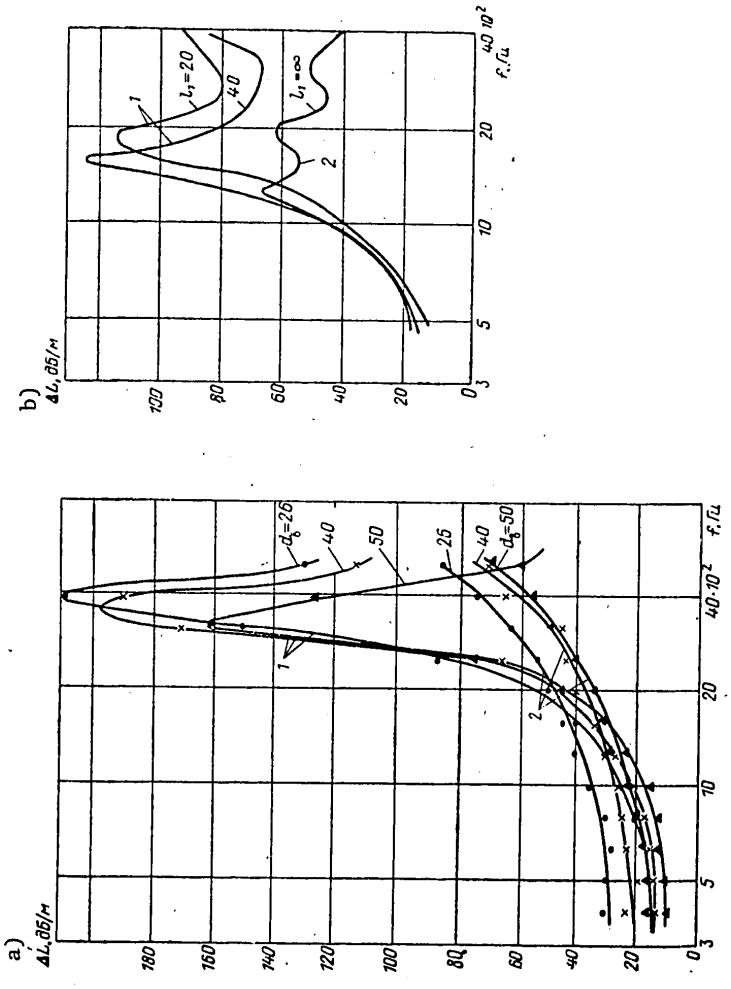

Figure 6.11. Comparison of attenuation in channel with cellular (2) and solid (1) liner; a -- VT-4S material, thickness d_1 = 20 mm, different air spaces d_a, in mm; b -- porolon, d_1 = 20 mm, different cell length l_1.

APPROVED FOR RELEASE: 2007/02/08: CIA-RDP82-00850R000200100009-9

APPROVED FOR RELEASE: 2007/02/08: CIA-RDP82-00850R000200100009-9

6.5. Reducer Noise and Ways to Reduce It

Factors That Influence Reducer Noise. The gear reducer is the main source of noise in steam turbine and gas turbine power plants. Acoustic levels in the engine room of a gas turbine ship, measured at full speed, are given in Figure 6.12. The sound levels, which are 98-101 dBA for a gas turbine engine, gradually increase to 112-113 dBA as one gets closer to the reducer.

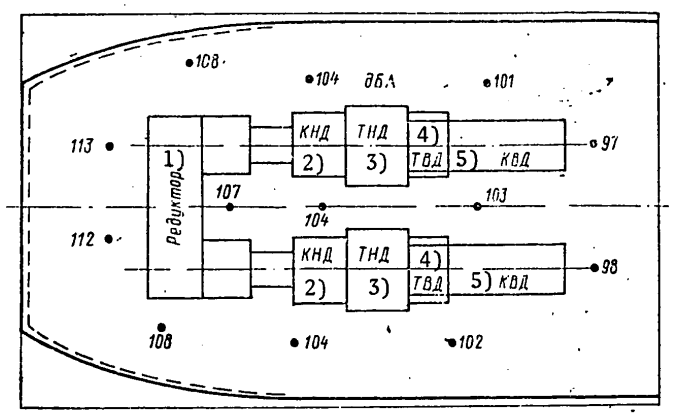

Figure 6.12. Sound levels in engine room of gas turbine ship "Parizhskaya kommuna."
Key: 1. Reducer
2. Low-pressure compressor
3. Low-pressure turbine
4. High-pressure turbine
5. High-pressure compressor

High-speed (turbine) and low-speed (diesel) reducers are used in marine power engineering. Low-speed reducers are used extensively in marine power plants with medium-speed diesel engines. Pinion, planetary and combined planetary-pinion reducers are used in marine main turbine reducer assemblies [11]. The necessary reducer noise reduction is about 10-20 dB. The acoustic levels of two-stage marine reducers of the pinion type, depending on their design and quality, vary in the 95-110 dBA range.

The basic cause of gear noise is the faulty production of the gear wheels and deformation of the teeth under stress. To assure smooth engagement it is necessary to strive for geometrically perfect meshing of the teeth and to prevent their deformation. It is impossible to completely satisfy both these requirements. Therefore, when the teeth mesh torque is transmitted unevenly and periodic deformations of the teeth occur, usually of the impact variety. These deformations, which coincide with the frequency of natural vibrations of the gear wheels and gear box, can cause all kinds of resonance phenomena, which amplify reducer noise [10].

APPROVED FOR RELEASE: 2007/02/08: CIA-RDP82-00850R000200100009-9

APPROVED FOR RELEASE: 2007/02/08: CIA-RDP82-00850R000200100009-9

Double helical, and less frequently helical gear wheels are used for high-speed marine reducrs, and helical, less frequently double helical gear wheels are used for low rpm reducers. Attempts to build quiet high rpm reducers with precision straight teeth have failed [20].

Reducer noise depends on the load and on the rotation frequency of the initial circumferences of the wheels. The vibration level on the gear box is plotted in Figure 6.13 as a function of the load distribution across the gear wheel rims of an experimental reducer [11]. The product of the load distribution nonuniformity coefficient k_d along the teeth and the rated specific load W_t is plotted on the abscissa axis. Uniform distribution of load across the rim is one of the most difficult problems of reducer design and of MTRA [Main turbine reducer assembly] operation. Flaws in the machining of rotating parts, elastic and thermal deformation of gears and wheels, misalignment of their axes due to deformation of the gear box, etc., are causes of poor distribution of load. The most common causes of deformation of MTRA parts and of misalignment of rotating parts on ships, discovered as a result of an inspection of the MTRA of a large number of heavy-displacement tankers, are depicted schematically in Figure 6.14 [23]. The most probable causes are: change of displacement and of the oil temperature in the oil sump; fluctuations of the torque and thrust of the screw shaft, and also of the sea water temperature and linear thermal expansion of the steam manifold that connects the turbine, etc.

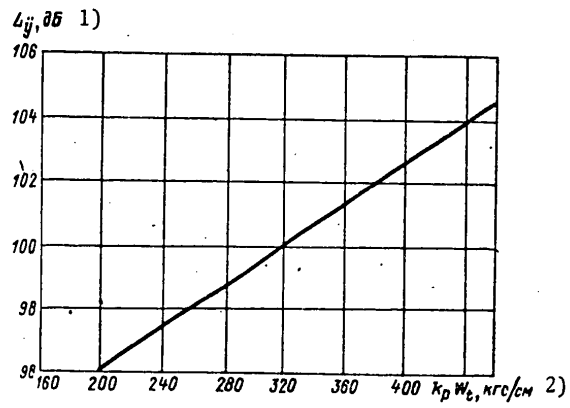

Figure 6.13. Vibration level of gear box as function of load distribution on teeth.
Key: 1. dB 2. k_dW_t, kg/cm

APPROVED FOR RELEASE: 2007/02/08: CIA-RDP82-00850R000200100009-9

APPROVED FOR RELEASE: 2007/02/08: CIA-RDP82-00850R000200100009-9

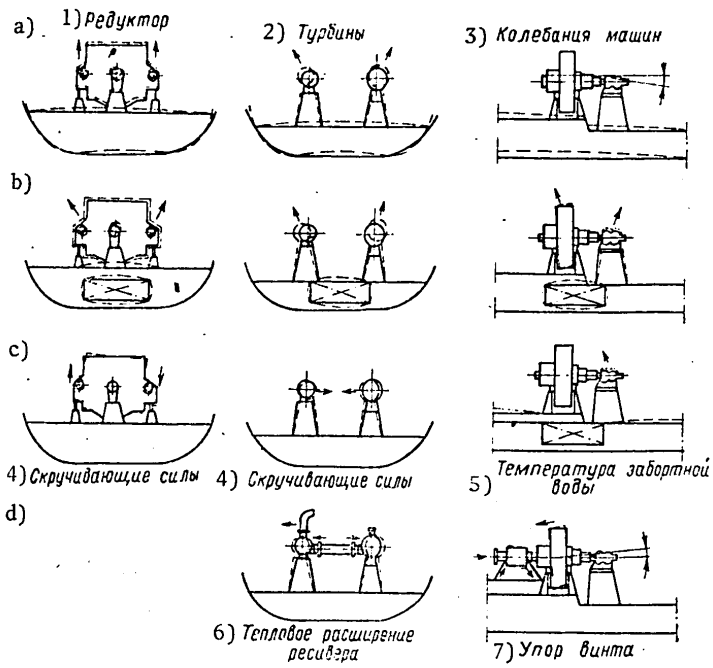

Figure 6.14. Causes of deformation of MTRA on ship: a -- influence of draft; b -- influence of oil temperature; c -- influence of forces; d -- influence of various factors.

Key: 1. Reducer
2. Turbines
3. Mechanical vibrations
4. Torsional forces
5. Sea water temperature
6. Thermal expansion of manifold
7. Screw thrust

Deformation of the reducer due to static forces contributes additional imprecision to the mating of gears, and noise increases. There have been cases when the noise level increased by 5 dBA and more as a result of deformation of the gear box.

MTRA reducer noise depends on the circumferential velocity of the wheels [3]:

$$L_p = L_0 + 10 \lg v_0^n,$$

where L_0 is the initial noise level, determined by the quality and design of the gear wheels; n for most marine reducers varies in the range n = 2-3; when there are many resonance matches it may increase to n = 5.

APPROVED FOR RELEASE: 2007/02/08: CIA-RDP82-00850R000200100009-9

APPROVED FOR RELEASE: 2007/02/08: CIA-RDP82-00850R000200100009-9

For quality reducers L_0 should not be more than 40 dB, and not more than 50 dB for reducers of satisfactory quality; a reducer with L_0 = 50-55 dB should be considered unsatisfactory [3]. If one judges by the noise level at a distance of 1 m from the gear box at full speed, the sound level should not exceed 95 dBA for a pinion reducer of good quality, and 95-100 dBA for a reducer of satisfactory quality. Reducers with noise exceeding 105 dBA should be considered unsatisfactory.

Planetary reducers have small dimensions and lower noise levels than pinion reducers due to a reduction of the specific loads on the teeth as a consequence of the more uniform transmission of torque through several satellites and lower circumferential velocities. Moreover, their smaller parts can be made with greater precision than the very large parts of pinion reducers. Planetary reducers make about the same noise as the very best pinion reducers [20].

The average noise levels of the MTRA reducer of a heavy-displacement tanker are given below:

Middle frequencies of octave bands, Hz	63	125	250	500	1000	2000	4000	8000	Total noise level, dBA
Noise levels, dB	97	93	93	93	91	83	79	70	94.5

A three-stage six-line combined reducer is used on the tanker. A differential transmission is used as the first stage and pinions as the second and third stages. The comparatively low circumferential velocity (v_0 = = 78.1 m/s), reduced loads on the teeth (due to the multiline power distribution) and high gear cutting precision result in the manufacture of a good-quality reducer with a noise level of 95 dBA.

Small planetary reducers with helical wheels, used for large medium rpm diesel engines, have sound levels of about 85 dBA at 1 m.

Ways to Reduce Reducer Noise. It was pointed out above that the noise of a reducer is influenced by its design features, which lead to a change of the specific load on the teeth and of the circumferential velocities of the wheels. In this respect the use of three-stage multiline and planetary reducers is always preferable from the standpoint not only of noise, but also of cost, size and weight [11, 20, 23].

To reduce the influence of deformations caused by various external forces an attempt is usually made to adapt the reducer to them. "Floating" couplings, gear couplings and special mounts for fastening the reducer to the foundation in order to neutralize the undesirable influence of displacements, misalignments of the shafts, fluctuations of torque and screw thrust, etc., are used for this purpose [11, 23].

APPROVED FOR RELEASE: 2007/02/08: CIA-RDP82-00850R000200100009-9

APPROVED FOR RELEASE: 2007/02/08: CIA-RDP82-00850R000200100009-9

One of the basic factors that determine reducer noise is production precision. High precision and quality of manufacture provide not only a low noise level, but also better reliability throughout the entire service life of a ship. Features of the manufacture of quiet main turbine reducer assembly pinion reducers with noise levels not exceeding 95 dBA can be traced by examining British Fairfield reducers with a power of up to 22,000 kW and more and with noise levels of 94-95 dBA. The most important parts are machined to a precision of $2 \cdot 10^{-6}$ mm. During the cutting of gears the temperature in the shops is maintained constant within ±0.3°C. The forgings, set upon the milling machine, are aligned to a precision of $6 \cdot 10^{-6}$ mm. Machines with a slowly rotating turntable are used for milling, which produces even more precise wheels. After being shaved the surfaces of the teeth have an error of less than $1 \cdot 10^{-6}$ mm. So-called selective shaving is utilized [6]; in addition, high-quality shaving is assured by preliminary hobbing of good quality. The gear boxes are bored with the alignment maintained within $8 \cdot 10^{-6}$ mm.

During the production of gear wheels it is important to maintain constant not only the temperature in the box, where the teeth are cut, but also the temperature of the milling machine itself, which heats up during operation [6]. There are other more or less effective ways to reduce noise. It is important during the production of a reducer to avoid resonance of induced and natural vibrations of the gear wheels. For this purpose the spectrum of natural vibrations of reducer assemblies, chiefly the wheels, is analyzed (Figure 6.15a), and the frequency of induced vibrations is calculated. Then a "coincidence curve" is plotted (Figure 6.15b), which shows the points of resonances as functions of the screw shaft rotation speed. It is important that the points of matchup not lie in the vicinity of the rated rotation frequency. Otherwise the natural vibration frequency must be increased or reduced by changing the rigidity of the wheels. If that cannot be done the wheels have to be deformed by fastening on the disk or rim materials with a high internal friction (plastic, lead disks, etc.).

Vibration from the gear wheels is transmitted to the reducer box through the bearings. To eliminate or to substantially reduce the noise the bearings are vibration-insulated with plastic or rubberized metal rings 1, inserted between the bearing and the box (Figure 6.15c). Transmission of high-frequency vibrations to the box is substantially reduced. One effective way to cut down on reducer noise is to replace the metal box with a plastic one (Figure 6.15d). Comparative tests of two-stage reducers with silumin (curve 1), glass fiber-reinforced plastic (curve 2) and fiber plastic (curve 3) demonstrated the significant advantages of plastic housings [12]. The noise level of a reducer with a fiber plastic housing is 21 dB lower than a reducer with a silumin housing.

Plastic gear boxes are also used for marine main turbine reducer assemblies [23]. The plastic reduces the weight of the reducer; this saves metal and improves the general appearance of the reducers. Plastic is also

APPROVED FOR RELEASE: 2007/02/08: CIA-RDP82-00850R000200100009-9

APPROVED FOR RELEASE: 2007/02/08: CIA-RDP82-00850R000200100009-9

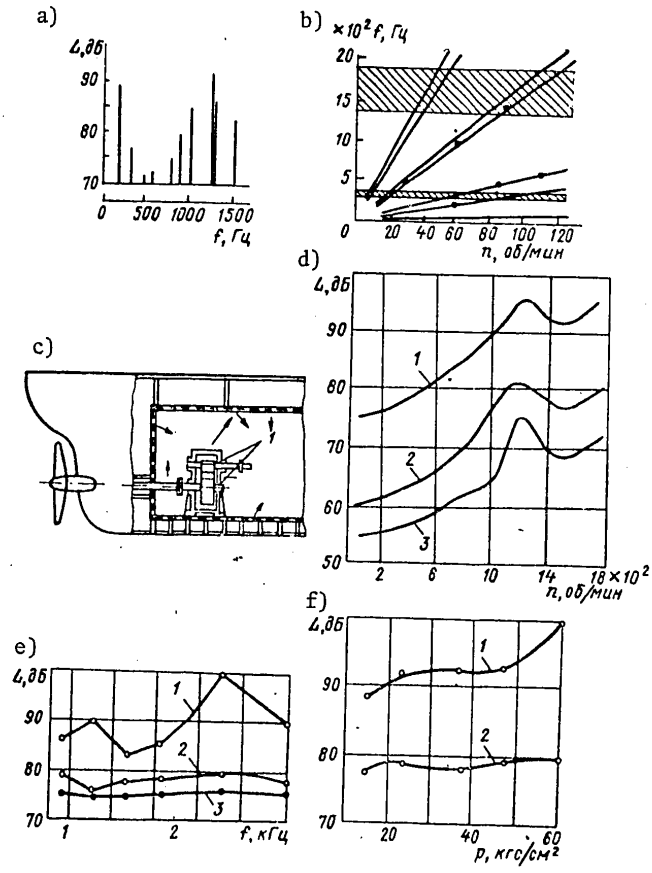

Figure 6.15. Estimation of effectiveness of ways to combat marine reducer noise. [дБ=dB; Гц=Hz; об/мин=rpm; кгс=kg]

extremely promsing for the manufacture of gear wheels, but it has not yet been ascertained whether it can be used for heavy-duty reducers.

Curves characterizing the noise level of gears made of different materials are shown in Figure 6.15e, f: 1 -- steel-steel, 2 -- steel-capron, 3 -- capron-capron. In principle it is sufficient to replace one of the two wheels of a mate with plastic; the noise level then drops by nearly 20 dB. Plastic gears are cheaper and much lighter, withstand dynamic loads satisfactorily, can run in low-quality lubricant and in fact without lubrication for a long time. Their chief deficiency is poor strength in

APPROVED FOR RELEASE: 2007/02/08: CIA-RDP82-00850R000200100009-9

APPROVED FOR RELEASE: 2007/02/08: CIA-RDP82-00850R000200100009-9

comparison with steel wheels. Therefore plastic transmissions may be used for light-duty reducers of auxiliary machinery.

The simplest way to decrease reducer noise on ships, particularly when other techniques are unsuitable for various reasons, is to install a sound-insulating housing.

6.6. Ship Pipe Valve Noise and Ways to Reduce It

Calculation of Valve Noise. Steam and gas pipes of marine steam turbine and gas turbine power plants with valves installed in them are high-frequency noise sources. The noise produced by valves consists of the noise generated by the valve itself and pipe noise. The latter is produced by the flow from the discharge of the valve and at critical flow rates is usually the predominant source of noise. When a pipe has a noisy valve in it the noise level of the supplying pipe is 10-25 dB lower than that of the discharge pipe. The noise level of a valve is estimated at a distance of 1 m from the wall of the discharge pipe in a cross section at a distance of 1 m beyond the valve. The noise levels of throttle valves reach 115-125 dBA. The acoustic vibration, propagating through the pipes and their brackets on the hull structures of the ship, can greatly exceed the noise level in nearby quarters. The spectra of noise in the engine room from a steam throttle valve (curve 2) in the control system of the main steam turbine power plant, of the discharge pipe beyond the valve at the point of rigid fastening of the pipe to the hull structure of the ship (curve 1), and in state rooms, located on the deck in the vicinity of the noise valve (the cross hatched region), are shown in Figure 6.16. The steam pressure drop in the valve is $p_1/p_2 = 15$. The conditional clearance of the valve is $d_c = 158$ mm. The steam flow rate is 70 tons/hr. Valve noise in the main steam and gas lines depends on a number of factors, primarily on the velocities permitted in the valve, on the dimensions and design features of the valve, on how well the pipes are sound-insulated, on the pressure drop, etc. At a subcritical gas flow, i.e., when $p_1/p_2 \leq \beta_{cr}$ (where p_1 and p_2 are the pressures in front of and after the valve, and β_{cr} is the critical pressure ratio), the acoustic power of a valve is proportional to the acoustic power of the jet discharged into the atmosphere. The acoustic power of a hot jet in the subsonic flow mode is determined by the formula

$$N = k\frac{\rho_m s v_m^8}{\rho c^5}, \qquad (6.6.1)$$

where k is a coefficient related to turbulent flow; ρ and c are the density of air and the speed of sound in air; ρ_m is the density of gas; v_m is the velocity of expanding gas; s is the pipe cross section at the discharge.

APPROVED FOR RELEASE: 2007/02/08: CIA-RDP82-00850R000200100009-9

APPROVED FOR RELEASE: 2007/02/08: CIA-RDP82-00850R000200100009-9

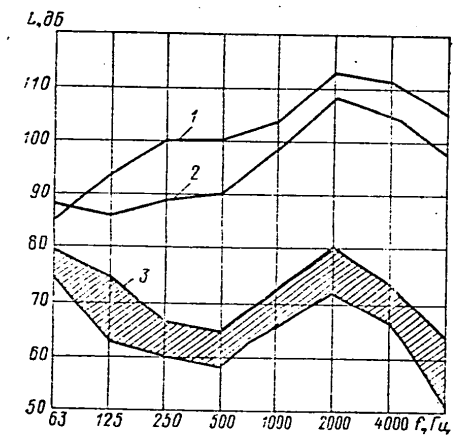

Figure 6.16. Octave spectra of acoustic pressure level produced by throttle valve in marine steam turbine power plant control system. Flow rate 70 tons/hr, p_1 = 30 kg/cm^2, p_2 = 2 kg/cm^2. [дБ=dB; Гц=Hz]

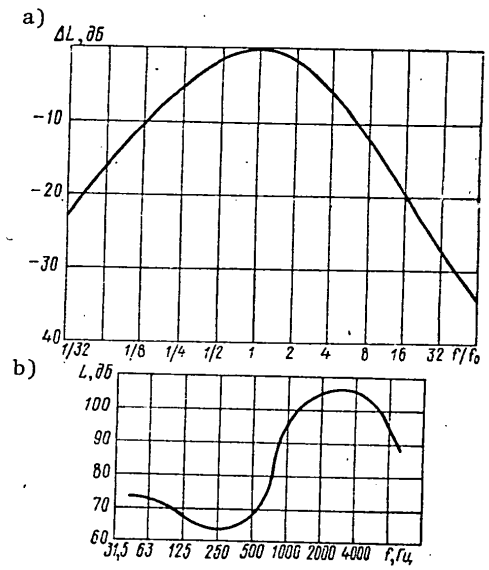

Figure 6.17. Spectra of jet and valve noises: a -- calculated relative noise spectrum of subsonic jet discharged into atmosphere; b -- noise spectrum of throttle valve. p_1 = = 21 kg/cm^2, p_2 = 6.4 kg/cm^2, medium -- natural gas.

APPROVED FOR RELEASE: 2007/02/08: CIA-RDP82-00850R000200100009-9

APPROVED FOR RELEASE: 2007/02/08: CIA-RDP82-00850R000200100009-9

According to formula (6.6.1) the acoustic power N at subcritical flow rates increases in proportion to the eighth power of the gas velocity at the nozzle discharge. Valves have about the same ratio for subcritical pressure drops p_1 and p_2; in the case of supercritical drops this function is proportional to $v_m^6 - v_m^7$.

The calculated noise spectrum of a jet as a function of frequency ratio f/f_0 is shown in Figure 6.17. Also given there is the typical noise spectrum of a control valve, operating under a supercritical pressure drop: $p_1 = 21$ kg/cm^2 and $p_2 = 6.5$ kg/cm^2. The maximum frequency f_0 of the spectrum in terms of amplitude is given by the Strouhal number St

[эф=ef]
$$St = f_0 \frac{d_{эф}}{\omega_m},$$

where d_{ef} is the effective orifice; v_m is the gas velocity in the critical cross section.

For a jet discharged into open space with pressure ratio $p_1/p_2 \approx 2$ the Strouhal number is $St \approx 0.5$. Strouhal number St decreases as the pressure ratio p_1/p_2 increases according to the formula

[kp=cr]
$$St = 0{,}2\left(\frac{p_1}{p_2} - \frac{p_1}{p_{кр}}\right)^{-1/2}.$$

Using the critical ratio $p_1/p_2 = 1.89$ and the critical flow coefficient C_f, it is possible to find a more exact equation for determining the Strouhal number for a valve [15]:

[кл=va]
$$St_{кл} = 0{,}2\left[p_1/p_2 - \left(\frac{1}{1 - 0{,}47C_f^2}\right)\right]^{-1/2}. \qquad (6.6.2)$$

Coefficient C_f represents the ratio of the valve transmission capacity C_v under critical and under the examined conditions. By definition $C_f^2 = \Delta p_{cr}/(p_1 - p_v)$, where $\Delta p_{cr} = p_1 - p_2$ for a critical flow, p_v is the pressure in the critical cross section of the valve.

The coefficient C_f is connected to the different parameter of flow through a valve by the expression [1]

$$G = 0{,}0207 C_v C_f \sqrt{\Delta p\,(p_1 + p_2)\,\rho},$$

APPROVED FOR RELEASE: 2007/02/08: CIA-RDP82-00850R000200100009-9

APPROVED FOR RELEASE: 2007/02/08: CIA-RDP82-00850R000200100009-9

where G, in tons/hr, is the mass flow rate; p_2, in kg/cm^2, is the absolute discharge pressure in critical flow; ρ_1, in t/m^3, is the density of gas (steam) for working intake parameters; $\Delta p = p_1 - p_2$ is the pressure drop.

The pressure recovery coefficient $K_{p.r}$, numerically $K_{p.r} = C_f$, is utilized in Soviet practice. Coefficient C_f varies from design to design, depending on the valve operating mode, within 0.2-1.0; in most cases C_f = 0.5-0.90.

The Strouhal number for valves according to calculated and experimental data does not exceed 0.2; usually St = 0.10-0.18 [15].

The acoustic power N_a of a valve is equal to the kinetic power W_k of the jet, multiplied by the acoustic efficiency η_{va}:

$$N_a = W_к \eta_{кл}, \tag{6.6.3}$$

where

$$W_к = \frac{\pi}{8g} \rho_m v_m^3 d_{эф}^2; \tag{6.6.4}$$

ρ_m is the density of the medium in the critical cross section. The value v_m in critical flows may be assumed equal to the speed of sound. The value η_{va} depends on pressure drop p_1/p_2 and on the coefficient C_f.

The generation of acoustic energy in valves is a complicated physical process, particularly for critical and supercritical pressure drops. Since the ratio p_1/p_2 in throttle valves usually is higher than critical it is worthwhile to examine just that operating mode.

When a compressed medium is discharged with critical and supercritical pressure ratio p_1/p_2 pulsating shock waves and flow turbulence, which cause strong vibration of the discharge pipe, are the determining factors in the generation of noise at the discharge from a valve. The change of η_{va} as a function of p_1/p_2 and C_f is plotted in Figure 6.18. As C_f increases, i.e., as the pressure recovery coefficient after the valve decreases, noise increases. This is physically explainable, since when $C_f = 1$ the kinetic energy after the valve is not converted to potential energy, but is converted entirely to thermal and acoustic energy, and when $C_f \to 0$ most of the kinetic energy of the flow after the valve reverts to potential energy. Valves that have small C_f and operate on a compressed medium make less noise. Conversely, the flow of incompressible fluids under the same conditions can cause cavitation phenomena, and valve noise increases.

APPROVED FOR RELEASE: 2007/02/08: CIA-RDP82-00850R000200100009-9

APPROVED FOR RELEASE: 2007/02/08: CIA-RDP82-00850R000200100009-9

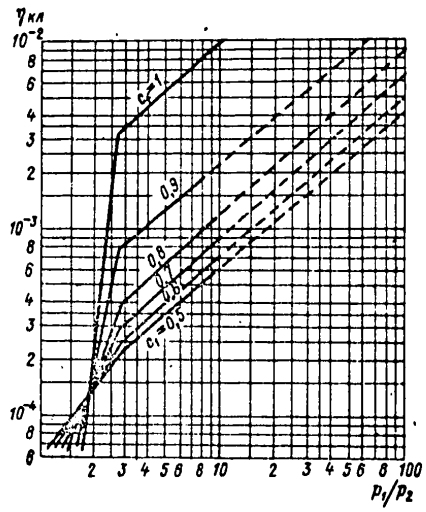

Figure 6.18. Function $\eta_{va} = f(p_1/p_2)$ [15].
[нл=va]

Acoustic efficiency η_{va} at the critical pressure ratio p_1/p_2 is not a function of valve design; therefore all curves meet at the same point. At approximately $p_1/p_2 = 2.8$ the curves bend, and after that acoustic power is proportional to the flow velocity to approximately the sixth power.

The effective cross section d_{ef} in a valve can be determined through the coefficients C_v and C_f:

$$d_{эф} = a\sqrt{C_v C_f}, \qquad (6.6.5)$$

where a is a constant.

The value C_v, like C_f, usually is indicated in the certification of a valve. In Soviet practice the transmission capacity is sometimes denoted by the symbol K. It represents the mass flow rate of a medium with a density of 1 t/m^3 at a pressure drop of 1 kg/cm^2 on a valve; numerically $K = 0.86C_v$.

The value C_v can be calculated by empirical relations [1]: for $p_1/p_2 \geq 2$ the coefficient C_v is

for steam

$$C_v = \frac{0{,}84Gk}{p_1}, \qquad (6.6.6)$$

APPROVED FOR RELEASE: 2007/02/08: CIA-RDP82-00850R000200100009-9

APPROVED FOR RELEASE: 2007/02/08: CIA-RDP82-00850R000200100009-9

for gas

$$C_v = \frac{G}{0{,}0182} \cdot \frac{1}{p_1\sqrt{\rho_1}}, \tag{6.6.7}$$

where G, in t/hr, is the mass flow rate; ρ, in t/m^3, is the density of steam (gas) for the working intake parameters; k is a correction factor for heating of steam above the saturation point. For saturated steam k = 1, and for superheated steam k = 1.023 + 0.0007 Δt, where Δt, in °C, is the temperature of the steam.

Bauman [15] proposed on the basis of equations (6.6.3) and (6.6.4) a formula for calculating the acoustic level L_{va}, in dBA, in control valves at a distance of 1 m for a blocked flow:

[кл=va; тр=p; д=d]

$$L_{кл} = 10 \lg (10^{11} a_1 \varkappa \eta_{кл} C_v C_f p_1 \rho_2) - R_{тр} + S_д, \tag{6.6.8}$$

where a_1 is a constant; κ is the ratio of the real pressure drop to critical, which for throttle valves can be estimated as $\kappa = (p_1 - p_2)/0.41p_1$; R_p is a parameter that takes into account the design features of a valve and the sound-insulating capacity of the discharge pipe.

Equation (6.6.8) shows that the acoustic power of a valve depends on the density of the medium in the valve; the term S_d takes into account the influence of that parameter. If for air it is assumed that $S_d = 0$, then conversion to a compressible medium of different composition for S_d, in dBA, can be done by the formula

$$S_д = 20 \lg (\rho_m/\rho)^2 + 23 (c_m/c), \tag{6.6.9}$$

where c_m and c are the speed of sound, respectively, in air and in gas (steam) at 17°C; ρ and ρ_m are the corresponding densities at the same temperature.

The values of S_d for different media are listed in Table 6.3.

The parameter R_p, in dBA, is given by the formula

$$R_{тр} = 17 \lg \left[\frac{1{,}47 \cdot 10^4 m \mathrm{St} n_к}{C_v C_f} \right] - 36, \tag{6.6.10}$$

where m is the surface mass of the pipe walls after a valve, in kg/m^2; n_k is a parameter that takes into account design features of a valve; $n_k = 1$ for a ball check valve; $n_k = 1.4$ for a gate valve, corner valve and pass valve, and $n_k = 2.2$ for a two-way double-seat valve.

APPROVED FOR RELEASE: 2007/02/08: CIA-RDP82-00850R000200100009-9

APPROVED FOR RELEASE: 2007/02/08: CIA-RDP82-00850R000200100009-9

Table 6.3. S_d for Different Media

Media	S_d, dBA
Saturated steam	-2
Superheated steam	-3
Natural gas	-1
Air	0
Carbon dioxide gas	+1
Propane	+1
Hydrogen	-10
Oxygen	+5

Table 6.4. R_p as Function of Diameter and Wall Thickness of Pipe

Pipe diameter d_p, in mm	Wall thickness δ_w, in mm	R_p, dBA
50	5	15.5
100	6	18.5
200	8	21.0
250	9.5	22.0
300	10.5	22.5
450	14.5	25.0

Villier [26] simplified the problem of calculating valve noise by plotting graphs (Figure 6.19), on the basis of which he determined the parameters that enter into the formula:

$$L_{кл} = S_p + S_v + S_e + S_д - R_{тр}. \quad (6.6.11)$$

The parameter R_p is taken as a function of the outside diameter of the discharge pipe and of wall thickness δ_w (Table 6.4).

When δ_w is doubled R_p increases by 4-5 dBA. The convergence of the calculated and measured acoustic pressure levels for some valve designs, operating in different modes, was ±3 dBA [15]. Valves with drops $p_1/p_2 > 0$ and higher values of C_v have the greatest scattering.

Example of How to Calculate Valve Noise. Given: p_1 = 30 kg/cm^2; p_2 = = 3 kg/cm^2, C_v = 250, C_f = 0.85, d_p = 200 mm, δ_w = 10 mm; corner valve, medium -- saturated steam. Using the graphs in Figure 6.19 determine: S_p = = 71 dBA, S_v = 44 dBA, S_e = 28 dBA, S_d = -2 (according to Table 6.3) and R_p = -22 dBA (according to Table 6.4). Substituting the values into formula (6.6.30), we find

APPROVED FOR RELEASE: 2007/02/08: CIA-RDP82-00850R000200100009-9

APPROVED FOR RELEASE: 2007/02/08: CIA-RDP82-00850R000200100009-9

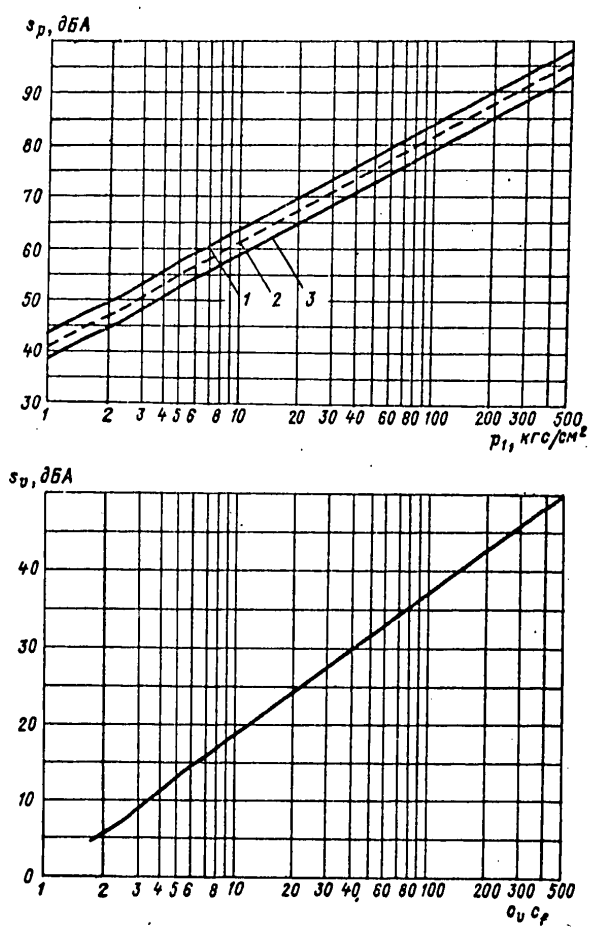

Figure 6.19. Graphs for calculating acoustic level of valves [26]. [ЭБА=dBA; кгс=kg]

$$L_{va} = 71 + 44 + 28 - 22 - 2 = 119 \text{ dBA}.$$

If the valve is inserted in a constricted part of the line, then to calculate the parameter S_e using the graphs in Figure 6.19 it is necessary, instead of the coefficient C_f, to use its product, multiplied by the ratio of the intake r and discharge R radii of the diffuser on the discharge side of the valve.

APPROVED FOR RELEASE: 2007/02/08: CIA-RDP82-00850R000200100009-9

APPROVED FOR RELEASE: 2007/02/08: CIA-RDP82-00850R000200100009-9

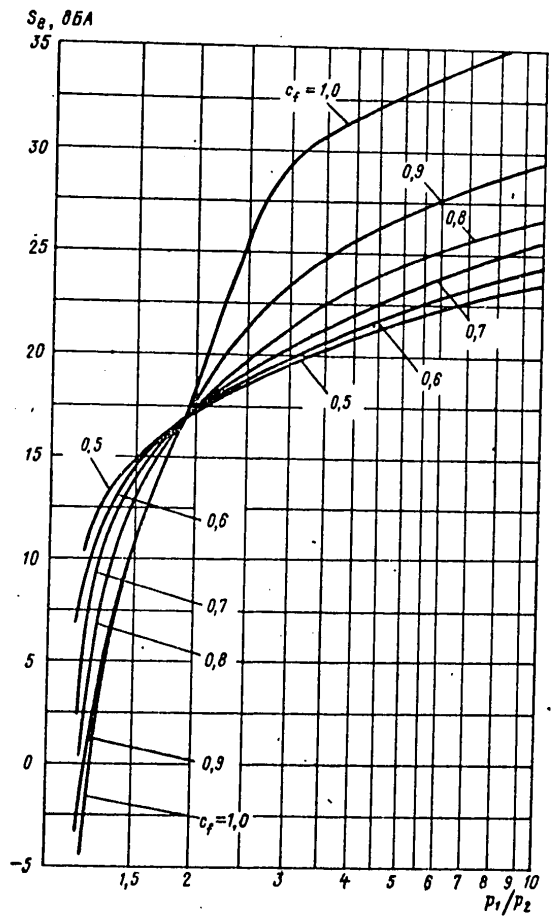

Figure 6.19 (continued).

Ways to Reduce Aerodynamic Noise of Control Valves and Pipes. Ship pipe noise is reduced by correctly regulating the parameters that are most responsible for aerodynamic valve noise. The main parameters that cause noise are:

valve geometry, which influences the pressure recovery coefficient C_f ($K_{p.r}$) and acoustic efficiency η_{va} of a valve. Reduction of the noise level due to this parameter is 10-12 dBA in individual cases;

APPROVED FOR RELEASE: 2007/02/08: CIA-RDP82-00850R000200100009-9

APPROVED FOR RELEASE: 2007/02/08: CIA-RDP82-00850R000200100009-9

effective orifice diameter d_{ef} of a valve, which influences noise approximately in proportion to the fourth power [15];

steam (gas) velocity v_{va}: if it is in the range v_{va} = 0.5-1.0M it influences noise to the eighth power; when $v_{va} \leq 0.5M$ to the sixth power [9]. This parameter is the most effective, and therefore attempts are made in practice to limit the discharge velocity to not more than 0.3M. By cutting the flow velocity in half it is possible to reduce noise by 20 dBA and more.

The velocities in the pipes themselves should be selected in accordance with the following requirements: the noise level at a distance of 1 m from an uninsulated steam pipe should not exceed 90, 80, 60 dBA, and steam velocities should not exceed 55, 40 and 30 m/s, respectively [21].

Most of the acoustic energy is radiated at a valve discharge in a branch pipe. The acoustic level at a distance of 1 m from diffusers of different sizes, installed in main pipelines and blown with air at velocities of from 0.33 to 1M [26] (M is the Mach number), is plotted in Figure 6.20. The diffuser intake diameters are equal to the conditional diameter d_c at the discharge flange. This example illustrates how flow velocity and valve dimensions influence real installations.

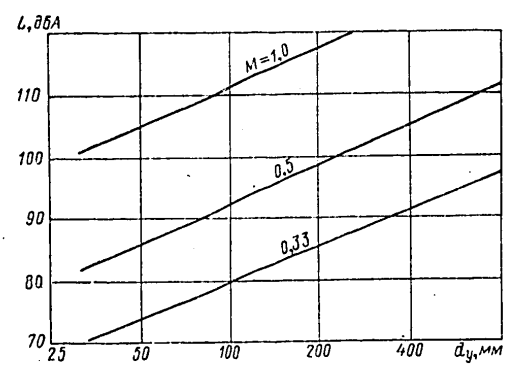

Figure 6.20. Acoustic level of pipe on discharge side of valve as function of diameter d_c and flow velocity M. [дБА=dBA; y=c]

If the noise level of a pipe must be reduced in accordance with standards by 5-10 dBA, sound insulation may be used on the walls of the discharge pipe (ordinary heat insulation with scorlupes, asbestos and glass wool encased in sheet metal, etc.). Sound insulation on the average is 2-5 dBA

APPROVED FOR RELEASE: 2007/02/08: CIA-RDP82-00850R000200100009-9

APPROVED FOR RELEASE: 2007/02/08: CIA-RDP82-00850R000200100009-9

per 1 cm of thickness of heat insulation. Noise can also be reduced by increasing the wall thickness of the discharge pipe (by 4-5 dBA when wall thickness is doubled). If noise must be reduced by 15-20 dBA an active silencer is installed immediately after the valve, or connected to the valve. In this case the supply pipe and the valve itself must also be sound-insulated (Figure 6.21). Otherwise the noise, propagating through the supply pipe, can lower the effect of the silencer by 5-10 dB.

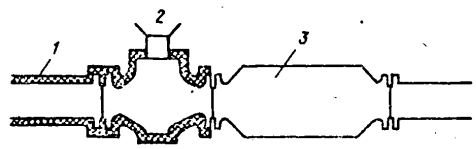

Figure 6.21. Diagram of silencer and sound insulation of supply pipe: 1 -- sound insulation; 2 -- valve; 3 -- silencer.

The usual element, a pipe in a pipe, is utilized in a silencer. The inside pipe is perforated, and the space between them is filled with sound-absorbing material, for example basalt wool, ultrafine glass fiber, etc. A silencer in the form of a single or several throttle plates (grilles) may be used. They are installed in the diffuser right after the valve; the diffuser cross section is increased in proportion to the increase of the specific volume of the medium. Some of the total pressure drop is lost on the throttle grilles, by virtue of which the ratio p_1/p_2 on a valve can be maintained at the required level. That is how the problem of reducing valve noise is solved.

Each throttle grille, consisting of two disks with offset holes, is calculated for the critical flow at the supply-delivery pressure ratio p_1/p_2 = = 2-4. Noise is generated on the throttle grilles, but because the flow is broken down into small jets a scale effect occurs, so that less noise is generated than when the same drop and flow rate are throttled in the valve. Noise is reduced due to deceleration of the flow in the holes and in the space between the disks, and also due to the interaction of the gas jets beyond the grille and shift of frequencies into a higher spectrum. Noise with a higher frequency spectrum is effectively isolated by the pipe walls. In order to shift the spectrum into the range of high-frequency noise it is necessary that the characteristic size of the jet be made as small as possible. Figure 6.22 shows how the low-frequency components of the noise spectrum are reduced by 10-15 dB when the stream flows through a throttle grille.

The design of a quiet valve, manufactured by the (Mazoneylan) firm of France, is illustrated in Figure 6.23. This is a Low-dB type of valve with a system of throttle grilles [26].

APPROVED FOR RELEASE: 2007/02/08: CIA-RDP82-00850R000200100009-9

APPROVED FOR RELEASE: 2007/02/08: CIA-RDP82-00850R000200100009-9

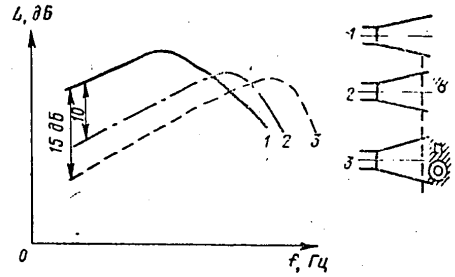

Figure 6.22. Change of spectrum of acoustic pressure level of open jet: 1 -- open jet with circular cross section; 2 -- jet flowing through perforated grille with round holes; 3 -- jet flowing through orifice with rectangular or annular cross section. [дБ=dB; Гц=Hz]

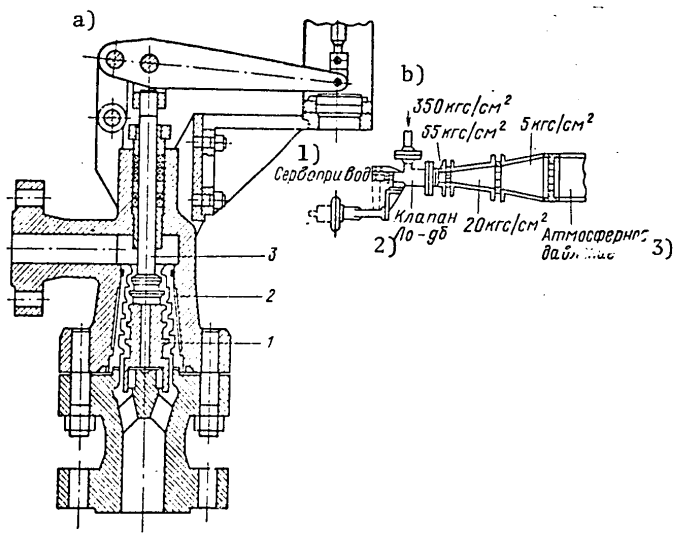

Figure 6.23. Quiet multistage Low-dB throttle valve (a) with throttle grille system (b) in delivery pipe.
Key: 1. Servodrive
2. Low-dB valve
3. Atmospheric pressure
[кгс=kg]

In throttle systems with a high flow rate and supercritical pressure drops ($p_1/p_2 \geq 10$) it is necessary to use special quiet valves, based on flow splitting, and valves with multistage throttling. Split flow valves are based on the same principle as throttle grilles, but unlike the grilles, which are calculated for a constant flow rate (about 75% of rated), the

APPROVED FOR RELEASE: 2007/02/08: CIA-RDP82-00850R000200100009-9

APPROVED FOR RELEASE: 2007/02/08: CIA-RDP82-00850R000200100009-9

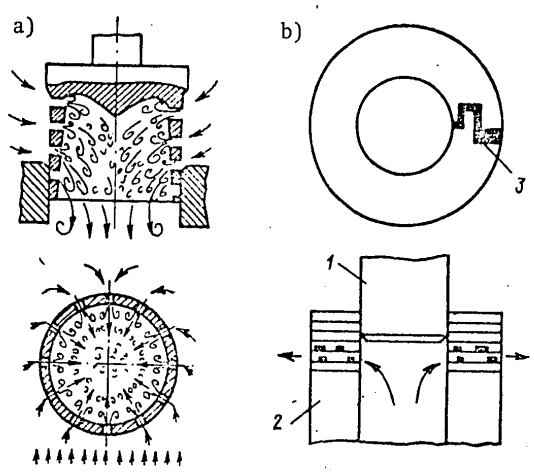

Figure 6.24. Design diagrams of split flow valves: a -- valve with perforated gate [17]; b -- valve with throttle disks. 1 -- gate; 2 -- disks; 3 -- cross section of throttling channel in disk.

valves operate effectively in variable modes. Split flow valve designs are illustrated in Figure 6.24. Quiet valves, in which there are gates with axial ridges (in the form of a gear), are, in principle, based on flow splitting. The flow passes through the valve through numerous grooves in the gate, each of which is shaped like a Venturi nozzle [18, 24].

Multistage throttle valves are used in throttling systems in which large pressure drops must be created.

The greatest reduction of noise in multistage throttle valves, similar to the one illustrated in Figure 6.23, is achieved when the pressure ratio is $p_1/p_2 \leq 5$. Valves can operate also with substantially larger p_1/p_2, but in this case there is less noise reduction. Staged piston 1 and seat 2 (see Figure 6.23) force the flow to change direction. Each stage creates a labyrinth with four corners and creates a large pressure drop, which limits the gas velocity. The areas of the stages increase in arithmetic progression, compensating the increase of volume of the gas due to expansion. When the valve is closed only the seat and stem are in contact. The steps do not touch the seat. The valve gate and the seat are made of ordinary austenitic stainless steel, and the seat surfaces are fused with Stellit. The moving part of this design has great hardness. Valve piston 1 and stem 3 have three veins, which reduces the possibility of vibration. Also, after the valve is opened the pressure is equalized. The use of a long-stroke servomotor for driving the valve and lever for shortening the stroke stabilizes the valve and increases its sensitivity.

APPROVED FOR RELEASE: 2007/02/08: CIA-RDP82-00850R000200100009-9

APPROVED FOR RELEASE: 2007/02/08: CIA-RDP82-00850R000200100009-9

A semiempirical formula was derived on the basis of studies of a large number of such valves for calculating noise L_a, in dBA, produced by Low-dB multistage throttle valves [26]:

[тр=p; д=d] $$L(A) = 18{,}5 \lg C_v + 28 \lg p_1 - 13 \lg p_2 + 20 \lg \frac{4}{y} + 46 - R_{тр} - S_д. \qquad (6.6.12)$$

The parameters C_v, p_1, p_2, R_p and S_d are analogous to those previously mentioned; y is the ratio of the cross section areas of the first and last valve stages (for Low-dB corner valves y = 4 or y = 2, depending on the type of valve-seat assembly; for double-seat valves y = 2). The measured noise levels of Low-dB valves at a distance of 1 m are 80-90 dBA; ordinary valves with the same parameters produce noise levels of 105-110 dBA. Quiet valves are 2-3 times more expensive than ordinary valves, but the cost is more than offset by a 5-10 times longer service life. Quiet throttle disk valves, as shown in Figure 6.24, are used for extremely large pressure drops.

The Problem of Reducing Vibration. Valve noise is an external manifestation of internal vibrations of a system. High-frequency vibration can produce undesirable consequences, involving the destruction of metering and control instrumentation. High-frequency vibration on the surfaces of uninsulated delivery pipes reaches 40-60g (g is the acceleration of gravity). It can lead to the loosening of bolt connections on mainline flanges and to the shearing of pipe bolts. Noisy pipes and valve assemblies, including steam, must be fastened with spring and rubberized metal shock absorbers to prevent structural noise from being transmitted to hull structures of a ship.

BIBLIOGRAPHY

1. Blagov, E. Ye. and B. Ya. Ivanitskiy, "Drossel'no-Reguliruyushchaya Armatura v Energetike" [Throttle-Control Hardware in Power Engineering], Moscow, Energiya, 1974.

2. "Bor'ba s Shumom" [Combatting Noise], edited by Ye. Ya. Yudin, Moscow, Stroyizdat, 1964.

3. Genkin, M. D. and V. K. Grinkevich, "Shum Reduktorov Sudovykh Dvigateley" [Marine Diesel Reducer Noise], Leningrad, Sudpromgiz, 1957.

4. Grigor'yan, F. Ye., V. I. Zinchenko and N. V. Pogrebnyak, "Calculation of Baffle Plate Mufflers with Small Air Spaces," TRUDY TSNIIMF [Proceedings of Central Scientific Research Institute of the Maritime Fleet], No 171, Leningrad, Transport, 1973, pp 21-31.

APPROVED FOR RELEASE: 2007/02/08: CIA-RDP82-00850R000200100009-9

APPROVED FOR RELEASE: 2007/02/08: CIA-RDP82-00850R000200100009-9

5. Grigor'yan, F. Ye., V. I. Zinchenko and N. V. Pogrebnyak, "Attenuation of Sound in Channels of Baffle Plate Mufflers with Small Spaces," TRUDY TSNIIMF, No 171, Leningrad, Transport, 1973, pp 31-49.

6. Zinchenko, V. I. and F. Ye. Grigor'yan, "Shum Sudovykh Gazoturbinnykh Ustanovok" [Marine Gas Turbine Power Plant Noise], Leningrad, Sudostroyeniye, 1969.

7. Idel'chik, A. M., "Spravochnik po Gidravlicheskim Soprotivleniyam" [Handbook on Hydraulic Resistances], Moscow, Gosenergoizdat, 1961.

8. Klyukin, I. I., "Bor'ba s Shumom i Zvukovoy Vibratsiyey na Sudakh" [Control of Noise and Acoustic Vibration on Ships], Leningrad, Sudostroyeniye, 1971.

9. Kuznetsov, V. M., A. G. Munin and Z. N. Naumenko, "Influence of Flow Velocity on Acoustic Power of Isothermic Subsonic Jet," "Trudy VI Vsesoyuznoy Akusticheskoy Konferentsii. Dokl. Zhl 1-2" [Proceedings of Sixth All-Union Acoustic Conference. Report Zh 1 1-2], Moscow, Izd-vo Akusticheskogo instituta AN SSSR, 1968.

10. Petrusevich, A. I., M. D. Genkin and V. K. Grinkevich, "Dinamicheskiye Nagruzki v Zubchatykh Peredachakh s Pryamozubymi Kolesami" [Dynamic Stresses in Spur Gear Transmissions], Moscow, AN SSSR, 1956.

11. "Reduktory Sudovykh Turboagregatov" [Reducers of Marine Turbine Power Plants], O. A. Pyzh, L. M. Garkavi, Yu. A. Derzhavets, et al, Leningrad, Sudostroyeniye, 1975.

12. Timofeyev, B. A., "Analysis of Noise of Reducers with Gear Boxes and Cover Plates Made of Different Materials," VESTNIK MASHINOSTROYENIYA [Herald of Machine-Building], 1962, No 10.

13. Khoroshev, G. A., Yu. I. Petrov and N. F. Yegorov, "Shum Sistem Ventilyatsii i Konditsionirovaniya Vozdukha" [Noise of Ventilation and Air Conditioning Systems], Leningrad, Sudostroyeniye, 1974.

14. Yudin, Ye. Ya. and S. N. Kuznetsov, "Analysis and Calculation of Compressor Suction Noise of Gas Turbine Power Plants," TEPLOENERGETIKA [Thermal Engineering], 1966, No 11.

15. Bauman, H. D., "On the Prediction of Aerodynamically Created Sound Pressure Level of Control Valves," Pap. Amer. Soc. Mech. Eng., 1970, NWA/FE-28.

16. Bonnet, P., "Les moyens modernes de lutte contre les bruits de detente de gas sous pression," GAZ D'AUJOURD'HUI, 1973, Vol 97, No 2, pp 43-48.

APPROVED FOR RELEASE: 2007/02/08: CIA-RDP82-00850R000200100009-9

APPROVED FOR RELEASE: 2007/02/08: CIA-RDP82-00850R000200100009-9

17. Detsch, F., "Betrag zur Abschatzung und Verminderung des Stromungslarms bei Ventilen," TECHN. INFORM ARMAT., 1972, Vol 7, P. 2-4, pp 88-97.

18. French, A. L., "Control Valve Noise," CANADIAN CONTROLS AND INSTRUMENTATION, September 1972, pp 25-30.

19. "Gas Turbine Sound and Its Reduction," STANDARDS NEMA, N SM-33, 1964.

20. Jones, T. P., "Fifteen Years of Development of Power Epicyclic Gears," THE INSTITUTE OF MARINE ENGINEERS TRANS., 1967, Vol 79, No 8, pp 273-303.

21. Kevin, A., "Causes and Cures of Noise in Steam Piping Systems," DES NEWS, 1973, Vol 28, No 9, pp 77, 79-80, 82.

22. McAuliffe, D. R., H. Morlock and F. M. Oran, "What to Do about Gas Turbine Noise," Paper Amer. Soc. Mech. Engrs., N AHGT-73, 1963.

23. Ross, G., "Turbines and Gearing for VLCC," IMAS, 1973.

24. Smagghe, P. and R. Villier, "Vannes speciales a faible niveau de bruit pour le gaz naturel," TECHNIQUES ET REALISATIONS INDUSTRIELLES, 1972, Vol 12, No 68.

25. "The Report of the Marine Reduction Gas Research Committee," The Ships Machinery Manufacturers Association of Japan, Vol 3, 1960, Tokyo, pp 4-7.

26. Villier, A., "Comment lutter contre le bruit produit par les vannes de reglage," INFORMATION CHIMIE, 1971, No 101, pp 191-194, 197-202.

APPROVED FOR RELEASE: 2007/02/08: CIA-RDP82-00850R000200100009-9

APPROVED FOR RELEASE: 2007/02/08: CIA-RDP82-00850R000200100009-9

CHAPTER 7. REDUCTION OF NOISE OF VENTILATION AND AIR CONDITIONING SYSTEMS

7.1. Noise Sources in Ventilation and Air Conditioning Systems

Marine ventilation and air conditioning systems are intended for ventilating ship rooms, for maintaining comfortable living conditions for crew and passengers in state rooms, social and service facilities. Noise sources in these systems are: blowers, air distribution, throttling and shutoff hardware, air humidifying instruments and machinery, mechanical and chemical air purification filters and other elements.

All ventilation and air conditioning systems, depending on noise levels, can be classified in terms of two principles: air velocity in ducts -- low- and high-velocity; location of refrigeration (heating) and treatment of air -- central, group central and self-contained independent room systems.

High-velocity air conditioning systems, in which the air velocity reaches 30-40 m/s (10-20 m/s in branch ducts), and the static blower pressure is 5,000-6,000 Pa, have been very popular in recent years. The machinery of these systems are lightweight and compact. However, the acoustic characteristics of high-velocity systems, due to high air velocities, are worse than of low-velocity systems, in which the air velocity does not exceed 10-15 m/s (5-7 m/s in branch ducts), and the static pressure is 1.2-1.8 thou. Pa.

One of the main units of ventilation and air conditioning systems on ships is the blower; it is not a principal source of noise. Centrifugal electric blowers are the most popular. Centrifugal blowers of the TsS (centrifugal ship) series are used in most of the ventilation and air conditioning systems of Soviet-built ships. They are single-stage electric blowers, whose radial blades of the squirrel cages are made of stamped sheet metal. The squirrel cage is pressed onto the motor shaft, and the snail is fastened to its flange. Head H, developed by blowers of the TsS series at $n = 300$ rpm and productivity $Q = 0.1\text{-}2.5\ m^3/s$, is 600-1,800 Pa. Blowers of the TsS series, in addition to dependability and economy, also have an important drawback -- they are extremely noisy. The generalized dependence of the integral noise level on the basic energy parameters of the blowers is given in Figure 7.1. As can be seen, the overall noise level for the

APPROVED FOR RELEASE: 2007/02/08: CIA-RDP82-00850R000200100009-9

APPROVED FOR RELEASE: 2007/02/08: CIA-RDP82-00850R000200100009-9

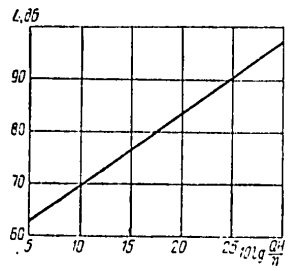

Figure 7.1. Total noise level of TsS series blowers as function of basic energy parameters. [дБ=dB]

most commonly utilized ship blowers, with the parameter 10 lg QH/η > 15 (where η is blower efficiency), reaches 80-100 dB. The spectral characteristics of the noise of some blowers of the TsS series are listed in Table 7.1.

The spectral makeup of the air noise of centrifugal blowers usually includes a continuous part and individual discrete components, which are 5-15 dB stronger than the continuous spectrum. A typical air noise spectrum of a centrifugal blower is shown in Figure 7.2.

The sources of the continuous part of the air noise spectrum of a centrifugal blower are eddy systems and individual eddies, formed in the ducts, primarily in the flow around the blades of the squirrel cage. The initial flow turbulence at the intake into the squirrel wheel exerts a substantial influence on the intensity and size of eddies, and consequently on the level and frequency of the noise. The source of the discrete components of air noise in single-stage centrifugal blowers without guides and flow straightening hardware is the interaction of the flow in the delivery cross section of the squirrel cage, which has uneven velocity, with the tongue of the discharge channel (snail). This noise component is called turbulent flow noise.

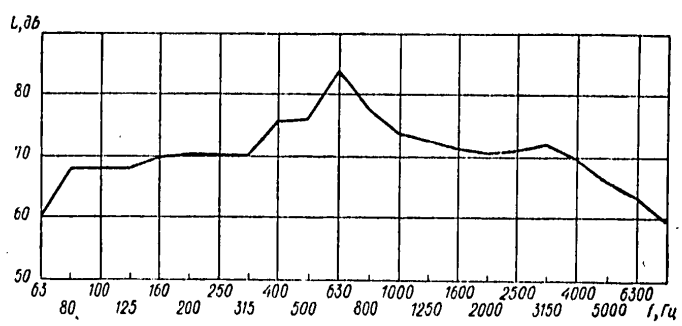

Figure 7.2. Typical air noise spectrum of centrifugal blower. [дБ=dB; Гц=Hz]

Axial fans are used considerably less frequently in ship ventilation and air conditioning systems than centrifugal blowers. The spectral makeup of the air noise of an axial fan, like that of a centrifugal blower, includes a continuous part and individual discrete components (Figure 7.3).

APPROVED FOR RELEASE: 2007/02/08: CIA-RDP82-00850R000200100009-9

APPROVED FOR RELEASE: 2007/02/08: CIA-RDP82-00850R000200100009-9

Table 7.1. Spectral Characteristics of Noise of TsS Series Blowers

1) Тип вентилятора	2) Общий уровень шума, дБ (r = 0.5 м)	3) Среднегеометрические частоты, Гц													
		70	100	140	200	280	400	560	800	1120	1600	2240	3200	4800	6400
5ЦС-6	71	57	56	59	61,5	62	62	58	59	61	59	55	56	55	—
11ЦС-6	74	61,5	62	61,5	63,5	61	61	62	65	65	60	64	64	56	50
3ЦС-11	71	56	59	60	61	58	69	56	54	54	56	52	54	52	49
8СЦ-11	75	64	63	68	69	62	67	63	60	65	65	58	60	56	49
30ЦС-11	85	69	74,5	74,5	80	75	75	72	74	73	69	71	73	66	62
63ЦС-11	94	84	84	83	90	79	83	79	75	71	73	68	70,5	68	63
3ЦС-17	72	52	55	59	61	60	59	66	64	62	57	56	55	52	46
8ЦС-17	77	66	66,5	69	63	67	64	64,5	69	62	60	61,5	56	52	46
40ЦС-17	88	70	74	75	78	76	79	74	76	80	72	74	74	70	67
80ЦС-17	95	74	81	77	82	80	88	93	82	79	78	77,5	77	72	69
3ЦС-24	70	61	54	50	54	52	57	55	56	55	55	55	53	50	—
8ЦС-24	78	60	62	64	70	66	69	64	69	69	62	63	67	58	54
45ЦС-24	87	68	71	72	71,5	71,5	76	77	76	79	79	76	76	70	66
90ЦС-24	95	80	84	82	83	78	85	84	85	82	86	82	82	80	77

Key: 1. Type of blower
2. Total noise level (r = 0.5 m)
3. Mean geometric frequencies, Hz [ЦС=TsS]

APPROVED FOR RELEASE: 2007/02/08: CIA-RDP82-00850R000200100009-9

APPROVED FOR RELEASE: 2007/02/08: CIA-RDP82-00850R000200100009-9

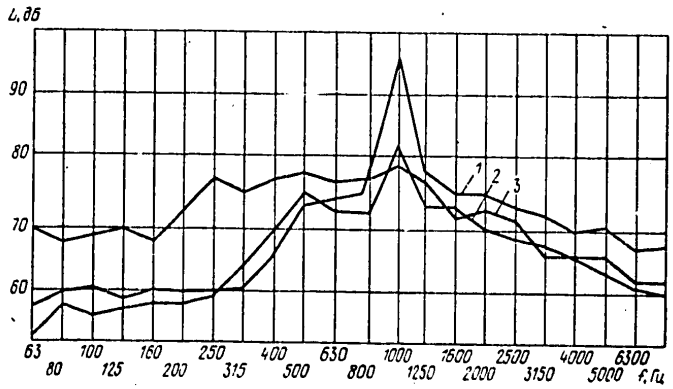

Figure 7.3. Typical air noise spectrum of axial fan at different productivities: 1 -- $Q = Q_{pot}$; 2 -- $Q > Q_{pot}$; 3 -- $Q < Q_{pot}$.

The continuous part of the noise spectrum (eddy noise) is of the same physical nature as of centrifugal blowers. In axial fans, which usually have a different kind of flow in the profile grilles in comparison with centrifugal blowers, and the flow past them is also virtually without separation, the main sources of eddy noise are pressure pulsations (of thrust) on the blades, related to the sliding of eddies from the trailing edge. The appearance of discrete components in the noise spectrum of axial fans is attributed basically to the displacement of some volume of air by the rotating blades (so-called rotation noise [1]) and to the interaction of the air stream with the guide vanes of the stator.

Rotation noise usually occurs in axial fans with a few blades ($z = 3$-5) [11]. The discrete noise components of fans with high-density grilles, $b/t > 0.5$, are on the same level as the continuous part of the spectrum. The noise density and frequency depend on the interaction of the air flow coming out of the working wheel of the rotor, with the guide vanes of the stator, on the ratio of the number of working wheel blades and the blades of the guide system, and also on the space between them.

The acoustic characteristics of marine axial fans depend to a great extent on their productivity: as productivity decreases ($Q < Q_{pot}$) the fan noise increases sharply. This is attributed to the onset of flow separation around the working blades. The low-frequency components (up to 500 Hz) increase sharply in the noise spectrum in these operating modes (see Figure 7.3). When fans operate in the high-productivity range ($Q > Q_{pot}$) the noise on high frequencies ($f > 1$ kHz) increases by 5-7 dB and the discrete component due to flow inhomogeneity also increases.

APPROVED FOR RELEASE: 2007/02/08: CIA-RDP82-00850R000200100009-9

APPROVED FOR RELEASE: 2007/02/08: CIA-RDP82-00850R000200100009-9

The main source of noise in an air conditioner is the built-in blower. Air conditioner blowers should be balanced very carefully in order to prevent the appearance of high noise levels on low frequencies.

The refrigeration compressors of self-contained room air conditioners are a source of intense vibrations, and therefore considerable attention is devoted to their vibration insulation.

The humidifiers of air conditioners with steam humidifying systems are a strong source of air noise. For instance, the UVP-72 humidifier, with a steam flow rate of 0.2 kg/s and pressure of $4 \cdot 10^5$ Pa, has a total noise level of 98 dB. Mufflers greatly reduce the noise levels of a humidifier in intermediate- and high-frequency ranges (Figure 7.4). The basic characteristics of a number of ship air conditioners are given in Table 7.2.

Marine ventilation and air conditioning systems are usually packed with plumbing fittings and various heating equipment (throttle dampers, slide gates and heaters). All these elements offer a certain amount of hydraulic resistance to the flow, passage through which is accompanied by strong turbulence, and consequently the emission of noise.

The acoustic power level of the noise generated by the passage of air through the hardware depends primarily on the flow velocity in front of it. Spectrograms of the discharge noise of the OVPCh brand refrigerator at different air flow velocities are given in Figure 7.5. As can be seen in the figure, an increase of velocity is accompanied by an increase of the noise level, particularly in the intermediate and high audio frequency ranges. The total noise level L_N of the equipment is proportional to the sixth power of the air flow velocity [11]. Audio frequency components of noise, the acoustic power of which is proportional to the flow velocity to the fourth power, occur in systems with short ducts. These audio frequency components fall in the infrasound frequency range in long systems (air ducts longer than 6 m), and their fundamental frequency is inaudible.

The heat exchangers of ventilation systems represent a collection of cylindrical rods, the flow separation around which produces noise. However, because the heat exchangers have many tubes the Strouhal frequency and its harmonics in the noise spectrum of these machines are not manifested explicitly, particularly when the noise is analyzed in the 1, 1/2 and 1/3 octave bands.

Noise sources in ventilation and air conditioning systems, in addition to hardware and heating equipment, are shaped parts (corners, T-branches, etc.) of the air ducts. The data in Figure 7.6 show that the noise in the low-frequency range, occurring in an intake T-branch at a flow velocity of 30 m/s, is somewhat louder than the noise of a blower with small parameters Q and H.

APPROVED FOR RELEASE: 2007/02/08: CIA-RDP82-00850R000200100009-9

APPROVED FOR RELEASE: 2007/02/08: CIA-RDP82-00850R000200100009-9

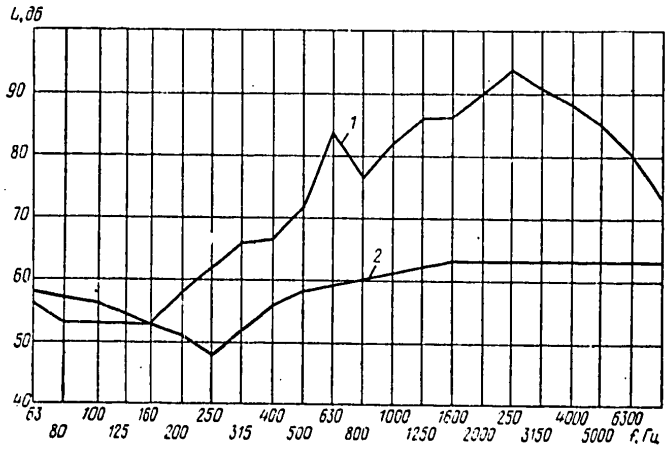

Figure 7.4. Spectrogram of airborne noise of UVP-72 humidifier: 1 -- without muffler; 2 -- with muffler. [дБ=dB; Гц=Hz]

The noise generation process in air distribution equipment is of the same character as in the duct work, except that the duct work noise occurs in the main air channel, experiences reflection at the discharge from the system and can be deadened with a muffler. The noise of air distribution equipment is generated directly in the ventilated room as a result of the flow of air around corners, through grates, grilles and other elements, located in the plane of the discharge hole.

Various distribution and control systems are used extensively, in addition to distribution hardware, in air conditioning systems. The noisiest of them are decorative ejection air distributors [2], the high noise level of which is attributed primarily to high velocities (up to 25 m/s) at the discharge from the air distribution apparatuses, necessary for forcing air through the heat exchanger. Even when sound-absorbing materials are used in decorative air distributors their noise is comparatively high; the total noise level is 65 dB.

The noise of air distribution equipment is the result of turbulence and depends primarily on the air flow velocity. As in the case of duct work, an increase of the flow velocity leads to a rapid increase of the noise level in the medium and high audio frequency ranges. The design features of air distributors also have an influence on the level of the noise which they produce. For instance, the noise of a swivel air distributor with the control in the "under plate" working position is 3-5 dB higher on intermediate and high frequencies than in the "onto plate" working position at the same flow velocity.

APPROVED FOR RELEASE: 2007/02/08: CIA-RDP82-00850R000200100009-9

APPROVED FOR RELEASE: 2007/02/08: CIA-RDP82-00850R000200100009-9

FOR OFFICIAL USE ONLY

Table 7.2. Basic Characteristics of Ship Air Conditioners

1) Тип кондиционера	2) Максимальная производительность, м³/с	3) Полное давление, Па	4) Тип электродвигателя или электровентилятора	5) Максимальная потребляемая мощность, кВт	6) Холодопроизводительность, ккал/ч	7) Общий уровень шума кондиционера, дБ: 8) вокруг агрегата	9) на всасывании	10) на нагнетании	11) Общая масса кондиционера, кг
12) Центральные высоконапорные кондиционеры (агрегаты) для одноканальной системы									
КИВ-19/17А	0,53	1700	Электродвигатель АОМ41-2	3,4	—	—	—	72,5	395
КТ-56/20	1,56±10%	2000	13) Электродвигатель АМТ61-2	10,7	—	92	—	—	850
КТ-90/30	2,5±10%	3000	Электродвигатель АМТ72-2	24,3	—	98	—	—	950
14) Центральные высоконапорные кондиционеры для двухканальной системы									
«Бриз-30» 15)	0,832	2400	17) Электровентилятор 40ЦС-34	7,65	53 900—58 000	75	86	75	1080
«Бриз-56»	1,56	2000	Электровентилятор 56ЦС-34	11,0	100 500—110 000	77	93	75	1525
«Пассат-30» 16)	0,832	2500	Электровентилятор 40ЦС-34	7,65	53 900—58 000	75	86	75	1040
«Пассат-48»	1,33	2200	Электровентилятор 56ЦС-34	11,0	86 000—95 000	77	92	75	1210
«Пассат-56»	1,56	2000	Электровентилятор 56ЦС-34	11,0	100 500—110 000	77	93	75	1360

KEY:
1. Type of air conditioner
2. Maximum capacity, m^3/s
3. Total pressure, Pa
4. Type of electric motor or electric blower
5. Maximum supply power, kW
6. Refrigeration capacity, kcal/hr
7. Total air conditioner noise level, dB
8. around unit
9. intake
10. discharge
11. Total weight of air conditioner, kg
12. High-pressure central air conditioners (units) for single-duct system
13. Electric motor
14. High-pressure central air conditioners for dual-duct system
15. "Briz"
16. "Passat"
17. Electric blower

[КИВ=KIV; ЦС=TsS]

FOR OFFICIAL USE ONLY

APPROVED FOR RELEASE: 2007/02/08: CIA-RDP82-00850R000200100009-9

APPROVED FOR RELEASE: 2007/02/08: CIA-RDP82-00850R000200100009-9

Air distribution systems of the "perforated deckhead" type are finding increasing application in ship air conditioning systems. They substantially reduce the amount of air being supplied to a conditioned room, and consequently they reduce the flow velocity. This is why air distributors of this type produce relatively little noise [9]. Systems in which air is supplied through a perforated grille at an intake air flow velocity of about 10 m/s, and 3 m/s in the holes, are the quietest of all existing systems.

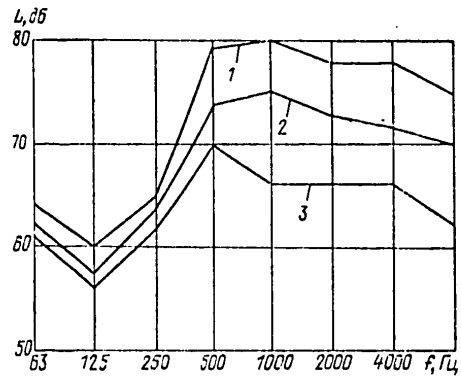

Figure 7.5. Spectrograms of air noise of OVPCh air refrigerator at different intake flow velocities: 1 -- v = 20 m/s; 2 -- v = 15 m/s; 3 -- v = 10 m/s. [дБ=dB; Гц=Hz]

The noise level in panel air distributors, in which air is supplied through perforated side plates, is vastly higher than in ordinary perforated panel air distributors, particularly on intermediate audio frequencies. Slotted air distributors in the form of an ordinary slot, without windows and guide nozzles, are comparatively quiet at air flow velocities of 10 m/s in the channel in front of the slot, and not higher than 5 m/s in the slot. The noise of all air distributors increases rapidly as the air velocity in the intake channel increases.

7.2. Reduction of Turbulence Noise and Nonuniform Flow Noise of Blowers

Reduction of Turbulence Noise. The acoustic power of the air noise emitted by blower vanes due to pressure pulsations on the vanes, is determined by the expression [10]

$$N = \frac{2\rho z \pi^3}{3bc^3} \int_x r_1 l_1(x) \left[1{,}5(r_1 + r_2) - \sqrt{r_1 r_2}\right]^2 \times \times v_1^4(x) f^2(x) \varepsilon^2(x) \left[\frac{\sin^2\beta_1}{\sin^2\beta_m}(x)\right] dx, \quad (7.2.1)$$

APPROVED FOR RELEASE: 2007/02/08: CIA-RDP82-00850R000200100009-9

APPROVED FOR RELEASE: 2007/02/08: CIA-RDP82-00850R000200100009-9

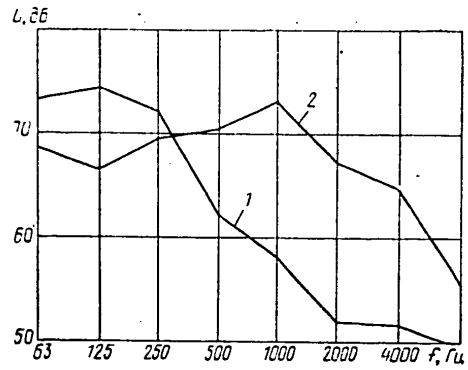

Figure 7.6. Spectrogram of air noise of supply T-branch 1 (branch angle 45°, branch channels have equal areas) and of centrifugal blower 2 ($Q = 0.222\ m^3/s$, $H = 2550$ Pa).

where ρ is the density of air, in kg/m^3; b, z are chord length, in m, and the number of fan blades; l_1 is the size of an eddy along the blade (on the x axis), in m; r_1, r_2 are the correlation radii of an eddy perpendicular to the blade surface and along the chord, in m; ε, f are the power and spectrum of boundary layer turbulence on the blade surface at the point of flow separation; v_1 is the velocity of the air flowing onto a blade, in m/s; β_1, β_m are the entrance angle and mean geometric angle of flow in the grille, °.

It follows from expression (7.2.1) that in order to reduce the acoustic power it is necessary to reduce the flow velocity and the turbulence characteristic and to optimize the blade array parameters for a given head and capacity. The optimum blade array parameters, according to the literature [10], have the following values:

Geometric entrance angle	$\beta_{b1} = (27\text{-}32)°$
Profile curvature	$\bar{f} = f/b = 0.07\text{-}0.08$ for $b/t < 1.0$
	$\bar{f} = 0.1\text{-}0.11$ for $b/t > 1.0$
Array density	$b/t = 1.5$ for $\bar{f} > 0.10$
	$b/t = 1.0$ for $\bar{f} < 0.10$
Angle of attack	$i = 3\ 5°$ for $\bar{f} \leq 0.07$
	$i = 0\ 3°$ for $\bar{f} \geq 0.07$

APPROVED FOR RELEASE: 2007/02/08: CIA-RDP82-00850R000200100009-9

APPROVED FOR RELEASE: 2007/02/08: CIA-RDP82-00850R000200100009-9

ON

BY

3 JULY 1980 I. I. KLYUKIN AND I. I. BOGOLEPOV 3 OF 6

APPROVED FOR RELEASE: 2007/02/08: CIA-RDP82-00850R000200100009-9

APPROVED FOR RELEASE: 2007/02/08: CIA-RDP82-00850R000200100009-9

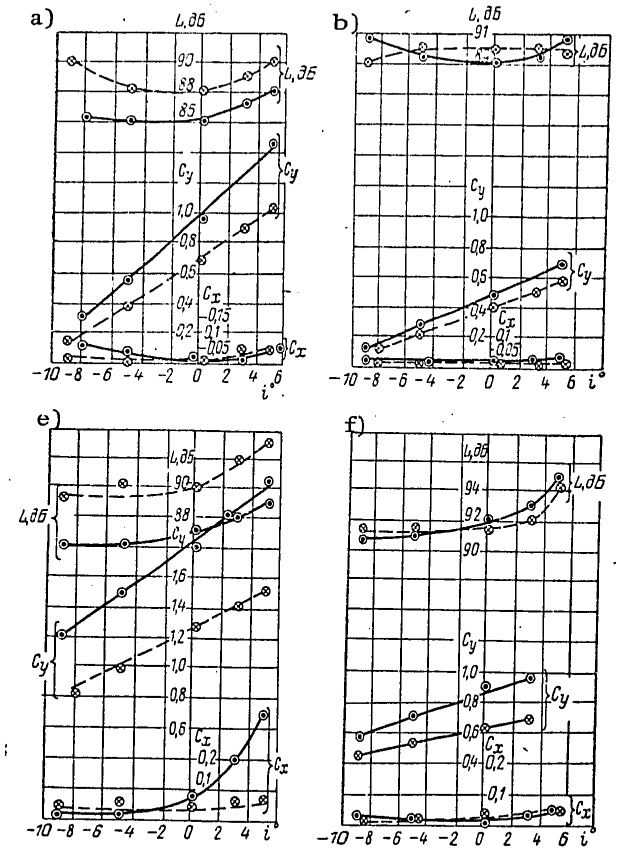

Figure 7.7. Aeroacoustic characteristics of plane blade arrays (v_1 = 60 m/s). Arrays: a -- TsZ-8 (.—. τ = 0.5, ×-× τ= 1.0); b -- TsZ-8 (.—. τ = 1.5, ×-× τ = 1.0); c -- Ts5-8 (.—. τ = 0.5, ×-× τ = 1.0); d -- Ts5-8 (.—. τ = 1.5, ×-× τ = 2.0); e -- Ts7-8 (.—. τ = 0.5, ×-× τ = 1.0); f -- Ts7-8 (.—. τ = 1.5, ×-× τ = = 2.0); g -- Ts11-8 (×-× τ = 1.0); h -- Ts11-8 (.—. τ = 1.5, ×-× τ = 2.0). [дБ=dB]

[Figure 7.7 continued on next page]

APPROVED FOR RELEASE: 2007/02/08: CIA-RDP82-00850R000200100009-9

APPROVED FOR RELEASE: 2007/02/08: CIA-RDP82-00850R000200100009-9

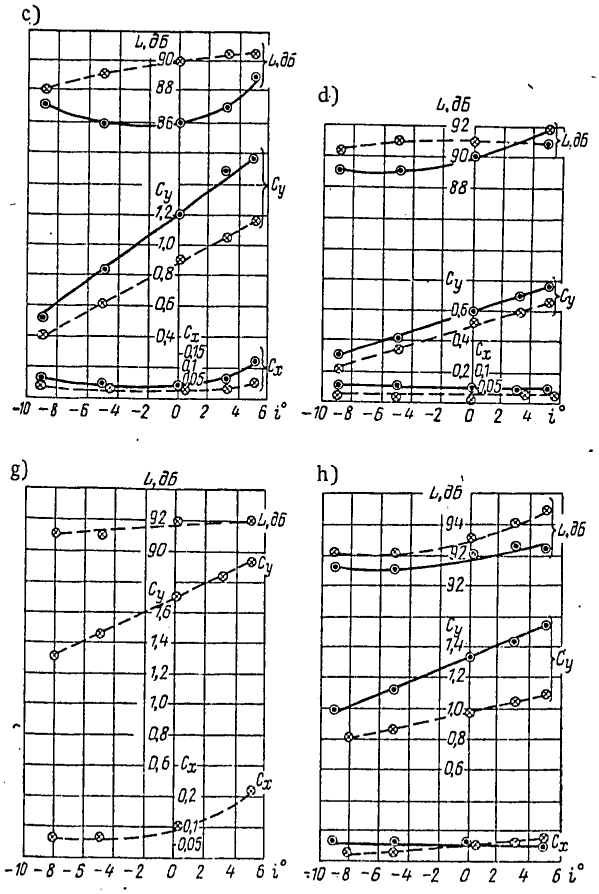

Figure 7.7 (continued).

APPROVED FOR RELEASE: 2007/02/08: CIA-RDP82-00850R000200100009-9

APPROVED FOR RELEASE: 2007/02/08: CIA-RDP82-00850R000200100009-9

The relative profile thickness within its range of change (0.06-0.12) has practically no influence on the noise level of a blade array.

The following requirements must be met during the design of quiet fans:

1) use a higher than usual fan pressure coefficient; for instance, if the recommended pressure coefficient of a stage for calculating the energy characteristics of fans is $\overline{H}$ = 0.15-0.20 for $c_a \leq 0.3$ and $\overline{H}$ = 0.25-0.3 for $c_a \leq 0.5$, then this coefficient for an axial fan with low noise levels should be $\overline{H} \geq 0.3$-0.35;

2) optimize the conditions of flow around the peripheral cross sections of the fan blades, which are the strongest noise sources;

3) eliminate strong components from the fan noise spectrum, produced by flow inhomogeneity on the frequency f = knz/60 (k = 1, 2, 3, ...; n is the rotation frequency of the fan, rpm);

4) select blade array parameters in accordance with the recommendations presented above and in consideration of the aerodynamic and acoustic characteristics of plane profile arrays, presented in Figure 7.7. Also given in the figure are the characteristics of arrays whose profile curvature varies from 3 to 11%, the array density from τ = 0.5 to τ = 2.0, and the angle of attack from -9 to +5°.

The intensity of the air noise emitted by a fan or by a guide device can be evaluated by the formula (for a point 1 m from the intake at an angle of 45° to its axis at v_1 = 60 m/s):

[р.к=f; п=р; к=r]

$$I_{\text{р.к}} = \frac{\pi I_{\text{п.с}}}{lb}(r_{\text{п}}^2 - r_{\text{к}}^2), \qquad (7.2.2)$$

where r_p, r_r are the peripheral and root radii of the fan wheel; l is blade height; $I_{p.c}$ is the intensity of the noise emitted by a profile array, equivalent to the peripheral cross section at v_1 = 60 m/s (determined by Figure 7.7).

The air noise level of a fan or the guide apparatus of a fan at a relative air flow velocity onto the peripheral cross section of the blade of v_1 = var is determined by the expression

$$L_{\text{п}} = 10 \lg \frac{I_{\text{р.к}}}{10^{-12}} + 60 \lg \frac{v_1 = \text{var}}{60}. \qquad (7.2.3)$$

By calculating several versions of the blading of axial fans and by determining through formula (7.2.3) their noise level it is possible to select the quietest version of blade array.

APPROVED FOR RELEASE: 2007/02/08: CIA-RDP82-00850R000200100009-9

APPROVED FOR RELEASE: 2007/02/08: CIA-RDP82-00850R000200100009-9

An effective means of reducing turbulence noise of squirrel cage blowers, in which flow separation usually occurs around the intake surfaces of the blade, is to use turbulizer grilles, installed on the intake and discharge edges of the working wheel and turning along with it. When turbulizers are installed on the intake edges of the vanes turbulization occurs in the air flow next to the vane surface. When this happens some of the energy of the main flow of the between-vane channel is transferred to the region of the turbulent boundary layer. Consequently the boundary layer profile changes and its pattern is filled out more completely, which leads to an increase of the stability of the boundary layer and shift of the point of separation downstream. As a result of this fan turbulence noise is reduced. Another positive effect of a turbulizer on the aeroacoustic characteristics of blade arrays is the fact that the eddies formed during flow through the turbulizer break large separation eddies down into smaller ones, the scale of which is determined by the parameters of the turbulizer. Here the total acoustic power, radiated by a blade array, is decreased.

The aeroacoustic efficiency of turbulizer grilles is determined by the following factors:

conditions of flow around blade arrays, which depend, in turn, on the type of profile, its curvature, angle of attack, density of the array, etc.;

parameters and dimensions of the turbulizers: wire diameter ρ_s, effective cross section coefficient S, and screen size of a turbulizer screen;

location of turbulizer in relation to the blade chord and screen size (if a discontinuous turbulizer is used).

The conditions of flow around a profile in an array can be characterized by one parameter -- the pattern of the distribution of velocity (pressure) on a profile (maximum dimensionless profile velocity $v_{m.d} = v_m/v_1$ and velocity gradient near peak velocity). The acoustic efficiency of turbulizers in various frequency ranges is plotted in Figure 7.8 as a function of $v_{m.d}$.

Turbulizers produce the greatest acoustic effect when their optimum parameters are determined by the expression

[c=s; м.б=m.d]

$$\left(s - \frac{\rho_c}{t_c}\right)_{opt} = 0{,}5 - 0{,}022\,(v_{м.б})^{11}, \qquad (7.2.4)$$

where t_s is the space separating the wires in the screen; S is the effective cross section coefficient of the screen.

The optimum value of S for virtually all array parameters ($v_{m.d}$ = 4-11), for arrays used in modern ship ventilators, falls within a rather narrow range (S_{opt} = 0.5-0.6).

APPROVED FOR RELEASE: 2007/02/08: CIA-RDP82-00850R000200100009-9

APPROVED FOR RELEASE: 2007/02/08: CIA-RDP82-00850R000200100009-9

When selecting turbulizer parameters it is important to consider the nature of the noise spectrum of the fan. If the greatest reduction of noise must be achieved in the low and intermediate frequency ranges (up to 2-3 kHz) it is advisable to use a screen turbulizer with a relatively large wire diameter (δ_s = 1-1.5 mm). The noise levels in this case may increase somewhat in the high-frequency range. To reduce the noise level in the entire audio frequency band it is desirable to use a turbulizer with a smaller wire diameter (δ_s = 0.4-0.8 mm), but the turbulizer will have somewhat less acoustic efficiency. In consideration of the conditions of air flow in centrifugal blowers it is desirable to install turbulizers at points of the length of the vanes next to the front disk. Blower pressure and efficiency losses in this case are negligible (Figure 7.9). The optimum screen turbulizer length for blowers of the TsS series is (0.4-0.5)l, where l is the length of the intake edge of the vane.

Turbulizers should also be installed on the delivery edges of the blades. Although the acoustic efficiency of these turbulizers is low, they still equalize the velocity field in between-vane channels, thereby promoting a certain amount of compensation of pressure and efficiency losses, which occur when turbulizers are used.

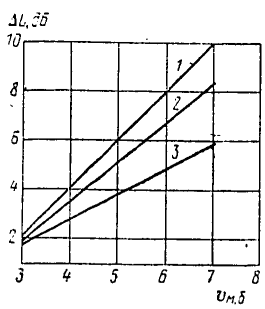

Figure 7.8. Reduction of noise level by screen turbulizers as function of maximum velocity on profile: 1 -- Δf = 20-1,350 Hz; 2 -- Δf = 20-5,600 Hz; 3 -- Δf = = 20-15,000 Hz. [дБ=dB; м.б= =m.d]

Semipermeable (perforated) blades (Figure 7.10) may also be used, in addition to turbulizers, for reducing turbulence noise, generated by a fan with separated flow past the blades. A perforation forces air to flow from the delivery surface of a blade to the suction surface. The point of flow separation is shifted downstream, and consequently the acoustic characteristics of the fan are improved.

To prevent a reduction of the noise level from detracting from the aerodynamic characteristics of blade arrays the perforation parameters must be selected in accordance with the graphs presented in Figure 7.11. If the maximum noise reduction is required and some sacrifice of the aerodynamic characteristics of the blowers can be tolerated, the perforation coefficient k = 0.15-0.20 should be used. In cases when the requirements on the energy characteristics are rigid the perforation coefficient must not exceed k = 0.08-0.12. Figure 7.12 shows, for instance, that when k = 0.18 and d_{hol} = 2.4 mm the noise reduction is 5-12 dB through the spectrum and the loss of blower efficiency is negligible

APPROVED FOR RELEASE: 2007/02/08: CIA-RDP82-00850R000200100009-9

APPROVED FOR RELEASE: 2007/02/08: CIA-RDP82-00850R000200100009-9

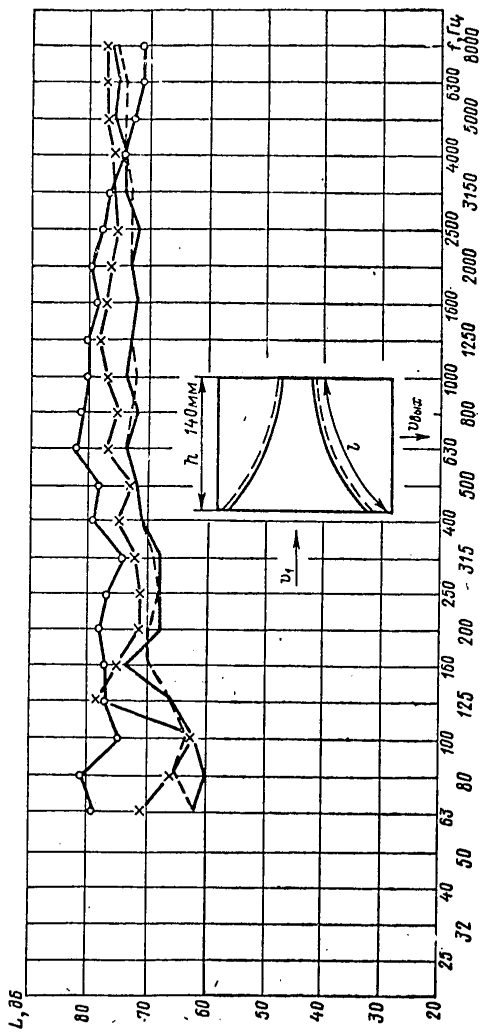

Figure 7.9. Noise spectrum of 45 TsS-24 blower (diagram of fan shown in center): o-o -- blower without screen (Q = 1.25 m^3/s, H = 264 Pa, η = 0.67); --- on intake side of screen 5.4 × 5.4 × 1.2, on discharge side of screen 2.5 × 2.5 × 0.6 (l = 80 mm, Q = = 1.25 m^3/s, H = 2440 Pa, η = 0.57); x-x on intake side of screen 5.4 × 5.4 × 1.2, on discharge side of screen 2.5 × 2.5 × 0.6 (l = 30 mm, Q = 1.25 m^3/s, H = 2590 Pa, η = = 0.59); —— on intake side of screen 5.4 × 5.4 × 1.2, on discharge side of screen 2.5 × 2.5 × 0.6 (Q = 1.25 m^3/s, H = 2330 Pa, η = 0.545). [дБ=dB; вых=out]

APPROVED FOR RELEASE: 2007/02/08: CIA-RDP82-00850R000200100009-9

APPROVED FOR RELEASE: 2007/02/08: CIA-RDP82-00850R000200100009-9

(1%). When k = 0.1 and d_{hol} = 1.8 mm the noise reduction for f < 4,000 Hz is 4-6 dB, but blower efficiency is 10% higher.

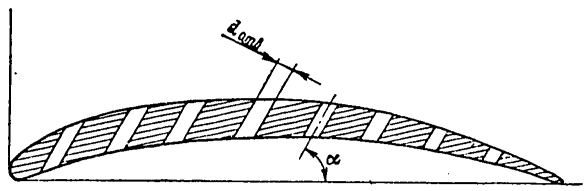

Figure 7.10. Diagram of perforated blade.

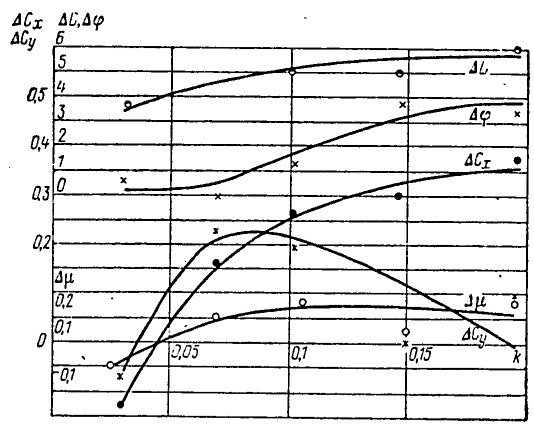

Figure 7.11. Effect of perforation coefficient k on aero-acoustic characteristics of plane blade arrays. $\Delta L = L_{ori.a} - L_{perf.a}$; $\Delta C_y = L_{perf.a} - L_{ori.a}$; $\Delta C_x = L_{ori.a} - L_{perf.a}$; $\Delta\phi = \Delta\beta_{perf.a} - \Delta\beta_{ori.a}$.

For the air velocities that are customary in ship ventilators the hole diameter in the blades should be in the range d_{hol} = 1-2 mm, where the smaller hole diameters correspond to arrays with better conditions of flow past the blades.

The optimum angle of inclination of the holes lies in the range α = 40-50°. When the angles of inclination of the holes are larger (α > 60°) the aerodynamic parameters of blade arrays (C_y, C_x) deteriorate (Figure 7.13); there is also a simultaneous reduction of acoustic efficiency. When

APPROVED FOR RELEASE: 2007/02/08: CIA-RDP82-00850R000200100009-9

APPROVED FOR RELEASE: 2007/02/08: CIA-RDP82-00850R000200100009-9

$\alpha < 40°$ the values ΔL, ΔC_y, ΔC_x are virtually unchanged and perforated blades with small α are much harder to manufacture.

The relative area of the perforated surface of a blade (in relation to the total blade area) $S = S_{perf}/bl$, exerts a considerable effect on the aerodynamic characteristics of perforated blades. Here b and l are chord length and blade length; $S_{perf} = (x_{hol} - x_{1hol} - x_{sep})l_{perf}$, where l_{perf} is the length of a perforated blade; x has the corresponding index of the chord coordinate: x_{sep} -- of the point of flow separation, x_{1hol} -- of the first row of holes, x_{hol} -- of the last row of holes.

If a blade is perforated through the entire length the equality

$$S = \frac{x_{hol} - x_{1hol} - x_{sep}}{b}$$

is valid.

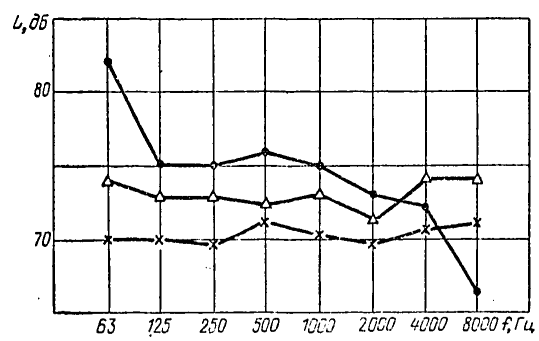

Figure 7.12. Spectrum of air noise of 40TsS-17 fan: .—. original fan with unperforated blades ($Q = 1.11\ m^3/s$; $H = 1545$ Pa; $\eta = 0.688$); Δ-Δ perforated blades ($k = 0.1$; $d_{hol} = 1.8$ mm; $H = 1505$ Pa; $\eta = 0.782$); ×-× perforated blades ($k = 0.18$; $d_{hol} = 2.4$ mm; $H = 1500$ Pa; $\eta = 0.678$). [дБ=dB; Гц=Hz]

The acoustic efficiency of perforated blades ΔL, plotted as a function of S (Figure 7.14), shows that when $S \geq 0.15$ the value of ΔL remains virtually constant at 5-6 dB of the total level. To take most complete advantage of the effect of perforation of blades the first 2-3 rows of holes should be in front of the points of flow separation, and the rest behind them.

APPROVED FOR RELEASE: 2007/02/08: CIA-RDP82-00850R000200100009-9

APPROVED FOR RELEASE: 2007/02/08: CIA-RDP82-00850R000200100009-9

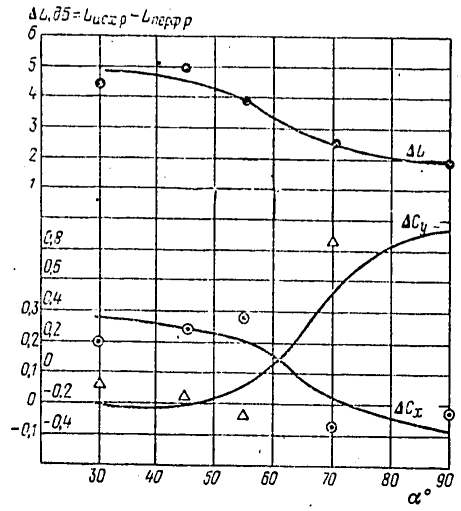

Figure 7.13. Influence of inclination angle of hole in blade on aeroacoustic characteristics of plane blade arrays. [дБ=dB; исх=ori; р=a; перф=perf]

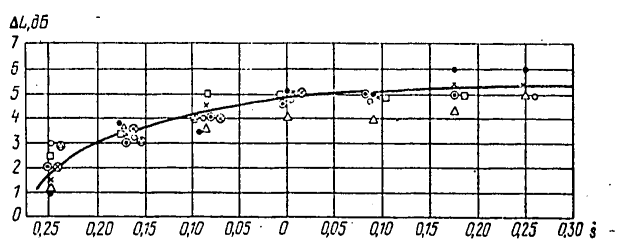

Figure 7.14. Effect of perforation area on acoustic efficiency.

The parameters of the blade arrays themselves also influence acoustic efficiency, in addition to perforation parameters. As is shown in the literature [10], perforated blades should be used when $v_{m.d} > 2.5$, i.e., when the flow past the blades is unsatisfactory. As profile thickness increases the acoustic efficiency decreases. For instance, when the relative profile thickness increases from 3 to 12% the reduction of noise ΔL decreases from 6 to 3 dB at constant ΔC_y and ΔC_x.

The acoustic efficiency of perforated blades also depends on the relative blade extension $\bar{l} = l/b$. When $\bar{l} < 1$ and secondary eddies appear the

APPROVED FOR RELEASE: 2007/02/08: CIA-RDP82-00850R000200100009-9

APPROVED FOR RELEASE: 2007/02/08: CIA-RDP82-00850R000200100009-9

coefficients C_y and C_x decrease and ΔL decreases simultaneously. Perforated blades should be used only when $\bar{l} \geq 1.25$.

Reduction of Noise from Irregular Flow. Acoustic pressure p on frequencies f = knz/60 (k = 1, 2, 3, ...), the source of which is flow irregularity, is determined by the expression

$$p = 4 \cdot 10^{-6} \frac{1}{rk\tau_1} \sin \frac{k\omega\tau_1}{2} \sin \frac{k\omega\tau_2}{2}, \qquad (7.2.5)$$

where r is the distance to the point of measurement, in m;

$$\tau_1 = \frac{t + \Delta x_3 - l \operatorname{tg}\theta - d/\cos\theta}{2\alpha R};$$
$$\tau_1 - \tau_2 = \frac{l \operatorname{tg}\theta + d/\cos\theta - \Delta x_3}{\alpha R}, \qquad (7.2.6)$$

Δx_3 is a parameter of the discharge flow velocity pattern, in m; t is the space between the blades; l is the height of the working blades in the delivery cross section; α is angular velocity; R is fan radius; θ is the angle of inclination of the body in the flow (the vanes of the flow straightening device, snail tongues) relative to the delivery edges of the blades; d is the thickness of the intake edge of the body in the flow.

The value of F, H is determined by the formula

[ct=st]

$$F = \frac{\pi d l}{2}\left(\Delta p_{\text{ст}} + \frac{\rho \Delta v^2}{4}\right), \qquad (7.2.7)$$

where $\Delta p_{st} = p'_{st} - p''_{st}$ is the maximum deficiency of static pressure in the aerodynamic medium;

$$\Delta v^2 = (v'_2)^2 - (v''_2)^2;$$

p'_{st}, v'_2 are the static pressure and flow velocity at the center of the between-blade channel; p''_{st}, v''_2 are the static pressure and flow velocity in the center of the aerodynamic medium.

It follows from expressions (7.2.5)-(7.2.7) that the following measures should be taken to reduce irregular flow noise.

1. Reduce the dimensions l, d of the intake parts of the flow straightening devices. This technique, however, cannot always be used, since the dimensions are usually determined by other considerations.

APPROVED FOR RELEASE: 2007/02/08: CIA-RDP82-00850R000200100009-9

APPROVED FOR RELEASE: 2007/02/08: CIA-RDP82-00850R000200100009-9

2. Reduce Δp_{st}, Δv, in particular, by increasing the space between the fan and the discharge edges of the flow straightener -- the snail tongues. The irregular flow noise level of axial fans can be reduced by ΔL = 14-15 dB by changing the relative axial space within the range ΔS_b = 0.1-1.0.

The dependence between ΔS_b and ΔL [10] is

$$\Delta S_б = 10^{\frac{\Delta L}{20}}. \qquad (7.2.8)$$

V. I. Zinchenko's formula for centrifugal compressors can be used for centrifugal blowers:

$$\Delta S_б = \frac{\Delta S}{D_2} \approx 0{,}17 \div 0{,}22, \qquad (7.2.9)$$

where D_2 is the diameter of the working wheel.

However, an increase of the axial and radial spaces detracts somewhat from the energy and weight and size parameters of blowers. For example, an increase of the space from $\Delta S = 0.03D_2$ to $\Delta S = 0.12D_2$ leads to a decrease of blower efficiency by 6-8% in addition to a decrease of the spectral component of irregular flow noise.

3. Change parameters τ_1 and τ_2 so that the trigonometric functions entering in formula (7.2.5) will be equal to zero. Since the parameters τ_1 and τ_2 are determined by angle of inclination θ of the body in the flow (7.2.6), the trigonometric functions will be equal to zero for some value of θ under otherwise identical conditions.

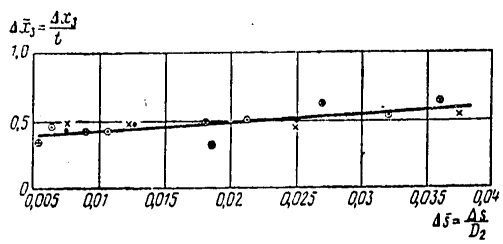

Figure 7.15. Parameter Δx_3 as function of radial space.

By solving the equations $k\omega\tau_1/2 = \pi m$; $k\omega\tau_2/2 = \pi m$, where m = 0, 1, 2, ..., for centrifugal blowers, we determine θ corresponding to p = 0:

$$\theta = \arccos \frac{(t + \Delta x_3)\, d + l\sqrt{(t + \Delta x_3)^2 + l^2 - d^2}}{(t + \Delta x_3)^2 + l^2}. \qquad (7.2.10)$$

APPROVED FOR RELEASE: 2007/02/08: CIA-RDP82-00850R000200100009-9

APPROVED FOR RELEASE: 2007/02/08: CIA-RDP82-00850R000200100009-9

It follows from formula (7.2.10) that the blade space, the length of the body in the flow and the parameter Δx_3 have the greatest effect on θ. The thickness of the leading edge has little effect on the angle of inclination, since $d \ll l$ in blowers.

To determine the parameter Δx_3 we may use data obtained for ship centrifugal blowers of the TsS series (Figure 7.15).

For axial blowers the angle of inclination of the blade of the flow straightening device can be determined by the formula

[p.k=f; пер=per]

$$\theta = \frac{180}{z_{\text{р.к}}} + \operatorname{arctg} \frac{t_{\text{пер}} + \Delta x_2 - a - d - l \cos \text{CAO}_2 \mp a_1}{l \sin \text{CAO}_2}, \qquad (7.2.11)$$

where z_f is the number of fan blades; t_{per} is the blade perforation space; $\Delta x_2 = (0.1\text{-}0.2)t_{mid}$ (t_{mid} is the blade space in the middle cross section); a, a_1 are values determined by the drawing of the fan blades and flow guide (Figure 7.16); a_1 has a plus sign when the vane of the flow guide is inclined toward the concave surface, and a minus sign when it is inclined toward the convex surface;

$$< \text{CAO}_2 = 90^\circ - \frac{180^\circ}{z_{\text{р.к}}}. \qquad (7.2.12)$$

The value of d in formulas (7.2.11) and (7.2.12) should be taken as the maximum blade thickness.

The use of a flow guide and snail with inclined blades has practically no effect on the energy characteristics of the machine, but it completely eliminates from the air noise spectrum of axial (Figure 7.7) and centrifugal (Figure 7.18) fans the component of noise due to flow irregularity.

One way to reduce irregular flow noise of axial fans is to optimize the ratio of the number of fan blades z_f to the flow guide device $z_{f.g}$. According to data in the literature [3], the following ratios of $z_{f.g}$ and z_f, depending on modulation index $\omega\tau_m$, are the best:

[c.a=f.g; p.k=f]

$\omega\tau_m$	2	3	4	5	6–7	8	9	10
$z_{\text{с.а}} - z_{\text{р.к}}$	5	6	7	8	10	12	13	15

APPROVED FOR RELEASE: 2007/02/08: CIA-RDP82-00850R000200100009-9

APPROVED FOR RELEASE: 2007/02/08: CIA-RDP82-00850R000200100009-9

The modulation index is determined by the expression

$$\omega\tau_m = \frac{2\pi n z_{\text{р. к.}}}{60} \cdot \frac{r \sin\beta}{C}, \qquad (7.2.13)$$

where β is the angle between the radius vector, drawn from the center PK to the measurement point, and the PK axis; r is the outside radius of the fan blades.

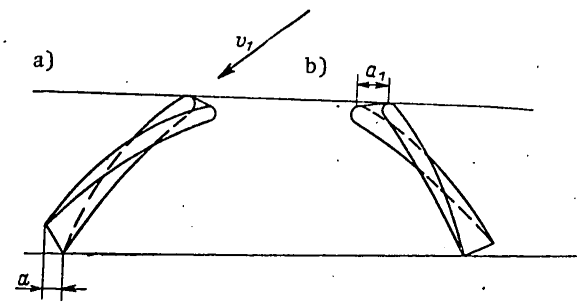

Figure 7.16. View of fan blades (a) and of guide vane (b) of axial blower stage.

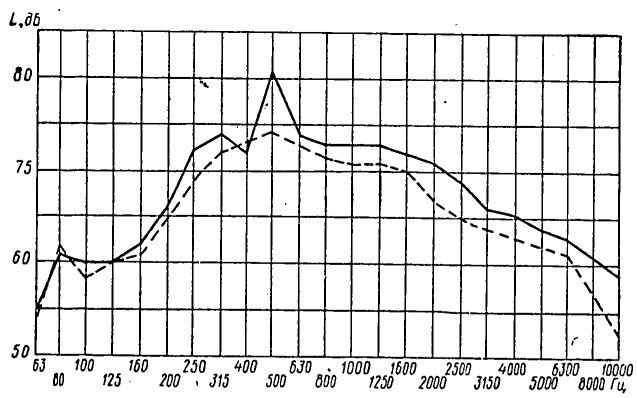

Figure 7.17. Air noise spectrum of axial blower. Guide vanes: —— serial; --- inclined. [дБ=dB; Гц=Hz]

In blowers with rather large $\omega\tau_m$ it is difficult to satisfy the equality $z_{f.g} - z_f = 10\text{-}15$, since this involves a sacrifice of energy parameters. For single-mode blowers the number of fan blades and the number of guide vanes may be determined by the expressions

$$\left.\begin{aligned} Jp_1'(\omega\tau_m) &= 0; \\ Jp_1''(\omega\tau_m) &= 0, \end{aligned}\right\}, \qquad (7.2.14)$$

where $p_1' = z_{f.g} - z_f$; $p_1'' = z_f$. When condition (7.2.14) is satisfied the value of $z_{f.g} - z_f$ can be minimum.

APPROVED FOR RELEASE: 2007/02/08: CIA-RDP82-00850R000200100009-9

APPROVED FOR RELEASE: 2007/02/08: CIA-RDP82-00850R000200100009-9

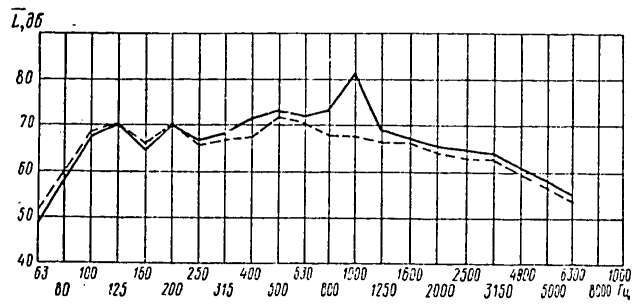

Figure 7.18. Air noise spectrum of centrifugal blower.
—— straight tongue; --- oblique tongue.

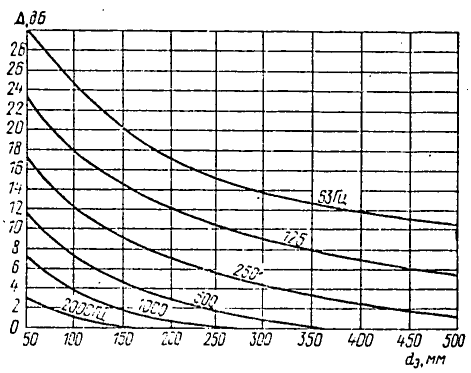

Figure 7.19. Graphs for determining reduction of noise due to reflection from open end of air duct.

The amplitude of acoustic pressure on frequency f = knz/60 can also be reduced by dephasing the pulses by using an uneven fan blade pitch [10]. For the first harmonic it is necessary that $I_0(2\pi\alpha_m/\alpha_0) = 0$, where $\alpha_0 = 2\pi/z_p$ is the pitch for unevenly spaced blades; α_m is the amplitude of the pitch nonuniformity. The first zero of the zero-order Bessel functions corresponds to an argument equal to 2.40; the second one to 5.52; the third to 8.65, etc. [4]. The corresponding maximum values of the relative amplitude of pitch nonuniformity are $(\alpha_m/\alpha_0)_{max} = 0.38, 0.88, 1.48$.

The amount of reduction of noise $\Delta L^{n.n}$ for a nonuniform pitch is plotted in Figure 7.19 as a function of d_e.

In spite of the fact that the number of waves of pitch nonuniformity has no effect on the amount of reduction of the noise level due to uneven flow, much attention must be devoted to the choice of λ, since λ determines the balance of the fan. When λ = 1 the blades are asymmetric, and the fan is

APPROVED FOR RELEASE: 2007/02/08: CIA-RDP82-00850R000200100009-9

APPROVED FOR RELEASE: 2007/02/08: CIA-RDP82-00850R000200100009-9

unbalanced. When $\lambda > 1$ the fans are balanced, which is preferable from the standpoint of vibration and strength characteristics.

7.3. Acoustic Calculation of Ventilation and Air Conditioning Systems

Reduction of the aerodynamic noise of blowers at the source (see §7.2) in most cases is not enough to assure acceptable noise conditions in rooms serviced by ventilation and air conditioning systems (VS and AC). Furthermore, at the comparatively high wind velocities that occur in these systems, parts of the duct work (branches and the elbows), hardware and air distribution systems are also sources of loud noise. In this connection the designers of VS and AC must solve the difficult problem of silencing these systems basically by selecting the best ventilation parameters, flow velocities, layouts and mufflers.

The acoustic calculation of VS and AC begins with the determination of the sources of noise and quantitative analysis of their intensity. Then the paths through which the noise propagates into rooms are found and acoustic energy losses that can occur are determined. The influence of the acoustic characteristics of these rooms on noise levels at given points is evaluated. Then the anticipated noise levels for a given room can be calculated and compared with standards and the required amounts of noise reduction can be determined.

As noise sources VS and AC systems are characterized by octave acoustic power levels, which must be known in order to calculate the noise levels that penetrate into a room through a branched ventilation system. The acoustic power levels are determined on the basis of the acoustic pressure levels, measured in accordance with the required conditions [7]. For rooms in which there are noise sources (ventilation units and air distributors), calculation of the anticipated noise levels can be limited to the octave acoustic pressure levels, measured on an acoustic test stand at a certain distance (usually 0.5 or 1 m) from these sources.

The acoustic calculation of VS and AC includes determination of the anticipated noise levels: in ventilator rooms, where ventilators and air conditioners are installed; in ventilated or air conditioned rooms; in rooms that contain transit ducts.

Calculation of Noise Levels in Ventilator Rooms. Ventilators and central air conditioners should be installed in ships in groups in special rooms -- ventilator rooms. This localizes the noise of the units and facilitates attainment of acceptable noise levels in adjacent state rooms and service rooms of the ship.

On the basis of design features that determine the propagation paths of noise produced by ventilators and air conditioners it is possible to view each of them as a set of three separate noise sources, which may be assumed to be independent, and to characterize them by their own noise levels or acoustic power. L_u and L_{Nu} are, respectively, the acoustic pressure level and acoustic power level, produced by a ventilator with

APPROVED FOR RELEASE: 2007/02/08: CIA-RDP82-00850R000200100009-9

APPROVED FOR RELEASE: 2007/02/08: CIA-RDP82-00850R000200100009-9

suction and delivery ducts leading into different rooms; L_{Nsuc} and L_{Ndel} are the acoustic power levels of aerodynamic noise, produced by a ventilator or air conditioner in ducts from the direction of the suction and delivery ducts. L_{suc} and L_{del} characterize the noise levels near open holes of the described ducts. Levels L_u and L_{suc} are known from the results of acoustic tests of ship ventilators, and L_u, L_{del} and L_{suc} are known from the results of acoustic tests of air conditioners. The relations that connect the acoustic power and noise levels of ventilation system (VS) and air conditioning (AC) equipment are presented below.

The values of L_u are the initial data for calculating the noise levels in ventilators, and L_{Nsuc} and L_{Ndel} are most often used for determining the anticipated noise levels in rooms equipped with VS and AC, and on open decks of a ship where there are holes, through which air is drawn in and discharged.

If the suction and delivery ducts of a ventilation unit are located outside of the ventilation room noise level L_r at a given point, in dB, the position of which is usually near the bulkhead that separates the ventilator room from the adjacent room, can be determined by the relation

[пом=r; ar=u]

$$L_{\text{пом}} = L_{\text{ar}} + \Delta L_{\text{пом}}. \qquad (7.3.1)$$

The correction factor ΔL_r, in dB, characterizing the influence of a room on the propagation of sound in it, is calculated by the formula

$$\Delta L_{\text{пом}} = 10 \lg \left[\frac{1}{4\pi r^2} + \frac{4(1-\alpha)}{\alpha S} \right] + \text{const}, \qquad (7.3.2)$$

where r is the distance between the unit and a given point in the ventilator room, in m; S is the total area of the surfaces that enclose the ventilator room, in m^2; α is the average sound absorption coefficient of the surfaces.

Information about coefficients α for the interior surfaces of ship rooms without special sound-absorbing wall coverings is presented in Chapter 11. The value of const depends on the distance from the unit at which levels L_u were determined under conditions of the shipbuilder's acoustic test stand. If this distance is 0.5 m, then const = 5 dB; for 1 m const = 11 dB.

If there are several units in the ventilator room it is necessary to calculate L_{r1}, L_{r2}, ..., L_r, which express the octave levels of the noise generated at a given point by each of the individual units. The total

APPROVED FOR RELEASE: 2007/02/08: CIA-RDP82-00850R000200100009-9

APPROVED FOR RELEASE: 2007/02/08: CIA-RDP82-00850R000200100009-9

octave levels L_r, in dB, of noise that occurs in the ventilator room during the operation of all the units are determined by logarithmic addition of the levels:

$$L_{пом} = 10 \lg \left(10^{0,1L_{пом\,1}} + 10^{0,1L_{пом\,2}} + \cdots + 10^{0,1L_{пом\,n}}\right). \qquad (7.3.3)$$

In cases when a ventilation unit takes in air directly from the ventilator room, the unit should be viewed as consisting of two independent noise sources, characterized by levels L_u and L_{suc}. These levels are usually presented in the technical documentation on ventilators and air conditioners. When there is one unit operating in a room with an open air intake duct L_r, in dB, is determined by the function

[вс=suc]

$$L_{пом} = 10 \lg \left[10^{0,1\,(L_{вс} + \Delta L_{пом\,1})} + 10^{0,1\,(L_{ar} + \Delta L_{пом\,2})}\right],$$

where ΔL_{r1} and ΔL_{r2} are determined by formula (7.3.2), respectively, for the distances between a given point in a room and the plane of the air intake opening of the suction duct of the unit, and the unit itself.

When there are several units in a ventilator room the total noise level is given by formula (7.3.3).

The octave noise levels L at a point 1 m from the plane of an open air intake or delivery duct of the ventilator unit are connected to the acoustic power levels L_N, in dB, by the function [10]

$$L_N + L + \Delta + 11, \qquad (7.3.4)$$

where Δ characterizes the attenuation of the acoustic power due to reflection from the plane of the delivery opening when it propagates from the duct into open space. It is determined by the graphs in Figure 7.19 on the basis of given frequency and equivalent diameter $d_e = 1.12\sqrt{S_d}$, where S_d is the cross section area of the duct. For cylindrical ducts d_e is the same as the diameter of the cross section.

The octave acoustic power levels L_{Nsuc}, in dB, radiated by a centrifugal blower into a duct from the suction side, can be calculated by the empirical formula

[в=b]

$$L_{N\,вс} = 10 \lg Q_в + n_в \lg H_в - 40 \lg f + 148, \qquad (7.3.5)$$

where Q_b is blower capacity, m^3/s; H_b is total pressure, Pa; f is the mean geometric frequencies of the octave bands, Hz; n_b is a coefficient, the values of which are presented below:

APPROVED FOR RELEASE: 2007/02/08: CIA-RDP82-00850R000200100009-9

APPROVED FOR RELEASE: 2007/02/08: CIA-RDP82-00850R000200100009-9

Frequency, Hz	63	125	250	500	1,000	2,000	4,000	8,000
n_b	7.5	10.0	12.5	15.0	17.5	20.0	22.5	25.0

With these relations it is possible to calculate noise levels L_{suc} of centrifugal blowers. It is important to note that formula (7.3.5) cannot be used for determining the noise levels of air conditioners, since they have built-in sound-absorbing structures that substantially reduce the aerodynamic noise levels of the blowers installed in them.

The noise levels in a room adjacent to the ventilator room $L_{a.r}$, in dB, are calculated by the formula [5]

[с.п=a.r; пом=r; пер=bul]

$$L_{с.п} = L_{пом} - R + 10 \lg S_{пер} - 10 \lg A_{с.п}, \qquad (7.3.6)$$

where R is the acoustic insulation of the bulkhead that separates the ventilator room from the adjacent room, dB; S_{bul} is the area of the bulkhead, m^2; $A_{a.r}$ is the sound absorption in the adjacent room, m^2.

Methods of determining the value R of ship bulkheads are described in Chapter 10, and methods of determining sound absorption A are given in Chapter 11. If the condition $L_{a.r} = L_{tol}$ must be satisfied, where L_{tol} are the tolerable noise levels, then it is possible, by solving equation (7.3.6) in terms of sound insulation R, to establish the values of R that must be assigned to the bulkhead that separates the ventilator room from an adjacent state room. It is obvious here that the noise levels produced by other sources must be at least 8-10 dB lower than the standard levels.

Calculation of Noise Levels in Rooms Equipped with VS and AC. The octave noise levels in a ventilated (air conditioned) room L_r, in dB, are represented in the general case by the logarithmic sum

[в=v; с=s; к=d]

$$L_{пом} = 10 \lg \left(10^{0,1 L_{пом.\,в}} + 10^{0,1 L_{пом.\,с}} + 10^{0,1 L_{пом.\,к}}\right), \qquad (7.3.7)$$

where $L_{r.v}$ are the octave noise levels of an operating ventilation unit, in dB; $S_{r.s}$ are the octave noise levels related to the passage of air through the ducts of the system, in dB; $L_{r.d}$ are the octave noise levels due to the passage of air through the air distribution devices, in dB.

In order to determine levels $L_{r.v}$ it is necessary to know the acoustic power levels radiated by the ventilator or air conditioner into the system, and its losses as the noise propagates from the ventilator to an examined room. Levels L_{Nsuc} and L_{Ndel} are calculated by formula (7.3.4) on the basis of known levels L_{suc} and L_{del} of air conditioners and ventilators.

APPROVED FOR RELEASE: 2007/02/08: CIA-RDP82-00850R000200100009-9

APPROVED FOR RELEASE: 2007/02/08: CIA-RDP82-00850R000200100009-9

For ventilators L_{del} usually are not measured, and therefore it is necessary to use relations found by analyzing the characteristic dimensions of the units, and on the basis of experimental data, in order to determine acoustic power levels L_{Ndel}. For ship centrifugal blowers $L_{Ndel} \approx L_{Nsuc}$ + + 4 dB in the entire octave frequency band, and for axial fans $L_{Ndel} \approx$ $\approx L_{Nsuc}$. Thus, if the suction noise levels are known it is possible to determine the acoustic power radiated by a blower into the delivery duct. Acoustic power levels L_{Nsuc} of centrifugal blowers can also be calculated by formula (7.3.5) on the basis of given energy parameters Q_b and H_b.

The great length of ventilation and air conditioning ducts, the branching of the systems and the presence in them of many profiled elements, hardware, technological equipment and control systems, are responsible for considerable losses of acoustic power in these systems. Data that characterize the attenuation of noise in straight sections of ducts are listed in Table 7.3 [10].

Table 7.3. Acoustic Power Losses in Straight Ducts, dB/m

1) Форма проходного сечения	2) Диаметр или ширина трубопровода, мм	3) Частоты октавных полос, Гц				
		63	125	250	500	≥1000
Круглая 4)	75—200	0,10	0,10	0,15	0,15	0,30
	200—400	0,06	0,10	0,10	0,15	0,20
	400—800	0,03	0,06	0,06	0,10	0,15
	800—1600	0,03	0,03	0,03	0,06	0,06
Прямоугольная 5)	75—200	0,60	0,60	0,45	0,30	0,30
	200—400	0,60	0,60	0,45	0,30	0,20
	400—800	0,60	0,60	0,30	0,15	0,15
	800—1600	0,45	0,30	0,15	0,10	0,06

Key: 1. Shape of cross section
2. Diameter or width of duct, mm
3. Frequencies of octave bands, Hz
4. Round
5. Rectangular

Most ship ventilation and air conditioning systems have comparatively small cross section dimensions of the ducts, many corners and are smooth. Under these conditions the average acoustic power losses per corner should be the following:

Frequency, Hz	63	125	250	500	1,000	2,000	4,000	8,000
Attenuation of acoustic power level, dB	0.05	0.10	0.15	0.20	0.25	0.30	0.35	0.40

APPROVED FOR RELEASE: 2007/02/08: CIA-RDP82-00850R000200100009-9

APPROVED FOR RELEASE: 2007/02/08: CIA-RDP82-00850R000200100009-9

These data refer to elbows with 45-90° turns. The reduction of acoustic power levels in elbows with angles smaller than 45° may be ignored; these ducts should be viewed as straight sections.

The acoustic power losses in certain kinds of ventilation and air conditioning hardware and equipment are presented in Table 7.4. As can be seen, filter cartridges have substantial losses. In other cases the losses occur only on frequencies above 1,000 Hz. It is important to remember that as the control gate closes the passage cross section the acoustic power losses in it increase.

Table 7.4. Acoustic Power Losses in Hardware, Filters and Heat Exchangers, dB

Type of equipment	Frequencies of octave bands, Hz							
	63	125	250	500	1000	2000	4000	8000
Ventilation flap valve	0	0	0	0	2	2	3	2
Bulkhead flap valve	0	0	0	0	2	3	4	3
Ordinary gate	0	0	1	2	4	4	5	5
Corner valve	0	1	3	4	4	6	6	5
Plate eliminator	0	0	1	1	1	0	0	0
Corner separator	0	1	3	4	4	6	6	5
Heat exchanger	0	0	1	1	1	1	1	2
Screen filter	0	0	0	1	1	1	2	3
Cartridge filter	8	8	10	12	20	24	28	25
Swivel air distributor	0	0	0	2	3	6	6	6
Swivel slotted air distributor	0	0	0	0	0	2	4	5
Perforated louver air distributor	0	0	0	1	1	3	5	5
Rotary louver air distributor	0	1	1	2	1	0	0	0
Airtight shutoff head	0	1	1	2	4	8	12	11
Mushroom shutoff head	0	1	1	2	4	8	12	11

Comments. 1. Data refer to hardware with completely open passage section. 2. For terminal grilles, screens and ventilator cowls losses are equal to zero on all frequencies.

Rather strong acoustic attenuation occurs in Soviet-manufactured standard air distribution and control systems. This is because they are lined with sound-absorbing materials. Information on noise attenuation in these systems are presented in the literature [10].

The reduction of the acoustic power level Δ_{br}, in dB, in a branch in comparison with the level in a main duct before the branch is determined by the formula

APPROVED FOR RELEASE: 2007/02/08: CIA-RDP82-00850R000200100009-9

APPROVED FOR RELEASE: 2007/02/08: CIA-RDP82-00850R000200100009-9

[отв=br; маг=ma]

$$\Delta_{отв} = 10 \lg \frac{\sum S_{отв}}{S_{отв}} + 10 \lg \left[\frac{\left(S_{маг}/\sum S_{отв} + 1\right)^2}{4S_{маг}/\sum S_{отв}} \right],$$

where S_{ma} and S_{br} are the cross section areas of the main duct in front of the branch and of the examined branch, respectively, in m^2; ΣS_{br} is the total cross section area of all the branches of an examined branch system, in m^2.

Reduction of the acoustic power level Δ_{cs}, in dB, due to an abrupt change (decrease or increase) of the cross section area of a duct is calculated by the formula

[сеч=cs]

$$\Delta_{сеч} = 10 \lg \frac{(S_1/S_2 + 1)^2}{4S_1/S_2},$$

where S_1 and S_2 are the cross section areas of the duct in front of and after the point of change, respectively.

Ventilation and air conditioning ducts are not characterized by great changes of cross section areas S_1 and S_2, and therefore losses Δ_{cs} may be ignored in most cases, particularly when the duct tapers from one cross section to the next.

If the acoustic power level L_{Nv}, radiated by a ventilator unit into a system, and its losses in elements of that system are known it is possible to determine noise levels $L_{r.v}$, in dB:

[пом=r; в=v; c=s]

$$L_{пом.\,в} = L_{Nв} - \sum \Delta_c + \Delta L_{пом}, \qquad (7.3.8)$$

where $\Sigma\Delta_s$, in dB, are the total acoustic power losses in the system, made up of the losses in straight parts of the ducts, corners and branches, in hardware, control and heating equipment, and of losses at the discharge from the system, determined by the graphs in Figure 7.20. Depending on what part is examined -- the intake or delivery, L_{Nv} may be replaced with L_{Nsuc} or L_{Ndel}; ΔL_r is determined by (7.3.2).

Octave acoustic power levels L_{Ns}, in dB, of noise that occurs as the air flows through hardware, elements of ducts and other ventilation and air conditioning equipment, can be established by the formula

[o.o=a.o; c=s; э=e; пр=fl]

$$L_{Nc} = L_{o.o} + m_c \lg v + 20 \lg d_э + q_c \lg \frac{S_{пр}}{S_0} - 61, \qquad (7.3.9)$$

APPROVED FOR RELEASE: 2007/02/08: CIA-RDP82-00850R000200100009-9

APPROVED FOR RELEASE: 2007/02/08: CIA-RDP82-00850R000200100009-9

where $L_{a.o}$ are the abstracted octave noise levels [10], in dB; v is the air flow velocity, in m/s; S_0 is the cross section area of the duct in the plane of the connecting flange of the hardware or other element, in m^2; d_e is the equivalent cross section diameter, in mm; S_{fl} is the cross section area of the flow part of the hardware, open to the passage of air, in m^2; m_s and q_s are coefficients, the values of which are listed in Table 7.5.

Table 7.5. Frequency Characteristics of Coefficients m_s and q_s

1) Коэффициенты	2) Частоты октавных полос, Гц							
	63	125	250	500	1000	2000	4000	8000
m_c	25	30	35	40	45	50	55	60
q_c	—15	—20	—25	—30	—35	—40	—45	—50

Key: 1. Coefficients [c=s] 2. Frequencies of octave bands, Hz

It has been established on the basis of test results of hardware and elements of ventilation and air conditioning ducts that levels $L_{a.o}$ do not depend on their dimensions and air intake velocity, or even on how open the passage cross section of control hardware is, which is characterized by the ratio S_{fl}/S_0. This also helped in the derivation of generalized relation (7.3.9).

Abstract octave levels $L_{a.o}$ for duct hardware and elements are listed in Table 7.6.

Noise level $L_{r.s}$, in dB, at a given point in a room, produced by a main duct element of a system, may be expressed as

$$L_{\text{пом. с}} = L_{\text{о. о}} + m_c \lg v + 20 \lg d_э + q_c \lg \frac{S_{\text{пр}}}{S_0} - \sum \Delta_c + \Delta L_{\text{пом}} - 72.$$

The sum $\Sigma\Delta_s$ is determined the same as in formula (7.3.8). The only difference is that a part of the system, located beyond the duct element whose noise is being calculated, is examined. In the general case the noise level produced in a room by all duct elements of a system will be represented by the logarithmic sum of the noise levels of each of the elements.

APPROVED FOR RELEASE: 2007/02/08: CIA-RDP82-00850R000200100009-9

APPROVED FOR RELEASE: 2007/02/08: CIA-RDP82-00850R000200100009-9

Table 7.6. Abstract Noise Levels $L_{a.o}$, in dB, of Duct Elements, Hardware and Equipment of Marine Ventilation and Air Conditioning Systems

	Elements, hardware	Frequencies of octave bands, Hz							
		63	125	250	500	1000	2000	4000	8000
Duct elements	Straight air duct	77	56	37	24	11	3	-5	-11
	Air duct with 30° corner	77	59	38	26	13	5	-3	-11
	Air duct with 60° corner	81	66	45	31	16	6	-2	-9
	Air duct with 90° corner	83	68	51	36	20	7	-1	-9
	Delivery T-piece, branch	88	72	53	41	26	9	-3	-11
	Branch in passage duct	81	69	51	36	21	6	-4	-11
Duct hardware	Corner separator	92	73	64	46	34	22	11	-1
	Corner valve	82	74	67	48	40	23	15	-7
	Ordinary gate	85	62	50	46	32	19	7	-7
	Throttle slide gate	72	56	38	26	18	10	4	-9
	Eliminator	77	63	57	47	41	36	30	21
	Ventilation flap	77	60	54	40	20	7	-3	-11
Air distribution hardware	Mushroom head	63	52	49	43	36	26	16	-6
	Terminal ventilator cowl with grille	57	41	30	22	15	14	7	-4
	Swivel louver air distributor	57	46	38	32	24	15	8	-2
	Swivel slotted air distributor	64	52	42	40	35	29	18	6
	Swivel air distributor	62	49	38	33	23	15	5	-2
	Terminal grille	60	47	40	37	30	25	15	4

The noise of an air distributor is radiated directly into the room in which it is installed. Therefore there are no acoustic power losses in this case, and noise levels $L_{r.d}$, in dB, are expressed by the relation

[пом=r; k=d;
o.o=a.o; c=s;
э=e; пр=fl]

$$L_{\text{пом. к}} = L_{\text{о. о}} + m_{\text{с}} \lg v + 20 \lg d_{\text{э}} + q_{\text{с}} \lg \frac{S_{\text{пр}}}{S_0} + \Delta L_{\text{пом}} - 72. \qquad (7.3.10)$$

The noise levels produced by an air distributor-control system in a room, calculated by formula (7.3.1), in which L_u is replaced by the appropriately measured noise levels of these systems. It is important to remember that the location of built-in control valves in air distribution and control systems has an effect on noise levels. Data illustrating this are presented in Figure 7.20.

When there are several air distribution systems in a room it is necessary once again to find a sum of the form (7.3.3). After levels $L_{r.v}$, $L_{r.s}$ and $L_{r.d}$ are calculated the total noise level is calculated by formula (7.3.7) and is compared with the tolerable values. By comparing $L_{r.v}$, $L_{r.s}$ and $L_{r.d}$ it is possible to determine sources of excessive noise and to find the best ways to reduce it.

APPROVED FOR RELEASE: 2007/02/08: CIA-RDP82-00850R000200100009-9

APPROVED FOR RELEASE: 2007/02/08: CIA-RDP82-00850R000200100009-9

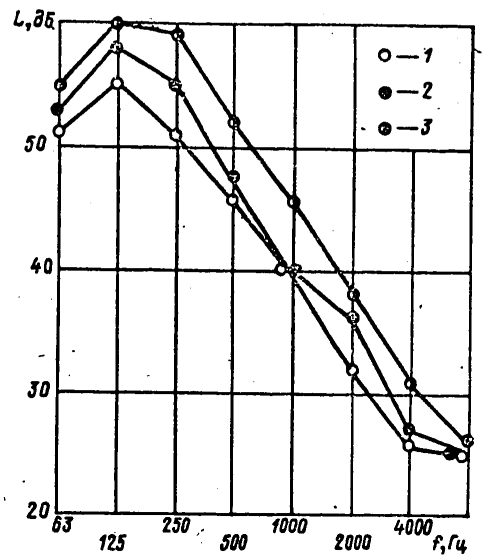

Figure 7.20. Octave noise levels 1 m from VSII-150/200 air distributor with only second channel open with 0.042 m^3/s air flow rate as function of location of control valve in channel. 1 -- gate completely open (90° opening); 2 -- 60° opening; 3 -- 45° opening. [дБ=dB; Гц=Hz]

The attenuation of levels $L_{r.v}$ and $L_{r.s}$ is most often accomplished by installing dampers in the systems. A reduction of $L_{r.d}$ can be achieved primarily by reducing velocity v in front of the air distributors, and by using quieter air distributors. Assuming $L_{r.d} = L_{tol}$ and solving equation (7.3.10) in terms of v it is possible to find the velocity at which an air distributor is virtually quiet. The smallest of the eight calculated values of velocity v must be used in order to make noise levels of an air distributor satisfy the tolerable levels in the entire frequency range.

Calculation of Noise Levels in Rooms with Transit Ventilation and Air Conditioning Ducts. Ventilation and air conditioning ducts that pass through the rooms of a ship are in many cases strong noise sources. The calculation of the levels of noise penetrating through the transit duct walls involves two problems. The first consists in determining the noise levels inside the duct, and the second in the determination of the sound-insulating effect of the duct walls. If the acoustic power levels, the calculation relations for which were given above, radiated by a ventilator unit into the system, are known noise levels $L_{du.v}$, in dB, generated by that unit in the transit duct, can be determined by the formula

APPROVED FOR RELEASE: 2007/02/08: CIA-RDP82-00850R000200100009-9

APPROVED FOR RELEASE: 2007/02/08: CIA-RDP82-00850R000200100009-9

[тр=du; в=v; с=s]

$$L_{\text{тр.в}} = L_{N\text{в}} - \sum \Delta_{\text{с}} - 10 \lg S_{\text{тр}},$$

where S_{du} is the cross section area of the duct, in m^2.

As before, depending on what part of the system is being examined, L_{Nv} should be replaced either with L_{Nsuc}, or with L_{Ndel}. The sum $\Sigma\Delta_s$ in the given case expresses the losses of acoustic power as the noise propagates from the unit to the midpoint of the transit duct.

In addition to the ventilator unit, its profiled elements and hardware, located in front of the transit part of the duct and beyond it, can influence the noise level in the duct. The total level $L_{du.s}$, in dB, is

$$L_{\text{тр.с}} = 10 \lg \left(10^{0,1 L_{\text{с}_1}} + 10^{0,1 L_{\text{с}_2}}\right),$$

where L_{s1} and L_{s2} are the noise levels in the duct as the air flow passes through elements of the system located, respectively, in front of and beyond the transit section of the duct, in dB.

Noise levels L_s, in dB, are calculated by the formula

[о.о=a.o; пр=fl]

$$L_{\text{с}} = L_{\text{о.о}} + m_{\text{с}} \lg v + q_{\text{с}} \lg \frac{S_{\text{пр}}}{S_0}.$$

When the hardware is completely open the last term in this formula vanishes.

The total noise level L_{du}, in dB, in a duct is represented by the sum

$$L_{\text{тр}} = 10 \lg \left(10^{0,1 L_{\text{тр.в}}} + 10^{0,1 L_{\text{тр.с}}}\right).$$

Noise level drop R_{du} in a duct and at a given point in a room depends on the size of the duct, the sound-insulating properties of its walls and the distance between it and a given point. It has been established on the basis of experimental data that for cylindrical ducts R_{du}, in dB,

$$R_{\text{тр}} = 10 \lg E + 20 \lg \delta_{\text{тр}} = 10 \lg h - 20 \lg f - 20 \lg d - 10 \lg \theta + 55,$$

and for rectangular ducts

$$R_{\text{тр}} = 20 \lg \delta_{\text{тр}} + 20 \lg \rho_{\text{тр}} + 10 \lg h - 20 \lg d_{\text{э}} - 10 \lg \theta + 17,$$

APPROVED FOR RELEASE: 2007/02/08: CIA-RDP82-00850R000200100009-9

APPROVED FOR RELEASE: 2007/02/08: CIA-RDP82-00850R000200100009-9

where E is the Young's modulus of the material from which the duct wall is made, in Pa; δ_{du} is the wall thickness of the duct, in mm; f is the frequency of the octave band, in Hz; d is the diameter of a cylindrical duct, in mm; ρ_{du} is the density of the duct wall material, in kg/m^3; d_e is the equivalent diameter of a rectangular duct; $\theta = \arctan l/h$ is the angle between rays emanating from a given point in a room and passing through the end points of a transit duct, in rad; l is the length of a duct within a room, in m; h is the shortest distance between a given point and the duct wall, in m.

Now noise level L_r, in dB, at a given point in a room can be expressed as

[пом=r; тр=du]

$$L_{пом} = L_{тр} - R_{тр} + \Delta L^*_{пом},$$

where ΔL^*_r is the increment of the noise level at a given point due to the acoustic energy reflected from the surface of the room, in dB.

The value ΔL^*_r, in dB, is determined by the formula [8]:

$$\Delta L^*_{пом} = 10 \lg \left(1 + 4x^2 \frac{1-\alpha}{\alpha}\right),$$

where $x = h/r_e$ is the dimensionless distance between the duct and given point; r_e is the radius of the equivalent sphere, the area of whose surface is equal to the sum of the area of the surfaces that enclose the examined room; α is the average sound absorption coefficient of the enclosing surfaces.

The value ΔL^*_r differs from correction factor ΔL_r presented above in that to determine it the levels at the points of a room and of the open space, separated from the noise source by exactly the same distance, are compared. However, correction factor ΔL_r expresses the difference between the noise levels at a point in the room, located at some distance r from the noise source, and the noise level produced by the same source in open space at a specific distance from it (1 m, for instance). ΔL_r may be positive and negative; however, increment ΔL^*_r is always positive.

A comparison of the values of noise level drop R_{du} of circular and rectangular ducts shows that under otherwise identical conditions the noise level drop of cylindrical ducts on low frequencies is 25-30 dB higher. This should be taken into consideration when selecting the shape of the cross sections of transit ducts.

APPROVED FOR RELEASE: 2007/02/08: CIA-RDP82-00850R000200100009-9

APPROVED FOR RELEASE: 2007/02/08: CIA-RDP82-00850R000200100009-9

In cases when the noise levels of a ventilation unit and duct work are attenuated appreciably by dampers, the noise characteristics of transit ducts are determined by the so-called turbulent boundary layer noise.

7.4. Ways to Reduce Noise of Ventilation and Air Conditioning Systems

The noise levels that occur in ship rooms during the operation of ventilation and air conditioning systems depend primarily on the noise characteristics of the blowers. The aerodynamic parameters of ventilation units, and consequently the noise levels are determined by the makeup, length, degree of branching of the systems and by the quality of their design and construction. In this connection it is necessary, to assure a quiet ventilation and air conditioning operating mode, to strive for simplicity and to minimize branching. This makes it possible to use comparatively low-pressure ventilation units, and that means less noise. The air flow rate in a system should not exceed the levels necessary for providing healthful air exchange in the serviced rooms. This notwithstanding, it would seem, the obvious rule, analysis of the causes of high noise in ship rooms, indicates that it is caused in many cases by the use in a system of blowers and air conditioners with exaggerated aerodynamic parameters. The tendency to overstate the pressure and capacity of blowers during the design of ventilation and air conditioning systems leads not only to increased noise levels in these units, exaggeration of data on the air exchange in rooms entails higher air flow velocities in the system. Consequently the noise levels that occur in the duct work, duct elements and air distributors increase. The use of ventilation units with a pressure margin necessitates the installation in ventilation and air conditioning systems of throttle systems, which are redundant. At high degrees of pressure throttling different kinds of gates and slides become strong noise sources, which determine the noise levels in ship rooms.

Operating experience shows that so-called control slides, built into air distribution systems and used for adjusting ventilation and air conditioning systems in accordance with the required delivery of air among rooms, exert an especially strong influence on the noise characteristics of marine air conditioning systems. In the general case the position of these controls can vary and can differ substantially from the completely open position, which affects the noise of the air distributor. A specific feature of these control valves is the fact that they are located right next to the discharge plane of the delivery duct. Data characterizing the influence of the length of a branch duct located immediately behind a throttle valve, at the level of the noise that it creates, are given in Figure 7.21. As can be seen, the noise levels of the slide valve in the 125-2,000 Hz range decrease as the length of the branch duct increases (within certain limits). It may be assumed that a slide valve will exert minimal influence on air distributor noise if it is installed about 1 m away from the distributor. Observing this rule in many cases reduces the noise in air conditioned rooms by 6-8 dB on frequencies of 125-2,000 Hz.

APPROVED FOR RELEASE: 2007/02/08: CIA-RDP82-00850R000200100009-9

APPROVED FOR RELEASE: 2007/02/08: CIA-RDP82-00850R000200100009-9

Ventilation units should be installed on shock absorbers, and the ducts should be connected to them through flexible absorbing pipes. This prevents the transmission of acoustic vibrations of ventilation units to ship hull structures, so that they do not cause noise in rooms distant from the ventilator room. An effort should be made when mapping ventilation and air conditioning duct routes to avoid routing them through state rooms and service rooms. Where fastened to ship structures ducts should have elastic vibration-insulating pads. The transit parts of ducts, passing through rooms, should be assembled, if possible, from cylindrical pipes. The exhaust vents of ventilation systems into the atmosphere should be so located that the noise penetrating through them will not be directed toward recreation areas, ship control stations and ward rooms.

Experience in the operation of marine air conditioning systems shows that single-duct high-velocity systems with additional conditioning of the air in state room conditioning units with built-in heat exchangers are the noisiest. Air conditioning systems that deliver air through perforated panel air distributors have the lowest noise levels. It should be borne in mind, however, that the noise characteristics of air distributors are determined not only by their design features, but also by the velocity of the air in them.

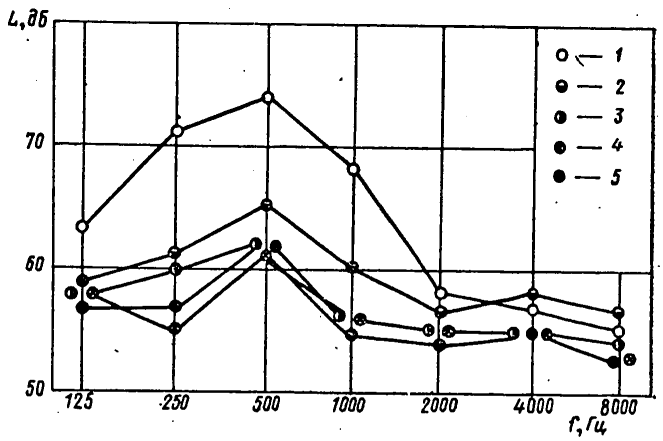

Figure 7.21. Noise characteristics of partly open round throttle valve as function of length of branch duct behind it. Branch duct length: 1 -- 100 mm; 2 -- 250 mm; 3 -- 500 mm; 4 -- 1,000 mm; 5 -- 2,000 mm. [дБ=dB; Гц=Hz]

The desirability of using mufflers and the choice of design, efficiency and location in a system are determined on the basis of the results of comparison of levels $L_{r.v}$, $L_{r.s}$ and $L_{r.d}$, which were calculated in the preceding section. Mufflers obviously can reduce the acoustic power level of

APPROVED FOR RELEASE: 2007/02/08: CIA-RDP82-00850R000200100009-9

APPROVED FOR RELEASE: 2007/02/08: CIA-RDP82-00850R000200100009-9

ventilator and duct work noise propagating through a system. If acoustic calculation of a system establishes that levels $L_{r.v}$ play a certain role in a particular room in the entire frequency band, or in just several octave bands, a muffler should be installed in the path of the ventilator noise. Duct work noise is reduced in the same way. The installation of one muffler in front of the air distributor can reduce ventilator and duct work noise simultaneously. However, in view of the comparatively long length of ventilation and air conditioning ducts and the fact that they can pass through rooms or in the immediate vicinity of them mufflers should be installed in most cases right after the ventilator (or in front of it if the problem is with the intake part of the system) and at the end of the system, after noisy duct work hardware.

If air distributor noise is the predominant noise efforts to improve living conditions in a room by installing mufflers may not produce positive results. The air distributor should be replaced with a less noisy one, or the air velocity in the duct in front of it should be reduced. But to maintain the required air exchange factor it is necessary to increase the number of distributors that service a given room. The effect of increasing the number of distributors ΔL_d, in dB, can be determined by the formula

[k=d; c=s] $$\Delta L_к = m_c \lg \frac{v_1}{v_2} - 10 \lg \frac{n_{к2}}{n_{к1}},$$

where ΔL_d is the reduction of the noise level, in dB; v_1 and v_2 are the flow velocities in front of the air distributors before and after an increase of their number, respectively; n_{d1}, n_{d2} are the numbers of air distributors before and after their number is increased, respectively.

The values of coefficient m_s are given in Table 7.5.

Air distributor noise levels cannot be reduced by installing duct mufflers. Therefore these levels are the natural limit to a reduction of noise in a given room.

Thus, when selecting the parameters of mufflers for reducing the noises of ventilators, duct work and duct hardware it is necessary to consider not only the required attenuation of the noise levels, but also the noise characteristics of the air distributors in a particular room. The desired effectiveness Δ_{muf}, in dB, of the installation of a muffler should be determined by the formulas:

for $L_{r.d} > L_{tol}$

[гл=muf; пом=r; в=v] $$\Delta_{гл} = 10 \lg \left(10^{0,1 L_{пом.\,в}} + 10^{0,1 L_{пом.\,с}}\right) - L_{пом.\,к} + 10;$$

APPROVED FOR RELEASE: 2007/02/08: CIA-RDP82-00850R000200100009-9

APPROVED FOR RELEASE: 2007/02/08: CIA-RDP82-00850R000200100009-9

for $L_{r.d} < L_{tol}$

[доп=tol] $$\Delta_{гл} = 10 \lg \left(10^{0,1 L_{пом.в}} + 10^{0,1 L_{пом.с}}\right) - L_{доп}.$$

The procedure for calculating Δ_{muf} for mufflers that are most often used in ship ventilation and air conditioning systems is explained below.

7.5. Noise Mufflers of Ship Ventilation and Air Conditioning Systems

Primarily dissipative mufflers, the attenuation of which is based on the absorption of acoustic energy by special liners, made of porous or fibrous sound-absorbing materials, are used for reducing noises that propagate the ducts of ship ventilation and air conditioning systems. It is customary to estimate the influence of a muffler on the noise level of a system on the basis of the frequency characteristic of the effect of installation, which in each octave band is found as the difference of the acoustic pressure levels at a given point near the delivery port of the system before and after the installation of a muffler [10].

The simplest of dissipative mufflers in terms of design that work well in the medium- and high-acoustic frequency ranges are mufflers of the sound-absorbing branch type (Figure 7.22), which are subdivided in accordance with the shape of the cross section into cylindrical and prismatic. Different kinds of mufflers, designed as 90° turns, are also used in ship ventilation and air conditioning systems in addition to straight sound-absorbing branches. A diagram of one of the three utilized modifications of mufflers is shown in Figure 7.23.

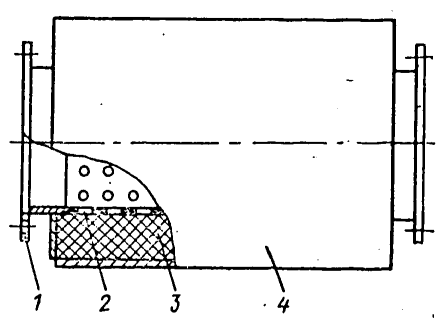

Figure 7.22. Structural diagram of sound-absorbing branch muffler: 1 -- flange; 2 -- perforated pipe; 3 -- sound-absorbing liner; 4 -- wall.

The passage cross section of a sound-absorbing branch is usually the same size as the ducts to which it is connected and is constant from end to end.

APPROVED FOR RELEASE: 2007/02/08: CIA-RDP82-00850R000200100009-9

APPROVED FOR RELEASE: 2007/02/08: CIA-RDP82-00850R000200100009-9

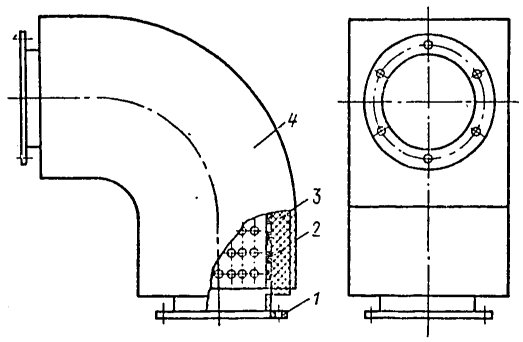

Figure 7.23. Structural diagram of prismatic sound-absorbing branch muffler in elbow form (see Figure 7.22 for explanation).

The internal perforated pipe is used for holding the sound-absorbing liner in the required position and for protecting it from being blown away by the air flow (the perforation coefficient is ≥ 0.2).

Grades E3-100 and E2-80 incombustible glass fibers and E3-200 glass screen (GOST 19907-74) are most often used as windproof linings in mufflers.

Test results of various researchers show that ventilation and air conditioning system mufflers whose sound-absorbing liners are made of loosely packed fibrous materials, such as grade VT-4 staple capron fiber mats (TU 17 RSFSR 5232-71) [TU: Technical Specification], VT-4s mats (TU RSFSR 17-2166-68), also made of capron fiber, and ATM-1 (MRTU 6-11-11-64) [MRTU: Interrepublic Technical Specifications] and III mats (STU 651-65 or STU 57/07-3-65) [STU: Sovnarkhoz Technical Specifications] mats, made of superfine glass fiber. The recommended density of capron fiber liners is 40-60 kg/m^3, and for superfine glass fiber mats it is 15-25 kg/m^3.

It has been established experimentally that a 50 mm thick sound-absorbing linear provides effective attenuation of ventilation and air conditioning noise and can be used in mufflers of sizes acceptable for ships. This is the standard liner thickness today for ship mufflers (of the sound-absorbing branch type), manufactured from standard drawings.

Frequency f_m, in Hz, on which the maximum attenuation of noise is provided by a sound-absorbing branch, is related to the dimensions of its passage cross section and loosely packed fibrous liner thickness by the empirical formula

[г=h; об=lin]

$$f_m = \frac{11200}{\sqrt{d_г \delta_{об}}},$$

APPROVED FOR RELEASE: 2007/02/08: CIA-RDP82-00850R000200100009-9

APPROVED FOR RELEASE: 2007/02/08: CIA-RDP82-00850R000200100009-9

where $d_h = 4S_0/\Pi$ is the hydraulic diameter of the muffler cross section, in cm; δ_{lin} is the thickness of the sound-absorbing liner, in cm; S_0 and Π are the area and perimeter of the muffler cross section, respectively.

Using frequency f_m as a standard unit it is possible on the basis of experimental data to determine the generalized frequency characteristic of the effect of installing a sound-absorbing branch muffler with a loosely packed sound-absorbing liner.

A study of the frequency characteristics of mufflers with different relative (expressed in calibers) length disclosed that the attenuation of acoustic energy in them is nonuniform. The first three calibers of a muffler (one caliber is equal in length to hydraulic diameter d_h [10]) work most effectively. Therefore that is the length that is used as the basic length for sound-absorbing branch type mufflers. A further increase of muffler length is accompanied by a slowdown of the rate of increase of its effectiveness. Noise attenuation $\Delta_{muf.c}$, in dB, of a muffler not longer than five calibers is fairly accurately determined by the empirical formula

[гл=muf; k=c] $$\Delta_{гл.к} = \Delta_{гл1}(1 + 3\lg K_{гл}),$$

where Δ_{muf1} is the noise attenuation of the first caliber of a muffler, the length of which in calibers is $K_{muf} \leq 5$, dB; $K_{muf} = l_{muf}/d_h$ is the length of the active part of the muffler, in which the sound-absorbing liner is installed.

Data on Δ_{muf1} as a function of dimensionless frequency f/f_m are presented in Table 7.7.

Table 7.7. Noise Attenuation of First Caliber of Sound-Absorbing Branch Muffler with Fiber Liner

1) Толщина облицовки, мм	2) Ослабление шума $\Delta_{гл1}$, дБ, при безразмерной частоте f/f_m								
	0,062	0,125	0,25	0,5	1	2	4	8	16
25	1	1	2	4	8	4	3	3	3
50	1	1,5	3	6	10	6	3,5	3,5	3,5
≥100	1	2	4	8	12	8	4	3,5	3,5

Key: 1. Liner thickness, mm
2. Noise attenuation Δ_{muf1}, dB, for dimensionless frequency f/f_m

APPROVED FOR RELEASE: 2007/02/08: CIA-RDP82-00850R000200100009-9

APPROVED FOR RELEASE: 2007/02/08: CIA-RDP82-00850R000200100009-9

The nonuniformity of noise attenuation is related to a change of character of the acoustic field as it propagates along a muffler. If the total energy of fast-attenuating normal waves of higher numbers predominates in the front of a muffler, the energy of the weak-attenuating fundamental wave, the leading edge of which, in a manner of speaking, slides along the surface of the sound-absorbing liner, begins to prevail after the third caliber. The difference of the rates of attenuation of waves of different numbers [6] also makes a contribution to the nonuniformity of different parts of a muffler and to its total effectiveness. After noise passes through the first five calibers of a muffler only the fundamental wave remains in the noise, for practical purposes, and the rate of attenuation of the wave remains constant through the entire length of the muffler. Stabilization of the character of the acoustic field in a muffler, in sections after the first 3-4 calibers, causes the attenuation of noise per caliber to become constant. The effect $\Delta_{muf.c}$, in dB, of installing a muffler longer than five calibers can be determined by the formula

[o=m] $$\Delta_{гл.к} = 3\Delta_{гл1} + \Delta_{гл.о}(K_{гл} - 5),$$

where $\Delta_{muf.m}$ is the attenuation, in dB, of the main normal wave by one caliber of a muffler.

For mufflers with 50 mm thick loosely packed fiber liners the values of $\Delta_{muf.m}$ are:

Dimensionless frequency f/f_m	0.062	0.125	0.25	0.5	1	2	4	8	16
Noise attenuation $\Delta_{muf.m}$, dB	0.5	0.5	1.5	2.0	2.5	3.0	2.5	2.0	2.0

The data presented above can be used for determining the frequency characteristics of the effect of installing sound-absorbing branch mufflers with VT-4, VT-4s and ATM-1 mat liners.

Elastic self-attenuating porous polyurethane, called brand PPU-E-40-1,2 poroplast, and manufactured in accordance with MRTU 6-05-1150-68, has come to be used in recent years as sound absorbent in marine mufflers. Poroplast is technologically easier to handle than fibrous sound absorbers. It is also more resistant to the air flow and does not require wind-protective covers. However, a poroplast liner is considerably less effective in the medium-frequency range than a fiber liner (Figure 7.24). Data on the attenuation of noise by sound-absorbing branch mufflers with poroplast liner are presented in Table 7.8. Data for cylindrical mufflers satisfactorily describe the effectiveness of mufflers with 100-200 mm effective cross sections. For determining the frequency characteristics of noise attenuation $\Delta_{muf\ 3}$, dB, of three caliber long cylindrical mufflers with 50 mm thick poroplast liners with diameters of 50-500 mm it is preferable to use the empirical relation

APPROVED FOR RELEASE: 2007/02/08: CIA-RDP82-00850R000200100009-9

APPROVED FOR RELEASE: 2007/02/08: CIA-RDP82-00850R000200100009-9

$$\Delta_{гл\,3} = a_{гл} + b_{гл} \lg \frac{d}{50},$$

where $\Delta_{muf\ 3}$ is the noise attenuation of a three caliber long muffler, in dB; a_{muf} and b_{muf} are parameters, the values of which are given in Table 7.9; d is the effective cross section diameter of a muffler, in mm.

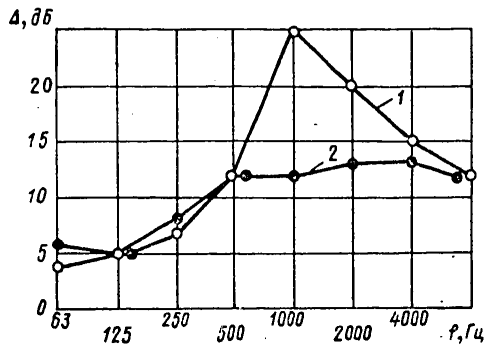

Figure 7.24. Comparison of efficiency of three caliber long sound-absorbing branch mufflers with 100 × 130 mm effective cross section with 50 mm thick grade VT-4 mat sound-absorbing liner (1) and PPU-E-40-1,2 poroplast (2). [дБ=dB; Гц=Hz]

Table 7.8. Effect, in dB, of Installation of Sound-Absorbing Branch Muffler with 50 mm Thick Poroplast Liners

1) Вид глушителя	2) Длина глушителя, в калибрах	3) Частоты октавных полос, Гц							
		63	125	250	500	1000	2000	4000	8000
4) Цилиндрический	3	3	5	9	12	15	16	16	14
	5	3	8	15	20	20	20	20	15
5) Призматический	3	4	6	8	9	11	13	13	12
	5	4	9	14	17	17	17	19	13

Key: 1. Kind of muffler
2. Muffler length, in calibers
3. Frequencies of octave bands, Hz
4. Cylindrical
5. Prismatic

APPROVED FOR RELEASE: 2007/02/08: CIA-RDP82-00850R000200100009-9

APPROVED FOR RELEASE: 2007/02/08: CIA-RDP82-00850R000200100009-9

Table 7.9. Values of Parameters a_{muf} and b_{muf}

1) Параметры	2) Частоты октавных полос, Гц							
	63	125	250	500	1000	2000	4000	8000
$a_{гл}$	3	5	9	9	10	10	10	10
$b_{гл}$	0	0	0	5	7	9	12	7

Key: 1. Parameter 2. Frequencies of octave bands, Hz

The efficiency of sound-absorbing mufflers with larger passage cross sections can be increased by installing in them sound-absorbing panels, which divide a muffler into several channels with smaller cross sections. Data on the effect of these plates are given in the literature [10].

It should be mentioned that the noise reduction capabilities of mufflers are not limitless. Their efficiency is limited both by the generation of noise as the air flow passes through a muffler and elements of a system that come after it, and by the existence of bypasses and detours through which acoustic energy is transmitted, for example through the perforated pipe and wall of a muffler.

BIBLIOGRAPHY

1. Gutin, L. Ya., "On Acoustic Field of Rotating Air Screw," ZHURNAL TEKHNICHESKOY FIZIKI [Journal of Technical Physics], 1936, No 5, pp 899-909.

2. Yel'nik, A. G., "Noise Reduction of Ship Air Conditioning Systems," TRUDY TSNIIMF [Proceedings of Central Scientific Research Institute of the Maritime Fleet], 1968, No 191, pp 83-86.

3. Kim, Ya. A., "Effect of Number of Blades of Rotor and Stator on Noise and Vibration of Blade Machines," "Akustika v Sudostroyenii. Materialy po Obmenu Opytom" [Acoustics in Shipbuilding. Materials on Exchange of Experience], Leningrad, Sudostroyeniye, 1974, pp 45-57.

4. Kim, Ya. A., "Influence of Nonuniform Fan Blade Pitch on Discrete Components of Noise and Vibration of Blade Machine," "Tezisy Dokladov VII Vsesoyuznoy Akusticheskoy Konferentsii" [Theses of Reports at 7th All-Union Acoustics Conference], Leningrad, 1971.

5. Klyukin, I. I., "Bor'ba s Shumom i Zvukovoy Vibratsiyey na Sudakh" [Combatting Noise and Acoustic Vibration on Ships], Leningrad, Sudostroyeniye, 1971.

APPROVED FOR RELEASE: 2007/02/08: CIA-RDP82-00850R000200100009-9

APPROVED FOR RELEASE: 2007/02/08: CIA-RDP82-00850R000200100009-9

6. Morz, F., "Kolebaniya i Zvuk" [Vibrations and Sound], Moscow, GITTL, 1949.

7. Osipov, G. L., D. Z. Lopashov and Ye. N. Fedoseyeva, "Izmereniye Shuma Mashin i Oborudovaniya" [Measurement of Noise of Machines and Equipment], Moscow, Izd-vo Komiteta standartov, mer i izmeritel'nykh priborov, 1968.

8. Rozenberg, L. L., "Influence of Average Sound Absorption Coefficient on Acoustic Force Level," ZHURNAL TEKHNICHESKOY FIZIKI, 1940, No 19, pp 1634-1638.

9. Seliverstov, V. M., "Raschety Sudovykh Sistem Konditsionirovaniya Vozdukha" [Calculation of Marine Air Conditioning Systems], Leningrad, Sudostroyeniye, 1971.

10. Khoroshev, G. A., Yu. I. Petrov and N. F. Yegorov, "Shum Sudovykh Sistem Ventilyatsii i Konditsionirovaniya Vozdukha" [Noise of Marine Ventilation and Air Conditioning Systems], Leningrad, Sudostroyeniye, 1974.

11. Yudin, Ye. Ya., "Issledovaniye Shuma Ventilyatornykh Ustanovok i Metodov Bor'by s Nim" [Analysis of Ventilator Noise and Ways to Control It], Moscow, Oborongiz, 1958.

12. Yudin, Ye. Ya. and A. V. Tolmachev, "Calculation of Noise Generated by Throttle and Control Devices in Air Ducts," VODOSNABZHENIYE I SANITARNAYA TEKHNIKA [Water Supply and Sanitation Engineering], 1969, No 11, pp 30-32.

APPROVED FOR RELEASE: 2007/02/08: CIA-RDP82-00850R000200100009-9

APPROVED FOR RELEASE: 2007/02/08: CIA-RDP82-00850R000200100009-9

CHAPTER 8. NOISE REDUCTION OF SHIP HYDRAULIC SYSTEMS, COMPRESSORS AND ELECTRICAL MACHINERY

8.1. Causes of Noise in Ship Hydraulic Systems

Noise Sources. Pumps and controls are the main sources of noise in ship hydraulic systems.

The intensity and spectral composition of air noise and vibrations of ship hydraulic equipment depend on design, on the pressure drops of local hydraulic resistances, velocity and temperature of the hydraulic fluid. The concentration of air in water also exerts a strong effect on the level of air noise and vibration.

The working processes of the basic types of control equipment are based on flow throttling principles. When critical pressure drops are reached throttling is accompanied by cavitation, which is a powerful source of acoustic energy. Therefore the vibration and noise characteristics of a hydraulic system are usually expressed as functions of the cavitation number, which connects the basic hydraulic flow parameters:

[k=c; п=v; ж=fl]

$$\sigma_{к} = \frac{p_2 - p_{п}}{\frac{c_{ж}^2}{2g}}, \qquad (8.1.1)$$

where p_2 is the fluid pressure in the flow after a control; p_v is the vaporization pressure at a given temperature; c_{fl} is the fluid flow velocity.

The experimental dependences [5] of the general acoustic noise and vibration levels on the cavitation number $L = f(\sigma_c)$ and $L_{\ddot{x}} = f(\sigma_c)$ for the basic types of marine hydraulic systems are plotted in Figures 8.1 and 8.2. The graphs show that at numbers $\sigma_c > 60$ acoustic noise and vibration have levels that do not exceed $L \leq 60$ dB and $L_{\ddot{x}} \leq 52$ dB. Air noise and vibration with $\sigma_c > 60$ are produced by turbulence, which precedes flow cavitation, and by vibrations of air bubbles, released in eddies and eddy zones.

APPROVED FOR RELEASE: 2007/02/08: CIA-RDP82-00850R000200100009-9

APPROVED FOR RELEASE: 2007/02/08: CIA-RDP82-00850R000200100009-9

As σ_c decreases from approximately 60 to the minimum value the noise and vibration levels increase suddenly due to the onset and intensification of cavitation.

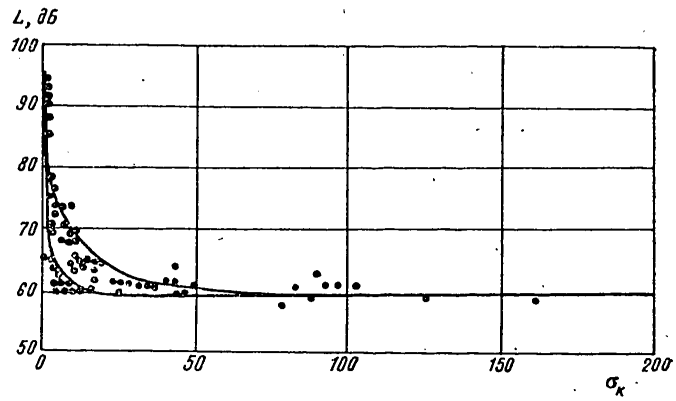

Figure 8.1. Acoustic noise level of hydraulic system as function of cavitation number. [дБ=dB; н=c]

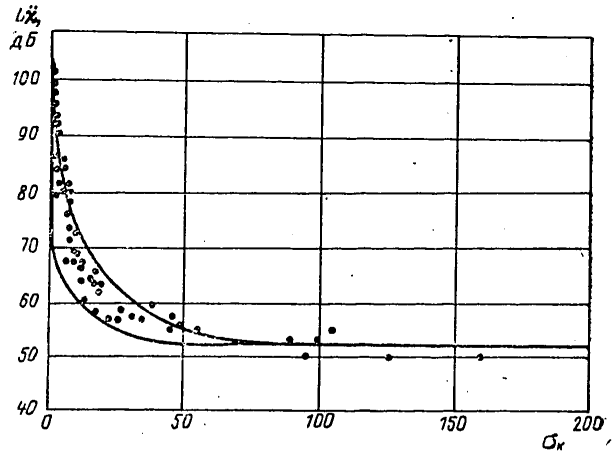

Figure 8.2. Vibration level of hydraulic system as function of cavitation number.

Two curves that bound the maximum and minimum acoustic noise and vibration levels of a system are given in Figures 8.1 and 8.2. The bottom curve corresponds to a system with low local impedances (ζ = 0.25-0.4), and the top to a system with high local impedances ($\zeta \approx 5$).

APPROVED FOR RELEASE: 2007/02/08: CIA-RDP82-00850R000200100009-9

APPROVED FOR RELEASE: 2007/02/08: CIA-RDP82-00850R000200100009-9

The acoustic noise and vibration levels of ship equipment on the hydraulic impedance coefficients for different values of σ_c are plotted in Figures 8.3 and 8.4. As can be seen, the noise and vibration levels for given numbers σ_c are higher in a system with high local impedances. And the noise and vibration levels increase faster with local impedances as σ_c gets smaller. The reason is that cavitation develops more slowly in a system with less cavitation impedance for the same values of σ_c.

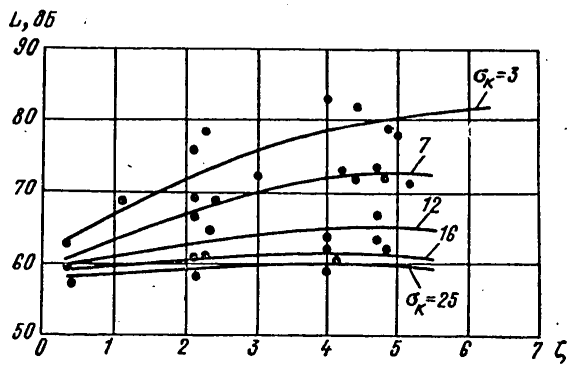

Figure 8.3. Acoustic noise level of system as function of hydraulic impedances.

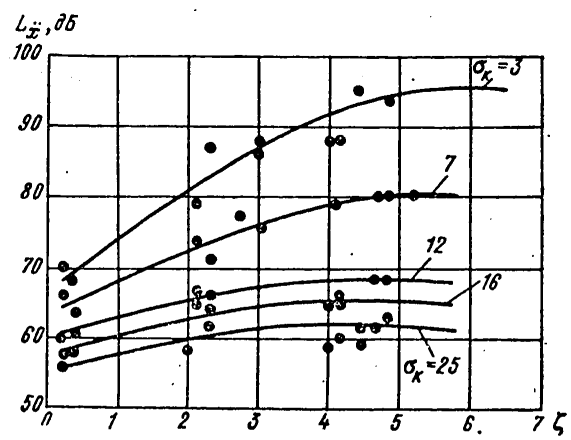

Figure 8.4. Vibration level of system as function of hydraulic impedances.

APPROVED FOR RELEASE: 2007/02/08: CIA-RDP82-00850R000200100009-9

APPROVED FOR RELEASE: 2007/02/08: CIA-RDP82-00850R000200100009-9

Vibration spectrograms of individual kinds of cutoff and control devices are shown in Figures 8.5 and 8.6, where it is obvious that high-frequency components in the spectra play a dominant role.

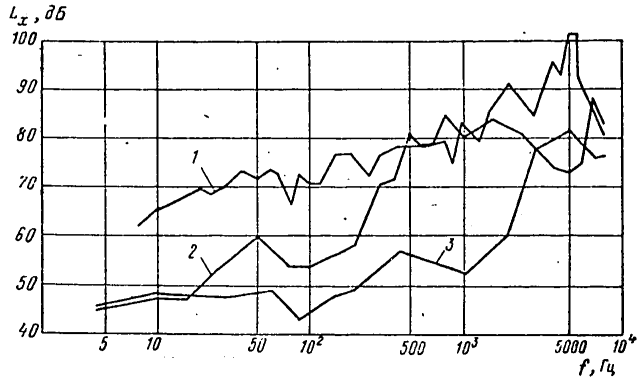

Figure 8.5. Vibration spectrograms of cutoff valves: 1 -- check valve, D_y = 100 mm; 2 -- gate valve, D_y = = 100 mm; 3 -- sluice valve, D_y = 100 mm. [дБ=dB; Гц=Hz]

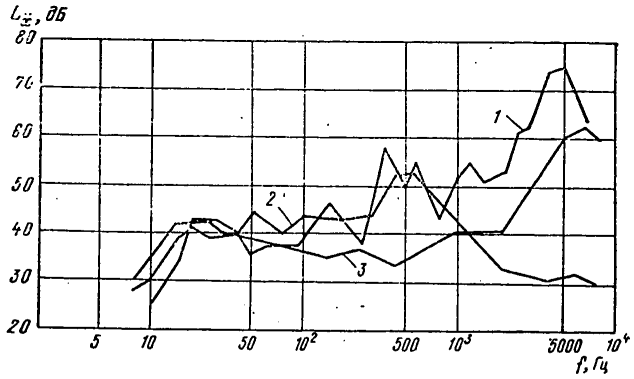

Figure 8.6. Vibration spectrograms of control valves: 1 -- throttle valve, D_y = 60 mm; 2 -- throttle valve, D_y = 40 mm; 3 -- reduction valve, D_y = 50 mm.

Approximation of experimental data produced the following approximate relations between the overall noise and vibration levels of marine hydraulic equipment on the cavitation number:

APPROVED FOR RELEASE: 2007/02/08: CIA-RDP82-00850R000200100009-9

APPROVED FOR RELEASE: 2007/02/08: CIA-RDP82-00850R000200100009-9

noise level L_{max}, in dB

[k=c]

$$L_{max} = 35e^{-0,12\sigma_K} + 60; \quad (8.1.2)$$

vibration level $L_{\ddot{x}\,max}$, in dB

$$L_{\ddot{x}=max} = 52e^{0,09\sigma_K} + 52. \quad (8.1.3)$$

The strongest noise source of the three main types of valves -- check, distribution and control, is control hardware, since the working process in a control valve is based on the flow throttling principle.

The best ways to reduce the noise of hydraulic equipment is to limit the pressure drops (per stage) to subcritical when cavitation begins to occur and to perfect the profiles of the flow passages. Results that have been achieved in this respect are extremely encouraging [1]. A few designs of the passage parts of multistage throttle valves, which provide a substantial reduction of noise and vibration in the entire spectrum in comparison with single-stage valves, calculated for the same parameters, are illustrated in Figure 8.7 as examples.

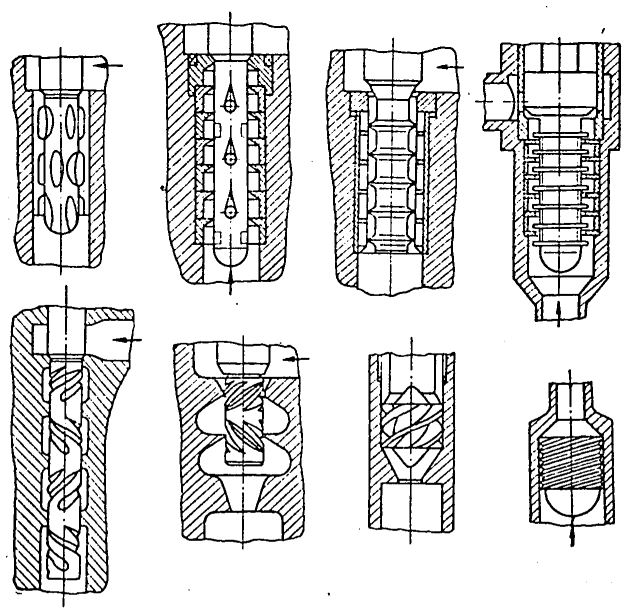

Figure 8.7. Design diagrams of flow passage parts of quiet throttle valving.

APPROVED FOR RELEASE: 2007/02/08: CIA-RDP82-00850R000200100009-9

APPROVED FOR RELEASE: 2007/02/08: CIA-RDP82-00850R000200100009-9

Other strong noise and vibration sources in hydraulic systems are certain final control devices, used chiefly in hydraulic control systems. The most vibration-active elements of these systems are various kinds of levers, slides and valves. Friction and impacts of contacting parts, in particular impacts of valves on seats in the valve cases, impacts and friction in couplings of the drives of slide valves, levers and in other assemblies, are other sources of noise and vibration, in addition to hydraulic factors (turbulence, pressure pulsations and cavitation).

Vibration and pressure pulsations, produced by pumps, fittings and hydraulic control mechanisms, are transmitted by the lines that connect the elements and also propagate through the fluid.

The propagation of perturbations in the flow, which takes place at the speed of sound, does not depend on the velocity of the fluid in the line. Pressure pulsations in hydraulic lines attenuate over very short distances from the source. This applies principally to straight sections of lines. Elbows, branches, flexible sleeves and various fittings in the path of the flow promote reflection, dissipation and conversion of pulsation energy. If these devices are not enough special antipulsation devices are connected to the hydraulic line system.

The most common type of antipulsation device is the air box. The operating principle of the air box is based on the accumulation of pressure pulses in the flow and subsequent equalization of these pulses by periodic compression and expansion of air, locked in a box. In modern air box designs the water and air cavities are separated by a rubber diaphragm, which prevents air from dissolving in the water.

Various cavities in a system -- tanks, receivers, etc., help considerably to reduce the intensity of flow pulsations. Air traps, installed in the highest parts of the lines, exert a double-edged effect on the reduction of the intensity of the flow pulsations -- they prevent interruption of the flow and they damp pressure vibrations by virtue of the elasticity of the air that accumulates in the air trap.

Antipulsation devices that reduce the activity of flow disturbances do not prevent resonance vibrations of pipes and of columns of liquid standing in them. To detune from resonance it is necessary that the ratio of the frequencies ω of the disturbing forces to the natural vibration frequencies ω_0 of the pipes or of the fluid standing in them fall outside of the range $0.75 > \omega/\omega_0 > 1.25$. The easiest way to accomplish resonance detuning is to change the length of line sections and the rigidity of the bearing surfaces.

Natural vibration frequencies f_0, in Hz, of fluid in lines can be determined by the following formulas:

APPROVED FOR RELEASE: 2007/02/08: CIA-RDP82-00850R000200100009-9

APPROVED FOR RELEASE: 2007/02/08: CIA-RDP82-00850R000200100009-9

for a straight pipe with both ends open

[эКВ=eq]

$$f_0 = \frac{c}{2l_{эКВ}}(2n - 1); \quad (8.1.4)$$

for a straight pipe with one end open

$$f_0 = \frac{c}{4l_{эКВ}}(2n - 1), \quad (8.1.5)$$

where c is the speed of sound in the liquid, in m/s; n is any positive integer; l_{eq} is the equivalent pipe length, in m, equal to $l + \Delta l$ for a pipe with one open end and $l + 2\Delta l$ for a pipe with both ends open.

According to Rayleigh the correction factor is $\Delta l = \pi r/4$, where r is pipe radius, in m.

The natural vibration frequency f_0, in Hz, of a column of water in a pipe with a box (collector) on the end can be found by the formula

$$f_0 = \frac{c}{2\pi}\sqrt{\frac{s}{Vl}}, \quad (8.1.6)$$

where s is the cross section of the pipe, m^3; V is the volume of the box, m^3; l is pipe length, m.

Ways to determine the natural vibration frequencies of a liquid in complicated plumbing systems are described in the literature [9].

The natural transverse vibration frequency f_0, in Hz, of individual sections of pipes is expressed in the general case by the relation

$$f_0 = \frac{\alpha^2}{2\pi l^2}\sqrt{\frac{EJ}{m}}, \quad (8.1.7)$$

where α is a coefficient that characterizes how the ends of an examined section of pipe are fastened; l is the length of an examined section, in m; E is the elasticity modulus, in Pa; J is the moment of inertia of the pipe cross section, in m^4; m is the weight of 1 m of length, in kg/m.

If a pipe is continuous it usually may be viewed as an unbroken beam. For multiple span beams with different distances between supports of identical rigidity the coefficient α for determining fundamental frequency is $\alpha = 3.14$. For a pipe with intermediate supports, viewed as a beam with fixed ends, this coefficient for fundamental vibrations, first and higher overtones are, respectively, $\alpha_0 = 4.78$; $\alpha_1 = 7.85$; $\alpha_n = 0.5[2(n + 1) + 1]\pi$ for $n > 1$.

A pipe with one intermediate support in the middle, which permits rotation in the cross section of the support, may be viewed as consisting of two

APPROVED FOR RELEASE: 2007/02/08: CIA-RDP82-00850R000200100009-9

APPROVED FOR RELEASE: 2007/02/08: CIA-RDP82-00850R000200100009-9

beams, each of which has a fixed end and a hinged end. The coefficients for the fundamental frequency, first and higher overtones of these beams will be $\alpha_0 = 3.93$; $\alpha_1 = 7.07$; $\alpha_n = \frac{4(n+1)+1}{4}\pi$ for $n > 1$.

For a pipe with fixed ends and intermediate pivot supports, forming three, four, five and six spans of identical length, the coefficients α_0 are, respectively, 3.55, 3.39, 3.30, 3.26. As the number of intermediate supports increases the dependence of vibrations on the manner in which the ends of the pipe are fastened decreases. The waveforms of the vibrations, inherent to a single-span beam with pivot supports and with the characteristic dimension l, equal to the span between supports, become the predominant forms of vibration. The values of α_0, α_1, α_n for such a beam are, respectively, π, 2π, $(n + 1)\pi$.

The methods whereby pipes are fastened to pumps and bearing structures (parts of the frame, bulkheads and foundations) have a considerable effect on the vibration and noise characteristics of pipes. To reduce the transmission of acoustic energy through pipes they are isolated from pumps with sound-insulating elements (vibration-insulating branches, siphons, flexible sleeves).

The noise level of a ship hydraulic system depends to a considerable degree on how well the operating modes of its elements are matched, since noise is minimized when all the parts of a system operate in the optimum modes. When designing ship hydraulic systems, therefore, it is important to make sure first of all that the pumps used in them operate in the optimum delivery mode. In particular, when several utilizers are connected in parallel to the same pump with a constant rotation frequency and individual utilizers are periodically turned off during the operation of the pump the flow rate for which they are accountable should be compensated by means of bypassing. Otherwise the turning on and off of recipients can lead to deviation of pump operation from the rated mode and, consequently, to an increase of noise. Bypassing is especially important in systems with impeller pumps, which run quietest at just one delivery rate, corresponding to impact-free intake of the flow into the impeller blades.

To minimize the deviation of pump parameters from the optimum mode in a system with a variable flow rate it is helpful to use variable speed pumps.

8.2. Hydrodynamic and Mechanical Noise Sources in Pumps[1]

General Premises. The vibration and noise characteristics of pumps are determined by the pumps themselves, by the motors that drive them and by transmission mechanisms (reducers, hydraulic transformers, clutches, etc.).

[1]This section was written by O. N. Sergeyeva.

APPROVED FOR RELEASE: 2007/02/08: CIA-RDP82-00850R000200100009-9

APPROVED FOR RELEASE: 2007/02/08: CIA-RDP82-00850R000200100009-9

Accordingly the spectral composition of noise and vibrations of pumps is attributed to hydrodynamic and mechanical sources. In many cases it exhibits components of electromagnetic origin from drive motors.

Impeller Pumps. The low-frequency range of the noise and vibrations of pumps of this type (centrifugal, axial, mixed flow, turbine) is determined by two kinds of sources: a) mechanical -- from unbalanced forces of inertia of the rotor, flaws in bearings and misalignment of rotors, which are manifested on the rotation frequency of a pump and on its harmonics; b) hydrodynamic -- from the force interaction of the blades with a variable pressure field, which can be seen in the spectra on the blade frequency and its higher-order components. The middle frequency range is filled basically with harmonics of the blade frequency and with components produced by turbulence in the flow passage part, and by vibrations of roller bearing parts.

The high-frequency range of the noise and vibration spectra of impeller pumps is determined principally by cavitation, and in precavitation modes by turbulence in the flow part. Different forms of cavitation exert a considerable influence on the intensity of the noise and vibration spectra in a wide frequency range. The total noise level of an impeller pump is plotted in Figure 8.8 as a function of the cavitation margin at a constant impeller rotation speed and on the impeller rotation speed for a constant cavitation margin. In the figure three critical modes are indicated, corresponding to the following: 0_{cr} -- development of cavitation in the radial space; I_{cr} -- developed profile cavitation, when the energy characteristics begin to deteriorate (the pressure drop is 2%); II_{cr} -- pump failure. The initial stages of cavitation are associated with the strongest noise. The initial cavitation number in impellers in consideration of the secondary influence of the basic parameters (the scale effect) is expressed by the relation

[k=c]

$$\sigma_{\kappa} = \frac{2g_2\Delta h}{u^{2+\alpha}}, \qquad (8.1.8)$$

where Δh is the absolute pressure in the flow; g is the acceleration of gravity; u is the circumferential velocity of the rotor; α is a coefficient that takes into account the influence of the scale effect (for impeller pumps $\alpha \approx 0.3$).

A change of delivery exerts an extremely strong influence on the noise level of impeller pumps. When the delivery deviates from the rated value in either direction the noise and vibration levels increase due to angles of attack different from zero at the impeller intake, which promotes earlier onset of cavitation. The experimental dependence of the relative initial cavitation number on the reduced delivery coefficient (Figure 8.9) is an indirect characteristic of the change of the noise level of an axial pump.

APPROVED FOR RELEASE: 2007/02/08: CIA-RDP82-00850R000200100009-9

APPROVED FOR RELEASE: 2007/02/08: CIA-RDP82-00850R000200100009-9

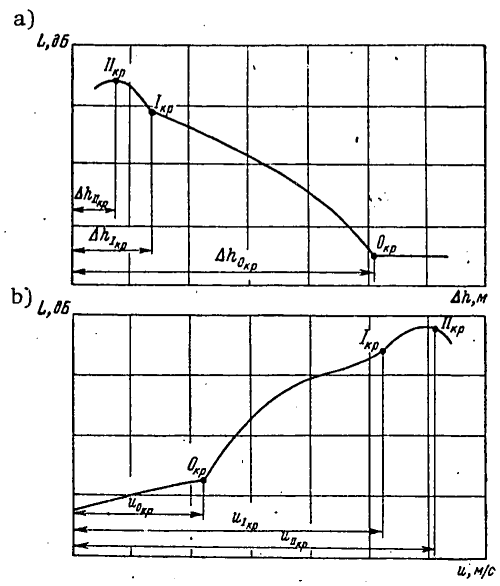

Figure 8.8. Total noise level of impeller pumps as function of: a -- cavitation margin; b -- circumferential velocity of impeller. [дБ=dB; kp=cr; c=s]

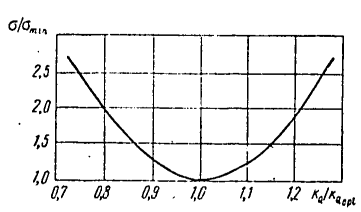

Figure 8.9. Relative initial cavitation number in axial pump as function of reduced delivery coefficient.

An examination of axial pumps that have operated for a long time often shows cavitation damage to the peripheral parts of the impellers and of the inner walls of the impeller chamber. This is indicative of the occurrence of slotted cavitation in the radial clearance.

The saturation of the spectrum with strong components from turbulization, pressure pulsations and cavitation creates conditions for the excitation of resonances of the individual pump elements in a wide frequency range, and of free vibrations of the impeller blades.

The main cause of strong noise in centrifugal pumps is intensive turbulization in the suction branch and also high irregularity of velocities in the discharge section of the suction branch. Consequently the flow strikes the impeller with substantially different pressures, velocities and directions. Strong turbulence also occurs at the impeller discharge and at the entrance

APPROVED FOR RELEASE: 2007/02/08: CIA-RDP82-00850R000200100009-9

APPROVED FOR RELEASE: 2007/02/08: CIA-RDP82-00850R000200100009-9

into the discharge branch. The formation of a hydrodynamic wake behind the rotating impellers leads to flow irregularity at the entrance into the flow guide or discharge branch.

Positive Displacement Pumps. The noise and vibrations of positive displacement (piston, gear) pumps are attributed to the nearly instantaneous change from suction pressure to delivery pressure and to the pulsed nature of the delivery of liquid into the discharge pipe. Components in the spectra of noise and vibrations of piston pumps are produced by valve impacts, pressure pulsations in the pumping chambers, pressure fluctuations in the delivery pipe and cavitation. One cause of noise in this type of pumps is the release of air in the stream of the pumped liquid. The intensity of noise and vibration here increases as the discharge pressure and rotation frequency increase.

A local increase of hydraulic pressure as the chamber between the gear teeth passes the seal is also a source of strong noise in gear pumps. Another cause of noise (in gear and screw pumps) is partial filling of the gear tooth chambers with liquid, which produces pulsation disturbances in the working elements.

The causes of noise in individual kinds of pumps are related to their design and technological features. They include: alternating inertial forces, caused by reciprocation of pistons in piston pumps and by the rotation of the teeth from the discharge to the suction cavity in gear pumps; friction of working parts; elastic deformations and vibrations of mated surfaces due to geometric errors in the machining of parts and assemblies.

Roller bearings are a common source of noise for all examined types of pumps. The main cause of noise in roller bearings is wear of the inner and outer races, and also flattening of the rollers. Friction bearings used in pumps produce primarily low-frequency components due to machining errors of the journals and hydrodynamic processes in the space between the journal and insert.

Jet Pumps. Noise in jet pumps is determined entirely by hydrodynamic processes. The main hydrodynamic processes are turbulization and turbulent pressure pulsations. The noise and vibration spectra of jet pumps, particularly in the high-frequency range, are uniform, and their levels usually are low and meet existing standards.

8.3. Ways to Reduce Pump Noise

Techniques for reducing pump noise and vibrations are classified in accordance with the causes as design, technological and operational. The most important opportunity for reducing pump noise during the design is to reduce the speeds of working parts (rotation of impellers, gears, screws and reciprocation pistons) and also the liquid flow velocity, since the

APPROVED FOR RELEASE: 2007/02/08: CIA-RDP82-00850R000200100009-9

APPROVED FOR RELEASE: 2007/02/08: CIA-RDP82-00850R000200100009-9

vibration levels of pumps due to mechanical sources are proportional to the square of velocity, and due to hydrodynamic sources -- to the fourth-sixth and higher power of velocity. The second opportunity is to make the most complete utilization of design techniques to reduce the intensity of perturbations or to completely eliminate them.

To improve the cavitation capacity of the impellers of centrifugal pumps, especially of the first stage of multistage pumps, it is necessary to reduce the diffusion of the annular suction channel, to use double-curvature blades with channels of larger rotation radii and to install guides on the seals to reduce turbulence in the flow as it enters the impeller from the seals.

The radial space between the impellers and guide must be increased with particular attention to reduction of the eccentricity of the radial clearance around the periphery of the impeller in order to reduce the intensity of discrete components on the blade frequency and its harmonics, caused by irregular pressure at the impeller discharge.

To adjust the onset of cavitation in axial pumps the flow part must be designed for a reduced power-speed coefficient with the use of cavitation-resistant profiles. The calculated values of circulation along the radius must be reduced sharply toward the periphery and gradually toward the radix. The amount and eccentricity of the radial clearance between the ends of the impeller blades and the chamber wall must also be minimized.

To reduce the amplitude of the pressure pulsations at the discharge of a centrifugal pump it is helpful to install additional short blades in the peripheral cross sections of the impeller blade channels. The suction flow into the next stage can be improved to reduce flow irregularity, turbulence and turbulent pressure pulsations by increasing the height of the guide channel and by making in it a large bladeless axially symmetric annular converging nozzle, by making an annular bladeless chamber around the periphery of the guide, by reducing the diffusivity of return channels, and in some cases by installing thin guide vanes in the return channels. However, the best organized flow is achieved by using guides with bladeless convergent return channels [6]. A schematic diagram of such a device is shown in Figure 8.10.

To reduce the intensity of the discrete component from flow irregularity after the impeller the discharge edges of the impeller blades and the leading edges of the guide vanes should not be parallel, the numbers of blades of the impeller and guide should not be multiples, and the number of impeller blades should be made odd.

Adapters should be tapered and the larger radii rounded off to the extent possible through the entire length of the flow part, including the suction and discharge branch pipes, to reduce turbulence noise.

APPROVED FOR RELEASE: 2007/02/08: CIA-RDP82-00850R000200100009-9

APPROVED FOR RELEASE: 2007/02/08: CIA-RDP82-00850R000200100009-9

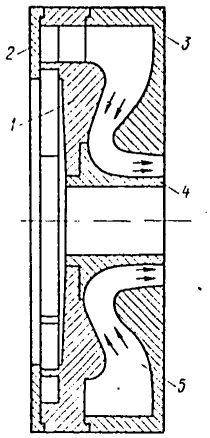

Figure 8.10. Guide of multistage centrifugal pump with bladeless annular convergent return channel: 1 -- case; 2 -- front wall; 3 -- rear wall; 4 -- seal; 5 -- bladeless annular convergent return channel.

The following measures are used to reduce the noise of piston pumps: the impacts of the valves on the seats are reduced by reducing the speed and weight of the valves; pressure pulsations in the delivery channel are reduced by increasing the number of cylinders and by installing air boxes in the pump discharge; the rigidities of the hydraulic unit and of parts that connect the hydraulic unit to the stand are increased.

The best way to reduce noise in positive displacement rotor pumps is to perfect production technology and especially to increase the production precision of the couplings of the moving parts (pistons, screws).

The third way to reduce pump noise is to detune pump elements from their natural vibration frequencies and the entire unit as a whole from the frequencies of perturbing forces.

A fourth possibility of reducing noise is to assemble pump units efficiently. The following measures must be taken into account here: single-unit assembly of pump systems (the drive and the pump have a common rotor and common chassis); the rotors are arranged vertically, are made light as possible and rigidity is made symmetric with respect to the rotation axis.

There is one more possible way of reducing pump noise, and that is to use vibration insulation and vibration damping techniques. The former include internal shock absorption, and the latter consists in the manufacture of case structures out of materials with a high decrement of vibrations and applying vibration-insulating coatings on them.

An effective measure for pump units is to install under the bearings elastic rings or special inserts, made of material with a high vibration decrement (laminated and metal fiber materials, rubber and plastic). The spectrogram in Figure 8.11 shows the effect of installing roller bearings in a single-stage horizontal centrifugal pump with inserts made of pressed copper fiber with a porosity of 70%, and the photograph in Figure 8.12 shows the position of the bearings in these inserts.

APPROVED FOR RELEASE: 2007/02/08: CIA-RDP82-00850R000200100009-9

APPROVED FOR RELEASE: 2007/02/08: CIA-RDP82-00850R000200100009-9

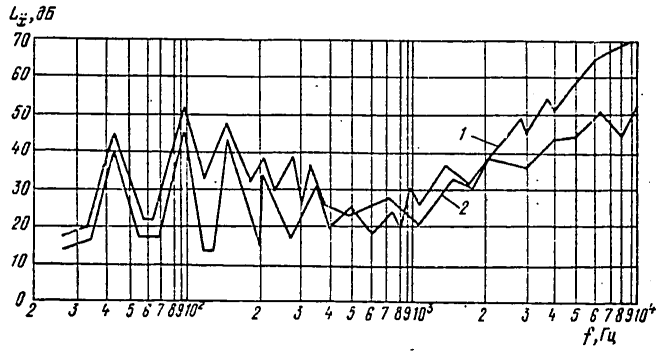

Figure 8.11. Effect of installing roller bearings in pressed copper fiber inserts on vibration level of centrifugal pump: 1 -- bearings without inserts; 2 -- bearings in inserts. [дБ=dB; Гц=Hz]

Elastic pads, pneumatic tire and leaf spring carriages, installed between the pump and pump stand, are used for absorbing acoustic energy on bearing lugs and flanges. The transmission of acoustic energy in pipes is reduced by using elastic inserts, elastic branch pipes, bellows, etc. (see Chapter 12).

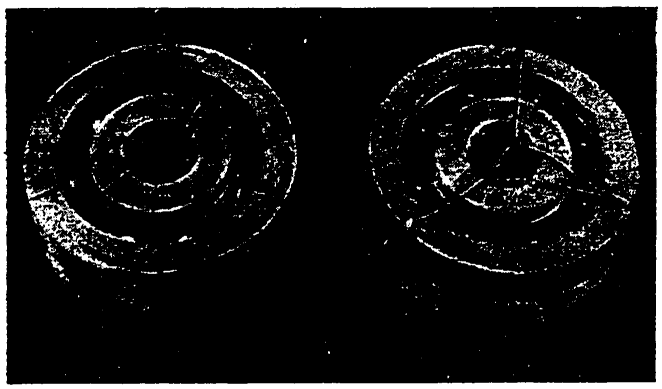

Figure 8.12. General view of roller bearings, inserted in pressed copper fiber inserts: left -- 30% porosity; right -- 70% porosity.

Pump noise is influenced to a great extent by production technology. Noise can be reduced by improving the production quality of pumps, precision of the machining and assembly of parts and units, by using quiet bearings, by balancing the rotors part by part and by balancing them in the assembled

APPROVED FOR RELEASE: 2007/02/08: CIA-RDP82-00850R000200100009-9

APPROVED FOR RELEASE: 2007/02/08: CIA-RDP82-00850R000200100009-9

form. One of the most important requirements of technology is standardization of the deviation of shapes and mating of joined surfaces in accordance with the tolerances of GOST 10356-63, which meet the requirements on pump noise.

Operational factors can predominate in pump noises under certain conditions. Therefore, to prevent excessive noise during operation it is important to observe specific operating conditions and to eliminate deformation and displacement of elements and assemblies under the influence of temperatures and pressures.

8.4. Noise and Vibration of Reciprocating Compressors[1]

The noise of reciprocating compressors is produced by the irregular speed and turbulence of air in suction systems (suction noise), and by radiation by the surfaces of parts and assemblies of the compressor, subjected to variable forces.

Nonuniform suction velocity produces strong noise components with frequencies that are multiples of the shaft rotation frequency. Noise related to turbulization is manifested in the medium- and high-frequency ranges, and it is strongest in the region corresponding to the eddy separation frequency in the channels at the time of the maximum piston velocity. Noise is especially strong when the frequency of turbulization and the natural frequency of the resonator cavity (8.1.6), formed by the cavity of the cylinder, coincide at specifically that time. Suction noise also increases if the vibration frequency of the intake valves matches the frequency to which the cylinder cavity is tuned at the instant of seating.

Suction noise is readily reduced on frequencies above 200 Hz by using mufflers in the form, for example, of an annular resonator with one or two cells, tuned to the loudest noise. Low-frequency noise, related to the variable intake velocity, cannot be muffled this way because the cells of an acoustic filter are ineffective within size limits that can be considered acceptable. To reduce low-frequency noise it is better to use a muffler with friction elements in the form of slots and holes, representing a parallel channel for the variable flow component.

One possible muffler design that can reduce intake noise to the level of the noise radiated by the surface of a compressor is illustrated in Figure 8.13 [8]. The attenuation in the 100-250 Hz band, inherent to this design, is 28-30 dB.

Intake noise can also be reduced without a muffler if the air is supplied to the intake pipe through a flexible rubber or reinforced rubber sleeve. The attenuation of noise for about a 20 caliber long sleeve is 10-15 dB in a wide frequency range. Less attenuation (about 10 dB) can be achieved by

[1]This section was written by V. D. Kurnatov.

APPROVED FOR RELEASE: 2007/02/08: CIA-RDP82-00850R000200100009-9

APPROVED FOR RELEASE: 2007/02/08: CIA-RDP82-00850R000200100009-9

using a flexible metal sleeve. The amount of muffling is determined as the difference of the noise levels without a muffler and with a muffler, measured at a distance of 0.5 m from the intake pipe in the former case and 0.5 m from the intake hole of the muffler or sleeve in the latter.

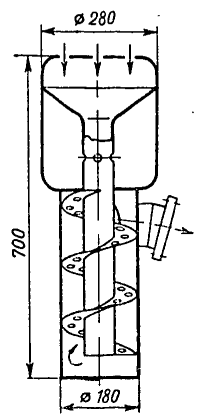

Figure 8.13. Intake noise muffler.

The noise radiated by the surface of a compressor is produced by forces of inertia and pressure, by the periodically deformed cylinder heads and walls, by pressure fluctuations in pipes and assemblies of between-stage connections, acting upon the compressor block through the crank-connecting rod assembly, and by impacts in bearings, drive and auxiliary mechanisms.

The design of a compressor and its arrangement determine the magnitude of unbalanced forces, their moments and the irregularity of the tilting moment. Unbalanced forces and moments are among the basic sources of low-frequency vibrations of ship compressors. The arrangement also influences the vibration and noise levels in the medium- and high-frequency ranges. In this case the influence of arrangement depends on the distance between a source of vibration and the bearing surfaces or radiating surfaces, and on the degree of attenuation of vibrations along the propagation path.

It may be assumed that low-level compressor noise and vibration can be assured by selecting the proper arrangement. In view of rigid requirements on vibration and noise characteristics it is important that centrifugal forces and forces of inertia of the first two orders from reciprocating masses be balanced. These forces can be balanced by using a multibank, including opposed-piston arrangement, or a special balancing mechanism. A multibank arrangement provides equalization of the tilting moment and a reduction of the vibration it produces. A moment with harmonics that do not exceed 10-12% of the average may be assumed satisfactory.

The dynamic effect of the tilting moment can also be reduced by placing the mounts close to the principal inertia axis of the machine. This reduces the rotation rigidity and natural vibration frequency f_n. This measure is justified in the range $f_n < 0.7f$, where f is the frequency of the strongest harmonics of the moment. This requirement corresponds to smaller coefficients of dynamicity and transmission of forces in comparison with the usual range $f_n = (0.7\text{-}2.7)f$ for rotation vibrations, so that both the transmitted moment and the amplitude of the vibrations of a machine are

APPROVED FOR RELEASE: 2007/02/08: CIA-RDP82-00850R000200100009-9

APPROVED FOR RELEASE: 2007/02/08: CIA-RDP82-00850R000200100009-9

reduced. In the limiting case of pivot support on the principal inertia axis ($f_n \to 0$), how much of the moment is transmitted is determined by the amount of friction in the support.

One form of vibrations that are produced by stresses, characteristic of a compressor, are bending vibrations of cantilever cylinders. The problem of reducing them consists in detuning the natural frequency of vibrations of this form far enough away from the frequency range that includes strong harmonics of normal force. The solution of the problem for a given rotation frequency consists in increasing the rigidity of the cantilever base. For the purposes of estimation one may assume the rigidity to be inadequate if the frequency of the indicated form of free vibrations in a crosshead-less machine is less than 25 times the shaft rotation frequency.

By examining the cylinder and head as a cantilever beam with mass m per unit length and with mass M suspended on the end, the approximate free vibration frequency can be determined by using relation (8.1.7). The influence of the suspended mass is taken into account in this relation by value α. In relation to point and distributed masses within $M/ml = 6\text{-}12$ one may use $\alpha = 0.8$ (here l is the length of the beam).

Cylinder vibrations produce noise, related to radiation not only by cylinder surfaces, but to a lesser degree also by the surfaces of the crank case and frame. Pipe vibrations are related to cylinder vibrations. They can increase compressor noise if the pipes between fastening points are too long. Additional fastening of pipes in a vibration loop eliminates the source of noise in this case and improves the reliability of pipe connections. The type of fastening that resists both transverse displacements of the pipe and rotation vibrations at a fastening point is preferable here.

The vibrations of pipes and of parts connected to them can be caused by pressure pulsations due to the periodic delivery of air. In this case vibrations can be reduced by changing the rigidity and by detuning the natural frequencies of the pipe with extra fasteners. Another way to reduce pipe vibrations is to lessen pressure pulsations. One way to do this is to use a buffer box, installed as close as possible to the cylinder. If the pipe connects two compressor stages the buffer box should be installed on the delivery side, since a stronger compression wave is generated than the rarefaction wave on the suction side.

If a buffer box is viewed as an acoustic filter of the expansion box type, its size can be determined by assigning the amount of deadening ΔL by the formula

$$\Delta L = 10 \lg \left[1 + \frac{1}{4} \left(m - \frac{1}{m} \right)^2 \sin 2\pi \frac{l_e}{\lambda} \right], \qquad (8.4.1)$$

where $m = s_2/s_1$ is the ratio of the cross section areas of the chamber and pipe; l_e is chamber length.

APPROVED FOR RELEASE: 2007/02/08: CIA-RDP82-00850R000200100009-9

APPROVED FOR RELEASE: 2007/02/08: CIA-RDP82-00850R000200100009-9

A filter best attenuates waves for which the ratio l_e/λ corresponds to values $\frac{1}{4}$ n, where n is a series of odd numbers, i.e., chamber length corresponds to an odd number of quarter waves. Vibrations with an even number of quarter waves through the length of the chamber are not attenuated.

Pressure vibrations in a pipe can also be attenuated with a throttle disk (diaphragm) or valve, installed at the point where the vibration velocity of standing waves is maximum. The greatest effect is achieved when the acoustic impedance of the disk is matched with the wave impedance of the pipe. The condition of matching is expressed by the relation [4]

[д=d]

$$\frac{d_д}{d} = \sqrt[4]{\frac{c_0}{c}}, \qquad (8.4.2)$$

where $c_0 = c_m(D/d)^2$ is the average velocity of the gas in the pipe, determined by the average piston velocity c_m; d_d, d, D are, respectively, the diameters of the hole in the diaphragm, pipe and cylinder.

8.5. Basic Noise Sources of Electrical Machinery

Classification of Noise. Noise produced by electrical machinery (EM) is subdivided into three categories: magnetic, mechanical and aerodynamic.

Magnetic noise is produced by electromagnetic forces, acting in the air gap between the rotor and stator. The main sources of mechanical noise in EM are rotor disbalance, dual rigidity of the rotor, bearings and brushes. Aerodynamic noise in EM occurs chiefly as a result of rotation of the rotor and fan in air. This is the predominant source of noise in EM with a rotor speed higher than 50 m/s.

A schematic diagram of a single-armature DC motor with basic noise sources is illustrated in Figure 8.14.

The noise of EM depends on its power, rotation frequency and design execution. The noise level L, in dB, of self-ventilated EM is proportional to nominal power N and to the square of the rotation frequency:

$$L \approx 10 \lg N + 20 \lg n + K. \qquad (8.5.1)$$

The value of K depends on design and technological features of a machine, and also on noise measurement conditions (8.5.1).

The requirements on noise characteristics depend on the purpose of EM. According to GOST 16372-70 different types of EM (with a nominal power more than 0.25 kW and nominal rotation speed of up to 4,000 rpm) are divided into five classes in terms of noise: 0, 1, 2, 3, 4. For ordinary class 1

APPROVED FOR RELEASE: 2007/02/08: CIA-RDP82-00850R000200100009-9

APPROVED FOR RELEASE: 2007/02/08: CIA-RDP82-00850R000200100009-9

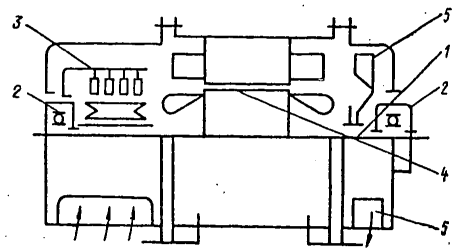

Figure 8.14. Basic noise sources of DC motor: 1 -- unbalanced rotor; 2 -- bearing noise; 3 -- brush noise; 4 -- magnetic noise; 5 -- fan noise.

AC and DC EM the average acoustic levels A, in dBA, at a distance of 1 m from the machine should not exceed the values indicated in Table 8.1.

Different noise sources can predominate in the noise of a machine, depending on the type, execution (roller bearings, friction bearings) and speed. A classification of basic noise sources of EM is given in Table 8.2; typical noise spectra are given with the fan not running.

Table 8.1. Noise Level of Electrical Machinery as Function of Power and Rotation Frequency

1) Номинальная мощность, кВт	2) Ориентировочные значения уровня шума, дБА, электрических машин при номинальной частоте вращения, об/мин				
	3) до 1000	1000—1500	1500—2200	2200—3000	3000—4000
0,25—1,50	64	68	70	71	75
1,50—4,00	67	72	74	76	80
4,00—15,00	74	78	82	85	89
15,00—45,00	80	85	87	89	93
45,00—132,00	85	92	95	97	100
132,00—400,00	90	96	98	100	104
400,00—1000,00	94	100	103	105	109

Key: 1. Rated power, kW
2. Approximate noise levels, dBA, of electrical machinery at nominal rotation frequency, rpm
3. up to 1,000

Magnetic Noise. The magnetic noise of EM occurs under the influence of alternating forces in the air gap (Figure 8.15). The forces in the air gap act upon the rotor and upon the stator. The rotor, which is the most stable and invariant component of EM, resists deformation very well. Magnetic noise in EM is produced chiefly by deformation of the stator. In

APPROVED FOR RELEASE: 2007/02/08: CIA-RDP82-00850R000200100009-9

APPROVED FOR RELEASE: 2007/02/08: CIA-RDP82-00850R000200100009-9

Table 8.2. Basic Noise Sources in Different Types of Electrical Machinery

Type of electrical machine	Execution	Basic noise sources	Typical noise spectrum
Large DC and AC electric motors (n ≤ 1,000 rpm)	Friction bearings	Magnetic forces, external fan, brushes	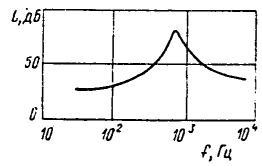
Medium and small AC and DC electric motors (n ≤ 1,500 rpm)	Friction bearings 1 Roller bearings 2	Magnetic forces, disbalance, built-in fan Bearings, magnetic forces, disbalance, built-in fan	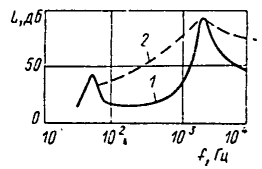

[дБ=dB; Гц=Hz]

APPROVED FOR RELEASE: 2007/02/08: CIA-RDP82-00850R000200100009-9

APPROVED FOR RELEASE: 2007/02/08: CIA-RDP82-00850R000200100009-9

Table 8.2 (continued)

Type of electrical machine	Execution	Basic noise sources	Typical noise spectrum
Medium and small AC and DC electric motors (n ≤ 3,000 rpm)	Friction bearings 1 Roller bearings 2	Disbalance, magnetic forces, built-in fan Bearings, disbalance, magnetic forces, built-in fan	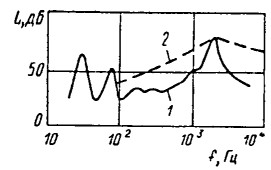
Large turbo-generators -- 100-500 MW (n > > 3,000 rpm)	Friction bearings	Disbalance, magnetic forces, built-in fans, brushes	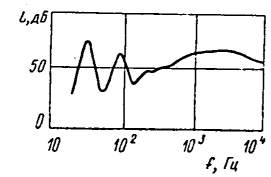
HF induction generators (n = = 1,500-3,000 rpm)	Friction bearings and roller bearings	Magnetic forces	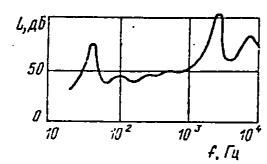

APPROVED FOR RELEASE: 2007/02/08: CIA-RDP82-00850R000200100009-9

APPROVED FOR RELEASE: 2007/02/08: CIA-RDP82-00850R000200100009-9

calculations the armature of a machine is usually represented as a cylindrical case, acted upon by a system of radial and tangential forces with wave number r, periodically changing in time and symmetric with respect to the circumference.

Magnetic noise is a function of the magnetic flux density, the number and form of poles, the number and form of slots and the geometry of the air space.

In the air space of an asynchronous motor there occurs, in addition to the main magnetic field, which produces torque on the shaft, a large number of higher field harmonics: higher harmonic winding fields, produced by non-sinusoidal distribution of the magnetic force in the air gap; tooth-like fields produced by the variable magnetic conductance in the air gap; higher field harmonics due to various asymmetries in the magnetic circuit; higher field harmonics due to asymmetric supply voltage; higher field harmonics due to saturation of the magnetic conductor.

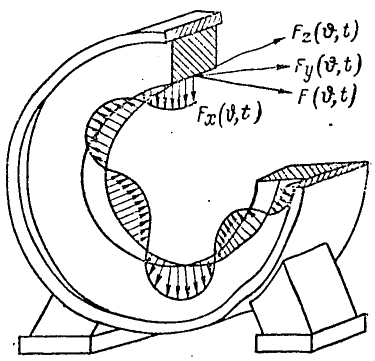

Figure 8.15. Effect of perturbing magnetic forces F (radial F_x, tangential F_y, axial F_z) on stator of electric motor.

In an asynchronous motor with a symmetric stator winding, with a whole number of pole and phase slots, higher field harmonics occur with the following numbers of pole pairs:

from the stator winding

$$\nu = p(2m_1q_1 + 1); \tag{8.5.2}$$

from the rotor winding

$$\mu = p(2m_2q_2 + 1) - \tag{8.5.3}$$

APPROVED FOR RELEASE: 2007/02/08: CIA-RDP82-00850R000200100009-9

APPROVED FOR RELEASE: 2007/02/08: CIA-RDP82-00850R000200100009-9

in the case of a phase winding

$$\mu = zq_2 + p - \tag{8.5.4}$$

in the case of a short-circuited winding ("squirrel cage");

from the sawtooth stator field

$$\nu_z = p\left(1 \pm \frac{z_1}{p} k\right). \tag{8.5.5}$$

from the sawtooth rotor field

$$\mu_z = p\left(1 \pm \frac{z_2}{p} k\right). \tag{8.5.6}$$

In these formulas: m_1, m_2 are the numbers of winding phases; p is the number of pole pairs of the main field; q_1 and q_2 = ±1, ±2, ±3, ...; z_1 and z_2 are the numbers of stator and rotor slots; k = 1, 2, 3, ...

The circular frequencies are, respectively:

for the stator fields

[ct=st]

$$\omega_{ст} = \omega_0 = 2\pi f_0; \tag{8.5.7}$$

for the rotor fields (in terms of the stator)

$$\omega_\mu = \omega_0 \left[\frac{\mu}{p}(1 - s) + s\right], \tag{8.5.8}$$

where f_0 is the power line frequency; s is the slip of the rotor relative to the main rotating stator field.

The magnetic inductions of the higher field harmonics are determined by the currents, winding parameters (number of turns, winding coefficients) and magnetic circuit (the size of the air gap and Carter's coefficient). The inductions of the serrated sawtooth-like harmonics are determined entirely by the parameters of the serrated stator and rotor zones (the shape of the slot and the size of the air gap). Favorable conditions are created for the excitation of many natural vibration frequencies of the stator. Wave number r is equal to the difference of the number of pole pairs of the interacting stator and rotor fields ν and μ:

$$r = |\nu - \mu|. \tag{8.5.9}$$

The frequencies of the resulting forms of deformation of the stator ring correspond to the orders of the active forces. The rigidity of the stator ring depends on the geometric dimensions of the stator and on the order of deformation (it is proportional to r^4 for $r \geq 2$). Therefore lower-order

APPROVED FOR RELEASE: 2007/02/08: CIA-RDP82-00850R000200100009-9

APPROVED FOR RELEASE: 2007/02/08: CIA-RDP82-00850R000200100009-9

magnetic forces, for which the amplitudes of dynamic deformations are maximum, play the biggest part in the generation of magnetic noise and vibration. For small asynchronous motors these low orders may be assumed to be $r \leq 4$, and for medium and large motors they are larger values of r (up to $r \leq 12$). Since the order of vibrations depends on the ratio of the numbers of stator and rotor slots z_1 and z_2 they must be selected such as to obtain the highest possible value of r.

The radial magnetic forces that act upon a unit area of the stator boring are determined by the expression

[МАГН=magn]

$$F_{\text{магн}} = \left[\frac{B_\delta(x, t)}{5000}\right]^2 \tag{8.5.10}$$

where $B_\delta(x, t)$ is the radial term of induction in the air gap.

The most important of the forces produced by the interaction of the stator and rotor field harmonics are those that are produced by the serrated harmonics. These forces can develop considerable deformations of the stator, particularly for low-order vibrations that occur in the case of poor selection of the ratios of the numbers of stator and rotor slots. Frequencies f, in Hz, of these forces are determined, respectively, by the formulas

$$f_1 = f_0\left[2 + \frac{z_2 k}{p}(1 - s)\right], \tag{8.5.11}$$

$$f_2 = f_0 \frac{z_2 k}{p}(1 - s), \tag{8.5.12}$$

where f_0 is the line voltage frequency; z_2 is the number of rotor slots; p is the number of pole pairs of the main stator field; $k = \pm 1, \pm 2, \pm 3, \ldots$

The process whereby magnetic noise is generated in synchronous motors is analogous to the process that takes place in asynchronous motors. The magnetic forces that subject the stator to periodic deformation occur due to interference of higher harmonic fields in the air gap. The laws responsible for winding and serrated harmonics of the stator in synchronous motors are exactly the same as in asynchronous motors. The difference between salient-pole synchronous motors and asynchronous motors is attributed to rotor design. In synchronous motors with massive rotors the HF components of noise are weakened considerably by the larger air gap between the stator and rotor and by the damping force of the rotor mass. The rotor field harmonics are determined by the magnetic conductance of the air gap. If $z_2 = 2p$ in salient-pole synchronous motors, we obtain the following expression for the number of pole pairs of the rotor field harmonics:

$$\eta_p = \left(1 \pm \frac{z_2}{p} k\right) = p(1 \pm 2k), \tag{8.5.13}$$

where $k = 1, 2, 3, \ldots$

APPROVED FOR RELEASE: 2007/02/08: CIA-RDP82-00850R000200100009-9

APPROVED FOR RELEASE: 2007/02/08: CIA-RDP82-00850R000200100009-9

By virtue of the symmetric design of the pole pieces of synchronous motors only equal phase harmonics of odd orders remain in the curve of the rotor field. These harmonics are determined by the following relation:

$$\eta_p = p\,(2q_3 - 1), \tag{8.5.14}$$

where $q_3 = 1, 2, 3, \ldots$

The circular frequency of these harmonics, expressed in terms of the stator with synchronous rotation of the pole piece, is

$$\omega_\eta = \frac{\eta}{\beta}\,\omega_0 = 2\pi f_0\,(2q_3 - 1). \tag{8.5.15}$$

As in asynchronous noise, magnetic noise in synchronous motors is produced chiefly by magnetic force waves of lower orders r, occurring due to the interaction of the stator and rotor field harmonics ν and η_r. Magnetic forces produced by the serrated stator field harmonics (particularly in open slot motors) are chiefly responsible for noise in synchronous motors in the idle mode. The resulting magnetic forces have the following orders:

$$r = 2p\left(q_3 - \frac{z_1}{p}\right), \tag{8.5.16}$$

where z_1 is the number of stator slots; 2p is the number of poles of the main field; $q_3 = 1, 2, 3, \ldots$

Frequencies f_r, in Hz, of these forces, will be $f_r = 2f_0q_3$, where $q_3 = 1, 2, 3, \ldots$

Magnetic noise produced by the fundamental wave of magnetic field rotation does not readily submit to suppression, particularly in two-pole 50 Hz asynchronous motors.

Magnetic noise also can occur, in principle, due to magnetostriction, i.e., due to a change of the shape and size of the ferromagnetic plates under the influence of periodic magnetic fields. However, a change of size of the active iron on acoustic frequencies in electric motors is usually insignificant, and magnetostriction noise does not reach the level of the noise produced by the attraction of magnetic masses.

Periodic electromagnetic forces in DC motors are caused by a periodic change of the magnetic conductance of the air gap under the poles as the serrated armature rotates. The frequency of the magnetic noise f_m, in Hz, is $f_m = \frac{zn}{60}\,i$, where z is the number of armature teeth; $i = 1, 2, 3, \ldots$

The only difference between magnetic noises of DC and AC motors is the fact that in the former stator deformation occurs under the influence of point forces, and in the latter it occurs under the influence of sinusoidally distributed forces.

APPROVED FOR RELEASE: 2007/02/08: CIA-RDP82-00850R000200100009-9

APPROVED FOR RELEASE: 2007/02/08: CIA-RDP82-00850R000200100009-9

Mechanical Noise. Mechanical noise is the result of many factors that happen inside a motor. The most typical of them are unbalanced rotor assemblies, roller bearings and the brushes on the commutator rings.

The level of the disbalance component of noise in electrical machinery nearly entirely depends on the process whereby the rotor is balanced. The type of EM is important only from the standpoint of sensitivity to subsequent changes in the distribution of mass. The front parts of the windings of motors with a wound rotor is especially vulnerable to displacement under the influence of centrifugal forces. Disbalance noise is manifested on rotation frequency $f_{rot} = n/60$.

GOST 12327-66 recommends residual disbalance for rigid rotors weighing from 3 to 1,000 kg. The tolerable levels of vibration of rigid rotors weighing more than 1,000 kg and of flexible rotors are usually established by in-factory standards.

In accordance with GOST 16921-71 there are eight classes of motors weighing from 0.25 to 2,000 kg: 0.28, 0.45, 0.7, 1.1, 1.8, 2.8, 4.5, 7.0. The index corresponds to the maximum tolerable vibration velocity for a given class; for example, 0.28 mm/s corresponds to the vibration class of 0.28, 0.45 mm/s corresponds to class 0.45, etc.

Disbalance in electrical machinery can change significantly, depending on the thermal condition of the rotor (thermal disbalance). An investigation of many different types of electrical machinery disclosed that when the thermal asymmetry of the rotor is 0.5°C thermal disbalance can be 5-6 times greater than residual (mechanical) disbalance.

Basically the following factors are responsible for uncompensated residual disbalance in the rotor: the absence of monolithic rotating windings (particularly in DC and synchronous motors), which leads to a constant change of residual disbalance, both in terms of magnitude and phase; unavoidable thermal asymmetry due to different thicknesses of the slot insulation; the existence of turn shorts in excitation windings; different cooling conditions, leading to thermal deformation of the rotor, etc. The most precise balancing obviously can be achieved in asynchronous motors with shorted rotors, in which the first critical velocity is higher than the working velocity. High-speed synchronous turbogenerators with massive rotors and tenons have higher residual disbalance per unit mass of the rotor than asynchronous generators. Moreover, synchronous turbogenerators, due to possible turn shorts in the excitation winding and failures of the rotor cooling system during operation, are less stable in relation to vibration (this is particularly characteristic of water-cooled rotors).

The armatures of DC motors and the salient-pole rotors of synchronous motors have higher residual disbalance than the above-examined motors. The strongest noise produced by disbalance occurs in motors with flexible rotors, in which the working velocity is higher than the 1st and 2nd

APPROVED FOR RELEASE: 2007/02/08: CIA-RDP82-00850R000200100009-9

APPROVED FOR RELEASE: 2007/02/08: CIA-RDP82-00850R000200100009-9

critical velocities of the rotor. The rotors of these motors are particularly sensitive to thermal asymmetry and often require thermal balance adjustment during operation in the rated mode.

Noise produced by double rigidity is not always heard, but it can be significant, particularly in turbogenerators. Double rigidity occurs because the large teeth in the slot zone of the turbogenerator barrel impart different rigidities to the rotor in the principal bending planes. Two complete cycles of change of rigidity, and accordingly two complete changes of bending, occur in each rotation of the rotor, causing noise with a double rotation frequency. This noise does not occur in vertical motors.

Sometimes the rotor journals of electrical machinery are not manufactured strictly symmetric; then the center of the rotor is displaced relative to the rotation axis and causes an inertial perturbing force, which acts upon the bearing. Out-of-round journals exert the strongest influence on the noise level in large high-speed EM with a journal diameter of 100-120 mm.

Bearing noise depends on the type of electric motor, since the characteristics of acoustic vibration and noise transmission vary from motor to motor. Ball bearings with their numerous parts, which experience relative displacement, produce noise on many frequencies, which are proportional to the rotation frequency of the inside bearing race, i.e., $f_\tau = k_\tau n/60$, where n is the shaft rotation frequency; k_τ is the proportionality coefficient for the τ-th perturbing harmonic, which depends on the microgeometry of the bearing surfaces and on bearing design.

The frequencies according to these formulas in application to electrical machinery can be calculated approximately. In real motors they can differ somewhat due to the existence of numerous sources of excitation, the complexity of the elastic system of the motor and the effect of the phase relations between the sources.

One source of mechanical noise in electrical machinery are the brushes and commutator. When the rotor rotates the commutator plates, striking the brushes, impart vibrations to the parts of the brush clamps and to the brushes themselves. The frequencies of the fundamental components of brush noise are determined by the formula

$$f_b = \frac{n}{60} z_c i,$$

where i = 1, 2, 3, ... are noise harmonics; z_c is the number of commutator plates.

A frequency analysis shows that the brush noise range is 1,000-8,000 Hz. It is manifested particularly strongly in large slow (up to 350 rpm) DC motors. In motors running at frequencies higher than 1,000 rpm this noise is overlapped by magnetic and aerodynamic noises.

APPROVED FOR RELEASE: 2007/02/08: CIA-RDP82-00850R000200100009-9

APPROVED FOR RELEASE: 2007/02/08: CIA-RDP82-00850R000200100009-9

Aerodynamic Noise. Aerodynamic, or fan noise in electric motors is produced by the rotating rotor itself, by the fan blades and by air passing through the ventilation channels and air cavities of the motor.

Ventilation noise has a wide-band spectrum. The fundamental frequency of fan blade noise is $f_{fan} = nz/60$, where z is the number of fan blades, and this frequency is sometimes distinguishable in noise of random frequency.

The aerodynamic noise level is determined basically by the type of fan, and not by the type of electric motor. For self-ventilating motors, cooled by a fan, pressed on the shaft of the motor, the aerodynamic noise level L, in dB, at a distance of 0.5 m from the case is determined by the formula $L = 10 \log N + 20 \log n + 5$; for sealed self-ventilating motors $L = 10 \log N + 20 \log n$; for sealed water-cooled motors $L = 10 \log N + 20 \log n - 10$, where N is motor power, in kW; n is the rotation frequency, in rpm. For independently ventilated (quiet running) motors, the noise of which is determined by the noise of the external fan, $L = 10 \log N + 80$, where N is the power of the electric fan, in kW.

8.6. Reduction of Noise of Electrical Machinery

Basic Principles. The noise of electrical machinery (EM) is reduced at the present time in two basic ways. The first is to reduce perturbing forces at the source, and the second is to reduce the noise on the propagation paths by appropriately changing the parameters of the structural parts of EM (rigidities, masses and damping elements).

Noise reduction techniques for EM are classified in Table 8.3 [3]. The design measures for reducing EM noise are: rake the rotor slots; make the roller bearings smaller; replace ball bearings with friction bearings; reduce the mass ratio of rotating and nonmoving motor parts; change the profile of the fan blades; reduce the rotor rotation frequency.

Perturbing inertial forces and noise produced by disbalance, out-of-round journals, double rotor rigidity, misaligned shafts, etc., depend mostly on manufacture precision and the quality of assembly.

Noise of EM can be reduced by using vibration- and sound-insulating systems to reduce the transmission of perturbing forces to external surfaces, reducing the noise radiated by the motor.

Reduction of Magnetic Noise. Magnetic noise is reduced primarily by reducing the periodic components of electromagnetic forces and by eliminating resonance in the mechanical system consisting of the frame and rotating rotor, i.e., by mismatching the natural vibration frequency of the frame and the frequency of perturbing forces. This is especially important in DC motors with the rotation frequency controlled in a wide range.

APPROVED FOR RELEASE: 2007/02/08: CIA-RDP82-00850R000200100009-9

APPROVED FOR RELEASE: 2007/02/08: CIA-RDP82-00850R000200100009-9

Table 8.3. Classification of Noise Reduction Techniques for Electrical Machinery

Cause of noise	Fundamental perturbation frequencies	Noise reduction techniques	Effectiveness of method, dB
Rotor disbalance	n/60	Static and dynamic balancing Elastic bearings Elastic inertial bearings Vertical installation of motor on horizontal shock absorbers	10-20 5-10 10-15 10-20
Double rigidity of rotor	2n/60	Cut extra slots Elastic damping bearings Elastic inertial bearings	10-20 10-12 10-15
Out-of-round rotor journals	2n/60	Careful maching of rotor journals Elastic, elastic damping, elastic inertial bearings	10-20 10-15
Friction bearings	n/60; tn/60	Careful machining of bearing surface, selection of proper lubricant	10-15
Roller bearings	$\frac{n}{60}$; $\frac{2n}{60}$; $\frac{z_{ш}n}{60}$; $\frac{n}{60}\cdot\frac{D_0}{d_{ш}}\left(1-\frac{d_{ш}^2}{D_0^2}\right)z_{ш}$; $\frac{D_0-d_{ш}}{2D_0}\cdot\frac{n}{60}$; $\frac{n}{120}\left(1+\frac{d_{ш}}{D_0}\right)z_{ш}$; $\frac{n}{60}\left(1\pm\frac{d_{ш}}{D_0}\right)\frac{z_в z_{ш}}{q}$	Use friction bearings Spring bearing stays Elastic, elastic inertial bearings Use special quiet bearings	20-25 10-15 10-15 10-20
Brushes	$\frac{z_c n}{60}$	Careful manufacture of commutator and contact ring relief Use appropriate soft grades of brushes	10-15 8-10
Magnetic circuit in motors: DC	$\frac{zn}{60}$	Rake armature slots Eccentric air gap Step poles Magnetic wedges Smooth armature Elastic magnetic suspension	10-15 6-12 10-15 10-20 15-30 10-15

APPROVED FOR RELEASE: 2007/02/08: CIA-RDP82-00850R000200100009-9

APPROVED FOR RELEASE: 2007/02/08: CIA-RDP82-00850R000200100009-9

Table 8.3 (continued)

Cause of noise	Fundamental perturbation frequencies	Noise reduction techniques	Effectiveness of method, dB
asynchronous	$f_0 \cdot \left[2 + \frac{z_2 k}{p}(1-s)\right]$; $f_0 \frac{z_2 k}{p}(1-s)$	Rake rotor or stator slots Use proper stator and rotor slots Elastic magnetic suspension	10-15 10-15 10-15
synchronous	$2f_0 k$	Rake stator slots Elastic magnetic suspension	10-15 10-15
Fan	$\frac{z_f n}{60}$	Use water cooling Install noise mufflers	10-20 10-15

The basic measures for reducing magnetic vibration and noise in EM are: cut raked rotor slots for all types of DC and AC electrical machinery; design an eccentric air gap for DC motors; select the proper ratio of the number of rotor and stator slots for asynchronous motors.

Raking the armature and rotor slots promotes a more uniform distribution of magnetic flux in the air gap and reduces the intensity of the serrated magnetic fields. The attainable reduction of magnetic noise in small- and medium-power motors is

$$\Delta L = 20 \lg f_{s\mu} = 20 \lg \frac{\sin\left(\frac{\mu}{p} \cdot \frac{a_s}{2}\right)}{\frac{\mu}{p} \cdot \frac{a_s}{2}}, \qquad (8.6.1)$$

where $f_{s\mu}$ is the skew factor; μ is the order of the strongest field harmonics; a_s is the rake angle of the slot; p is the number of pole pairs.

In small- and medium-power motors it is customary to rake the slots by one tooth division (of the stator or rotor), which reduces the magnetic noise and vibration by 10-15 dB.

An eccentric air gap in DC motors reduces magnetic induction on the pole edges, i.e., magnetic flux pulsation and perturbing forces. This reduces magnetic noise by 2-5 dB. The use of a combination of raked slots and eccentric air gap produces the greatest effect in terms of the reduction of magnetic noise in DC motors.

The choice of the proper ratio of the numbers of stator and rotor slots is very important for reducing magnetic noise in asynchronous electric motors. There are many recommendations regarding the proper choice of slot ratio

APPROVED FOR RELEASE: 2007/02/08: CIA-RDP82-00850R000200100009-9

APPROVED FOR RELEASE: 2007/02/08: CIA-RDP82-00850R000200100009-9

[2, 3, 8, 11]. However, there are no universal rules that are equally suitable in terms of the reduction of magnetic noise in small and large motors. The reason is that the resonance properties of the iron packs depend on the size of the motors. Therefore, when selecting the ratio z_1/z_2 for the purpose of reducing magnetic noise it is necessary to examine each individual small, medium and large motor separately.

Step poles, which reduce magnetic noise by 10-15 dB, are used for DC motors. Sometimes it is also recommended, for reducing magnetic vibration, to drive magnetic wedges into the armature and rotor slots. This promotes a more uniform distribution of induction in the air gap and thus reduces perturbing forces. Wedges reduce vibration in the serrated frequency range by up to 18 dB without a sacrifice of the energy indices of the motor.

Reduction of Mechanical Noise. As was mentioned earlier, the disbalance component very often determines the overall noise level in EM. The basic method for reducing it is careful static and dynamic balancing. The rotor must be balanced in its own bearings in order to reduce dynamic disbalance. It is recommended that the rotor be balanced in assembled form, i.e., when all parts are mounted on it, including the fan, rings or commutator, etc.; otherwise there is no guarantee of the required precision, even if the parts to be assembled are balanced separately. Extra slots (dummy slots) are cut in the large teeth.

Elastic and elastic inertial EM mechanical and magnetic noise reduction techniques are examined below.

Changing to friction bearings is a radical means of reducing bearing noise. Friction bearings are already being used today in the construction of numerous large machines by virtue of their great bearing capacity and dependability. However, the use of friction bearings in small and medium machines is difficult for design and operational considerations (in particular, an efficient lubrication system is needed, etc.).

The problem of reducing bearing noise is solved in three independent steps: development and use of roller bearings with improved noise characteristics; vibration damping and absorption of vibrations transmitted to the frame of a machine; creation of the most favorable operating conditions for the bearings in a machine.

Experience in the electrical industry has shown that it is best from the standpoint of noise reduction to use single-race radial ball bearings in electrical machinery; other types of bearings, as a rule, produce a higher noise level.

To reduce brush noise it is recommended that a high-quality forged commutator be used, carefully surface finished to minimize deviation from cylindricity. The brush clamp must be sufficiently rigid, and the gaps

APPROVED FOR RELEASE: 2007/02/08: CIA-RDP82-00850R000200100009-9

APPROVED FOR RELEASE: 2007/02/08: CIA-RDP82-00850R000200100009-9

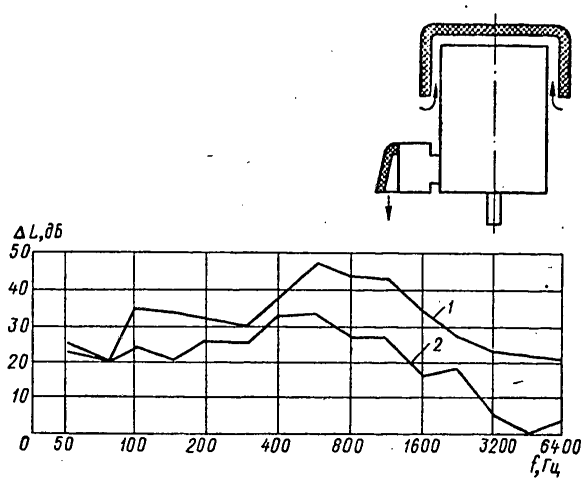

Figure 8.16. Noise mufflers of self-ventilating electric motor and their efficiency: 1 -- motor without muffler; 2 -- motor with muffler. [дБ=dB; Гц=Hz]

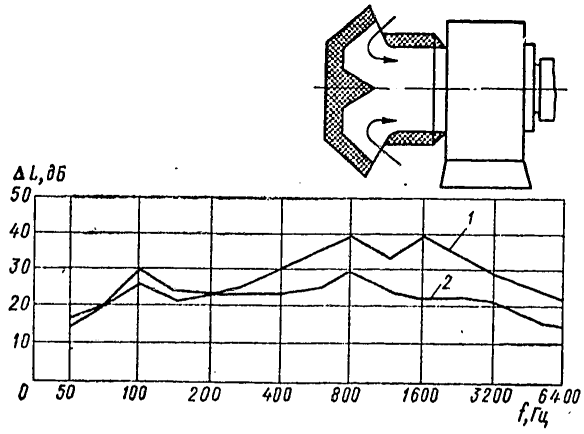

Figure 8.17. Noise muffler of electric fan and its efficiency: 1 -- fan without muffler; 2 -- fan with muffler.

between the brush and brush box must be minimized. Noise can be reduced by 8-10 dB by selecting soft grades of brushes, which wear in well.

Reduction of Aerodynamic Noise. In self-ventilating large motors, in which air is sucked in from the atmosphere and vented into the atmosphere, noise

APPROVED FOR RELEASE: 2007/02/08: CIA-RDP82-00850R000200100009-9

APPROVED FOR RELEASE: 2007/02/08: CIA-RDP82-00850R000200100009-9

can be reduced by 6-9 dB by replacing self-ventilation with induced ventilation using an external fan. The amount of noise reduction in sealed self-ventilating motors depends on the thickness and mass of the walls of the air ducts. In large motors with thin-wall brushes the brushes must be covered on the inside with a muffler. In independently (induced) ventilated motors noise is determined by the external fan. Therefore an effort must be made to use quiet fans. In water-cooled motors the power bars that extend from the case and the slots in the case must be carefully sealed. Water cooling provides 8-10 dB more reduction of aerodynamic noise in comparison with air cooling.

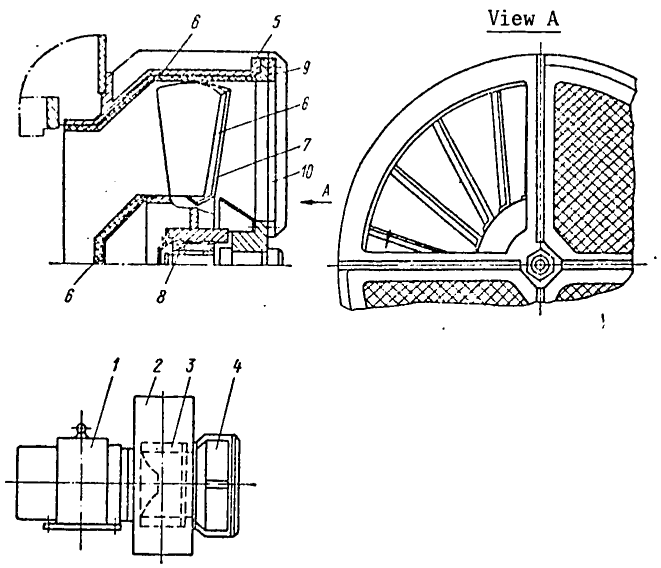

Figure 8.18. Fan muffler: 1 -- electric motor; 2 -- snail; 3 -- fan blades; 4 -- muffler; 5 -- muffler case; 6 -- sound-absorbing material; 7 -- duraluminum muffler vanes; 8 -- ball bearing; 9 -- cross piece; 10 -- metal screen.

One effective way to reduce aerodynamic noise in electrical machinery is to install mufflers (Figures 8.16 and 8.17). The efficiency of the mufflers depends on the area and thickness of the sound-absorbing material. In many mufflers the air flow is diverted by 90-180° for the most effective deadening of noise.

Illustrated in Figure 8.18 is a muffler, which differs from familiar ones in that a fan with vanes, which overlap each other and are covered on the inside with a sound-absorbing material, is inserted in the air flow, rotating on its axis under the influence of the air stream. The muffler is

APPROVED FOR RELEASE: 2007/02/08: CIA-RDP82-00850R000200100009-9

APPROVED FOR RELEASE: 2007/02/08: CIA-RDP82-00850R000200100009-9

attached to an electric fan, which contains a motor and blower. When the motor is turned on the fan is turned by the air flow without offering much resistance to it; the fan serves at the same time as an acoustic screen. A muffler of this design reduces the aerodynamic noise of an electric fan by 8-10 dB.

Built-in Elastic Vibration Absorption. With this technique elastic and elastic inertial elements, which substantially reduce mechanical and magnetic noise, are installed in a machine or outside of it. Local internal vibration- and noise-insulation are created as a result of the insertion of additional elastic elements. These flexible couplers can be placed in the rotor bearings or built into the bearing and magnetic assemblies.

Elastic magnetic suspension is used extensively in electrical machinery for reducing magnetic noise [2]. Some versions of elastic suspensions are shown in Figure 8.19. The efficiency of an elastic suspension increases as its rigidity decreases. At the same time a reduction of the rigidity of a suspension can lead to the appearance of intolerable eccentricity between the rotor and stator, and for this reason deformation limiters must be incorporated in the designs.

In spite of the variety of designs, all suspensions share in common the existence of a certain number of elastic elements (springs) with a particular rigidity coefficient K for a given type of machine. The suspension designs have elastic elements with different cross sections (usually made in the form of plates or webs that react to bending) and are inserted and fastened in a machine in different ways.

The main aspect of the determination of the parameters of an elastic suspension is to find the natural frequency f_n. To achieve the desired effect, as is known, the natural frequency of a suspension must be different from the frequency of the perturbing force by a factor of at least 3-4. The minimum possible value of f_n can be determined by the formula $f_n = 5/\sqrt{\delta}$, where δ is the maximum sag of the elastic element of the suspension under the mass of the stator, which does not exceed 10% of the air space.

To avoid resonance f_n must differ considerably from the rotation frequency of electrical machinery.

The total coefficient of radial rigidity is determined on the basis of the known frequency f_n: $K = 4\pi^2 m f_n$, where m is the stator mass.

If an elastic element is broken down conditionally into N separate elements, each of which represents a web, fastened on both sides, rigidity coefficient K_1 of such an element may be assumed to be K/2N. On the other hand, as is known, the rigidity coefficient of such a web is determined by the

APPROVED FOR RELEASE: 2007/02/08: CIA-RDP82-00850R000200100009-9

APPROVED FOR RELEASE: 2007/02/08: CIA-RDP82-00850R000200100009-9

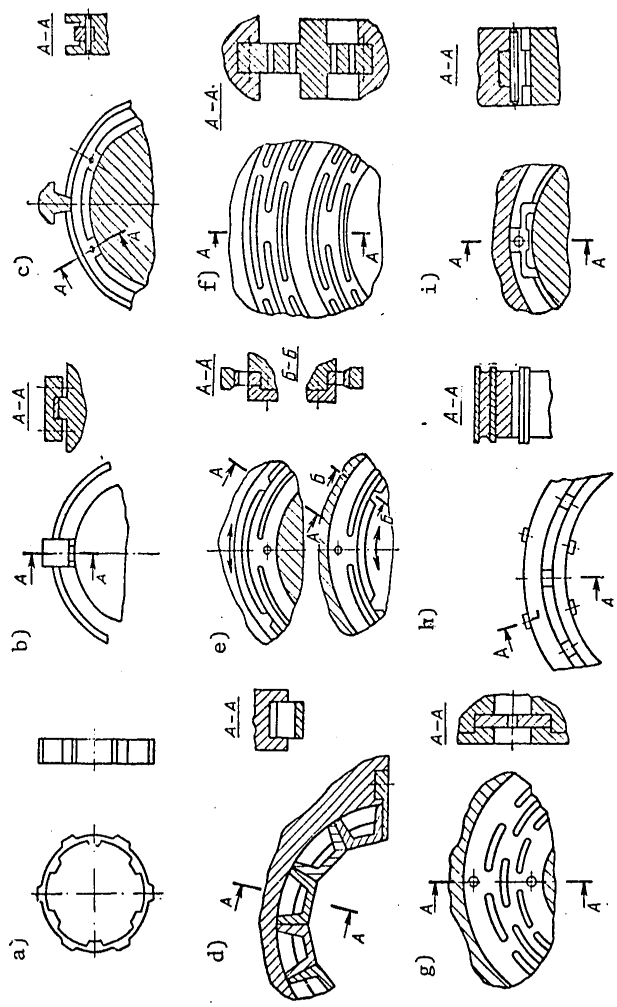

Figure 8.19. Designs of elastic and inertial elastic sound-insulating elements of electrical machinery: a -- ring with bilateral lugs; b -- ring with straps; c -- ring with vertical ears; d -- assembly of elastic webs; e -- ring with notched periphery; f -- ring with two elastic stages; g -- ring with three rows of concentric notches; h -- "double smooth spacer" elastic stage; i -- self-adapting elastic webs.

APPROVED FOR RELEASE: 2007/02/08: CIA-RDP82-00850R000200100009-9

APPROVED FOR RELEASE: 2007/02/08: CIA-RDP82-00850R000200100009-9

formula $K_1 = 12EJ/l^3$, where E is Young's modulus; $J = bh^3/12$ is the moment of inertia of the web; l, b, h are the length, width and height of the web, respectively.

If K_1 is known it is possible to select the dimensions of the elastic element, which satisfy the requirements of structural strength, and also to determine the effectiveness of the elastic suspension by the formula $\Delta L = 2rN \log \left|1 - \gamma \frac{M\omega^2}{K}\right|$, where M is the total weight of the machine; $\gamma = \mu/(1 + \mu)^2$, and $\mu = m/M - m$.

Experience shows that elastic suspensions can reduce magnetic vibrations and noise by 10-15 dB.

One way to reduce acoustic vibration and noise on the rotation frequency, as is known, is to use elastic bearings. The resonance frequencies of a system can be adjusted by changing the rigidity of the bearings, by inserting elastic elements in them. Internal elastic inertial noise reduction expands opportunities to reduce low-frequency mechanical components of electrical machinery noise. Inertial elements (antivibrators) are inserted in elastic couplings. A built-in elastic inertial noise-insulating unit consists in the general case of a top elastic element, intermediate mass and bottom elastic element. The elastic element of an antivibrator with inertial mass is fastened to the intermediate mass.

BIBLIOGRAPHY

1. Blagov, E. Ye. and B. Ya. Ivnitskiy, "Drossel'no-Reguliruyushchaya Armatura v Energetike" [Throttle-Control Hardware in Power Engineering], Moscow, Energiya, 1974.

2. "Bor'ba s Shumom" [Noise Abatement], edited by Ye. Ya. Yudin, Moscow, Stroyizdat, 1964.

3. "Vibratsiya Energeticheskikh Mashin. Spravochnoye Posobiye" [Vibration of Electrical Machinery. A Textbook], edited by N. V. Grigor'yev, Leningrad, Mashinostroyeniye, 1974.

4. "Kolebaniya i Vibratsii v Porshnevykh Kompressorakh" [Vibrations in Reciprocating Compressors], Leningrad, Mashinostroyeniye, 1972. Authors: Yu. A. Vidyakin, G. F. Kondrat'yeva, F. P. Petrova, et al.

5. Duan, N. I. and N. M. Yegorov, "Vibroacoustic Characteristics of Ship Plumbing," SUDOSTROYENIYE [Shipbuilding], 1962, No 3, pp 14-17.

6. Karelin, V. Ya., "Kavitatsionnyye Yavleniya v Tsentrobezhnykh i Osevykh Nasosakh" [Cavitation Phenomena in Centrifugal and Axial Pumps], Moscow, Mashinostroyeniye, 1975.

APPROVED FOR RELEASE: 2007/02/08: CIA-RDP82-00850R000200100009-9

APPROVED FOR RELEASE: 2007/02/08: CIA-RDP82-00850R000200100009-9

7. Kurnatov, D. V. and N. A. Stoyanova, "Noise Muffler for Variable Velocity Flow," SUDOSTROYENIYE, 1972, No 12, pp 33-35.

8. Lazaronts, D. F. and P. Bikir, "Shum Elektricheskikh Mashin i Transformatorov" [Noise of Electrical Machinery and Transformers], Moscow, Energiya, 1973.

9. "Raschet i Proyektirovaniye Sistem Truboprovodov. Spravochnoye Posobiye" [Calculation and Design of Plumbing Systems. A Textbook], Moscow, Gostoptekhizdat, 1961.

10. Timoshenko, S. P., "Kolebaniya v Inzhenernom Dele" [Vibrations in Engineering], Moscow, Nauka, 1967.

11. Shubov, I. G., "Shum i Vibratsiya Elektricheskikh Mashin" [Noise and Vibration of Electrical Machinery], Leningrad, Energiya, 1974.

APPROVED FOR RELEASE: 2007/02/08: CIA-RDP82-00850R000200100009-9

APPROVED FOR RELEASE: 2007/02/08: CIA-RDP82-00850R000200100009-9

CHAPTER 9. REDUCTION OF NOISE OF OPERATING ENGINES AND OTHER SYSTEMS

9.1. Engine Noise in Ship Rooms

The engines of modern ships are sources of loud noise in many aft compartments. The following types of engines are considered to be sources of loud noise: screws, air screws, fountain engines and rudder screws. Each of the mentioned types of engines is characterized by its own noise features.

Screws. The basic physical causes of noise during the operation of a screw are:

periodic forces that occur in water due to hydrodynamic loads on the blades (the force component of the sound of rotation);

periodic displacement of water due to the corporeality of the screw blades (the volume component of the sound of rotation);

generation of sound by turbulent flow past the screw blades (turbulent noise);

acoustic pulses that accompany the collapse of cavitation bubbles (cavitation noise).

The stream that flows through a screw, for several reasons (the hull lines of the stern are asymmetric with respect to the axis of the screw, parts of the hull protrude in front of the screw, etc.), is inhomogeneous in relation both to the periphery, and to the radius of the screw disk. This leads to a periodic change of the elements of the axial and tangential thrust and pressure against the water. The frequency of change of these parameters is nz (n is the rotation frequency of the screw, in revolutions per second, and z is the number of blades). Because the blades have finite cross section dimensions their "force" and "volume" actions upon the water are impulsive in nature and consequently can have harmonics with a frequency that is a multiple of nz.

APPROVED FOR RELEASE: 2007/02/08: CIA-RDP82-00850R000200100009-9

APPROVED FOR RELEASE: 2007/02/08: CIA-RDP82-00850R000200100009-9

The "force" and "volume" components of acoustic pressure can be calculated at the present time if the circulation of the flow velocity around the blades is known as a function of radius and rotation angle (Figure 9.1).

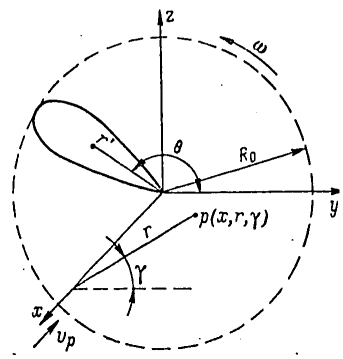

Figure 9.1. Calculation of pulsating pressures.

In accordance with [8] the force component is

$$p(x, r, \gamma, t) = \frac{\rho}{2\pi}\int_0^{R_0} \Gamma(r', t)\, D(x, \gamma) \times \frac{1}{R_1}\, dr', \qquad (9.1.1)$$

where x, r, γ are the cylindrical coordinates of a point in space in the coordinate system that moves along with the screw; t is time; ρ is the density of the liquid; $R_1 = [x^2 + r^2 + r'^2 - 2rr' \cos(\gamma - \omega t)]^{1/2}$ is the distance between the point in space and a point on the screw blade; ω is the angular velocity of the screw; $D(x, \gamma) = \omega r' \frac{\partial}{\partial x} - \frac{v_p}{\partial r'}\frac{\partial}{\partial x}$ is a differential operator; v_p is the axial component of the velocity of the incident flow, averaged across the screw disk; Γ(r', t) is the circulation of the flow velocity around an element of the screw blade, located at radius r'.

The velocity circulation and the coefficients of its expansion into a Fourier series with arguments kωt are assumed to be known.

The harmonic components of the force pressure of the screw, operating in a uniform flow, are determined and tabulated in the literature [23]. The components of pressure on a frequency that is a multiple of nz are

$$p_k = \frac{P}{\pi R_0^2}\left[-\frac{\lambda_p}{\pi} A_k \sin k\alpha + B_k \cos k\alpha\right], \qquad (9.1.2)$$

where P is screw thrust; $\lambda_p = v_p/nD$ is the relative approachability of the screw; R_0 is screw radius; α is the angle between a blade and a line to a calculated point; A_k and B_k are the harmonic components of pressure; k = = mz, where m = 1, 2, 3, ...

The coefficients for several first harmonics, computed for several values of x/R_0 and r/R_0, are listed in Tables 9.1 and 9.2 (x is the distance between the center of the screw along its axis in the direction of the flow, and r is the distance from the axis to a calculated point).

APPROVED FOR RELEASE: 2007/02/08: CIA-RDP82-00850R000200100009-9

APPROVED FOR RELEASE: 2007/02/08: CIA-RDP82-00850R000200100009-9

Table 9.1. Expansion Coefficients A_k

x/R_0	r/R_0	A_3	A_4	A_5	A_6	A_8	A_{10}
0	1,2	0,381	0,285	0,216	0,164	0,095	0,055
	1,3	0,267	0,185	0,130	0,093	0,048	0,024
	1,4	0,192	0,123	0,081	0,053	0,024	0,011
0,1	1,2	0,362	0,266	0,200	0,149	0,084	0,064
	1,3	0,257	0,175	0,122	0,086	0,043	0,031
	1,4	0,186	0,118	0,077	0,050	0,022	0,015
0,2	1,2	0,313	0,220	0,158	0,114	0,060	0,031
	1,3	0,230	0,152	0,102	0,069	0,033	0,015
	1,4	0,171	0,105	0,066	0,042	0,018	0,008

Table 9.2. Expansion Coefficients B_k

x/R_0	r/R_0	B_3	B_4	B_5	B_6	B_8	B_{10}
0	1) Любое	0	0	0	0	0	0
0,1	1,2	0,085	0,065	0,049	0,037	0,021	0,011
	1,3	0,045	0,033	0,023	0,017	0,008	0,006
	1,4	0,025	0,017	0,011	0,008	0,004	0,002
0,2	1,2	0,128	0,094	0,069	0,051	0,027	0,019
	1,3	0,073	0,051	0,035	0,025	0,012	0,008
	1,4	0,043	0,028	0,018	0,012	0,005	0,003

Key: 1. Arbitrary

Example. A five-bladed tanker screw with n = 110 rpm produces 156 ton thrust. Screw radius is 3.4 m. The pressure in the vicinity of the screw, according to (9.1.2), should be $p_k \leqslant \frac{P}{\pi R_0^2}\sqrt{\left(\frac{\lambda_p}{\pi}A_k\right)^2 + B_k^2}$. For the fundamental harmonic at a distance of 0.7 m from the screw disk and 4.5 m from the screw axis $A_5 = 0.102$, $B_6 = 0.035$, $A_{10} = 0.015$, $B_{10} = 0.006$.

At a speed of 18 knots the relative approach is $\lambda_p = \frac{18 \cdot 0{,}515 \cdot 60}{110 \cdot 6{,}8} = 0{,}74$.

The computations yield $p_5 = 1.82 \cdot 10^3$ Pa; $p_{10} = 2.93 \cdot 10^2$ Pa.

Due to the inhomogeneity of the flow these values increase by a factor of 3-4 [8]. In view of this, by converting to acoustic pressure levels we obtain: on 9.2 Hz $L = 20 \log \frac{1.82 \cdot 10^3 \cdot 4}{2 \cdot 10^{-5}} = 170$ dB; on 18.4 Hz

APPROVED FOR RELEASE: 2007/02/08: CIA-RDP82-00850R000200100009-9

APPROVED FOR RELEASE: 2007/02/08: CIA-RDP82-00850R000200100009-9

$L = 20 \log \frac{2.93 \cdot 10^2 \cdot 4}{2 \cdot 10^{-5}} = 155$ dB. As the example shows, the frequency of the strongest components of rotation noise is in the infrasonic region (this is typical of most screws). The amplitudes of HF (acoustic) harmonics diminish rapidly as frequency increases. The fall is approximately 15 dB per octave.

For real screws the amplitudes of the harmonics of the volume component of rotation sound, the frequencies of which fall in the audio frequency range, are vastly smaller than the amplitudes of the harmonics of the force component. Therefore the former may be ignored during calculation of acoustic pressures.

Measurements of noise and acoustic vibration in the aft compartments show that the noise spectrum of noncavitating screws is mixed, even in the low-frequency region; in addition to audio components there is noise with a continuous spectrum. The flow velocity relative to the screw blades reaches 30-50 m/s across much of the radius. The Reynolds number for a flow around blade elements becomes 10^7-10^8. In this case the boundary layer of the liquid, flowing past the blades, is an emitter of sound. The spectral density of the acoustic pressure can be approximated through the relation [8]

$$p(f) = \frac{56{,}3\tau_w^2\delta^*}{u_\infty[1 + e^{3{,}9(f\delta^*/u_\infty)^{0{,}625}}]}, \qquad (9.1.3)$$

where τ_w is the tangential force of friction on the blade surface; δ^* is the thickness of the displaced turbulent boundary layer; u_∞ is flow velocity.

The characteristics of flow past a plane surface may be used for estimating the order of magnitude of pressure [8]:

$$\tau_w = 0{,}1315\rho\nu^{1/7}u_\infty^{13/7}l^{-1/7};$$
$$\delta^* = 0{,}0206l \cdot Re_l^{-1/7}, \qquad (9.1.4)$$

where Re_l is the Reynolds number, $Re_l = \frac{lu}{\nu}$ (l is profile length); u is flow velocity; ν is the kinematic viscosity, for water at 20°C $\nu = 1.0 \cdot 10^{-6}$ m²/s.

Example. In the preceding example the circumferential velocity in the blade cross section with $R = 0.85R_0$ is u = 31 m/s. The blade width in this cross section is l = 1.0 m, and the Reynolds number is

$$Re_l = \frac{30 \cdot 1{,}0}{1{,}0 \cdot 10^{-6}} = 3 \cdot 10^7.$$

APPROVED FOR RELEASE: 2007/02/08: CIA-RDP82-00850R000200100009-9

APPROVED FOR RELEASE: 2007/02/08: CIA-RDP82-00850R000200100009-9

Substituting the necessary values into formulas (9.1.4), we obtain τ_w = = 1,000 Pa; $\delta^* = 1.76 \cdot 10^{-3}$ m. As a result of substitution of these values into formula (9.1.3) and averaging in the octave bands we find the acoustic pressure levels in the 145-155 dB range in the 100-1,000 Hz frequency range.

Cavitating screws produce the strongest noise in rooms. The cause of the noise is the collapse of cavitation bubbles, which occur near the blade surface at points where the pressure drops to some critical value and water loses solidity. The popping of bubbles is accompanied by an acoustic pulse. The intensity of cavitation noise depends on the number of bubbles and their diameter, on the time intervals between the formation of bubbles and on the concentration of gas in water. All these factors are random, and therefore cavitation noise should be viewed as a random pulse process [8]. The size of the cavitation volume is determined by the geometry of the blades and by the velocity field in the screw disk. The inhomogeneity of the velocity field in the screw disk causes a periodic change of the attack angle of any cross section of the blade (Figure 9.2), which leads to modulation of cavitation noise by frequency nz.

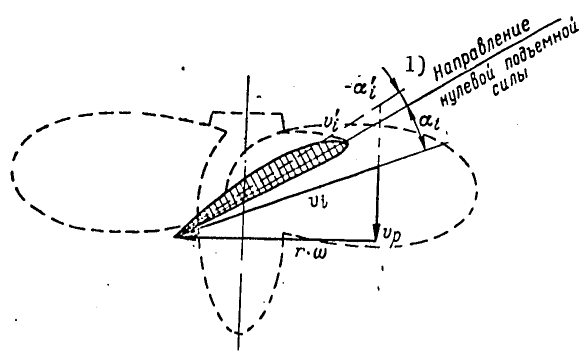

Figure 9.2. Diagram of velocities on blade.
Key: 1. Zero thrust line

Under otherwise identical conditions the inhomogeneity of the flow in the screw disk amplifies cavitation and increases cavitation noise.

Cavitation occurs not only on the screw blades, but also on certain protruding parts of the hull (struts), located in front of the screw. As a result a flow that represents a mixture of water and cavitation bubbles flows around the blades at certain rotation angles. This phenomenon exacerbates even more the calculation of cavitation noise.

If the acoustic pressure near a screw is known the acoustic vibration levels of the part of the exterior hull above the screw can be estimated, and then the noise levels in aft compartments can be calculated, using the described part of the exterior hull as a reference bulkhead (see Chapter 15).

APPROVED FOR RELEASE: 2007/02/08: CIA-RDP82-00850R000200100009-9

APPROVED FOR RELEASE: 2007/02/08: CIA-RDP82-00850R000200100009-9

The outer hull plating is located on the air-water interface. It can be shown [16] that, excluding cases of very great thicknesses, the outer hull plating may be viewed as a locally reacting surface, the resistance of which is determined by impedance $i\omega m$, which does not depend on the angle of incidence (m is mass per unit area). Then the following relation will exist between the acoustic pressure levels under the hull and the vibration levels of the hull:

$$N_v = L - 20 \lg (1{,}5 \cdot 10^6 + i\omega m) + 49, \qquad (9.1.5)$$

where N_v is the vibration velocity of the hull (relative to $v_0 = 5 \cdot 10^{-8}$ m/s), in dB; L is the acoustic pressure level under the outer hull, in dB; m is mass per unit area of the outer hull plating, in kg/m^2.

If the acoustic pressure levels are not known the vibration levels of the outer hull N_v, in dB, located above the screw, operating in the strong cavitation mode, can be estimated through the empirical formula

$$N_v = 54 \lg nR_0 + \Delta' + \Delta''(1 - \alpha) + \Delta''', \qquad (9.1.6)$$

where n is the rotation frequency, in revolutions per second; R_0 is screw radius, in m; Δ' is a correction factor that takes into account the frequency characteristic of the interaction of the cavitating screw and the hull, in dB; Δ'' is a correction factor that takes into account the distance between the screws and the hull and the angle of inclination of the screw shaft, in dB; α is a coefficient that takes into account the influence of velocity with the screw and hull in different relative positions; Δ''' is a correction factor that takes into account the mass of the outer hull plating, in dB.

Correction factor Δ' acquires the following values as a function of frequency:

f, Гц	63	125	250	500	1000	2000	4000	8000
Δ', дБ	54	50	47	40	32	26	15	10

Correction factor Δ'' and coefficient α are determined by the graphs in Figures 9.3 and 9.4 as functions of the ratio r/R_0 (r is the distance between the center of the screw and the outer hull, and R_0 is screw radius), angle of inclination of the screw shaft and speed of the ship.

The correction factor Δ''' is

$$\Delta''' = 20 \lg \frac{1 + 1{,}6 \cdot 10^{-3} f}{1 + 4{,}4 \cdot 10^{-4} mf}, \qquad (9.1.7)$$

where m is the mass of the outer lining per unit area, in kg/m^2.

APPROVED FOR RELEASE: 2007/02/08: CIA-RDP82-00850R000200100009-9

APPROVED FOR RELEASE: 2007/02/08: CIA-RDP82-00850R000200100009-9

Table 9.3. Calculation of Outer Hull Vibration Levels

1) Параметр	2) Частоты октавных полос, Гц							
	63	125	250	500	1000	2000	4000	8000
$I_1 = 54 \lg n\ R_0$	48	48	48	48	48	48	48	48
$I_2 = \Delta_1$	54	50	47	40	32	26	15	10
$I_3 = \Delta^{\prime\prime} (1 - \alpha)$	1	1	1	1	1	1	1	1
$I_4 = \Delta'''$	0	0	0	0	0	0	0	0
$N_0 = I_1 + I_2 + I_3 + I_4$	103	99	96	89	81	75	64	59

Key: 1. Parameter 2. Frequencies of octave bands, in Hz

Example. Calculate the vibration of a 10 mm thick steel hull plating, located above a screw with a radius of 2.0 m (Figure 9.5). The rotation frequency of the screw is n = 4 rev/s, the speed of the ship is 12 m/s, the angle of inclination of the screw shaft is 3°, and the ratio r/R_0 = 1.3 (Table 9.3).

The vibration levels in the last row of Table 9.3 for a bulkhead, located above the screws, are used as the initial data for calculating the noise levels in aft compartments. For example, determine the noise levels in room III. The calculation can be done graphoanalytically (see Chapter 15). We number the bulkheads; we call the bulkhead located immediately above the screw number 0. Using the formulas and nomograms in §15.5, we calculate the vibration levels of the bulkheads that enclose room II, after which we determine the noise levels, radiated by those bulkheads, and the total noise levels in room II. The noise levels in room II are used as the initial data for calculating the noise levels in examined room III by the procedure used for distant compartments. The calculations yield the following levels of the spectral components of noise in the octave frequency bands:

[Гц=Hz; дБ=dB]									
	f, Гц	63	125	250	500	1000	2000	4000	8000
	L, дБ	100	95	88	80	76	71	60	50

Air Screws. Air screws are one of the main sources of noise for ships that utilize dynamic lift principles. Noise is produced by the periodic force of the blades, acting upon a medium, and by the displacement of air masses (the "force" and "volume" components of fan noise), and by the separation of eddies from the trailing edges of the blades (eddy noise). A characteristic feature of modern air screws is the fact that the frequencies of the first harmonics of fan noise are in the audio frequency range, and not in the infrasonic range, as in the case of screws.

To calculate the amplitude of acoustic pressure in the far field of an air screw on frequency f = mn it is customary to use L. Ya. Gutin's formula

APPROVED FOR RELEASE: 2007/02/08: CIA-RDP82-00850R000200100009-9

APPROVED FOR RELEASE: 2007/02/08: CIA-RDP82-00850R000200100009-9

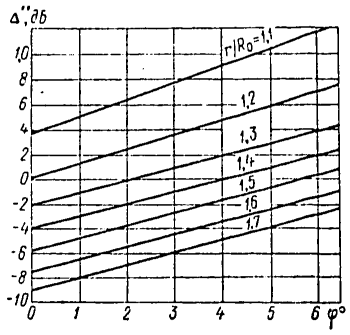

Figure 9.3. Correction factor Δ'' as function of angle of inclination of screw shaft.

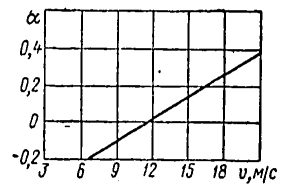

Figure 9.4. Correction factor α as function of ship speed.

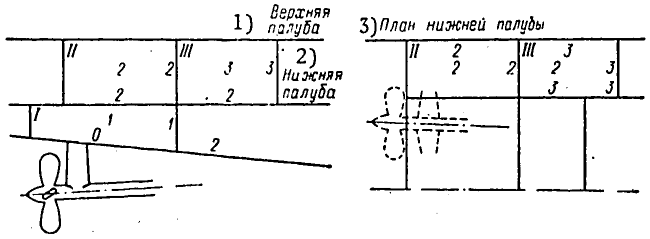

Figure 9.5. Calculation of noise level.
Key: 1. Upper deck 3. Lower deck plan
2. Lower deck

[э=е]

$$p(f, r, \theta) = \frac{mnz}{c_0 r}\left| -P\cos\theta + M\frac{c_0}{2\pi n R_э}\right| J_{mz}\left(\frac{2\pi mnz}{c_0} R_э \sin\theta\right), \qquad (9.1.8)$$

where m is the number of harmonic; n is the rotation frequency of the air screw, in rev/s; z is the number of blades; r is the distance between the center of the screw and the calculated point; c_0 is the speed of sound in air; P and M are, respectively, the thrust and torque of the screw; $R_e = 0.8R_0$ (R_0 is screw radius); J_{mz} is a first-kind Bessel function; θ is the angle between a line to the calculated point and the screw axis (the axis is aimed in the direction of travel of the screw).

The results of calculation by formula (9.1.8) agree satisfactorily with the experimental data for screws with peripheral velocities less than the speed of sound. In the case of high harmonics and near- and supersonic circumferential velocities the calculated and measured acoustic pressures differ

APPROVED FOR RELEASE: 2007/02/08: CIA-RDP82-00850R000200100009-9

APPROVED FOR RELEASE: 2007/02/08: CIA-RDP82-00850R000200100009-9

substantially. The circumferential velocities of air screws used on ships sometimes reach (0.9-1.1)M (M is the Mach number). In this case preference should be given to initial data obtained from stand tests for calculating noise.

Rudder Systems (RS). RS sometimes produce unacceptably high-level noise in nearby compartments. The total noise levels at a distance of 1 m from modern RS are 111-110 dB, and vibration levels near RS reach 90-95 dB. RS with an adjustable pitch screw are used most frequently in Soviet shipbuilding. The screw is usually driven by an electric motor with a constant rotation frequency through an articulated reducer. The reducer and blade pitch control mechanism are installed in a water-tight gondola, which is located in the RS shaft.

Narrow-band analysis of RS noise and vibration and comparison of the acoustic characteristics in different operating modes lead to the conclusion that noise and vibration on frequencies of up to 400-500 Hz are produced in approximately equal measure by the interaction of the gears of the articulated reducer and operation of the screw. On frequencies above 500 Hz screw cavitation noise predominates. The results of acoustic test stand measurements at the shipyards may be used as the initial data for forecasting the noise levels in ship compartments. A comparison of the results of measurements on ships and on stands disclosed certain discrepancies in the frequency characteristics (up to 7 dB in individual bands) of noise and vibrations and under natural and test stand conditions, but the integral levels are virtually the same.

9.2. Methods of Reducing Screw and Other Engine Noise

There are two ways to reduce the noise produced by engines in ship compartments: reduce the acoustic pressure on the hull by changing engine operating conditions; reduce hull vibration and the transmission of vibration to ship compartments without changing engine operating mode.

The acoustic pressure under the hull is reduced by decreasing the inhomogeneity of the flow, the maximum distance between the screw and hull and screw shaft struts, and by reducing the downwash of the flow.

One way to reduce flow inhomogeneity is to secure the screw shaft without struts, as recommended by the Leningrad Institute of Water Transport (LIVT) for small ships. The reduction of the vibration level of the outer hull ΔN, in dB, for a cantilever screw (in comparison with one fastened to a strut) is characterized by the following figures:

[Гц=Hz; дБ=dB]									
f, Гц	63	125	250	500	1000	2000	4000	8000
ΔN, дБ . . .	9	7	7	6	5	4	3	3

Several techniques have been proposed for reducing acoustic vibrations of the outer hull near the screws. Some of them utilize N. N. Babayev's

APPROVED FOR RELEASE: 2007/02/08: CIA-RDP82-00850R000200100009-9

APPROVED FOR RELEASE: 2007/02/08: CIA-RDP82-00850R000200100009-9

concept [8], according to which the section of the bottom immediately above the screw is replaced by a flexible element, which receives the screw pressure and reduces the transmission of acoustic vibration to hull structures [11, 19].

The pressure may be absorbed by elastic skin, placed over the hull in a recess (Figure 9.6), or by a membrane, covering a slot in the bottom (Figure 9.7). Deep wells with a spring-loaded piston inside may also be used (Figure 9.8). High pressure is picked up by the piston, but vibration is not transmitted to the hull due to the vibration-insulating fastening of the piston. The efficiency of these systems is 10-12 dB in the entire audio frequency band.

The mass of the part of the bottom directly over the screw can be increased to reduce the vibration of the outer plating. To do this the bottom is covered with concrete, bitumen or other massive material that is resistant to vibration.

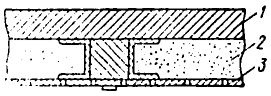

Figure 9.6. Vibration-damping elastic skin: 1 -- outer skin; 2 -- elastic layer; 3 -- perforated skin.

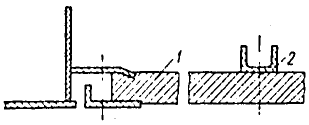

Figure 9.7. Rubber membrane: 1 -- membrane; 2 -- keel.

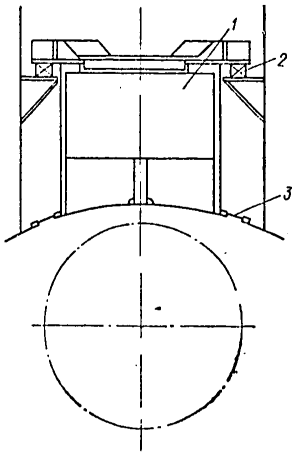

Figure 9.8. Spring-loaded piston: 1 -- piston; 2 -- elastic element; 3 -- seal.

APPROVED FOR RELEASE: 2007/02/08: CIA-RDP82-00850R000200100009-9

APPROVED FOR RELEASE: 2007/02/08: CIA-RDP82-00850R000200100009-9

The area over the screw to be covered should be $(1.2\text{-}1.4)D^2$, where D is screw diameter. The average mass of the skin per unit area should be 4-5 times greater than the mass of the bottom in the vicinity of the screw. The thickness of the cover should decrease from the center to the periphery by a ratio of 2.0-2.5. The use of massive coatings reduces noise in aft compartments by 4-6 dB [4].

An air shroud may be used for reducing pressure pulsations picked up by the outer skin[1]. Air is forced through several slots or holes in the outer skin in front of the screw to create a shroud. It is entrained by the flow toward the stern, forming a layer consisting of a mixture of air and water. The acoustic impedance of this layer is much less than the impedance of water. This produces a substantial sound-insulating effect of 8-10 dB on low and intermediate frequencies of the audio frequency band.

Ordinary design measures may be used in addition to the above-described specific techniques for reducing screw noise: "room in room" sounding insulation, vibration-absorbing coatings, vibration insulation of bulkhead joints and other methods of reducing structural noise, like the ones examined below.

According to the literature [1], the circumferential velocity of the blades should be reduced and the number of blades increased in order to reduce the noise of an air screw with a given thrust. However, this recommendation refers only to screws with subsonic velocities at the ends of the blades.

One important way to reduce noise is to use synchrophased screws. The rotation frequencies of all screws are maintained equal to a high precision with the aid of a special system, and the blades of each screw are held in a certain position in relation to the blades of the others. According to the literature [1], the noise levels at individual points can be reduced by 5-7 dB by means of synchrophasing. Low-frequency noise can be reduced substantially by placing the screws in an annular shroud. The effect, produced primarily by relieving the stress on the blades, is a reduction of 5-8 dB.

The noise of rudder systems can be reduced both by general design techniques and by special measures. General design techniques include increasing the rigidity of the RS shaft and fastening the shaft to just the bottom bulkhead and sides without a rigid connection to the deck above the RS. The bottom in the vicinity of the foundation of RS should be poured with concrete, bitumen or other massive and vibration-resistant material for a distance of five or six frame spaces, just as is recommended for reducing screw noise.

---

[1]Satt att dampa buller fran fartygspropellrar (Method of Reducing Screw Noise), Swedish Patent No. 322705, dated 13 April 1970, B63 No. 21/30.

APPROVED FOR RELEASE: 2007/02/08: CIA-RDP82-00850R000200100009-9

APPROVED FOR RELEASE: 2007/02/08: CIA-RDP82-00850R000200100009-9

Another effective way to reduce noise is to line the inside of the rudder system shaft with an elastic material [3]. Materials whose wave impedances are much less than the wave impedance of water are used for this purpose: sponge rubber and polyvinyl chloride foam. To prevent separation of the liner from the shaft the elastic material is covered with thin sheet metal.

The thickness of the elastic layer in constructions that are used in practice is 10-15 mm. The acoustic vibration levels of the rudder system are reduced by 15-20 dB as a result of lining. The reduction of air noise is less and is 8-10 dB.

9.3. Noise Interference on Bridge and Ways to Reduce It[1]

Statistical Characteristics of Noise Interference and Acceptable Standards. The types of noise interference on the bridge are noise levels in the wheelhouse and navigator room and on the bridge wings. Noise interference on the bridge should be viewed basically from the standpoint of navigation safety, i.e., audibility of sound signals from oncoming ships, intelligibility of voice commands, etc. In accordance with the plan of CEMA standards, the PS-55 curve is used as the acceptable standard in rooms of the bridge. However, this standard, as will be shown, does not assure audibility of acoustic signals from oncoming ships at certain distances.

The existing health standards call for the use of the PS-40 limiting noise spectrum for the bridge. The actual noise levels in the wheelhouse and navigator room, and also on the bridge wings of seagoing transport ships, based on TsNIIMF [Central Scientific Research Institute of the Maritime Fleet] data, are given in Figure 9.9. Curves of the probability distribution of acoustic pressure levels, on the basis of which noise levels can be calculated, are given in Figure 9.10 for the same rooms. The data were obtained as the result of measurements on 75 seagoing transport ships of different types. The M curves in Figure 9.9 correspond to the universal mean. As can be seen by the curves, the greatest excess above the PS-45 curve occurs in the 500-2,000 Hz octave bands.

The required reduction of noise in the wheelhouse and navigator room, according to PS-45, is 6-10 dB for 25% of the ships, 13-17 dB for 50%, and 20-25 dB for the remaining 25%.

Audibility of Acoustic Signals. The new International Rules on Collision Avoidance of Ships at Sea (MPPSS-72), approved by the International Convention (IMKO) and adopted on 1 January 1976, stipulate: the range of audibility of acoustic signals, their frequency spectrum and acoustic pressure levels, depending on the size of ships (Table 9.4). The Rules of the USSR Register specify that acoustic signals should be audible at a distance of 2 miles, irrespective of the size of ships.

[1]This section was written by V. I. Zinchenko and L. A. Tatsi.

APPROVED FOR RELEASE: 2007/02/08: CIA-RDP82-00850R000200100009-9

APPROVED FOR RELEASE: 2007/02/08: CIA-RDP82-00850R000200100009-9

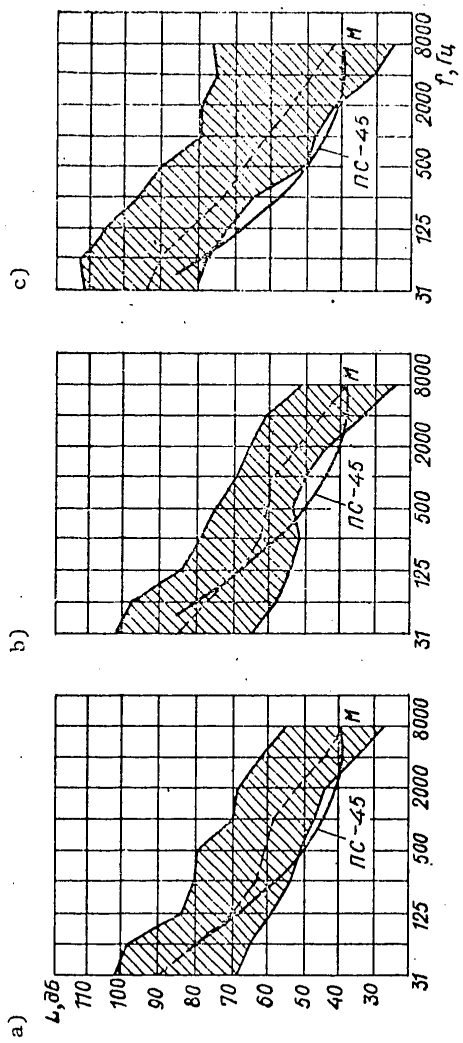

Figure 9.9. Noise levels in bridge rooms of seagoing transport ships (measurements taken on 75 ships): a -- in wheelhouse; b -- in navigator room; c -- on bridge wing. [дБ=dB; Гц=Hz; ПС=PS]

APPROVED FOR RELEASE: 2007/02/08: CIA-RDP82-00850R000200100009-9

APPROVED FOR RELEASE: 2007/02/08: CIA-RDP82-00850R000200100009-9

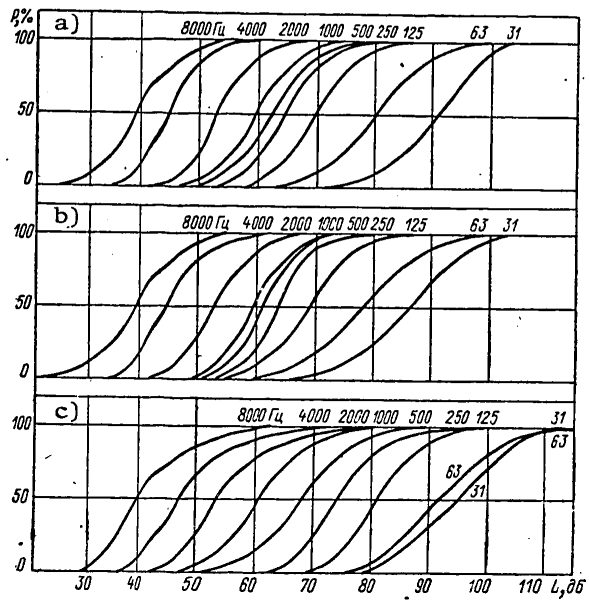

Figure 9.10. Curves of probability distribution of acoustic pressure levels, P%, in bridge rooms: a -- in wheelhouse; b -- in navigator room; c -- on bridge wing. [дБ=dB; Гц=Hz]

The audibility of a whistle depends on its acoustic pressure level, attenuation in the atmosphere and level of noise interference on the receiving end. The receiving end is usually the wing of the bridge and wheelhouse. The overall levels and frequencies of the fundamental tone of certain modern signal systems, used on ships, are listed in Table 9.5.

According to MPPSS-72 the acoustic level of a ship's own signal at listening stations should not exceed 110 dBA, and if possible not more than 100 dBA. In most cases a ship's whistle may be installed not farther than 20-30 m from the bridge. At that distance the acoustic pressure level will be 25-30 dB lower than at a distance of 1 m. Therefore, in accordance with MPPSS-72 requirements, the acoustic signal level at 1 m should, if possible, not exceed 130 dBA, and levels above 140 dBA are unacceptable.

On the basis of experimental investigations the optimum frequency band for acoustic signals is 180-700 Hz ± 10%. Therefore the noise interference level at listening stations on board a ship in two octave frequency bands: 250 and 500 Hz, which cover the 177-709 Hz range, is extremely important.

APPROVED FOR RELEASE: 2007/02/08: CIA-RDP82-00850R000200100009-9

APPROVED FOR RELEASE: 2007/02/08: CIA-RDP82-00850R000200100009-9

Table 9.4. MPPSS-72 Requirements on Acoustic Signal Systems of Seagoing Ships

Length of ship, m	Acoustic pressure level in third-octave bands at 1 m from whistle, in dB	Recommended fundamental frequency of whistle, Hz	Audibility range in nautical miles
200 and more	143	70-200	2.0
75 and more, but less than 200	138	130-350	1.5
20 and more, but less than 75	130	250-700	1.0
Less than 20	120	--	0.5

The spectrum of a whistle is ruled (discrete) in character. The maximum level of the frequency components depends on the design of the whistle and on how it is tuned; it does not always appear on the fundamental frequency (Figure 9.11).

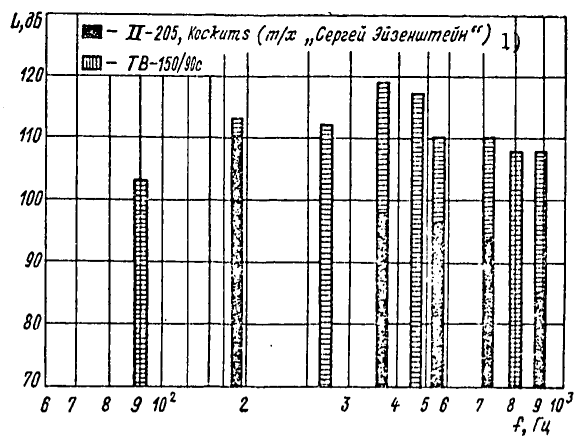

Figure 9.11. Sample spectra of acoustic pressure levels of ship foghorns. [дБ=dB; c=s; Гц=Hz]
Key: 1. (motor ship "Sergey Eyzenshteyn")

Calculation of Audibility of Acoustic Signals. According to the standards of the acoustic signal committee of the International Association of Beacon Services (IABS), the audibility range should be determined as a function of the noise interference level inherent to 84% of the large merchant ships [7].

APPROVED FOR RELEASE: 2007/02/08: CIA-RDP82-00850R000200100009-9

APPROVED FOR RELEASE: 2007/02/08: CIA-RDP82-00850R000200100009-9

Table 9.5. Acoustic Characteristics of Certain Modern Marine Acoustic Signal Systems [12]

1) Марка	2) Общий уровень на расстоянии, м		3) Частота основного тона, Гц	4) Страна-изготовитель
	$r = 10$	$r = 1$		
5) Воздушные тифоны				
ТВ 100/180	124	144	180	СССР
ТВ 100/165	126	146	165	СССР 6)
ТВ 150/90$_c$	130	150	90	СССР
100EA	124	144	200	Япония
150EA	127	147	110	Япония 7)
ТА 100/200	124	144	200	Швеция
КТ 150/165	125	145	165	Швеция
КТ 150/130	127	147	130	Швеция 8)
КТ 230/75	131—133	151—153	75	Швеция
9) Электротифоны				
ТЭ-1	125	145	110	СССР
ТЭ-2	126	146	90	СССР 6)
МН-75	123	143	140	Япония
МН-220	128	148	113	Япония 7)
МА 18/75	131—135	151—153	75	Швеция
МА 18/90	127—131	147—151	90	Швеция 8)
МА 18/130	123—127	143—147	130	Швеция
10) Паровые свистки				
230/75	131—133	151—153	75	Швеция
Т300МЕ	129	149	125	Швеция
Т20	128	148	165	Швеция

Key:
1. Brand
2. Total level at distance, in m
3. Fundamental frequency, in Hz
4. Manufacturer
5. Air foghorns
6. USSR
7. Japan
8. Sweden
9. Electric foghorns
10. Steam whistles

The results of measurements of the sound levels on the bridges of ships with probabilities of 84% and 90%, based on data of TsNIIMF [Central Scientific Research Institute of the Maritime Fleet], IMKO-Sweden and the IABS organization, are presented in Table 9.6. The data were obtained on the basis of numerous measurements, and their results agree satisfactorily in the 250 and 500 Hz octave bands. The interference levels in the wheelhouse in the 250 and 500 Hz octave bands may be assumed, on the average, to be 75 and 70 dB, respectively, and 83 and 76 dB on the bridge wings. In third-octave bands, in consideration of the manner in which the spectra fall off, the levels are 3 dB lower.

Curves that show the useful signal level that will be heard on the bridge with a probability of 50% at the corresponding interference level in the

APPROVED FOR RELEASE: 2007/02/08: CIA-RDP82-00850R000200100009-9

APPROVED FOR RELEASE: 2007/02/08: CIA-RDP82-00850R000200100009-9

Table 9.6. Noise interference Levels on Bridges of Sea-going Ships, in dB [7]

1) Источник данных и место измерения	2) Количество судов (из числа обследованных), %	3) Уровни звукового давления, дБ, в октавных полосах частот, Гц								
		31	63	125	250	500	1000	2000	4000	8000
4) Фирма MAMC (Швеция)	84	—	89	82	79	74	71	71	—	—
5) Фирма IMKO (Швеция)	90	104	91	82	75	68	65	62,5	60,5	60
6) ЦНИИМФ (СССР):										
штурманская рубка	84	95	87	75	68	66	65	69	51,5	47
рулевая рубка	84	97	88	77	71	67	65	58	51	46
крылья ходового мостика	84	104	103	87	8	76	70	64	57	49

Key: 1. Source of data and measurement point
2. Number of ships (of total investigated), %
3. Acoustic pressure levels, dB, in octave frequency bands, Hz
4. IABS firm (Sweden)
5. IMKO firm (Sweden)
6. TsNIIMF (USSR): navigator's room wheelhouse bridge wings

third-octave bands, are given in Figure 9.12. The curves were plotted by Oguro Hideo on the basis of Soviet investigations and data of other authors. For example, at interference levels in the third-octave bands 250 and 500 Hz, equal to 73 and 67 dB, respectively, as was shown, an acoustic signal will be audible with a probability of 50% only if its level is 73 and 67 dB, respectively. Before a signal can be heard with a probability of 90% its level must be approximately 3 dB higher, i.e., 76 and 66 dB, and 82 and 72 dB, respectively, on the bridge wings. If these values and the whistle level at a distance of 1 m or 10 m are known (see Table 9.6), it is possible to calculate the range of audibility of ship signals at the corresponding interference levels and at the PS-45 acceptable level at a distance of r = 1 mile and r = 2 miles.

The acoustic pressure level decreases with distance because the acoustic energy diminishes due to the spherical propagation of the wave front, losses due to the conversion of acoustic energy to thermal and bending of acoustic rays due to the influence of wind and temperature gradients, and also due to atmospheric turbulence.

APPROVED FOR RELEASE: 2007/02/08: CIA-RDP82-00850R000200100009-9

APPROVED FOR RELEASE: 2007/02/08: CIA-RDP82-00850R000200100009-9

The reduction of signal level due to the spherical propagation of the leading edge of an acoustic wave L_r, in dB, can be calculated with sufficient accuracy by the formula

$$L_r = L_{r_0} - 20 \lg \frac{r}{r_0}, \qquad (9.4.1)$$

where L_r and L_{r_0} are the acoustic pressure levels of the signal at distances r and r_0 = 1 m (or 10 m).

The attenuation of the acoustic pressure level ΔL_1 due to the conversion of acoustic energy to thermal energy as a result of molecular absorption, humidity, thermal conductivity and certain other factors, is comparatively minor and depends on the frequency of the sound [20]. The values of attenuation are listed below:

f, Hz	ΔL_1, dB/mile
50	0,13—0,7
100	0,16—1,4
200	0,32—2,1
400	3,2—3,4
800	5,8—10,8

The wind, temperature gradient with altitude and the turbulence of the atmosphere, which produce additional attenuation, exert a substantially strong influence on the reduction of signal level. Wind and temperature gradients distort acoustic rays and produce a so-called dead zone, or acoustic shadow, in which signal audibility falls additionally by 20-3 dB. An acoustic shadow is formed usually on the windward side of the sound source (sound propagates against the wind), at a distance of 100-500 m, depending on the elevation of the source and receiver (Figure 9.13).

For the point of reception, located at height h_2, distance r to the boundary of an acoustic shadow is calculated by the approximate formula [10]

$$r + \sqrt{2 \frac{c_0}{dc/dh} (\sqrt{h_1} + \sqrt{h_2})}, \qquad (9.4.2)$$

where h_1 is the elevation of the source above sea level; c_0 is the speed of sound at the surface of the water; dc/dh is the gradient of the speed of sound; $\frac{c_0}{dc/dh}$ is the radius of curvature of an acoustic ray.

An acoustic shadow can also be formed in calm weather, when acoustic rays are curved only by a temperature gradient. Curves of additional attenuation of signals under the influence of weather conditions (Figure 9.14) were plotted on the basis of studies of the audibility of acoustic signals at sea [21]. The principles of attenuation are close to the values of

APPROVED FOR RELEASE: 2007/02/08: CIA-RDP82-00850R000200100009-9

APPROVED FOR RELEASE: 2007/02/08: CIA-RDP82-00850R000200100009-9

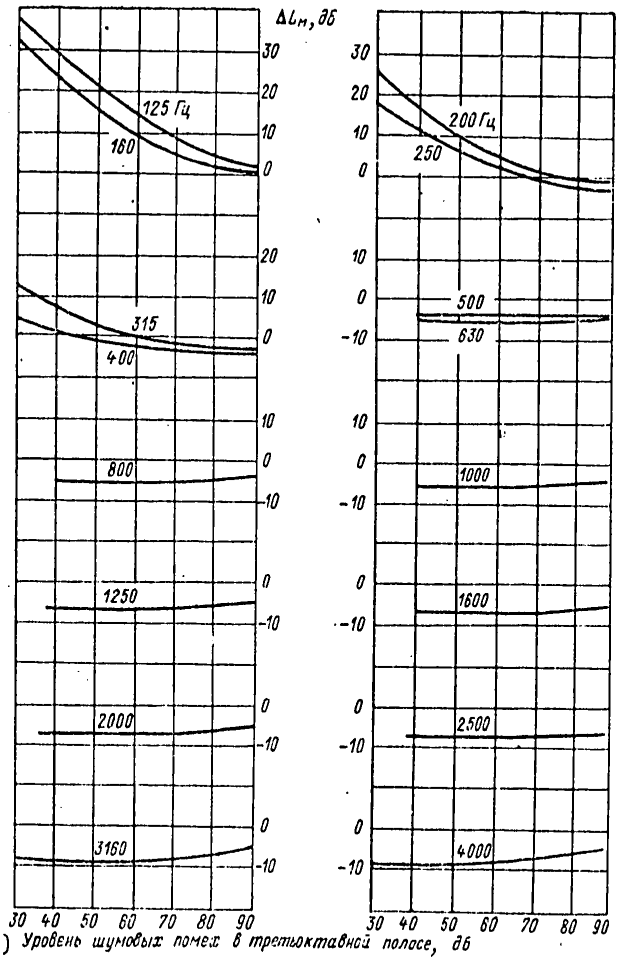

Figure 9.12. Curves for determining levels of acoustic signal heard on noise interference background.
Key: 1. Noise interference level in third-octave band, dB [ДБ=dB; Гц=Hz]

Winer and Keat [24], determined on land. The additional attenuation on the leeward side is attributed primarily to atmospheric turbulence and depends on the frequency of the sound.

APPROVED FOR RELEASE: 2007/02/08: CIA-RDP82-00850R000200100009-9

APPROVED FOR RELEASE: 2007/02/08: CIA-RDP82-00850R000200100009-9

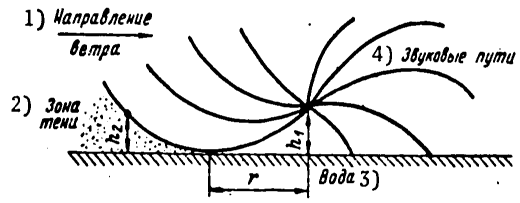

Figure 9.13. Formation of acoustic shadow.
Key: 1. Wind direction 3. Water
2. Shadow zone 4. Acoustic rays

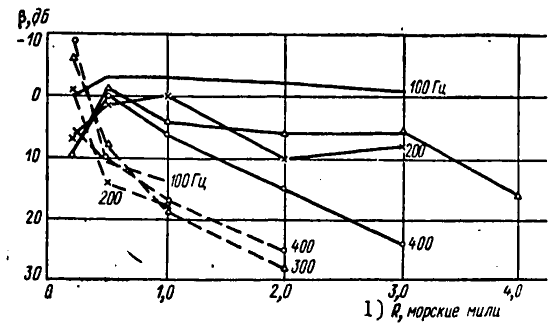

Figure 9.14. Curves of additional attenuation of sound [21]: —— leeward side; --- windward side.
Key: 1. R, nautical miles

Histograms of the attenuation of acoustic signals in the atmosphere at a distance of 2 miles are given in Figure 9.15. As can be seen by the graphs, the additional attenuation due to wind and atmospheric turbulence is quite substantial.

Ye. S. Prokhorov and I. I. Epshteyn [12], on the basis of studies of the audibility of ship signals on rivers and reservoirs, proposed nomograms for calculating the audibility range. Nomograms for two octave bands -- 250 and 500 Hz, are presented in Figure 9.16. The difference of the acoustic pressure levels of a signal at a distance of 10 m from the whistle and at the point of reception are plotted on the ordinate axis. It was assumed in the calculations that the probability that a signal will be audible on the listening end will be 90% if the level of the incoming signal and the interference level are equal. Fog contributes practically no attenuation [12].

The levels of acoustic signals at distances of 1 and 2 miles of certain modern ship whistles, calculated on the basis of the above procedure in

APPROVED FOR RELEASE: 2007/02/08: CIA-RDP82-00850R000200100009-9

APPROVED FOR RELEASE: 2007/02/08: CIA-RDP82-00850R000200100009-9

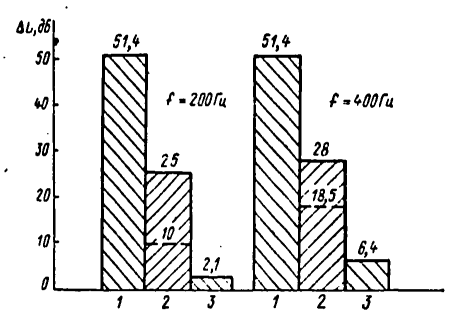

Figure 9.15. Quantitative estimation of acoustic attenuation at distance of 2 nautical miles: 1 -- diminution of level due to spherical wave front propagation; 2 -- additional attenuation (--- with wind, —— against wind); 3 -- molecular and classic absorption. [дБ=dB; Гц=Hz]

consideration of the curves in Figure 9.14, are presented in Table 9.7. The results show that the levels of the acoustic signals on the listening end are substantially lower than the interference levels, and in most cases the whistle will be heard neither from 2 miles, nor from 1 mile.

Table 9.7. Acoustic Pressure Levels of Certain Ship Horns at Distances of 1 and 2 Miles at Wind Velocity U = 2-8 m/s [12, 21]

Indices	Type of horn			
	150EA	TA 100/130	TA 100/200	TB 150/90s
Fundamental horn frequency, Hz	110	130	200	360*
Total level α, dB, at distance r_0 = = 10 m	127	126	124	130
Acoustic pressure level of signal at 1 mile:				
downwind	85	84	78	80
upwind	67.5	66.5	60	66
Likewise at 2 miles:				
downwind	77.5	70.5	70	70
upwind	58	57	54	49

*Spectral component with highest level.

APPROVED FOR RELEASE: 2007/02/08: CIA-RDP82-00850R000200100009-9

APPROVED FOR RELEASE: 2007/02/08: CIA-RDP82-00850R000200100009-9

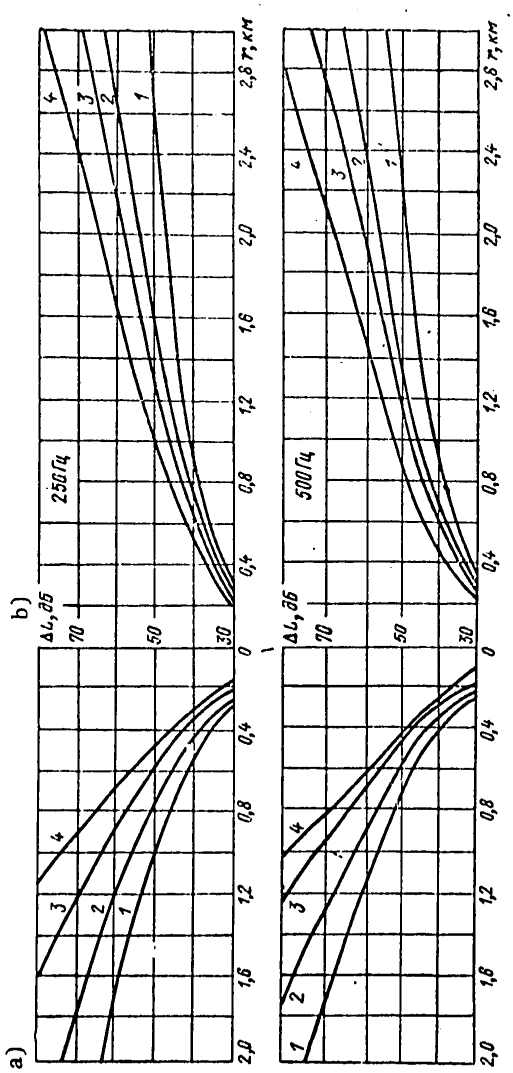

Figure 9.16. Nomograms for calculating audibility range of acoustic signals against wind (a) and with wind (b) at different wind velocities: 1 -- v = 0.5-2.0; 2 -- v = = 2-5; 3 -- v = 5-10; 4 -- v = 10-15.

APPROVED FOR RELEASE: 2007/02/08: CIA-RDP82-00850R000200100009-9

APPROVED FOR RELEASE: 2007/02/08: CIA-RDP82-00850R000200100009-9

Table 9.8. Necessary Signal Level, in dB, on Reception End for Audibility with 90% Probability

Noise interference level	Type of foghorn			
	150EA	TA 100/130	TA 100/200	TV 150/90s
Actual on 84% of ships:				
wheelhouse	85	85	74	68
bridge wings	95	95	86	76
Not more than PS-45	77	77	62	49
Not more than PS-55	81	81	71	58

The minimum necessary acoustic signal levels, audible with 90% probability on a background of actual noise interference at listening stations, and on a background of noise interference that does not exceed the PS-45--PS-55 limiting spectra, are given in Table 9.8. A comparison of the data in Tables 9.8 and 9.7 shows that before acoustic signals can be audible in accordance with the requirements of MPPSS and the Rules of the USSR Register, the noise interference levels must not exceed the PS-45 spectra.

Intelligibility of Speech. Interference noise levels on the bridge exert a strong influence on the intelligibility of commands and instructions.

The mean interference noise levels in four octave frequency bands -- 500, 1,000, 2,000 and 4,000 Hz, are important for determining the intelligibility of speech. The maximum distances at which normal speech is assumed to be satisfactorily intelligible (95% intelligibility, which corresponds to the discrimination of approximately 50% of the logatoms, or 90% of the words [15, 18]), and the maximum distances at which rather loud speech can be understood satisfactorily (shouting is excluded), are given in Table 9.9 as functions of the interference level.

On ships with the interference level indicated in Table 9.6, normal speech is satisfactorily intelligible in wheelhouses at a distance of not farther than 0.5 m, and on the bridge wings not farther than 0.15 m, and loud voice not more than 0.85 m and 0.20 m, respectively. Before speech can be satisfactorily intelligible when commands are conveyed by a loud voice from a distance of 7-8 m, i.e., from a distance common for medium ships, between the helmsman, standing at the wheel, and the navigator standing on the bridge, the interference level must not exceed 40-45 dB on frequencies of 500, 1,000, 2,000, 4,000 Hz, which corresponds approximately to PS-45.

Ways to Reduce Noise Interference. The techniques for reducing engine and boiler room ventilation and exhaust noise, the noise of air conditioning systems and structural noise from screws and engines are examined in the corresponding sections of this handbook. They consist in the installation of effective noise mufflers in the exhaust and intake of the ventilation

APPROVED FOR RELEASE: 2007/02/08: CIA-RDP82-00850R000200100009-9

APPROVED FOR RELEASE: 2007/02/08: CIA-RDP82-00850R000200100009-9

Table 9.9. Maximum Distances, m, at Which Speech is Considered Satisfactorily Intelligible

Speech interference level*, dB	Kind of speech	
	normal voice	loud voice
35	7.5	11.5
40	4.5	8.4
45	2.3	4.6
50	1.3	2.6
55	0.75	1.5
60	0.42	0.85
65	0.23	0.56
70	0.13	0.20

*Determined on the basis of test results

system, vibration insulation of the exhaust stacks of diesel engines, separation of the air intakes of the ventilation system and room exhausts from the bridge by the maximum possible distance. To reduce structural noise the wheelhouse and navigator room are installed on shock absorbers, and other acoustic insulation techniques are used.

The strongest noise interference in the wheelhouse and navigator room on frequencies above 250 Hz is produced by electronic and radio navigation gear, including the gyrocompass with repeaters on the bridge wings, course recorder, automatic steering system, radar, radio direction finder, echo sounder, log, windshield wipers, etc.

Consoles that include clusters of control instruments of a ship and its power plant are installed in modern vessels. The results of measurement of the noises of several navigation instruments, most widely used on ships, are presented in Figure 9.17; the average values of these instruments, based on measurements on 10-12 ships, are presented. The noise level of instruments of the same brand may vary in a wide range. The noise sources of most navigation instruments are contactless micromotors, principally selsyn motors. The noise level of a contactless selsyn is not stable and depends on the rotation angle of its rotor and varies strongly from machine to machine. Particularly noisy selsyns account for about 20% of the selsyns used in marine instruments. Cases when one noisy selsyn exceeds the noise level in the wheelhouse or on the deck by 10-15 dB are not uncommon [2].

The choice of the right bearings for the friction moment is especially important. The highest class of bearings, for example classes a and AB with not more than 10-micron radial play, and with subsequent spinning and break-in of the bearings for 2-12 hours, should be used for selsyns.

Alternating electromagnetic forces are a direct cause of displacement of the rotor in bearings. Therefore the micromotors must be carefully adjusted in assembled form in the final analysis in order to reduce the noise in navigation instruments.

APPROVED FOR RELEASE: 2007/02/08: CIA-RDP82-00850R000200100009-9

APPROVED FOR RELEASE: 2007/02/08: CIA-RDP82-00850R000200100009-9

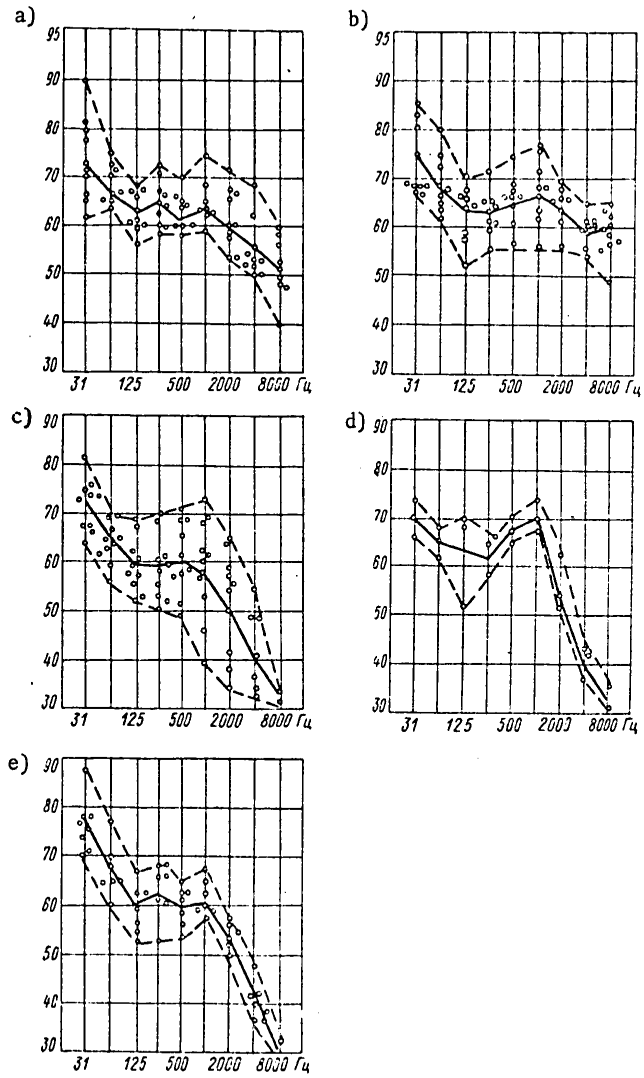

Figure 9.17. Noise spectra of certain navigation instruments used on ships [12]: a -- indicator of NEL-5 echo sounder; b -- NEL-5 recording echo sounder; c -- course recorder (34A instrument); d -- log repeater (5D instrument); e -- type AR automatic steering system.

APPROVED FOR RELEASE: 2007/02/08: CIA-RDP82-00850R000200100009-9

APPROVED FOR RELEASE: 2007/02/08: CIA-RDP82-00850R000200100009-9

APPROVED FOR RELEASE: 2007/02/08: CIA-RDP82-00850R000200100009-9

APPROVED FOR RELEASE: 2007/02/08: CIA-RDP82-00850R000200100009-9

Vibrations are transmitted through the chassis and are amplified by the case of an instrument. Therefore vibration insulation of the chassis from the case is an effective way to reduce the noise of navigation instruments at the source. Vibration insulation can be accomplished with shock absorbers. Combining instruments in consoles is quite effective on ships if the instruments are acoustically insulated by the console cabinet, and indicator instruments are tightly sealed by a sound-insulating transparent window. The noise of navigation instruments can be reduced by 25-30 dB by using appropriately the measures explained above.

The windshield wiper is an instrument of the wheelhouse that is rarely turned on. However, it is turned on, as a rule, during poor weather and poor visibility, i.e., at times when special quiet is necessary for hearing signals. Therefore its noise should not exceed the level of interference on the bridge.

Noisy cooling fans are used in electronic and radio navigation gear. When setting up these instruments mufflers should be installed on the suction end discharge sides and quiet fans should be used.

Noise control at the source should include perfected electromechanical systems and the development of fundamentally new devices on semiconductors and integrated circuits.

BIBLIOGRAPHY

1. "Aviatsionnaya Akustika" [Aviation Acoustics], edited by A. G. Munin and V. Ye. Kvitka, Moscow, Mashinostroyeniye, 1973.

2. Grigor'yan, F. Ye., "Shum Sudovykh Navigatsionnykh Priborov" [Noise of Marine Navigation Instruments], Leningrad, Transport, 1973. (TRUDY TsNIIMF [Proceedings of the Central Scientific Research Institute of the Maritime Fleet], No. 171).

3. Daletskiy, K. P. and I. I. Klyukin, "Reduction of Screw Noise in Ship Rooms," TRUDY LKI [Proceedings of Leningrad Shipbuilding Institute], 1972, No 77, pp 11-16.

4. Zefirov, L. B., "Experience in Noise Control on 'Volgodon' Type Ships," SUDOSTROYENIYE [Shipbuilding], 1967, No 2, pp 5-8.

5. Klyukin, I. I., "Bor'ba s Shumom i Zvukovoy Vibratsiyey na Sudakh" [Noise and Acoustic Vibration Control on Ships], Leningrad, Sudostroyeniye, 1971.

6. Kovrigin, S. D., "Bor'ba s Shumami v Grazhdanskikh Zdaniyakh (Udarnyye i Strukturnyye Shumy)" [Noise Control in Civilian Buildings (Impact and Structural Noises), Moscow, Gosstroyizdat, 1969.

APPROVED FOR RELEASE: 2007/02/08: CIA-RDP82-00850R000200100009-9

APPROVED FOR RELEASE: 2007/02/08: CIA-RDP82-00850R000200100009-9

7. Kovchegov, L. P. and N. A. Kubachev, "Vliyaniye Shumovykh Pomekh na Dal'nost' Slyshimosti Zvukovykh Signalov" [Influence of Noise Interference on Audibility Range of Acoustic Signals], Moscow, Izd-vo Reklambyuro MMF, 1975 ("Sbornik Trudov 'Sudovozhdeniye'" [Symposium "Ship Navigation], No 16, pp 78-85).

8. Miniovich, I. Ya., A. D. Pernik and V. S. Petrovskiy, "Gidrodinamicheskiye Istochniki Shuma" [Hydrodynamic Sources of Noise], Leningrad, Sudostroyeniye, 1972.

9. Oguro Hideo, "Audibility of Ship Acoustic Signals," SEMPAKU, 1968, Vol 12, No 41, pp 58-64 (in Japanese).

10. Osipov, G. L., "Zashchita Zdaniy ot Shuma" [Protecting Buildings from Noise], Moscow, Stroyizdat, 1972.

11. Panenko, S. M., "Features of Noise Control on Dredges 'Chernoye More' and 'Baltiyskoye More'," SUDOSTROYENIYE, 1967, No 2, pp 8-11.

12. Prokhorov, Ye. S. and I. I. Epshteyn, "Zvukovaya Signalizatsiya Sudov na Rekakh i Vodokhranilishchakh" [Acoustic Signaling of Ships on Rivers and Reservoirs], Gor'kiy, GIVT, 1973.

13. "Sanitarnyye Normy i Pravila po Oranicheniyu Shuma na Territoriyakh i v Pomeshcheniyakh Proizvodstvennykh Predpriyatiy" [Sanitation Rules on Limitation of Noise on Land and in Rooms of Industrial Enterprises], No. 785-69, Moscow, Minzdrav, 1970.

14. "Sredstva Zvukoizolyatsii i Zvukopogloshcheniya v Sudovykh Pomeshcheniyakh" [Methods of Acoustic Insulation and Acoustic Absorption in Ship Compartments], LIVT, 1967.

15. French, N. R. and J. K. Steinberg, "Factors That Influence Speech Intelligibility," JASA, 1949, No 19, pp 90-119.

16. Shenderov, Ye. L., "Volnovyye Zadachi Gidroakustiki" [Wave Problems in Hydroacoustics], Leningrad, Sudostroyeniye, 1972.

17. Yaskevich, A. P. and Yu. G. Zubarov, "Novyye Mezhdunarodnyye Pravila Preduprezhdeniya Stolknoveniy Sudov v More (MPPSS)" [New International Rules on Ship Collision Avoidance at Sea (MPPSS)], Moscow, Transport, 1975.

18. Beranek, L. L., "Noise and Vibration Control, New York, 1971.

19. Geicke, K., "Wirkung schallweicher Beschichtungen im Propellerbereich auf die Einleitung von Schwingungen in der Ausenhaut," SCHIFF UND HAFEN, 1975, Vol 27, No 3, pp 222-223.

APPROVED FOR RELEASE: 2007/02/08: CIA-RDP82-00850R000200100009-9

APPROVED FOR RELEASE: 2007/02/08: CIA-RDP82-00850R000200100009-9

20. Harris, M., "Handbook of Noise Control," New York-Toronto-London, 1957.

21. Hideo Ogura and Masayuki Tsuchiya, "Study of Acoustic Signal Propagation over Ocean Water," Report of Ship Research Institute, 1973, 10, 1, pp 1-17.

22. Ort, A., "Korperschalldammung von elastisch gelagerten Propeller-Brunnen," SCHIFF UND HAFEN, 1975, Vol 27, No 3, pp 223-224.

23. Pohl, K. H., "Das Instationare Druckfeld in der Umgebung eines Schiffspropellers und die ihm benachbarten Platten erzeugten periodischen Kraften," SCHIFFSTECHNIK, 1959, 32, pp 107-116.

24. Winer, F. and D. Keat, "Experimental Study of Propagation of Sound over Ground," JASA, 1959, Vol 31, No 6, p 724.

APPROVED FOR RELEASE: 2007/02/08: CIA-RDP82-00850R000200100009-9

APPROVED FOR RELEASE: 2007/02/08: CIA-RDP82-00850R000200100009-9

CHAPTER 10. ACOUSTIC INSULATION ON SHIPS

10.1. Importance of Acoustic Insulation on Ships

Acoustic insulation is one of the most effective ways of reducing noise produced by the propagation of acoustic vibrations from one room to another (Figure 10.1). With acoustic insulation it is possible to reduce the transmission of noise through paths 1, 2 and 3 from room I to room II. Bypass 4 reduces the effectiveness of acoustic insulation. Soundproofing structures are used extensively on ships for acoustic covers for machines and screens, control centers, air ducts and, importantly, bulkheads, decks and partitions that separate rooms with noise sources from quiet rooms. The basic types of soundproofing ship structures are shown in Figure 10.2.

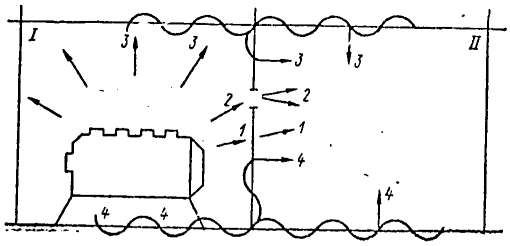

Figure 10.1. Paths of propagation of noise from one room to another.

In double-wall structures a liner can be attached to the hull with the aid of acoustic or sound-insulating bridges. Acoustic bridges are ordinary parts, used for fastening a liner to the hull. Sound-insulating bridges are special fasteners, which substantially reduce the transmission of sound from the hull to the liner and thus improve the soundproofing of a double-wall structure.

10.2. Basic Principles of Acoustic Insulation

The term "acoustic insulation" is used for describing an acoustic structure, a physical process, and also for numerical description of the process.

APPROVED FOR RELEASE: 2007/02/08: CIA-RDP82-00850R000200100009-9

APPROVED FOR RELEASE: 2007/02/08: CIA-RDP82-00850R000200100009-9

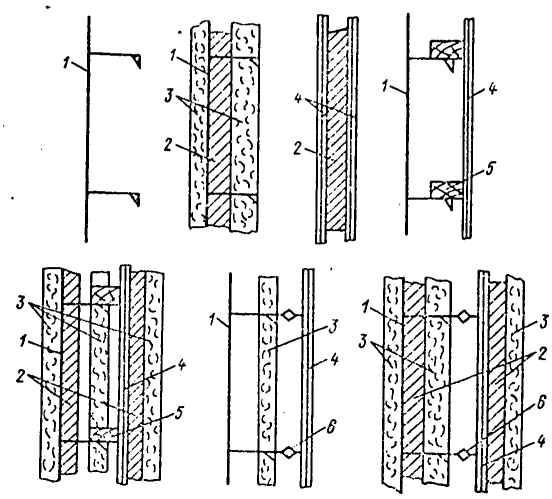

Figure 10.2. Types of soundproofing ship structures:
1 -- hull structure; 2 -- vibration-damping material;
3 -- sound-absorbing material; 4 -- liner; 5 -- acoustic bridge; 6 -- sound-insulating bridge.

Acoustic insulation is analyzed numerically with the aid of transmission coefficient τ (the term "penetration coefficient" is also used), which is equal to the ratio of the flux of acoustic energy passing through an examined cross section of a bulkhead to the flux of acoustic energy striking that cross section. The inverse transmission coefficient is acoustic insulation capacity r.

Transmission coefficient τ is related to scatter coefficient δ and reflection coefficient ε by the equation that expresses the law of conservation of energy, specifically $\delta + \varepsilon + \tau = 1$.

If α is the absorption coefficient, then $\alpha + \varepsilon = 1$. The acoustic insulation coefficient (the term "acoustic insulation" is most often used) R, in dB, is

$$R = 10 \lg r = -10 \lg \tau = -10 \lg (\alpha - \delta). \qquad (10.2.1)$$

The International Standardization Organization recommends the use of the terms penetration coefficient and acoustic insulation coefficient [19].

It is important to distinguish between acoustic insulation R and the acoustic pressure drop $\Delta L = L_1 - L_2$. For a soundproofing partition,

APPROVED FOR RELEASE: 2007/02/08: CIA-RDP82-00850R000200100009-9

APPROVED FOR RELEASE: 2007/02/08: CIA-RDP82-00850R000200100009-9

separating two reverberative rooms in the absence of bypasses, this difference in ship structures may be 5-10 dB.

Acoustic insulation in consideration of bypasses is sometimes called the actual acoustic insulation [5].

In addition to the above interpretation, according to which acoustic insulation does not depend on the coordinates of the points in space in front of and behind a partition, the concept of local acoustic insulation is also utilized. In this case the acoustic flux behind a partition in the Fraunhofer zone of open or of enclosed space is examined in the presence of and in the absence of the partition. The fact that acoustic insulation depends on the point of observation (its localization in space) necessitates the determination in this case of the spatial spectra that occur when sound passes through a partition [14].

When plane acoustic waves strike the interface between two semi-infinite media (Figure 10.3), in which longitudinal waves propagate, acoustic insulation R, in dB, is

$$R = 20\lg\left(\sqrt{\frac{Z_1}{Z_2}} + \sqrt{\frac{Z_2}{Z_1}}\right) - 6, \qquad (10.2.2)$$

and the normal acoustic resistances (impedances) are

$$Z_1 = \frac{\rho_1 c_1}{\cos\vartheta_1} \quad \text{and} \quad Z_2 = \frac{\rho_2 c_2}{\cos\vartheta_2}, \qquad (10.2.3)$$

where ϑ_1 is the angle of incidence of acoustic waves; ϑ_2 is the angle of transmission of acoustic waves. The other values with the subscript 1 refer to the first medium, and the values with the subscript 2 to the second.

Impedance Mismatch Principle. It follows from formula (10.2.2) that when impedances Z_1 and Z_2 are equal acoustic insulation is equal to zero. To increase acoustic insulation it is necessary to increase the difference (mismatch) of the impedances of the first and second media. This situation is called the impedance mismatch principle. To achieve good acoustic insulation it is necessary to have a substantial mismatch of impedances, and the amount of acoustic insulation does not change when the acoustic waves propagate in the opposite direction. The impedance mismatch principle is applied to any partition, medium and type of acoustic wave.

Determination of Acoustic Insulation by Input Impedance. The ratio of the acoustic pressure to the normal component of vibration velocity, taken on the interface, from which sound propagates from the opposite side of the interface, is called input impedance. The formula for the input impedance of the j-th layer of thickness s, in which just longitudinal waves propagate, acquires the form [4]

APPROVED FOR RELEASE: 2007/02/08: CIA-RDP82-00850R000200100009-9

APPROVED FOR RELEASE: 2007/02/08: CIA-RDP82-00850R000200100009-9

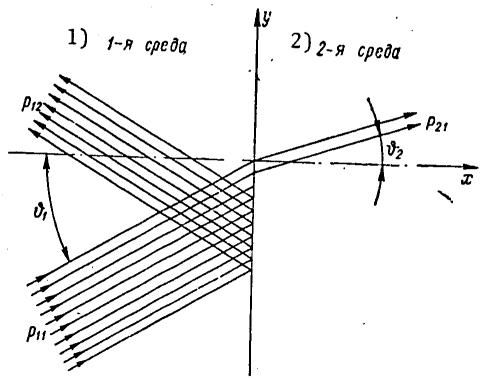

Figure 10.3. Transmission of acoustic waves through interface between two media.
Key: 1. 1st medium 2. 2nd medium

[вх=in]

$$Z_{\text{вх}}^{(j)} = \frac{Z_{(j+1)} - iZ_j \operatorname{tg} k_j s_j}{Z_j - iZ_{(j+1)} \operatorname{tg} k_j s_j}. \tag{10.2.4}$$

The layers are calculated from the side of the medium that the acoustic waves enter behind the partition. A soundproofing partition consisting of n layers, R in dB, is determined by the formula

$$R = 20 \lg \left| \prod_{j=1}^{j=n} \frac{Z_j + Z_{\text{вх}}^{(j+1)}}{Z_{(j+1)} + Z_{\text{вх}}^{(j+1)}} e^{ik_{(j+1)} s_{(j+1)}} \right|. \tag{10.2.5}$$

Determination of acoustic insulation by input impedance is the most general way of calculating the acoustic insulation of infinite (or of large-area, in practice) partitions.

Law of Mass. The input impedance of an extremely thin single layer with air on both sides, and with a large input impedance is, according to formula (10.2.4),

$$Z_{\text{вх}} = \frac{\rho c}{\cos \vartheta} - i\omega m, \tag{10.2.6}$$

where ϑ is the angle of transmission of acoustic waves through the layer; m is the surface mass of the layer.

Substituting this expression in (10.2.5) we obtain acoustic insulation R, in dB, relative to the partition according to the "law of mass" for any angle of incidence of acoustic waves:

$$R = 10 \lg \left[1 + \left(\frac{\omega m \cos \vartheta}{2\rho c} \right)^2 \right]. \tag{10.2.7}$$

APPROVED FOR RELEASE: 2007/02/08: CIA-RDP82-00850R000200100009-9

APPROVED FOR RELEASE: 2007/02/08: CIA-RDP82-00850R000200100009-9

It follows from the formula that in addition to the mass of the partition, the angle of incidence of acoustic waves also exerts an important influence on acoustic insulation. This phenomenon is called the component effect [16]. In the case of tangential incidence of acoustic waves the acoustic insulation is equal to zero, and in the case of normal incidence it reaches the maximum value.

In diffusive incidence of sound acoustic insulation R, in dB, is

$$R = 20 \lg fm + 20 \lg \frac{\pi}{\rho c} - 10 \lg \lg \left[1 + \left(\frac{\pi f m}{\rho c} \right)^2 \right] - 3{,}6. \qquad (10.2.8)$$

This formula may also be written in the form

$$R = a_1 \lg (f + a_2) + a_3 \lg (m + a_4) + a_5. \qquad (10.2.9)$$

The values a_1-a_5 are corrected on the basis of experimental data and then formulas are derived for engineering calculations. That, in particular, is how all the formulas presented in this chapter were derived.

For ship bulkheads, sides, partitions, etc., made of steel, duraluminum and plywood with thicknesses of from 1 to 12 mm, and with rigidity ribs extending in one direction at a height of not more than 30 times the thickness of the plate, and with frame spaces of from 500 to 1,000 mm, formula (10.2.9) acquires the form

$$R = 14{,}5 \, [\lg (fm + 100) - 2], \qquad (10.2.10)$$

where f is the mean geometric third-octave frequency band, in Hz; m is the surface mass of the partition, in kg/m^2.

Acoustic insulation is determined by the law of mass by just one partition parameter, namely the surface mass, and it increases monotonically with frequency. The formula of the law of mass conservation is valid for thin barriers with a thickness of less than 1/6 the bending wavelength in them, and for the $2f_r \leq f \leq 0.5f_{cr}$ frequency range, where f_r is the first resonance frequency of the partition and f_{cr} is its critical frequency. There should be a nearly diffusive acoustic field on both sides of such a partition, and there should be no bypasses through which the sound can penetrate.

The law of mass conservation is the fundamental law that determines the acoustic insulation of thin partitions. In cases when it is valid either materials with high density must be used to increase acoustic insulation, or the thickness of a partition must be increased. Steel has the highest density of materials used on ships, but lead is considered to be a better material for acoustic insulation. Thin tin-plated lead foils should be

APPROVED FOR RELEASE: 2007/02/08: CIA-RDP82-00850R000200100009-9

APPROVED FOR RELEASE: 2007/02/08: CIA-RDP82-00850R000200100009-9

used on ships when especially effective and reliable noise suppression is required [8].

10.3. Acoustic Insulation of Single-Wall Structures

Physical Principles. Most ship hull structures are thin-wall constructions. In such structures sound propagates primarily in the form of bending waves, which are readily excited by acoustic air waves and which readily radiate acoustic energy into surrounding space.

Let us examine the basic principles of acoustic insulation of single-wall structures in application to bending waves, for the case of the simultaneous propagation of these waves in an endless plate. The impedance of such a plate for induced bending waves, which is expressed as the ratio of the difference between the acoustic pressures on both sides of the plate to its vibration velocity [16], is

[и=b]

$$Z_{\text{и}} = i\left[\omega m - \frac{E_f J(1+i\eta)\,\omega^3 \sin^4\vartheta}{c^4(1-\sigma^2)}\right], \qquad (10.3.1)$$

where ϑ is the angle of incidence of the acoustic waves on the plate; c is the speed of sound in air; J is the moment of inertia of a unit width of the plate.

In addition to induced bending waves, caused by the incidence of acoustic waves on the plate, free bending waves can also propagate in and on the plate. The velocity of these waves is

$$c_{\text{и}} = \sqrt{2\pi f}\cdot\sqrt[4]{\frac{E_f J}{m(1-\sigma^2)}}, \qquad (10.3.2)$$

and wavelength is

[п=lo]

$$\lambda_{\text{и}} = \sqrt{1{,}8\frac{c_{\text{п}} s}{f}}, \qquad (10.3.3)$$

where s is the thickness of the plate; c_{lo} is the velocity of longitudinal acoustic waves in the plate.

Formula (10.3.2) does not take into account internal losses, but for ship construction materials they are negligible and therefore have little effect on the velocity of free bending waves.

If in formula (10.3.1) the expression enclosed in braces is equal to zero, a plate with small internal losses will not offer resistance to external acoustic pressure. In this case acoustic insulation is nil on the matching wave frequency:

$$f_0 = \frac{c^2}{2\pi\sin^2\vartheta}\sqrt{\frac{m(1-\sigma^2)}{E_f J}}. \qquad (10.3.4)$$

APPROVED FOR RELEASE: 2007/02/08: CIA-RDP82-00850R000200100009-9

APPROVED FOR RELEASE: 2007/02/08: CIA-RDP82-00850R000200100009-9

The following relation exists on that frequency between lengths λ of acoustic waves in air and λ_b of free bending waves in the plate:

[и=b]

$$\lambda = \lambda_{\text{и}} \sin \sigma. \tag{10.3.5}$$

The lowest matching wave frequency is called the critical frequency:

[кр=cr; п=lo]

$$f_{\text{кр}} = \frac{c^2}{2\pi s} \sqrt{\frac{12\rho(1-\sigma^2)}{E_f}} \approx 0{,}55 \frac{c^2}{sc_{\text{п}}}. \tag{10.3.6}$$

On frequencies below critical the matching wave phenomenon cannot occur and acoustic insulation for this reason cannot have a minimum. On higher frequencies the bending wave velocity becomes asymptotic to the Rayleigh surface wave velocity as frequency increases.

The domain of the laws that are inherent to bending waves is limited to a thin plate, which should satisfy the relation

$$s < 0{,}05 \frac{c_{\text{п}}}{f}. \tag{10.3.7}$$

The frequency above which, according to bending wave theory, sound insulation does not exist, can be calculated by the formula

$$f_{\text{в}} \approx 0{,}05 \frac{c_{\text{п}}}{s}. \tag{10.3.8}$$

The acoustic insulation of an infinite plate (i.e., a very large plate in practice) R_p, in dB, is determined by the formula

$$R_{\text{п}} = 10 \lg \left\{ \left[1 + \eta \frac{\omega^3}{c^4} \frac{E_f J}{(1-\sigma^2)} \frac{\sin^2\vartheta \cos\vartheta}{2\rho c} \right]^2 + \left(\frac{\cos\vartheta}{2\rho c} \right)^2 \left[\omega m - \frac{\omega^3 E_f J}{c^4 (1-\sigma^2)} \sin^4\vartheta \right]^2 \right\}. \tag{10.3.9}$$

According to this formula acoustic insulation on frequencies below the critical frequency obeys the law of mass conservation. On frequencies equal to the critical frequency and higher acoustic insulation is determined by the internal losses in the plate and by the bending rigidity of the plate. This has been confirmed experimentally.

Calculation of Acoustic Insulation. A single-wall ship partition is examined in engineering calculation of acoustic insulation as a thin plate with large dimensions, which always has rigidity ribs. The range of application of the graphoanalytical method presented below for calculating acoustic insulation of single-wall partitions has the following constraints.

The minimum linear dimension l of a room (height, width or length) on both sides of the structure intended for acoustic insulation, should be

APPROVED FOR RELEASE: 2007/02/08: CIA-RDP82-00850R000200100009-9

APPROVED FOR RELEASE: 2007/02/08: CIA-RDP82-00850R000200100009-9

$$l \geq 8\lambda_{cr}, \qquad (10.3.10)$$

where λ_{cr} is the bending wavelength on the critical frequency.

The second constraint pertains to the bottom and top boundaries of the calculated frequency range. The bottom boundary of the calculated frequency range of acoustic insulation should be approximately one octave higher than the first resonance frequency of the single-wall partition. It is determined to an accuracy satisfactory for practice by the formula

$$f_{bot} = c/l, \qquad (10.3.11)$$

where l is the minimum linear dimension of the partition, in m.

The top boundary of the calculated frequency range is determined by formula (10.3.8).

The acoustic insulation of single-wall structures (Figure 10.4) is calculated as follows [2].

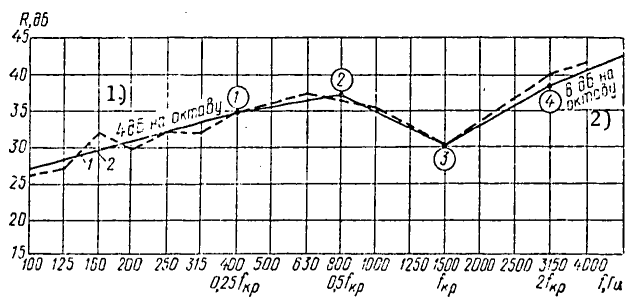

Figure 10.4. Calculation of acoustic insulation of steel bulkhead. Seven millimeter thick plate with welded No. 12 bulb-plate rigidity ribs; 1 -- theory; 2 -- experiment. [дБ=dB; кр=cr; Гц=Hz]
Key: 1. 4 dB per octave 2. 8 dB per octave

1. The critical frequency of a given material for a single-wall plate structure of a given thickness is calculated by formula (10.3.6).

2. Four values of the abscissa: $0.25f_{cr}$, $0.5f_{cr}$, f_{cr} and $2f_{cr}$, are marked off, as shown in Figure 10.4, on the coordinate grid (the mean geometric third-octave frequency bands f, in Hz, are plotted on the abscissa axis in logarithmic scale, and acoustic insulation R, in dB, is plotted on the ordinate axis).

APPROVED FOR RELEASE: 2007/02/08: CIA-RDP82-00850R000200100009-9

APPROVED FOR RELEASE: 2007/02/08: CIA-RDP82-00850R000200100009-9

3. For the above-mentioned four abscissas four ordinates are marked off in accordance with the data in Table 10.1.

Table 10.1. Ordinates for Plotting Calculation Curve of Acoustic Insulation

1) Материал конструкции	2) Плотность, кг/м³	3) Звукоизоляция, дБ, на частотах			
		$0{,}25f_{кр}$	$0{,}5f_{кр}$	$f_{кр}$	$2f_{кр}$
4) Сталь	7800	35	37	30	39
5) Титан	4500	31	33	26	35
6) Алюминиево-магниевые сплавы	2800	29	31	23	31
7) Стеклопластик	1700	28	31	28	34
8) Фанера	800	26	29	26	32
9) Стекло силикатное	2500	32	34	27	34
10) Стекло органическое	1200	34	36	30	38

Key: 1. Construction material
2. Density, kg/m³
3. Acoustic insulation, in dB, on frequencies
4. Steel
5. Titanium
6. Aluminum-magnesium alloys
7. Glass-reinforced plastic
8. Plywood
9. Silicate glass
10. Organic glass

[kp=cr]

4. The four points thus obtained (see Figure 10.4) are connected with straight lines, and then a straight line is drawn from the first point toward lower frequencies downward with an inclination of 4 dB per octave, and a straight line is drawn from the fourth point toward higher frequencies, upward with an inclination of 8 dB per octave.

The limiting deviations of the calculated values of acoustic insulation from the experimental values do not exceed 5 dB with an estimated reliability of 0.95. The errors will be smaller if the rigidity ribs go in the same direction at distances more than 0.5 m apart, and their height should not exceed 30 times the plate thickness. We note that the calculated values of acoustic insulation left of point 1 correspond to the law of conservation of mass, and consequently to formula (10.2.10).

Acoustic Insulation of Single-Side Partition with Soundproofing. One effective way to improve the acoustic insulation of thin single-wall partitions is to use lightweight sound-absorbing materials, covering an entire insulated partition surface in a uniform layer. This produces a two-layer structure consisting of the single-wall structure with acoustic insulation R_1 and soundproofing layer, which increases acoustic insulation by ΔR_1. The acoustic insulation of a single-wall partition with soundproofing is

APPROVED FOR RELEASE: 2007/02/08: CIA-RDP82-00850R000200100009-9

APPROVED FOR RELEASE: 2007/02/08: CIA-RDP82-00850R000200100009-9

$$R = R_1 + \Delta R_1, \qquad (10.3.12)$$

where R_1 is calculated by the above-described graphoanalytic method.

The additional acoustic insulation of a single-wall partition with soundproofing, applied snugly on the structure to a thickness of 20-100 mm, can be calculated by the formulas

$$\Delta R_1 = 8{,}7 \lg s\beta \text{ for } s\beta > 1 \text{ and } \Delta R_1 = 0 \text{ for } s\beta \leqslant 1, \qquad (10.3.13)$$

where s is the thickness of the soundproofing material, in mm; β is the attenuation coefficient for that material, in 1/cm.

Attenuation coefficient β for basic soundproofing materials used in shipbuilding are listed in Table 10.2. Lining single-wall bulkheads with soundproofing is used extensively in rooms with noise sources (the engine compartments of ships, ventilation rooms, etc.), in soundproofing covers of machinery, and in control centers.

Acoustic Insulation of Single-Wall Partition with Holes. Holes can have an appreciable effect on acoustic insulation and must always be taken into account during the design and manufacture of soundproofing structures.

The acoustic insulation of four plates made of 3 mm thick duraluminum is plotted in Figure 10.5 as a function of frequency. The plates differ in that the first (curve 1) has a 1 mm wide 1,000 mm long slit, which divides it into two equal halves; the second plate (curve 2) has 16 9 mm diameter holes, uniformly distributed on the surface of the plate; the third plate (curve 3) has a single hold right in the middle, with a diameter of 36 mm; the fourth plate is solid and has no holes (curve 4). The total area of the holes in all the plates with holes is identical.

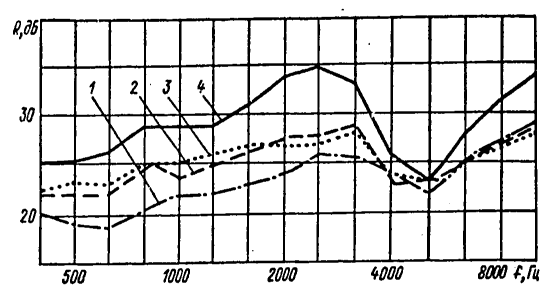

Figure 10.5. Acoustic insulation of 3 mm thick duraluminum panels with 1,000 mm^2 hole area as function of frequency: 1 -- plate with one slit; 2 -- plate with 16 holes; 3 -- plate with one hole; 4 -- plate with no holes.

APPROVED FOR RELEASE: 2007/02/08: CIA-RDP82-00850R000200100009-9

APPROVED FOR RELEASE: 2007/02/08: CIA-RDP82-00850R000200100009-9

Table 10.2. Attenuation Coefficient β, in 1/cm

1) Звукопоглощающий материал	2) Частоты октавных полос, Гц							
	63	125	250	500	1000	2000	4000	8000
3) Теплозвукоизоляционный материал АТМ-1	0,014	0,020	0,035	0,080	0,142	0,198	0,220	0,220
4) Поропласт полиуретановый эластичный самозатухающий	0,026	0,074	0,122	0,190	0,300	0,370	0,420	0,500
5) Теплоизоляционный материал марки ВТ-4	0,016	0,041	0,066	0,082	0,091	0,120	0,130	0,130
6) Теплоизоляционный материал марки ВТ-4С	0,014	0,033	0,053	0,062	0,081	0,140	0,170	0,170
7) Теплоизоляционный материал марки АТИМСС	0,012	0,028	0,044	0,058	0,082	0,190	0,200	0,200
8) Плиты из штапельного стекловолокна	0,014	0,038	0,061	0,083	0,105	0,132	0,156	0,176
9) Плиты полужесткие минераловатные на фенольной связке	0,018	0,061	0,104	0,150	0,180	0,320	0,450	0,470

Key: 1. Soundproofing material
2. Frequencies of octave bands, in Hz
3. ATM-1 heat-insulation material
4. Elastic self-attenuating polyurethane poroplast
5. VT-4 heat insulation
6. VT-4S heat insulation
7. ATIMSS heat insulation
8. Staple glass fiber panels
9. Semirigid phenol-bonded rock wool panels

As can be seen in the figure, even small holes and the slit can reduce the acoustic insulation in a wide frequency range by approximately 10 dB. It also follows from Figure 10.5 that one large round hold and a group of small round holes with the same area reduces the acoustic insulation of a panel by about the same amount, whereas a slit with the same area reduces the acoustic insulation of a panel to a much greater extent in a considerable frequency range (below the critical frequency).

Thus, slots and holes reduce acoustic insulation basically on frequencies below critical, and a slot is worse in that frequency range than holes. Slots and holes can have a negligible influence on acoustic insulation on the critical frequency. On frequencies above critical slots and holes again exert a negative effect on acoustic insulation, and the shape of holes has no effect on the deterioration of acoustic insulation; their area is more important.

APPROVED FOR RELEASE: 2007/02/08: CIA-RDP82-00850R000200100009-9

APPROVED FOR RELEASE: 2007/02/08: CIA-RDP82-00850R000200100009-9

Slots and holes in ships can greatly detract from acoustic insulation of doors and windows in soundproof control centers, in ward rooms, etc. The elimination of these weak points in acoustic insulation is the prerequisite for the successful control of noise.

10.4. Acoustic Insulation of Double-Wall Structures

Physical Principles. It has long been known in the practice of noise control that the acoustic insulation of double-wall partitions can be substantially more effective than of a single-wall structure of equal mass. That is why many soundproof partitions on modern ships are based on the use of double-wall structures with layers of air and soundproofing materials between the walls. These structures are made by lining ship rooms. The liner is installed some distance from the main hull structure (bulkhead, side, deck, etc.).

If the space between the panels of a double-wall structure is filled with a soft porous material and its absolute characteristic impedance is close to that of air (which for modern sound-absorbing materials is, for practical purposes, the case), then the acoustic insulating capacity of the double-wall structure for acoustic waves with normal incidence is

[И=i]

$$r = \left| \left(1 + \frac{Z_{и1}}{2Z_0}\right)\left(1 + \frac{Z_{и2}}{2Z_0}\right) \cdot e^{d\beta} - \frac{Z_{и1}Z_{и2}}{4Z_0^2} \cdot e^{-d\beta} (\cos 2kd - i \sin 2kd) \right|^2, \quad (10.4.1)$$

where Z_{i1} and Z_{i2} are the impedances of the first and second panels.

An analysis of the formula shows that the specific way to improve the acoustic insulation of a double-wall structure is to increase distance d between the panels and attenuation constant β of the soundproofing layer. When the values of dβ are large enough the effects of acoustic insulation of the panels and of soundproofing between the panels (in dB) are independent of each other and the acoustic insulation R, in dB, of the double-wall structure is maximum when the mass is minimum:

$$R = 10 \lg \left| 1 + \frac{Z_{и1}}{2Z_0} \right|^2 + 10 \lg \left| 1 + \frac{Z_{и2}}{2Z_0} \right| + 0\beta d\beta. \quad (10.4.2)$$

If there is little absorption of sound between the panels the acoustic insulation of the double-wall structure on the lowest frequencies, when $kd \ll 1$, is equivalent to the acoustic insulation of a single-wall structure with the same total surface mass as two panels.

In the low-frequency range, when $\cos kd \approx 1$ and $\sin kd \approx kd$, the acoustic insulation is minimum. A double-wall structure behaves in this case like a system with concentrated parameters in the mass-elasticity-mass system.

APPROVED FOR RELEASE: 2007/02/08: CIA-RDP82-00850R000200100009-9

APPROVED FOR RELEASE: 2007/02/08: CIA-RDP82-00850R000200100009-9

The panels function as mass here, and air functions as the elastic element between them. For ship structures, however, the attainment of this minimum usually does not matter much.

The acoustic insulating properties of a double-wall structure that are important in practice are manifested on medium and high frequencies. It is specifically on these frequencies that the acoustic insulation of a double-wall structure can substantially exceed the acoustic insulation of a single-wall structure of the same mass. The acoustic insulation in the indicated frequency range has several successive maxima and minima, and the minima are attributed to the resonances of the layer between the panels, and the maxima to antiresonances. The extent of the minima of acoustic insulation on the frequency axis is negligible in comparison with the extent of increased acoustic insulation. The installation of even a little soundproofing material between the panels sharply increases the minima of acoustic insulation, which greatly improves the acoustic insulation of a double-wall structure on medium and high frequencies.

Experimental data that show how much a soundproofing material, installed between panels, affects the acoustic insulation of a double-wall structure, are plotted in Figure 10.6. The first panel is made of 4 mm thick duraluminum, and the second of 1 mm thick steel; the distance between the panels is 60 mm. Curve 1 shows the acoustic insulation of a double-wall structure when all the space between the panels is filled with ultrafine glass fiber. Curve 2 characterizes the acoustic insulation of the same structure, but with one-half the air space between the panels filled with ultrafine glass fiber (30 mm thick soundproofing layer). Curve 3 corresponds to the case when there is no soundproofing between the panels and there is only a 60 mm thick layer of air. It is noteworthy that the first and second panels do not have acoustic bridges.

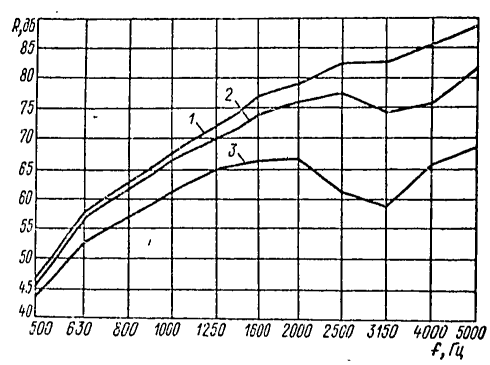

Figure 10.6. Acoustic insulation of double-wall structure with soundproofing. [дБ=dB; Гц=Hz]

APPROVED FOR RELEASE: 2007/02/08: CIA-RDP82-00850R000200100009-9

APPROVED FOR RELEASE: 2007/02/08: CIA-RDP82-00850R000200100009-9

The increase of acoustic insulation due to soundproofing increases with frequency and reaches 20-25 dB in the indicated case, which, naturally, is not the limit. It is important in practice that the main increase of acoustic insulation come from filling just one-half the air space between the panels with soundproofing.

Acoustic Bridges. The sound insulation of double-wall partitions depends to a great extent on the structural connection between the panels, which is made up of acoustic or sound-insulating bridges. The effect of acoustic and soundproofing bridges on acoustic insulation is illustrated in Figure 10.7, where test data on the structure illustrated in Figure 10.6, but without soundproofing, are plotted. The acoustic bridges, as can be seen by the data, can reduce acoustic insulation by 10-15 dB in an extremely wide frequency range.

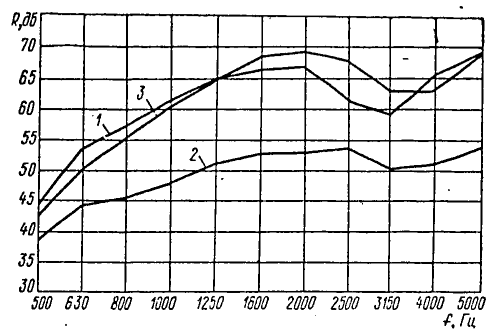

Figure 10.7. Acoustic insulation of double-wall structure with acoustic bridges: 1 -- acoustic insulation without acoustic bridges; 2 -- acoustic insulation with acoustic bridges; 3 -- acoustic insulation with soundproofing bridges.

Three types of soundproofing bridges -- inertial, elastic and combined, may be used in ship structures for reducing this harmful effect for acoustic insulation.

Inertial bridges should be used for double-wall partitions, in which the critical frequencies of the first and second panels exceed 5,000-8,000 Hz (the top limit is preferable). The acoustic insulation properties of an inertial bridge are determined by its mass, which usually should satisfy the requirement

[г=b]

$$M \geqslant \frac{s_1^2 \sqrt{\rho_1 E_1}}{f_{r1}}, \qquad (10.4.3)$$

APPROVED FOR RELEASE: 2007/02/08: CIA-RDP82-00850R000200100009-9

APPROVED FOR RELEASE: 2007/02/08: CIA-RDP82-00850R000200100009-9

where s_1 is the thickness of the hull structure or liner, in m; ρ_1 is the density of the material of which the hull structure or liner is made, in kg/m^3; E_1 is the dynamic Young's modulus of the material from which the hull structure or linear is made, in Pa.

The first boundary frequency (see below) also enters in formula (10.4.3). It is calculated by the formula

$$f_{r1} = \frac{850}{\sqrt{d}} \sqrt{\frac{m_1 + m_2}{m_1 m_2}}, \qquad (10.4.4)$$

where m_1 is the surface mass of the first panel, in kg/m^2; m_2 is the surface mass of the second panel, in kg/m^2; d is the distance between the panels, in m.

Mass M is calculated separately for the hull structure and for the liner, and then the larger value is taken. An inertial bridge should be made of steel, bronze or other solid material in the form of a cylinder or ball.

Elastic bridges should be used for massive and rigid double-wall ship partitions, in which the critical frequencies of the first and second panels lie below 3,000-5,000 Hz. The acoustic properties of an elastic bridge are determined entirely by its rigidity, which should satisfy the following requirement:

$$D = \frac{ES_M}{h} \leqslant s_1^2 f_{r1} \sqrt{\rho_1 E}, \qquad (10.4.5)$$

where E is the static Young's modulus of the elastic material, in Pa; S_m is the cross section area of the elastic element, in m^2; h is the length of the elastic element, in m.

Rigidity D of an elastic bridge is calculated separately for the hull structure and for the liner, and then the smaller value is taken. It is recommended that a porous rubber (with closed pores), soft monolithic rubber, etc., be used as the elastic element. For this purpose it is helpful to use different shock absorbers, for example those used for protecting instruments from vibration. The rigidity of the shock absorber is determined by the formula

$$D = P_{rat}/\Delta h, \qquad (10.4.6)$$

where P_{rat} is the rated load on the shock absorber, H; Δh is the deformation of the shock absorber under the influence of the rated load, in m.

Combined bridges should be used for double-wall partitions in cases when the critical frequency of the hull structure is less than approximately

APPROVED FOR RELEASE: 2007/02/08: CIA-RDP82-00850R000200100009-9

APPROVED FOR RELEASE: 2007/02/08: CIA-RDP82-00850R000200100009-9

5,000 Hz and the critical frequency of the liner is higher than approximately 8,000 Hz. Mass M and rigidity D of the elastic element of a combined bridge are determined by the formulas presented above.

Soundproofing bridges are effective in the frequency range above the first boundary frequency f_{b1}. The number of bridges should be minimized, but sufficient to assure that the liner is securely fastened to the hull structure. The distance between the bridges should be not less than 500 m and they should be spaced uniformly apart over the entire surface of the structure. Soundproofing bridges should also be placed along the edge of the liner.

Calculation of Acoustic Insulation. The distance between the panels of double-wall structures on ships is usually 50-150 mm. The engineering calculation presented below of the acoustic insulation of double-wall structures with soundproofing bridges is intended for distances in that range. Each panel of a double-wall structure should meet all the requirements on the calculation of the acoustic insulation of single-wall structures.

The calculations are done in the third-octave frequency bands and the results are plotted in graphic form, in much the same way as for single-wall structures. The first boundary frequency is determined first by formula (10.4.4). The acoustic insulation in the frequency range below the first boundary frequency $R_{1,2}$, in dB, obeys the law of mass conservation; it is calculated by the formula

$$R_{1,2} = 14{,}5\,[\lg f + \lg(m_1 + m_2) - 2]. \qquad (10.4.7)$$

The acoustic insulation of a double-wall structure, determined by this formula, is virtually the same as that determined for a single-wall structure with the same surface mass.

Additional acoustic insulation appears on frequencies above the first boundary frequency. The second boundary frequency is calculated by the formula

$$f_{b2} = \frac{8{,}500}{d}, \qquad (10.4.8)$$

where d is the distance between the panels, in cm.

Acoustic insulation on frequencies between the first and second boundary frequencies increases linearly on a logarithmic frequency scale. On frequencies above the second boundary frequency the acoustic insulation of a double-wall structure depends little on the distance between the panels. It is determined by the formula

APPROVED FOR RELEASE: 2007/02/08: CIA-RDP82-00850R000200100009-9

APPROVED FOR RELEASE: 2007/02/08: CIA-RDP82-00850R000200100009-9

$$R_{1,2} = \Phi_R (R_1 + R_2), \tag{10.4.9}$$

where R_1 and R_2 are the acoustic insulation values of the first and second panels, in dB.

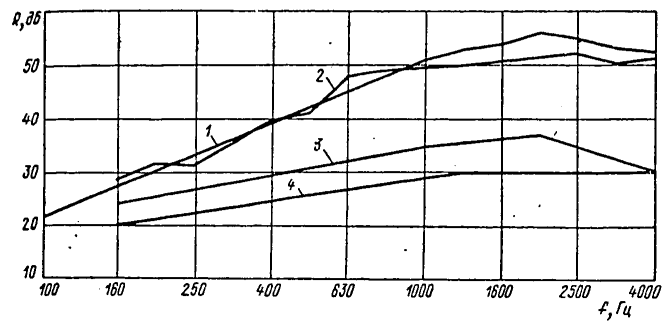

Figure 10.8. Acoustic insulation of double-wall ship partition. First wall 3 mm steel, second wall 12 mm plywood; distance between walls 90 mm; 1 -- calculated curve of acoustic insulation $R_{1,2}$; 2 -- experimental curve of acoustic insulation $R_{1,2}$; 3 -- calculated curve of acoustic insulation of hull structure R_1; 4 -- calculated curve of acoustic insulation of liner R_2. [дБ=dB; Гц=Hz]

The numerical coefficient Φ_R is determined by the formula

[г=b]

$$\Phi_R = 0{,}80 + 0{,}10\frac{f}{f_{г2}} \text{ for } \frac{f}{f_{г2}} < 10,$$
$$\Phi_R = 0{,}90 \text{ for } \frac{f}{f_{г2}} \geqslant 10, \tag{10.4.10}$$

where f is the third-octave frequency band, for which the acoustic insulation is calculated, in Hz; f_{b2} is the second boundary frequency, in Hz.

The calculated curve of the acoustic insulation of a double-wall structure is plotted in the coordinate grid examined above, in which the first and second boundary frequencies are plotted first. On frequencies above the first boundary frequency the acoustic insulation is calculated by formula (10.4.7), and on frequencies above the second boundary frequency by formula (10.4.9). The region between the first and second boundary frequencies is connected with a straight line. The result is the calculated curve of the acoustic insulation of a double-wall ship structure.

APPROVED FOR RELEASE: 2007/02/08: CIA-RDP82-00850R000200100009-9

APPROVED FOR RELEASE: 2007/02/08: CIA-RDP82-00850R000200100009-9

The theoretical and experimental curves of the acoustic insulation of a double-wall ship partition with an air space between the panels are presented in Figure 10.8.

Table 10.3. Efficiency of Soundproofing in Double-Wall Structures

1) Третьоктавные полосы частот, Гц	2) Значения дополнительной звукоизоляции $\Delta R_п$, дБ
3) 160 и ниже	0
200	1
250	2
315	3
400	4
500	5
630	6
800	7
1000	8
1250	9
4) 1600 и выше	10

Key: 1. Third-octave frequency bands, Hz
2. Amount of additional acoustic insulation ΔR_p, dB
3. 160 and below
4. 1,600 and above

To increase the acoustic insulation of a double-wall structure it is advisable to install between the panels a soundproofing material. It should be installed in a uniform layer with a thickness of from 1/2 to 2/3 of the distance between the panels. If the density of the material thus installed is less than 20 kg/m^3 the attenuation constant is higher than 0.1 cm^{-1} and the speed of sound in the material is less than 200 m/s, the additional acoustic insulation, gained by installing the soundproofing material between the panels, can be determined in the first approximation by the data in Table 10.3. The calculated values of the acoustic insulation of a double-wall structure with a layer of soundproofing material between the panels is

[п=р] $$R_{1,2п} = R_{1,2} + \Delta R_п,$$

where $R_{1,2}$ are the calculated values of the acoustic insulation of the double-wall structure without the soundproofing material between the panels, determined by the procedure described above.

The average values of the experimental data are presented in Table 10.3. When different soundproofing materials are used it must be remembered that the additional acoustic insulation, achieved by using the soundproofing material increases as the impedance of the soundproofing material decreases and as its attenuation constant increases.

10.5. Planning of Acoustic Insulation of Ship

Planning of the acoustic insulation of a ship starts with the determination of the required acoustic insulation, which provides low enough acoustic pressure levels (not higher than the permissible standards) in an insulated room.

Acoustic insulation R_{req}, in dB, can be calculated by the formula

APPROVED FOR RELEASE: 2007/02/08: CIA-RDP82-00850R000200100009-9

APPROVED FOR RELEASE: 2007/02/08: CIA-RDP82-00850R000200100009-9

[тр=req; доп=per] $$R_{тр} \geqslant L - L_{доп} + 10\lg\frac{S}{A}, \quad (10.5.1)$$

where L is the acoustic pressure level in a room with a noise source, in dB; L_{per} is the permissible acoustic pressure level in the insulated room, in dB; S is the area of the partitioning, through which the noise penetrates into the insulated room, in m^2; A is the total soundproofing of the insulated room, in m^2.

The acoustic pressure levels in a room with a noise source can be determined by full-scale measurements on a prototype ship by calculation. The acceptable acoustic pressure levels in an insulated room must correspond to GOST SSBT 12.1.003-76: "Noise. General Safety Requirements" and to industrial standards documents. The required acoustic insulation is determined in third-octave frequency bands in the 63 to 8,000 Hz range. The ratio S/A may be assumed equal to one in the first approximation.

After the required amount of acoustic insulation is determined the structure that provides that acoustic insulation is designed. The development of the structure is the main objective of the planning of ship acoustic insulation.

Walls that separate the engine room or other room with powerful noise sources from other (living or service) rooms of a ship must have the greatest amount of acoustic insulation. The acoustic insulation of state room and corridor walls should meet the requirement on the reduction of routine noise that penetrates into state rooms from adjacent rooms. The envelope of the spectrum of the maximum routine noise levels is shown in Figure 10.9. The average required values of acoustic insulation from routine noise are given in Figure 10.10.

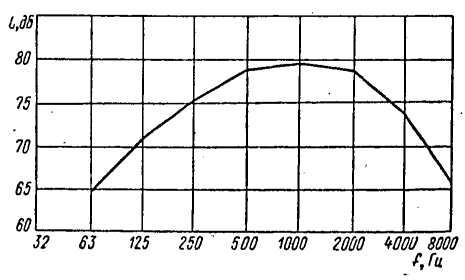

Figure 10.9. Maximum routine noise levels.
[дБ=dB; Гц=Hz]

Soundproofing ship structures are developed either by calculation, as was mentioned above, or by using ready-made structures, the acoustic insulating

APPROVED FOR RELEASE: 2007/02/08: CIA-RDP82-00850R000200100009-9

APPROVED FOR RELEASE: 2007/02/08: CIA-RDP82-00850R000200100009-9

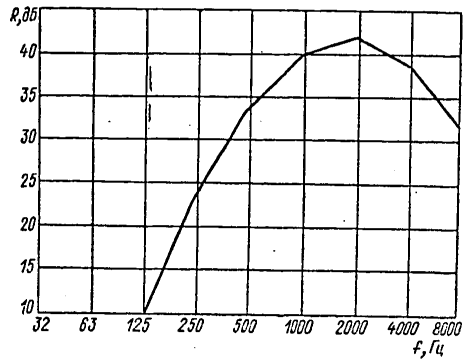

Figure 10.10. Average values of required insulation of state room partitions and corridor walls.

effectiveness of which is determined experimentally. The latter approach is often more convenient. This section pertains to the second approach to the planning of ship soundproofing.

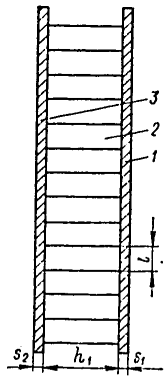

Figure 10.11. Diagram of sotoplast-filled panel: 1 -- first panel; 2 -- honeycomb filter; 3 -- second panel.

The main ship soundproofing partitions are single-wall structures. The sound insulation of single-wall structures, the thickness and material of which cover virtually the entire range of the values used for ships, is given in Table 10.4. The acoustic insulation of decks and bulkheads of transport and merchant ships, afforded by all main structures, is given in Table 10.5, and of state room partitions and corridor walls, used on all types of ships for all purposes, in Table 10.6. The acoustic insulation of hydrofoil ships is summarized in Table 10.7 [2].

Designers have been devoting increasing attention in recent years to honeycomb structures. The acoustic insulation of a large series of standard panels with sotoplast honeycomb plastic filler is given in Table 10.8, and the design of such a panel is illustrated in Figure 10.11. The table was compiled on the basis of the results of measurements of the acoustic insulation of the described structures. The measurement procedure met the recommendations of the International Standardization Organization [19]. The measurements were conducted in third-octave frequency bands of a virtually diffusive acoustic field at dozens of points in high-level and low-level chambers. The limiting measurement error was 1 dB with a probability of not less than 0.95. For this reason the values of acoustic insulation in the table are reliable enough.

APPROVED FOR RELEASE: 2007/02/08: CIA-RDP82-00850R000200100009-9

APPROVED FOR RELEASE: 2007/02/08: CIA-RDP82-00850R000200100009-9

Table 10.4. Acoustic Insulation of Single-Wall Structures, in dB

1) Материал	2) Толщина, мм	3) Масса 1 м² полотна, кг	4) Частоты октавных полос, Гц							
			63	125	250	500	1000	2000	4000	8000
5) Сталь	1,0	7,8	12	16	20	24	29	33	36	34
	2,0	15,6	16	20	24	29	33	36	34	34
	3,0	23,4	19	23	27	31	35	37	30	39
	4,0	31,2	21	25	29	33	36	34	34	41
	5,0	39,0	22	26	30	34	37	32	36	42
	6,0	46,8	23	27	31	35	37	30	39	43
	8,0	62,4	24	28	32	36	34	33	40	44
	10,0	78,0	26	30	34	36	32	36	42	46
	15,0	117,0	28	32	36	35	33	40	44	48
6) Алюминиево-магниевые сплавы	1,0	2,8	6	10	14	18	22	26	29	27
	2,0	5,6	10	14	18	22	26	29	27	25
	3,0	8,4	12	16	20	24	28	31	22	30
	4,0	11,2	14	18	22	26	29	27	25	32
	5,0	14,0	15	19	23	27	30	24	28	33
	7,0	19,6	17	21	25	29	28	24	31	35
	10,0	28,0	19	23	27	30	24	27	33	37
7) Стеклопластик	3,0	5,1	9	13	17	21	25	29	31	32
	5,0	8,5	12	16	20	24	28	31	31	34
	8,0	13,6	15	19	23	27	30	31	33	37
	10,0	17,0	17	21	25	28	31	31	34	38
8) Фанера	4,0	3,2	8	12	16	20	24	27	27	27
	5,0	4,0	9	13	17	21	25	28	26	29
	8,0	6,4	12	16	20	24	27	27	27	32
	10,0	8,0	13	17	21	25	28	25	29	33
	12,0	9,6	15	19	23	26	28	26	30	34
9) Железобетон	20,0	52,0	27	31	36	40	35	41	45	49
	30,0	78,0	29	34	38	38	38	43	47	51
	40,0	104,0	31	36	40	35	41	45	49	53
	50,0	130,0	33	37	38	37	42	46	50	54
	70,0	182,0	35	39	36	40	44	48	52	56
	100,0	260,0	38	38	37	42	46	50	55	59
10) Стекло силикатное	2,0	5,0	12	16	20	24	28	32	30	33
	3,0	7,5	14	18	22	26	30	34	29	38
	5,0	12,5	17	21	25	29	33	30	36	41
	7,0	17,5	19	23	27	31	33	31	39	43
	10,0	25,0	21	25	28	33	30	36	42	44
	12,0	30,0	22	26	30	34	29	38	42	46
	15,0	37,5	24	28	32	32	33	40	44	48
11) Стекло органическое	2,0	2,4	9	13	17	21	25	28	32	35
	3,0	3,6	11	15	19	23	26	30	34	34
	5,0	6,0	14	18	22	26	30	33	35	31
	7,0	8,4	16	20	24	27	31	35	32	35
	10,0	12,0	18	22	26	30	33	35	31	39
	16,0	19,2	21	25	28	32	35	31	37	41

Key:
1. Material
2. Thickness, mm
3. Mass per 1 m^2 of plating, kg
4. Frequency of octave bands, Hz
5. Steel
6. Aluminum-magnesium alloys
7. Glass-reinforced plastic
8. Plywood
9. Reinforced concrete
10. Silicate glass
11. Organic glass

APPROVED FOR RELEASE: 2007/02/08: CIA-RDP82-00850R000200100009-9

APPROVED FOR RELEASE: 2007/02/08: CIA-RDP82-00850R000200100009-9

Table 10.5. Acoustic Insulation of Decks and Bulkheads of Transport and Merchant Ships, in dB

1) Схема конструкции	2) Описание конструкции	3) Масса 1 м² конструкции, кг	4) Частоты октавных полос, Гц							
			63	125	250	500	1000	2000	4000	8000
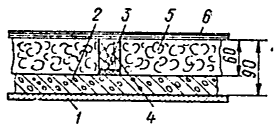	5) *1* — сталь (s = 6,0 мм); *2* — мастика «Нева»; (s=30 мм); *3* — прокладка из губчатой резины (s = = 5,0 мм); *4* — обрешетник; *5* — звукопоглотитель АТМ 1; *6* — фанера (s = 10,0 мм)	88.4	30	39	48	52	53	53	55	59
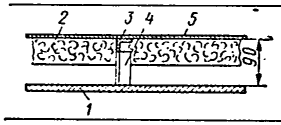	6) *1* — сталь (s = 6.0 мм); *2* — звукопоглотитель АТМ-1 (s = = 40 мм); *3* — обрешетник; *4* — коротыш; *5* — алюминиево-магниевый сплав (s = 2 мм)	52,8	26	31	41	47	48	48	50	55
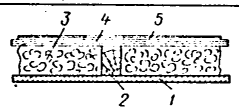	7) *1* — сталь (s = 6,0 мм); *2* — обрешетник; *3* — звукопоглотитель из штапельного стекловолокна (s = 50 мм); *4* — фанера (s = = 12,0 мм); *5* — слоистый пластик (s = 1,5 мм)	61,0	26	29	37	44	45	45	47	51
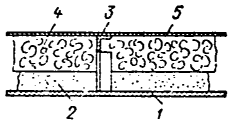	8) *1* — сталь (s = 3.0 мм); *2* — материал ФС-7 (s = 30 мм); *3* — обрешетник; *4* — звукопоглотитель из штапельного стекловолокна (s = 60,0 мм); *5* — сталь (s = = 1,0 мм)	37,2	23	32	41	46	50	53	56	59

Key: 1. Diagram of structure
2. Description of structure
3. Mass per 1 m^2 of structure
4. Frequency of octave bands, Hz
5. 1 - steel (s = 6.0 mm); 2 - "Neva" mastic (s = = 30 mm); 3 - sponge rubber pad (s = 5.0 mm); 4 - stud; 5 - ATM-1 sound absorber; 6 - plywood
6. 1 - steel (s = 6.0 mm); 2 - ATM-1 sound absorber (s = 40 mm); 3 - stud; 4 - bolster; 5 - aluminum-magnesium alloy (s = 2 mm)
7. 1 - steel (s = = 6.0 mm); 2 - stud; 3 - staple glass fiber sound absorber; 4 - plywood; 5 - laminated plastic (s = 1.5 mm)
8. 1 - steel (s = = 3.0 mm); 2 - FS-7 material (s = 30 mm); 3 - stud; 4 - staple glass fiber sound absorber (s = = 60.0 mm); 5 - steel (s = 1.0 mm)

APPROVED FOR RELEASE: 2007/02/08: CIA-RDP82-00850R000200100009-9

APPROVED FOR RELEASE: 2007/02/08: CIA-RDP82-00850R000200100009-9

Table 10.5 (continued)

1) Схема конструкции	2) Описание конструкции	3) Масса 1 м² конструкции, кг	4) Частоты октавных полос, Гц							
			63	125	250	500	1000	2000	4000	8000
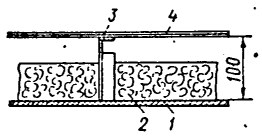	9) 1 — сталь (s = 3,0 мм); 2 — звукопоглотитель из штапельного стекловолокна (s = 60,0 мм); 3 — обрешетник; 4 — слоистый пластик (s = 3,0 мм)	30,6	19	30	41	46	49	51	52	53
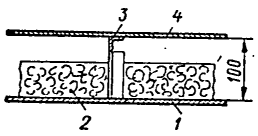	10) 1 — сталь (s = 3,0 мм); 2 — звукопоглотитель из штапельного стекловолокна (s = 60,0 мм); 3 — обрешетник; 4 — сталь (s = = 1,0 мм)	34,2	25	35	44	49	53	54	55	56
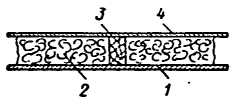	11) 1 — сталь (s = 3,0 мм); 2 — звукопоглотитель из штапельного стекловолокна (s = 50,0 мм); 3 — обрешетник; 4 — алюминиево-магниевый сплав (s = 1,0 мм)	28,7	20	25	34	42	46	49	50	51

Key: 9. 1 - steel (s = 3.0 mm); 2 - staple glass fiber sound absorber (s = = 60.0 mm); 3 - stud; 4 - laminated plastic (s = 3.0 mm)

10. 1 - steel (s = 3.0 mm); 2 - staple glass fiber sound absorber (s = = 60.0 mm); 3 - stud; 4 - steel (s = 1.0 mm)

11. 1 - steel (s = 3.0 mm); 2 - staple glass fiber sound absorber (s = 50.0 mm); 3 - stud; 4 - aluminum-magnesium alloy (s = 1.0 mm)

APPROVED FOR RELEASE: 2007/02/08: CIA-RDP82-00850R000200100009-9

APPROVED FOR RELEASE: 2007/02/08: CIA-RDP82-00850R000200100009-9

Table 10.5 (continued)

Схема конструкции	Описание конструкции	Масса 1 м² конструкции, кг	Частоты октавных полос, Гц							
			63	125	250	500	1000	2000	4000	8000
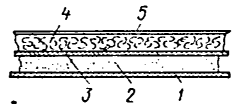	12) *1* — алюминиево-магниевый сплав (s = 3,0 мм); *2* — материал ПХВ-1 (s = 30,0 мм); *3* — пластмасса «Агат» (s = 2,5 мм); *4* — звукопоглотитель ВТ-4 (s = = 30,0 мм); *5* — гидрозащитная пленка	16,5	27	27	28	32	38	45	49	56
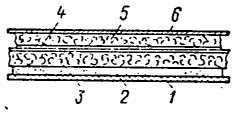	13) *1* — алюминиево-магниевый сплав (s = 3,0 мм); *2* — вибропоглощающая мастика ВД-17 (s = 30 мм); *3* — пенополиуретан (s = 30 мм); *4* — фольга (s = = 0,1 мм); *5* — звукопоглотитель ВТ-4 (s = 30,0 мм); *6* — алюминиево-магниевый сплав (s=1,0 мм)	24,7	28	30	40	44	47	51	52	59
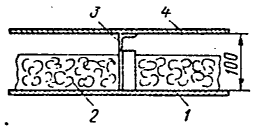	14) *1* — сталь (s = 3,0 мм); *2* — штапельное стеклоплокно (s = = 60 мм); *3* — обрешетник; *4* — алюминиево-магниевый сплав (s = 1,0 мм)	29,2	20	29	40	47	51	53	54	55

Key: 12. 1 - aluminum-magnesium alloy (s = 3.0 mm); 2 - PKhV-1 material (s = 30.0 mm); 3 - "Agat" plastic (s = 2.5 mm); 4 - VT-4 sound absorber (s = = 30.0 mm); 5 - water-proof film

13. 1 - aluminum-magnesium alloy (s = 3.0 mm); 2 - VD-17 vibration-absorbing mastic (s = 30 mm); 3 - polyurethane foam (s = 30 mm); 4 - foil (s = 0.1 mm); 5 - VT-4 sound absorber (s = 30.0 mm); 6 - aluminum-magnesium alloy (s = = 1.0 mm)

14. 1 - steel (s = 3.0 mm); 2 - staple glass fiber (s = 60 mm); 3 - stud; 4 - aluminum-magnesium alloy (s = 1.0 mm)

APPROVED FOR RELEASE: 2007/02/08: CIA-RDP82-00850R000200100009-9

APPROVED FOR RELEASE: 2007/02/08: CIA-RDP82-00850R000200100009-9

Table 10.6. Acoustic Insulation of State Room Partitions and Corridor Bulkheads, in dB

1) Схема конструкции	2) Описание конструкции	Масса 1 м² конструкции, кг/м²	4) Частоты октавных полос, Гц							
			63	125	250	500	1000	2000	4000	8000
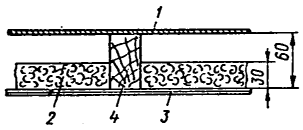	5) 1 — сталь (s = 2,0 мм); 2 — звукопоглотитель АТМ-1 (s = 30 мм); 3 — слоистый пластик (s = 2,0 мм); 4 — брусок 40×60 мм	18,7	21	19	28	42	47	50	50	54
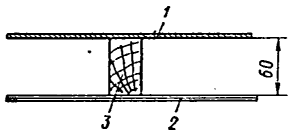	6) 1 — сталь (s = 2,0 мм); 2 — слоистый пластик (s = 2,0 мм); 3 — брусок 40×60 мм	18,4	21	17	23	34	43	48	49	52
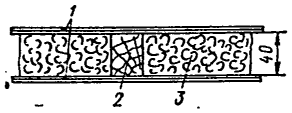	7) 1 — слоистый пластик (s = 3 мм); 2 — брусок 40×40 мм; 3 — звукопоглотитель АТМ-1 (s = 40 мм)	8,8	19	14	15	30	40	48	52	52

Key: 1. Diagram of structure
2. Description of structure
3. Mass per square meter of structure
4. Frequency of octave bands, Hz
5. 1 - steel (s = 2.0 mm); 2 - ATM-1 sound absorber (s = 30 mm); 3 - laminated plastic (s = 2.0 mm); 4 - stud 40 × 60 mm
6. 1 - steel (s = 2.0 mm); 2 - laminated plastic (s = 2.0 mm); 3 - stud 40 × 60 mm
7. 1 - laminated plastic (s = = 3 mm); 2 - stud 40 × 40 mm; 3 - ATM-1 sound absorber (s = 40 mm)

APPROVED FOR RELEASE: 2007/02/08: CIA-RDP82-00850R000200100009-9

APPROVED FOR RELEASE: 2007/02/08: CIA-RDP82-00850R000200100009-9

Table 10.6 (continued)

1) Схема конструкции	2) Описание конструкции	Масса 1 м² конструкции, кг/м²	4) Частоты октавных полос, Гц							
			63	125	250	500	1000	2000	4000	8000
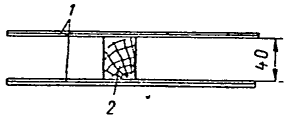	8) 1 — слоистый пластик (s = 3,0 мм); 2 — брусок 40×40 мм	8,4	19	14	13	19	30	41	48	48
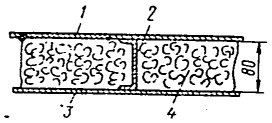	9) 1 — сталь (s = 2,0 мм); 2 — швеллер № 8; 3 — алюминиево-магниевый сплав (s = 2,0 мм); 4 — звукопоглотитель АТМ-1 (s = 80 мм)	22,0	24	30	41	47	48	52	54	54
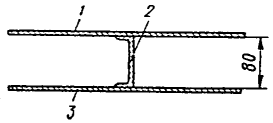	10) 1 — сталь (s = 2,0 мм); 2 — швеллер № 8; 3 — алюминиево-магниевый сплав (s = 2,0 мм)	21,2	24	20	31	37	42	48	52	52
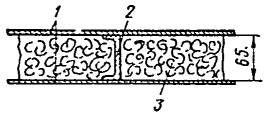	11) 1 — алюминиево-магниевый сплав (s = 2,0 мм); 2 — швеллер № 6,5; 3 — звукопоглотитель АТМ-1 (s = 65 мм)	11,8	21	18	33	43	48	52	52	52

8. 1 - laminated plastic (s = = 3.0 mm); 2 - stud 40 × 40 mm
9. 1 - steel (s = 2.0 mm); 2 - No. 8 channel bar; 3 - aluminum-magnesium alloy (s = 2.0 mm); 4 -- ATM-1 sound absorber (s = 80 mm)
10. 1 - steel (s = 2.0 mm); 2 - No. 8 channel bar; 3 - aluminum-magnesium alloy (s = 2.0 mm)
11. 1 - aluminum-magnesium alloy (s = 2.0 mm); 2 - No. 6.5 channel bar; 3 - ATM-1 sound absorber (s = 65 mm)

APPROVED FOR RELEASE: 2007/02/08: CIA-RDP82-00850R000200100009-9

APPROVED FOR RELEASE: 2007/02/08: CIA-RDP82-00850R000200100009-9

FOR OFFICIAL USE ONLY

Table 10.6 (continued)

1) Схема конструкции	2) Описание конструкции	Масса 1 м² конструкции, кг 3)	4) Частоты октавных полос, Гц							
			63	125	250	500	1000	2000	4000	8000
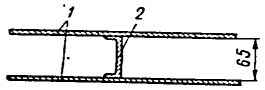	12) 1 — алюминиево-магниевый сплав (s = 2,0 мм); 2 — швеллер № 6,5	11,2	21	18	22	29	37	45	48	48
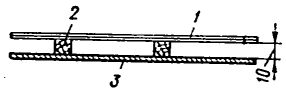	13) 1 — слоистый пластик (s = = 2.0 мм); 2 — брусок 20×10 мм; 3 — алюминиево-магниевый сплав (s = 3.0 мм)	11,2	22	22	21	22	29	37	43	49
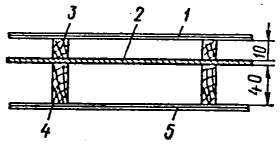	14) 1 — слоистый пластик (s = = 2.0 мм); 2 — алюминиево-магниевый сплав (s = 3.0 мм); 3 — брусок 20×10 мм; 4 — брусок 20×40 мм; 5 — фанера (s = 2.0 мм)	12,8	22	22	17	23	35	46	55	60

12. 1 - aluminum-magnesium alloy (s = 2.0 mm); 2 - No. 6.5 channel bar

13. 1 - laminated plastic (s = 2.0 mm); 2 - stud 20 × 10 mm; 3 - aluminum-magnesium alloy (s = 3.0 mm)

14. 1 - laminated plastic (s = 2.0 mm); 2 - aluminum-magnesium alloy (s = 3.0 mm); 3 - stud 20 × 10 mm; 4 - stud 20 × 40 mm; 5 - plywood (s = = 2.0 mm)

FOR OFFICIAL USE ONLY

APPROVED FOR RELEASE: 2007/02/08: CIA-RDP82-00850R000200100009-9

APPROVED FOR RELEASE: 2007/02/08: CIA-RDP82-00850R000200100009-9

FOR OFFICIAL USE ONLY

Table 10.7. Acoustic Insulation of Hydrofoil Ships, in dB

1) Схема конструкции	2) Описание конструкции	Масса 1 м² конструкции, кг/м²	4) Частоты октавных полос, Гц							
			63	125	250	5000	1000	2000	4000	8000
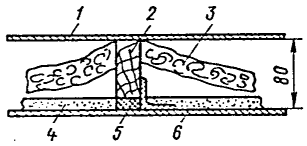	5) *1* — алюминиево-магниевый сплав (s = 2,0 мм); *2* — брусок 20×70 мм; *3* — звукопоглотитель ВТ-4С (s = 20 мм); *4* — пенопласт ПХВ-1 (s = 10 мм); *5* — резина губчатая 10×20 мм; *6* — алюминиево-магниевый сплав (s = 3,0 мм)	15,4	22	22	33	43	50	53	55	58
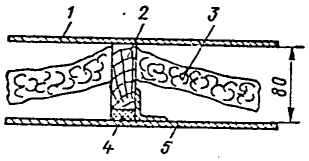	6) *1* — алюминиево-магниевый сплав (s = 2,0 мм); *2* — брусок 20×70 мм; *3* — звукопоглотитель ВТ-4С (s = 20 мм); *4* — резина губчатая 10×20 мм; *5* — алюминиево-магниевый сплав (s = 3,0 мм)	14.4	21	21	30	39	46	51	53	55
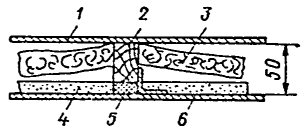	7) *1* — алюминиево-магниевый сплав (s = 2,0 мм); *2* — брусок 20×40 мм; *3* — звукопоглотитель ВТ-4С (s = 20 мм); *4* — пенопласт ПХВ-1 (s = 10 мм); *5* — резина губчатая 10×20 мм; *6* — алюминиево-магниевый сплав (s = 3,0 мм)	15.4	22	22	29	39	48	52	54	54

1. Diagram of structure
2. Description of structure
3. Mass per square meter of structure
4. Frequency of octave bands, Hz
5. 1 - aluminum-magnesium alloy (s = 2.0 mm); 2 - stud 20 × 70 mm; 3 - VT-4S sound absorber (s = 20 mm); 4 - PKhV-1 foam plastic (s = 10 mm); 5 - soft rubber 10 × 20 mm; 6 - aluminum-magnesium alloy (s = 3.0 mm)
6. 1 - aluminum-magnesium alloy (s = 2.0 mm); 2 - stud 20 × × 70 mm; 3 - VT-4S sound absorber (s = 20 mm); 4 - soft rubber 10 × 20 mm; 5 - aluminum-magnesium alloy (s = = 3.0 mm)
7. 1 - aluminum-magnesium alloy (s = = 2.0 mm); 2 - stud 20 × 40 mm; 3 - VT-4S sound absorber (s = 20 mm); 4 - PKhV-1 foam plastic (s = 10 mm); 5 - sponge rubber 10 × 20 mm; 6 - aluminum-magnesium alloy (s = = 3.0 mm)

FOR OFFICIAL USE ONLY

APPROVED FOR RELEASE: 2007/02/08: CIA-RDP82-00850R000200100009-9

APPROVED FOR RELEASE: 2007/02/08: CIA-RDP82-00850R000200100009-9

Table 10.7 (continued)

1) Схема конструкции	2) Описание конструкции	Масса 1 м² конструкции, кг	4) Частоты октавных полос, Гц							
			63	125	250	500	1000	2000	4000	8000
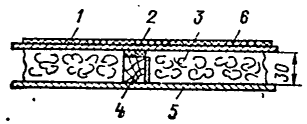	8) 1 — алюминиево-магниевый сплав (s = 2,0 мм); 2 — резина губчатая 5×15 мм; 3 — звукопоглотитель ВТ-4С (s = 30 мм); 4 — брусок 15×25 мм; 5 — алюминиево-магниевый сплав (s = 2,0 мм); 6 — линолеум (s = 3,0 мм)	16,3	23	23	25	36	44	49	53	54
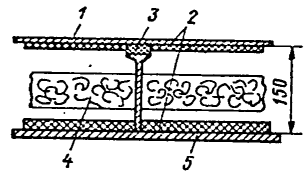	9) 1 — алюминиево-магниевый сплав (s = 1,0 мм); 2 — вибропоглощающее покрытие с незатвердевающей связкой; 3 — губчатая резина 20×10 мм; 4 — звукопоглотитель АТМ-1 (s = 70 мм); 5 — алюминиево-магниевый сплав (s = 3,0 мм)	18,9	24	28	40	48	52	54	56	58
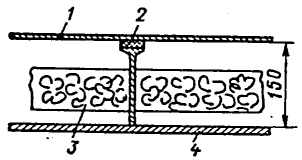	10) 1 — алюминиево-магниевый сплав (s = 1,0 мм); 2 — губчатая резина 20×10 мм; 3 — звукопоглотитель АТМ-1 (s = 70 мм); 4 — алюминиево-магниевый сплав (s = 3,0 мм)	11,9	22	21	31	39	45	52	56	58

8. 1 - aluminum-magnesium alloy (s = 2.0 mm); 2 - sponge rubber 5 × 15 mm; 3 - VT-4S sound absorber (s = 30 mm); 4 - stud 15 × 25 mm; 5 - aluminum-magnesium alloy (s = 2.0 mm); 6 - linoleum (s = 3.0 mm)

9. 1 - aluminum-magnesium alloy (s = = 1.0 mm); 2 - vibration-absorbing coating with nonhardening binder; 3 - sponge rubber 20 × 10 mm; 4 - ATM-1 sound absorber (s = 70 mm); 5 - aluminum-magnesium alloy (s = = 3.0 mm)

10. 1 - aluminum-magnesium alloy (s = 1.0 mm); 2 - sponge rubber 20 × × 10 mm; 3 - ATM-1 sound absorber (s = = 70 mm); 4 - aluminum-magnesium alloy (s = 3.0 mm)

APPROVED FOR RELEASE: 2007/02/08: CIA-RDP82-00850R000200100009-9

APPROVED FOR RELEASE: 2007/02/08: CIA-RDP82-00850R000200100009-9

Table 10.8. Acoustic Insulation of Sotoplast-Filled Panels, in dB

1) Материал и размеры конструктивных элементов панели, мм						2) Частоты октавных полос, Гц							
3) 1-я стенка		4) 2-я стенка		5) Соты									
6) Материал	s_1	6) Материал	s_2	6) Материал	l	h_1	63	125	250	500	1000	2000	4000	8000
7) Стеклопластик	2	7) Стеклопластик	5	Стеклоткань 8)	14	10	19	21	25	31	33	29	29	40
»	2	»	5	Хлопчатобумажная ткань 9)	5	10	18	21	26	30	32	27	31	42
»	2	»	5	То же 11)	5	40	23	24	26	24	25	30	39	46
»	2	»	5	Стеклоткань 8)	5	40	26	25	26	25	26	34	41	48
»	2	»	5	Хлопчатобумажная ткань 9)	7	10	21	21	25	30	30	27	29	38
»	2	»	5	То же 11)	14	10	25	23	24	31	34	33	30	39
»	5	»	5	Стеклоткань 8)	5	20	18	18	24	28	25	28	37	45
»	2	»	5	Хлопчатобумажная ткань 9)	14	40	19	18	24	29	28	29	34	42
»	5	»	5	То же 11)	5	20	15	18	24	30	26	27	34	43
10) Слоистый пластик	5	10) Слоистый пластик	5	Стеклоткань 8)	5	40	17	17	21	23	25	31	39	46
11) То же	5	11) То же	5	»	5	20	21	17	24	26	22	30	37	44
»	2	»	2	»	5	40	17	17	19	22	23	29	36	42
»	2	»	2	»	5	20	22	15	22	23	20	26	32	39
7) Стеклопластик	2	7) Стеклопластик	2	Хлопчатобумажная ткань 9)	5	20	17	18	21	24	20	22	28	37
»	2	»	2	Стеклоткань 8)	5	20	20	19	22	24	20	25	32	38
»	2	»	2	Хлопчатобумажная ткань 9)	5	40	19	17	21	21	21	28	34	40
»	2	»	2	Стеклоткань 8)	5	40	18	17	21	20	21	29	35	42
»	2	»	5	»	5	10	23	22	26	31	29	26	34	42
»	2	»	5	»	7	10	27	23	27	31	31	25	32	42
»	2	»	5	Хлопчатобумажная ткань 9)	7	40	20	17	23	25	24	27	34	43
»	2	»	5	Стеклоткань 8)	7	40	24	22	22	22	21	28	36	43
»	2	»	5	»	14	40	22	23	24	24	22	25	34	42
»	2	»	5	Хлопчатобумажная ткань 9)	5	40	22	20	22	24	23	29	36	44
»	5	»	5	Стеклоткань 8)	5	40	27	25	24	24	24	31	38	44
—	—	»	5	»	5	40	24	20	24	31	38	45	45	48
—	—	»	5	»	14	40	18	17	23	29	34	43	41	40

Key:
1. Material and dimensions of structural elements of panel, mm
2. Frequencies of octave bands, Hz
3. 1st panel
4. 2nd panel
5. Honeycomb
6. Material
7. Glass-reinforced plastic
8. Glass fiber cloth
9. Cotton cloth
10. Laminated plastic
11. Same

APPROVED FOR RELEASE: 2007/02/08: CIA-RDP82-00850R000200100009-9

APPROVED FOR RELEASE: 2007/02/08: CIA-RDP82-00850R000200100009-9

The basic recommendations presented below must be taken into consideration in all cases during the planning of ship acoustic insulation.

The critical frequency of a single-wall soundproofing structure should be higher as possible than the calculated frequency range. It is important that the critical frequencies of the hull and liner in double-wall soundproofing structures differ by at least one octave. The air space in double-wall structures with soundproofing bridges must be at least 100 mm thick and be half filled with soundproofing material. If soundproofing structures are located in places with high acoustic vibrations they must have a vibration-absorbing coating. Special attention must be devoted to the sealing of cracks and holes in sound-insulating structures (windows, doors, cable passages, etc.). The only permissible type of connection between the liner and hull structure in double-wall soundproofing structures are soundproofing bridges, and they should also be installed along the edges of the structure.

Practice in Soviet and foreign shipbuilding has shown that a further increase of the quality and effectiveness of acoustic insulation can be achieved on the basis of a modular system. Such a system consists in the use of standardized soundproofing elements, the dimensions of which, just as the dimensions of ship rooms, are multiples of a selected module. Soundproofing modules are manufactured industrially, irrespective of the shape of a ship hull, and eliminate the need for fitting operations on a ship during the installation of acoustic insulation.

The development of acoustic insulation should begin in the earliest possible planning stage. It is first necessary to select the type of acoustic insulation and determine its basic parameters, which assure the required reduction of sound. In the next planning stage drawings of the soundproofing structures are made, and these drawings should indicate the best ratios of acoustic and nonacoustic requirements, including production technology and testing of acoustic insulation during operation.

10.6. Soundproofing Shields and Booths[1]

Application of Shields and Booths. Soundproof shields and booths are ways of achieving local sound control. They are most effective for reducing noise on open decks; they are less effective in closed rooms due to the reflection of sound from the walls. Acoustic shielding depends to a great extent on the directivity of the noise source, and directive sources are much easier to shield than sources that radiate sound uniformly in all directions. Directive sources are those noise sources in which the maximum acoustic pressure level exceeds the minimum level by more than 5 dB (the turbochargers of certain engines, with axial air intake, etc.).

[1]This section was written by E. A. Gomzikov.

APPROVED FOR RELEASE: 2007/02/08: CIA-RDP82-00850R000200100009-9

APPROVED FOR RELEASE: 2007/02/08: CIA-RDP82-00850R000200100009-9

When shields are installed in a room their effectiveness increases the closer they are placed near the source. Soundproofing should be installed on the noise source side of the shields, when the shield is as close as possible to the source, and also in partly open bulkheads.

The best way to achieve local sound control is to use closed booths. The reduction of noise in booths depends on the sound-insulating properties of the enclosures, the amount of acoustic absorption inside the booth and the vibration insulation of bearing structures of the booth. Plane shields are used on the ships basically for reducing noise in work places near engines and ventilation openings, and near stations of the main distribution panel and steam generators. Panels, wells, partitions and quiet units also have a screening effect, in addition to special acoustic shields. Partly open partitions and closed booths are used for reducing sound at engine control stations, on steam generators, where telephones are installed and at cargo loading stations on decks.

The necessary local noise reduction technique is determined on the basis of how much higher a noise level is at a particular point than the acceptable levels. The efficiency of local noise reduction systems ΔL, in dB, is evaluated by the expression

$$\Delta L = L_1 - L_2, \qquad (10.6.1)$$

where L_1 is the noise level at a calculated point in the absence of local sound reduction devices; L_2 is the same after noise reducers are installed, in dB.

The effectiveness is calculated for a point located on a line passing through the center of the shielding device and in the center of a booth, and for directive sources for a point on the axis of the noise source, passing also through the center of the shield.

Plane Shield on Open Deck. For a nondirectional noise source shield effectiveness ΔL_s is determined graphically (Figure 10.12) in accordance with parameter N, which should be found through the formula

$$N = 0{,}05\sqrt{f}\,\sqrt[4]{\frac{d^2}{1+4(r/l)^2}}, \qquad (10.6.2)$$

where f is the calculated frequency, in Hz; l is the average length of the shield, in m; r is the distance between the shield and the noise source, in m; d is the distance between the shield and the calculated point behind the shield, in m.

The dimensions l, r, d are given in Figure 10.13.

APPROVED FOR RELEASE: 2007/02/08: CIA-RDP82-00850R000200100009-9

APPROVED FOR RELEASE: 2007/02/08: CIA-RDP82-00850R000200100009-9

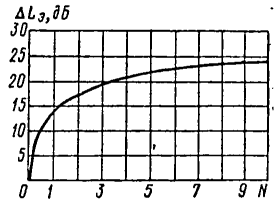

Figure 10.12. Effectiveness of plane shield on open deck for nondirectional noise source. [э=s; дБ=dB]

For a directional noise source shield effectiveness $\Delta L_{s.d}$, in dB, is calculated by the formula

[э=s; н=d]

$$\Delta L_{э.н} = -10\lg[\Phi^2(\theta) + 10^{-0,1R}], \qquad (10.6.3)$$

where $\Phi(\theta) = r_\theta/r$ is the shielding coefficient, which depends on angle θ (Figure 10.14), and the smaller of two angles θ_1 and θ_2 is taken as θ; r is a value equal to the distance between point 0 and point 0° (Figure 10.15); r_θ is equal to the distance between point 0 and the intersection of a ray, drawn at angle θ to the curve corresponding to the calculated coefficient γ, the axial concentration coefficient of the source, determined in accordance with Figure 10.16 as a function of parameter ka; k = f/54 is the wave number, in 1/m; a is the radius of the source, in m; R is the acoustic insulation of the shield, in dB.

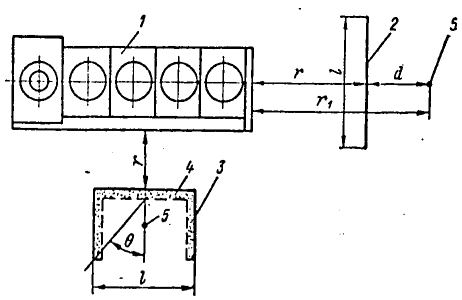

Figure 10.13. Diagram (in plan) of shield that shields work position from engine noise: 1 -- engine; 2 -- plane shield; 3 -- plane shield with hood; 4 -- soundproofing; 5 -- calculation point (work place).

Plane Shield in Room. Effectiveness ΔL_s, in dB, of a shield in a room for a nondirectional noise source is calculated by the formula

$$\Delta L_э = 10\lg\frac{\Phi_н Q + 50r_1^2}{\frac{\Phi_н Q}{25N} + 50r_1^2(1 - \alpha_э K_п)}, \qquad (10.6.4)$$

APPROVED FOR RELEASE: 2007/02/08: CIA-RDP82-00850R000200100009-9

APPROVED FOR RELEASE: 2007/02/08: CIA-RDP82-00850R000200100009-9

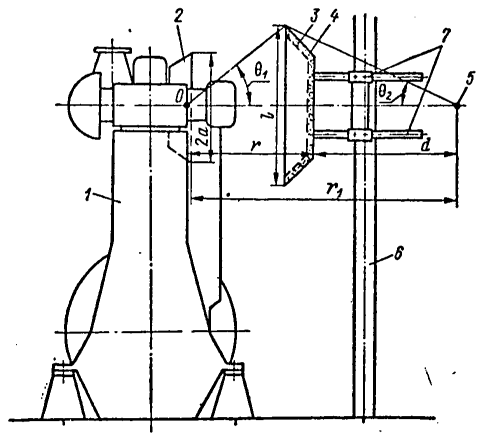

Figure 10.14. Diagram of turbocharger shield: 1 -- engine; 2 -- turbocharger; 3 -- plane shield with shroud; 4 -- soundproofing; 5 -- calculation point; 6 -- post; 7 -- fasteners.

where Φ_n is the front to rear ratio, which characterizes the location of a nondirectional noise source in a room: near the center of a room $\Phi_n = 1$, in the center of one of the walls $\Phi_n = 2$, on the surface of two walls at mid-height of a room $\Phi_n = 4$, and in the corner of a room $\Phi_n = 8$; $r_1 = r + d$ is the distance between the noise source and the calculation point behind the shield, in m; α_s is the sound absorption coefficient of the surface of the shield facing the source; $K_c = b/r_c < 1$ is a coefficient that takes into account the coverage of the noise source by the shield (the dimensions b and r_c are indicated in Figure 10.17); Q is a constant of the room (see §15.3).

If the shield is coated with a soundproofing material on the noise source side and is set up in the area where direct noise is strongest ($r \leq r_{sur}$)

[гр=sur]

$$r_{гр} = 0{,}14\sqrt{\Phi_н Q}, \qquad (10.6.5)$$

then there will be a reduction ΔL_{so} of the noise of the source, which must be taken into consideration for points outside of the shielded zone. This reduction ΔL_{so}, in dB, is determined by the formula

[и=so; п=c]

$$\Delta L_и = -10\lg(1 - \alpha_э K_п). \qquad (10.6.6)$$

APPROVED FOR RELEASE: 2007/02/08: CIA-RDP82-00850R000200100009-9

APPROVED FOR RELEASE: 2007/02/08: CIA-RDP82-00850R000200100009-9

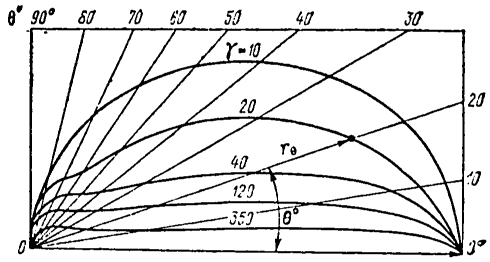

Figure 10.15. Diagram for determining shielding of directional noise source.

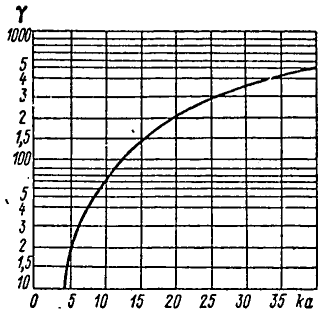

Figure 10.16. Diagram for determining axial concentration coefficient of noise source.

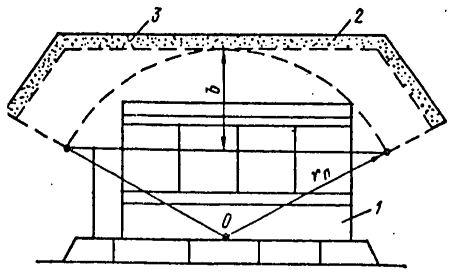

Figure 10.17. Diagram of coverage of nondirectional noise source by shield: 1 -- engine; 2 -- shield with shroud; 3 -- soundproofing.

Effectiveness $\Delta L_{s.d}$, in dB, of a shield in a room with a directional noise source is

APPROVED FOR RELEASE: 2007/02/08: CIA-RDP82-00850R000200100009-9

APPROVED FOR RELEASE: 2007/02/08: CIA-RDP82-00850R000200100009-9

[э=s; н=d]

$$\Delta L_{э.н} = 10 \lg \frac{\gamma Q + 50 r_1^2}{\gamma Q \Phi^2(\theta) + 50 r_1^2 [1 - \alpha_э (1 - \Phi(\theta))]}. \quad (10.6.7)$$

Enclosure Shield on Open Deck. Shield effectiveness $\Delta L_{s.e}$ for a nondirectional noise source is calculated by the formula

[o=e]

$$\Delta L_{э.о} = \Delta L_э + 10 \lg \frac{1}{1 - \cos\theta}, \quad (10.6.8)$$

where ΔL_s is the effectiveness of a plane shield, in dB, determined graphically (Figure 10.12); θ is the angle of the shield (Figure 10.13).

For a directional noise source effectiveness $\Delta L_{s.e.d}$, in dB, is

$$\Delta L_{э.о.н} = \Delta L_{э.н} + 10 \lg \frac{1}{1 - \cos\theta}, \quad (10.6.9)$$

where $\Delta L_{s.d}$ is the effectiveness of a plane shield, determined by formula (10.6.3).

Enclosure Shield in Room. The effectiveness of an enclosure in a room for a nondirectional noise source is calculated by the formula

[cp=av]

$$\Delta L_{э.о} = 10 \lg \frac{S_э \alpha_{ср.э} (\Phi_н Q + 50 r^2)}{50 r^2 S_0}, \quad (10.6.10)$$

where S_s is the total area of the shield enclosures, including the opening, in m^2; S_0 is the area of the opening, in m^2; $\alpha_{av.s}$ is the average sound absorption coefficient in the enclosure (for calculations one may use $\alpha_{av.s} = 1$ for an opening, $\alpha_{av.s} = 0.1$ for wood surfaces, $\alpha_{av.s} = 0.07$ for metal surfaces, and $\alpha_{av.s} = 0.04$ for glazed surfaces).

For a directional noise source $\Delta L_{s.c.d}$, in dB, is given by the formula

[п=c; c=w]

$$\Delta L_{э.п.н} = 10 \lg \frac{(\gamma Q + 50 r^2) \cdot 10^{0.1R} + S_э \alpha_{ср.э}}{50 r^2 (S_c + S_0 \cdot 10^{0.1R}) + \gamma S_c Q}, \quad (10.6.11)$$

where S_w is the area of the walls of the enclosure, in m^2.

The acoustic effect of an enclosure, installed in a room, regardless of the type of noise source, can be increased by aiming the opening toward a wall lined with soundproofing, or by installing a special shield with soundproofing [15]. This increase $\Delta L_{s.e.b}$, in dB, is

[k=b]

$$\Delta L_{э.о.к} = -10 \lg \frac{4 a_к (1 - \alpha_к)(a_к - t)}{(2 a_к - t)^2}, \quad (10.6.12)$$

APPROVED FOR RELEASE: 2007/02/08: CIA-RDP82-00850R000200100009-9

APPROVED FOR RELEASE: 2007/02/08: CIA-RDP82-00850R000200100009-9

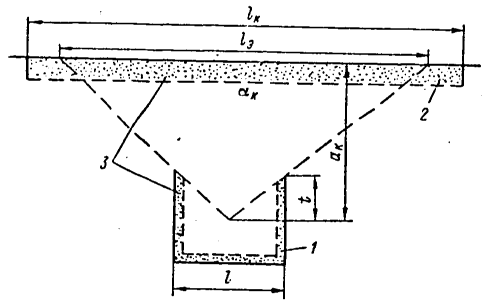

Figure 10.18. Diagram of barrier in front of partly open bulkhead: 1 -- bulkhead; 2 -- barrier; 3 -- soundproofing.

where α_b is the sound absorption coefficient of the liner of the barrier or special shield; a_b, t are linear dimensions (Figure 10.18).

Formula (10.6.12) is valid for the conditions $l \leq a$ and $l_b \geq l_s$.

Closed Booth. The effectiveness of a closed booth in terms of air noise ΔL_b, in dB, is calculated for any type of source by the formula

$$\Delta L_к = -10 \lg \sum_{i=1}^{n} \frac{S_i}{10^{0,1R_i} \alpha_{ср} S_n}, \qquad (10.6.13)$$

where S_i is the area of the i-th wall of the booth, in m^2; R_i is the acoustic insulation of the i-th wall, in dB; α_{av} is the average sound absorption coefficient in the booth; S_c is the total enclosure are of the booth, in m^2; n is the number of enclosures exposed to noise.

Data on the effectiveness of local sound reduction devices (shields and booths) are presented in Table 10.9 for directional and nondirectional sources: turbochargers, engines, etc. The data are based on measurements (see Figure 10.14 for designations).

10.7. Acoustic Insulation of Ship Machinery

The problem of reducing noise on ships to established standards can be solved most economically in many cases by using special soundproofing devices (SPD), which form a closed soundproofing shield around the source.

The basic parts of sound-insulating systems are the frame and wall panels. The structure also includes hardware, with which the panels are installed, fastened to the frame and connections are sealed. SPD also must have

APPROVED FOR RELEASE: 2007/02/08: CIA-RDP82-00850R000200100009-9

APPROVED FOR RELEASE: 2007/02/08: CIA-RDP82-00850R000200100009-9

Table 10.9. Effectiveness of Shields and Booths, dB

Local noise reduction device and installation features	Structural design and measurement conditions	Frequencies of octave bands, Hz					
		250	500	1,000	2,000	4,000	8,000
Plane shield in open space 0.5 m from directional noise source (a = 0.2 m)	1. Shield dimensions 1 × 1 m, material -- plywood (δ = 10 mm)						
	d = 0.5 m	3	2	15	21	33	31
	d = 1.5 m	0	1	10	20	29	27
	2. Shield dimensions 0.5 × 0.3 m, material -- plywood (δ = 10 mm)						
	d = 0.5 m	0	0	3	7	13	16
	d = 1 m	0	0	3	6	12	7
Plane shield in open space 0.5 m from nondirectional noise source	Shield dimensions 1 × 1 m, material -- plywood (δ = 10 mm)						
	d = 0.5 m	0	3	10	14	12	14
	d = 1 m	0	2	10	12	10	12
Plane shield in engine room of cargo motor ship 1.5 m from engine	Shield dimensions 1 × 1.5 m, material -- steel (δ = = 2 mm), room constant Q = = 50-300 m^2						
	d = 0.7 m	0	2	3	4	7	6
Plane shield with soundproofing in engine room of motor tugboat over engine (r = 0.4 m)	Shield dimensions 1 × 1.2 m, material -- steel (δ = = 1.5 mm), soundproofing -- staple glass fiber (δ = = 50 mm)						
	d = 0.3 m	2	5	6	6	6	5
	Engine noise reduction	1	2	2	3	2	4
Plane shield in room 0.5 m from directional noise source (a = 0.2 m)	Shield dimensions 1 × 1 m, material -- plywood (δ = 4 mm), soundproofing -- staple glass fiber (δ = 50 mm), room constant Q = 30-70 m^2: shield without soundproofing (d = = 0.5 m)	0	2	2	11	21	23
	shield with soundproofing	0	2	10	14	24	26

APPROVED FOR RELEASE: 2007/02/08: CIA-RDP82-00850R000200100009-9

APPROVED FOR RELEASE: 2007/02/08: CIA-RDP82-00850R000200100009-9

Table 10.9 (continued)

Local noise reduction device and installation features	Structural design and measurement conditions	Frequencies of octave bands, Hz					
		250	500	1,000	2,000	4,000	8,000
Plane shield with soundproofing installed in engine room of cargo motor ship 0.5 m from turbocharger of engine	Shield dimensions 1 × 1 m, material -- steel (δ = 1.5 mm), soundproofing -- staple glass fiber (δ = 40 mm); on background of mechanical engine noise (d = 1m)	0	0	5	11	12	14
Enclosure with soundproofing, installed in room	Shield dimensions 2 × 1 × 0.7 m, material -- plywood (δ = 4 mm), soundproofing -- VT-3 (δ = 30 mm), room constant Q = 30-70 m^2 r = 0.8 m	7	8	9	9	10	12
	in center of enclosure r = 2.3 m	4	4	5	5	6	7
Boiler partition (open at top), installed in engine room of cargo motor ship 1.5 m from engine	Partition dimensions 3 × 3 × 2.5 m, material -- steel (δ = 3 mm); at center of partition	3	4	5	5	4	6
Soundproof SEU control center, permanently installed in engine room of motor tugboat (engines and diesel generators on shock absorbers)	Dimensions of booth 5 × 3 × 2.5 m, construction of booth: steel (δ = 4 mm), foam plastic FF (δ = 40 mm), plywood (δ = 4 mm), plastic (δ = 1.5 mm), double glazed windows (δ = 5 mm), in center of booth	25	27	29	32	34	33
Soundproof control booth installed in engine room of floating crane on AKSSM shock absorbers	Booth dimensions 1.8 × 1.3 × 2 m, construction of booth enclosure steel (δ = 5 mm); foam plastic FF (δ = 40 mm), rock wool (δ = 50 mm),						

APPROVED FOR RELEASE: 2007/02/08: CIA-RDP82-00850R000200100009-9

APPROVED FOR RELEASE: 2007/02/08: CIA-RDP82-00850R000200100009-9

Table 10.9 (continued)

Local noise reduction device and installation features	Structural design and measurement conditions	Frequencies of octave bands, Hz					
		250	500	1,000	2,000	4,000	8,000
	steel (δ = 2 mm), double glazed windows (δ = 4 mm), in center of booth	30	32	34	36	38	45

Comment. The measured effectiveness of soundproofing systems is zero on frequencies of 63-125 Hz, and the effectiveness of soundproof booths is 20-23 dB.

devices that prevent an unacceptable increase of temperature and pressure and dangerous concentration of oil vapors in the space under state rooms, and also serve for venting vapors and for repairing leaks in systems. The effective acoustic insulation of passages through SPD walls for engine control levers and mounts, and of fasteners that tie the entire sound-insulating system to the foundation, is extremely important.

However, the main sound-insulating elements are the panels, which along with the frame form the walls of the device (here the frame plays a secondary role). The frames of all soundproofing devices are multihinged rolled steel rod frames. Transverse connections with longitudinal connections and with the base frame are made detachable.

SPD are made in the shape of shallow boxes and consist of a main skin, body, soundproofing material and perforated liner. A typical SPD wall panel is illustrated in Figure 10.19. The main skin functions as the sound-insulating element. It is made of thin sheet metal and reinforced plastic and is designed as a "sandwich" structure (alternating layers of metal and polymer). The panel body forms the side walls and serves to increase the rigidity and to protect the soundproofing material along the edges of the panel. The metal parts of the panel are argon arc-welded and spot welded on cement. This kind of connection assures not only the necessary rigidity, but also air tightness, without producing great thermal deformations.

The sound-absorbing elements of the panel are made in the form of packages. Their shape and length and width dimensions match the panel cells into which they are inserted. The packages should not be less than 50 mm thick. A material based on ultrafine glass or rock wool is recommended as the soundproofing. The packages are waterproofed with films, which should not be more than 25 micron thick. A perforated aluminum-magnesium alloy liner, not thicker than 1 mm, is placed on the inside of the panel. The perforations should cover 25% of the total liner area. The liner holds the soundproofing material in the panel and protects it from mechanical damage.

APPROVED FOR RELEASE: 2007/02/08: CIA-RDP82-00850R000200100009-9

APPROVED FOR RELEASE: 2007/02/08: CIA-RDP82-00850R000200100009-9

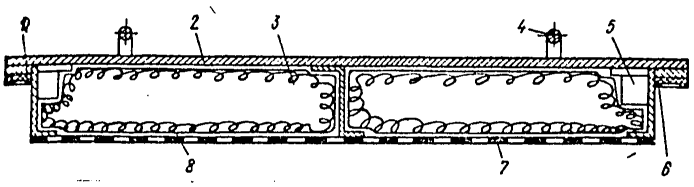

Figure 10.19. Typical soundproofing device wall panel:
1 -- panel body; 2 -- main skin; 3 -- soundproofing material; 4 -- handle; 5 -- lock; 6 -- gasket; 7 -- interior perforated liner; 8 -- protective film.

Panel to frame connections may be sealed by the most popular and easiest technique -- with elastic soft porous gaskets with closed pores. The space between the engine and soundproofing device walls may be ventilated through a system of special channels. Ventilation by natural convection usually is not enough to assure the necessary air exchange. Therefore a combined system, in which two low-pressure fans are used in addition to natural ventilation, are often utilized in soundproofing devices. Air is circulated into and from the space under rooms through special mufflers. The design of such a muffler is shown in Figure 10.20. As can be seen in the figure, the panels with the ventilation channels are in the form of thin-wall boxes, but the walls are higher than the panels of the SPD itself, and one solid and two perforated liners are additionally installed on the inside of each wall, parallel to the outside liner. The height of the ventilation channel is 25 mm and width is 210 mm. The slot-like cross section of the channel and its great length provide adequate sound insulation.

Special seals (Figure 10.21) are installed to prevent sound from penetrating from the space under cabins through pipe and cable holes. Small pipes are combined into bundles, each of which is drawn through one seal.

It is also important to take measures to limit the shifting of soundproofing devices during rolling and vibration. This is best done by installing fasteners that hold SPD to the foundation of vibration-damping elements. The foundation for SPD, as is shown in Figure 10.22, may be: the ship foundation (Figure 10.22a); engine block (Figure 10.22b); intermediate frame (Figure 10.22c). However, because the required vibration insulation of a fastener increases with the level of vibration of the foundation, preference should be given to fastening to the ship foundation.

Measurements of the acoustic effect of the noise reduction of SPD for a ship compressor disclosed (Figure 10.23) that SPD reduces noise in a wide frequency range by an average of 17 dB (curve 1). This applies to all versions of testing (different suspensions, perforated or solid liner, soundproofed panels and panels without soundproofing), except one, when the compressor draws air from the space under the cabins; in this case the effectiveness of a system decreases on low frequencies by about 10 dB (Figure 10.23, curve 2). On medium and high frequencies the noise reduction effect is the same.

APPROVED FOR RELEASE: 2007/02/08: CIA-RDP82-00850R000200100009-9

APPROVED FOR RELEASE: 2007/02/08: CIA-RDP82-00850R000200100009-9

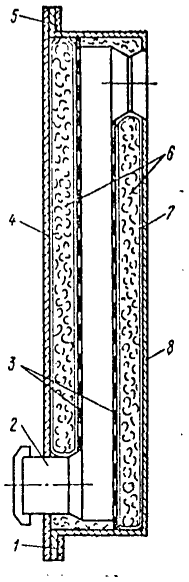

Figure 10.20. Noise muffler (wall panel of ventilation channel): 1 -- frame; 2 -- outside branch; 3 -- perforated liner; 4 -- main skin; 5 -- gasket; 6 -- soundproofing material; 7 -- protective film; 8 -- inside liner.

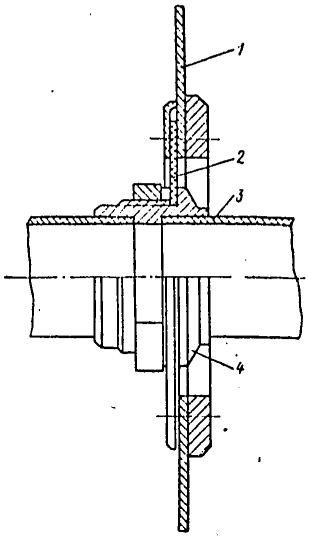

Figure 10.21. Soundproof gasket for passage of pipe through wall of hood: 1 -- main liner; 2 -- rubber diaphragm; 3 -- pipe; 4 -- seal.

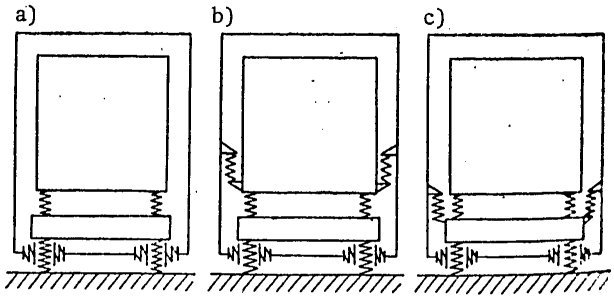

Figure 10.22. Diagrams showing how soundproof hood is fastened: a -- to ship foundation; b -- to engine block; c -- to intermediate frame.

APPROVED FOR RELEASE: 2007/02/08: CIA-RDP82-00850R000200100009-9

APPROVED FOR RELEASE: 2007/02/08: CIA-RDP82-00850R000200100009-9

Other important results of measurements of the effectiveness of SPD are presented in Figure 10.24. Curve 1 corresponds to the case when external pipes are not insulated and the walls are not sealed. The use of SPD reduced noise by 2-13 dB in the medium- and high-frequency ranges in the absence of pipes and connections (Figure 10.24, curve 2). Sealing slots and holes in places where the panels are next to the block, on the floor and around locks increase the effectiveness of SPD by another 5-8 dB on high frequencies (Figure 10.24, curve 3). The described measures substantially increased the acoustic insulation of SPD, but the maximum possible acoustic insulation for a given wall structure still could not be achieved (Figure 10.24, curve 4). In real SPD structures, obviously, if acoustic insulation is incorporated in the design of the machine itself, all kinds of mechanical noise can be reduced to acceptable levels. The acoustic insulation of machinery saves more materials and space in the hull of a ship than the acoustic insulation of rooms. The combining of machinery into modules substantially reduces the cost of acoustic insulation and improves its reliability and effectiveness.

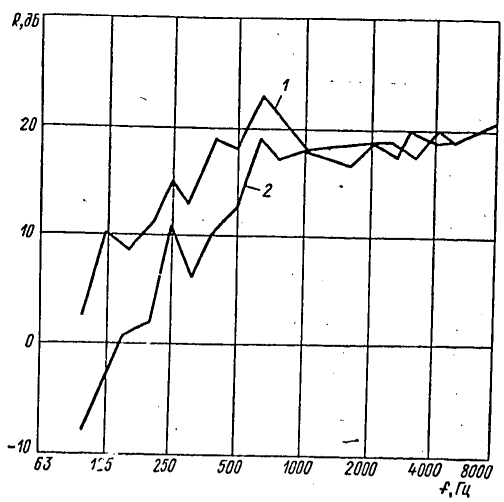

Figure 10.23. Effectiveness of unsealed soundproofing system: 1 -- air drawn from outside of soundproofing device through muffler; 2 -- air drawn from basement space of soundproofing device. [дБ=dB; Гц=Hz]

APPROVED FOR RELEASE: 2007/02/08: CIA-RDP82-00850R000200100009-9

APPROVED FOR RELEASE: 2007/02/08: CIA-RDP82-00850R000200100009-9

Table 10.10. Basic Materials for Soundproofing Structures

1) Наименование материала	2) Плотность (объемная масса) ρ_m, кг/м³	3) Динамический модуль упругости E, Н/м²	4) Коэффициент Пуассона μ	5) Коэффициент внутренних потерь η	6) Скорость продольных звуковых волн в стержнях $c_п$, м/с	7) Удельное акустическое сопротивление $\rho_m c_п$, кг/(м²·с)	8) Характеристика горючести по данным СНИЛ ВНИИПО	Условия применения материала по данным Министерства здравоохранения СССР: 9) 10) насыщенность (не более)	11) температура °С (не более)	12) воздухообмен
13) Алюминиевые сплавы (ГОСТ 4784—74)	2800	$7,2\cdot10^{10}$	0,30	$5\cdot10^{-4}$	5100	$1,4\cdot10^{7}$	Негорючий 14)	—	—	—
15) Армоцемент и железобетон	2500	—	—	$1,0\cdot10^{-2}$	—	—	»	—	—	—
	2600	—	—	$1,0\cdot10^{-2}$	—	—	» 17)	—	—	—
16) Листовой конструкционно-отделочный стеклопластик марки ЛТСД	1800	$1,4\cdot10^{10}$	—	$1,0\cdot10^{-2}$	2800	$5,0\cdot10^{6}$	Трудногорючий (K = 0,47)	3,5 м²/м³ 20)	50	18) Трехкратный
19) Материал слоистый листовой ВИПОНИТ	2500	—	—	$2,0\cdot10^{-1}$	—	—	— 23)	11 м открытых кромок на 1 м³	60	Четырехкратный
22) Пиломатериалы хвойных пород (ГОСТ 8486—66)	510	$1,17\cdot10^{10}$	0,45	$1,5\cdot10^{-2}$	4800	$2,5\cdot10^{6}$	Трудногорючий (после глубокой пропитки антипиреном), $K = 0,21\div0,27$	—	—	21) —
24) Пластик для судостроения бумажно-слоистый декоративный трудносгораемый	1400	—	—	—	—	—	25) Трудногорючий ($K = 0,43\div0,48$, J = 2)	—	—	—
26) Пластик трудносгораемый бумажно-слоистый	1400	$1,3\cdot10^{10}$	0,30	$2,0\cdot10^{-2}$	3100	$4,3\cdot10^{6}$	Трудновоспламеняющийся ($K = 0,96\div1,12$, $J = 21,4\div24,6$)	27) Допущен после термообработки		
28) Плиты негорючие конструкционно-отделочные. Асбосилит	800	$3\cdot10^{9}$	0,56	$1,0\cdot10^{-2}$	1900	$1,5\cdot10^{6}$	Негорючий 14)	—	—	—
29) Сталь	7800	$21\cdot10^{10}$	$2,0\cdot10^{-1}$	$1,0\cdot10^{-4}$	5200	$4,0\cdot10^{7}$	»	—	—	—
30) Стекла для судовых иллюминаторов: закаленные (ГОСТ 9421—71) и незакаленные (ГОСТ 1041—58)	2500	$6,7\cdot10^{10}$	—	$3,0\cdot10^{-3}$	5200	$1,3\cdot10^{7}$	»	—	—	—
31) Стекло органическое конструкционное (ГОСТ 15809—70)	1180	$4,3\cdot10^{9}$	$4,0\times10^{-1}$	$2,5\cdot10^{-2}$	6000	$7,1\cdot10^{6}$	32) Горючий	0,02 кг/м²	28	—
33) Стеклопластик на основе полиэфирной смолы	1700	$2,1\cdot10^{10}$	$1,0\times10^{-1}$	$1,3\cdot10^{-2}$	3500	$6,0\cdot10^{7}$	25) Трудновоспламеняющийся (K = 1,0, J = 17)	—	—	—

[Key on next page]

APPROVED FOR RELEASE: 2007/02/08: CIA-RDP82-00850R000200100009-9

APPROVED FOR RELEASE: 2007/02/08: CIA-RDP82-00850R000200100009-9

Key to Table 10.10:

1. Material
2. Density ρ_m, kg/m^3
3. Dynamic elasticity modulus E, N/m^2
4. Poisson's ratio μ
5. Internal loss coefficient η
6. Longitudinal acoustic wave velocity in rods c_{lo}, m/s
7. Specific acoustic resistance $\rho_m c_{lo}$, kg/(m^2·s)
8. Combustibility according to SNIL VNIIPO [not further identified] data
9. Application of material according to data of USSR Ministry of Health
10. installation density (not to exceed)
11. temperature, °C (not to exceed)
12. air exchange
13. Aluminum alloys (GOST 4784-74)
14. Incombustible
15. Reinforced cement and reinforced concrete
16. Grade LTSD finishing glass-reinforced plastic
17. Flame-retardant
18. Triple
19. VIPONIT laminated sheet
20. 11 m of exposed edges per cubic meter
21. Quadruple
22. Pine lumber (GOST 8486-66)
23. Flame-retardant (after pressure treatment with antipyrine)
24. Shipbuilding plastic, flame-retardant decorative cardboard
25. Flame-retardant
26. Flame-retardant plastic, cardboard
27. Acceptable after heat treatment
28. Incombustible finishing panels. Asbosilit
29. Steel
30. Porthole glass (GOST 9421-71) and untempered glass (GOST 1041-58)
31. Construction organic glass (GOST 15809-70)
32. Combustible
33. Polyester-base glass-reinforced plastic

APPROVED FOR RELEASE: 2007/02/08: CIA-RDP82-00850R000200100009-9

APPROVED FOR RELEASE: 2007/02/08: CIA-RDP82-00850R000200100009-9

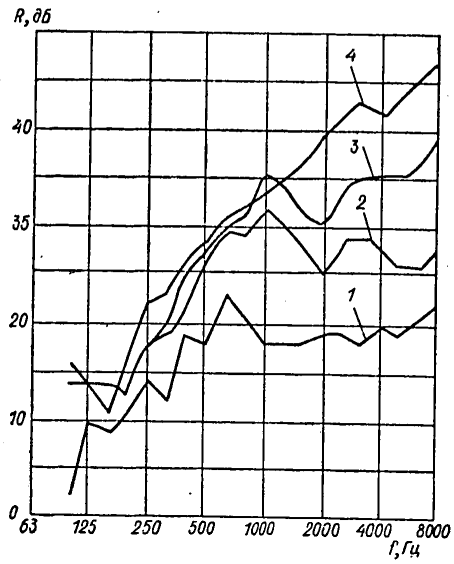

Figure 10.24. Effectiveness of sealed soundproofing system: 1 -- before sealing and insulation of pipes; 2 -- after insulation of pipes; 3 -- after additional sealing of connections; 4 -- maximum effectiveness, achieved under laboratory conditions. [дБ=dB; Гц=Hz]

10.8. Materials for Marine Acoustic Insulation and Soundproofing Structures[1]

The materials used for reducing noise on ships must meet a whole set of requirements, including efficiency, manufacturability, performance reliability, ergonomic suitability and other indices. The general requirements are incombustibility (at least flame retardant) and nontoxicity. The use of materials that do not meet these requirements is prohobited or strictly limited.

Materials for Sound-Insulating Structures. The materials that are used in sound-insulating structures are divided by purpose and acoustic effect into main and auxiliary. Main materials include sheet materials, used for making hull structures and for finishing rooms: metals, reinforced concrete, reinforced cement, asbosilit, plywood, laminated plastics, glass, etc. Auxiliary materials include decking and vibration-absorbing carpets, heat insulation, air space fillers for double-wall soundproofing structures, vibration-insulating spacers, etc.

[1]This section was written by V. M. Frolkova with G. S. Beregova and T. A. Firkovich.

APPROVED FOR RELEASE: 2007/02/08: CIA-RDP82-00850R000200100009-9

APPROVED FOR RELEASE: 2007/02/08: CIA-RDP82-00850R000200100009-9

Table 10.11. Basic Materials for Soundproofing Structures

Material	Description of material	Density, kg/m^3	Dimensions, m		
			length	width	thickness
Grade ATM-1 heat insulation	Mat consisting of layer of loose superfine staple glass fibers, bonded with phenol formaldehyde resin, and cemented to aluminum foil, PETF polyethylene terephthalate film or STF impregnated glass fiber cloth (or uncemented). No. 20 low-boron glazed fiber	$0.01 \cdot 10^3$	5.5-6.0	0.55-0.60	0.020; 0.025; 0.030; 0.040; 0.050 (at pressure of 100 N/m^2
Grade BZM sound-absorbing products	Mats made of layer of loose staple long-fiber superfine basalt fibers not smaller than 1 and not larger than 3 micron in diameter, lined with glass cloth	$(0.02-0.03) \cdot 10^3$	0.5-1.0	0.5-1.0	0.030-0.200
Discharge-free rock wool soundproofing panels	Ready-made for assembly, manufactured in two grades:				
	ZP/O - with perforated face	190	0.5	0.5	0.020
	ZP/S - with nonperforated face	150	0.5	0.5	0.020

APPROVED FOR RELEASE: 2007/02/08: CIA-RDP82-00850R000200100009-9

APPROVED FOR RELEASE: 2007/02/08: CIA-RDP82-00850R000200100009-9

The nomenclature, classification and characteristics of basic materials, approved by the USSR Ministry of Health for use in ship rooms, are listed in Table 10.10, where the average internal loss coefficients and elasticity moduli of materials are given for the 100 to 2,000 Hz frequency range at 20°C. The combustibility index K of the materials according to GOST 17088-71 is indicated and combustibility groups (J) according to the Rules of the USSR Register are explained.

Materials for Soundproofing Structures. The materials used in soundproofing structures are classified by purpose and acoustic effect as basic sound-absorbing, and auxiliary materials. Basic materials are indicated in Table 10.11. The best in terms of properties (efficiency, incombustibility, nontoxicity, weight and manufacturability) are mats made of superfine glass and basalt fiber.

Table 10.12. Acoustic Characteristics of ATM-1 Heat- and Acoustic Insulation (Density 10 kg/m^3)

1) Частота звука, Гц	2) Коэффициент распространения $\gamma_m = \alpha_m + i\beta_m$, 1/м	3) Волновое сопротивление $W_m = W_{rm} + iW_{im}$
250	3,2+i6,0	2,40—i1,0
315	4,8+i9,0	2,20—i0,75
400	6,0+i13,5	2,00—i0,55
500	8,0+i18,0	1,85—i0,48
630	10,0+i21,0	1,80—i0,40
800	12,0+i26,0	1,75—i0,38
1000	14,2+i32,0	1,70—i0,35
1250	16,1+i38,0	1,62—i0,31
1600	18,0+i44,0	1,60—i0,30
2000	19,8+i51,0	1,58—i0,29
2500	20,5+i60,0	1,50—i0,27
3150	21,0+i69,0	1,50—i0,25
4000	22,0+i74,0	1,50—i0,25
5000	22,0+i80,0	1,50—i0,25
6300	22,0+i82,0	1,50—i0,25
8000	22,0+i84,0	1,50—i0,25

Table 10.13. Acoustic Characteristics of Ultrasuperfine Basalt Fiber Cloth and Grade BZM Products (Density 17-20 kg/m^3)

1) Частота звука, Гц	2) Коэффициент распространения $\gamma_m = \alpha_m + i\beta_m$, 1/м	3) Волновое сопротивление $W_m = W_{rm} + iW_{im}$
250	8,0+i18,0	3,72—i1,00
315	9,0+i19,0	3,75—i1,05
400	10,0+i20,0	3,70—i1,11
500	11,0+i22,0	3,63—i1,20
630	14,0+i25,0	3,56—i1,31
800	17,0+i29,0	3,42—i1,47
1000	25,0+i33,0	3,12—i1,55
1250	29,0+i39,0	2,64—i1,54
1600	32,0+i46,0	2,43—i1,46
2000	34,0+i54,0	2,27—i1,25
2500	35,0+i63,0	2,14—i1,10
3150	36,0+i71,0	2,03—i0,97
4000	37,0+i78,0	1,94—i0,86
5000	38,0+i85,0	1,85—i0,78
6300	38,0+i93,0	1,77—i0,70
8000	38,0+i100,0	1,72—i0,65

Key: 1. Frequency of sound, Hz
2. Propagation coefficient
3. Wave impedance

The acoustic characteristics of the basic sound-absorbing materials are listed in Tables 10.12-10.14. Auxiliary materials include films for lining sound-absorbing materials (Table 10.15).

The physical mechanism of the absorption of sound by sound-absorbing materials is examined in Chapter 11.

10.9. Measurement of Acoustic Insulation

The acoustic insulation of ship bulkheads can be measured with sufficient accuracy and reliability with the aid of the system illustrated in

APPROVED FOR RELEASE: 2007/02/08: CIA-RDP82-00850R000200100009-9

APPROVED FOR RELEASE: 2007/02/08: CIA-RDP82-00850R000200100009-9

Table 10.14. Acoustic Characteristics of Soundproofing Discharge-Free Rock Wool Panels (Density 130 kg/m^3)

1) Частота звука, Гц	2) Коэффициент распространения $\gamma_m = \alpha_m + i\beta_m$, 1/м	3) Волновое сопротивление $W_m = W_{rm} + iW_{im}$
250	17,0+i13,0	1,80−i1,94
315	18,0+i16,0	1,75−i1,80
400	18,0+i20,0	1,72−i1,62
500	19,0+i24,0	1,69−i1,48
630	20,0+i46,0	1,65−i1,23
800	21,0+i34,0	1,60−i1,14
1000	22,0+i39,0	1,50−i1,00
1250	24,0+i43,0	1,40−i0,87
1600	28,0+i48,0	1,30−i0,78
2000	31,0+i54,0	1,24−i0,70
2500	37,0+i60,0	1,18−i0,65
3150	41,0+i65,0	1,15−i0,62
4000	45,0+i71,0	1,13−i0,58
5000	48,0+i76,0	1,12−i0,55
6300	50,0+i82,0	1,10−i0,54
8000	52,0+i87,0	1,09−i0,50

Key: 1. Frequency of sound, Hz
2. Propagation coefficient
3. Wave impedance

Figure 10.25. Both acoustic measurement chambers of the instrument (or one of them) are mounted on wheels, so that complex structures of any length can be measured by placing them between chambers. By virtue of the mobility of the chambers it is possible to use them independently of each other with real noise sources. The boundary conditions in the chambers for testing an object can be regulated and adjusted with a special mechanism.

A schematic diagram of an instrument for measuring acoustic insulation is shown in Figure 10.26. Each chamber may be both a high-level, and a low-level chamber. The acoustic system produces high-intensity noise through loudspeakers; there is also a mechanical noise generator. The entire metering process is controlled from a remote control panel.

With an acoustic insulation meter it is possible to check a variety of ship structures: sound-insulating panels, windows, portholes, etc. The acoustic insulation of large structures should be measured with this instrument on models.

To determine the experimental values of acoustic insulation it is necessary to measure the energy levels of acoustic pressure L_1 in the high-level chamber, L_2 in the low-level chamber, and reverberation time T. The R values of acoustic insulation, in dB, are determined for a given frequency band by the formula

$$R = L_1 - L_2 + 10 \lg \frac{ST}{0{,}16V}, \qquad (10.9.1)$$

where S is the area of the opening between the chambers, in m^2; V is the volume of the low-level chamber, in m^3.

Instruments for measuring acoustic insulation are described in detail in the literature [9], and the determination of the acoustic insulation measurement precision is examined in [2].

APPROVED FOR RELEASE: 2007/02/08: CIA-RDP82-00850R000200100009-9

APPROVED FOR RELEASE: 2007/02/08: CIA-RDP82-00850R000200100009-9

Table 10.15. Properties of Films for Facing Loose Fiber Materials in Soundproofing Structures

1) Наименование материала	2) Плотность, кг/м³	3) Размеры, м		6) Масса 1 м², кг	7) Предел прочности при растяжении, Н/м² (не менее)	8) Паропроницаемость, кг/(м²·сут)	9) Характеристика горючести пленки по данным СНИЛ ВНИИПО	10) Условия применения пленки по данным Министерства здравоохранения СССР	
		4) толщина	5) ширина					11) насыщенность, м²/м²	12) температура, °С
13) Пленка полиамидная ПМ	1420	$40 \cdot 10^{-6}$	1,20	0,057	$1000 \cdot 10^5$	$1,70 \cdot 10^2$	14) Трудногорючая ($K < 0,2$; $J = 0$)	2	100
15) Пленка типа Саран (Крехалон)	1650	$30 \cdot 10^{-6}$	0,6—0,8 16) (до 1,6 в развернутом виде)	0,049	$650 \cdot 10^5$	$0,40 \cdot 10^{-2}$	17) Трудновоспламеняющаяся ($K < 0,57$; $J < 1$)	—	—
18) Стеклоткань марки СТФ	1000	$50 \cdot 10^{-6}$	0,65	0,050	19) Прочность на разрыв полоски $(25 \times 100) \cdot 10^{-6}$ м не менее 90 Н	$1,07 \cdot 10^{-2}$	20) Трудногорючая ($K = 0,42$)	1	60
21) Пленка полиэтилентерефталатная:									
22) общего назначения	1400	$25 \cdot 10^{-6}$ $50 \cdot 10^{-6}$	1,50	0,035 0,070	$1300 \cdot 10^5$	$0,80 \cdot 10^{-2}$ $0,25 \cdot 10^{-2}$	23) Горючая	2	60
24) электроизоляционная	1400	$25 \cdot 10^{-6}$	0,65	0,035	$1200 \cdot 10^5$	—		1	100
25) Пленка полиэтиленовая (ГОСТ 10354—63)	930	$25 \cdot 10^{-6}$ $50 \cdot 10^{-6}$	1,4	0,023 0,046	$100 \cdot 10^5$	$0,20 \cdot 10^{-2}$ $0,16 \cdot 10^{-2}$	26) Горючая	—	—

[Key on next page]

APPROVED FOR RELEASE: 2007/02/08: CIA-RDP82-00850R000200100009-9

APPROVED FOR RELEASE: 2007/02/08: CIA-RDP82-00850R000200100009-9

Key to Table 10.15:

1. Material
2. Density, kg/m^3
3. Dimensions, m
4. thickness
5. width
6. Weight per 1 m^2, kg
7. Tensile strength, N/m^2 (not less than)
8. Vapor permeability, $kg/(m^2 \cdot day)$
9. Combustibility of film according to SNIL VNIIPO data
10. Application of film according to data of USSR Ministry of Health
11. installation density, m^2/m^3
12. temperature, °C
13. PM polyamide film
14. Flame-retardant
15. Saran type film (Krekhalon)
16. (up to 1.6 unrolled)
17. Flame-retardant
18. Grade STF glass fiber cloth
19. Rupture strength of strip $(25 \times 100) \cdot 10^{-6}$ m not less than 90 N
20. Flame-retardant
21. Polyethylene terephthalate film:
22. general purpose
23. Combustible
24. electrical insulation
25. Polyethylene film (GOST 10354-63)
26. Combustible

APPROVED FOR RELEASE: 2007/02/08: CIA-RDP82-00850R000200100009-9

APPROVED FOR RELEASE: 2007/02/08: CIA-RDP82-00850R000200100009-9

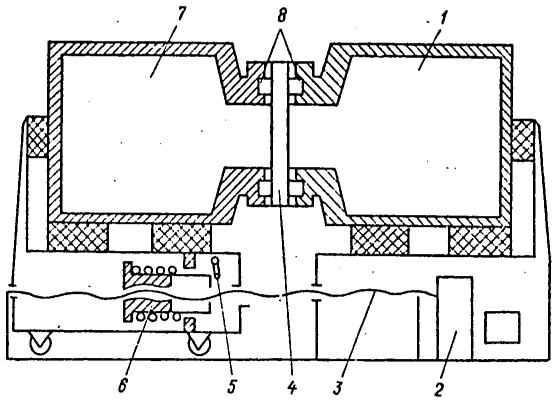

Figure 10.25. Diagram of instrument for measuring acoustic insulation: 1, 7 -- acoustic measurement chambers; 2 -- electric motor; 3, 6 -- set screw and lock nut; 4 -- test structure; 5 -- end switch; 8 -- insulators.

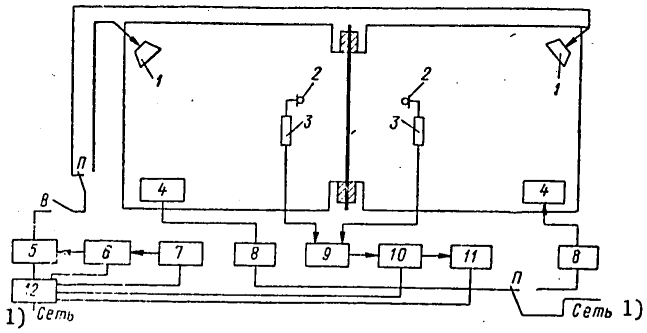

Figure 10.26. Schematic diagram of acoustic insulation meter: 1 -- acoustic radiator; 2, 3 -- microphone with preamplifier; 4 -- mechanical noise generator; 5 -- power amplifier; 6 -- acoustic filters; 7 -- white noise generator; 8 -- autotransformer; 9 -- microphone switch; 10 -- spectrometer; 11 -- level recorder; 12 -- stabilizer.
Key: 1. Line

APPROVED FOR RELEASE: 2007/02/08: CIA-RDP82-00850R000200100009-9

APPROVED FOR RELEASE: 2007/02/08: CIA-RDP82-00850R000200100009-9

10.10. Personal Acoustic Insulation Gear[1]

There are three types of acoustic insulation, or antinoise devices: internal or endaural -- earplugs, inserts and tampons which are inserted in the outer ear passage and do not require fastening; mixed or "half-plugs," worn over the entrance to the outer auditory passage and requiring fastening with a headband; outer wear or extraural -- earmuffs and helmets. Plugs, inserts or tampons are usually adequate at a total noise level not exceeding 100 dB; they reduce noise to the acceptable level. Earmuffs should be worn at a total noise level of 100 to 125 dB. If the noise exceeds 125 dB it is recommended that a helmet be worn in addition to endaural devices.

Researchers have been devoting attention in recent years to ultrafine polymer fiber, used extensively in Petryanov filter cloth (FPP-15), and made by electrostatic spinning of perchlorovinyl resin. Petryanov cloth was first used for personal noise safety purposes in the form of noise-proof tampons by A. I. Vozhzhova, V. V. Perelygin, L. S. Basova, et al. These personal safety devices passed extensive long-term tests under actual sailing conditions and produced positive results. The fabric has a fiber diameter of 1 to 1.5 micron. It is nonhygroscopic and retains its structure at temperatures up to +60°C. The noiseproof tampon is made in the form of a ball, one-half of which is drawn to a point to facilitate removal from the ear. Petryanov cloth has residual electrical resistance and sticks to the fingers. Therefore the tampon, to impart to it the tampon shape which it must retain, is coated with a thin (5 to 10 micron) elastic film consisting of 2% alcohol solution of polyvinyl butyral. By virtue of the elasticity of the film the tampon can be squeezed in the fingers to insert it into the outer ear passage, where the tampon swells and completely fills it (this is the essential condition for effective protection against noise). The tampons can be washed and are intended for repeated usage, and therefore a special pencil case with a cap is provided so that they can be stored in a shirt pocket.

It is recommended that Petryanov cloth be used in the form of disposable earplugs of the "berusha" type (designed by I. V. Petryanov-Sokolov, I. K. Razumov, L. N. Shkarinov, et al) for protecting large contingents of workers for an entire work shift. Berushas are pads measuring 4 × 4 cm, weighing 150 ± 10 mg, cut from FP-Sh soundproofing material. The material consists of ultrafine polymer fibers, reinforced with coarser fibers (from 3 to 100 micron in diameter) of the same polymer. To use the earplugs the worker folds the pad on the diagonal, rolls it into a cone and, inserting the point into the ear passage, packs in the plug with his finger.

The effectiveness of endaural personal safety devices is given in Table 10.16, and the effectiveness of earmuffs is given in Table 10.17. The most

[1]This section was written by A. I. Vozhzhova.

APPROVED FOR RELEASE: 2007/02/08: CIA-RDP82-00850R000200100009-9

APPROVED FOR RELEASE: 2007/02/08: CIA-RDP82-00850R000200100009-9

effective and easiest to use are earmuffs with liquid or viscous filler, in particular G. I. Petrova's outfit. It consists of a metal headband and muffs in the form of aluminum cups with flanges, covered with polyvinyl chloride pads, filled with glycerine. F. A. Kulikov's earmuffs are of similar design. They consist of metal cups with snugly fitting pads, also filled with glycerine. Earmuffs developed in East Germany, Hungarian ear boxes and earmuffs developed by VTsNIIOT [All-Union Scientific Research Institute of Work Safety] VTsSPS [All-Union Central Trade-Union Council] belong to the same group.

Table 10.16. Noiseproofing Effectiveness of Endaural Safety Devices

1) Типы втулок, тампонов и вкладышей	2) Среднее ослабление шума, дБ, на частотах, Гц						
	125	250	500	1000	2000	4000	8000
3) Антифоны Оропакс (ГДР)	—	20	22	26	35	38	—
4) Неопреновые однородные втулки $v = 29$	31	31	31	34	37	41	41
5) Неопреновые втулки MSA $v = 30$	29	29	34	36	37	31	41
6) Винилитовые втулки типа v-51R	15	20	22	25	32	30	35
7) Ушные пробки (Венгрия)	25	30	25	25	35	40	25
8) Тампоны из ультратонкого волокна ФПП-15	8	10	15	22	25	32	—
9) Вкладыши из ФП-III	15	18	18	24	26	36	31
10) Требования ГОСТ 15762—70	10	12	15	17	25	30	30

Key:
1. Type of plug, tampon, insert
2. Average noise attenuation, dB, on frequencies, Hz
3. Oropaks antiphones (GDR)
4. Uniform neoprene plugs v = 29
5. MSA neoprene plugs v = 30
6. Type v-51R vinylite plugs
7. Hungarian earplugs
8. FPP-15 ultrafine fiber tampons
9. FP-Sh inserts
10. GOST 15762-70 requirements

Liquid or viscous-filled earmuffs with a snugly fitting ring should be used in extremely high noise levels. Dry porous elastic-filled or air-filled earmuffs should be used in other cases.

Under actual sailing conditions personal safety gear is selected in accordance with the noise situation and nature of the work being done. For instance, during occasional stays in extremely noisy rooms, and when standing watches in them that do not require movement of the head and body, G-63 outfits with Z-63 muffs (ordinary and in the communications version, i.e., equipped with telephones and laryngophones) should be used. When doing work requiring movement of the head and body the type ShSh-1 helmets, equipped with the same Z-63 and ShSh-II earmuffs, and also equipped with headsets and laryngophones, i.e., communications helmets, should be used.

APPROVED FOR RELEASE: 2007/02/08: CIA-RDP82-00850R000200100009-9

APPROVED FOR RELEASE: 2007/02/08: CIA-RDP82-00850R000200100009-9

Table 10.17. Effectiveness of Soundproofing Earmuffs

1) Типы наушников и страна-изготовитель	2) Среднее ослабление шума, дБ, на частотах, Гц						
	125	250	500	1000	2000	4000	8000
3) Гарнитур шумозащитный типа ГШ-1 (СССР)	20	22	25	27	27	37	—
4) Противошумные наушники клепальщиков типа ПН-2К (СССР)	14	15	20	20	30	34	40
5) Противошумные наушники типа Вд-1/63 (ГДР)	6	7	10	18	29	26	19
6) Защитные футляры (ВНР)	15	20	30	30	40	35	30
7) Противошумные наушники избирательного действия конструкции В. С. Байдина (СССР)	7	11	14	22	35	47	38
8) Противошумные наушники типа ЕМ (Канада)	5	6	16	25	29	27	23
9) Наушники типа MSA (США)	7	9	12	18	32	48	35
10) Прямолинейный звуковой протектор (США)	17	20	32	38	37	45	42
11) Требования ГОСТ 15762—70 (масса пары наушников — до 0,5 кг, сила прижатия — не более 0,8 кгс)	12	15	20	25	30	35	—

Key: 1. Type of earmuff and manufacturer
2. Average noise attenuation, dB, on frequencies, Hz
3. GSh-1 protective outfit (USSR)
4. PN-2K riveter earmuffs (USSR)
5. Vd-1/63 earmuffs (GDR)
6. Safety cups (Hungary)
7. V. S. Baydin's selective action earmuffs (USSR)
8. Type EM earmuffs (Canada)
9. Type MSA earmuffs (United States)
10. Straight sound protector (United States)
11. GOST 15762-70 requirements (weight of pair of earmuffs -- up to 0.5 kg, pressure -- not more than 0.8 kg)

Actual tests on small high-speed ships have shown that crew members who use the type PT FPP-15 antinoise tampons, antinoise outfits and helmets, in addition to vibration-damping clothing and personal mat overalls do not exhibit significant changes with respect to auditory and other sensory systems of the body.

BIBLIOGRAPHY

1. "Aviatsionnaya Akustika" [Aviation Acoustics], edited by A. G. Munin and V. Ye. Kvitk, Moscow, Mashinostroyeniye, 1973.

2. Bogolepov, I. I. and E. I. Avferonok, "Zvukoizolyatsiya na Sudakh" [Acoustic Insulation on Ships], Leningrad, Sudostroyeniye, 1970.

APPROVED FOR RELEASE: 2007/02/08: CIA-RDP82-00850R000200100009-9

APPROVED FOR RELEASE: 2007/02/08: CIA-RDP82-00850R000200100009-9

3. Bogolepov, I. I. and G. L. Osipov, "Sovremennyye Akusticheskiye Materialy v Stroitel'stve i Promyshlennosti" [Modern Acoustic Materials in Construction and Industry], LDNTP, 1977.

4. Brekhovskikh, L. I., "Volny v Sloistvykh Sredakh" [Waves in Lamellar Media], Moscow, Izd-vo AN SSSR, 1957.

5. Zaborov, V. I., L. N. Klyachko and G. S. Rosin, "Zashchita ot Shuma i Vibratsii v Chernoy Metallurgii" [Protection from Noise and Vibration in Ferrous Metallurgy], Moscow, Metallurgiya, 1976.

6. "Zvukoizoliruyushchiye i Zvukopogloshchayushchiye Konstruktsii v Stroitel'stve i Na Transporte" [Acoustic-Insulating and Soundproofing Structures in Construction and Transportation], edited by I. I. Bogolepov, LDNTP, 1974.

7. "Zvukoizoliruyushchiye i Zvukopogloshchayushchiye Konstruktsii v Praktike Bor'by s Shumom" [Acoustic-Insulating and Soundproofing Structures in Noise Control], edited by I. I. Bogolepov, LDNTP, 1977.

8. Klyukin, I. I., "Bor'ba s Shumom i Zvukovoy Vibratsiyey na Sudakh" [Noise and Acoustic Vibration Control on Ships], Leningrad, Sudostroyeniye, 1971.

9. Klyukin, I. I. and A. Ye. Kolesnikov, "Akusticheskiye Izmereniya v Sudostroyenii" [Acoustic Measurements in Shipbuilding], Leningrad, Sudostroyeniye, 1968.

10. Lyamshev, L. M., "Otrazheniye Zvuka Tonkimi Plastinkami i Obolochkami v Zhidkosti" [Reflection of Sound by Thin Plates and Shells in Liquid], Moscow, Izd-vo AN SSSR, 1955.

11. Osipov, G. L., "Acoustic Insulation of Walls with Window and Door Openings," in the book: "Voprosy Zvukoizolyatsii i Arkhitekturnoy Akustiki" [Problems of Acoustic Insulation and Acoustic Architecture], Moscow, Gosstroyizdat, 1959, pp 49-87.

12. Rybak, S. A. and B. D. Tartakovskiy, "Some Applications of Matrix of Conversion to Plane Wave Theory in System of Elastic Films," AKUSTICHESKIY ZHURNAL [Acoustics Journal], 1962, Vol VIII, No 1, pp 119-123.

13. "Spravochnik Proyektirovshchika. Zashchita ot Shuma" [Designer's Handbook. Protection from Noise], edited by Ye. Ya. Yudin, Moscow, Stroyizdat, 1974.

14. Shenderov, Ye. L., "Volnovyye Zadachi Gidroakustiki" [Wave Problems in Hydroacoustics], Leningrad, Sudostroyeniye, 1972.

APPROVED FOR RELEASE: 2007/02/08: CIA-RDP82-00850R000200100009-9

APPROVED FOR RELEASE: 2007/02/08: CIA-RDP82-00850R000200100009-9

15. Borner, H., "Uber die Wirkung offener akustischer Schirme in Innerraumen," HOCHFREQUENZTECHNIK UND ELEKTROAKUSTIK, 1960, Vol 69, No 9, pp 36-43.

16. Cremer, L., "Theorie der Schalldammung dunner Wande bei schragen Einfall," AKUSTISCHE ZEITSCHRIFT, 1942, Vol 7, No 3, pp 81-104.

17. Heckl, M., "Die Schalldammung von homogenen Einfachwanden endlicher Flasche," ACUSTICA, 1960, Vol 10, No 2, pp 98-108.

18. Josse, R. and C. Lamure, "Transmission du son par une paroi simple," ACUSTICA, 1964, Vol 14, No 5, pp 266-280.

19. "ISO Recommendation R140-1960. Field and Laboratory Measurements of Airborne and Impact Sound Transmission."

APPROVED FOR RELEASE: 2007/02/08: CIA-RDP82-00850R000200100009-9

APPROVED FOR RELEASE: 2007/02/08: CIA-RDP82-00850R000200100009-9

CHAPTER 11. SOUNDPROOFING OF SHIPS

11.1. Application of Soundproofing Structures[1]

General Principles. One way to reduce airborne noise on a ship is to use sound-absorbing structures, placed on the partitions of ship rooms or on the inside of it. These structures reduce the intensity of acoustic waves reflected from surfaces. Sound-absorbing materials, installed inside of a room, also reduce the intensity of direct sound. Acoustic absorbers reduce the airborne noise level not only inside of a room containing a noise source, but also in adjacent rooms.

How well rooms are protected from noise by soundproofing structures depends on the acoustic properties of the room before and after soundproofing. These characteristics are determined by the following: the initial average sound absorption coefficient in the room in the absence of the soundproofing material, the area on which soundproofing structures can be applied, and the acoustic absorption coefficient of the structure utilized. The distance between the noise source and the point at which the effectiveness of soundproofing is determined also plays a part.

Lining with soundproofing material is effective in cases when the average sound absorption coefficient in a room after being lined increases by at least a factor of 2.

The values of α_{av} for ship rooms, the walls of which are lined with soundproofing structures, are presented in Figure 11.1.

An example of the reduction of the airborne noise levels in source rooms, achieved by using sound-absorbing structures made of ATM-1 material with a thickness of 50 mm, installed at a distance of 50 mm from the bulkhead, is given in Table 11.1.

The liner area comprises 20% and 40% of the total room enclosure area; the resulting effect can be 5-7 dB. Sound-absorbing structures must be used in

[1]This section was written by E. I. Avferonok and G. S. Beregova.

APPROVED FOR RELEASE: 2007/02/08: CIA-RDP82-00850R000200100009-9

APPROVED FOR RELEASE: 2007/02/08: CIA-RDP82-00850R000200100009-9

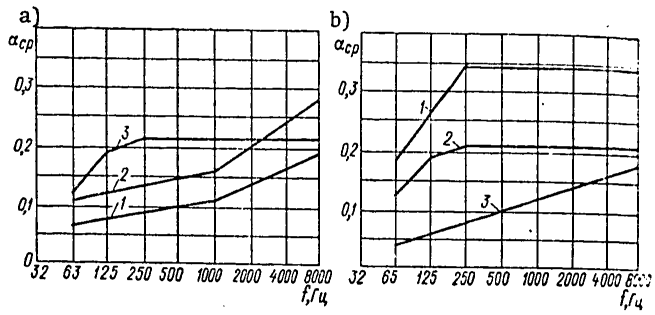

Figure 11.1. Values of α_{av} for ship rooms: a -- transport and industrial ships. 1 -- low saturation rooms (rooms with auxiliary machinery, refrigerator rooms, steering gear compartments); 2 -- engine and boiler rooms; 3 -- stations, wheelhouses, cabins, salons and ward rooms; b -- hydrofoil ships [11]. 1 -- passenger salons; 2 -- cabins and wheelhouses; 3 -- engine compartments. [ср=av; Гц=Hz]

rooms with low initial absorption, for example rooms for auxiliary machinery, ventilation partitions, insulated control booths, etc.

Structures with a porous absorber, made in the form of flat panels (Figure 11.2), in which the sound-absorbing material is installed tightly against the ship hull (bulkhead, deck, etc.), or at some distance from it, with the perforated lining protected from mechanical damage, are most commonly used on modern ships. Thin airtight films are used to protect rooms from dust, which certain loose fiber materials release, and also to prevent the absorbers themselves from becoming moist with fuel and oil vapors.

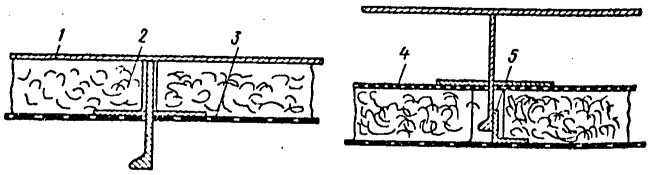

Figure 11.2. Soundproofing structures with porous absorber: 1 -- element of ship hull; 2 -- sound absorber; 3 -- perforated backing; 4 -- screen; 5 -- bracket.

Space absorbers in the form of pyramids (Figure 11.3), installed on bulkheads, sides and ceilings of rooms, are used less frequently. Their advantages are ease of installation and somewhat better effectiveness. These pyramids, with a base area of 500 × 500 mm and a height of 200 mm,

APPROVED FOR RELEASE: 2007/02/08: CIA-RDP82-00850R000200100009-9

APPROVED FOR RELEASE: 2007/02/08: CIA-RDP82-00850R000200100009-9

Table 11.1. Effectiveness of Soundproofing Structures in Rooms

1) Схема конструкции	2) Процент площади, занятой конструкцией	3) Расстояние от источника, м	4) Постоянная помещения	5) Снижение уровня воздушного шума, дБ, на частотах, Гц							
				63	125	250	500	1000	2000	4000	8000
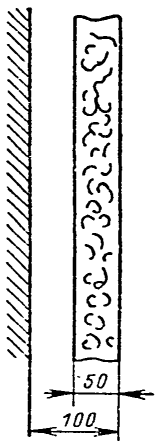	20	5—20	2—20	0	0	4	5	4	4	4	4
			20—100	0	0	4	5	4	4	4	4
			100—500	0	0	3	4	3	3	3	3
		2	2—20	0	0	3	5	3	3	3	3
			20—100	0	0	2	4	2	2	2	2
			100—500	0	0	1	3	1	1	1	1
		1	2—20	0	0	3	4	3	3	3	3
			20—100	0	0	2	3	2	2	2	2
			100—500	0	0	1	2	1	1	1	1
	40	5—20	2—20	0	0	6	7	6	6	6	5
			20—100	0	0	6	7	6	6	6	5
			100—500	0	0	5	6	5	5	5	4
		2	2—20	0	0	5	7	5	5	5	5
			20—100	0	0	4	6	4	4	4	4
			100—500	0	0	2	4	2	2	2	2
		1	2—20	0	0	4	6	4	4	4	4
			20—100	0	0	3	5	3	3	3	2
			100—500	0	0	1	2	1	1	1	1

Key: 1. Diagram of structure
2. Percentage of area covered by structure
3. Distance from source, m
4. Room constant
5. Reduction of airborne noise level, dB, on frequencies, Hz

APPROVED FOR RELEASE: 2007/02/08: CIA-RDP82-00850R000200100009-9

APPROVED FOR RELEASE: 2007/02/08: CIA-RDP82-00850R000200100009-9

and with a 30 mm thick capron fiber filler, were installed on the ceiling and bulkheads of the engine room of a motor ship, on an area of approximately 20% of the total area of all the surfaces. The resulting average sound absorption coefficient increased by a factor of 1.5-2 in the entire frequency range, which yielded a reduction of the airborne noise level in the engine compartment by 3-4 dB. The noise in the dining room, located right behind the engine room, also decreased by 8-10 dB due, in addition to the sound absorption effect, also to some increase of the acoustic insulation of the deck (Figure 11.4).

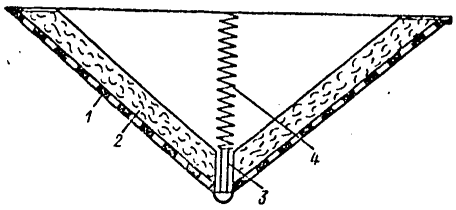

Figure 11.3. Sound-absorbing pyramid: 1 -- perforated lining; 2 -- soundproofing material; 3 -- rod; 4 -- spring.

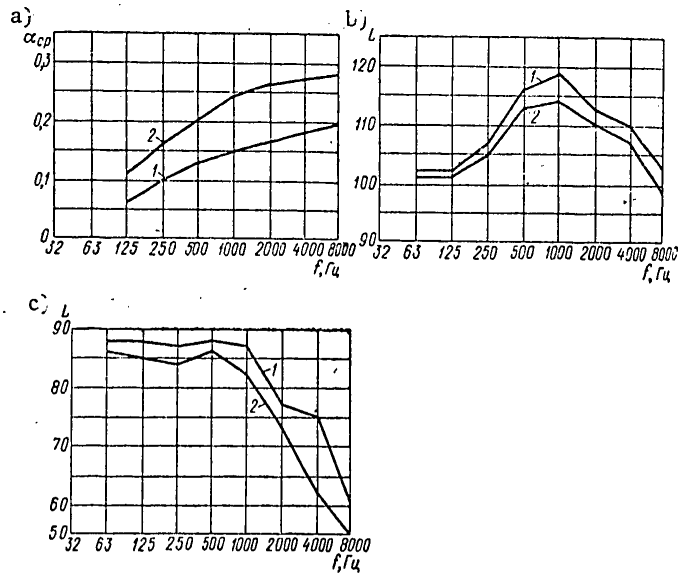

Figure 11.4. Average sound absorption coefficient (a) and airborne noise levels in engine room (b) and in dining room (c) of motor ship "Sputnik": 1 -- before installation of pyramids; 2 -- after installation of pyramids. [ср=av; Гц=Hz]

APPROVED FOR RELEASE: 2007/02/08: CIA-RDP82-00850R000200100009-9

APPROVED FOR RELEASE: 2007/02/08: CIA-RDP82-00850R000200100009-9

Resonance soundproofing structures, like flat and space structures, are not yet used extensively on ships due to problems in manufacture and rather large sizes.

Soundproofing structures are also used on ships in swimming pools, movie halls, etc., for providing the best conditions for enjoying music and speech; in air ducts, ventilation shafts and exhaust stacks for reducing propagating noises; in noise mufflers; for lining bulkheads and shields located near noise sources and on the inner walls of the hoods of machinery and mechanisms for improving their sound-insulating properties.

Sound-absorbing materials are also used extensively for improving the effectiveness of acoustic insulation structures.

The sound-absorbing structures and materials used on ships must be sufficiently fireproof and vibration-resistant and must not emit dust and toxic substances above the maximum permissible concentration [1, 11, 15].

11.2. Wave Parameters. Porous Panel. Resonant Sound Absorbers

The sound-absorbing properties of materials and structures are characterized by reflection coefficient β, equal to the amplitude ratio of reflected and incident waves; β is a function of the acoustic impedance Z_a of the interface, which is equal to the ratio of the acoustic pressure to the normal component of vibration velocity $\dot{\xi}_n$ [17]:

$$Z_a = \frac{p}{\dot{\xi}_n} = R_a + iX_a, \tag{11.2.1}$$

where R_a is the active, and X_a the reactive components of acoustic impedance.

In normal incidence

$$Z_a = \frac{Z+\beta}{Z-\beta}; \quad Z_1 = \frac{Z_a}{Z}; \quad \beta = \frac{Z_a - Z}{Z_a + Z}. \tag{11.2.2}$$

The sound absorption coefficient (SAC) is

$$\alpha = 1 - |\beta|^2; \quad \alpha = \frac{4R_1}{(R_1+1)^2 + X_1^2}. \tag{11.2.2a}$$

In these formulas $Z_1 = R_1 + iX_1$; $Z = \rho c$ is the specific acoustic impedance of air, $\rho c = 410$ Pa•m/s.

APPROVED FOR RELEASE: 2007/02/08: CIA-RDP82-00850R000200100009-9

APPROVED FOR RELEASE: 2007/02/08: CIA-RDP82-00850R000200100009-9

The wave parameters of an acoustic medium are the propagation coefficient γ_m and wave impedance W_m. In a medium with losses $W_m = W_{mr} + iW_{mi}$; $\gamma_m = \alpha_m + i\beta_m$, where α_m is the attenuation coefficient; β_m is the wave number. W_m and γ_m describe the acoustic behavior of a medium. They are related to density ρ_m and to the bulk elasticity modulus K_m for a harmonic process by the equations [18]:

$$\gamma_m = i\omega\sqrt{\frac{\rho_m}{K_m}}; \quad W_m = \sqrt{K_m\rho_m}. \tag{11.2.3}$$

In porous materials porosity P must be taken into account, i.e., the ratio of pore volume to total volume. For a porous medium $K'_m = K_m/P\kappa$, where κ is the ratio of specific heats for constant pressure and volume.

For a harmonic process and a wave propagating in a porous material

$$\begin{gathered} i\omega\rho_m\dot{\xi} = \gamma_m p; \quad \rho_m = \frac{m\rho}{P} - \frac{i\sigma_c}{\omega} = \rho_{mr} - i\rho_{mi}; \\ K'_m = K'_{mr} + iK'_{mi} = \frac{1}{P\varkappa}[K_{mr} + iK_{mi}], \end{gathered} \tag{11.2.4}$$

where m is a structural constant; σ_c is the impedance constant.

Expression (11.2.4) is valid for the average air pressure in a fibrous material [2]:

$$\begin{gathered} \gamma_m = i\omega\sqrt{\left(\frac{m\rho}{P} - i\frac{\sigma_c}{\omega}\right)P\varkappa(K_{mr} + iK_{mi})^{-1}}; \\ W_m = \sqrt{\left(\frac{m\rho}{P} - i\frac{\sigma_c}{\omega}\right)(K_{mr} + iK_{mi})(P\varkappa)^{-1}}. \end{gathered} \tag{11.2.5}$$

For κ it is customary to use $\kappa = 1$ for an adiabatic, and $\kappa = 1.4$ for an isothermal process in a material. From (11.2.5) we have

$$\rho_{mr} - i\rho_{mi} = W_m\gamma_m\frac{1}{i\omega}; \tag{11.2.6}$$

$$K_{mr} + iK_{mi} = \frac{i\omega W_m}{\gamma_m}; \tag{11.2.7}$$

$$\frac{\rho_{mr}}{\rho} = \frac{m}{P} = (\beta_m W_{mr} - \alpha_m W_{mi})\frac{1}{\rho ck}; \tag{11.2.8}$$

$$|\omega\rho_{mi}| = \sigma_c = |\alpha_m W_{mr} + \beta_m W_{mi}|; \tag{11.2.9}$$

$$K_{mr} = \frac{(W_{mr}\beta_m + W_{mi}\alpha_m)k}{\alpha_m^2 + \beta_m^2}; \tag{11.2.10}$$

$$K_{mi} = \frac{(W_{mr}\alpha_m + W_{mi}\beta_m)k}{(\alpha_m^2 + \beta_m^2)}. \tag{11.2.11}$$

APPROVED FOR RELEASE: 2007/02/08: CIA-RDP82-00850R000200100009-9

APPROVED FOR RELEASE: 2007/02/08: CIA-RDP82-00850R000200100009-9

Porous Panel. A rigid panel with holes, called perforations, is used in sound-absorbing structures. The inertial impedance of one hole with area s_0 and diameter d [17] is

$$iX_a = i\omega M' = i\omega\rho \frac{s_0^2}{K} = i\omega\rho s_0 (l + 2l'), \tag{11.2.12}$$

where M' is conjugate mass; K is conductance.

The inertial impedance per unit area of a perforated panel, standardized to Z, is

$$iX_1 = i\omega \frac{s}{cK}, \tag{11.2.13}$$

where $K = \frac{s_0}{(l + 2l')}$; t' is the correction factor for the end of a hole.

The active acoustic impedance of a hole attributed to the viscosity of the air flowing through it is

$$R_0 = \frac{32\mu (l + 2l')}{d^2} \tag{11.2.14}$$

for $d\sqrt{\frac{\omega\rho}{8\mu}} = \eta < 1$ (where μ is the coefficient of dynamic viscosity for air).

For $\eta \geq 10$

$$R_0 = 2 (l + 2l') \sqrt{2\rho\mu\omega} \cdot \frac{1}{d}. \tag{11.2.15}$$

The specific dimensionless acoustic impedance R_1 of a panel is

$$R_1 = \frac{sR_0}{s_0\rho c}. \tag{11.2.16}$$

Formulas are given in Table 11.2 for calculating K, t' of holes of different shape in cells of different configuration: for a square hole with side a in a square cell with side a_1; for a round hole with diameter d in a circular cell with diameter d_1 and a square cell with side a_1. The value t' can be found in Figure 11.5, where $2t' = \sqrt{s_0} I(\zeta)$; $I(\zeta)$ is the ordinate of the point with abscissa ζ, where $\zeta = a/a_1$, d/d_1 (curves 1, 2) and $\zeta = d/a_1$ (curve 3). For $\zeta \leq 0.4$ [20]

$$2l' = \sqrt{s_0}\, 0{,}96 (1 - 1{,}25\zeta). \tag{11.2.17}$$

Resonant acoustic absorbers (RAA) are a perforated panel, installed at distance l_1 from a rigid wall. Losses in RAA are caused either by the friction of air in the holes, or by friction in a cloth or screen type of material, inserted in the holes.

APPROVED FOR RELEASE: 2007/02/08: CIA-RDP82-00850R000200100009-9

APPROVED FOR RELEASE: 2007/02/08: CIA-RDP82-00850R000200100009-9

Table 11.2. Calculation of K, t' for Holes of Different Shape

1) Площадь ячейки	2) Площадь отверстия	3) Толщина ячейки	4) Поправка на конец	5) Проводимость
∞	$\frac{\pi d^2}{4} s_0$	0 t	$\pi d/8$ $\pi d/8$	d $\pi d^2/4 \left(t + \frac{\pi d}{4}\right)$
$\frac{\pi d_1^2}{4}$	$\frac{\pi d^2}{4} s_0$	0 t	$\pi d/8F\left(\frac{d}{d_1}\right)$	$dF(d/d_1)^*$ $\pi d^2/4 \left[t + \frac{\pi d}{4F(d/d_1)}\right]$
$\frac{\pi d_1^2}{4}$, a_1^2	$\frac{\pi d^2}{4}$; a^2	0 t	$0{,}48a_1(1-1{,}25\zeta)$; $0{,}48\sqrt{\frac{\pi d^2}{4}}(1-1{,}25\zeta)$ $\left(\zeta \leqslant 0{,}4;\ \zeta = \frac{d}{d_1};\ d/a_1;\ a/a_1\right)$	$s_0/0{,}96\sqrt{s_0}(1-1{,}25\zeta)$ $s_0/[t + 0{,}96\sqrt{s_0}(1-1{,}25\zeta)]$
a_1^2	$a_1 a$ 6) Щель	0 t	$\frac{a_1}{2\pi}\ln\frac{1}{\eta} - 0{,}338$ (на единицу длины щели)[7]	$\frac{\pi a}{\frac{a_1}{2\pi}\ln\frac{a}{a_1} - 0{,}338}$ $\frac{1}{\left(t + \frac{a_1}{2\pi}\ln\frac{a}{a_1} - 0{,}338\right)}$

$^* F\left(\frac{d}{d_1}\right) \approx \left(1 - 1{,}47\frac{d}{d_1} + 0{,}47\frac{d^3}{d_1^3}\right)^{-1}$

Key: 1. Cell area
2. Hole area
3. Cell thickness
4. Correction factor for end
5. Conductance
6. Slit
7. (per unit length of slit)

APPROVED FOR RELEASE: 2007/02/08: CIA-RDP82-00850R000200100009-9

APPROVED FOR RELEASE: 2007/02/08: CIA-RDP82-00850R000200100009-9

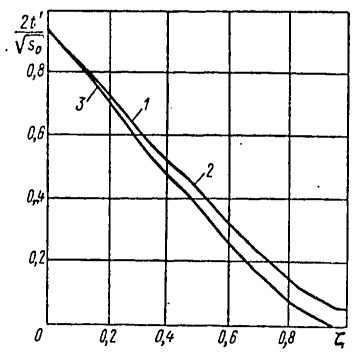

Figure 11.5. End correction factor for holes of different shape: $\zeta = d/d_1$; $\zeta = a/a_1$ (1, 2); $\zeta = d/a_1$ (3); d, d_1 -- diameters of hole and cell; a, a_1 -- sides of square holes and cell.

The parameters of RAA are the following: s (the area of a cell, in which there is one hole), and also the values s_0, l_1, R_1, σ_c, for which the sound absorption coefficient will be greater than or equal to prescribed value α_1 in the frequency range f_1-f_2, calculated by the formulas

$$l_i = \frac{c\alpha_1\left(1 - \frac{f_i}{f_2}\right)}{4\pi f_1 \sqrt{1-\alpha_i}}; \qquad (11.2.18)$$

$$R_1 = \frac{2-\alpha_i}{\alpha_i};$$

$$\frac{s}{K} = \frac{2c\sqrt{1-\alpha_i}}{\pi\alpha_1(f_2 - f_1)} = B. \qquad (11.2.19)$$

For a specified panel thickness t and diameter d, a_1, the distance between holes in a square cell with $s = a_1^2$, is determined (for $s/k \geq 4$) by the formula [2]:

$$a_i = \frac{1{,}05d^2 \pm \sqrt{1{,}1d^4 + 3{,}53Bd(t + 0{,}85d)}}{2(t + 0{,}85d)}. \qquad (11.2.20)$$

The specific impedance of a material, inserted in holes, is

$$\sigma_c = \frac{s_0 Z(2-\alpha_i)}{s\alpha_i} = \frac{\pi d^2 Z(2-\alpha_1)}{4a_1^2\alpha_i}. \qquad (11.2.21)$$

If the losses in the holes are caused only by the viscosity of air, diameter d is not assigned, but is determined by the expression

$$d^2 = \frac{32\mu\sqrt{1-\alpha_i}}{(f_2 - f_1)(2-\alpha_1)}. \qquad (11.2.22)$$

APPROVED FOR RELEASE: 2007/02/08: CIA-RDP82-00850R000200100009-9

APPROVED FOR RELEASE: 2007/02/08: CIA-RDP82-00850R000200100009-9

11.3. Laminated Soundproofing Structures. Space Absorbers. Membrane Acoustic Absorbers

Laminated Acoustic Absorbers. Laminated absorbers consist of layers of different materials (sometimes with a panel). The simplest structure is a layer of material, applied on a wall with impedance Z_2. In normal incidence the input impedance of the structure is

$$Z_1' = \frac{W_{m1} Z_{12} \operatorname{ch} \gamma l + W_{m1} \operatorname{sh} \gamma l}{Z_{1,2} \operatorname{sh} \gamma l + W_{m1} \operatorname{ch} \gamma l} = \frac{W_m}{Z} \operatorname{cth} (\gamma l + \varphi), \qquad (11.3.1)$$

where l is the thickness of the layer; ϕ is the phase shift contributed by impedance $Z_{1,2}$; Z_2, W_m, Z' are normal to Z, which is denoted by the subscript 1; $W_m/Z = W_{m1}$.

For $Z_{12} \to \infty$ (a rigid wall) [10]:

$$Z_1' \approx \frac{\sigma_c l}{3Z} + \frac{K_{m1}}{\omega l Z} + i\left(\frac{\omega m l}{c 3P} - \frac{K_{mr}}{\omega l Z}\right). \qquad (11.3.1a)$$

For materials with large σ_c, for example $\frac{\sigma_c l}{3Z} \gg \frac{K_{ml}}{\omega l Z}$; $R_1 \approx \frac{\sigma_c l}{3Z}$. For bulk materials $\frac{\sigma_c l}{3Z} \ll Kmi \frac{1}{\omega l Z}$. For a layer, applied at distance l_1 from a rigid wall (for $K_m \approx K_{mr}$), the input impedance is

[сл=lay]

$$Z_{1cл}' \approx \frac{\sigma_c (P\varkappa l + l_1)}{3ZP\varkappa} + i\left[\frac{\omega m (P\varkappa l + l_1)}{c 3P^2 \varkappa} - \frac{c}{\omega (P\varkappa l + l_1)}\right]. \qquad (11.3.2)$$

Formulas (11.3.1a) and (11.3.2) are valid to a frequency that is 30-40% higher than the resonance frequency of the layer (determined by the condition $X_{1lay} = 0$).

On low frequencies soundproofing structures in the form of a layer are ineffective. Absorption on these frequencies is improved by using a perforated panel, applied snugly or loosely to a sheet on the incidence side. In the case of loose contact the impedance [2] is

[k=c]

$$Z_{1к}' = Z_{1cл} + i \frac{\omega}{c} \frac{s}{s_0} (2l' + l). \qquad (11.3.3)$$

In snug contact

$$Z_{1к} = Z_{1cл} + \frac{\sigma_c s}{Z s_0} l' + i \frac{\omega}{c} [(m+1) l' + l]. \qquad (11.3.4)$$

APPROVED FOR RELEASE: 2007/02/08: CIA-RDP82-00850R000200100009-9

APPROVED FOR RELEASE: 2007/02/08: CIA-RDP82-00850R000200100009-9

The maximum acoustic absorption coefficient (AAC) α_{max} is achieved when $f = f_{res}$. If the resonance frequency f_{res} is given and it is required to determine $(P\varkappa l + l_1)$ and s/K, then

[рез=res]
$$\frac{m(P\varkappa l + l_1)^2}{(3P^2\varkappa)^2} + \frac{s(P\varkappa l + l_1)}{K} = \frac{c_0^2}{4\pi^2 f_{res}^2}. \qquad (11.3.4a)$$

The best practical values must be selected from combinations of the values of $(P\varkappa l + l_1)$ and s/K. If the AAC must not only be maximum on frequency $f = f_{res}$, but also have a certain value $\alpha_{max} = \alpha_1$, the parameters of a structure (with a snug fit) are calculated by the following formulas [2]:

$$(P\varkappa l + l_1) = \frac{sP\varkappa}{2}\left[\frac{(m+1)R_1}{\sigma_1} \pm \sqrt{(m+1)^2\left(\frac{R_1}{\sigma_1}\right)^2 - \frac{c_0^2}{3P^2\varkappa\pi f_{res}^2}}\right]; \qquad (11.3.5)$$

$$R_1 = (2-\alpha_1) \pm \sqrt{(2-\alpha_1)^2 - \alpha_1} = \frac{\sigma_1(P\varkappa l + l_1)}{3P^2\varkappa} + \frac{\sigma_1 s}{2K}; \qquad (11.3.6)$$

$$\frac{s}{K} = 2\left[R_1 - \frac{\sigma_1^2(P\varkappa l + l_1)}{3P^2\varkappa}\right] = B; \quad \sigma_1 = \frac{\sigma_c}{Z}. \qquad (11.3.7)$$

Cell distance a_1 for given t and d are determined by expression (11.2.20).

Example of Calculation. For a structure with f_{res} = 400 Hz find $\alpha_1 = 1$. Determine l, l_1, a_1 and R_1, if m = 2, P = 0.98, $\sigma_1 = 0.2$.

The panel has $d = 5 \cdot 10^{-3}$ m, $t = 2 \cdot 10^{-3}$ m. The formulas yield $R_1 = 1.1(P\varkappa l + l_1) = 0.13$ m; $l = 0.05$ m; $l_1 = 6 \cdot 10^{-2}$ m, $a_1 = 1.8 \cdot 10^{-2}$ m.

The values of α are: for f = 200 Hz $\alpha = 0.83$; for f = 400 Hz $\alpha = 1$; for f = 1,000-1,200 Hz $\alpha = 0.85$; for f = 2,000 Hz $\alpha = 0.5$.

It is recommended that one more layer of material be applied on the acoustic incidence side of the panel to improve the absorption characteristics. If the frequency, for which α_1' on the boundary of the range of AAC is smaller than desired, is f_1', then the thickness of the top layer may be calculated by the formulas [5]

$$l_2 = \frac{c\left(n + \frac{1}{2}\right)\pi - \delta_0}{2\pi f_1' \sqrt{m\varkappa}};$$
$$\delta_0 = \operatorname{arctg} 2\,[X - W'_{mi}]/(R - W'_{mr})^2 + (X - W'_{mi})^2, \qquad (11.3.8)$$

where R, X are components of the acoustic impedance of the bottom layer (next to the panel), but expressed in fractions of W_m (of the wave impedance

APPROVED FOR RELEASE: 2007/02/08: CIA-RDP82-00850R000200100009-9

APPROVED FOR RELEASE: 2007/02/08: CIA-RDP82-00850R000200100009-9

of the material of which the top layer is made), and taken on frequency f_1', and W'_{mr} and W'_{mi} are the active and inertial wave impedances of the material of the top layer, but expressed in fractions of Z.

If on the above-described structure is applied a layer of the same material with $l_2 = 2 \cdot 10^{-2}$ m (based on calculation data), it is possible to reach the value $\alpha = 0.8$ for f = 200 Hz, $\alpha = 0.99$ for f = 2,000 Hz and $\alpha = 0.9$ for f = = 1,600 Hz.

Influence of Film on Acoustic Absorption of Porous Material. This influence is determined basically by the inertia of the film, i.e., by surface mass M_s. Films with $M_s < 0.020$ kg/m^2 have no influence on the acoustic absorption coefficient. The values $M_s = 0.020$-0.070 kg/m^2 are taken into account by adding to the inertial impedance of the material the through impedance of the film X_2:

[п=s]
$$X_2 = \omega M_п; \quad X_{i2} = \frac{M_п \omega}{Z},$$

where M_s is the surface mass of the film, kg/m^2.

Consequently $X_{1c} = X_1 + X_{12}$.

Given in Table 11.3 are the values of X_2 of films, used for lining fiber materials. Films with $M_s \geq 0.070$ kg/m^2 should not be used, since they substantially reduce the acoustic absorption coefficient on high frequencies.

Space Acoustic Absorbers. Space absorbers (SA) are designed as separate bodies (spheres, cubes, cones, etc.), made of sound-absorbing materials, sometimes with a perforated cover. The working area of the absorber varies due to diffraction. This variable area is called the effective area. The ratio of effective area Q_a to the actual area of a space absorber expresses the change of the number of units of absorption due to the use of a material not in the form of a film, but in the form of a space absorber. This value, called the conditional acoustic absorption coefficient α_c^e, for an absorber in the form of a sphere with radius r, covered with a film of material with impedance $R_1 + iX_i = Z_1$, which should be local[1] in normal incidence, is calculated by the formula [3, 4]

[y=c; п=a]
$$\alpha_y = \frac{s}{kr} \sum_{n=0}^{\infty} \frac{(2n+1) R_1 \sin(\delta_п - \delta'_п)}{\frac{D_п}{D'_п} + 2\left[X_1 \cos(\delta_п - \delta'_п) + R_1 \sin(\delta_п - \delta'_п) + \frac{D_п}{D'_п}(X_1^2 + R_1^2)\right]}, \quad (11.3.9)$$

[1] Impedance that does not depend on the angle of incidence is called local impedance.

APPROVED FOR RELEASE: 2007/02/08: CIA-RDP82-00850R000200100009-9

APPROVED FOR RELEASE: 2007/02/08: CIA-RDP82-00850R000200100009-9

Table 11.3. Reactive Component X_2 of Through Impedance of Films

1) Тип пленки	2) Толщина пленки, м²	3) Поверхностная масса, кг/м²	4) Частоты октавных полос, Гц							
			63	125	250	500	1000	2000	4000	8000
5) Полиимидная ПМ	$40 \cdot 10^{-6}$	0,057	0,05	0,11	0,21	0,43	0,85	1,70	3,41	6,82
6) Типа Саран (Крехалон)	$30 \cdot 10^{-6}$	0,049	0,05	0,09	0,18	0,37	0,74	1,48	2,96	5,92
7) Стеклоткань марки СТФ	$50 \cdot 10^{-6}$	0,050	0,05	0,09	0,19	0,37	0,75	1,49	2,99	5,98
8) Полиэтилентерефталатная	$25 \cdot 10^{-6}$	0,035	0,03	0,06	0,13	0,26	0,52	1,05	2,09	4,19
	$50 \cdot 10^{-6}$	0,070	0,07	0,13	0,26	0,52	1,05	2,09	4,19	8,37
9) Полиэтиленовая	$25 \cdot 10^{-6}$	0,023	0,02	0,04	0,08	0,17	0,34	0,69	1,37	2,75
	$50 \cdot 10^{-6}$	0,046	0,04	0,08	0,17	0,34	0,69	1,37	2,75	5,50

Key: 1. Type of film
2. Thickness of film, m^2
3. Surface mass, kg/m^2
4. Frequencies of octave bands, in Hz
5. Polyimide PM
6. Saran (Krekhalon)
7. Grade STF glass fiber cloth
8. Polyethylene terephthalate
9. Polyethylene

where $D_a(kr)$, $D'_a(kr)$, $\delta_a(kr)$, $\delta'_a(kr)$ are the amplitudes and phases of the spherical Bessel functions and their derivatives, $k = \omega/c$.

Formula (11.3.9) is also applicable for calculating α_c of a cube with side $a_1 = r/0.64$, but the resulting values should be reduced by a factor of 1.25. The calculated values of α_c as a function of kr for R_1 and X_1, taken as parameters, are nomograms. One such nomogram is presented in Figure 11.6, where it is seen that the character of the dependence of α_c on kr varies for reactive impedances of different signs: when $X_1 < 0$ α_c is maximum, and when $X_1 > 0$ all the curves decline gradually as kr increases.

To maximize absorption in the low-frequency range, i.e., where $kr < 1$, it is necessary that R_1 and X_1 have the values

$$X_1 = -\frac{kr}{1 + (kr)^2},$$
$$R_1 = \frac{(kr)^2}{1 + (kr)^2}. \qquad (11.3.10)$$

APPROVED FOR RELEASE: 2007/02/08: CIA-RDP82-00850R000200100009-9

APPROVED FOR RELEASE: 2007/02/08: CIA-RDP82-00850R000200100009-9

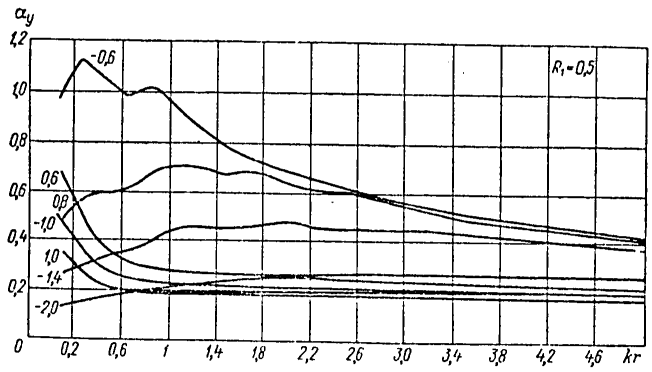

Figure 11.6. Nomogram for determining acoustic absorption coefficient on basis of known components X_1 and R_1 of local impedance of surface of space absorber, or for determining X_1 and R_1 for given AAC. [y=c]

The conditions of maximum absorption for $kr \gtrless 1$ are plotted in general form in Figure 11.7. A set of n space absorbers will be most effective when the absorbers are placed at distances apart, such that areas Q_a will not overlap. Then the total number of absorption units, contributed by the n space absorbers, will be $Q_a = n\pi r^2 \alpha_c$ m^2.

Membrane Acoustic Absorbers. These are absorbers whose front wall has pliancy; they include a resonant acoustic absorber (RAA) with a pliant front wall. For such RAA the resonance frequency depends on the ratio ω_1/ω_2 between the resonance frequencies, where ω_1 is the frequency of the cavity and ω_2 is the frequency of the wall.

The calculation is presented for a cell with area s. Let $\omega_1 = \sqrt{\beta_1/M_1}$; $\omega_2 = \sqrt{\beta_2/M_2}$; $\beta_1 = \rho c^2/sl_1$ is the elasticity of the cavity resonator (air space); $\beta_2 = e_2/s_2$; e_2 is the specific elasticity of the cell; $M_1 = m_1/s_2$; $m_1 = s_0 p(t + 2t')$ is the mass of the air in the hole plus the connected mass; $M_2 = m_2/s^2$ is the mass of the cell.

When $M_1/M_2 = \mu < 1$ and $\omega_1/\omega_2 < 1$ [16]

$$\omega_{01}^2 \approx \omega_1^2 \left[1 - 1/1 + \mu\left(\frac{\omega_2^2}{\omega_1^2} - 1\right)\right];$$
$$\omega_{02}^2 \approx \omega_2^2 \left[1 + \frac{[1 - (2-\mu)]\,\omega_1^2}{\omega_2^2}\right] \Big/ 1 + \mu\left[\frac{\omega_2^2}{\omega_1^2} - 1\right]. \qquad (11.3.11)$$

APPROVED FOR RELEASE: 2007/02/08: CIA-RDP82-00850R000200100009-9

APPROVED FOR RELEASE: 2007/02/08: CIA-RDP82-00850R000200100009-9

There turn out to be two resonance frequencies, and $\omega_{01} < \omega_1$; $\omega_{02} > \omega_2$. If $\omega_1 > \omega_2$ there again are two resonance frequencies:

$$\omega_{01}^2 \approx \omega_1^2 (1+\mu); \quad \omega_{01} > \omega_1; \quad \omega_{02}^2 \approx \omega_2^2 \left(1 + \frac{2\beta_2}{\beta_1}\right). \tag{11.3.12}$$

When $\omega_1 = \omega_2$ there is one resonance frequency:

$$\omega_0^2 = \frac{\mu\left(1+\frac{R_2}{R_1}\right)}{1+\mu\left(\frac{R_2}{R_1}\right)^2}. \tag{11.3.13}$$

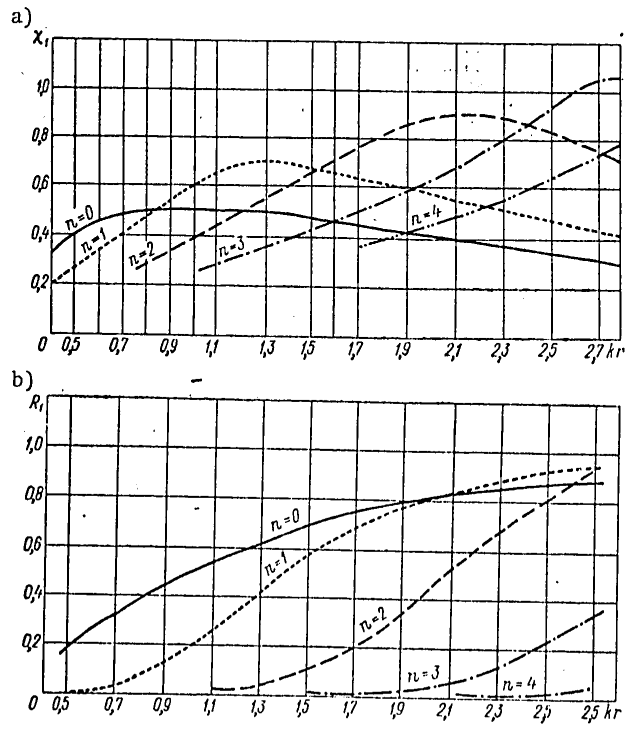

Figure 11.7. Reactive (a) and active (b) components of local surface impedance of spherical space absorber (as functions of kr), corresponding to perfect absorption of spherical wave of given order (n = 0, 1, 1, 3, 4, ...).

The absorption characteristic of a front wall with little damping of sound may show a valley on that frequency.

APPROVED FOR RELEASE: 2007/02/08: CIA-RDP82-00850R000200100009-9

APPROVED FOR RELEASE: 2007/02/08: CIA-RDP82-00850R000200100009-9

If the wall has no holes it is a membrane absorber, the resonance frequency of which is

$$\omega = c\sqrt{(\beta_1 + \beta_2)\frac{1}{\Delta l_2}}. \qquad (11.3.14)$$

11.4. Soundproofing Structures with Oblique and Diffusive Incidence

All the calculations in §11.2 and §11.3 pertain to the case of normal incidence of sound on structures. In practice it is possible to experience oblique incidence, or nearly diffusive incidence, when all angles of incidence are equiprobable, and the acoustic energy density in the room has a uniform distribution.

However, if the field in a room was also diffuse before the installation of a structure, the diffusivity usually will remain after the installation due to acoustic absorption. In practice it is necessary to deal with conditions that are nearly diffuse. In oblique incidence of sound the impedance is standardized in fractions of $Z/\cos\theta$ (denoted by the symbol "), and therefore the factor $\cos\theta$ appears. If the normal component of vibration velocity ξ_p^* depends on incidence angle θ, the impedance is called nonlocal.

For resonant acoustic absorbers, in which the air space is separated into compartments with a width smaller than λ,

$$Z_0'' = R_1\cos\theta + i\left[\frac{\omega s\cos\theta}{ck} - \operatorname{ctg}\frac{\omega l}{c}\right]\cos\theta \qquad (11.4.1)$$

If there are no compartments, then the impedance [8] is

$$Z_0'' = R_1\cos\theta + i\left[\frac{\omega s\cos\theta}{ck} - \operatorname{ctg}\left(\frac{\omega l\cos\theta}{c}\right)\right]. \qquad (11.4.2)$$

Here $a_1 \leq 0.2\lambda$, which means that the connected mass is independent of θ. In the case of resonant acoustic absorbers without compartments the acoustic absorption coefficient is maximum on the very same frequency for all θ, but α_{max} will be different. In the latter case the maximum AAC will fall on different frequencies for different θ.

The impedance of a layer applied on a rigid wall [21] is

$$Z_0'' = (W_{m1}\cos\theta/Z\cos\psi)\operatorname{cth}(\gamma l\cos\psi). \qquad (11.4.3)$$

where $\cos\psi = \sqrt{1 + \frac{k^2\sin^2\theta}{\gamma^2}}$; ψ is the complex angle of refraction.

APPROVED FOR RELEASE: 2007/02/08: CIA-RDP82-00850R000200100009-9

APPROVED FOR RELEASE: 2007/02/08: CIA-RDP82-00850R000200100009-9

For small $\gamma_m l$ [7]

$$Z_0'' \approx ik \frac{m\cos\theta}{P}\left(1-\frac{i}{\Omega}\right)\left[\frac{1}{ik^2\left(\sin^2\theta - m - \frac{im}{\Omega}\right)} - \frac{l}{3}\right], \qquad (11.4.4)$$

where $\Omega = \omega/\omega_0$; ω_0 is the characteristic frequency, equal to $\omega_0 = \sigma_c P/m\rho$.

When $\Omega < 1$

$$Z_0'' \approx \frac{i\cos\theta}{P}\left[\frac{\omega m l}{3c} - \frac{c}{\omega l}\right] + \frac{3\rho\omega}{\sigma_c P^2}\sin^2\theta_1\cos\theta + \\ + \frac{\sigma_c l}{3Z}\cos\theta = iY_1\cos\theta + R_0'', \qquad (11.4.5)$$

where Y_1 is the local reactive component of the impedance of the film.

Consequently, when $\Omega < 1$ only the reactive component of the acoustic impedance is local.

The impedance of a very thick film ($l \to \infty$) is

$$Z_\infty = \frac{Z\sqrt{m}\left(1-\frac{i}{\Omega}\right)}{\sqrt{\left(1-\frac{i}{\Omega}-\frac{\sin^2\theta}{m\varkappa}\right)P^2\varkappa}}; \qquad (11.4.6)$$

$$\Omega < 1: \quad Z_{0\infty} = \sqrt{\frac{\sigma}{2\rho\omega P}}\cos\theta\,(1-i); \qquad (11.4.6a)$$

$$\alpha_\theta = \frac{\frac{4\cos\theta\sqrt{m}}{P\sqrt{2\Omega}}}{\left(\frac{\sqrt{m}\cos\theta}{P\sqrt{2\Omega}}+1\right)^2 + \left(\frac{\sqrt{m}\cos\theta}{P\sqrt{2\Omega}}\right)^2}. \qquad (11.4.7)$$

Maximum absorption corresponds to the condition $\cos\theta = P\sqrt{2\Omega}/\sqrt{m}$.

When $\Omega > 1$ (bulk materials)

$$Z_0'' = \cos\theta\sqrt{m}\cdot\frac{1}{\sqrt{1-\frac{\sin^2\theta\varkappa P}{m}}}. \qquad (11.4.8)$$

The impedance of a layer, installed at distance l_1 from a rigid wall [15], is

$$Z_0'' = \frac{W_{m_1}\cos\theta\left[\frac{W_{m_1}\cos\theta}{\cos\psi}\operatorname{sh}(\gamma_m l\cos\psi) - i\operatorname{ctg}kl_1\cos\theta\operatorname{sh}(\gamma_m l\cos\psi)\right]}{\cos\psi\left[-i\operatorname{ctg}(kl_1\cos\theta)\operatorname{sh}(\gamma_m l\cos\psi) + \frac{W_{m_1}\cos\theta}{\cos\psi}\operatorname{ch}(\gamma_m l\cos\psi)\right]}. \qquad (11.4.9)$$

APPROVED FOR RELEASE: 2007/02/08: CIA-RDP82-00850R000200100009-9

APPROVED FOR RELEASE: 2007/02/08: CIA-RDP82-00850R000200100009-9

If the angular function Z''_θ or α is known it is possible to calculate the diffuse acoustic absorption coefficient:

for plane absorbers

[Д=d] $$\alpha_Д = 2\int_0^{\pi/2} \alpha_\theta \sin\theta\cos\theta\, d\theta, \quad (11.4.10)$$

for space absorbers

[y=c] $$\alpha_Д = 4\alpha_y. \quad (11.4.11)$$

11.5. Acoustic Absorption in High Acoustic Pressure Levels[1]

A level at which an amplitude function of impedance and of the acoustic absorption coefficient of sound-absorbing materials appears, in addition to the frequency dependence, is called a high acoustic pressure level (HPL). Impedance exhibits greatest nonlinearity in perforated panels, starting with HPL ≈ 100 dB, i.e., at levels that are frequent on ships. The dependence of impedance and the acoustic absorption coefficient on HPL can be determined experimentally or calculated by empirical formulas.

Data from measurements of linear impedance and of stationary flux impedance σ_c as a function of velocity [22] are used for calculating the impedance of a thin film of porous material in the nonlinear range. In the linear range acoustic and hydrodynamic impedances R and σ_c are virtually identical. At amplitudes of vibration velocity (for σ_c -- at flux velocities), exceeding several meters per second, the values of R and σ_c begin to increase with velocity, and a one-to-one relationship exists between them.

The components of the impedance of a thin film of porous material with σ_c = = 5 in the linear range, are plotted in Figure 11.8 as functions of HPL. The calculated and measured values of the active component of impedance agree quite well. The reactive part of acoustic impedance depends less on velocity and stays in the linear mode longer.

The specific impedance of a single hole in a panel with HPL $R = R_0 + k\rho\dot{\xi}$, where the nonlinear additive is proportional to the amplitude of the vibration velocity in the hole, is $\dot{\xi}(k \approx 1)$.

When $\dot{\xi} > \dot{\xi}_{crit}$ the additive becomes many times greater than R_0 and entirely determines the active losses in the hole. The value $R = \rho\dot{\xi}$ is the limiting

[1]This section was written by I. V. Lebedeva.

APPROVED FOR RELEASE: 2007/02/08: CIA-RDP82-00850R000200100009-9

APPROVED FOR RELEASE: 2007/02/08: CIA-RDP82-00850R000200100009-9

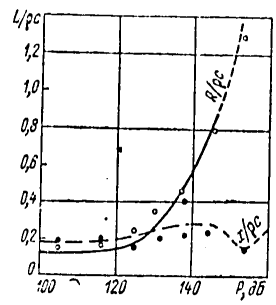

Figure 11.8. Comparison of experimental and theoretical (calculated) components of impedance of thin porous film: σ_c = 5 rel, f = 1,250 Hz, $l_1 = \lambda/4$. [дБ=dB]

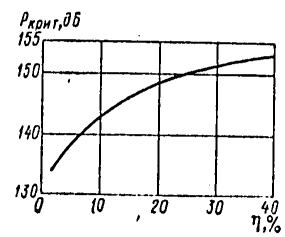

Figure 11.9. Boundary acoustic pressure levels of nonlinear impedance as functions of perforation coefficient η. [крит=crit]

value for the specific impedance of a hole of any diameter with HPL. In consideration of the transformation of impedance from a hole to a cell in a panel, this circumstance can be used for achieving high acoustic absorption coefficients with large-diameter holes in high-intensity fields. Thin panels exhibit stronger nonlinear effects.

Nonlinear effects are strongest when $\dot{\xi}_{crit} > 10$ m/s. In practice it is better to use not $\dot{\xi}_{crit}$, but the boundary HPL p_{crit}, in Pa, of the incident sound, which for the resonance frequency is estimated through the empirical formula [19]:

[крит=crit]

$$p_{крит} = 62 + 2090\,\eta + 140\,\eta^2. \qquad (11.5.1)$$

The boundary values of HPL (above which the nonlinear term prevails), calculated by this formula, are given in Figure 11.9 as functions of perforation coefficient η. Modern technology creates levels that exceed p_{crit}, even for η = 40% (p_{crit} = 153.2 dB). The deviation of these values of impedance from linear begins at substantially lower velocities ($\dot{\xi} > 1$ m/s) and at correspondingly smaller HPL.

Nonlinearity R can be expressed by the so-called "nonlinear end correction factor" Δ_{nl}:

[нл=nl]

$$R = \frac{\sqrt{8\mu\omega\rho}}{d}(t + 2t' + \Delta_{нл}). \qquad (11.5.2)$$

APPROVED FOR RELEASE: 2007/02/08: CIA-RDP82-00850R000200100009-9

APPROVED FOR RELEASE: 2007/02/08: CIA-RDP82-00850R000200100009-9

For holes with the parameters 0.5 cm $\leq$ d $\leq$ 2 cm, η = 0.5-10% one may use the empirical dependence of the relative value Δ_{nl}/d on HPL (in decibels):

$$\log(\Delta_{нл}/d) = -1{,}685 + 0{,}0185p. \qquad (11.5.3)$$

The reactive component of the acoustic impedance of a hole with HPL exceeding p_{crit} is assumed to decrease to one-half of the linear value. In consideration of this, and by determining R in accordance with (11.5.2), it is possible to calculate the frequency characteristic of absorption for different HPL values. As the impedance of a hole in the case of ordinary perforation (η = 1-12%) increases α_{max} increases in the range of HPL values from 120 to approximately 140 dB, and then it begins to decrease, and the resonance absorption curve expands. The resonance frequency increases as the reactive component of impedance decreases.

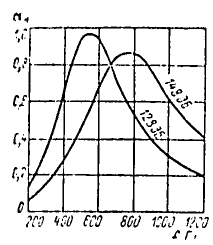

Figure 11.10. Frequency characteristic of absorption coefficient of panel with hole d = 0.2 cm for different acoustic pressure levels.

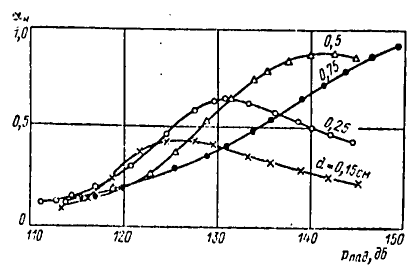

Figure 11.11. Amplitude function of acoustic absorption coefficient of holes with different diameter (f = = 1,000 Hz, $l_1 = \lambda/4$).

The results of the calculation are plotted in Figure 11.10; they coincide satisfactorily with the experimental data for a hole with the parameters t = 0.16 cm; d = 0.2 cm; η = 1.45%; l_1 = 4.8 cm.

The sound absorption coefficient of holes with d = 0.15, 0.25, 0.5, 0.75 cm in a cell with a diameter of 2.35 cm for $l_1 = \lambda/4$, in normal incidence, is plotted in Figure 11.11 as a function of HPL (the measurements were done with an interferometer, f = 1,000 Hz) [13]. The sound absorption coefficient quickly reaches its maximum value, which is low, as R increases in a panel with a small-diameter hole. Large-diameter holes are more effective.

Nonlinear phenomena in HPL substantially alter the absorption characteristic and often increase acoustic absorption, which should be taken into consideration during the design of acoustic absorbers for deadening high-intensity noise.

APPROVED FOR RELEASE: 2007/02/08: CIA-RDP82-00850R000200100009-9

APPROVED FOR RELEASE: 2007/02/08: CIA-RDP82-00850R000200100009-9

11.6. Measurement of Acoustic Absorption[1]

Acoustic Interferometry. This method is used for measuring the acoustic absorption coefficient (AAC) and impedance in normal instruments. A specimen is placed in one end of a hollow cylindrical or square tube with rigid walls. The diameter of the specimen is the same as the cross section of the tube. A radiator, driven by an acoustic frequency generator, is placed in the other end of the tube. The receiver is a probe (a hollow metal tube 3-4 mm in diameter), inserted in the tube and connected to a capsule containing a microphone. Potential from the microphone is applied to a metering amplifier with a filter (to eliminate harmonics). The acoustic waves, striking the specimen, are reflected and produce standing waves in the tube.

The probe may introduce distortions, and therefore the so-called correction factor for the probe must be determined. To do this a plate is placed over the end of the tube and the coordinate of the first minimum, which in this case should be theoretically at a distance of $\Delta_1 = \lambda/4$, is marked. The difference between the calculated and measured values of Δ_1 is the correction factor for the probe. The frequency dependence of this correction factor must be determined and taken into account during the measurements.

The top frequency boundary, up to which measurements may be conducted, is $f_b = 2 \cdot 10^6/d_1$ for a cylindrical interferometer with diameter d_1, and for a square interferometer with side a_1 it is $f_b = c/2a_1$. The frequency at which measurements can be taken in an interferometer with length l is $f = c/4l$.

To measure the AAC it is necessary to measure the pressure at the maximum p_{max} and minimum p_{min} of the standing wave:

$$\alpha = \frac{4d}{2d + d^2 + 1}; \quad d = \frac{p_{max}}{p_{min}}. \tag{11.6.1}$$

To measure impedance it is also necessary, in addition to d, to determine Δ_1 and calculate phase shift 2δ:

$$2\delta = \frac{2\pi(\Delta_1 - \lambda/4)}{\lambda/2}; \tag{11.6.2}$$

The components of impedance are calculated by the formulas

$$X_1 = \frac{(d^2 - 1)\sin 2\delta}{(d^2 + 1) - (d^2 - 1)\cos 2\delta};$$
$$R_1 = \frac{2d}{(d^2 + 1) - (d^2 - 1)\cos 2\delta}. \tag{11.6.3}$$

[1] I. V. Lebedeva contributed to this section.

APPROVED FOR RELEASE: 2007/02/08: CIA-RDP82-00850R000200100009-9

APPROVED FOR RELEASE: 2007/02/08: CIA-RDP82-00850R000200100009-9

X_1 and R_1 can also be determined on the basis of the impedance diagram [17].

Measurement of Wave Parameters W_m and γ_m. This method is based on measurement of impedance Z_1' of a film with thickness l of the analyzed material, placed on a rigid wall, and of impedance Z_1'' of a film, applied over the wall at distance $l_1 = \lambda/4$:

$$\frac{W_m}{Z} = W_{m_1} = \sqrt{Z_1' Z_1''}; \tag{11.6.4}$$

$$\gamma_m = \frac{1}{l}\left\{\frac{1}{4}\ln\frac{(1+R)^2+X^2}{(1-R)^2+X^2}\right\} - \\ -\frac{i}{l}\operatorname{arctg}\left[n\pi+\frac{\pi}{2}+\frac{R+1}{X}\right]-\frac{i}{l}\operatorname{arctg}\left[n\pi-\frac{1-R}{X}\right]; \tag{11.6.5}$$

where R and X are the real and imaginary components of $\sqrt{Z_1''/Z_1'}$.

The values of W_m and γ_m can also be determined by measuring impedance Z_1' of layer l on a rigid wall, and of layer $2l$ - Z_1'' (also on a rigid wall). If $Z_1'/Z_1'' = u + iv$, then the expressions

$$\beta_m = \frac{1}{4l}\arccos\frac{1\mp\sqrt{1-2[(u-1)^2+v^2]^2+[(u+1)^2+v^2]^2}}{(u-1)^2+v^2}; \tag{11.6.6}$$

$$\alpha_m = \frac{1}{4l}\operatorname{arcch}\frac{1\mp\sqrt{1-2[(u-1)^2+v^2]^2+[(u+1)^2+v^2]^2}}{(u-1)^2+v^2} \tag{11.6.7}$$

are used for determining α_m and β_m ($\gamma_m = \alpha_m + i\beta_m$). The radical is determined by the conditions $\alpha_m \geq 0$, $\beta_m \geq 0$. The wave impedance is

$$\frac{W_m}{Z} = \frac{Z_1'}{\operatorname{cth}(\alpha_m + i\beta_m)\, l} = W_{mr}' + iW_{mi}'. \tag{11.6.8}$$

The values of K_m and ρ_m are calculated by (11.2.7, 8), whence

$$\rho_{mr} = \frac{m\rho}{P} \qquad |\rho_{mi}| = \frac{\sigma_c}{\omega}. \tag{11.6.9}$$

The value $\sigma_c = |\rho_{mi}\omega|$ on some frequency may coincide with the impedance of the stationary flux, determined as the ratio of the pressure drop to the space velocity.

Reverberation Technique. The reverberation technique is used for measuring the acoustic absorption coefficient in a diffuse acoustic field, generated in reverberation chambers (RC), which are large irregular rooms with smooth walls, which reflect sound well. RC must have a separate foundation or a floating floor for insulation from external noise and vibrations. The recommended volume for RC is 200 ± 20 m^3; structures that are used in practice are tested in them.

APPROVED FOR RELEASE: 2007/02/08: CIA-RDP82-00850R000200100009-9

APPROVED FOR RELEASE: 2007/02/08: CIA-RDP82-00850R000200100009-9

An RC is a three-dimensional vibrating system, in which a certain spectrum of natural frequencies is excited by an acoustic signal. Width B of the resonance curves is determined by the losses in RC, which occur both on boundary surfaces, and in the air mass. The absorption of RC walls is characterized by the average acoustic absorption coefficient $\bar{\alpha} = \Sigma\alpha_i S_i / \Sigma S_i$ (α_i is the AAC of a surface with area S_i), and the absorption in the space is determined by the absorption coefficient m in air.

The acoustic characteristic of losses in a room is the standard reverberation time T -- the segment of time during which the intensity of sound, after the source is turned off, falls to one-millionth (i.e., by 60 dB), and the pressure to one-thousandth of the initial values. In RC with $\bar{\alpha} \leq 0.1$ T, in seconds, is determined by Sebin's formula

$$T = \frac{0{,}16V}{\bar{\alpha}s + 4mV}. \qquad (11.6.10)$$

Eyring's formula is more exact for $\bar{\alpha} > 0.1$:

$$T = \frac{0{,}16V}{-s\ln(1-\bar{\alpha}) + 4mV}. \qquad (11.6.11)$$

Due to the frequency dependence of $\bar{\alpha}$ and m the reverberation time decreases monotonically as frequency increases. According to GOST T_0 in a vacant chamber with a volume of 200 m^3 should be $T_0 \geq 5$ s on low frequencies (starting at 100 Hz) and $T_0 \geq 2$ s on 4 kHz.

The field in RC is assumed to be diffuse if the natural vibration frequencies are so close that the frequency distance between them is $\Delta f \leq B/3$. This condition limits the effective range of RC on the low-frequency end: $f_b = 2{,}000\sqrt{T/V}$, where V, in m^3, is the volume of RC.

The high-frequency end is limited by the strengthening of attenuation in air, as a result of which the direct sound from the source begins to predominate.

Acoustic absorption in a diffuse field is determined by measuring the reverberation time T_0 in an empty chamber and the reverberation time T in the chamber with the specimen. Then the acoustic absorption coefficient of the analyzed material with area S_1 is

[Д=d]

$$\alpha_д = \bar{\alpha} + \frac{0{,}16V}{S_1}\left[\left(\frac{1}{T} - \frac{1}{T_0}\right) - 25\,(m - m_0)\right]. \qquad (11.6.12)$$

The first term takes into account the absorption of surface of RC shielded by the specimen (usually $\bar{\alpha} \ll \alpha$, and for calculation purposes it may be

APPROVED FOR RELEASE: 2007/02/08: CIA-RDP82-00850R000200100009-9

APPROVED FOR RELEASE: 2007/02/08: CIA-RDP82-00850R000200100009-9

ignored). The last term is related to the change of absorption in air due to changes of temperature and humidity during the time of measurements.

T_0 and T should be measured under the identical conditions. Then

$$\alpha_{д} = \frac{0{,}16V}{S_1}\left(\frac{1}{T} - \frac{1}{T_0}\right). \qquad (11.6.13)$$

The measured values of α for a specimen of limited size, due to the so-called "boundary effect," caused by diffraction on the boundary of the specimen, depend on the area of the specimen and may exceed unity [12]. For an RC with a volume of 200 m^3 it is recommended that specimens with an area of 10-12 m^2 be used in the form of a rectangle with a side ratio of 0.7:1. The specimen is mounted flush against the floor or its sides are covered with wood strips to eliminate absorption by the side surfaces.

Diffusers in the form of randomly oriented, easily folded sheets of rigid material, commensurable in size with wavelength, are suspended in RC to maintain diffusivity after the sound-absorbing specimen is set up. A homogeneous field in the stationary mode and linear decline of the acoustic pressure level in decibels, during the time of reverberation, are indirect indications of diffusivity.

The frequency dependence of the acoustic absorption coefficient should be measured with third-octave bands of white noise with the measured values of α_d expressed in terms of the mean geometric frequencies of the band. The values of T, averaged in time (three tests at one point) and in space (the microphone is set up in three positions) should be substituted into (11.6.13). To obtain statistical experimental data the test points should be separated by distance $l \geq \lambda/2$ from the walls, absorbing specimen, sound source and each other.

The recordings, made with a recording instrument, are processed in the pressure drop range of from -5 to -35 dB from the stationary level. The reverberation time is determined on the basis of the slope of the reverberation curves with a special protractor, included in the test instrument kit. Recordings with a nonlinear curve are not used in the calculation.

The values of α may also be measured in reverberation chambers in the stationary mode, using the so-called "method of intensities." The energy density, or the mean square acoustic pressure in the empty chamber $\langle p_0^2 \rangle$ and in the chamber with the specimen $\langle p_1^2 \rangle$, proportional to the energy density, at the same source output power is determined for this purpose. After determining the total absorption A_0 in the empty chamber for T_0 using the relation $\frac{\langle p_0^2 \rangle}{\langle p_1^2 \rangle} = A_1/A_0$ the total absorption in the chamber with the specimen A_1 and the diffuse acoustic absorption coefficient of the specimen are calculated. The advantage of measuring the AAC in the stationary mode is

APPROVED FOR RELEASE: 2007/02/08: CIA-RDP82-00850R000200100009-9

APPROVED FOR RELEASE: 2007/02/08: CIA-RDP82-00850R000200100009-9

that its precision does not have any effect on the constant interference level. The mean acoustic power of the sources is also determined in the stationary mode:

$$N = \frac{A_0}{4\rho c} \langle p_0^2 \rangle .$$

Measurements can be conducted in the stationary mode not only with third-octave, but also with narrower noise bands, with multitone and discrete frequencies. In these cases the acoustic field in the reverberation chamber is described, respectively, by the average measured value, by the limits of deviation from the average (for example of standard dispersion σ^2), and by the fiducial probability of these limits $P\langle\overline{p}^2\rangle$. In an inhomogeneous field, generated by a pure tone, the standard dispersion $\overline{p}^2$ of a single measurement is equal to one. Precision increases by a factor of n after averaging for n statistically independent points of the room: $\sigma_1^2 = 1/n$. When averaging is done with continuous motion on some trajectory of length l the number of equivalent statistically independent points is $n = 1 + 2l/\lambda$.

If the test signal consists of i statistically independent frequencies additional averaging in terms of frequency is done at each point: $\sigma_2 = 1/i$. Frequencies separated by an interval wider than the bandwidth of the resonance curve of the RC in that range are statistically independent frequencies. The equivalent number of statistically independent components in the noise band of width Δf_n is determined by the approximate formula $i = 1 + \frac{\Delta f_n T_0}{6.9}$. The relation is satisfied with a high degree of accuracy when $\Delta f_n T_0 \gg 20$, which is easy to achieve in RC [14].

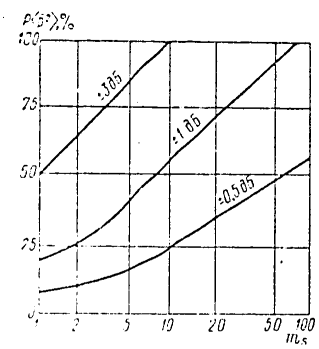

Figure 11.12. Fiducial probability of mean square pressure, averaged in terms of space and frequency, for different tolerable measurement precisions.

Since averaging in terms of frequency and space may be assumed to be independent processes, the standard dispersion of the arithmetic mean of n measurements with an i-component signal is $\sigma_3 = 1/m_s$, where $m_s = n \cdot i \cdot n$.

The function $P\langle\overline{p}^2\rangle$ is plotted in Figure 11.12 as a function of the parameter m_s for different tolerable measurement precisions. For a given confidence range of the measured mean square pressure, expressed in decibels, and given fiducial probability (in percentage points), it is possible to find on the curves the value of the parameter m_s, and thus to establish the test

APPROVED FOR RELEASE: 2007/02/08: CIA-RDP82-00850R000200100009-9

APPROVED FOR RELEASE: 2007/02/08: CIA-RDP82-00850R000200100009-9

conditions. For instance, if the necessary precision is such that $\langle\overline{p^2}\rangle$ is determined in the range of ±1 dB with a probability of 80%, then averaging must be done for about 30 points when working with a pure tone.

BIBLIOGRAPHY

1. "Aviatsionnaya Akustika" [Aviation Acoustics], edited by A. G. Munin and V. Ye. Kvitk, Moscow, Mashinostroyeniye, 1973.

2. Velizhanina, K. A., "On Calculation of Porous Acoustic Absorbers with Perforated Panel," AKUSTICHESKIY ZHURNAL [Acoustics Journal], 1968, XIV, No 1, pp 50-55.

3. Velizhanina, K. A. and L. A. Borisov, "Studies of Space Absorbers in Field of Plane Acoustic Wave and in Diffuse Field," VESTNIK MOSKOVSKOGO UNIVERSITETA. FIZIKA, ASTRONOMIYA [Herald of Moscow University. Physics, Astronomy], 1967, No 4, pp 77-83.

4. Velizhanina, K. A. and L. A. Borisov, "Space Acoustic Absorbers," in the book: "Bor'ba s Shumom i Zvukoizolyatsiya" [Noise Control and Acoustic Insulation], Moscow, NIISF, 1969.

5. Velizhanina, K. A. and R. D. Kisenishskaya, "Investigation of Sound-Absorbing Systems in Wide Frequency Range," in the book: "Bor'ba s Shumom i Zvukoizolyatsiya," Moscow, NIISF, 1969.

6. Velizhanina, K. A., N. P. Voronina and Ye. S. Kodymskaya, "Investigations of Impedance of Sound-Absorbing Systems in Oblique Incidence," AKUSTICHESKIY ZHURNAL, 1971, XVII, No 2, pp 229-234.

7. Velizhanina, K. A. and Ye. S. Kodymskaya, "Analysis of Behavior of Sound-Absorbing Systems in Oblique Incidence," "Trudy 11-y Akusticheskoy Konferentsii" [Transactions of 11th Acoustics Conference] Bratislava, 1973.

8. Vital', K. A., "On Oblique Acoustic Incidence on Resonant Absorber," ZHTF [Journal [Journal of Technical Physics], 1940, Vol 10, No 12, pp 980-987.

9. GOST 16297-70. Izdeliya i Stroitel'nyye Materialy. Metody Akusticheskikh Ispytaniy [Products and Construction Materials. Acoustic Testing Techniques].

10. Yegorov, N. F., "Acoustic Absorption by Thin Fiber Sheets," AKUSTICHESKIY ZHURNAL, 1969, VI, No 2, pp 219-222.

11. Zinchenko, V. I. and V. K. Zakharov, "Snizheniye Shuma na Sudakh" [Reduction of Noise on Ships], Leningrad, Sudostroyeniye, 1968.

APPROVED FOR RELEASE: 2007/02/08: CIA-RDP82-00850R000200100009-9

APPROVED FOR RELEASE: 2007/02/08: CIA-RDP82-00850R000200100009-9

12. Lebedeva, I. V., "On Method of Measuring Acoustic Absorption Coefficient in Reverberation Chamber," AKUSTICHESKIY ZHURNAL, 1962, VIII, No 3, pp 334-340.

13. Lebedeva, I. V., "Measurement of Acoustic Properties of Perforated Panels at High Acoustic Pressure Levels," in the book: "Zvukoizoliruyushchiye i Zvukopogloshchayushchiye Konstruktsii v Stroitel'stve i na Transporte" [Acoustic Insulating and Soundproofing Structures in Construction and Transportation], LDNTP, 1974, pp 88-91.

14. Lebedeva, I. V. and A. A. Shkol'nikova, "Analysis of Reverberant Field in Stationary Mode," VESTNIK MOSKOVSKOGO UNIVERSITETA, 1971, No 6, pp 649-654.

15. Osipov, G. L., "Zashchita ot Shuma" [Noise Safety], Moscow, Stroyizdat, 1972.

16. Rzhevkin, S. N., "Resonant Acoustic Absorber with Pliant Front Wall," ZHTF, 1946, XIV, No 4.

17. Rzhevkin, S. N., "Kurs Lektsiy po Teorii Zvuka" [Course of Lectures on Theory of Sound], Moscow, Izd-vo MGU, 1960.

18. Tsvikker, K. and K. Kosten, "Zvukopogloshchayushchiye Materialy" [Soundproofing Materials], Moscow, IL, 1952.

19. Blackman, A. W., "Effect of Nonlinear Losses on the Design of Absorbers for Combustion Instabilities," AM. ROCKET, 1960, 30.

20. Ingard, U., "On the Theory and Design of Acoustic Resonators," J. ACOUST. SOC. AMERICA, 1953, Vol 25, No 6, pp 1037-1061.

21. Pyett, J. S., "The Acoustic Impedance of a Porous Layer at Oblique Incidence," ACOUST., 1953, 3, pp 375-382.

22. Zorumski, W. E. and T. L. Parrot, "Nonlinear Acoustic Theory for Thin Porous Sheets," NASA, SP-189, 1968.

APPROVED FOR RELEASE: 2007/02/08: CIA-RDP82-00850R000200100009-9

APPROVED FOR RELEASE: 2007/02/08: CIA-RDP82-00850R000200100009-9

CHAPTER 12. VIBRATION DAMPING OF MARINE MACHINERY

12.1. Purpose and Classification of Vibration-Damping Shock-Absorbing Structures and Fasteners

Purpose and Kinds of Structural Shock Absorption. Structural shock absorption consists in the use of a special mounting, called a shock absorber, which eliminates direct contact between a machine and bearing structures and other external connections to it, thereby preventing the transmission of undesirable dynamic forces.

Shock absorption for the purpose of protecting something from dynamic forces that propagate from neighboring structures is called passive shock absorption. The case when a vibration-damped object is a source, or contains a source of dynamic forces, from which nearby structures or equipment must be protected, is called active shock absorption. Thus, the purpose of active shock absorption is to insulate a source of undesirable dynamic forces.

Active shock absorption is characterized by the direct action of force upon the vibration-damped object, i.e., the direct application to it of dynamic forces (Figure 12.1a), when the points of application of forces often do not coincide with mechanical contacts between the object and surrounding structures. In passive shock absorption the vibration-damped object is subjected to so-called kinematic forces: the vibrations of fasteners to bearing structures are external forces that cause an object to vibrate (Figure 12.1b).

Unprotected machinery sometimes experiences considerable vibration due to the fact that it, along with its foundation and (or) other bearing structures, constitutes a vibrating system that resonates with the forces acting upon it. In this case the installation of a shock-absorbing mount removes the system from resonance by changing its natural frequency.

A shock-absorbing mount is a vibration-damping (sound-insulating) foundation when it reduces the transmission of vibrations or of forces that produce vibration. The ensuing discussion pertains to vibration-damping shock-absorbing mounts, and the dynamic forces to be isolated are assumed

APPROVED FOR RELEASE: 2007/02/08: CIA-RDP82-00850R000200100009-9

APPROVED FOR RELEASE: 2007/02/08: CIA-RDP82-00850R000200100009-9

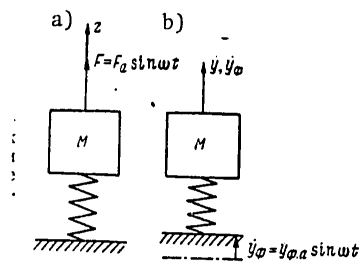

Figure 12.1. Active (a) and passive (b) vibration-damping shock absorption. [ϕ=f]

to be harmonic or consisting of harmonic components.

Classification of Shock-Absorbing Structures. A shock-absorbing mount consists of individual shock-absorbing structures, the relative position and characteristics of which are determined entirely by the characteristics of the mount. Shock-absorbing structures that are parts of shock-absorbing mounts are classified as follows:

bearing absorbers that, with the ship in the upright position (in the absence of roll and trim), bear the entire weight of a machine;

nonbearing shock absorbers, also called thrusts, which prevent intolerable movements of a machine relative to the foundation and surrounding machinery during rolling and at large trim angles. If displacements of a machine must be limited by bearing absorbers, thrusts are not necessary;

inserts (bellows, hose joints, flexible branches, flexible sleeves and hoses) in pipes connected to a machine;

shock-absorbing inserts (flexible couplings) in shafts connected to a machine;

flexible sections of cables connected to a machine.

The last three types of shock-absorbing structure are vibration-damping systems of nonbearing connections of mechanisms (pipes, shafts, cables).

Single-Stage and Two-Stage Fastening. A shock-absorbing fastener, in which all shock absorbers operate in parallel, is called a single-stage fastener. Two series-connected single-stage fasteners make up a two-stage shock-absorbing fastener and as its component parts are called absorbing stages. The inside stage is directly connected to the protected mechanism, and the outside stage is connected to the bearing structures. Intermediate structures, for example mounts or frames, are inserted between the stages, connecting them.

Effectiveness of Shock Absorption. The effectiveness of vibration-damping shock absorption can be judged on the basis of the attainable reduction of vibration and dynamic forces at characteristic points of a protected structure. In the steady state harmonic mode it is convenient to compare

APPROVED FOR RELEASE: 2007/02/08: CIA-RDP82-00850R000200100009-9

APPROVED FOR RELEASE: 2007/02/08: CIA-RDP82-00850R000200100009-9

the amplitude y_a, $\dot{y}_a$, $\ddot{y}_a$ or effective[1] y_{ef}, $\dot{y}_{ef}$, $\ddot{y}_{ef}$ vibration displacements y, velocities $\dot{y}$ or accelerations $\ddot{y}$ without shock absorption with the corresponding values y_a^{sa}, $\dot{y}_a^{sa}$, $\ddot{y}_a^{sa}$, y_{ef}^{sa}, $\dot{y}_{ef}^{sa}$, $\ddot{y}_{ef}^{sa}$ with shock absorption. Each pair of compared values is used to compute the ratio

[ам=sa; эф=ef]
$$k_* = \frac{y_a^{ам}}{y_a} = \frac{y_{эф}^{ам}}{y_{эф}} = \frac{\dot{y}_a^{ам}}{\dot{y}_a} = \frac{\dot{y}_{эф}^{ам}}{\dot{y}_{эф}} = \frac{\ddot{y}_a^{ам}}{\ddot{y}_a} = \frac{\ddot{y}_{эф}^{ам}}{\ddot{y}_{эф}}. \qquad (12.1.1)$$

If the examined values pertain to the same point of a structure and to the same direction of vibration, then the effectiveness of shock absorption for a given point and given direction is determined entirely by k_*. In this case k_* expresses the fraction of the dynamic force applied to the examined point of the structure in the absence of shock absorption, which penetrates there through the shock absorbers.

The reduction of vibration is characterized by the absorption effectiveness coefficient

$$k_e = 1 - k_*. \qquad (12.1.2)$$

This coefficient is positive when shock absorption produces a positive effect and it increases with its effectiveness, but it cannot be greater than one.

The difference E, in dB, of the vibration levels of a given direction at a given point is called absorption effectiveness (for the given point and direction):

[Э=E]
$$Э = 20 \lg \frac{y_a}{y_a^{ам}} = 20 \lg \frac{\ddot{y}_{эф}}{\ddot{y}_{эф}^{ам}} = 20 \lg k_*^{-1} = 20 \lg (1 - k_э)^{-1}. \qquad (12.1.3)$$

The comparative analysis of vibration intensity, used in formula (12.1.3) and in the ensuing discussion, is essentially a comparative analysis of the specific kinetic energy of vibration at points, the vibrations of which are being examined. If a protected structure receives from a shock-absorbing mount a harmonic force F^{sa} or moment M^{sa} instead of the same force (i.e., of the same direction and frequency) F or moment M that acts upon it in the absence of shock absorption, the effectiveness E, in dB, of shock absorption in relation to the same kind of force is

$$Э = 20 \lg \frac{F_a}{F_a^{ам}} = 20 \lg \frac{F_{эф}}{F_{эф}^{ам}}, \qquad (12.1.4)$$

or

$$Э = 20 \lg \frac{\mathfrak{M}_a}{\mathfrak{M}_a^{ам}} = 20 \lg \frac{\mathfrak{M}_{эф}}{\mathfrak{M}_{эф}^{ам}}. \qquad (12.1.5)$$

[1]The so-called effective value of any harmonic variable, as is known, is $\sqrt{2}$ times smaller than its amplitude value.

APPROVED FOR RELEASE: 2007/02/08: CIA-RDP82-00850R000200100009-9

APPROVED FOR RELEASE: 2007/02/08: CIA-RDP82-00850R000200100009-9

The corresponding effectiveness coefficient in terms of the external force (F or M) is determined by expression (12.1.2), in which

$$k_* = \frac{F_a^{\text{ам}}}{F_a} = \frac{F_{\text{эф}}^{\text{ам}}}{F_{\text{эф}}} \tag{12.1.6}$$

or

$$k_* = \frac{\mathfrak{M}_a^{\text{ам}}}{\mathfrak{M}_a} = \frac{\mathfrak{M}_{\text{эф}}^{\text{ам}}}{\mathfrak{M}_{\text{эф}}}.$$

The mounting of machinery without shock absorbers, usually called rigid mounting, in the simplified examination of many problems, is often assumed to exhibit the ideal properties of absolute rigidity and inertialessness. An absolutely rigid contact is assumed to exist on all the contact surfaces between the machine and surrounding structures in so-called rigid fastening, which is usually utilized in practice. The characteristics of vibration and of the perturbing forces that cause it, which correspond to this assumption, are indicated by the superscript "r." The same explanatory superscript is given to the symbols of the values k_*, k_e, E if they are computed under this assumption; thus, in the special case at hand the symbols k_*^r, k_e^r, E^r will be used.

The effectiveness of a shock-absorbing mount, determined in relation to the case of an absolutely rigid inertialess support, is called vibration damping VD, in dB:

[ВИ=VD; ж=r; э=e]

$$\text{ВИ} = \text{Э}^{\text{ж}} = L^{\text{ж}} - L^{\text{ам}} = 20\lg\frac{y_{\text{э}}^{\text{ж}}}{y_a^{\text{ам}}} = 20\lg\frac{\ddot{y}_{\text{эф}}^{\text{ж}}}{\ddot{y}_{\text{эф}}^{\text{ам}}} = -20\lg k_*^{\text{ж}}. \tag{12.1.7}$$

The analogous special modifications of expressions (12.1.4) and (12.1.6) are

$$\text{ВИ} = \text{Э}^{\text{ж}} = 20\lg\frac{F_a^{\text{ж}}}{F_a^{\text{ам}}} = 20\lg\frac{F_{\text{эф}}^{\text{ж}}}{F_{\text{эф}}^{\text{ам}}}, \tag{12.1.8}$$

$$k_*^{\text{ж}} = \frac{F_a^{\text{ам}}}{F_a^{\text{ж}}} = \frac{F_{\text{эф}}^{\text{ам}}}{F_{\text{эф}}^{\text{ж}}}, \tag{12.1.9}$$

and of expressions (12.1.5) and (12.1.6) the equations

$$\text{ВИ} = \text{Э}^{\text{ж}} = 20\lg\frac{\mathfrak{M}_a^{\text{ж}}}{\mathfrak{M}_a^{\text{ам}}} = 20\lg\frac{\mathfrak{M}_{\text{эф}}^{\text{ж}}}{\mathfrak{M}_{\text{эф}}^{\text{ам}}}, \tag{12.1.10}$$

$$k_*^{\text{ж}} = \frac{\mathfrak{M}_a^{\text{ам}}}{\mathfrak{M}_a^{\text{ж}}} = \frac{\mathfrak{M}_{\text{эф}}^{\text{ам}}}{\mathfrak{M}_{\text{эф}}^{\text{ж}}}. \tag{12.1.11}$$

An absolutely rigid inertialess mount transfers intact the dynamic forces applied to it. The coefficient of transmission of dynamic forces through such a mount is unity.

APPROVED FOR RELEASE: 2007/02/08: CIA-RDP82-00850R000200100009-9

APPROVED FOR RELEASE: 2007/02/08: CIA-RDP82-00850R000200100009-9

Shock Absorbers and Absorbing Mounts as Two-Ended Mechanical Links, Analogous to Electrical Quadrupoles. In a chain that transmits harmonic longitudinal vibrations, a shock-absorbing fastener may be viewed as a two-ended passive mechanical link or combination of two-ended mechanical links, each of which is analogous to an electrical quadrupole. An individual shock absorber may be represented in like fashion as being a two-ended mechanical link or combination of such links.

A conditional diagram of a two-ended passive (i.e., not containing sources of vibration energy) mechanical link along with the forces acting upon it and velocities imparted to it, is shown in Figure 12.2a. The diagram does not reveal the internal structure of the link, which can vary. From the outside, to the left end (input) of the link, is applied disturbing force F_1, and to the right end (output) is applied reaction F_2 from the mechanical system on the right. Force F_1, which produces reaction F_2, also gives rise to velocities $\dot{y}_1$ at the input and $\dot{y}_2$ at the output of the two-ended link. The forces are assumed to be positive when they are exerted from the ends to the inside of the link. The direction from the input of the link to its output is assumed positive for both velocities.

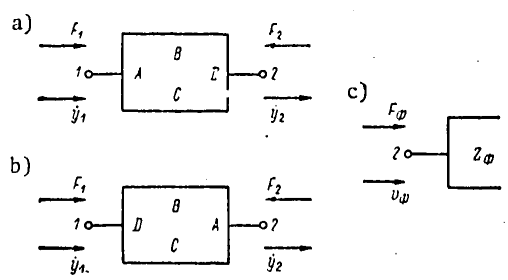

Figure 12.2. General diagram of double-ended mechanical link with harmonic disturbing force F applied to input (point 1) (a); analogous diagram for inverted link (b); mechanical impedance Z_f connected at point 2, loading output of double-ended link (c). [ϕ=f]

In the steady state harmonic mode, when the forces and velocities change in time with some angular frequency ω, the relation between them is determined by the equation system

$$\left.\begin{aligned} F_1 &= AF_2 + B\dot{y}_2; \\ \dot{y}_1 &= CF_2 + D\dot{y}_2. \end{aligned}\right\} \qquad (12.1.12)$$

Here A, B, C, D are called the characteristic coefficients of a two-ended link, connected together by the relation

APPROVED FOR RELEASE: 2007/02/08: CIA-RDP82-00850R000200100009-9

APPROVED FOR RELEASE: 2007/02/08: CIA-RDP82-00850R000200100009-9

$$AD - BC = 1. \tag{12.1.13}$$

All characteristic coefficients depend in the general case on frequency ω and, for a fixed frequency, are constant complex numbers. Of them A and D are dimensionless, B is measured in mechanical impedance and C in mobility (mechanical conductance), which is the inverse mechanical impedance. Linear two-ended mechanical links, the characteristic coefficients of which do not depend on the amplitude values of forces F_{1a}, F_{2a} and of velocities $\dot{y}_{1a}$, $\dot{y}_{2a}$, are examined below.

Equation system (12.1.12) may be written as the matrix equation

$$\begin{bmatrix} F_1 \\ \dot{y}_1 \end{bmatrix} = A_0 \begin{bmatrix} F_2 \\ \dot{y}_2 \end{bmatrix}, \tag{12.1.14}$$

where

$$A_0 = \begin{bmatrix} A & B \\ C & D \end{bmatrix} \tag{12.1.15}$$

is the matrix of the characteristic coefficients; its determinant $|A_0|$, as can be seen by (12.1.13), is equal to unity for the rule of signs which we are using for forces and velocities.

By rotating a two-ended mechanical link (see Figure 12.2a) in the plane of the drawing by 180°, so that the input and output change places, we obtain the inverse of the original link (see Figure 12.2b). The matrix of this characteristic coefficient can be obtained from matrix (12.1.15) by interchanging coefficients A and D. In the general case a given external disturbing force F_1, applied first to one and then to the other end after inverting the two-ended link, produces reactions F_2 and velocities $\dot{y}_1$ and $\dot{y}_2$ of different magnitudes. In the special case when A = D the inversion of a two-ended link changes nothing; it is called a symmetric link. The input mechanical impedance Z_f of this part of a mechanical system (see Figure 12.2c), which may be viewed as the foundation, or supporting part of a structure, and whose input, i.e., the point where it is attached to the examined two-ended link, is acted upon by force $F_f = F_2$ and acquires velocity $\dot{y}_f = \dot{y}_2$, determines the relationship between these variables:

[ϕ=f]

$$\frac{F_2}{\dot{y}_2} = -Z_\phi = \frac{F_\phi}{\dot{y}_\phi}. \tag{12.1.16}$$

The positive direction of force F_f and velocity $\dot{y}_f$ is opposite the positive direction of reaction F_2 and thus coincides with the positive direction of velocities $\dot{y}_1$, $\dot{y}_2$ and force F_1. Here

APPROVED FOR RELEASE: 2007/02/08: CIA-RDP82-00850R000200100009-9

APPROVED FOR RELEASE: 2007/02/08: CIA-RDP82-00850R000200100009-9

$$\left.\begin{aligned}\dot{y}_1 &= F_1\frac{CZ_\phi + D}{AZ_\phi + B} = \frac{F_1}{Z_{1\phi}};\\ \dot{y}_2 &= \dot{y}_\phi = \frac{F_\phi}{Z_\phi} = \frac{F_1}{AZ_\phi + B}.\end{aligned}\right\} \qquad (12.1.17)$$

The input mechanical impedance of a two-ended link along with the mechanical impedance Z_f connected to its output will be

$$Z_{1\phi} = \frac{F_1}{\dot{y}_1} = \frac{AZ_\phi + B}{CZ_\phi + D}. \qquad (12.1.18)$$

Relations (12.1.12) and (12.1.16) are taken into consideration in the right hand side of expressions (12.1.17).

If Z_f is very large the output end of the mechanical link will be virtually fixed, i.e., $\dot{y}_2 = \dot{y} = 0$. Then, as follows from (12.1.18), Z_{1f} acquires the value

$$Z_{10} = \frac{A}{C}. \qquad (12.1.19)$$

If the output of a two-ended link is free, i.e., $Z_f = 0$, then $F_2 = F_f = 0$ and Z_{1f} will be

$$Z_{1*} = \frac{B}{D}. \qquad (12.1.20)$$

In electrical engineering terms (12.1.19) is often called dry run impedance and (12.1.20) is called the short circuit impedance. The inverse values

$$\left.\begin{aligned}M_{10} &= \frac{1}{Z_{10}} = \frac{C}{A};\\ M_{1*} &= \frac{1}{Z_{1*}} = \frac{D}{B}\end{aligned}\right\} \qquad (12.1.21)$$

are called the input mobilities of a two-ended mechanical link with fixed and free inputs, respectively.

If mechanical impedance Z_f is connected to the output of an inverted mechanical link, then instead of (12.1.18), (12.1.19) and (12.1.20) we will have, respectively,

$$\left.\begin{aligned}Z'_{1\phi} &= \frac{B + DZ_\phi}{A + CZ_\phi};\\ Z'_{10} &= \frac{D}{C};\\ Z'_{2*} &= \frac{B}{A}.\end{aligned}\right\} \qquad (12.1.22)$$

APPROVED FOR RELEASE: 2007/02/08: CIA-RDP82-00850R000200100009-9

APPROVED FOR RELEASE: 2007/02/08: CIA-RDP82-00850R000200100009-9

Sometimes (12.1.22) is called the inverse dry run impedance and (12.1.2) the inverse short circuit impedance.

The values

$$\left.\begin{aligned} M'_{10} &= \frac{1}{Z'_{10}} = \frac{C}{D}; \\ M'_{1*} &= \frac{1}{Z'_{1*}} = \frac{A}{B} \end{aligned}\right\} \qquad (12.1.23)$$

express the input mobilities of an inverted two-ended mechanical link with fixed and free ends, respectively.

Relations (12.1.12) may be rewritten for forces, and then, in consideration of (12.1.13), they are written as

$$\begin{bmatrix} F_1 \\ F_2 \end{bmatrix} = Z \begin{bmatrix} \dot{y}_1 \\ \dot{y}_2 \end{bmatrix}, \qquad (12.1.24)$$

where

$$Z = \begin{bmatrix} \frac{A}{C} & -\frac{1}{C} \\ \frac{1}{C} & -\frac{D}{C} \end{bmatrix} \qquad (12.1.25)$$

is the matrix of mechanical impedances, which serve as coefficients for velocities.

The inverse matrix of (12.1.25)

$$M = Z^{-1} = \begin{bmatrix} \frac{D}{B} & -\frac{1}{B} \\ \frac{1}{B} & -\frac{A}{B} \end{bmatrix} \qquad (12.1.26)$$

is the matrix of mobilities which serve as coefficients for forces F_1 and F_2, when velocities $\dot{y}_1$ and $\dot{y}_2$ are expressed through them in consideration of (12.1.13). The corresponding matrix equation acquires the form

$$\begin{bmatrix} \dot{y}_1 \\ \dot{y}_2 \end{bmatrix} = M \begin{bmatrix} F_1 \\ F_2 \end{bmatrix}. \qquad (12.1.27)$$

The elements of each of matrices (12.1.25), (12.1.26) are expressed through three of the four characteristic coefficients, which are the elements of matrix (12.1.15). To reconvert from (12.1.25) or from (12.1.26) to matrix (12.1.15) the three elements (characteristic coefficients) of the latter are written directly, and the fourth may be found from relation (12.1.13). This function owes its existence, in particular, to the fact that the non-diagonal elements of each of matrices (12.1.25) and (12.1.26) differ from each other in sign only.

APPROVED FOR RELEASE: 2007/02/08: CIA-RDP82-00850R000200100009-9

APPROVED FOR RELEASE: 2007/02/08: CIA-RDP82-00850R000200100009-9

Series- and Parallel-Connected Two-Ended Mechanical Links. Two series-connected two-ended mechanical links (Figure 12.3a), the properties of which are determined by the matrices of characteristic coefficients A_1 and A_2, are equivalent to one link with the characteristic matrix

$$A_0 = A_1 A_2. \tag{12.1.28}$$

Equation (12.1.28) is expanded as

$$\begin{bmatrix} A & B \\ C & D \end{bmatrix} = \begin{bmatrix} A_1A_2 + B_1C_2; & A_1B_2 + B_1D_2 \\ C_1A_2 + D_1C_2; & C_1B_2 + D_1D_2 \end{bmatrix}. \tag{12.1.29}$$

Expression (12.1.28) is generalized to the case of an arbitrary number of series-connected two-ended mechanical links. To find the characteristic matrix of the equivalent compound link it is necessary to multiply the characteristic matrices of the component links in the same order as the links follow each other from the input to the output of the compound link (this is the same direction as for the equivalent and all component series-connected links).

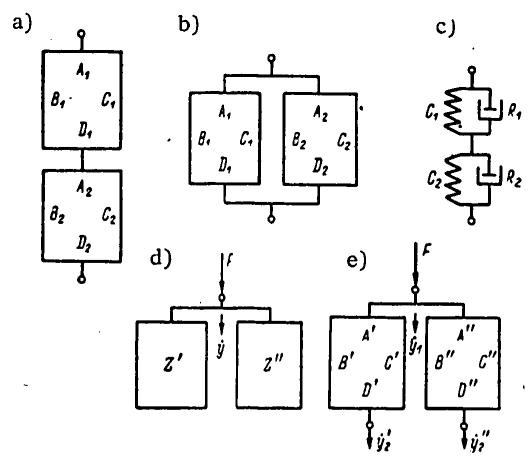

Figure 12.3. Series- (a) and parallel-connected (b) two-ended mechanical links; two series-connected elastic links (c); simplest branching systems (d, e).

The following recursive equations may be used for computing the characteristic coefficients of a chain of three and more series-connected links:

a) if the two-ended links that comprise the chain are numbered from the input to the output, so that the input of the (n + 1)-st link is connected to the output of the n-th:

APPROVED FOR RELEASE: 2007/02/08: CIA-RDP82-00850R000200100009-9

APPROVED FOR RELEASE: 2007/02/08: CIA-RDP82-00850R000200100009-9

$$\left.\begin{aligned}
A^*_{n+1} &= A^*_n\left(A_{n+1} + \frac{C_{n+1}}{C_n} D_n\right) - A^*_{n-1}\frac{C_{n+1}}{C_n};\\
B^*_{n+1} &= B^*_n\left(D_{n+1} + \frac{B_{n+1}}{B_n} A_n\right) - B^*_{n-1}\frac{B_{n+1}}{B_n};\\
C^*_{n+1} &= C^*_n\left(A_{n+1} + \frac{C_{n+1}}{C_n} D_n\right) - C^*_{n-1}\frac{C_{n+1}}{C_n};\\
D^*_{n+1} &= D^*_n\left(D_{n+1} + \frac{B_{n+1}}{B_n} A_n\right) - D^*_{n-1}\frac{B_{n+1}}{B_n};
\end{aligned}\right\} \qquad (12.1.30)$$

b) if the component links are numbered from output to input, so that the output of the (n + 1)-st link is connected to the input of the ends:

$$\left.\begin{aligned}
A^*_{n+1} &= A^*_n\left(A_{n+1} + \frac{B_{n+1}}{B_n} D_n\right) - A^*_{n-1}\frac{B_{n+1}}{B_n};\\
B^*_{n+1} &= B^*_n\left(A_{n+1} + \frac{B_{n+1}}{B_n} D_n\right) - B^*_{n-1}\frac{B_{n+1}}{B_n};\\
C^*_{n+1} &= C^*_n\left(D_{n+1} + \frac{C_{n+1}}{C_n} A_n\right) - C^*_{n-1}\frac{C_{n+1}}{C_n};\\
D^*_{n+1} &= D^*_n\left(D_{n+1} + \frac{C_{n+1}}{C_n} A_n\right) - D^*_{n-1}\frac{C_{n+1}}{C_n}.
\end{aligned}\right\} \qquad (12.1.31)$$

The asterisk in formulas (12.1.30) and (12.1.31) denotes the characteristic coefficients of a chain (equivalent to a two-ended link), the number of elements of which is indicated by the subscript of these coefficients. The other values (without asterisks) are the characteristic coefficients of the links of the chain; the number of link is indicated by the subscript of the coefficient.

Two parallel-connected two-ended links with characteristic coefficients A_1, B_1, C_1, D_1 and A_2, B_2, C_2, D_2 (Figure 12.3b) are equivalent to one, the characteristic coefficients of which are

$$\left.\begin{aligned}
A &= \frac{A_1C_2 + A_2C_1}{C_1 + C_2}; \quad B = B_1 + B_2 + \frac{(A_1 - A_2)(D_1 - D_2)}{C_1 + C_2};\\
C &= \frac{C_1C_2}{C_1 + C_2}; \quad D = \frac{C_1D_2 + C_2D_1}{C_1 + C_2}.
\end{aligned}\right\} \qquad (12.1.32)$$

Matrix Z of the mechanical impedances of the equivalent link, determined by formula (12.1.25), is the sum of the analogous matrices Z_1 and Z_2, each of which describes one of the parallel-connected links:

$$Z = Z_1 + Z_2. \qquad (12.1.33)$$

Equation (12.1.33) may be written in the expanded form

APPROVED FOR RELEASE: 2007/02/08: CIA-RDP82-00850R000200100009-9

APPROVED FOR RELEASE: 2007/02/08: CIA-RDP82-00850R000200100009-9

$$\begin{bmatrix} \frac{A}{C} & -\frac{1}{C} \\ \frac{1}{C} & -\frac{D}{C} \end{bmatrix} = \begin{bmatrix} \frac{A_1}{C_1} + \frac{A_2}{C_2}; & -\frac{1}{C_1} - \frac{1}{C_2} \\ \frac{1}{C_1} + \frac{1}{C_2}; & -\frac{D_1}{C_1} - \frac{D_2}{C_2} \end{bmatrix}. \qquad (12.1.34)$$

Expressions (12.1.33) and (12.1.34) are easily applied to an arbitrary number of parallel-connected two-ended mechanical links. For example, in the case of a one-dimensional mechanical system, a single-stage shock-absorbing fastener is viewed as a compound two-ended link, described by the matrix

$$Z = \sum_{i=1}^{n} Z_i, \qquad (12.1.35)$$

where Z_i is the matrix of the mechanical impedances of the i-th shock absorber.

The diagrams and characteristic coefficients of the simplest idealized two-ended mechanical links are given in Table 12.1. These links are (numbered in the same order as in the table):

1) absolutely rigid (nondeformable) inertialess link;

2) absolutely rigid mass M;

3) inertialess spring with rigidity C (compliance C^{-1});

4) damper with viscous friction, proportional to the first power of the rate of deformation of the link (R is the viscous friction coefficient).

Table 12.1. Simplest Two-Ended Mechanical Links and Their Characteristic Coefficients

1) Характеристические коэффициенты	2) Схема звена			
	1	2	3	4
A	1	1	1	1
B	0	$i\omega M$	0	0
C	0	0	$i\frac{\omega}{C}$	$\frac{1}{R}$
D	1	1	1	1

Key: 1. Characteristic coefficients 2. Diagram of link

APPROVED FOR RELEASE: 2007/02/08: CIA-RDP82-00850R000200100009-9

APPROVED FOR RELEASE: 2007/02/08: CIA-RDP82-00850R000200100009-9

ON

BY

3 JULY 1980 I. I. KLYUKIN AND I. I. BOGOLEPOV 5 OF 6

APPROVED FOR RELEASE: 2007/02/08: CIA-RDP82-00850R000200100009-9

APPROVED FOR RELEASE: 2007/02/08: CIA-RDP82-00850R000200100009-9

The characteristic coefficients of more complicated two-ended links with bunched constants, representing combinations of the simplest links, can be computed with the aid of the above equations on the basis of the known characteristic coefficients of the simplest links (2, 3, 4).

Here the following circumstances must be taken into account.

1. Connecting to a chain of series-connected two-ended links an absolutely rigid inertialess link (1 in Table 12.1) does not change the characteristics of the chain and need not be indicated in the diagrams of chain systems.

2. When $C \to \infty$ link 3, and when $R \to \infty$ link 4 behave as absolutely rigid inertialess link 1.

3. An absolutely rigid link (1 or 2 in Table 12.1), parallel-connected to other two-ended links, precludes relative displacements of the ends of each of them but does not always preclude internal deformations of those links.

4. If among the simplest links that make up a compound two-ended link, there is no link with mass (2 in Table 12.1), characteristic coefficient B of the compound link is equal to zero and the dimensionless coefficients A and D are equal to unity.

Now, in the case of series-connected compound links, characteristic coefficient C of the compound link is equal to the sum

$$C = \sum_{i=1}^{n} C_i \qquad (12.1.36)$$

of the like coefficients, belonging to the n links that comprise it.

5. To parallel-connected component links corresponds, as can be seen by (12.1.35), the relation

$$C^{-1} = \sum_{i=1}^{n} C_i^{-1}. \qquad (12.1.37)$$

According to this relation the inverse characteristic coefficient C of the compound link is found by adding like inverse coefficients of all n component links.

6. If the component links are inertialess springs (see link 3 in Table 12.1) expression (12.1.36) changes to the formula

$$C^{-1} = \sum_{i=1}^{n} C_i^{-1} \qquad (12.1.38)$$

for the series-connected case, when the compliance (inverse rigidity) of the chain of springs is found by adding their compliances.

In exactly the same way we derive from expression (12.1.37) the formula

APPROVED FOR RELEASE: 2007/02/08: CIA-RDP82-00850R000200100009-9

APPROVED FOR RELEASE: 2007/02/08: CIA-RDP82-00850R000200100009-9

$$C = \sum_{i=1}^{n} C_i \tag{12.1.39}$$

for the total rigidity of parallel-connected springs.

7. If the components of a link -- dampers with coefficients R_i of viscous friction, proportional to the first power of velocity (link 4 in Table 12.1), expressions (12.1.36) and (12.1.37) reduce, respectively, to the formulas

$$R = \left(\sum_{i=1}^{n} R_i^{-1}\right)^{-1} \tag{12.1.40}$$

and

$$R = \sum_{i=1}^{n} R_i. \tag{12.1.41}$$

The first of these formulas can be used to compute the viscous friction coefficient of a system of series-connected dampers, and the second parallel-connected dampers.

8. As can be seen by Table 12.1, an inertialess spring (link 3) and viscous damper (link 4) have the identical characteristic coefficients A, B, D.

9. The parallel connection of a spring and damper produces a compound viscoelastic link (see the diagram of link 1 in Table 12.2) with the characteristic coefficients

$$\left.\begin{aligned} &A = D = 1; \quad B = 0; \\ &C = \frac{i\omega}{C + i\omega R} = \frac{i\omega}{\tilde{C}} = \left(R + \frac{C}{i\omega}\right)^{-1} = \frac{\omega}{C}\,\frac{\frac{\omega R}{C} + i}{1 + \frac{\omega^2 R^2}{C^2}}. \end{aligned}\right\} \tag{12.1.42}$$

The value

$$\tilde{C} = C + i\omega R$$

is called the complex viscosity of a link, and the inverse

$$\tilde{C}^{-1} = C^{-1}\,\frac{1 - i\frac{\omega R}{C}}{1 + \frac{\omega^2 R^2}{C^2}}$$

is the complex compliance.

10. The summary complex rigidity of n parallel-connected viscoelastic links along the resulting compound two-ended link is

APPROVED FOR RELEASE: 2007/02/08: CIA-RDP82-00850R000200100009-9

APPROVED FOR RELEASE: 2007/02/08: CIA-RDP82-00850R000200100009-9

Table 12.2. Some Compound Two-Ended Mechanical Links and Their Characteristic Coefficients

2) Характеристические коэффициенты	1) Схема звена 1	2	3
	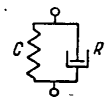	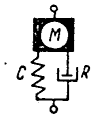	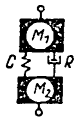
A	1	$1-\dfrac{\frac{\omega^2 M}{C}}{1+\frac{\omega^2 R^2}{C^2}}+ i\dfrac{\frac{\omega R}{C}\,\frac{\omega^2 M}{C}}{1+\frac{\omega^2 R^2}{C^2}}$	$1-\dfrac{\frac{\omega^2 M_1}{C}}{1+\frac{\omega^2 R^2}{C^2}}+ i\dfrac{\frac{\omega R}{C}\,\frac{\omega^2 M_1}{C}}{1+\frac{\omega^2 R^2}{C^2}}$
B	0	$i\omega M$	$-\omega(M_1+M_2)\dfrac{\frac{\omega R}{C}\,\frac{\omega^2}{C}\,\frac{M_1 M_2}{M_1+M_2}}{1+\frac{\omega^2 R_2}{C^2}}+ i\omega(M_1+M_2)\left(1-\dfrac{\frac{\omega^2}{C}\,\frac{M_1 M_2}{M_1+M_2}}{1+\frac{\omega^2 R^2}{C^2}}\right)$

KEY: 1. Diagram of link 2. Characteristic coefficients

APPROVED FOR RELEASE: 2007/02/08: CIA-RDP82-00850R000200100009-9

APPROVED FOR RELEASE: 2007/02/08: CIA-RDP82-00850R000200100009-9

Table 12.2 (continued)

C	$\frac{1}{R+\frac{C}{i\omega}}=\frac{\omega}{C}\frac{\frac{\omega R}{C}}{1+\frac{\omega^2R^2}{C^2}}+i\frac{\omega}{C}\frac{1}{1+\frac{\omega^2R^2}{C^2}}$		
D	1	1	$1-\frac{\frac{\omega^2M_2}{C}}{1+\frac{\omega^2R^2}{C^2}}+i\frac{\frac{\omega R}{C}\frac{\omega^2M_2}{C}}{1+\frac{\omega^2R^2}{C^2}}$
2) Характеристические коэффициенты	1) Схема звена		
	4		
	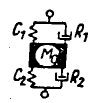		
A	$1-\frac{\frac{\omega^2M_0}{C_2}}{1-\frac{\omega^2R_2^2}{C_2^2}}+i\frac{\frac{\omega R^2}{C_2}\frac{\omega^2M_0}{C_2}}{1+\frac{\omega^2R_2^2}{C_2^2}}$		
B	$i\omega M_0$		

APPROVED FOR RELEASE: 2007/02/08: CIA-RDP82-00850R000200100009-9

APPROVED FOR RELEASE: 2007/02/08: CIA-RDP82-00850R000200100009-9

Table 12.2 (continued)

2) Характеристические коэффициенты	1) Схема звена
	4
C	$\frac{\omega}{C_1}\frac{\frac{\omega R_1}{C_1}}{1+\frac{\omega^2R_1^2}{C_1^2}}+\frac{\omega^2}{C_2}\frac{\frac{\omega R_2}{C_2}}{1+\frac{\omega^2R_2^2}{C_2^2}}-\frac{\omega}{C_1}\frac{\omega^2M_0}{C_2}\frac{\frac{\omega R_1}{C_1}+\frac{\omega R_2}{C_2}}{\left(1+\frac{\omega^2R_1^2}{C_1^2}\right)\left(1+\frac{\omega^2R_2^2}{C_2^2}\right)}+$ $+i\left[\frac{\frac{\omega}{C_1}}{1+\frac{\omega^2R_1^2}{C_1^2}}+\frac{\frac{\omega}{C_2}}{1+\frac{\omega^2R_2^2}{C_2^2}}-\frac{\omega}{C_1}\frac{\omega^2M_0}{C_2}\frac{1-\frac{\omega R_1}{C_1}\frac{\omega R_2}{C_2}}{\left(1+\frac{\omega^2R_1^2}{C_1^2}\right)\left(1+\frac{\omega^2R_2^2}{C_2^2}\right)}\right.$
D	$1-\frac{\frac{\omega^2M_0}{C_1}}{1+\frac{\omega^2R_1^2}{C_1^2}}+i\frac{\frac{\omega R_1}{C_1}\frac{\omega^2M_0}{C_1}}{1+\frac{\omega^2R_1^2}{C_1^2}}.$

2) Характеристические коэффициенты	1) Схема звена
	5
	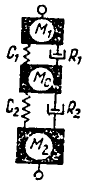
A	$1-\frac{1}{\left(1+\frac{\omega^2R_1^2}{C_1^2}\right)\left(1+\frac{\omega^2R_2^2}{C_2^2}\right)}\left[\frac{\omega^2M_1}{C_1}\left(1+\frac{\omega^2R_2^2}{C_2^2}\right)+\omega^2\frac{M_0+M_1}{C_2}\left(1+\frac{\omega^2R_1^2}{C_1^2}\right)-\right.$

APPROVED FOR RELEASE: 2007/02/08: CIA-RDP82-00850R000200100009-9

APPROVED FOR RELEASE: 2007/02/08: CIA-RDP82-00850R000200100009-9

Table 12.2 (continued)

	$-\frac{\omega^2 M_1}{C_1}\frac{\omega^2 M_0}{C_2}\left(\frac{\omega R_1}{C_1}+\frac{\omega R_2}{C_2}\right)\Big]+\frac{i}{\left(1+\frac{\omega^2 R_1^2}{C_1^2}\right)\left(1+\frac{\omega^2 R_2^2}{C_2^2}\right)}\Big[\frac{\omega R_1}{C_1}\frac{\omega^2 M_1}{C_1}\left(1+\frac{\omega^2 R_2^2}{C_2^2}+\right.$ $\left.+\omega^2\frac{M_0+M_1}{C_2}\frac{\omega R_2}{C_2}\left(1+\frac{\omega^2 R_1^2}{C_1^2}\right)-\frac{\omega^2 M_1}{C_1}\frac{\omega^2 M_0}{C_2}\left(\frac{\omega R_1}{C_1}+\frac{\omega R_2}{C_2}\right)\Big]$
B	$-\omega(M_0+M_1+M_2)\left[\frac{\omega^2 M_1}{C_1}\frac{M_0+M_2}{M_0+M_1+M_2}\frac{\frac{\omega R_1}{C_1}}{1+\frac{\omega^2 R_1^2}{C_1^2}}\left(1-\frac{\frac{\omega^2}{C_2}\frac{M_0 M_2}{M_0+M_2}}{1+\frac{\omega^2 R_2^2}{C_2^2}}\right)+\right.$ $\left.+\frac{\omega^2 M_2}{C_2}\frac{M_0+M_1}{M_0+M_1+M_2}\frac{\frac{\omega R^2}{C_2}}{1+\frac{\omega^2 R_2^2}{C_2^2}}\left(1-\frac{\frac{\omega^2}{C_1}\frac{M_0 M_1}{M_0+M_1}}{1+\frac{\omega^2 R_1^2}{C_1^2}}\right)\right]+$ $+i\omega(M_0+M_1+M_2)\left[1-\frac{\frac{\omega^2 M_1}{C_1}\frac{M_0-M_2}{M_0+M_1+M_2}}{1+\frac{\omega^2 R_1^2}{C_1^2}}-\frac{\frac{\omega^2 M_2}{C_2}\frac{M_0+M_1}{M_0+M_1+M_2}}{1+\frac{\omega^2 R_2^2}{C_2^2}}+\right.$ $\left.+\frac{M_0}{M_0+M_1+M_2}\frac{\omega^2 M_1}{C_1}\frac{\omega^2 M_2}{C_2}\frac{1-\frac{\omega R_1}{C_1}\frac{\omega R_2}{C_2}}{\left(1+\frac{\omega^2 R_1^2}{C_1^2}\right)\left(1+\frac{\omega^2 R_2^2}{C_2^2}\right)}\right]$
C	3) Как у звена 4
D	$1-\frac{1}{\left(1+\frac{\omega^2 R_1^2}{C_1^2}\right)\left(1+\frac{\omega^2 R_2^2}{C_2^2}\right)}\Big[\frac{\omega^2 M_2}{C_2}\left(1+\frac{\omega^2 R_1^2}{C_1^2}\right)+\omega^2\frac{M_0+M_2}{C_1}\left(1+\frac{\omega^2 R_2^2}{C_2^2}\right)-$ $-\frac{\omega^2 M_0}{C_1}\frac{\omega^2 M_2}{C_2}\left(\frac{\omega R_1}{C_1}+\frac{\omega R_2}{C_2}\right)\Big]+\frac{i}{\left(1+\frac{\omega^2 R_1^2}{C_1^2}\right)\left(1+\frac{\omega^2 R_2^2}{C_2^2}\right)}\Big[\frac{\omega R_2}{C_2}\frac{\omega^2 M_2}{C_2}\left(1+\frac{\omega^2 R_1^2}{C_1^2}\right)+$ $+\omega^2\frac{M_0+M_2}{C_1}\frac{\omega R_1}{C_1}\left(1+\frac{\omega^2 R_2^2}{C_2^2}\right)-\frac{\omega^2 M_0}{C_1}\frac{\omega^2 M_2}{C_2}\left(\frac{\omega R_1}{C_1}+\frac{\omega R_2}{C_2}\right)\Big]$

KEY: 3. Same as of link 4

APPROVED FOR RELEASE: 2007/02/08: CIA-RDP82-00850R000200100009-9

APPROVED FOR RELEASE: 2007/02/08: CIA-RDP82-00850R000200100009-9

$$\tilde{C} = \sum_{i=1}^{n} \tilde{C}_i = \sum_{i=1}^{n} C_i + i\omega \sum_{i=1}^{n} R_i = C + i\omega R. \tag{12.1.43}$$

Its characteristic coefficients are determined by the combination of expressions (12.1.42) and (12.1.43). Rigidity C and viscous friction coefficient R, as can be seen by (12.1.43), can be calculated by formulas (12.1.39) and (12.1.41).

11. The series connection of n viscoelastic links produces a compound two-ended chain with the complex rigidity

$$\tilde{C} = \left(\sum_{i=1}^{n} \tilde{C}_i^{-1}\right)^{-1} = C + i\omega R. \tag{12.1.44}$$

Its characteristic coefficients are determined by the set of expressions (12.1.42) and (12.1.43). The resulting (effective) rigidity C and viscous friction coefficient R of a compound link can be determined, respectively, by expressions (12.1.38) and (12.1.40), on the condition that the correspondence between rigidity C_i and viscous friction coefficient R_i is the same for all n links. It is also the same, of course, for parameters C and R of a compound link.

In the general case, when the mentioned requirement is not satisfied, each of the values of C and R is a complex function of all C_i and R_i and of circular frequency ω.

For example, when n = 2 (see Figure 12.3c)

$$\left.\begin{aligned} C &= \frac{C_1C_2}{C_1+C_2}\left\{1+\frac{\omega R_1}{C_1}\frac{\omega R_2}{C_2}\frac{\frac{R_2}{R_1}\left(1-\frac{C_2}{C_1}\frac{R_1}{R_2}\right)^2}{\left(1+\frac{C_2}{C_1}\right)^2\left[1+\left(\omega\frac{R_1+R_2}{C_1+C_2}\right)^2\right]}\right\}, \\ R &= \frac{R_1R_2}{R_1+R_2}\left\{1+\frac{\frac{R_2}{R_1}\left(1-\frac{C_2}{C_1}\frac{R_1}{R_2}\right)^2}{\left(1+\frac{C_2}{C_1}\right)^2\left[1+\left(\omega\frac{R_1+R_2}{C_1+C_2}\right)^2\right]}\right\}. \end{aligned}\right\} \tag{12.1.45}$$

Diagrams of certain compound two-ended mechanical links and the formulas for determining their characteristic coefficients are presented in Table 12.2. These links, the properties of which are of independent importance, are often parts of substantially more complicated chain and branched mechanical systems, including a variety of shock-absorbing structures and fasteners.

Idealized mechanical links with bunched constants are illustrated in Tables 12.1 and 12.2. All real elements of shock-absorbing structures are physical parts with distributed mass, rigidity and friction. To analyze

APPROVED FOR RELEASE: 2007/02/08: CIA-RDP82-00850R000200100009-9

APPROVED FOR RELEASE: 2007/02/08: CIA-RDP82-00850R000200100009-9

the characteristic of shock-absorbing fasteners in a wide frequency range a system with bunched constants, which approximates an individual element or a whole shock-absorbing structure usually must be made more complicated as frequencies get higher. A system with distributed constants is more stable in this respect. At the same time the nature and boundaries of its tolerable discreteness are determined by its properties. In many cases it is convenient to view a shock-absorbing structure as a system consisting of elements with bunched and distributed constants.

The simplest two-ended mechanical link with distributed constants is an elastic prismatic rod, through which propagate longitudinal waves. The prismatic working part of a shock absorber may be considered in such a rod in the first approximation. Its characteristic coefficients are

$$\left.\begin{aligned} A_a = D_a &= \cos\frac{\omega l}{c}\,\mathrm{ch}\,\frac{\omega^2 \varkappa l}{2cE} + i\sin\frac{\omega l}{c}\,\mathrm{sh}\,\frac{\omega^2\varkappa l}{2cE};\\ B_a &= \frac{ES}{c}\left(1+\frac{\omega^2\varkappa^2}{2E^2}+i\,\frac{\omega\varkappa}{2E}\right)\left(\cos\frac{\omega l}{c}\,\mathrm{sh}\,\frac{\omega^2\varkappa l}{2cE}+i\sin\frac{\omega l}{c}\,\mathrm{ch}\,\frac{\omega^2\varkappa l}{2cE}\right);\\ C_a &= \frac{c}{ES}\,\frac{\cos\frac{\omega l}{c}\,\mathrm{sh}\,\frac{\omega^2\varkappa l}{2cE}+i\sin\frac{\omega l}{c}\,\mathrm{ch}\,\frac{\omega^2\varkappa l}{2cE}}{1+\frac{\omega^2\varkappa^2}{2E^2}+i\,\frac{\omega\varkappa}{2E}}. \end{aligned}\right\} \qquad (12.1.46)$$

Here l is the length of the rod; S is its cross section area; E is the normal elasticity modulus of the rod material; κ is a coefficient that takes into account friction;

$$c = \sqrt{\frac{E}{\rho}} \qquad (12.1.47)$$

is the speed of sound in a material with density ρ.

The mass of a rod (of a prismatic working part of a shock absorber) is

$$M_a = \rho l S, \qquad (12.1.48)$$

and its longitudinal rigidity is

$$C_a = \frac{ES}{l}. \qquad (12.1.49)$$

The simplest case of a branched uniform mechanical system is depicted schematically in Figure 12.3d, e. Harmonic force F is distributed between both branches in proportion to their input mechanical impedances Z' and Z''. Thus

$$\left.\begin{aligned} F &= F' + F'';\\ \frac{F'}{F''} &= \frac{Z'}{Z''}. \end{aligned}\right\} \qquad (12.1.50)$$

Input velocity $\dot{y}_1$ of both branches is identical:

APPROVED FOR RELEASE: 2007/02/08: CIA-RDP82-00850R000200100009-9

APPROVED FOR RELEASE: 2007/02/08: CIA-RDP82-00850R000200100009-9

$$\dot{y}_1 = \frac{F}{Z' + Z''} = \frac{F'}{Z'} = \frac{F''}{Z''}. \qquad (12.1.51)$$

In the special case when each of the branches of a system can be reduced to a two-ended link with an unloaded output and with characteristic coefficients, respectively, A', B', C', D' and A", B", C", D" (Figure 12.3e),

$$Z' = \frac{B'}{D'}; \quad Z'' = \frac{B''}{D''}. \qquad (12.1.52)$$

The output velocities of the two links

$$\left.\begin{aligned} \dot{y}_2' &= \frac{F'}{B'} = \frac{F}{B' + B''\dfrac{D'}{D''}}; \\ \dot{y}_2'' &= \frac{F''}{B''} = \frac{F}{B'' + B'\dfrac{D''}{D'}} \end{aligned}\right\} \qquad (12.1.53)$$

are, in the general case, different; here

$$\frac{\dot{y}_2'}{\dot{y}_2''} = \frac{D''}{D'}. \qquad (12.1.54)$$

If, however, D' = D", then $\dot{y}_2' = \dot{y}_2''$, and combining the outputs, which converts the system shown in Figure 12.3e to the one in Figure 12.3b, does not alter the operating mode of the links. If a disturbance is applied not to the end of the chain system, but to the end of one of the intermediate links, it will propagate in both directions from the point of application and the system should be viewed as a branch system, consisting of two branches with a common input. An example is the case when some kind of mechanism, a source of vibration, is inserted on an intermediate frame between the shock-absorbing stages of a two-stage shock-absorbing mount.

The general relations that characterize transmission of steady state harmonic forces through a shock-absorbing fastener, represented as a passive two-ended mechanical link, derived directly from basic equations (12.1.12) and expressions that are connected with them. To emphasize that the characteristic coefficients belong to a shock-absorbing fastener (or, depending on circumstances, to a separate shock absorber or a group of shock absorbers), their literal designations are given the corresponding subscripts.

As can be seen in Figure 12.4, a shock-absorbing mount rests on a foundation, the input mechanical impedance of which, measured on the shock absorber side, is Z_f. The machine or other insulated object, supported by a shock-absorbing mount, has the mechanical impedance Z_m, measured on the mount side.

APPROVED FOR RELEASE: 2007/02/08: CIA-RDP82-00850R000200100009-9

APPROVED FOR RELEASE: 2007/02/08: CIA-RDP82-00850R000200100009-9

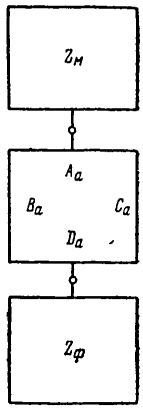

Figure 12.4. Two-ended mechanical link as shock absorber in mechanical chain system. [ϕ=f]

Force F_a is applied to the input of a shock-absorbing mount, whereupon harmonic forces are transmitted from the working machine to the input of the mount, and force F_f is applied to the foundation from the output of the mount. The points of application of these forces complete harmonic oscillations with velocities $\dot{y}_a$ and y_f, respectively. The expressions for the amplitude values of the velocities $\dot{y}_{aa}$ at the input and $\dot{y}_{fa}$ at the output of the shock absorbers are

$$[\phi=f] \qquad \left.\begin{aligned} \dot{y}_{a\,a} &= \frac{F_{a\,a}}{|Z_{a\,\phi}|} = F_{a\,a}\left|\frac{C_a Z_\phi + D_a}{A_a Z_\phi + B_a}\right|; \\ \dot{y}_{\phi a} &= \frac{F_{\phi a}}{|Z|_\phi} = \frac{F_{a\,a}}{|A_a Z_\phi + B_a|}, \end{aligned}\right\} \qquad (12.1.55)$$

where

$$Z_{a\,\phi} = \frac{A_a Z_\phi + B_a}{C_a Z_\phi + D_a}.$$

The values

$$\left.\begin{aligned} \bar{\beta}_{aF} &= \frac{F_\phi}{F_a} = \left(A_a + \frac{B_a}{Z_\phi}\right)^{-1}; \\ \bar{\beta}_{a\dot{y}} &= \frac{\dot{y}_\phi}{\dot{y}_a} = (C_a Z_\phi + D_a)^{-1} \end{aligned}\right\} \qquad (12.1.56)$$

express the complex coefficients of transmission of harmonic force and harmonic vibration to the foundation by the shock-absorbing mount. They tell the scale and phase of the force passing through the shock absorbers in relation to the force applied to the input of the shock-absorbing mount. We note that

$$\frac{\bar{\beta}_{aF}}{\bar{\beta}_{a\dot{y}}} = \frac{Z_\phi}{Z_{a\,\phi}}. \qquad (12.1.57)$$

Expressions (12.1.56) express the transfer properties of any two-ended mechanical link.

The moduli of the complex transfer functions are the ratios of the effective values or amplitude values of the forces and velocities and are called the transfer functions of harmonic force and harmonic vibration of a shock-absorbing mount in relation to the foundation. In contrast to the complex coefficients, they do not take into account the phase of the transmitted force:

APPROVED FOR RELEASE: 2007/02/08: CIA-RDP82-00850R000200100009-9

APPROVED FOR RELEASE: 2007/02/08: CIA-RDP82-00850R000200100009-9

[ф=f]

$$\left.\begin{aligned}\beta_{aF} &= \frac{F_{\text{ф}\,\text{a}}}{F_{a\,\text{a}}} = \left|A_a + \frac{B_a}{Z_\text{ф}}\right|^{-1};\\ \beta_{a\dot{y}} &= \frac{\dot{y}_{\text{ф}\,\text{a}}}{\dot{y}_{a\,\text{a}}} = |C_a Z_\text{ф} + D_a|^{-1}.\end{aligned}\right\} \qquad (12.1.58)$$

The force absorption coefficient $F^{\text{г}}_{\text{fa}}$, in relation to the force that would be transmitted to the foundation by an absolutely rigid fastener, is

[ж=r]

$$k_{\text{aм}} = \frac{F^{\text{ж}}_{\text{ф}\,\text{a}} - F_{\text{ф}\,\text{a}}}{F^{\text{ж}}_{\text{ф}\,\text{a}}} = \left|1 - \frac{Z_\text{м} + Z_\text{ф}}{A_a Z_\text{ф} + B_a + Z_\text{м}(C_a Z_\text{ф} + D_a)}\right|. \qquad (12.1.59)$$

This coefficient determines the relative reduction of the vibration of the foundation in comparison with an absolutely rigid mount:

$$k_{\text{aм}} = \frac{\dot{y}^{\text{ж}}_{\text{ф}\,\text{a}} - \dot{y}_{\text{ф}\,\text{a}}}{\dot{y}^{\text{ж}}_{\text{ф}\,\text{a}}}. \qquad (12.1.60)$$

The difference of the vibration levels on a shock-absorbing mount, calculated in decibels, is

[в=v]

$$\Pi_\text{в} = 20\lg\left|\frac{\dot{y}_a}{\dot{y}_\text{ф}}\right| = 20\lg\frac{\dot{y}_{a\,\text{a}}}{\dot{y}_{\text{ф}\,\text{a}}} = -20\lg\beta_{a\dot{y}} = 20\lg|C_a Z_\text{ф} + D_a|. \qquad (12.1.61)$$

Here, as in the other cases of comparison of the characteristics of harmonic vibration on the same frequency, the ratio of the amplitude values or effective values not only of velocities, but also of displacements and accelerations, can be written under the logarithm sign.

The logarithmic difference of forces on a shock-absorbing mount, also measured in decibels, is

$$\Pi_F = 20\lg\left|\frac{F_a}{F_\text{ф}}\right| = 20\lg\frac{F_{a\,\text{a}}}{F_{\text{ф}\,\text{a}}} = -20\lg\beta_{aF} = 20\lg\left|A_a + \frac{B_\text{a}}{Z_\text{ф}}\right|. \qquad (12.1.62)$$

Vibration damping VD, in dB, provided by a shock-absorbing mount in relation to an absolutely rigid mount, according to expression (12.1.7) will be

[ВИ=VD]

$$\text{ВИ} = 20\lg\left|\frac{F^{\text{ж}}_\text{ф}}{F^{\text{aм}}_\text{ф}}\right| = 20\lg\left|\frac{\dot{y}^{\text{ж}}_\text{ф}}{\dot{y}^{\text{aм}}_\text{ф}}\right|$$

or

$$\text{ВИ} = 20\lg\left|\frac{A_a Z_\text{ф} + Z_\text{м}(C_a Z_\text{ф} + D_a)}{Z_\text{м} + Z_\text{ф}}\right| = -20\lg(1 - k_{\text{aм}}). \qquad (12.1.63)$$

Effectiveness E, in dB, of the replacement of a mount without absolute rigidity by a shock-absorbing mount is determined by the difference of vibration damping values VD and VD', expressed, respectively, in terms of the new and replaced mounts, the latter of which has the characteristic coefficients A', B', C', D':

APPROVED FOR RELEASE: 2007/02/08: CIA-RDP82-00850R000200100009-9

APPROVED FOR RELEASE: 2007/02/08: CIA-RDP82-00850R000200100009-9

[Э=E]
$$Э = ВИ - ВИ' = 20 \lg \left| \frac{A_a Z_ф + B_a + Z_м (C_a Z_ф + D_a)}{A'_a Z_ф + B'_a + Z_м (C'_a Z_ф + D'_a)} \right|. \quad (12.1.64)$$

If the value of VD' is negative in some frequency range, the effectiveness of the new mount in this range will be greater than the vibration damping VD provided by it in relation to an absolutely rigid mount.

It follows from (12.1.61) and (12.1.62) that the difference, measured in decibels, is

$$П_в - П_F = 20 \lg \left| \frac{Z_ф}{Z_{aф}} \right|. \quad (12.1.65)$$

The difference between the vibration levels on shock absorbers and of the vibration damping values afforded by them, also measured in decibels, is

$$П_в - ВИ = 20 \lg \left| \frac{Z_м + Z_ф}{Z_м + Z_{aф}} \right|. \quad (12.1.66)$$

If mechanical impedance Z_m of an insulated machine is large in comparison with Z_f and Z_{af}, (12.1.66) will be close to zero, so that VD, in dB, is

$$ВИ \approx 20 \lg | C_a Z_ф + D_a |. \quad (12.1.67)$$

If the terms containing Z_f in the numerator and denominator of expression (12.1.63) predominate, then the VD, in dB, is

$$ВИ \approx 20 \lg | A_a + C_a Z_м |. \quad (12.1.68)$$

When harmonic vibration propagates to an insulated machine from the foundation expression (12.1.63) for vibration damping remains valid, just like the right hand side of expression (12.1.59). The shock absorption coefficient in this case obviously determines the relative amount of reduction of vibration of the insulated machine and of the force transmitted to it, which produces vibration. Here the difference of the vibration levels on the shock absorbers (from the foundation to the insulated machine, which, as before, is assumed to be connected to the input of the shock-absorbing mount, which in this case transmits the disturbances from its output to the input) $П_{fm}$, in dB, is

$$П_{фм} = 20 \lg | A_a + C_a Z_м |. \quad (12.1.69)$$

12.2. Calculation of Effectiveness of Vibration-Damping Mounts Using Electromechanical Analogies, Matrix Procedures and Orthogonal Polynomials

Calculation Using Electromechanical Analogies. Examples of equivalent electrical diagrams are presented in Chapter 1. Analysis by determining the input impedance can be used for comparatively simple designs, but

APPROVED FOR RELEASE: 2007/02/08: CIA-RDP82-00850R000200100009-9

APPROVED FOR RELEASE: 2007/02/08: CIA-RDP82-00850R000200100009-9

other methods, for example the loop current technique, are better for analyzing complex designs.

Example. We will determine the differences of the vibration levels and the values of vibration damping in a two-stage shock-absorbing system (without friction), resting on a foundation with finite impedance.

A diagram of the system, which indicates the mechanical parameters and parameters of the vibration process in its different elements, is shown in Figure 12.5a. Figure 12.5b shows the equivalent electrical diagram of the device. Loop currents I_1, I_2, I_3, the currents in the branches and the impedance of the elements are indicated.

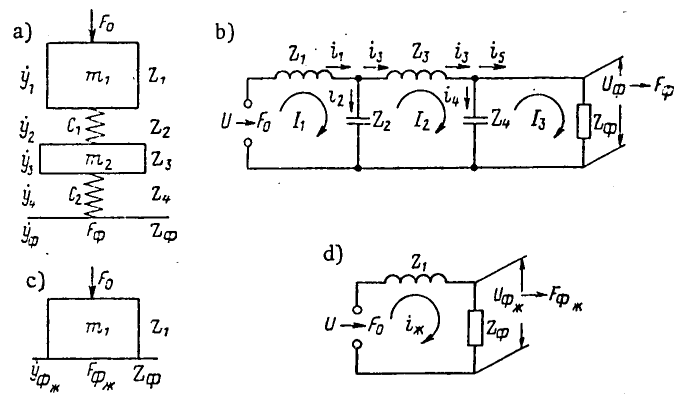

Figure 12.5. Calculation of acoustic effect of shock absorption using electromechanical analogies (loop currents technique). [ф=f; ж=r]

The equations of the potentials in the circuits in this case will be

$$\left.\begin{aligned}(Z_1+Z_2)I_1-Z_2I_2=U;\\ -Z_2I_1+(Z_2+Z_3+Z_4)I_2-Z_4I_3=0;\\ -Z_4I_2+(Z_4+Z_\phi)I_3=0.\end{aligned}\right\}\qquad(12.2.1)$$

Three loop currents are easily determined with the aid of this equation system. The currents in the branches, corresponding to the vibration velocities of the different elements, and the output voltage, corresponding to the vibration force on the foundation, are

[ф=f]

$$\left.\begin{aligned}i_1\to\dot{y}_1=I_1;\ i_2\to\dot{y}_2=I_1-I_2;\ i_3\to\dot{y}_3=I_2;\\ i_4\to\dot{y}_4=I_2-I_3;\ i_5\to\dot{y}_\phi=I_3;\ U_\phi\to F_\phi=Z_\phi i_\phi.\end{aligned}\right\}\qquad(12.2.2)$$

APPROVED FOR RELEASE: 2007/02/08: CIA-RDP82-00850R000200100009-9

APPROVED FOR RELEASE: 2007/02/08: CIA-RDP82-00850R000200100009-9

The impedances of the elements of this system for a harmonic vibration process are[1]

$$\left.\begin{aligned} Z_1 = j\omega m_1;\ Z_2 = \frac{C_1}{j\omega};\ \ Z_3 = j\omega m_2; \\ Z_4 = \frac{C_2}{j\omega};\ \ Z_\text{ф} = X + jY. \end{aligned}\right\} \qquad (12.2.3)$$

We will determine below the values that characterize the acoustic effect of vibration damping. From expressions (12.2.2) in consideration of I_1, I_2, I_3 according to (12.2.1) and impedances according to (12.2.3), it follows that:

the difference of the vibration velocities in the first shock absorption stage is

$$\Pi_{1\dot{y}} = \frac{\dot{y}_1}{\dot{y}_3} \to \frac{i_1}{i_3},$$

and in the second stage

$$\Pi_{2\dot{y}} = \frac{\dot{y}_3}{\dot{y}_5} \to \frac{i_3}{i_5};$$

the differences of the vibration velocities and of the forces on the entire shock absorption system are

$$\Pi_{\dot{y}} = \frac{\dot{y}_1}{\dot{y}_5} \to \frac{i_1}{i_5};\ \ \Pi_F = \frac{F_0}{Z_\text{ф}\dot{y}_\text{ф}} \to \frac{F_0}{Z_\text{ф} i_5};$$

the difference of the vibration forces transmitted from the mounts of a machine to the foundation is

[л=mo]
$$\Pi_{F\text{л}} = \frac{F_0 - j\omega m_1 \dot{y}_1}{Z_\text{ф}\dot{y}_\text{ф}} \to \frac{F_0 - j\omega m_1 i_1}{Z_\text{ф} i_5}.$$

To determine the vibration damping of a two-stage shock absorber it is necessary also to examine a system, corresponding to a rigid mount of a machine (without an extra frame, Figures 12.5c, d). The current i_r in it, corresponding to the vibration velocity of the foundation with a rigid mount, is

[ж=r; ф=f]
$$i_\text{ж} \to \dot{y}_\text{ж} = \frac{U}{Z_1 + Z_\text{ф}}.$$

The total vibration damping of the two stages of the shock absorbers is

[ВИ=VD]
$$\text{ВИ} = \frac{\dot{y}_\text{ж}}{\dot{y}_\text{ф}} = \frac{F_\text{фж}}{F_\text{ф}} \to \frac{U_\text{фж}}{U_\text{ф}} = \frac{i_\text{ж}}{i_5}.$$

[1]Here and in the ensuing analysis (until the end of the chapter) $\sqrt{-1}$ is denoted not through i, but through j. This is done in order to avoid confusion with current i [see, for instance, formula (12.2.2)].

APPROVED FOR RELEASE: 2007/02/08: CIA-RDP82-00850R000200100009-9

APPROVED FOR RELEASE: 2007/02/08: CIA-RDP82-00850R000200100009-9

Calculation by Matrix Method (Using Primarily Fundamentals of n-Pole Theory). The fundamentals of the acoustic calculation of the effect of installing shock absorbers using the tool of mechanical quadrupoles were presented in the preceding section. The coefficients of the quadrupoles, corresponding to complex vibration-damping elements, are determined basically experimentally. Considerable possibilities for analysis are available also if the coefficients of the equivalent vibration-damping elements of quadrupoles are found directly from the known physical constants of the material of the elements and from their geometric dimensions. This kind of representation is perfectly valid for shock absorbers with the simplest vibration-damping elements (elastic pads and KAS [not further identified] absorbers) and for certain nonbearing structures.

For this kind of homogeneous mechanic element with distributed parameters (including dissipative) and with harmonic longitudinal vibrations, the coefficients of the equivalent quadrupole, entering in formula (1.7.1) and its analogies are (see, for example, [6]):

$$\left.\begin{aligned} A &\cong \operatorname{ch}[(\alpha + jk)\,l] = D; \\ B &\cong \rho c\left(1 + j\frac{\eta}{2}\right) S \operatorname{sh}[(\alpha + jk)\,l] \approx \rho c S \operatorname{sh}[(\alpha + jk)\,l]; \\ C &\cong \frac{1 - j\frac{\eta}{2}}{\rho c S} \operatorname{sh}[(\alpha + jk)\,l] \approx \frac{1}{\rho c S} \operatorname{sh}[(\alpha + jk)\,l]. \end{aligned}\right\} \qquad (12.2.4)$$

Here l and S are the length and cross section area of a given element of a vibration conductor; k is the wave number; α is the dissipation constant, $\alpha = \frac{\omega}{c}\frac{\eta}{2}$; c is the speed of sound in the material $\eta \leq 0.3$ is the loss coefficient.

For the homogeneous part of any vibration conductor with longitudinal symmetry the diagonal terms of the matrix of the coefficients (A and D) are equal to each other.

In the case of extremely small losses, which can be the case in a metallic vibration conductor, $\alpha \approx 0$, and the coefficients of the elementary mechanical quadrupole with distributed constants are

$$\left.\begin{aligned} A &= \operatorname{ch} jkl = \cos kl = D; \\ B &= \rho c S \operatorname{sh} jkl = j\rho c S \sin kl; \\ C &= \frac{1}{\rho c S} \operatorname{sh} jkl = \frac{j}{\rho c S} \sin kl. \end{aligned}\right\} \qquad (12.2.5)$$

These coefficients for low-frequency vibrations are given in matrices (1.7.8) and (1.7.9). In consideration of these expressions and of the dependence for series-connected (mechanically) elements, expressed by

APPROVED FOR RELEASE: 2007/02/08: CIA-RDP82-00850R000200100009-9

APPROVED FOR RELEASE: 2007/02/08: CIA-RDP82-00850R000200100009-9

matrix (1.7.3), we may write for the system illustrated in Figure 12.5a the equation (the symbols are indicated in the figure):

[ф=f]
$$\begin{bmatrix} F_0 \\ \dot{y}_1 \end{bmatrix} = \begin{bmatrix} 1 & j\omega m_1 \\ 0 & 1 \end{bmatrix} \begin{bmatrix} 1 & 0 \\ \frac{j\omega}{C_1} & 1 \end{bmatrix} \begin{bmatrix} 1 & j\omega m_2 \\ 0 & 1 \end{bmatrix} \begin{bmatrix} 1 & 0 \\ \frac{j\omega}{C_2} & 1 \end{bmatrix} \begin{bmatrix} F_\text{ф} \\ \dot{y}_\text{ф} \end{bmatrix}. \qquad (12.2.6)$$

From this and analogous equations we can derive two algebraic equations by multiplying the matrices using the "row by column" rule [3].

With the relation $F_f = Z_f \dot{y}_f$ we can determine from equation (12.2.6) the differences of the vibration forces on a structure. The analogous expression for a rigid mount (Figure 12.5c) will be

[н=r]
$$\begin{bmatrix} F_0 \\ \dot{y}_\text{фж} \end{bmatrix} = \begin{bmatrix} 1 & j\omega m_1 \\ 0 & 1 \end{bmatrix} \begin{bmatrix} F_\text{фж} \\ \dot{y}_\text{фж} \end{bmatrix}, \qquad (12.2.7)$$

whence, in combination with the equality $F_{fr} = Z_f \dot{y}_{fr}$ and the results of calculation by formula (12.2.6), we can determine the vibration damping of a structure, which, in dB, is

$$20 \lg \left| \frac{F_\text{фж}}{F_\text{ф}} \right|.$$

For bending vibrations the equation of an elementary quadrupole will acquire the form (the symbols are given in Figure 1.24)

[и=b]
$$\begin{bmatrix} \dot{y}_{1n}/\omega \\ \dot{\varphi}_1/\omega \\ M_1 \\ F_1 \end{bmatrix} = \begin{bmatrix} S(k_\text{и}l) & \frac{1}{k_\text{и}} T(k_\text{и}l) & \frac{1}{k_\text{и}^2 B} U(k_\text{и}l) & \frac{1}{k_\text{и}^3 B} V(k_\text{и}l) \\ k_\text{и} V(k_\text{и}l) & S(k_\text{и}l) & \frac{1}{k_\text{и} B} T(k_\text{и}l) & \frac{1}{k_\text{и}^2 B} U(k_\text{и}l) \\ k_\text{и}^2 B U(k_\text{и}l) & k_\text{и} B V(k_\text{и}l) & S(k_\text{и}l) & \frac{1}{k_\text{и}} T(k_\text{и}l) \\ k_\text{и}^3 B T(k_\text{и}l) & k_\text{и}^2 B U(k_\text{и}l) & k_\text{и} V(k_\text{и}l) & S(k_\text{и}l) \end{bmatrix} \times \begin{bmatrix} \dot{y}_{2n}/\omega \\ \dot{\varphi}_{2n}/\omega \\ M_2 \\ F_2 \end{bmatrix}, \qquad (12.2.8)$$

where k_b is the wave number for bending vibrations; B = EJ is the bending rigidity; $S(k_b l)$, $T(k_b l)$, $U(k_b l)$, $V(k_b l)$ are Krylov functions [4]. The matrices in equation (12.2.8) are obtained from matrices presented in the literature [4] by means of certain transformations (introduction of k_b and B and utilization of $\dot{y}$ and $\dot{\phi}$ instead of y and ϕ).

Calculation of Parameters of Vibration Process in Branched Shock-Absorbing System by Matrix Procedure. Let several units [8], corresponding to machines installed on an n-stage shock-absorbing system, be installed on a common shock-absorbing frame (Figure 12.6a). When the top of one unit is acted upon by vibration force F_0 the transformation matrix of a unit will be

APPROVED FOR RELEASE: 2007/02/08: CIA-RDP82-00850R000200100009-9

APPROVED FOR RELEASE: 2007/02/08: CIA-RDP82-00850R000200100009-9

$$M_{j=1} = \prod_{i=1}^{n_1} (M_i),$$

where M_i are the matrices of the elements of the unit. To determine the reaction of the other units to the frame it is necessary to find their input impedances on the frame side. The transformation matrix of the j-th unit on the frame side is equal to the product of the matrices of the elements from bottom to top:

[бл=u]
$$\prod_{i=n_j}^{1} (M_i) = \begin{bmatrix} A_{бл_j} & B_{бл_j} \\ C_{бл_j} & D_{бл_j} \end{bmatrix},$$

where n_j is the number of elements in the j-th branch. To determine the input impedance of the j-th unit on the frame side it is necessary to determine it from the frame and to apply to it an arbitrary vibration force F_{in}. Here the equation

[вх=in; вых=out]
$$\begin{bmatrix} F_{вх} \\ \dot{y}_{вх} \end{bmatrix} = \begin{bmatrix} A_{бл_j} & B_{бл_j} \\ C_{бл_j} & D_{бл_j} \end{bmatrix} \begin{bmatrix} 0 \\ \dot{y}_{вых} \end{bmatrix}$$

is valid, where $\dot{y}_{in}$ and $\dot{y}_{out}$ are the vibration velocities at the input and output of the unit. According to the last equation the input impedance of the j-th unit is

$$Z^{\uparrow}_{вх_j} = \frac{F_{вх}}{\dot{y}_{вх}} = \frac{B_{бл_j}}{D_{бл_j}}.$$

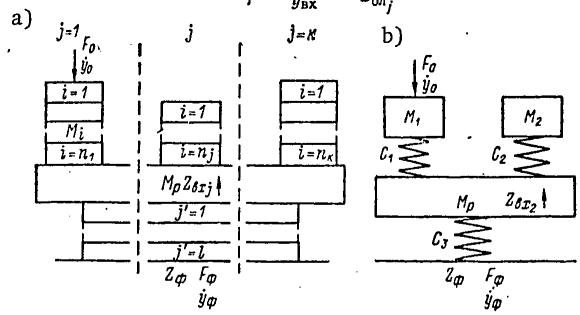

Figure 12.6. Calculation of effect of branched shock-absorbing systems. [ф=f; вх=in; p=fr]

It can be shown [8] that the input impedances of branches on the frame side enter in the calculation system as dipoles, i.e., their summary (except the first branch) transformation matrix is

APPROVED FOR RELEASE: 2007/02/08: CIA-RDP82-00850R000200100009-9

APPROVED FOR RELEASE: 2007/02/08: CIA-RDP82-00850R000200100009-9

$$\begin{bmatrix} 1 & \sum_{j=2}^{k} Z^{*}_{\text{вх}_j} \\ 0 & 1 \end{bmatrix} = \begin{bmatrix} 1 & \sum_{j=2}^{k} \frac{\text{В}_{\text{бл}_j}}{\text{D}_{\text{бл}_j}} \\ 0 & 1 \end{bmatrix}.$$

The overall matrix equation for vibrations in a structure will acquire the form

[p=fr]
$$\begin{bmatrix} F_0 \\ \dot{y}_0 \end{bmatrix} = \prod_{i=1}^{n_1} (M_i) \times \begin{bmatrix} 1 & \sum_{j=2}^{k} \frac{\text{В}_{\text{бл}_j}}{\text{D}_{\text{бл}_j}} \\ 0 & 1 \end{bmatrix} \times M_{\text{p}} \times \prod_{j'=1}^{l} (M_{j'}) \times \begin{bmatrix} F_{\text{ф}} \\ \frac{F_{\text{ф}}}{Z_{\text{ф}}} \end{bmatrix}, \qquad (12.2.9)$$

where M_{fr} is the transformation matrix of the frame, and $M_{j'}$ is the same for the j'-th vibration-damping element under the frame (the number of elements is l, see Figure 12.6a).

Thus, by introducing the input impedances of extra branches it is possible to reduce the total transformation matrix of a branched structure to the product of a series of matrices, i.e., to a form characteristic of non-branched, chainlike structures.

From (12.2.9) we can derive an equation for determining the effect of vibration damping of one or several vibration-damping elements in a branched structure. In the structure illustrated in Figure 12.6a let us determine the combined effect of the vibration damping of two elements: of some element in a branch, where force F_0 is applied (to this element we assign the subscript s), and the t-th element in the assembly, located under the frame. It follows from equation (12.2.9) that

[ж=r; ф=f]
$$\begin{bmatrix} F_0 \\ \dot{y}_{0\text{ж}} \end{bmatrix} = \prod_{i=1}^{s-1} (M_i) \times \text{E} \times \prod_{i=s+1}^{n_1} (M_i) \times \begin{bmatrix} 1 & \sum_{j=2}^{k} \frac{\text{В}_{\text{бл}_j}}{\text{D}_{\text{бл}_j}} \\ 0 & 1 \end{bmatrix} \times$$
$$\times M_{\text{p}} \times \prod_{j'=1}^{t-1} (M_{j'}) \times \text{E} \times \prod_{j'=t+1}^{l} (M_{j'}) \times \begin{bmatrix} F_{\text{фж}} \\ \frac{F_{\text{фж}}}{Z_{\text{ф}}} \end{bmatrix}, \qquad (12.2.10)$$

where unit matrices E indicate the locations of the absolished elements; the subscript "r" in the expression for the vibration velocity at the input and vibration force at the output of the structure refers to a rigid connection between the elements, contiguous with the absolished elements.

By taking F_{fr} from (12.2.10) and F_f from (12.2.9), we can determine the total vibration effect of the s-th and t-th elements under the given conditions.

APPROVED FOR RELEASE: 2007/02/08: CIA-RDP82-00850R000200100009-9

APPROVED FOR RELEASE: 2007/02/08: CIA-RDP82-00850R000200100009-9

If the vibration force acts not in one branch, but in m branches, then, by writing for each of the branches an equation of the type (12.2.9) and determining from them forces F_{fi} on the foundation, we can find the total average vibration force $F_{f\Sigma}$ on the foundation using the expression

$$F_{\phi\Sigma} = \sqrt{\sum_{i=1}^{m} (F_{\phi i})^2}\,.$$

For a simpler structure, consisting of two branches (Figure 12.11b), acted upon by relatively low-frequency vibration, equation (12.2.9) is simplified:

[вх=in; p=fr]

$$\begin{bmatrix} F_0 \\ \dot{y}_0 \end{bmatrix} = \begin{bmatrix} 1 & j\omega M_1 \\ 0 & 1 \end{bmatrix} \begin{bmatrix} 1 & 0 \\ \frac{j\omega}{C_1} & 1 \end{bmatrix} \begin{bmatrix} 1 & Z^{\uparrow}_{\text{вх}_2} \\ 0 & 1 \end{bmatrix} \begin{bmatrix} 1 & j\omega M_p \\ 0 & 1 \end{bmatrix} \begin{bmatrix} 1 & 0 \\ \frac{j\omega}{C_3} & 1 \end{bmatrix} \begin{bmatrix} F_\phi \\ \frac{F_\phi}{Z_\phi} \end{bmatrix}. \qquad (12.2.11)$$

The symbols of the parameters of the elements, which on these frequencies represent bunched mass and rigidity, are given in Figure 12.6.

The input impedance of the second branch "from the bottom" $Z^{\uparrow}_{in2}$ can be found from the equation

$$\begin{bmatrix} A_2 & B_2 \\ C_2 & D_2 \end{bmatrix} = \begin{bmatrix} 1 & 0 \\ \frac{j\omega}{C_2} & 1 \end{bmatrix} \begin{bmatrix} 1 & j\omega M_2 \\ 0 & 1 \end{bmatrix},$$

whence

$$Z^{\uparrow}_{\text{вх}_2} = \frac{B_2}{D_2} = j\omega M_2 \frac{1}{1 - \left(\frac{\omega}{\omega_{02}}\right)^2}, \qquad (12.2.12)$$

where ω_{02} is the partial circular frequency of the second branch:

$$\omega_{02} = \sqrt{\frac{C_2}{M_2}}\,.$$

Using equation (12.2.11) we can determine the difference of vibration forces F_0/F_f, and expressing the terms of the last matrix in this equation in the form $\dot{y}_f Z_f$ and $\dot{y}_f$, we can determine the difference of vibration velocities $\dot{y}_0/\dot{y}_f$ in the analogous shock absorber system.

Substituting, as before, rigidity matrices C_1 or C_2 (or both together) with unit matrices, we can determine from the equation thus derived the vibration force (or velocity) on the foundation with these shock absorbers eliminated (i.e., when the corresponding elements M_1 and M_{fr} are rigidly fastened). Then, by comparing the vibration parameters on the rigidly fastened foundation and with shock absorbers, we can determine their vibration damping. To determine the effect of shock absorption with some

APPROVED FOR RELEASE: 2007/02/08: CIA-RDP82-00850R000200100009-9

APPROVED FOR RELEASE: 2007/02/08: CIA-RDP82-00850R000200100009-9

inertial element excluded we replace the matrix in (12.2.11), corresponding to that inertial element, with the unit matrix.

Calculation of Acoustic Effect of Installation of Shock Absorber Using Orthogonal Polynomials. This method is an extension of the quadrupole technique in application to chain structures consisting of n series-connected identical component complexes (assemblies), each of which, in turn, may consist of m vibration elements (in the special case n or m may be equal to unity). Orthogonal polynomials of the Hegenbauer type of a complex argument are used for this purpose. The identity of recursive relations, demonstrated by Parody [2] for the described polynomials and for passive linear electric (and consequently mechanical) quadrupoles, is the foundation of this approach. The method is examined in the literature [7] in application to complex vibration-damping systems, and the expressions that follow are taken from the cited work.

In the general case the difference of the vibration forces and vibration velocities for a structure of n identical assemblies (Figure 12.7a) (the symbols are in the figure) is

$$\frac{F_0}{F_n} = t_1 C^1_{n-1}(x) - C^1_{n-2}(x); \tag{12.2.13}$$

$$\frac{\dot{y}_0}{\dot{y}_n} = t_2 C^1_{n-1}(x) - C^1_{n-2}(x), \tag{12.2.14}$$

where

$$t_1 = A_a + \frac{B_0}{Z_\Phi}; \quad t_2 = C_a Z_\Phi + D_a; \tag{12.2.15}$$

A_a, B_a, C_a, D_a are the coefficients of the mechanical quadrupoles that are equivalent to each of the identical assemblies of elements. The Hegenbauer polynomials entering in formulas (12.2.13) and (12.2.14), of somewhat lower orders (the number of assemblies is usually small in vibration technology) for the generating function, equal to unity, are expressed as

$$\left.\begin{array}{ll} C^1_0(x) = 1; & C^1_2(x) = 4x^2 - 1; \\ C^1_1(x) = 2x; & C^1_3(x) = 8x^3 - 4x. \end{array}\right\} \tag{12.2.16}$$

The argument of the polynomials is

$$x = \frac{1}{2}(A_a + D_a). \tag{12.2.17}$$

From equations (12.2.13) and (12.2.14), in consideration of the trivial relation $F_n = Z_f \dot{y}_n$, we can derive the input mechanical impedance of a structure, closed on impedance Z_f:

$$Z_{\text{вх}} = \frac{F_0}{\dot{y}_0} = Z_\Phi \frac{t_1 C^1_{n-1}(x) - C^1_{n-2}(x)}{t_2 C^1_{n-1}(x) - C^1_{n-2}(x)}. \tag{12.2.18}$$

APPROVED FOR RELEASE: 2007/02/08: CIA-RDP82-00850R000200100009-9

APPROVED FOR RELEASE: 2007/02/08: CIA-RDP82-00850R000200100009-9

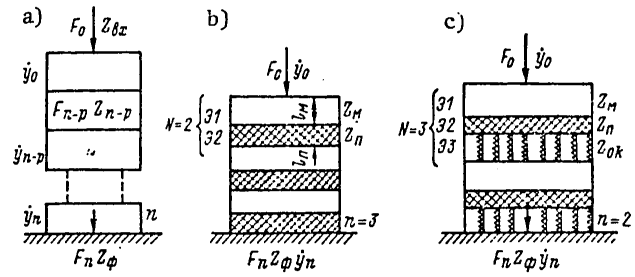

Figure 12.7. Calculation of multiple assembly chain vibration damping systems using orthogonal polynomials. [вх=in; ф=f; Э=E]

We also present expressions for the vibration force, vibration velocity and mechanical impedance at the input of the p-th assembly from the end of a structure closed on impedance Z_f:

$$F_{n-p} = [t_1 C^1_{p-1}(x) - C^1_{p-2}(x)]\, F_n = \frac{t_1 C^1_{p-1}(x) - C^1_{p-2}(x)}{t_1 C^1_{n-1}(x) - C^1_{n-2}(x)} F_0; \qquad (12.2.19)$$

$$\dot{y}_{n-p} = [t_2 C^1_{p-1}(x) - C^1_{p-2}(x)]\, \dot{y}_n = \frac{t_2 C^1_{p-1}(x) - C^1_{p-2}(x)}{t_2 C^1_{n-1}(x) - C^1_{n-2}(x)} \dot{y}_0, \qquad (12.2.20)$$

[ф=f]

$$Z_{n-p} = \frac{F_{n-p}}{\dot{y}_{n-p}} = Z_\phi \frac{t_1 C^1_{p-1}(x) - C^1_{p-2}(x)}{t_2 C^1_{p-1}(x) - C^1_{p-2}(x)}. \qquad (12.2.21)$$

The application of some of the expressions derived above for determining the differences of vibration on complex (multistage) structures and their vibration damping is examined below.

Three-Stage Shock Absorber on Foundation with Arbitrary Impedance. In this case there will be three series-connected identical assemblies (n = 3), each consisting of two elements E1 and E2, N = 2 (Figure 12.7b).

From expressions (12.2.13)-(12.2.17) for n = 3 we find the differences of the vibration forces and velocities on the structure in the form

$$\Pi'_F = \frac{F_0}{F_n} = \left(A_a + \frac{B_0}{Z_\phi}\right)[(A_a + D_a)^2 - 1] - (A_a + D_a); \qquad (12.2.22)$$

$$\Pi'_{\dot{y}} = \frac{\dot{y}_0}{\dot{y}_n} = (C_a Z_\phi + D_a)[(A_a + D_a)^2 - 1] - (A_a + D_a). \qquad (12.2.23)$$

In the last expressions the coefficients of the compound quadrupoles, equivalent to each of the assemblies, are determined by multiplying the matrices of two components of the assemblies of elementary quadrupoles [see (1.7.3)]:

[п=p]

$$\begin{bmatrix} A_a & B_a \\ C_a & D_a \end{bmatrix} = \begin{bmatrix} A_м & B_м \\ C_м & A_м \end{bmatrix} \begin{bmatrix} A_п & B_п \\ C_п & A_п \end{bmatrix},$$

APPROVED FOR RELEASE: 2007/02/08: CIA-RDP82-00850R000200100009-9

APPROVED FOR RELEASE: 2007/02/08: CIA-RDP82-00850R000200100009-9

where the subscript "m" indicates the parameters of metal structures (the machine and intermediate frames), and the subscript "p" indicates the parameters of elastic pads.

In consideration of the expressions for the coefficients of quadrupoles with losses [formula (12.2.4)], the parameters of compound quadrupoles in this case are written as

$$\left.\begin{aligned} A_a &= \operatorname{ch}(\gamma l)_м \operatorname{ch}(\gamma l)_п + \frac{Z_м}{Z_п}\operatorname{sh}(\gamma l)_м \operatorname{sh}(\gamma l)_п; \\ B_a &= Z_п \operatorname{ch}(\gamma l)_м \operatorname{sh}(\gamma l)_п + Z_м \operatorname{sh}(\gamma l)_м \operatorname{ch}(\gamma l)_п; \\ C_a &= \frac{1}{Z_м}\operatorname{sh}(\gamma l)_м \operatorname{ch}(\gamma l)_п + \frac{1}{Z_п}\operatorname{ch}(\gamma l)_м \operatorname{sh}(\gamma l)_п; \\ D_a &= \frac{Z_п}{Z_м}\operatorname{sh}(\gamma l)_м \operatorname{sh}(\gamma l)_п + \operatorname{ch}(\gamma l)_м \operatorname{ch}(\gamma l)_п. \end{aligned}\right\} \quad (12.2.24)$$

The following symbols are used in the last expressions for brevity:

$$\left.\begin{aligned} Z_м &= (\rho c S)_м\left(1 + j\frac{\eta_м}{2}\right); \quad Z_п = (\rho c S)_п\left(1 + j\frac{\eta_п}{2}\right); \\ \gamma_м &= \frac{\omega}{c_м}\frac{\eta_м}{2} + j\frac{\omega}{c_м}; \quad \gamma_п = \frac{\omega}{c_п}\frac{\eta_п}{2} + j\frac{\omega}{c_п}. \end{aligned}\right\} \quad (12.2.25)$$

Two-Stage Shock Absorber with Deadened Mounts on Foundation with Finite Impedance. In this case n = 2, N = 3 (Figure 12.7c). The differences of the vibration forces and vibration velocities, according to expressions (12.2.13)-(12.2.17), are expressed as

$$\Pi'_F = \frac{F_0}{F_n} = \left(A_a + \frac{B_a}{Z_ф}\right)(A_a + D_a) - 1, \quad (12.2.26)$$

$$\Pi'_{\dot{y}} = \frac{\dot{y}_0}{\dot{y}_n} = (C_a Z_ф + D_a)(A_a + D_a) - 1. \quad (12.2.27)$$

The coefficients A_a, B_a, C_a, D_a are determined in this case by the products of three matrices, corresponding to the elements E1, E2, E3 [7].

The vibration damping of certain elements of a vibration conductor is determined by comparing the vibration forces (or velocities) on the foundation in the absence of a given element and with it installed. By using Hegenbauer polynomials it is possible to find the vibration damping for two cases.

1. Identical elements (for example, vibration-damping pads) are absolished immediately in all assemblies of the structure. When some element is excluded from all assemblies of a structure the true vibration damping of the elements excluded from the calculation is expressed as the ratio

APPROVED FOR RELEASE: 2007/02/08: CIA-RDP82-00850R000200100009-9

APPROVED FOR RELEASE: 2007/02/08: CIA-RDP82-00850R000200100009-9

[ВИ=VD]

$$\text{ВИ} = \frac{F_{n\,N}}{F_{n\,N-1}} = \frac{\dot{y}_{n\,N}}{\dot{y}_{n\,N-1}}, \tag{12.2.28}$$

where N is the number of elements in the assembly.

When the number of assemblies is n = 2 and the number of elements in them is N = 3 (see Figure 12.7c) the true vibration damping of two stages of shock absorbers is

[ф=f]

$$\text{ВИ} = \frac{F_{n\,n=2,\,N=3}}{F_{n\,n=2,\,N=2}} = \frac{(A_{a\,N=3} + B_{a\,N=3}/Z_{\text{ф}})(A_{a\,N=3} + D_{a\,N=3}) - 1}{(A_{a\,N=2} + B_{a\,N=2}/Z_{\text{ф}})(A_{a\,N=2} + D_{a\,N=2}) - 1}, \tag{12.2.29}$$

where the coefficients with the subscript N = 3 are taken from (12.2.24).

2. Several identical assemblies (or one) are abolished simultaneously. By comparing the vibration force on the foundation with the total number of assemblies (for example, see Figure 12.7b) and on the foundation with the number of assemblies minus one, we find the vibration damping of the excluded assembly in the form

$$\text{ВИ} = \frac{F_{n\,n=3,\,N=2}}{F_{n\,n=2,\,N=2}} = \frac{(A_{a\,N=2} + B_{a\,N=2}/Z_{\text{ф}})\left[(A_{a\,N=2} + D_{a\,N=2}) - 1\right] - (A_{a\,N=2} + D_{a\,N=2})}{(A_{a\,N=2} + B_{a\,N=2}/Z_{\text{ф}})(A_{a\,N=2} + D_{a\,N=2}) - 1}, \tag{12.2.30}$$

where the coefficients A_a, B_a, C_a, D_a are taken from the literature [7].

Vibration Damping with Diffuse Vibration Field in Vibration-Damped Object (Vibration-Active Mechanism) and in Foundation. The vibration field in metal structures on medium and high acoustic frequencies can be diffuse under certain conditions. For the derivation in which we are interested we will use the successive approximation procedure. When the machine is rigidly fastened to the foundation the average energy density w_{m+f} in this combined space (Figure 12.8a) is

$$\omega_{\text{м+ф}} = \frac{E}{V_{\text{м}} + V_{\text{ф}}}, \tag{12.2.31}$$

where E is the energy of the vibration source (assumed to be constant); V_m and V_f are the volumes of the mechanism and foundation.

Through VD' we denote the "original" vibration damping effectiveness of a shock-absorbing mount, characterized approximately by the ratio of vibration energy E, radiated in the mechanism, to energy E', transmitted through the shock absorbers into the foundation (Figure 12.8b):

$$\text{ВИ}' \cong E/E'. \tag{12.2.32}$$

APPROVED FOR RELEASE: 2007/02/08: CIA-RDP82-00850R000200100009-9

APPROVED FOR RELEASE: 2007/02/08: CIA-RDP82-00850R000200100009-9

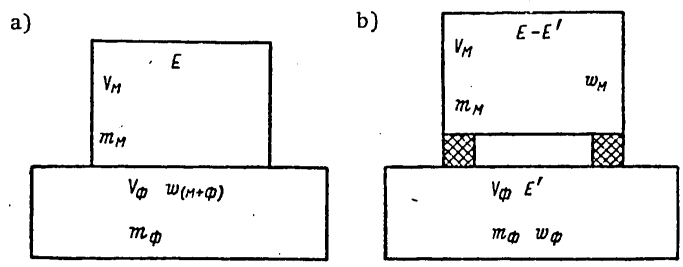

Figure 12.8. Determination of influence of foundation parameters on vibration-damping effectiveness of shock absorber.

The energy density in the foundation in the presence of shock absorbers is

$$w_\Phi = E'/V_\Phi. \tag{12.2.33}$$

From the above expressions we find the shock-absorbing effectiveness of the shock absorbers under these conditions in the form

$$\text{ВИ} = \frac{w_{M+\Phi}}{w_\Phi} = \frac{E}{E'}\frac{V_\Phi}{V_M+V_\Phi} = \text{ВИ}'\frac{V_\Phi}{V_M+V_\Phi}. \tag{12.2.34}$$

If the average densities of the mechanism and foundation are equal, then, as follows from the last equation, in a diffuse acoustic field

$$\text{ВИ} = \text{ВИ}'\frac{m_\Phi}{m_M+m_\Phi}, \tag{12.2.35}$$

where m_m and m_f are the masses of the mechanism and foundation, respectively.

As can be seen, the vibration-damping effectiveness of the shock-absorbing mount increases with the ratio of the mass of the foundation to the mass of the machine. When $m_f/m_m \geq 2$ the loss of acoustic insulation does not exceed 3 dB in comparison with the case of an infinitely massive foundation.

Difference of Vibration on Shock Absorbers as Function of Mass Ratio of Foundation and Machine. The vibration energy density in a vibration-damped machine is

$$w_M = \frac{E-E'}{V_M}\Big|_{E'\ll E} \cong \frac{E}{V_M}.$$

The difference Π_e of the vibration energy on the shock absorbers is equal to the ratio of w_m to w_f [see (12.2.33)]:

[э=e]

$$\Pi_э = \frac{EV_\Phi}{V_M E'} = \text{ВИ}'\frac{V_\Phi}{V_M}\Big|_{\rho_M=\rho_\Phi} = \text{ВИ}'\frac{m_\Phi}{m_M}. \tag{12.2.36}$$

APPROVED FOR RELEASE: 2007/02/08: CIA-RDP82-00850R000200100009-9

APPROVED FOR RELEASE: 2007/02/08: CIA-RDP82-00850R000200100009-9

From (12.2.36) and (12.2.35) we find the ratio of the difference of the vibration energy to vibration damping:

$$\frac{\Pi_э}{ВИ} = 1 + \frac{m_ф}{m_м}. \qquad (12.2.37)$$

Thus, the larger the ratio m_f/m_m the more the difference of the vibration of the shock absorbers exceeds their vibration damping, even though the latter also increases [see formula (12.2.35)].

In two-stage shock absorbers on a foundation with an arbitrary impedance the relationship between the difference of vibration and vibration damping is more complicated, and the difference between the gradient and vibration damping is greater than in single-stage shock absorbers [9].

12.3. Energy Analysis of Effectiveness of Shock-Absorbing Mounts

It is often difficult to give an exact description of vibration-damping systems in terms of kinematic parameters. In such cases it is helpful to use energy parameters [11].

To analyze the effectiveness of shock absorbers (of shock-absorbing structures) we will use the following energy parameters:

vibration power, absorbed by the vibration-damping system, N_a;

energy absorption coefficient Π_{aw}, determined as the ratio of powers N_{af} and N_f, where N_{af} is the vibration power absorbed in the shock absorber-foundation system:

[ф=f]

$$\Pi_{aw} = \frac{N_{aф}}{N_ф};$$

energy vibration-damping coefficient $B_w = N_f^0/N_f$, determined as the ratio of power N_f^0, radiated into the foundation in the absence of shock absorption, to power N_f, radiated into the foundation in the presence of shock absorption.

Case of Unidirectional Vibrations of Machine with One Point of Contact with Shock Absorber. The shock absorber absorbs the power

[xx=id;
кз=sc]

$$N_a = N_{aф} - N_ф = \frac{|\dot{q}_{эф}|^2}{|Z_ф + Z_{axx}|^2}\{\mathrm{Re}\,[Z_{a\,xx}(Z_ф + Z_{a\,кз})(Z_{a\,xx} + Z_ф)^*] - \mathrm{Re}\,Z_ф\,|Z_{a\,xx}(Z_{a\,xx} - Z_{a\,кз})|\} = \frac{|\dot{q}_{эф}|^2}{|Z_{aм} + Z_ф|^2}\{\mathrm{Re}\,[Z_{aм}\,|Z_{aм} + Z_ф|^2 - Z^2_{aмф}(Z_{aм} + Z_ф)^*] - |Z_{aмф}|^2\,\mathrm{Re}\,Z_ф\},$$

APPROVED FOR RELEASE: 2007/02/08: CIA-RDP82-00850R000200100009-9

APPROVED FOR RELEASE: 2007/02/08: CIA-RDP82-00850R000200100009-9

Where Z_{aid}, Z_{asc}, Z_f are the impedances of the shock absorber (in the idle and short circuit modes) and foundation; Z_{am}, Z_{amf} are the input and transient impedances of the shock absorbers.

The energy absorption coefficient of a shock absorber [11] is

$$\Pi_{aw} = \frac{\mathrm{Re}\,[Z_{a\,\text{xx}}\,(Z_\text{ф} + Z_{a\,\text{кз}})\,(Z_{a\,\text{xx}} + Z_\text{ф})^*]}{|\,Z_{a\,\text{xx}}\,(Z_{a\,\text{xx}} - Z_{a\,\text{кз}})\,|\,\mathrm{Re}\,Z_\text{ф}} = \frac{\mathrm{Re}\,[Z_\text{ам}\,|\,Z_\text{ам} + Z_\text{ф}\,|^2 - Z^2_\text{амф}\,(Z_\text{ам} + Z_\text{ф})^*]}{|\,Z_\text{амф}\,|^2\,\mathrm{Re}\,Z_\text{ф}}.$$

The vibration energy damping coefficient of the shock absorber is

$$B_w = \frac{(Z_\text{ф} + Z_{a\,\text{xx}})^2\,|\,Z_\text{ф}\,(Z_0 + Z_{a\,\text{xx}}) + Z_{a\,\text{xx}}\,(Z_0 + Z_{a\,\text{кз}})\,|}{|\,Z_0 + Z_\text{ф}\,|^2\,[Z_{a\,\text{xx}}\,(Z_{a\,\text{xx}} - Z_{a\,\text{кз}})]} = \frac{|\,(Z_\text{м} + Z_\text{ам})\,(Z_\text{ам} + Z_\text{ф}) - Z^2_\text{амф}\,|^2}{|\,Z_\text{м} + Z_\text{ф}\,|^2\,|\,Z_\text{амф}\,|^2}.$$

It is often desirable to determine the energy vibration parameters on the basis of the impedances of the shock absorber and vibration velocities of the machine and foundation. This can be done, since the gradient on a shock absorber is a function of Z_f and the influence of Z_f on the vibration energy flux in the foundation, and also the amount of absorption of energy in the shock absorbers can be taken into account [11]:

$$N_\text{ф} = \frac{1}{2}\,\mathrm{Re}\,(Q_\text{ф}\dot{q}^*_\text{ф}) = -\frac{1}{2}\,|\,\dot{q}_\text{ф}\,|^2\,\mathrm{Re}\,Z_\text{ф} - \frac{1}{2}\,\mathrm{Re}\,(Z_\text{амф}\dot{q}\dot{q}^*_\text{ф}) = \frac{1}{2}\,|\,\dot{q}_\text{ф}\,|^2\left[\mathrm{Re}\,Z_\text{аф} + \mathrm{Re}\,(Z_\text{амф}\Pi_{a\dot{q}})\right];$$

$$N_{a\text{ф}} = \frac{1}{2}\,\mathrm{Re}\,(Q\dot{q}^*) = \frac{1}{2}\,|\,\dot{q}\,|^2\,\mathrm{Re}\,Z_\text{ам} + \frac{1}{2}\,\mathrm{Re}\,(Z_{a\text{фм}}\dot{q}^*\dot{q}_\text{ф}) = \frac{1}{2}\,|\,q\,|^2\left[\mathrm{Re}\,Z_\text{ам} + \mathrm{Re}\left(\frac{Z_\text{амф}}{\Pi_{a\dot{q}}}\right)\right] = \frac{1}{2}\,|\,\dot{q}\,|^2\left[\mathrm{Re}\,Z_\text{ам} + \frac{\mathrm{Re}\,(Z_\text{амф}\Pi^*_{a\dot{q}})}{|\,\Pi_{a\dot{q}}\,|^2}\right] = \frac{1}{2}\,|\,\dot{q}_\text{ф}\,|^2\,|\,\Pi_{a\dot{q}}\,|^2\left[\mathrm{Re}\,Z_\text{ам} + \frac{\mathrm{Re}\,(Z_\text{амф}\Pi^*_{a\dot{q}})}{|\,\Pi_{a\dot{q}}\,|}\right],$$

$$N_a = \frac{1}{2}\,|\,\dot{q}_\text{ф}\,|^2\,[\,|\,\Pi_{a\dot{q}}\,|^2\,\mathrm{Re}\,Z_\text{ам} + \mathrm{Re}\,Z_\text{аф} + \mathrm{Re}\,(Z_\text{амф}\Pi^*_{a\dot{q}}) + \mathrm{Re}\,(Z_\text{амф}\Pi_{a\dot{q}})].$$

The energy absorption coefficient of a shock absorber is

$$\Pi_{aw} = -\frac{|\,\Pi_{a\dot{q}}\,|^2\,\mathrm{Re}\,Z_\text{ам} + \mathrm{Re}\,(Z_\text{амф}\Pi^*_{a\dot{q}})}{\mathrm{Re}\,Z_\text{аф} + \mathrm{Re}\,(Z_{a\text{фм}}\Pi_{a\dot{q}})}.$$

APPROVED FOR RELEASE: 2007/02/08: CIA-RDP82-00850R000200100009-9

APPROVED FOR RELEASE: 2007/02/08: CIA-RDP82-00850R000200100009-9

In a symmetric shock absorber

$$\Pi_{aw} = \frac{|\Pi_{a\dot{q}}|^2 \operatorname{Re} Z_{\text{ам}} + \operatorname{Re}\left(Z_{\text{амф}} \Pi^*_{a\dot{q}}\right)}{\operatorname{Re} Z_{\text{ам}} + \operatorname{Re}\left(Z_{\text{амф}} \Pi_{a\dot{q}}\right)},$$

[ф=f]

$$N_a = \frac{1}{2} |\dot{q}_\phi|^2 \left[\operatorname{Re} Z_{\text{ам}} \left(|\Pi_{a\dot{q}}|^2 - 1\right) + \operatorname{Im} Z_{\text{амф}} \operatorname{Im} \Pi_{a\dot{q}}\right].$$

The effect of vibration damping of vibration energy by shock absorbers is attributed to the establishment of conditions for the vibration force that acts in a source that are unfavorable for the excitation of vibrations in foundation structures. If a machine rigidly fastened to a foundation is acted upon by the force Q_f

[и=s]

$$Q_\phi = Q^{\text{и}} \frac{Z_\phi}{Z_{\text{м}} + Z_\phi},$$

the ratio between the vibration powers, absorbed in the machine N_m and radiated in the foundation N_f is

$$\frac{N_{\text{м}}}{N_\phi} = \frac{\operatorname{Re} Z_{\text{м}}}{\operatorname{Re} Z_\phi}. \qquad (12.3.1)$$

Let us examine vibrations in the frequency range up to wave resonances inside a shock absorber. In this frequency range the input impedance of a shock absorber is equal to the transient impedance and is elastic in nature:

$$Z_a = \frac{S_a (1 + j\eta_a)}{j\omega},$$

where η_a is the loss coefficient.

Then

$$Z_{a\phi} = \frac{Z_a Z_\phi}{Z_a + Z_\phi}$$

and

$$\operatorname{Re} Z_{a\phi} = \frac{\operatorname{Re} Z_\phi |Z_a|^2 + \operatorname{Re} Z_a |Z_\phi|^2}{|Z_a|^2 + |Z_\phi|^2 + 2 (\operatorname{Re} Z_a \operatorname{Re} Z_\phi + \operatorname{Im} Z_a \operatorname{Im} Z_\phi)}.$$

With shock absorbers (in the examined frequency range) the foundation is acted upon by the force

$$Q_{a\phi} = Q^{\text{и}} = \frac{Z_{a\phi}}{Z_{\text{м}} + Z_\phi}.$$

Usually $Z_a < Z_f$, and then

$$Z_{a\phi} \approx Z_a \text{ and } Q_{a\phi} \approx \frac{Z_a}{Z_{\text{м}} + Z_a}.$$

In this connection, and also because internal vibration forces on frequencies above the frequency of free vibrations of a machine on shock absorbers $Z_m > Z_a$ is expended basically on the excitation of vibrations of the machine itself

APPROVED FOR RELEASE: 2007/02/08: CIA-RDP82-00850R000200100009-9

APPROVED FOR RELEASE: 2007/02/08: CIA-RDP82-00850R000200100009-9

$$\frac{N_{\text{м}}}{N_{a\phi}} = \frac{\operatorname{Re} Z_{\text{м}}}{\operatorname{Re} Z_a}. \tag{12.3.2}$$

For example, when the loss coefficient in the material of a shock absorber is small ($\eta_a \to 0$) and $Z_a < Z_f$

$$\operatorname{Re} Z_{a\phi} \approx \operatorname{Re} Z_\phi \frac{|Z_a|^2}{|Z_\phi|^2} \approx \frac{\operatorname{Re} Z_\phi}{|\Pi_{\dot{q}}|^2}, \tag{12.3.3}$$

where $\Pi_{\dot{q}}$ is the gradient of vibration on the shock absorber.

The expression for N_m/N_{af} acquires the form

$$\frac{N_{\text{м}}}{N_{a\phi}} = \frac{\operatorname{Re} Z_{\text{м}}}{\operatorname{Re} Z_\phi} |\Pi_{\dot{q}}|^2. \tag{12.3.4}$$

A comparison of (12.3.1) with (12.3.4) shows that with a shock absorber the energy absorbed in the machine in relation to the energy radiated increases by a factor of $|\Pi_{\dot{q}}|^2$ in comparison with the case of a machine without a shock absorber. The reason for this is that in the case when a machine is installed on shock absorbers only the $1/|\Pi_{\dot{q}}|^2$-th fraction of the active impedance of the foundation is connected to the machine [see expression (12.3.3)]. The ratio between the powers absorbed in a machine in the absence of shock absorption N_m and with it N_m^a is

$$\frac{N_{\text{м}}^a}{N_{\text{м}}} = \left| \frac{Z_{\text{м}} + Z_\phi}{Z_{\text{м}} + Z_a} \right|^2.$$

When $Z_a < Z_m < Z_f$

$$\frac{N_{\text{м}}^a}{N_{\text{м}}} \approx \left| \frac{Z_\phi}{Z_{\text{м}}} \right|^2,$$

i.e., the energy absorbed in the machine increases sharply.

Let us examine three characteristic cases.

1. The case when $Z_f \gg Z_m \gg Z_a$ and $\eta_a \gg \eta_f$. Then $\operatorname{Re} Z_{af} \gg \operatorname{Re} Z_a$ and

$$\Pi_{aw} \approx \frac{\operatorname{Re} Z_a}{\operatorname{Re} Z_\phi} \frac{|Z_\phi|^2}{|Z_a|^2}, \quad B_\omega \approx \frac{|Z_{\text{м}}|^2}{|Z_a|^2}. \tag{12.3.5}$$

The relation between the coefficients of absorption and vibration damping in terms of energy is

$$\frac{B_\omega}{\Pi_{aw}} = \frac{\operatorname{Re} Z_\phi}{\operatorname{Re} Z_a} \frac{|Z_{\text{м}}|^2}{|Z_\phi|^2}.$$

In the case when there is no active impedance in the shock absorbers ($\eta_a = 0$) $\operatorname{Re} Z_{a\phi} = \operatorname{Re} Z_\phi \frac{|Z_a|^2}{|Z_\phi|^2}$ and, as can be seen by (12.3.5), $\Pi_{aw} = 1$. This is obvious, since in the absence of losses in a shock absorber all the energy radiated by the machine is transmitted into the foundation.

APPROVED FOR RELEASE: 2007/02/08: CIA-RDP82-00850R000200100009-9

APPROVED FOR RELEASE: 2007/02/08: CIA-RDP82-00850R000200100009-9

Then

$$\frac{B_w}{\Pi_{aw}} = \frac{|Z_м|^2}{|Z_a|}.$$

In the case at hand the vibration power radiated into the shock absorber-foundation system is proportional to the active impedance of the shock absorber:

[ф=f; и=s]

$$N_{a\phi} = \frac{|Q^и|^2}{|Z_м|^2} \operatorname{Re} Z_a \approx \operatorname{Re} Z_a.$$

Under these conditions the use of a shock absorber with a large η_a leads to some increase of N_{af}, but the power absorbed by the shock absorber increases simultaneously:

$$\Pi_{aw} \approx \frac{\operatorname{Re} Z_a}{\operatorname{Re} Z_\phi} |\Pi_{\dot{q}}|^2 \approx \frac{\operatorname{Re} Z_a}{\operatorname{Re} Z_\phi} \frac{(\operatorname{Im} Z_\phi)^2}{(\operatorname{Im} Z_a)^2 (1+\eta_a^2)}.$$

As a result the power radiated into the foundation is

$$N_\phi = \frac{N_{a\phi}}{\Pi_{aw}} \approx (1+\eta_a^2). \qquad (12.3.6)$$

Expression (12.3.6) shows, for example, that when the coefficient η_a increases from 0.15 to 0.3 the power radiated into the foundation increases by 7%.

2. The case when $Z_m \gg Z_f \gg Z_a$. In this case the excitation of the shock absorber-foundation system is kinematic in nature. The vibration velocity of the foundation changes in proportion to the vibration gradient on the shock absorbers. Therefore the vibration damping coefficient in terms of vibration velocity $B_{\dot{q}}$ is equal to the vibration gradient: $B_{\dot{q}} \approx \Pi_{\dot{q}}$.

The expressions for coefficients Π_{aw} and B_w are

$$\Pi_{aw} \approx \frac{\operatorname{Re} Z_{a\phi}}{\operatorname{Re} Z_\phi} |\Pi_{\dot{q}}|^2 \approx \frac{\operatorname{Re} Z_a}{\operatorname{Re} Z_\phi} |\Pi_{\dot{q}}|^2 \quad (\text{for } Z_a < Z_\phi \text{ and } \eta_a \geqslant \eta_\phi);$$

$$B_w = \frac{|Z_a + Z_\phi|^2}{|Z_a|^2} |\Pi_{\dot{q}}|^2;$$

$$\frac{B_w}{\Pi_{aw}} \approx \frac{\operatorname{Re} Z_a}{\operatorname{Re} Z_\phi}; \quad \text{for } \eta_a \to 0 \ \frac{B_w}{\Pi_{aw}} |\Pi_{\dot{q}}|^2.$$

3. The case when $Z_f \gg Z_m$ and $Z_f \gg Z_a$. Then

$$\Pi_w \approx \frac{\operatorname{Re} Z_a}{\operatorname{Re} Z_\phi} \frac{|Z_\phi|^2}{|Z_a|^2}; \quad B_w \approx \frac{|Z_м + Z_a|^2}{|Z_a|^2}.$$

APPROVED FOR RELEASE: 2007/02/08: CIA-RDP82-00850R000200100009-9

APPROVED FOR RELEASE: 2007/02/08: CIA-RDP82-00850R000200100009-9

Case of Unidirectional Vibrations of Machine-Shock Absorber-Foundation System with Multipoint Contact. The vibration power radiated into the foundation is calculated in this case by the formula

$$N_\Phi = \frac{1}{2}\sum_{n=1}^{m} |\dot{q}_\Phi^n| \operatorname{Re} Z_\Phi^{nn} + \sum_{\substack{n=1\\k\neq n}}^{m}\sum_{k=1}^{m} \operatorname{Re}\left(Z_\Phi^{nk}\dot{q}_\Phi^n \dot{q}_\Phi^{k*}\right),$$

where Z_f^{nn} and Z_f^{nk} are the point and transient impedances of the foundation; $\dot{q}_f^n$, $\dot{q}_f^k$ are the vibration velocities of the foundation at points n and k, i.e., in contrast to the previous case, additional information is needed about the transient impedance of the foundation and the degree of interaction of the vibration velocities at different points of the foundation [11].

The energy flux through each shock absorber, and then through all the shock absorbers, can be calculated on the basis of data on the impedance of the shock absorbers and on the vibration velocities at their inputs and outputs:

$$N_\Phi = \sum_{n=1}^{m} \frac{1}{2}\operatorname{Re}\left(Q_\Phi^n \dot{q}_\Phi^{n*}\right) = -\frac{1}{2}\sum_{n=1}^{m} |\dot{q}_\Phi^n|^2 \left[\operatorname{Re} Z_{a\Phi}^{nn} + \operatorname{Re}\left(Z_{a\text{м}\Phi}^{nn}\Pi_{a\dot{q}}^{nn}\right)\right];$$

$$N_{a\Phi} = \sum_{n=1}^{m} \frac{1}{2}\operatorname{Re}\left(Q^n \dot{q}^{n*}\right) = \sum_{n=1}^{m} \frac{1}{2}|\dot{q}^n|^2 \left[\operatorname{Re} Z_{a\text{м}}^{nn} + \frac{\operatorname{Re}\left(Z_{a\text{м}\Phi}^{nn}\Pi_{a\dot{q}}^{nn*}\right)}{|\Pi_{a\dot{q}}|^2}\right] =$$

$$= \sum_{n=1}^{m} \frac{1}{2}|\dot{q}_\Phi^n|^2 \left[|\Pi_{a\dot{q}}^{nn}|^2 \operatorname{Re} Z_{a\text{м}}^{nn} + \operatorname{Re}\left(Z_{a\text{м}\Phi}^{nn}\Pi_{a\dot{q}}^{nn*}\right)\right].$$

If the shock-absorbing mount consists of identical symmetric shock absorbers, which provide the average vibration gradient $\langle\Pi_{a\dot{q}}\rangle$, then W_a and Π_{aw} can be determined by the approximate formulas

$$N_a = \frac{m}{2}\langle|\dot{q}_\Phi|^2\rangle \left[\operatorname{Re} Z_{a\text{м}}^{nn}\left(\langle|\Pi_{a\dot{q}}|^2\rangle - 1\right) + \operatorname{Im} Z_{a\text{м}\Phi}^{nn} \operatorname{Im}\langle\Pi_{a\dot{q}}\rangle\right],$$

$$\Pi_{aw} = \frac{\langle|\Pi_{a\dot{q}}|^2\rangle \operatorname{Re} Z_{a\text{м}}^{nn} + \operatorname{Re}\left(Z_{a\text{м}\Phi}\langle\Pi_{a\dot{q}}^*\rangle\right)}{\operatorname{Re} Z_{a\text{м}}^{nn} + \operatorname{Re}\left(Z_{a\text{м}\Phi}\langle\Pi_{a\dot{q}}\rangle\right)},$$

where $\langle|\dot{q}_f|^2\rangle$ is the mean square vibration velocity of the foundation at the points of contact with the shock absorbers.

General Case of Vibrations of Machines. The vibration power, absorbed by a vibration-damping system, is determined through the force matrix $\overline{Q}$, vibration velocity matrix $\overline{\dot{q}}$ and mechanical impedance matrix $\overline{Z}$:

APPROVED FOR RELEASE: 2007/02/08: CIA-RDP82-00850R000200100009-9

APPROVED FOR RELEASE: 2007/02/08: CIA-RDP82-00850R000200100009-9

$$N_a = \frac{1}{2}\,\mathrm{Re}\,[\bar{Q}\dot{\bar{q}}^{*\prime} - \bar{Q}_\phi \dot{\bar{q}}_\phi^{*\prime}] = \mathrm{Re}\,\frac{1}{2}\,[(\bar{Z}_{aM}\dot{\bar{q}})\,\dot{\bar{q}}^{*\prime} + (\bar{Z}_{aM\phi}\dot{\bar{q}})\,\dot{\bar{q}}^{*\prime} + (\bar{Z}_{aM\phi}\dot{\bar{q}})\,\dot{\bar{q}}_\phi^{*\prime} + (\bar{Z}_{a\phi}\dot{\bar{q}}_\phi)\,\dot{\bar{q}}_\phi^{*\prime}].$$

When a machine is characterized as a generator of forces $\bar{Q}_0$, reduced to the points of contact with the shock absorber, the formula for computing N_a can be written in the form

$$N_a = \mathrm{Re}\,\{[\bar{Z}_a\,(\bar{Z}_{0\phi} + \bar{Z}_a)^{-1}\,\bar{Q}_0]\,[(\bar{Z}_a + \bar{Z}_{0\phi})^{-1}\,\bar{Q}_0]^*\},$$

$$\bar{Z}_a = \begin{bmatrix} \bar{Z}_{aM} & \bar{Z}_{aM\phi} \\ \bar{Z}_{aM\phi} & \bar{Z}_{a\phi} \end{bmatrix}, \qquad \bar{Z}_{0\phi} = \begin{bmatrix} \bar{Z}_0 & 0 \\ 0 & \bar{Z}_\phi \end{bmatrix}.$$

The matrix of impedances of foundation structures is

$$\bar{Z}_\phi = \begin{bmatrix} \bar{Z}_\phi^{11} & \bar{Z}_\phi^{12} & \dots & \bar{Z}_\phi^{1m} \\ \bar{Z}_\phi^{21} & \bar{Z}_\phi^{22} & \dots & \bar{Z}_\phi^{2m} \\ \dots & \dots & \dots & \dots \\ \bar{Z}_\phi^{m1} & \bar{Z}_\phi^{m2} & \dots & \bar{Z}_\phi^{mm} \end{bmatrix},$$

where Z_f^{11}, Z_f^{12}, ..., Z_f^{kn} are 6-th-order quadratic matrices

$$\bar{Z}_\phi^{kn} = \begin{bmatrix} Z_{11\phi}^{kn} & Z_{12\phi}^{kn} & \dots & Z_{16\phi}^{kn} \\ Z_{21\phi}^{kn} & Z_{22\phi}^{kn} & \dots & Z_{26\phi}^{kn} \\ \dots & \dots & \dots & \dots \\ Z_{61\phi}^{kn} & Z_{62\phi}^{kn} & \dots & Z_{66\phi}^{kn} \end{bmatrix}.$$

The absorption coefficient is expressed through the vibration velocity and mechanical impedance of the vibration-damping structure:

$$\Pi_\omega = \frac{\mathrm{Re}\,\{[\bar{Z}_{aM}\dot{\bar{q}}]\,\dot{\bar{q}}^{*\prime} + [\bar{Z}_{aM\phi}\dot{\bar{q}}_\phi]\,\dot{\bar{q}}^{*\prime}\}}{\mathrm{Re}\,\{[\bar{Z}_{aM\phi}\dot{\bar{q}}]\,\dot{\bar{q}}_\phi^{*\prime} + [\bar{Z}_{a\phi}\dot{\bar{q}}]\,\dot{\bar{q}}_\phi^{*\prime}\}}.$$

The vibration-damping coefficient is

$$B_\omega = \frac{Re\,[(\bar{Z}_\phi\dot{\bar{q}}_\phi)\,\dot{\bar{q}}_\phi^{*\prime}]}{Re\,\{[\bar{Z}_\phi\,(\bar{Z}_\phi + \bar{Z}_0)^{-1}\,\bar{Q}_0]\,[(\bar{Z}_\phi + \bar{Z}_0)^{-1}\,\bar{Q}_0]^{*\prime}\}},$$

where

$$\dot{\bar{q}}_\phi = (\bar{Z}_\phi + \bar{Z}_{a\phi})^{-1}\,\bar{Z}_{a\phi M}\,[\bar{Z}_0 + \bar{Z}_{aM} + \bar{Z}_{aM\phi}\,(\bar{Z}_\phi + \bar{Z}_{a\phi})^{-1}\,\bar{Z}_{a\phi M}]^{-1}\,\bar{Q}_0.$$

If a vibration-damping system is constructed of n shock absorbers the general equations for N_f and N_a may be reduced to the form

APPROVED FOR RELEASE: 2007/02/08: CIA-RDP82-00850R000200100009-9

APPROVED FOR RELEASE: 2007/02/08: CIA-RDP82-00850R000200100009-9

$$N_{\text{ф}} = -\frac{1}{2}\,\mathrm{Re}\sum_{n=1}^{m}\sum_{i=1}^{6}|\dot{q}^{n}_{i\text{ф}}|^{2}\sum_{j=1}^{6}\left(Z^{nn}_{ij\,\text{амф}}\Pi^{nn}_{iia\dot{q}}K^{n}_{ji} + Z^{nn}_{ij\,\text{Аф}}K^{n}_{ji\,\text{ф}}\right),$$

$$N_{\text{a}} = \frac{1}{2}\,\mathrm{Re}\sum_{n=1}^{m}\sum_{i=1}^{6}|\dot{q}^{n}_{i}|^{2}\sum_{j=1}^{6}\left(Z^{nn}_{ij\,\text{Ам}}K^{n}_{ij} + Z^{nn}_{ij\,\text{Аф}}\frac{K^{n}_{ji\text{ф}}}{\Pi^{nn}_{iia\dot{q}}}\right),$$

where $K^{n}_{ij} = \frac{\dot{q}^{n}_{i}}{\dot{q}^{n}_{i}}$; $K^{n}_{ij\,\text{ф}} = \frac{\dot{q}^{n}_{j\text{ф}}}{\dot{q}^{n}_{i\text{ф}}}$ are coefficients that characterize the relationship of vibrations in different directions at the same point of contact between the shock absorber and machine and between the shock absorber and foundation, respectively;

$$\Pi^{n}_{awi} = -|\Pi^{nn}_{iia\dot{q}}|^{2}\,\frac{Re\sum_{j=1}^{6}|K^{n}_{ij}|^{2}\left(Z^{nn}_{ij\,\text{Ам}}K^{n}_{ji} + Z^{nn}_{ij\,\text{Амф}}\frac{K^{n}_{ij\text{ф}}}{\Pi^{nn}_{iia\dot{q}}}\right)}{Re\sum_{j=1}^{6}|K^{n}_{ij\,\text{ф}}|^{2}\left(Z^{nn}_{ij\,\text{амф}}\Pi^{nn}_{iia\dot{q}}K^{n}_{ij} + Z^{nn}_{ij\text{аф}}K^{n}_{ij\text{ф}}\right)}.$$

When concepts of generalized effective mechanical impedances are used the values N_a, Π_{aw} and B_w in the general case of vibrations of a machine-shock absorber-foundation system are determined, respectively, by the formulas of the first part of this section.

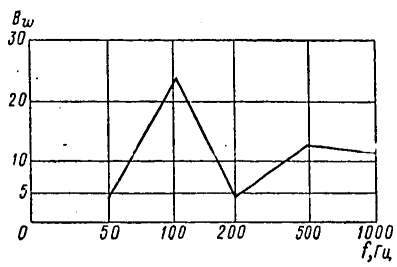

Figure 12.9. Vibration-damping coefficient of shock-absorbing mount of geared turbine unit (in terms of vibration energy). [Гц=Hz]

The calculated frequency characteristics of coefficient B_w of the vibration energy damping of the shock-absorbing mount of a geared turbine unit are presented in Figure 12.9 as an example.

12.4. Marine Shock Absorbers

Requirements on Marine Shock Absorbers. Most of the specific requirements imposed on marine shock absorbers stem from general and special requirements on shock-absorbing mounts for marine machinery. A shock-absorbing mount must satisfy the following conditions:

APPROVED FOR RELEASE: 2007/02/08: CIA-RDP82-00850R000200100009-9

APPROVED FOR RELEASE: 2007/02/08: CIA-RDP82-00850R000200100009-9

serve its basic function, i.e., have the required vibration-damping or antishock characteristics, or both simultaneously, depending on its purpose;

be dependable in operation;

have sufficient static and dynamic (including vibration) strength;

have adequate service life, during which time the characteristics must remain constant or change within tolerable limits;

must not cause an appreciable deterioration of the operating conditions of the vibration-damped machinery or hamper its servicing;

must not create interference in the operation of other installations, machines and systems;

be simple in manufacture, assembly and operation;

have the minimum weight and dimensions;

must not produce excessive amplification of running vibration, transmitted from the foundation of the vibration-damped machinery;

must not permit excessive deviations and displacements of the vibration-damped machinery during rolling and static inclination of the ship;

have a built-in alarm for all cases when the elastic element of the shock absorbers can fail and the vibration-damped machine can separate from its mount;

be resistant to the environment and temperature and to media and temperatures in which the vibration-damped machinery can influence the performance of the mount.

Additional specific requirements may be imposed on individual shock absorbers, depending on their functional purpose. For example, the requirements on flexible couplings, installed in shafts, are the following:

reliable transmission of the maximum torque to the utilizer in consideration of possible overloads and simultaneous prevention of dangerous torsional vibrations;

minimum radial rigidity, so that the elastic reactions in accordance with the existing standards on bending and displacement of the drive line and vibrations of the shock absorbers will be minimum;

tolerable static deformations in all directions, sufficient for possible relative static displacements of coupling shafts that can occur during assembly and operation;

APPROVED FOR RELEASE: 2007/02/08: CIA-RDP82-00850R000200100009-9

APPROVED FOR RELEASE: 2007/02/08: CIA-RDP82-00850R000200100009-9

maximum possible play in the event of radial and axial impact deformation.

Flexible inserts in the pipes connected to vibration-damped marine machinery must meet the following additional requirements:

withstand the hydraulic pressure established by technical documentation during tests for strength and tightness;

permit static deformations in all directions, sufficient to provide static displacements of one point of connection of a flexible insert in relation to another, which can occur under operating conditions;

withstand without a loss of tightness and strength (in the inner cavity, filled with fluid under the working pressure) impact deformation by the amount of play in all directions;

be as thrustless as possible or have little thrust, caused by the internal pressure of the working fluid[1].

Basic Kinds of Shock-Absorbing Structures. The following kinds of marine shock absorbers are used:

rubberized metal bonded shock absorbers, in which the elastic rubber element is vulcanized to the metal parts (hardware) of the shock absorber;

rubberized metal assembled shock absorbers, made up of individual rubberized parts and metal hardware;

rubberized metal bonded assemblies, made up of separate bonded rubberized metal elastic elements and metal hardware;

metal shock absorbers with metallic elastic elements;

shock absorbers with rubber and metal elastic elements that operate together;

shock absorbers with a pneumatic elastic element.

The following are used as flexible inserts in pipes: bonded rubberized metal branch pipes; assembled rubberized metal branch pipes; rubberized cloth and rubberized metal sleeves and hoses; reinforced rubber sleeves; metal bellows; flexible metal hoses; assembled branch pipes with elastic rubberized cord elements.

---

[1]Thrust is defined as the force applied to a pipe from a flexible insert, causing the pipe to shift under the influence of the working pressure created in it.

APPROVED FOR RELEASE: 2007/02/08: CIA-RDP82-00850R000200100009-9

APPROVED FOR RELEASE: 2007/02/08: CIA-RDP82-00850R000200100009-9

The following are used as flexible inserts in shafts: bonded rubberized metal couplings; assembled clutches with rubber or rubberized metal inserts; pneumatic tire clutches; couplings with metal elastic elements; assembled couplings with rubberized cord elastic elements.

Some Shock Absorber Designs and Their Basic Characteristics. The most common shock absorbers in shipbuilding are bonded rubberized metal shock absorbers. An example is the AKSS (insured bonded marine shock absorber) shock absorber, the design of which is illustrated in Figure 12.10. Its metal hardware is designed so that damage to the connection between the rubber and metal will not lead to failure of the shock absorber. The two main varieties of this type of shock absorber are the AKSS-M and AKSS-I [1, 6, 10]. They are manufactured with standard metal hardware. AKSS-I shock absorbers have less static and dynamic (vibration) rigidities than the AKSS-M shock absorbers of the same size.

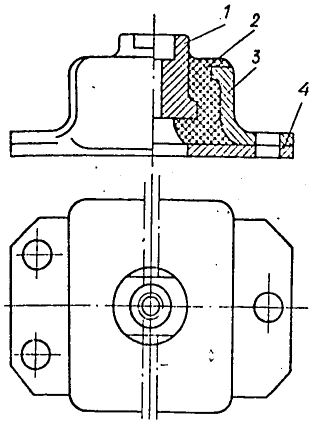

Figure 12.10. AKSS shock absorber: 1 -- bearing bushing; 2 -- rubber; 3 -- bracket; 4 -- base plate.

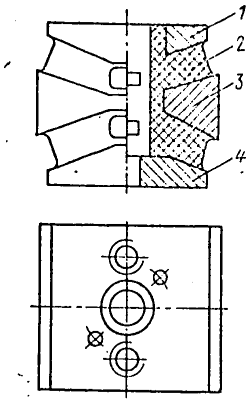

Figure 12.11. APM shock absorber: 1 -- top plate; 2 -- rubber; 3 -- middle piece; 4 -- base plate.

The basic characteristics of the AKSS-M and AKSS-I shock absorbers and certain other types are listed in Table 12.3.

The following types of shock absorbers are used extensively: bonded rubberized metal shock absorbers of the KAS design (marine bonded shock absorber), arch, ADP (double plate), ADPN (double plate with inclined rubber insert), ADPU (double plate with beveled rubber insert), APM (with a middle piece), ESA-100 bonded rubberized metal elements of assembled shock absorbers, etc.

APPROVED FOR RELEASE: 2007/02/08: CIA-RDP82-00850R000200100009-9

APPROVED FOR RELEASE: 2007/02/08: CIA-RDP82-00850R000200100009-9

Table 12.3. Basic Characteristics of Certain Marine Shock Absorbers

1) Тип амортизатора	2) Количество типоразмеров в типоряду	3) Диапазон номинальных статических нагрузок на амортизатор *, даН	4) Величина свободного хода в амортизаторе *, мм	5) Деформация сжатия под номинальной нагрузкой *, мм	6) Частота поступательных свободных колебаний амортизатора под номинальной статической нагрузкой от массы механизма *, Гц
7) АКСС-М	11	9,8—392	7—12	0,6—0,9	27—37
АКСС-И	9	24,5—392	7—12	1,0—1,5	16—22,5
Арочный	6	245—1970	35	7,0—10,7	6—7,5
АПС	4	98—685	18,4—20,5	3,5—9,5	6,5—11,5
АДП	7	490—2160	30—33	0,5—1,0	22,5—30
КАС	5	5,8—68,5	20—25	0,8—1,2	19,5—22
АПМ	12	157—1670	25—35	2,0—5,8	8—15,5
АКМ	4	392—1670	30	4,5—5,1	9—9,5
ЭСА-100	1	98	30	4,5	9,5
АСТ	6	78,5—295	18—25	1,9—5,8	7—14,5
АПР	4	196—491	20—25	8,3—17,1	6,1—7,9
АССП	6	1—78,5	20	0,8—2,0	14—21
А1	13	0,44—11,0	7—10	1,6	13,5— 14
А2	10	0,44—11,0	7—10	1,6	13,5— 14
АКПО	8	0,3—30	25—40	2,5	9,5—10,5

* Характеристика относится к случаю нагружения амортизатора в вертикальном направлении.

Key:
1. Type of shock absorber
2. Number of typical dimensions in typical series
3. Range of rated static loads on shock absorber*, N
4. Play in shock absorber*, mm
5. Compressive deformation under rated load*, mm
6. Frequency of reciprocating free vibrations of shock absorber under rated static load from weight of machine*, Hz

*The characteristic refers to the vertical load on the shock absorber.

7. AKSS-M
AKSS-I
Arch
APS
ADP
KAS
APM
AKM
ESA-100
AST
APR
ASSP
A1
A2
AKPO

The APM type of shock absorber with a middle piece (Figure 12.11) is analogous to some extent to two series-connected dual-plate shock absorbers. However, the shape that is imparted to the middle piece gives it rather large moments of inertia. This promotes the attenuation of bending

APPROVED FOR RELEASE: 2007/02/08: CIA-RDP82-00850R000200100009-9

APPROVED FOR RELEASE: 2007/02/08: CIA-RDP82-00850R000200100009-9

vibrations that pass through the shock absorber. By virtue of the filtering action of the middle piece the vibration-damping properties of the shock absorber are superior to those of a dual-plate shock absorber with the identical vertical stiffness.

An assembled rubberized metal shock absorber of the AST type with a donut-shaped rubber elastic element is illustrated in Figure 12.12.

Effective shock absorbers of the AKM (ship multielement shock absorber) type, assembled from compact elastic elements of the ESA-100 type, are convenient for the design of mounts.

Cylindrical (sleeve) rubberized metal shock absorbers, which may be bonded, assembled-bonded and assembled, are of considerable importance. The elastic rubber cushion of these shock absorbers may also be designed as sectional elements.

Spring-rubber shock absorbers of the APR type (Figure 12.13) and APS rubber pneumatic shock absorbers (Figure 12.14) are other examples of assembled bonded shock absorbers. The APS shock absorber has high vibration-damping properties because an air cushion and rubber, primarily shear-loaded, are used as the elastic elements. In APR shock absorbers the series-connected metal spring and shear-loaded elastic rubber elements provide good vibration-damping properties. During the assembly of a shock absorber initial compressive and shear deformation are imparted to the elastic rubber elements of both inserts by tightening the inside metal rings of the inserts. This increases the fatigue strength of the elastic elements.

Metal shock absorbers with metal elastic elements are also used in shipbuilding. They include the AKPO (ship spring one-turn), AFD (with friction damping) and AD (damped equalized frequency). Although these shock absorbers are metal devices, the set of each one of them includes a rubber piece, which acts as a buffer (the AKPO and AFD types) and parts of a damping system (the AD type).

All metal shock absorbers of the Vibrashok type with an elastic element made of pressed wire structures, are also used.

The basic characteristics of certain flexible inserts for ship plumbing are presented in Table 12.4.

PRMS and PRMS-T (Figure 12.15) are rubberized metal fittings of bonded design. A set of fittings includes an elastic stop, intended for limiting the deformation of axial extension due to the influence of hydraulic pressure in a plumbing system. The PRMS and PRMS-T fittings are acoustic insulators and protective (antiimpact) flexible inserts; they have compliance in all directions.

APPROVED FOR RELEASE: 2007/02/08: CIA-RDP82-00850R000200100009-9

APPROVED FOR RELEASE: 2007/02/08: CIA-RDP82-00850R000200100009-9

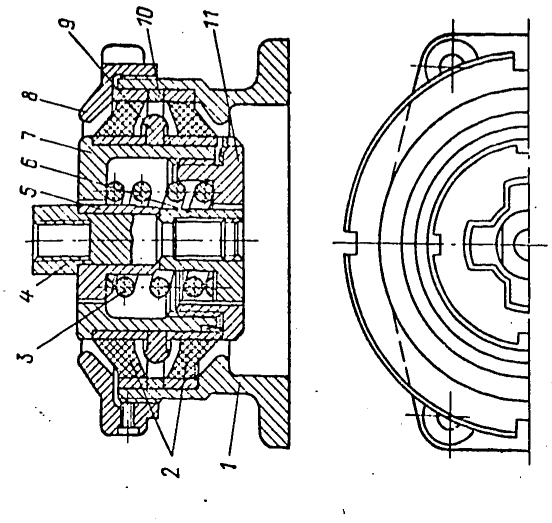

Figure 12.13. APR shock absorber: 1 -- case; 2 -- rubberized metal inserts; 3 -- spring; 4 -- core; 5 -- top bushing; 6 -- bottom bushing; 7 -- top cap; 8 -- adjustment nut; 9 -- stop; 10 -- ring; 11 -- bottom plate.

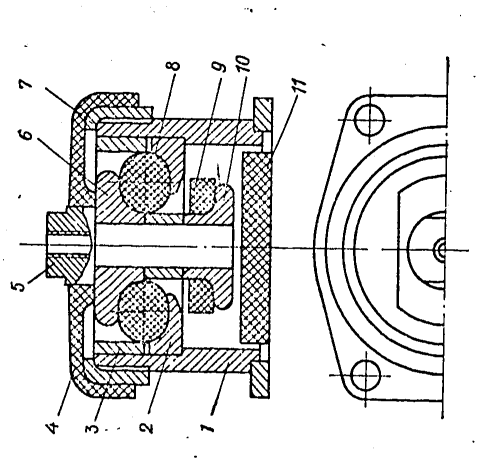

Figure 12.12. AST shock absorber: 1 -- case; 2 -- bottom bearing ring; 3 -- top bearing ring; 4 -- rubber cup; 5 -- rod; 6 -- top bushing; 7 -- nut; 8 -- rubber donut; 9 -- top rubber buffer; 10 -- bottom bushing; 11 -- bottom rubber buffer.

APPROVED FOR RELEASE: 2007/02/08: CIA-RDP82-00850R000200100009-9

APPROVED FOR RELEASE: 2007/02/08: CIA-RDP82-00850R000200100009-9

Table 12.4. Basic Characteristics of Certain Flexible Inserts for Ship Plumbing

Type of flexible insert	Conventional clearance D_c, mm	Conventional pressure p_c, kPa	Working pressure p_w, kPa	Fluid temperature, K	Transported medium
PRMS	80-150	2,450	2,450	For air 268-323, for other media 268-343	Solar and machine oil, petroleum, fuel, sea and fresh water, distillate, air
PRMS-T	80-150 80-150	2,450 2,450	2,450 1,570	271-308 278-358	Sea and fresh water, distillate
PRMK	80-150 150-250	588 588	588 From 95% vacuum	271-358	Turbine oil, sea and fresh water, distillate
KSG KSRM KSNP	70-400 100-400 800-1160	245 980 98	167 980 From 98% vacuum	773 353 573	Gases, air Sea water Steam
GMSh	20-50	6,270	From vacuum up to 6,270	423	Fresh water, oil, petroleum products, condensate, air and freon
RA	10 10-32 50-100	19,600 9,800 3,920	19,600 4,900 3,920	For sea water 268-318 For fresh water 271-318, for other media up to 363	Sea and fresh water, fuel, oil

In PRMK bonded rubberized metal fittings the elastic element and seal are rubber rings of rectangular cross section. The rubber rings are inserted between the flanges and a metal ring, in which there are special grooves for them, and they are assembled with steel tie bolts.

The PRMK fittings are simply a protective flexible insert and have compliance in the transverse direction. In the direction of axial compression they have little compliance and they do not function in the direction of axial extension. Displacements are compensated in the axial direction by virtue of the compliance of the pipe or with the aid of a second fitting, installed at an angle of 90° to the first.

Durite fittings, which are rubber sleeves and hoses, reinforced with cloth or metal wire, are used for vibration-damping fresh and sea water, fuel and

APPROVED FOR RELEASE: 2007/02/08: CIA-RDP82-00850R000200100009-9

APPROVED FOR RELEASE: 2007/02/08: CIA-RDP82-00850R000200100009-9

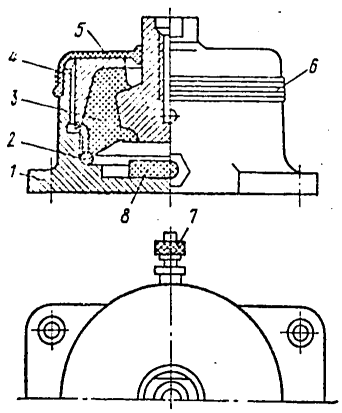

Figure 12.14. APS shock absorber: 1 -- case; 2 -- rubber gasket; 3 -- bonded rubberized metal insert; 4 -- cap; 5 -- cup; 6 -- steel wire; 7 -- fitting; 8 -- rubber cushion.

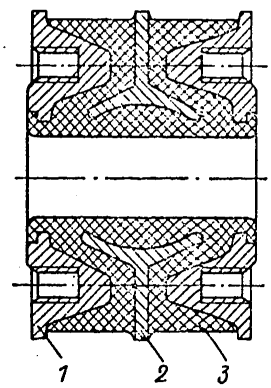

Figure 12.15. PRMT-T fitting (without stop): 1 -- connecting flange; 2 -- middle ring; 3 -- rubber cushion.

oil pipes. Durite hoses and couplings are manufactured with an inside diameter of from 1 to 90 mm for a working pressure of up to 490 kPa. Rubberized cloth pressure sleeves, designed for a pressure of up to 980 kPa, and manufactured with an inside diameter of from 3 to 150 mm, are used in fresh water lines. Sleeves that operate to a pressure of up to 9,800 kPa are used in high-pressure hydraulic lines. The ends of the durite sleeves have special clamps, and the ends of the sections of pipe to be connected have annular ridges.

Reinforced rubberized sleeves with annular connecting hardware in the form of flanges and end pieces, are also used. An example is the type RA reinforced sleeve.

Laminated metal bellows compensators, bulkhead gaskets (USP) and flexible metal hoses GMSh (Figure 12.16) also find extensive application. Flexible inserts of these types have high temperature resistance and are also resistant to various aggressive media. The design of a low-pressure bellows compensator of the KSN type, intended for fresh water and oil systems, is illustrated in Figure 12.17. The high temperature resistance of bellows compensators enables them to be used in exhaust pipes and steam lines, where rubber structures cannot be used.

Bonded rubberized metal couplings, in which the rubber piece is vulcanized to metal flanges, are used extensively for insulating the shafting of relatively small marine machinery. Bonded rubberized metal couplings (Figure 12.18) of the flange type RMSF and of the annular type RMSK

APPROVED FOR RELEASE: 2007/02/08: CIA-RDP82-00850R000200100009-9

APPROVED FOR RELEASE: 2007/02/08: CIA-RDP82-00850R000200100009-9

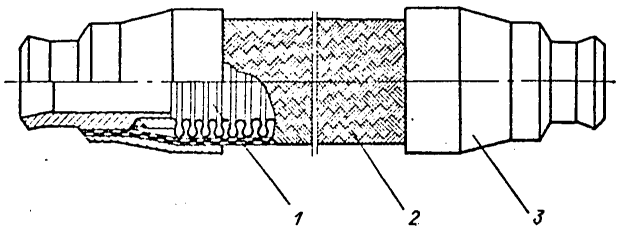

Figure 12.16. GMSh flexible metal hose: 1 -- bellows shell; 2 -- metal braid; 3 -- connecting hardware.

[1, 6, 10] are used most extensively. The standard series of RMSF couplings consists of eight typical dimensions, designed for transmitting nominal torque from 4.9 to 1,470 N·m, and the RMSK series of couplings has four typical sizes for transmitting torque from 98.1 to 1,470 N·m.

Bonded rubberized metal couplings are capable of withstanding great stresses without damage. In some designs rubber inserts, which absorb compression, are installed to prevent the elastic element from separating from the flanges under overloads. An example is the Metalastik coupling.

Assembled couplings with rubber or rubberized metal inserts are often used in main engine shafting. One possible design of such a coupling is shown in Figure 12.19. In this coupling the cylindrical rubber elements are installed parallel to the axis of the coupling; there are designs in which these elements are placed in the radial direction. The basic deficiency of these couplings is their low radial deformability.

Wooden ratchet couplings with elastic rubber elements of rectangular cross section, installed without precompression between the teeth of the wheel and the rim of the clutch, are extremely simple in design. Their deficiency is the fact that only one-half of the elastic elements are used for transmitting torque. The other half receives load when the drive wheel of the clutch changes direction.

Pneumatic tire clutches, which usually include a release mechanism [1, 10], have high vibration-damping effectiveness. The problem with these clutches is that they get out of balance, so that when the shaft rotates they become sources of additional perturbing forces.

Perifleks couplings with an elastic element in the form of a one-piece rubberized cord rim or annular cup, can be used for transmitting torque of up to 34,000 N·m and more [1].

12.5. Calculation of Shock-Absorbing Mounts of Marine Machinery

During the design of a shock-absorbing mount its basic qualities must be evaluated, including effectiveness and capacity for normal operation of

APPROVED FOR RELEASE: 2007/02/08: CIA-RDP82-00850R000200100009-9

APPROVED FOR RELEASE: 2007/02/08: CIA-RDP82-00850R000200100009-9

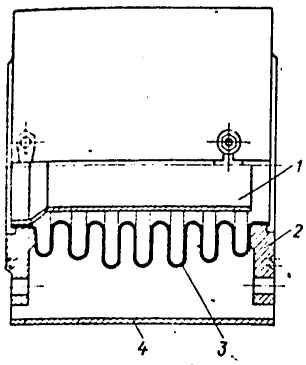

Figure 12.17. KSN low-pressure bellows compensator: 1 -- guide; 2 -- connecting flange; 3 -- bellows shell; 4 -- protective case.

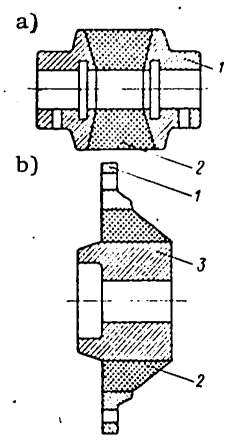

Figure 12.18. Bonded rubberized metal couplings of RMSF (a) and RMSK (b) types: 1 -- flange; 2 -- rubber pad; 3 -- hub.

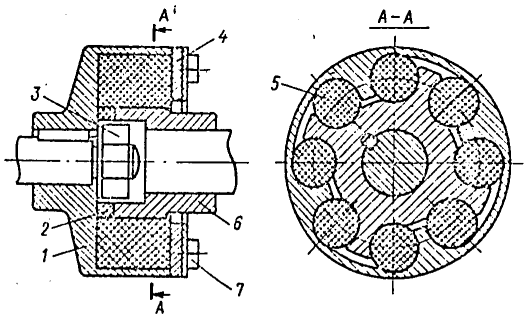

Figure 12.19. Assembled rubberized metal coupling: 1 -- driving half; 2 -- rubber ring; 3 -- lock nut; 4 -- cap; 5 -- cylindrical rubber insert; 6 -- driven half; 7 -- bolt.

the mount itself and of the machinery installed upon it. Calculations, done in successive planning stages, help to carry out such an analysis. These calculations are most often done for purposes of checking; corrections can be incorporated in a design, depending on the results of the calculations.

APPROVED FOR RELEASE: 2007/02/08: CIA-RDP82-00850R000200100009-9

APPROVED FOR RELEASE: 2007/02/08: CIA-RDP82-00850R000200100009-9

In order to do the calculations it is necessary to have data on the rigidity of shock absorbers. The static and dynamic rigidities of shock absorbers, and consequently of shock-absorbing mounts, can vary considerably. This is particularly true of shock absorber structures with rubber elements. Rigidity is also dependent to a great extent on temperature, which is a characteristic feature of rubber products.

The dynamic rigidity of a shock absorber in the vibration mode is called the vibration rigidity. For comparatively low amplitude deformation, in the frequency range corresponding to the free vibrations of a vibration-damped machine on shock absorbers, and also to the running vibration frequencies of the ship, the vibration rigidity of structures with rubber elastic elements usually can be assumed to be approximately constant.

The static rigidity characteristics of shock absorbers are determined from force-deformation diagrams, recorded during the deformation of specimens at rates of from one to several millimeters per minute. The rigidities corresponding to this mode of deformation can be only conditionally referred to as static. They are larger than the values that can be achieved when deformation is measured a few hours or 1-2 days after the application of a constant load. During that period the deformation becomes virtually completely stabilized if the load does not exceed the tolerable limit (at a given temperature), after which the rubber begins to creep and break up. The static rigidities of shock absorbers, determined by the method indicated above, with the corresponding correction factor for shrinkage, can be used for analyzing deformations caused by long-term constant load.

Short-term dynamic deformations and loads, which are safe for rubber elements of shock absorbers, can be many times greater than the tolerable static deformations. Under the influence of sharp impacts, which deform a shock-absorbing structure at high rates, the so-called impact rigidity, or dynamic impact rigidity, is manifested. It is usually greater than the above-mentioned vibration rigidity, determined for the relatively low-frequency range.

Static Calculations. The usual static calculations are the following:

determination of the deformations of a shock-absorbing mount and of loads borne by individual shock absorbers from weight of vibration-damped machine with ship in upright position;

determination of deflections of vibration-damped machine from equilibrium in list, trim and roll; determination of related stresses on shock-absorbing structures and strength testing of the latter;

determination of deformations of shock-absorbing mounts and individual shock-absorbing structures as a result of application of static working

APPROVED FOR RELEASE: 2007/02/08: CIA-RDP82-00850R000200100009-9

APPROVED FOR RELEASE: 2007/02/08: CIA-RDP82-00850R000200100009-9

loads (for example, forces of thrust in pliant elements of pipes; tilting moment from drive shaft, connected to vibration-damped engine or reducer).

The deflection of a vibration-damped machine from its usual equilibrium position on a ship as a result of roll and trim is determined in the following way. Coordinate system Oxyz, rigidly connected to the ship, is so selected that in usual equilibrium the main central axes of inertia of the vibration-damped machine coincide with the coordinate axes. Its center of gravity coincides with the coordinate origin. The Ox axis of the coordinate system is horizontal and is drawn to the bow; the Oy axis is transverse; the Oz axis is vertical from bottom to top. To positive list angle ϕ_{li} corresponds list to the port, to positive trim angle ψ_{tr} corresponds trim to the bow (Figure 12.20).

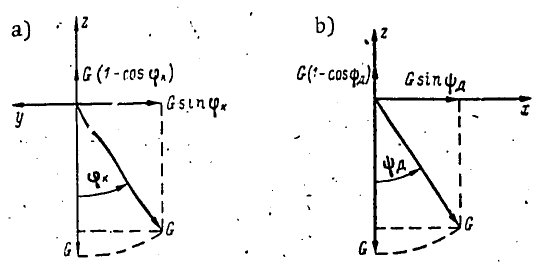

Figure 12.20. Determination of forces caused by shifting of vibration-damped machinery relative to bearing structures: a -- in list; b -- in trim. [н=li; д=tr]

A vibration-damped machine with weight G is displaced by forces of gravity

[н=li]
$$\left.\begin{aligned} F_y &= -G\sin\varphi_к; \\ F_z &= G(1-\cos\varphi_к), \end{aligned}\right\} \qquad (12.5.1)$$

applied at its center and corresponding to list angle ϕ_{li}, and by forces

[д=tr]
$$\left.\begin{aligned} F_x &= G\sin\psi_д; \\ F_z &= G(1-\cos\psi_д), \end{aligned}\right\} \qquad (12.5.2)$$

which occur at trim angle ψ_{tr}.

With a matrix of the compliances of a shock-absorbing mount, tied to the above-described Oxyz coordinate system, it is possible to immediately convert to the calculation of reciprocating and rotation displacements of a vibration-damped machine, caused by forces (12.5.1) or (12.5.2), and expressed in the same coordinate system. The compliance matrix or rigidity matrix, tied to some coordinate system, and which is usually quite simple

APPROVED FOR RELEASE: 2007/02/08: CIA-RDP82-00850R000200100009-9

APPROVED FOR RELEASE: 2007/02/08: CIA-RDP82-00850R000200100009-9

in structure (with a rather large number of zero elements), is often available. In such a case it is helpful to reduce forces (12.5.1) and (12.5.2) to a coordinate system that provides a simple compliance or rigidity matrix of a vibration-damping mount.

The displacements of a vibration-damped machine and the deformations of a shock-absorbing mount under the influence of any static forces should be analyzed in the same way.

The partial center of rigidity of a vibration-damped machine can be aligned with the center of gravity by tilting the rigidity axes of the shock absorbers by the appropriate angle [1, 6, 10]. This not only eliminates rotary displacements of the vibration-damped machine relative to the listing ship, but it also reduces its transverse deviation. When selecting the angle of inclination it is important to consider also the change of load on the shock absorber.

Dynamic Calculations. The vibration rigidity of a shock-absorbing mount, calculated on the basis of the vibration rigidities of the shock absorbers, is used for calculating the free and induced vibrations of a vibration-damped machine on shock absorbers. If the same relationship between the static and vibration rigidities is valid for all the shock absorbers, all the vibration rigidities of the shock-absorbing mount can be found by multiplying its corresponding static rigidities by the same coefficient.

The free vibration frequencies of a vibration-damped machine on the shock absorber should be as low as possible, since this affords better vibration damping. At the same time they should be as far away as possible from the frequencies of disturbing forces, capable of causing strong vibration in a vibration-damped machine. The frequency range that is devoid of such forces is sometimes rather narrow. When the frequencies of free vibrations of a vibration-damped machine on shock absorbers are concentrated in that range it must be considered that the narrow spectrum of the natural frequencies may be the cause of stronger vibrations when the power plant and screws pass through resonance or operate in certain modes. Methods of calculating frequencies and the corresponding formulas are presented in the literature [1, 6, 10].

Calculation of induced vibrations in a rigidly mounted machine on shock absorbers which along with the machine comprise a linear vibrating system, involves in the general case a separate examination of the problem for each principal coordinate and subsequent adding of the solutions obtained, expressed in the same generalized coordinates.

12.6. Vibration Damping of Nonbearing Connections of Machinery

Considerable acoustic energy, often exceeding the energy transmitted to the foundation through shock absorbers, can be transmitted from a machine

APPROVED FOR RELEASE: 2007/02/08: CIA-RDP82-00850R000200100009-9

APPROVED FOR RELEASE: 2007/02/08: CIA-RDP82-00850R000200100009-9

through nonbearing connections. Moreover, plumbing controls and hardware can be an additional source of strong vibrations in a wide frequency range.

If a shock-absorbing mount is used for the purpose of vibration-damping the nonbearing connections, fastened to the vibration-damped machine should have the corresponding qualities.

The main rules on the design execution of vibration-damping shock absorbers for nonbearing connections are the following:

nonbearing connections should be vibration-damped through their entire length, no matter how far they extend from the place where the vibration-damped mechanism is installed;

structural elements of vibration dampers with substantial damping should be installed in places where elements of nonbearing connections are directly connected to bearing ship structures;

the minimum number of fasteners should be used;

the input mechanical impedance of structures where nonbearing connections are fastened to bearing ship structures should be compatible with the vibration-damping capabilities of the shock absorbers of nonbearing connections;

elements of vibration-damping shock absorbers of nonbearing connections should protect the nonbearing connections from external static and dynamic loads, related to ship operating conditions. These loads can be produced, for example, by forces of inertia that occur due to running vibration of the hull, rolling, collisions during sailing in ice, etc;

elements of shock absorbers of nonbearing connections should permit free movement of the vibration-damped machinery without violating the basic vibration-damping plan and without changing its basic characteristics.

The conditions of vibration damping require the installation in shafting of flexible vibration-damping couplings and damping links at shaft bearings. These links are especially important in cases when the bearing is between the vibration-damped mechanism and the vibration-damping coupling or when it is a source of vibration (for example, roller bearings). In this connection it is desirable to design the shafting such that the vibration-damping coupling will be between the vibration-damped machine and the nearest bearing.

In cases when a connection of shafting to a machine does not have the required radial compliance due to the use of a vibration-damping coupling with great rigidity, universal joints, torsion shafts or two couplings, separated by an intermediate shaft, may be installed with the shaft in series-connected fashion [1, 6].

APPROVED FOR RELEASE: 2007/02/08: CIA-RDP82-00850R000200100009-9

APPROVED FOR RELEASE: 2007/02/08: CIA-RDP82-00850R000200100009-9

Vibration-damping structures used for shock absorption of pipes include flexible branches, reinforced sleeves and hoses for water, fuel and oil lines, branches for steam pipes, ventilation ducts and exhaust pipes, and also shock-absorbing pipe hangers (see §12.4). Hangers are usually assembled or bonded rubberized metal structures, equipped with a strap for fastening the pipe (Figure 12.21). Sometimes hangers have an extra elastic element next to the rubber element in the form of a leaf or coil spring. Shock absorbers with transition bars and straps are suitable for use as vibration-damping pipe hangers for liquids and steam.

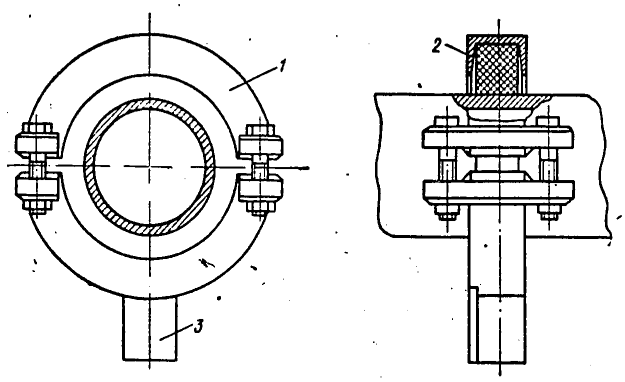

Figure 12.21. Type APTK shock-absorbing ring pipe hanger:
1 -- band; 2 -- rubber ring; 3 -- tail piece.

Where cables are connected to a vibration-damped machine they are usually bent in the form of a spiral or loop, which gives it compliance, reduces the transmission of vibrations through it and prevents damage due to vibrations and shaking [1, 6, 10].

The following requirements must be taken into consideration when flexible inserts are installed in plumbing:

if the flexible inserts are subjected to forces of axial thrust it is recommended, to reduce the influence of these forces on the shock-absorbing mount, that the inserts be so installed that their axis is aimed at the center of rigidity of the shock-absorbing mount, and when two or several inserts are installed in pipes of the same machine an attempt should be made to provide complete or partial compensation of thrust forces that occur in them;

it is recommended that pipes be connected to vibration-damped machinery at the points with the least relative displacements (static and dynamic) or to reduce the deformations of flexible inserts and pipes;

APPROVED FOR RELEASE: 2007/02/08: CIA-RDP82-00850R000200100009-9

APPROVED FOR RELEASE: 2007/02/08: CIA-RDP82-00850R000200100009-9

the clearance between a pipe, connected to a vibration-damped machine, and objects and structures surrounding it should be selected in consideration of the play of the shock-absorbing mount in the corresponding direction.

It is usually recommended that the total rigidity of all nonbearing connections (shafts, pipes, cables, etc.), connected to a vibration-damped machine, be minimum in each direction and not exceed: for main machines 50% of the total rigidity of the shock absorbers of the vibration-damping mount; for auxiliary machinery, instruments and apparatus 20% of the total rigidity of the shock absorbers of the vibration-damping mount.

The total rigidity of pipes and cables (the rigidity of flexible inserts in shafting is ignored), connected to a vibration-damped primary machine, should be minimal in each direction and should not exceed 20% of the rigidity of the shock absorbers of the vibration-damping mount.

Rubber reinforced sleeves and hoses, rubberized cord thrustless branches and couplings with high compliance and play, should be used as flexible inserts in nonbearing connections to machinery, installed on low-frequency shock-absorbing mounts.

During the planning of plumbing noise produced by media flowing through the pipes should be minimized. In particular, the tolerable velocity of the medium must be determined in consideration of the greatest amount of reduction of plumbing noise; sudden changes of flow direction should be avoided by using expanding and converging adapters; round elbows should be used instead of square elbows; the optimum bending radius for reducing noise is 3-5 pipe diameters; quiet valves and other control hardware should be used when possible; multistage flow throttling systems should be used when necessary, and pressure pulsation dampers should be used when possible.

The following requirements must be taken into account when selecting the configuration of pipes, design and location of hardware:

the effect of forces from the working fluid pressure in pipes connected to a machine on the shock-absorbing mount can be reduced by properly positioning and aiming the points of connection to the machine;

the proper grouping of plumbing and control hardware facilitates its installation on a common shock-absorbing mount.

The fundamental vibration frequencies of a system are determined by the technical delivery documentation of a machine and by vibration and acoustic test data. The entire range of velocities must be taken into consideration for machinery, the moving parts of which have different travel velocities.

The location of flexible inserts and pipe hangers and their orientation in space are determined in consideration of the following requirements:

APPROVED FOR RELEASE: 2007/02/08: CIA-RDP82-00850R000200100009-9

APPROVED FOR RELEASE: 2007/02/08: CIA-RDP82-00850R000200100009-9

the influence of thrust forces of flexible inserts on the vibration-damped mechanism should be reduced by using primarily thrustless structures and by installing them in the proper places;

two flexible inserts should be installed in a pipe: one near a machine (not more than 5 pipe diameters from the flange of the machine), and the other right next to bearing hull structures (bulkheads, decks, bottom decking and hull);

special vibration-damping fasteners should be used for grouped plumbing and control hardware and for heavy hardware and systems;

vibration-damping hangers should be oriented such that the displacements of plumbing due to impact loads will be minimal in all directions;

vibration-damping hangers should be fastened to rigid hull structures (deck girders and beams, interconnected bulkheads, walls and superstructures, and also to ribs and stringers of the ship's hull);

access should be provided to flexible inserts and vibration-damping hangers for inspection and replacement when necessary.

When selecting elastic elements it is important to remember that they must meet the following requirements: they must be loaded in consideration of the forces produced by thermal expansion of plumbing and by bending of hull structures; they must be insulated from low-level vibration frequencies; the displacement of plumbing due to dynamic forces must be minimized.

To achieve the required vibration damping it is desirable that the ratio of the lower vibration frequencies in a system to the frequency of free vibrations of the elastic element of a hanger under the rated load be not less than three or four.

When laying out the locations where pipe hangers are fastened to bearing structures try to make sure that the ratio of the rigidity of the bearing structures where hangers are fastened to them to the vibration rigidity of the elastic element of the hanger be 100 and higher (ratios smaller than 20 are not acceptable).

Ways of Improving Vibration-Damping Effectiveness of Pipe Hangers. When inspections reveal inadequate vibration-damping effectiveness of hangers on a ship an effort must be made to alter the bearing structures in such a way as to reduce vibrations to tolerable levels in places where hangers are fastened to them. To do this it is necessary to have the right information about the character of changes of the input mechanical impedance of the bearing structure due to structural changes of it. The increment of vibration-damping provided by a rubber-spring vibration-damping hanger as a result of various structural changes of the bearing structure, is given in Figure 12.22.

APPROVED FOR RELEASE: 2007/02/08: CIA-RDP82-00850R000200100009-9

APPROVED FOR RELEASE: 2007/02/08: CIA-RDP82-00850R000200100009-9

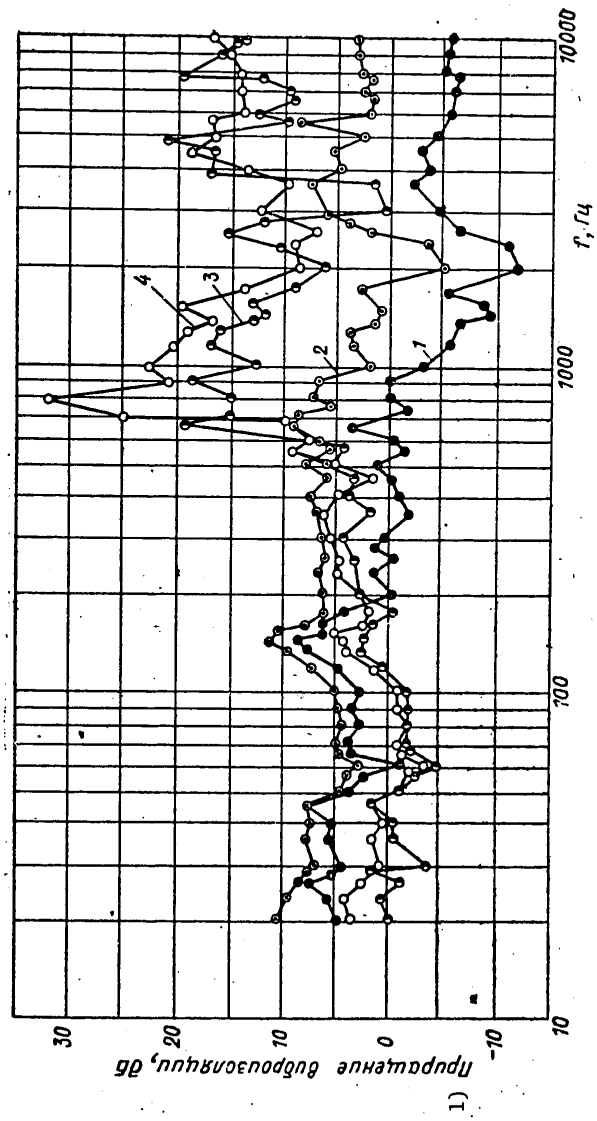

Figure 12.22. Increment of vibration damping provided by shock-absorbing hanger as a result of fastening to bearing structure: 1 -- reinforcing rib; 2 -- reinforcing rib and concentrated mass; 3 -- concentrated mass; 4 -- concentrated mass, additionally fastened by arc-welding rivets. [Гц=Hz]
Key: 1. Vibration damping increment, dB

APPROVED FOR RELEASE: 2007/02/08: CIA-RDP82-00850R000200100009-9

APPROVED FOR RELEASE: 2007/02/08: CIA-RDP82-00850R000200100009-9

If the transmission of vibrations through shock-absorbing hangers must be reduced on relatively low acoustic frequencies the most effective way is to fasten the bearing plate with a reinforcing rib, so that it will be rigidly connected between the space framing. It must be remembered in this case that the transmission of vibrations to a bearing structure can increase considerably in the high-frequency range.

By installing concentrated masses in the form of heavy plates where shock-absorbing hangers are fastened it is possible to greatly increase their vibration-damping effectiveness on frequencies higher than the lowest free vibration frequency of the bearing structure.

The installation of concentrated mass and simultaneous fastening of the bearing structure with a reinforcing rib reduce the transmission of vibrations through a vibration-damping hanger in a wide frequency range. The positive increment of vibration damping of a hanger on high frequencies is a little smaller than in the case when just one concentrated mass is installed, due to the negative effect of the reinforcing rib.

12.7. Measurement of Vibration Damping of Shock-Absorbing Mounts

The vibration-damping properties of shock-absorbing mounts are determined experimentally by measuring vibration levels, dynamic forces and vibration powers.

Vibration sensors for measurements should be installed on the heads of bolts, which fasten vibration-damping elements to a machine or foundation (or to a pipe).

The vibration gradient is usually measured on each shock absorber and branch pipe, both in terms of the total vibration level in the low and medium frequency ranges, and on individual frequencies in in individual frequency bands.

The first measurement establishes the "condition" of a shock absorber (for example, if the rubber pad is broken the total level gradient, according to experience, approaches zero). The second measurement provides a detailed evaluation of the effectiveness of a shock-absorbing mount.

The components of vibrations in three mutually perpendicular directions are measured. The spectra of the gradient are plotted for each of the directions of vibration.

The information obtained is processed by one of two methods. One: the vibration "gradient field" on a shock-absorbing mount is plotted and the vibration gradients on all shock absorbers are indicated on the curves (Figure 12.23). Two: the difference of the levels of the mean square vibrations around the periphery of a vibration-damping mount is determined

APPROVED FOR RELEASE: 2007/02/08: CIA-RDP82-00850R000200100009-9

APPROVED FOR RELEASE: 2007/02/08: CIA-RDP82-00850R000200100009-9

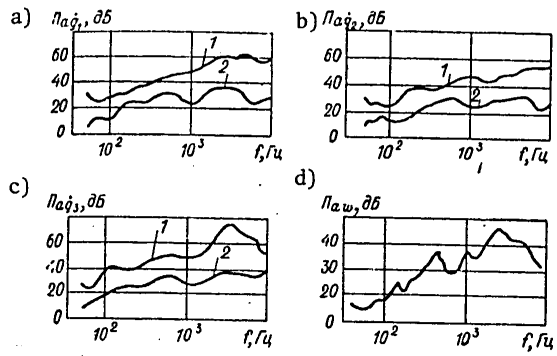

Figure 12.23. Frequency characteristics of gradients on shock-absorbing mount of diesel engine: a -- gradient $\Pi_{a\dot{q}_1}$ of vibration on x axis; b -- gradient $\Pi_{a\dot{q}_2}$ of vibration on y axis; c -- gradient $\Pi_{a\dot{q}_3}$ of vibration on z axis (1, 2 -- maximum and minimum gradients); d -- gradient of vibration energy. [дБ=dB; Гц=Hz]

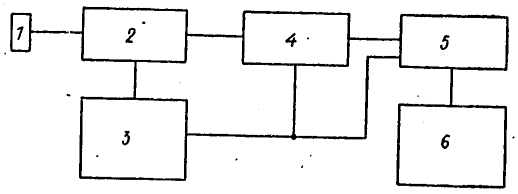

Figure 12.24. Schematic diagram of instrument for measuring mean square (around the perimeter of a mount) vibration level: 1 -- vibration receiver with preamplifier; 2 -- heterodyne filter; 3 -- control generator; 4 -- level recorder; 5 -- digital coding system; 6 -- perforator.

on the flange of the machine and on the flange of the foundation for each direction of vibration. This method has physical meaning in relation to the determination of the vibration-damping properties of a mount as a whole, since the mean square vibration levels are proportional to the flux of vibration energy through the analyzed cross section of the shock-absorbing mount.

The frequency characteristic of the energy gradients on a shock-absorbing mount is given in Figure 12.23.

APPROVED FOR RELEASE: 2007/02/08: CIA-RDP82-00850R000200100009-9

APPROVED FOR RELEASE: 2007/02/08: CIA-RDP82-00850R000200100009-9

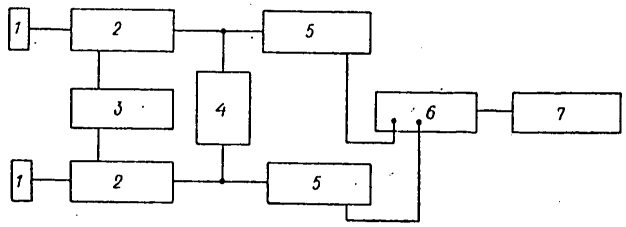

Figure 12.25. Schematic diagram of instrument for measuring combined vibration gradient: 1 -- vibration receiver with preamplifier; 2 -- filters; 3 -- control generator; 4 -- oscillograph; 5, 7 -- level recorders; 6 -- correlator.

During step-by-step measurement of vibrations at different points the mean square vibration at the different points is determined with the aid of an instrument, a block diagram of which is illustrated in Figure 12.24. Simpler meters, assembled from standard instruments, may be used. Foundation vibrations thus measured, with and without a shock-absorbing mount, are used for determining the vibration damping of a mount in terms of the kinematic parameter [5, 9].

The energy parameters for analyzing the vibration properties of a shock absorber can be determined, as was mentioned above, by direct measurement of radiated power [11]. The powers radiated through the machine-shock absorber and shock absorber-foundation cross sections can also be determined on the basis of measurement data on the combined vibration gradients. The combined gradients are measured with an instrument, a schematic diagram of which is shown in Figure 12.25.

BIBLIOGRAPHY

1. Belyakovskiy, N. G., "Konstruktivnaya Amortizatsiya Mekhanizmov, Priborov i Apparatury na Sudakh" [Structural Vibration Damping of Machines, Instruments and Equipment on Ships], Leningrad, Sudostroyeniye, 1965.

2. Brillyuen, L. and M. Parody, "Rasprostraneniye Voln v Periodicheskikh Strukturakh" [Wave Propagation in Periodic Structures], Moscow, IL, 1959.

3. Yefimov, N. V., "Kvadratichnyye Formy i Matritsy" [Quadratic Forms and Matrices], Moscow, Nauka, 1967.

4. Ivovich, V. A., "Perekhodnyye Matritsy v Dinamike Uprugikh Sistem" [Conversion Matrices in Dynamics of Elastic Systems], Moscow, Mashinostroyeniye, 1969.

APPROVED FOR RELEASE: 2007/02/08: CIA-RDP82-00850R000200100009-9

APPROVED FOR RELEASE: 2007/02/08: CIA-RDP82-00850R000200100009-9

5. Il'kov, V. K. and V. I. Popkov, "Vibrations of Complex Active Mechanical Systems," "Akusticheskaya Dinamika Mashin i Konstruktsiy" [Acoustic Dynamics of Machines and Structures], Moscow, Nauka, 1973.

6. Klyukin, I. I., "Bor'ba s Shumom i Zvukovoy Vibratsiyey na Sudakh" [Control of Noise and Acoustic Vibration on Ships], Leningrad, Sudostroyeniye, 1971.

7. Klyukin, I. I., "Transmission and Insulation of Longitudinal Waves in Chain Structures of Inertial and Elastically Dissipative Elements," TRUDY LKI [Proceedings of Leningrad Shipbuilding Institute], 1972, No 77, pp 3-9.

8. Klyukin, I. I., "Propagation and Insulation of Vibrations in Branched Mechanical Structures with Open and Closed Branch Ends," TRUDY LKI, 1975, No 97, pp 3-9.

9. Klyukin, I. I., "On Criteria of Vibration Damping and Relations between Them," AKUSTICHESKIY ZHURNAL AN SSSR [Acoustics Journal of the USSR Academy of Sciences], 1975, No 5, pp 747-750.

10. Naydenko, O. K. and P. P. Petrov, "Amortizatsiya Sudovykh Dvigateley i Mekhanizmov" [Vibration Damping of Ship Engines and Machinery], Leningrad, Sudpromgiz, 1962.

11. Popkov, V. I., "Vibroakusticheskaya Diagnostika i Umen'sheniye Vibroaktivnosti Sudovykh Mekhanizmov" [Vibroacoustic Diagnostics and Reduction of Vibration Activity of Marine Machinery], Leningrad, Sudostroyeniye, 1974.

APPROVED FOR RELEASE: 2007/02/08: CIA-RDP82-00850R000200100009-9

APPROVED FOR RELEASE: 2007/02/08: CIA-RDP82-00850R000200100009-9

CHAPTER 13. VIBRATION DAMPING OF SHIP HULL STRUCTURES

13.1. Basic Principles and Laws of Vibration Damping for Bending Waves

The ability of barriers to insulate hull structures from propagating elastic waves of vibration energy from vibration sources is defined as vibration damping.

Vibration damping VD, in dB, is the attenuation of the energy of vibrations of a structure after insulating barriers are installed between it and vibration sources:

[ВИ=VD]

$$\text{ВИ} = 10 \lg \langle \dot{w}_{21} \rangle - 10 \lg \langle w_{22} \rangle, \qquad (13.1.1)$$

where w_{21}, w_{22} are the vibration energy densities of the structure behind a barrier before and after its installation.

Both additional structural elements (vibration-impeding masses VIM, elastic pads, etc.), and all inhomogeneities of the shell of a hull structure (stiffening ribs, changes of inertial and rigidity parameters, etc.) are defined as barriers.

Vibration amplitude transmission coefficient T through a barrier on an infinite plate (rod) is used extensively for analyzing the vibration-damping capacity of barriers:

$$\text{ВИ} = -10 \lg \left[|T|^2 \frac{m_2}{m_1} \right], \qquad (13.1.2)$$

where m_1, m_2 are the masses of a plate (rod) before and after a barrier.

In the case of a diffuse field of incident waves energy techniques are utilized, and vibration damping is given by the formula

$$\text{ВИ} = -10 \lg \langle T^2 \rangle_0. \qquad (13.1.3)$$

where $\langle T^2 \rangle_\theta$ is the average vibration energy transmission coefficient in terms of incidence angle.

APPROVED FOR RELEASE: 2007/02/08: CIA-RDP82-00850R000200100009-9

APPROVED FOR RELEASE: 2007/02/08: CIA-RDP82-00850R000200100009-9

Vibration level gradients ΔL on a barrier are usually found as a direct result of measurements:

$$\Delta L = 10 \lg \langle w_{12} \rangle - 10 \lg \langle w_{22} \rangle, \qquad (13.1.4)$$

These gradients may differ considerably from the attainable vibration damping, depending on the resonance properties and vibration absorption in plates, divided by a barrier.

Vibration damping as a physical process is the result of the reflection of elastic vibration waves, propagating in a hull structure, from an inhomogeneity (barrier). The expressions for reflection coefficient R and transmission coefficient T of traveling bending waves on a plate with an arbitrary symmetric barrier are

$$R = [1 - iB]^{-1} - [1 - iA]^{-1};$$
$$T = 1 - [1 - iB]^{-1} - [1 - iA]^{-1}, \qquad (13.1.5)$$

where

[пл=pl]

$$A = \frac{K_x \left[K_{\text{пл}}^2 (1 + a)\delta - 1\right]}{C_1 D K_{\text{пл}}^2 (1 - a) + C_3 \delta / D};$$

$$\delta = \frac{C_1 D (1 + a) K_{\text{пл}}^2 - K'}{K' K_{\text{пл}}^2 (1 - a) + C_3 / D};$$

$$B = \frac{1 + (1 - a)\zeta}{\zeta K_x C_2 / (D K_{\text{пл}}^2) - C_0 K_x K_{\text{пл}}^2 D (1 + a)};$$

$$\zeta = \frac{1 + C_0 D K' K_{\text{пл}}^2 (1 - a)}{1 + a - C_2 K' / (D K_{\text{пл}}^2)};$$

$a = (1 - \mu) K_y^2 / K_{pl}^2 = (1 - \mu) \sin^2 \theta$; θ is the angle of incidence of a wave; K_{pl}, D are the wave number of the bending waves and bending stiffness of the plate, and $K_x = K_{pl} \cos \theta$, $K_y = K_{pl} \sin \theta$, $K' = K_{pl}\sqrt{1 + \sin^2 \theta}$. Coefficients C_i entering in these expressions depend on the type of barrier and express its shear and bending compliance and dynamic rigidities in relation to moments and forces:

[cp=av]

$$C_0 = \frac{\Delta z}{2Q_{\text{cp}}}; \quad C_1 = \frac{\Delta \varphi}{2M_{\text{cp}}}; \quad C_2 = \frac{\Delta M}{2\varphi_{\text{cp}}}; \quad C_3 = \frac{\Delta Q}{2z_{\text{cp}}}, \qquad (13.1.6)$$

where the symbol Δ denotes a jump (difference), and the subscript "av" is the average value of the corresponding physical parameter on both sides of a barrier. For the most characteristic barriers these coefficients are:

APPROVED FOR RELEASE: 2007/02/08: CIA-RDP82-00850R000200100009-9

APPROVED FOR RELEASE: 2007/02/08: CIA-RDP82-00850R000200100009-9

vibration-impeding mass (VIM) on a plate

$$C_0 = 0,\ C_2 = -0{,}5\,[GKK_y^2 - \rho I_p \omega^2],$$
$$C_1 = 0,\ C_3 = -0{,}5\,[BK_y^4 - \rho s \omega^2], \qquad (13.1.7)$$

where GK and B are the torsional and bending stiffnesses of VIM, and I_p is the polar moment of inertia of the cross section of VIM;

elastic pad in joint of plates

$$C_0 = -L_y\,(G_y s_y)^{-1},\ C_2 = 0,$$
$$C_1 = -L_y\,(E_y I_y)^{-1},\ C_3 = 0, \qquad (13.1.8)$$

where $G_y s_y$ and $E_y I_y$ are the shear and bending stiffnesses of the pad, and $2L_y$ is the thickness of the pad;

hinged barrier in plate joint

$$C_0 = -2L^2\,[GKK_y^2 - \rho I_p \omega^2]^{-1},\ C_2 - 0,$$
$$C_3 = -0{,}5\,[BK_y^4 - \rho s \omega^2]^{-1},\ C \to \infty, \qquad (13.1.9)$$

where 2L is the distance between the axes of the hinges.

In a plane bending wave one-half the vibration energy flux is produced by the transmission of moments and angles of rotation of the cross sections of the plate parallel to the leading edge of the wave, and the other half is the result of the transmission of shear forces and displacements in the described cross sections. Limiting just one of these characteristics of a bending wave of a barrier (for instance, making the moment in a hinge equal to zero) does not counteract the transmission of vibration energy through the plate at the expense of the other pair of characteristics, which do not depend on the constrained characteristic (force and displacement in the case of a hinge). Therefore the vibration damping of the simplest barriers (a hinge, bearings, movable clamp) is only 3 dB.

When bending waves propagate through a barrier at oblique angles the equality of the four characteristics (displacement, rotation angle, moment and force) that describe the transmission of bending wave energy is violated. In this case placing a constraint on displacements (a bearing) or on shear forces (conventional cross section) provides greater vibration damping than the other two methods -- the use of a hinge or moving clamp.

A direct way to achieve total vibration damping is to set two independent characteristics of the bending wave equal to zero at the same time. Examples of perfect barriers are: a hinged bearing ($M = 0$, $z = 0$); a fixed bearing ($\phi = 0$, $z = 0$); complete cross section ($M = 0$, $Q = 0$); fixed cross section ($\phi = 0$, $Q = 0$).

APPROVED FOR RELEASE: 2007/02/08: CIA-RDP82-00850R000200100009-9

APPROVED FOR RELEASE: 2007/02/08: CIA-RDP82-00850R000200100009-9

The vibration-damping properties of specific barriers are determined by how well some barrier realizes the constraints imposed on the reciprocating force and rotary moment characteristics of the vibrations of a plate.

13.2. Vibration Damping of Vibration-Impeding Masses and Stiffening Ribs

A vibration-impeding mass (VIM) is a metal beam, usually of square cross section, installed in the joints of the plates of ship structures for the purpose of preventing the transmission through them of acoustic vibrations due to a change of impedance. VIM is most often installed in T-shaped and straight-line joints of plates.

A stiffening rib (SR) with an elongate cross section may be viewed from the standpoint of vibration damping as a VIM, if the height of the cross section of the SR is less than 1/6 of the bending wavelength. This requirement is satisfied if the inequality $K_b H < 1$ is valid, where K_b is the wave number of bending vibrations in a plate with thickness t, equal to the thickness of SR, and H is the height of SR.

Vibration Damping of VIM in Straight Plate Joint. VIM is installed in a straight joint in the manner illustrated in Figure 13.1. Its vibration damping is calculated by formula (13.1.3). The transmission coefficient $\langle T^2 \rangle$ of the diffusive field of bending waves in a plate is

[пл=pl; и=b; н=t]

$$\langle T^2 \rangle \approx \frac{m_{пл}\left[K_{и.м} + K_{к.м}\left(1 + K_{и.пл}a/2\right)K_{и.пл}^{-2} r^{-2}\right]}{m_м K_{и.пл}^2}, \qquad (13.2.1)$$

where $m_m = ab\rho_m$; $m_{pl} = h_{pl}\rho_{pl}$; ρ_m, ρ_{pl} are, respectively, the density of VIM and of the plate on which it is installed; $K_{b.pl}$ is the wave number of bending vibrations of a plate; $K_{b.m}$, $K_{t.m}$ are the wave numbers of bending and torsional vibrations of VIM: $r = \sqrt{5/12}b$ is the radius of inertia of the VIM cross section relative to the line of intersection of the planes of symmetry of the plate and VIM.

The values a, b and h_{pl} are explained in Figure 13.1. The value $K_{b.m}$ is determined for the bending vibrations of VIM perpendicular to the plate. The values a and b are selected from the condition

[н=bot]

$$a = b \geqslant 0{,}213\sqrt{\frac{10 f_{пл}^4}{f_н}}, \qquad (13.2.2)$$

where f_{bot} is the bottom frequency of the range in which VIM is supposed to perform effectively (VD $\geq$ 5 dB), Hz; t_{pl} is expressed in meters.

Vibration Damping of VIM in T-Joint of Plates. The vibration damping of VIM in this kind of joint (see Figure 13.1) in relation to bending waves,

APPROVED FOR RELEASE: 2007/02/08: CIA-RDP82-00850R000200100009-9

APPROVED FOR RELEASE: 2007/02/08: CIA-RDP82-00850R000200100009-9

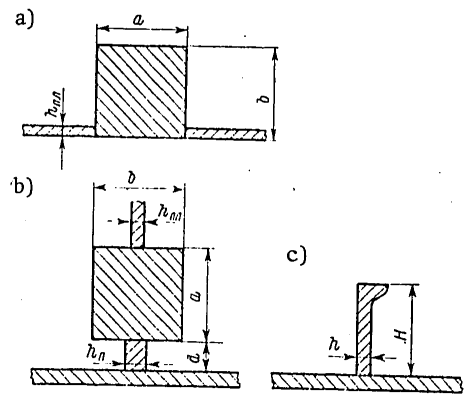

Figure 13.1. Structures connecting plate and vibration-impeding mass: a -- straight joint; b -- T-joint; c -- stiffening rib on plate. [пл=pl]

incident on VIM from a vertical plate, is determined by formula (13.1.3). The value $\langle T^2 \rangle$ entering in this formula is in this case

[н=t; и=b; пл=pl]

$$\langle T^2 \rangle \approx \frac{8K_{\text{к. м}}\left(1+K_{\text{н. пл}}a/2\right)^2 m_{\text{пл}}}{3K^4_{\text{н. пл}} m_{\text{м}} r^2_{\text{м}}}, \qquad (13.2.3)$$

where $m_{pl} = \rho_{pl} t_{pl}$;

$$r_{\text{м}} = \left[\frac{a^2}{6} + \left(\frac{a}{2}+d\right)^2\right]^{1/2}$$

is the radius of inertia of the cross section of VIM relative to the line of intersection of the planes of symmetry of the plate.

The values $K_{t.m}$, $K_{b.pl}$, h_{pl} and ρ_{pl} in expression (13.2.3) are the same as in formula (13.2.1), and $K_{b.pl}$, h_{pl} and ρ_{pl} refer to a vertical plate. If calculation by formula (13.1.3) yields VD < 0 dB it is recommended that VD = 0 dB be used.

Formula (13.2.3) explains possibilities for increasing the vibration damping of VIM. This can be done, in particular, by increasing r_m. It is for this very purpose that a spacer with height d is placed in a joint. The values of d can be arbitrarily large, but not greater than 1/6 of the bending wavelength in the spacer. This requirement is observed when the inequality

[п=sp; в=top]

$$\frac{t_{\text{п}}}{d^2} \geqslant \frac{3{,}6 f_{\text{в}}}{10^3} \qquad (13.2.4)$$

APPROVED FOR RELEASE: 2007/02/08: CIA-RDP82-00850R000200100009-9

APPROVED FOR RELEASE: 2007/02/08: CIA-RDP82-00850R000200100009-9

is satisfied, where t_{sp} is the thickness of the spacer; f_{top} is the top frequency of the band in which VIM is required to perform effectively, Hz; t_{sp} and d are expressed in meters. When this inequality is not satisfied the installation of a vibration-damping VIM will not correspond to the case of installation in a linear plate joint.

The desirability of using a spacer is determined by the inequality

$$d \geq 0.3a, \tag{13.2.5}$$

which corresponds to a 3 dB and larger increment of vibration damping of VIM. The cross section of VIM is selected from the condition

[H=bot]

$$a = b \geq 10^3 \sqrt{\frac{10 t_{пл}^3}{f_н}}; \tag{13.2.6}$$

here f_{bot} is the bottom frequency of the range in which the VIM is required to perform effectively (VD $\geq$ 5 dB), Hz, and t_{pl} is expressed in meters.

Vibration Damping of Stiffening Ribs. The vibration damping of a stiffening rib (see Figure 13.1) is determined by formula (13.1.3). The transmission coefficient $\langle T^2 \rangle$ of bending wave energy in this formula, on frequencies above

[п=lo]

$$f_0 = \frac{0{,}08 c_п t}{H^2}, \tag{13.2.7}$$

(where c_{lo} is the velocity of longitudinal waves in SR, and t and H are explained in Figure 13.1), is

$$\langle T^2 \rangle = 0.2. \tag{13.2.8}$$

Thus the vibration damping of SR on frequencies $f > f_0$ is 7 dB. On frequencies $f < f_0$ the coefficient $\langle T^2 \rangle$, in accordance with the above explanation, is determined for SR by formula (13.2.1). On frequencies higher than f_1, determined by formula

$$f_1 = \frac{c_п}{4H}, \tag{13.2.9}$$

vibration damping of a stiffening rib diminishes gradually to zero on frequency $f_2 = 2f_1$. On frequencies above f_2 vibration damping of stiffening ribs is infinitesimal; they behave as though they are "disconnected" from the hull and exert only a negligible influence on the propagation of bending waves.

Vibration Damping of VIM and Stiffening Ribs Fastened Elastically to Hull. The elastic fastening of VIM to the hull can be used for effective

APPROVED FOR RELEASE: 2007/02/08: CIA-RDP82-00850R000200100009-9

APPROVED FOR RELEASE: 2007/02/08: CIA-RDP82-00850R000200100009-9

vibration damping in ship structures. Here spacers made of vibration-absorbing materials are placed between the VIM and hull (Figure 13.2). The vibration damping of this kind of VIM is manifested in the frequency range

$$f_3 < f < f_4, \tag{13.2.10}$$

where f_3 is the frequency attributed to the resonance of torsional vibrations of VIM on the spacer, determined by the formula

$$f_3 = \frac{1}{2\pi}\sqrt{\frac{E_y b_y^3}{12 h_y \rho J_м}}, \tag{13.2.11}$$

and f_4 is the frequency attributed to the resonance of transverse vibrations of VIM on the spacer, determined by the formula

$$f_4 = \frac{1}{2\pi}\sqrt{\frac{E_y b_y}{m_м h_y}}. \tag{13.2.12}$$

Here E_y, b_y, h_y are the elasticity modulus, width and thickness of the spacer; m, ρJ_m are the mass and inertia moment of the VIM per unit length.

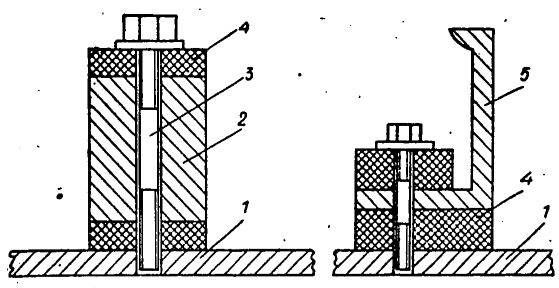

Figure 13.2. Diagrams of elastic joints between hull and vibration-impeding masses and stiffening ribs: 1 -- hull; 2 -- vibration-impeding mass (VIM); 3 -- bolt; 4 -- elastic spacer; 5 -- stiffening rib.

In the frequency range $f_3 < f < f_4$ the vibration damping of VIM in relation to a diffuse field of bending waves can be approximated by the formula

[ВИ=VD]

$$\text{ВИ} \approx -10\lg[\langle T^2\rangle + 0{,}025], \tag{13.2.13}$$

where $\langle T^2\rangle$ is calculated by formula (13.2.1).

APPROVED FOR RELEASE: 2007/02/08: CIA-RDP82-00850R000200100009-9

APPROVED FOR RELEASE: 2007/02/08: CIA-RDP82-00850R000200100009-9

On frequencies outside of range (13.2.10) vibration damping diminishes to zero when the frequency deviates by more than an octave. The angular and frequency dependences of vibration damping are given in the literature [5]. The compliance of the fastening of VIM can cause a reduction of vibration damping, even in the case of a simple joint between the VIM and hull (weld), if the VIM is not fastened firmly enough to the hull.

The amount of energy absorption of incident bending waves in an elastic spacer between VIM and a plate is determined by the absorption coefficient α_t

[п=р]

$$\alpha_T = 1 - |T|^2 - |R_n|^2, \qquad (13.2.14)$$

where R_p is the coefficient of reflection from the plate.

On frequency f_3 the absorption coefficient may reach $\alpha_t \approx 0.15$, and on frequency f_4 it is $\alpha_t \approx 0.45$ when the loss coefficient of the material from which the elastic spacer is made is $\eta \approx 1$. Therefore spacers made of vibration-absorbing materials, installed between ribs and the hull, can be an effective means of reducing vibrations of a ship hull.

13.3. Vibration Damping of Plate Joints

Various plate joints of ship structures, which destroy the homogeneity of structures, form a natural barrier to bending waves. The most characteristic are three kinds of plate joints: L, T and cross joints (Figure 13.3).

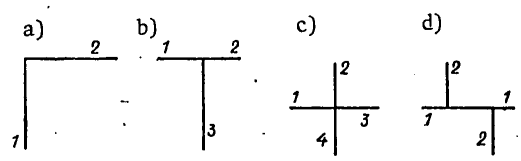

Figure 13.3. Diagrams of different kinds of plate joints: a -- L-joint; b -- T-joint; c -- cross; d -- offset.

Vibration Damping of Plate Joints for Plane Bending Wave with Normal Incidence. The energy transmission coefficient τ_{nk} of bending waves from plate k into plate n for the practical important case of plates of the identical material is

$$\tau_{kn} = \frac{2\chi_{nk}^{2,5}}{\left(\sum_{m=1}^{p} \chi_{mk}^{2,5}\right)^2}, \qquad (13.3.1)$$

APPROVED FOR RELEASE: 2007/02/08: CIA-RDP82-00850R000200100009-9

APPROVED FOR RELEASE: 2007/02/08: CIA-RDP82-00850R000200100009-9

where $\chi_{nk} = t_{pl\ n}/t_{pl\ k}$; $\chi_{mk} = t_{pl\ m}/t_{pl\ k}$; p is the number of plates involved in a joint; t_{pl} is the thickness of the corresponding plates.

In the special case $\chi_{mk} = 1$; $\tau_{nk} = \tau = 2p^{-2}$, and consequently the vibration damping of a joint VD, in dB, is

$$VD = 20 \log p - 3. \qquad (13.3.2)$$

Figure 13.4 shows the vibration damping of two T-joints, in one of which $t_{pl\ 1} = t_{pl\ 2}$ with variable $t_{pl\ 3}$, and in the other $t_{pl\ 1} = t_{pl\ 3}$ with variable $t_{pl\ 2}$. As can be seen, the thickness of the plate, the vibrations in which we are not interested, should be increased as much as possible. A decrease of plate thickness is effective in relation to a plate in which vibrations must be reduced.

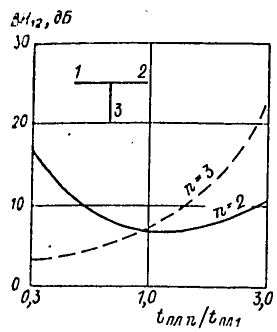

Figure 13.4. Vibration damping of T-joint of plates. [дБ=dB; пл=pl]

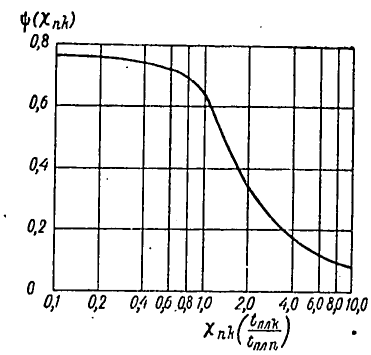

Figure 13.5. $\psi(\chi_{nk})$ as function of χ_{nk}.

Vibration Damping of Plate Joints for Diffuse Bending Wave Field. The energy transmission coefficient, averaged in terms of the angle of incidence on a joint is in this case

$$\langle \tau_{nk} \rangle = \tau_{nk} \psi(\chi_{nk}), \qquad (13.3.3)$$

where τ_{nk} is determined by formula (13.3.1) and $\psi(\chi_{nk})$ graphically using Figure 13.5.

In particular, if $\chi_{nk} = 1$, then $\psi(\chi_{nk}) = 2/\pi$. As can be seen, the energy of bending waves in a diffuse field passes through a plate joint with less intensity than in the case of normal incidence. The reason is that the

APPROVED FOR RELEASE: 2007/02/08: CIA-RDP82-00850R000200100009-9

APPROVED FOR RELEASE: 2007/02/08: CIA-RDP82-00850R000200100009-9

oblique waves in a diffuse field pass through a joint with greater attenuation.

Plate joints similar to the one illustrated in Figure 13.3d, called offset joints, are encountered in shipbuilding practice. These joints have greater vibration damping than cross joints on frequencies above

[н=bot; пл=pl; п=lo]

$$f_н = \frac{16 t_{пл\,2}^3 c_{п2}}{\pi^4 l^4}, \qquad (13.3.4)$$

where $t_{pl\ 2}$ is the thickness of the offset plates; $c_{lo\ 2}$ is the longitudinal wave velocity in the second plate; l is the distance between the plates.

The high vibration damping of this kind of joint is attributed to its higher impedance in relation to bending moment, and on frequencies above

[в=top]

$$f_в = \frac{c_{п1} t_{пл\,1}}{2\pi^2 l^2} - \qquad (13.3.5)$$

to the existence of two barriers, instead of one, in the propagation path of bending waves. The vibration damping of a joint with offset branches VD, in dB, is:

on frequencies above f_{top}

[ВИ=VD]

$$ВИ = 20 \lg \left[\frac{\pi}{4} \left(2 + \chi_{21}^{2,5}\right)^2 \right]; \qquad (13.3.6)$$

on frequencies below f_{bot}

$$ВИ = 10 \lg \left[\pi \left(1 + \chi_{21}^{2,5}\right)^2\right]; \qquad (13.3.7)$$

on frequencies in the range f_{bot}-f_{top}

$$ВИ = 10 \lg \left[\pi \left(1 + \frac{\beta_0}{2} + \frac{\beta_0^2}{8}\right) \right], \qquad (13.3.8)$$

where

$$\beta_0 = \frac{2 m_{пл\,2} c_{п2}}{m_{пл\,1} c_{п1}} \left(\frac{K_{п1} l}{2}\right)^2.$$

Calculations by formulas (13.3.6) and (13.3.7) for the case $\chi_{21} = 1$ yield, respectively, 17 and 11 dB. The vibration damping of a cross joint with $t_{pl\ 1} = t_{pl\ 2} = t_{pl\ 3} = t_{pl\ 4}$, according to formula (13.3.3), is 11 dB. As can be seen, on a frequency above f_{bot} the vibration damping of a cross joint with offset branches is 6 dB higher. The value of this frequency for l = 0.05 m and $t_{pl\ 1} = t_{pl\ 2}$ = 0.01 m is 124 Hz, and f_{top} = 1,000 Hz.

To satisfy condition $f_{top} > f_{bot}$, and consequently, to make sure that expressions (13.3.6), (13.3.7) and (13.3.8) are valid, it is necessary to satisfy the inequality

APPROVED FOR RELEASE: 2007/02/08: CIA-RDP82-00850R000200100009-9

APPROVED FOR RELEASE: 2007/02/08: CIA-RDP82-00850R000200100009-9

$$l > \frac{4t_{\text{пл}}}{\pi}. \qquad (13.3.9)$$

13.4. Vibration Damping of Periodic Barriers

A characteristic feature of ship hull structures and of other engineering installations, is the uniform spacing, or periodicity, of stiffening ribs, which serve as a natural barrier to bending waves that propagate in the hull.

Because the plates between barriers are finite in size resonance properties of the hull are manifested, with the result that the vibration-damping effect of several barriers is substantially lower than the sum of the vibration-damping effects of the individual barriers in the system. Furthermore, when barriers are spaced periodically on the surface of a hull ranges of frequencies and of angles of incidences appear, in which bending waves pass through a chain of barriers unattenuated. Thus, in these frequency ranges, sometimes called "transparent ranges," vibration damping decreases to nil, and vibrations can be attenuated only by using vibration-absorbing structures.

The attenuation of vibrations in a periodic space system is described by propagation constant μ, which expresses, per unit length, the natural logarithm of the ratio of the combined amplitudes of vibrations at corresponding points on neighboring spans:

$$W(x+L) = e^{\pm\mu L} W(x), \qquad (13.4.1)$$

$$\mu = \pm\frac{1}{L}\ln\frac{W(x+L)}{W(x)}. \qquad (13.4.2)$$

For barriers with zero moment impedance ($Z_\mu = 0$) and finite force impedance Z_F, the propagation constant is given by the equation

[н=b]

$$\frac{\sin(K_\text{н}L)}{\cos(K_\text{н}L) - \operatorname{ch}(\mu L)} - \frac{\operatorname{sh}(K_\text{н}L)}{\operatorname{ch}(K_\text{н}L) - \operatorname{ch}(\mu L)} - \frac{4DK_\text{н}}{i\omega Z_F} = 0. \qquad (13.4.3)$$

For barriers of an arbitrary type the propagation constant can be found from a simpler equation, which is valid for $K_b L \gg 1$, i.e., when the distance between barriers is greater than one-half the bending wavelength in the hull:

$$\operatorname{ch}(\mu L) = \frac{1}{|T|}\cos(K_x L - \gamma), \qquad (13.4.4)$$

where γ is the phase of transmission coefficient T; $\gamma = \ln T \cdot \ln |T|$.

As the frequency or incidence angle changes the propagation constant μ gradually acquires real and imaginary values, which correspond to the alternation of transparent zones and attenuation zones of bending waves in a plate with barriers, spaced periodically apart.

APPROVED FOR RELEASE: 2007/02/08: CIA-RDP82-00850R000200100009-9

APPROVED FOR RELEASE: 2007/02/08: CIA-RDP82-00850R000200100009-9

In the case of a diffuse field of vibrations near the source the maximum attenuation of vibrations in a frequency band that covers several transparent and attenuation zones may be found from the formula

$$\Delta L_1 = 10 \lg \frac{\alpha}{\langle T \rangle}, \qquad (13.4.5)$$

where α is a coefficient that varies in the range of 1 to $\pi/2$.

Formula (13.4.5) is applicable in the case of a hull without vibration-absorbing devices; in this formula <T> is the average modulus of the transmission coefficient through a single barrier.

When the hull contains a damped section, in which attenuation due to vibration-absorbing devices is 6 dB and more, the gradient of vibrations between the original section, which contains the source, and the damped section will be

$$\Delta L_2 = 10 \lg \frac{2}{\langle T^2 \rangle} \qquad (13.4.6)$$

in which the attenuation of vibrations due to the natural structural damping of the hull is ignored.

For the most common barriers of the vibration-impeding mass and stiffening rib types $\langle T^2 \rangle$ is determined by formula (13.2.1), and <T> is determined as follows:

[и=b; п=lo; п=ba; к=t]

$$\langle T \rangle = \frac{2}{\pi} \left\{ \langle T_{\text{и}}^2 \rangle L_{\text{п}} \frac{K_{\text{и.п}}}{K_{\text{пр}} \langle T^2 \rangle} + \langle T_{\text{к}}^2 \rangle \ln \frac{2}{\langle T_{\text{к}}^2 \rangle} \right\}, \qquad (13.4.7)$$

where $\langle T_b^2 \rangle$, $\langle T_t^2 \rangle$ is the mean square modulus of the transmission coefficient due to bending and torsional resonances of VIM, respectively [4].

13.5. Influence of Features of Ship Structures on Vibration Damping of Barrier

The vibration damping of a barrier, installed in the propagation path of bending waves, is also influenced by features of ship structures, such as the dimensions of their elements, connected liquid, the curvature of structures and fastening hardware in them.

Influence of Size of Structural Elements. Elements of ship structures are bent plates without stiffening ribs or plates fastened to the frame space (stiffening ribs, girders, etc.). The former include, for example, bearing plates of plate foundations, used extensively on ships for installing machinery; the second variety consists of decking, bulkheads, hull plating, etc. (Figure 13.6).

APPROVED FOR RELEASE: 2007/02/08: CIA-RDP82-00850R000200100009-9

APPROVED FOR RELEASE: 2007/02/08: CIA-RDP82-00850R000200100009-9

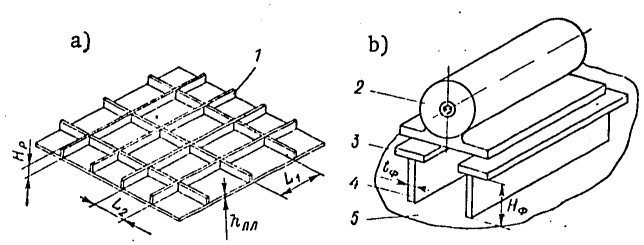

Figure 13.6. Typical elements of ship structures: a -- ribbed plate (bulkhead with stiffening ribs); b -- isotropic plate (plate foundation). 1 -- stiffening ribs; 2 -- machine; 3 -- mounting plate; 4 -- bearing plate; 5 -- hull structure. [пл=pl; ф=f]

The vibration damping of a barrier, installed in a joint between an isotropic plate and adjacent constructions, depends on its dimensions. If a plate has enough area the waves reflected from a barrier will attenuate entirely in it and will not return to the barrier. In this case the barrier behaves as an obstacle, installed in the joint of endless plates, and its vibration damping can be calculated by the formulas presented in §13.2. The essential condition is that the inequality

[пл=pl; п=lo]

$$\frac{s_{пл}}{L} > \frac{2c_п\langle\tau\rangle}{\pi\omega\eta} \qquad (13.5.1)$$

be satisfied, where c_{lo} and η are the longitudinal wave velocity and loss coefficient of the plate; L is the perimeter of the connecting line between the plate and adjacent structures; $\langle\tau\rangle$ is the transmission coefficient of diffuse bending wave energy through the joint between the plate and adjacent structures to the point where the barrier is installed.

If condition (13.5.1) is not satisfied plate dimensions begin to have an effect on the vibration damping of a barrier. Vibration damping in this case is calculated by formula (13.7.1). The dimensions of a ribbed plate, around whose edges is installed a barrier to bending waves, will not influence its vibration damping if the inequality

$$\frac{s_{пл}}{L} > \frac{1}{\pi}\sqrt{\frac{c_п L\langle\tau_p\rangle}{\eta f}} \qquad (13.5.2)$$

is satisfied, where L is the average distance between the stiffening ribs, fastened to the plate; $\langle\tau_p\rangle$ is the coefficient of transmission of the diffuse bending wave energy through a stiffening rib. More about this is said in §13.7.

Influence of Curvature of Hull Structures. This influence is manifested on frequencies below so-called circular frequency f_c, which is the frequency of cophasal radial vibrations

APPROVED FOR RELEASE: 2007/02/08: CIA-RDP82-00850R000200100009-9

APPROVED FOR RELEASE: 2007/02/08: CIA-RDP82-00850R000200100009-9

[k=c]

$$f_к = \frac{c_п}{2\pi R}, \tag{13.5.3}$$

where R is the radius of curvature.

In the frequency range $f < 0.25f_c$ vibration damping decreases and can be approximated by the formula

[ВИ=VD]

$$ВИ = -10 \lg [\langle T^2 \rangle + 0{,}1], \tag{13.5.4}$$

where $\langle T^2 \rangle$ is calculated by formula (13.2.1). In the frequency range $0.25f_c \leq f \leq f_c$ vibration damping increases and approaches the vibration damping of a barrier on a plane plate.

Influence of Liquid in Contact with Hull. This influence also leads in most cases to a decrease of vibration damping. In the first approximation on low frequencies it can be taken into account by replacing in the formulas in §13.1 and §13.2 the value m_{pl} with

$$m = m_{pl} + m_{liq}, \tag{13.5.5}$$

where $m_{liq} = \rho_{liq}/K_b$, and by changing the wave number of the bending vibrations of the plate:

[и=b; пл=pl; ж=liq]

$$K_и \approx K_{пл} \sqrt{1 + \frac{\rho_ж}{K_{пл} m_{пл}}}. \tag{13.5.6}$$

The vibration damping of barriers is influenced also, in addition to the covibrating mass of liquid, by the acoustic energy flux propagating in the liquid along the plating. This factor is manifested basically on high frequencies, approaching the so-called critical frequency f_{cr}, kHz, which for most ship plates in water is beyond the limits of the audio frequency range:

[kp=cr]

$$f_{кр} \approx \frac{23}{t}, \tag{13.5.7}$$

where t is the thickness of a steel plate, cm.

More exact estimates can be found with the aid of materials presented in [5].

Influence of Stiffening Rib Framing. This influence also leads to a decrease of vibration damping of barriers. There is a difference between the influence of stiffening ribs that are parallel to a barrier and of stiffening ribs that intersect it. For instance, stiffening ribs that intersect a barrier reduce the attainable vibration damping on a plate to the value

APPROVED FOR RELEASE: 2007/02/08: CIA-RDP82-00850R000200100009-9

APPROVED FOR RELEASE: 2007/02/08: CIA-RDP82-00850R000200100009-9

$$VD_{max} \approx 10 \log (2K_{pl} l), \qquad (13.5.8)$$

where l is the distance between neighboring stiffening ribs.

Stiffening ribs that are parallel to a barrier reduce the vibration damping to a lesser extent, but in this case the vibration damping still decreases:

$$VD = VD_{ba} - \Delta, \qquad (13.5.9)$$

where VD_{ba} is the vibration damping of a single barrier, estimated by the formulas in §13.1 and §13.2, and the correction factor

$$\Delta \approx -10 \lg \langle T_p \rangle \qquad (13.5.10)$$

takes into account how much the vibration field between stiffening ribs differs from diffuse; for real structures of ship framing this correction factor may reach Δ = 5-8 dB.

13.6. Vibration Damping as Function of Vibration Absorption

In real ship structures the vibration damping of a barrier to bending waves depends on the vibration absorption in the structures. We shall explain this relationship by way of example of a plate, divided by a barrier with length L into two equal parts with a total area s_{pl}. The vibration damping of such a barrier in relation to the energy of a diffuse bending wave field, generated in one-half of the plate, is

[ВИ=VD; пл=pl;
и=b; п=1o]

$$ВИ = 10 \lg \left[1 + \frac{\pi \eta_{пл} s_{пл} \omega}{2 c_{и.п} \langle \tau \rangle L} \right], \qquad (13.6.1)$$

where $\langle\tau\rangle$ is the transmission coefficient of the energy of the diffuse bending wave field through the barrier; η_{pl} is the loss coefficient of the plate, which determines vibration absorption.

If the losses in a plate are such that $\pi\eta_{pl}s_{pl}\omega \ll 2c_{b.1o}(\tau)L$, then $VD \to 0$, and consequently a barrier exhibits no vibration damping. The reason is that the energy of bending waves, reflected from the barrier, returns to it and gradually penetrates into the insulated part of the plate.

When the inequality $\pi\eta_{pl}s_{pl}\omega \gg 2c_{b.1o}(\tau)L$, VD >> 0 dB is satisfied. In this case the energy of bending waves, reflected by a barrier, is completely absorbed and does not go back into the insulated part of the plate. The interaction of energy with a barrier becomes virtually a one-time process, and the vibration damping of a barrier is similar to that of endless plates.

APPROVED FOR RELEASE: 2007/02/08: CIA-RDP82-00850R000200100009-9

APPROVED FOR RELEASE: 2007/02/08: CIA-RDP82-00850R000200100009-9

For a plate with insufficient losses, if the inequality

$$\eta_{пл} < \frac{\langle\tau\rangle c_{н.п} L}{\pi^2 f s_{пл}} \qquad (13.6.2)$$

is valid, a vibration-absorbing coating should be used (see Chapter 14). If there are limited opportunities for using such a coating it should be applied on the plate with the larger area, whether or not it is driven by vibrations or insulated.

13.7. Efficiency Analysis of Ship Vibration-Damping Techniques

Efficiency of Vibration-Damping Techniques for Ship Structures Consisting of Isotropic Plates. These structures include, for example, the bed plate (see Figure 13.6). The effectiveness of a vibration-damping device VD, in dB, installed between the bearing plates of such a bed plate and the ship structure, is determined by the formula

[ф=f]

$$ВИ = 10 \lg \left(1 + \frac{2\pi^2 f \eta_ф H_ф}{\langle\tau\rangle c_{н.ф}}\right), \qquad (13.7.1)$$

where η_f and $c_{b.f}$ refer to the bearing plates of the foundation; H_f is the height of the foundation (see Figure 13.6); $\langle\tau\rangle$ is the coefficient of transmission of the energy of a diffuse bending wave field through the joint between the bearing plates and the hull, determined by the formulas in §13.2 and §13.3 in consideration of the vibration-damping device installed in the seam. When H_f and $c_{b.f}$ vary around the perimeter of the foundation their averages are taken.

In the general case the efficiency of a vibration-damping device, separating an isotropic plate from the rest of the hull VD, in dB, is

$$ВИ = 10 \lg \left(1 + \frac{2\pi^2 f \eta_{пл} s_{пл}}{\langle\tau\rangle L_{пл} c_{н.пл}}\right), \qquad (13.7.2)$$

where s_{pl} and L_{pl} is the area and perimeter of the joint between the plate and the rest of the hull.

Formulas (13.7.1) and (13.7.2) are valid when conditions (13.5.2) and (13.6.2) are satisfied.

Efficiency of Vibration-Damping Systems Installed on Ribbed Plates on Circular Contour Around Vibration Source. The efficiency of these VD systems, in dB, is determined by the formula

$$ВИ = 10 \lg [1 + 2 I_1(\gamma R) K_1(\gamma R) \gamma R \sigma], \qquad (13.7.3)$$

where R is the radius of the contour; $I_1(\gamma R)$, $K_1(\gamma R)$ are cylindrical functions [6]:

APPROVED FOR RELEASE: 2007/02/08: CIA-RDP82-00850R000200100009-9

APPROVED FOR RELEASE: 2007/02/08: CIA-RDP82-00850R000200100009-9

$$\sigma = \frac{\langle\tau_0\rangle}{\langle\tau\rangle}\gamma l; \quad \gamma = \sqrt{\frac{2\pi f\eta}{\langle\tau_0\rangle c_{\text{ш}} l}};$$

l is the average distance between the stiffening ribs that fasten the plate; $\langle\tau_0\rangle$, $\langle\tau\rangle$ are the transmission coefficients of the diffuse bending wave field through a stiffening rib and through the vibration-damping system, respectively; η and c_b refer to a ribbed plate.

In the range $\gamma R < 2$ an increase of radius R leads to an increase of vibration damping, as is shown in Figure 13.7.

If the inequality $\gamma R < 2$ is satisfied formula (13.7.3) acquires the form

[ВИ=VD]

$$\text{ВИ} \approx 10 \lg \left(1 + \frac{\langle\tau_0\rangle}{\langle\tau\rangle}\gamma l\right). \qquad (13.7.4)$$

As can be seen, vibration damping here does not depend on distance R between the source and vibration-damping system.

Thus it is not desirable to increase R above $R > 2/\gamma$. The source should be placed near the center of the contour, formed by the vibration-damping system. If the source is shifted relative to the center of the contour by more than $a = 0.65/\gamma$ the vibration damping of the system will decrease by more than 1 dB in comparison with the values calculated by formula (13.7.3).

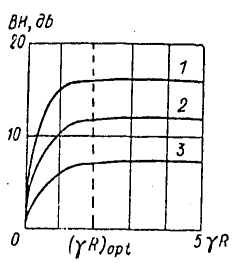

Figure 13.7. VD as function of γR. 1 -- $\sigma = 45$; 2 -- $\sigma = 15$; 3 -- $\sigma = 4.5$. [ВИ=VD]

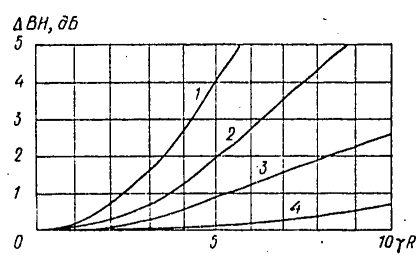

Figure 13.8. ΔVD as function of γR. 1 -- $l_1/l_2 = 3$; 2 -- $l_1/l_2 = 2$; 3 -- $l_1/l_2 = 1.5$; 4 -- $l_1/l_2 = 1.2$.

If the plate is fastened by stiffening ribs, different distances apart in mutually perpendicular directions, the vibration-damping systems should be set up such that there will be about the same number of stiffening ribs between it and the source in all directions. The gain in vibration damping ΔVD, in dB, thus achieved in comparison with the case when the system is set up on a circular contour with radius R with the identical perimeter is determined by the formula

APPROVED FOR RELEASE: 2007/02/08: CIA-RDP82-00850R000200100009-9

APPROVED FOR RELEASE: 2007/02/08: CIA-RDP82-00850R000200100009-9

$$\Delta ВИ = 10 \lg \left[I_0(\varepsilon\nu) + \frac{\varepsilon K_0(\nu) I_1(\varepsilon\nu)}{K_0(\nu)} \right], \qquad (13.7.5)$$

where $\nu = \gamma R$; $\varepsilon = \frac{1 - \sqrt{\frac{l_2}{l_1}}}{1 + \sqrt{\frac{l_2}{l_1}}}$; $\gamma = \frac{1}{2}(\gamma_1 + \gamma_2)$; l_1, l_2 are the distances between the stiffening ribs in mutually perpendicular directions ($l_2 \leqslant l_1$); γ_1, γ_2 are the values of γ in the same directions.

The dependence of ΔVD on γR is plotted in Figure 13.8 for different ratios l_1/l_2.

If several sources (machines) are installed on a hull structure (deck, bulkhead, etc.), the vibration-damping system should be installed around the contour of the structure. The surface of the structure inside the contour on which the system is installed should be faced with a vibration-damping coating (see Chapter 14).

13.8. Personal Vibration Safety Gear[1]

Vibrations on ships still occasionally exceed health standards, causing undesirable effects on people, in spite of the extensive application of prophylactic and safety techniques.

Personal safety gear is divided into two basic groups, depending on where vibration is received [3]. The first group includes devices that protect humans from general vibration, i.e., from vibrations of the deck and decking, and from rooms where crew members rest and sleep. This group consists of the following: shock-absorbing floors, vibration-damping bunks and sofas and personal mats; special foot wear with a vibration-damping sole and foot wear with vibration-damping insoles; pneumatic trusses and belts.

The second group includes devices intended for protection from local vibration, specifically: protective gloves, mittens and sleeves -- suede and leather, with sponge rubber or latex foam liner, and a variety of anti-vibration devices (antivibrators), used extensively in the designs of hand tools.

Both general and local vibrations sometimes are experienced on a sailing ship, when not only the decks and rest areas vibrate, but also hand rails, valves, control wheels, etc., with which people come into contact.

Personal safety gear should be selected in consideration of specific conditions, determined by the parameters of vibration, the effective time τ_e

[1]This section was written by A. I. Vozhzhova.

APPROVED FOR RELEASE: 2007/02/08: CIA-RDP82-00850R000200100009-9

APPROVED FOR RELEASE: 2007/02/08: CIA-RDP82-00850R000200100009-9

of the buildup of individual pulses produced by the stiffness of vibration, the possibility that vibration will exceed the maximum tolerable levels, and the point of application of vibration to the body.

The vibration-damping platform proposed by S. S. Zhikharev and B. L. Ivanov for protection against general vibration and for absorbing aperiodic jolts, is used as a shock-absorbing stand at the work stations of cutter crew members. "Floating" on springs, the platform, measuring 300 × 400 mm, is installed in a metal frame and is fastened to the deck. Four leaf springs and a 30 mm thick sponge rubber pad are used for absorbing low-frequency mechanical vibrations. The space between the frame and moving platform (5 mm) provides free movement in the vertical direction without tilting and shifting in the horizontal plane. This enables a person standing on the platform to maintain balance as the ship rolls.

Vibration-damping mats for personal use, made of sponge rubber (Figure 13.9a), and developed by A. I. Vozhzhova, V. V. Perelygin and Yu. N. Gromov, are manufactured by the Sverdlovsk sponge rubber and ebonite products factory. The mats consist of a collection of 2-3 sheets of sponge rubber of different density and thickness, glued together. The difference in the thickness of the sheets and the selection of different sheets of sponge rubber with the necessary porosity reduce the amplitude of vibration. Mat dimensions are 400 × 600 and 400 × 1,200 mm, and thickness is 50 mm; the mat is covered on both sides with grooved oil-resistant rubber sheet 1, which protects the mat from destruction by petroleum products. The mats help to stabilize the position of the body and reduce vibrations (for example, by a factor of 2.5-3 on frequencies of 20-30 Hz) in places where there are changes of thickness. The results of long-term testing of the mats on a sailing ship recommend them for extensive adoption in water transportation.

A sponge rubber (beige) pad with a density of 0.4 g/cm^3 (measuring 600 × × 450 × 74-200 mm), with 50 mm deep depressions with a diameter of 45 mm in the bottom side of the pad for inserting springs, reduces the amplitude of vibration by a factor of 12 on 25 Hz and completely damps it on 30 Hz. This pad can be used, in particular, in the design of bunks, sofas, armchairs and other furniture.

Antivibration belts also are included among personal vibration-damping gear. A belt pushes the internal organs against the back wall of the abdominal cavity and limits their movement. This is extremely important for protection against vibrations and jolts with frequencies close to the natural vibration frequencies of the mobile human internal organs, or which coincide with them, which involves the possibility of amplification of the harmful effect of mechanical vibrations due to resonance. Belts can be made of natural or artificial leather, stitched many times (to impart great stiffness) with buckle fasteners. There are also pneumatic belts consisting of two rubber strips, cemented on the periphery, which are inflated with

APPROVED FOR RELEASE: 2007/02/08: CIA-RDP82-00850R000200100009-9

APPROVED FOR RELEASE: 2007/02/08: CIA-RDP82-00850R000200100009-9

air. Worn on the body, the belt presses the internal organs against the rear wall of the abdominal cavity and thus immobilizes them.

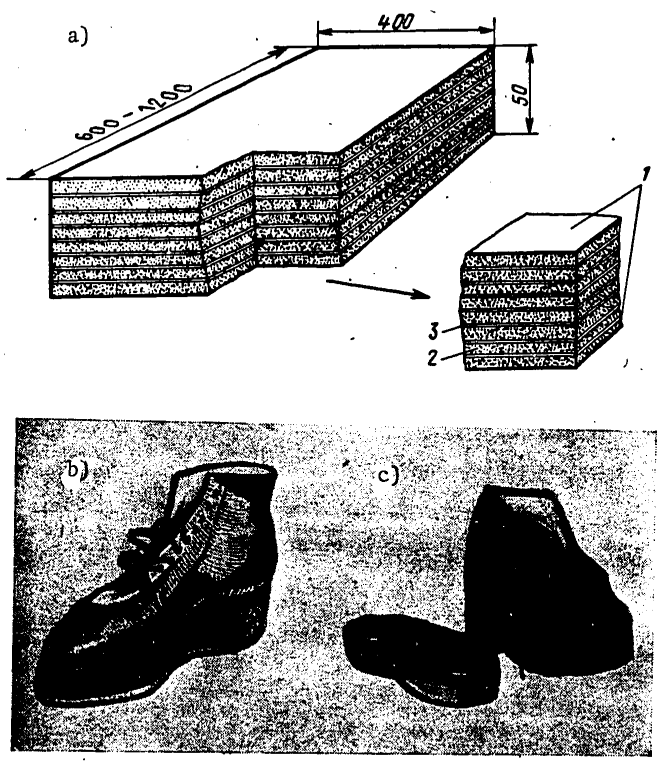

Figure 13.9. Personal vibration safety gear: a -- personal mat; b -- special shoe with damping sole; c -- boot designed by G. I. Rumyantsev for vibration-damping insoles.

Since general vibration on a sailing ship is transmitted to the human body basically through the lower extremeties, vibration-damping foot gear plays a very important role, since it provides protection from vibration and at the same time can be worn on duty involving walking about the ship. Foot wear of this kind should reduce the amplitude of vibration in a rather wide frequency range (from 3 to 300 Hz) and hold the foot in the normal physiological position, permitting the arch, a physiological damper, to be utilized to the fullest extent, and affording the body the necessary balance during rolling and aperiodic jolts.

APPROVED FOR RELEASE: 2007/02/08: CIA-RDP82-00850R000200100009-9

APPROVED FOR RELEASE: 2007/02/08: CIA-RDP82-00850R000200100009-9

The vibration-damping foot gear (designed by A. I. Vozhzhova, M. I. Groysman, et al), manufactured by the "Skorokhod" foot wear association in Leningrad, is effective on ships. They are boots with a 40 mm thick vibration-damping sole (Figure 13.9b). The walking part of the sole and the heel are made of grooved oil-resistant Mipora microporous rubber, and the cutaway part of the sole and the heel are painted with oil-resistant lacquer. An important design feature of the foot gear is the fact that it incorporates the use of layers of vibration-damping sponge rubber, varying in density and elasticity, with a density of 0.25-0.30 g/cm^3, one of which is perforated. The heel is made as a sponge rubber wedge with a density of 0.4-0.5 g/cm^3 [1]. The above-mentioned association also has developed and is manufacturing experimental work boots of special design for vibration-damping insoles of double thickness -- 24 mm. The top of the boot is made of perforated leather to provide access to air.

A lightweight shoe for motor operators -- sandal with a vibration-damping insole, with a leather top and leather sole (designed by A. I. Vozhzhova), is a more comfortable shoe that keeps the feet from overheating and sweating (which is extremely important under conditions of high temperatures in engine rooms and during sailing in the tropics). The shoe provides the necessary inner space in consideration of the 12 mm thick insole. The insole, made of porous sponge rubber, is lined on the foot side with soft leather. On the toe and ball end (the widest part of the foot) the insole is sewn into the sandal, and on the heel end it is free. The vibration-damping insoles, cut from sheets and leather, can be fashioned into an ordinary shoe, Russian leathers and rubbers and boots. In these cases the thickness of the insole is 12 mm for shoe sizes up to 40 and 16 mm for shoes larger than size 40.

13.9. Measurement of Vibration Damping[1]

The vibration damping of elements of ship hull structures is usually measured on models in the form of the corresponding connections of rods and plates. A "measuring rod" [5], a schematic diagram of which is presented in Figure 13.10, is used, as a rule, for this purpose. The setup is a rod, to one end of which is fastened an elastic wave driver, and the other end is driven into sand (to eliminate reflection of elastic waves from it). To obtain reliable data with the "measuring rod" device the reflection coefficient of elastic waves should not exceed 1%. To achieve this the following requirements must be observed:

1) the length of the section of the rod l_k, driven into sand, should be connected with the frequency at which the measurement starts by the relation

$$l_k \geq 1{,}5\lambda_{max}, \tag{13.9.1}$$

[1]This section was written by S. V. Budrin.

APPROVED FOR RELEASE: 2007/02/08: CIA-RDP82-00850R000200100009-9

APPROVED FOR RELEASE: 2007/02/08: CIA-RDP82-00850R000200100009-9

where λ_{max} is the maximum elastic wavelength in the rod in the measured frequency range;

2) the part of the rod driven into the sand should be wedge-shaped to provide better matching of the mechanical impedances of the sand and rod;

3) sand must cemented to the surface of the wedge to improve mechanical contact between the rod and sand;

4) the layer of sand that covers the rod should have a gradually increasing thickness;

5) the sand mass must be 200-900% of the mass of the wedge. Reduction of reflection from the end of the rod driven into the sand is facilitated by adding filings in the amount of 10-20% by volume to the sand where the rod is inserted into it.

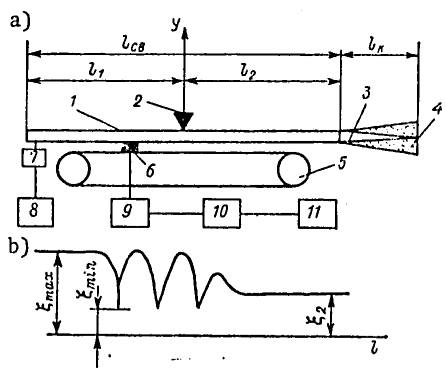

Figure 13.10. Diagram of "measuring rod" setup (a) and sample recording on magnetic tape (b): 1 -- rod; 2 -- analyzed barrier; 3 -- wedge; 4 -- sand; 5 -- device for transporting vibration receiver along rod; 6 -- vibration receiver; 7 -- vibrator; 8 -- acoustic generator; 9 -- amplifier; 10 -- analyzer; 11 -- level recorder. [CB=fr]

To measure the vibration-damping properties of the joints of rods the ends of all the rods except the driven one are placed in sand. The length of the free (not immersed in sand) part of the rod l_{fr} should satisfy the condition $l_{fr} \geq 4\lambda_{max}$. This condition limits the frequency range on the low end. The barrier to be analyzed is set up in the middle of the free section of the rod. The diameter of the contact between the vibration

APPROVED FOR RELEASE: 2007/02/08: CIA-RDP82-00850R000200100009-9

APPROVED FOR RELEASE: 2007/02/08: CIA-RDP82-00850R000200100009-9

receiver and rod should be $d \leq \lambda_{a.t}$, where $\lambda_{a.t}$ is the elastic wavelength on the top boundary frequency of the analyzed frequency band.

Vibration damping can be determined with the measuring rod by the following methods.

Standing Wave Method. In this method the interference of waves that strike a barrier and are reflected from it is utilized. As a result of interference standing waves form in front of a barrier.

The amplitude reflection coefficient is

$$R = \frac{|\ddot{\xi}_{max}| - |\ddot{\xi}_{min}|}{|\ddot{\xi}_{max}| + |\ddot{\xi}_{min}|}, \qquad (13.9.2)$$

where $\ddot{\xi}_{max}$ and $\ddot{\xi}_{min}$ are the maximum and minimum amplitudes of acceleration of the standing wave.

Denoting $\alpha = \frac{|\ddot{\xi}_{max}|}{|\ddot{\xi}_{min}|}$, we obtain for VD, in dB,

[ВИ=VD]

$$\text{ВИ} = 10 \lg \frac{(1+\alpha)^2}{4\alpha}. \qquad (13.9.3)$$

Vibration damping VD is plotted in Figure 13.11 as a function of α.

The standing wave method is used to determine vibration damping if it does not exceed 5-7 dB.

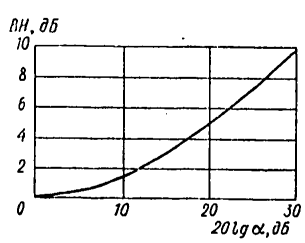

Figure 13.11. VD as function of α. [ВИ=VD; дБ=dB]

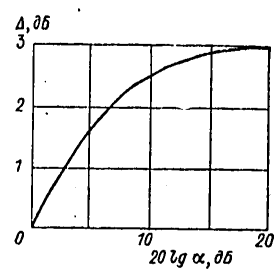

Figure 13.12. Δ as function of α.

Vibration Level Gradient Method. When the vibration damping of a barrier exceeds 5 dB measurement by comparing the maximum levels of the standing wave in front of a barrier $|\ddot{\xi}_{max}|$ with the level of the traveling wave $|\ddot{\xi}|_2$ is more reliable. The vibration damping of an analyzed barrier is calculated in relation to $\alpha = \frac{|\ddot{\xi}_{max}|}{|\ddot{\xi}_2|}$ as follows:

APPROVED FOR RELEASE: 2007/02/08: CIA-RDP82-00850R000200100009-9

APPROVED FOR RELEASE: 2007/02/08: CIA-RDP82-00850R000200100009-9

$$\text{ВИ} = 20 \lg \alpha - \Delta. \qquad (13.9.4)$$

The correction factor Δ for different α values is presented in Figure 13.12.

Triple Point Method. Vibration damping can be determined by measuring the amplitude of vibrations at three points on a section of rod $l \leq x \leq 0$ (Figure 13.13). The points on the rod are selected such that, first, the distances between the middle and the outer points will be identical (Δl), and, second, distances l_3 and $l-l_1$ will be equal to or greater than $\lambda/3$.

Reflection coefficient R is

$$R = -\gamma + \sqrt{\gamma^2 - 1},$$

where

$$\gamma = \frac{m - \cos 2\beta}{m - 1} \cos \alpha - \frac{\sin 2\beta}{m - 1} \sin \alpha;$$

$$\operatorname{tg} \alpha = \frac{n - m}{m + n - 2} \operatorname{tg} \beta;$$

$$\left| \frac{\ddot{\xi}_{01}}{\ddot{\xi}_{02}} \right|^2 = m;$$

$$\left| \frac{\ddot{\xi}_{03}}{\ddot{\xi}_{02}} \right|^2 = n;$$

$$R \Delta l = \beta.$$

Vibration damping is

$$\text{ВИ} = -10 \lg (1 - \gamma^2 + \gamma \sqrt{\gamma^2 - 1}). \qquad (13.9.5)$$

The success of this method depends on how carefully the vibration receivers are calibrated and on how closely the useful signal corresponds to the ideal signal.

Input Mechanical Impedance Method. This method is based on a change of the input mechanical impedance of a semi-infinite rod when a barrier is placed on it. If an electrodynamic driver is used for measuring mechanical impedance the desired vibration damping is

$$\text{ВИ} = 10 \lg \left| \frac{\gamma\beta}{\sin \alpha} \right|, \qquad (13.9.6)$$

where

$$\gamma = \left| \frac{\ddot{\xi}_{m0}}{\ddot{\xi}_0} \right|;$$

$$\beta = \frac{\omega M}{Z_0 F};$$

APPROVED FOR RELEASE: 2007/02/08: CIA-RDP82-00850R000200100009-9

APPROVED FOR RELEASE: 2007/02/08: CIA-RDP82-00850R000200100009-9

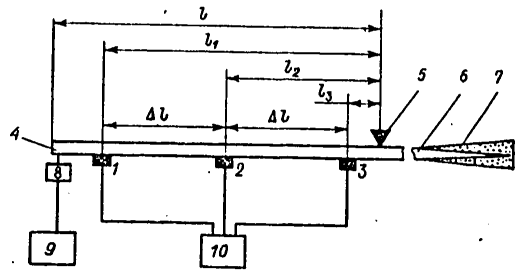

Figure 13.13. Measurement of vibration damping by triple point method: 1, 2, 3 -- vibration receivers; 4 -- rod; 5 -- analyzed barrier; 6 -- wedge; 7 -- sand; 8 -- vibrator; 9 -- acoustic generator; 10 -- vibration meter.

$\dot{\xi}_{m0}$ is the amplitude of the vibration velocity of the magnetic system of the electrodynamic driver; $\dot{\xi}_0$ is the amplitude of the vibration velocity of the rod at the point of excitation; M is the mass of the magnetic system of the electrodynamic driver; α is the phase shift between the vibrations of the magnetic system of the driver and the rod at the point of excitation; Z_{0F} is the characteristic impedance of the rod in relation to force.

With the "measuring rod" it is possible to measure the vibration damping of a barrier in relation to a plane elastic wave with normal incidence.

In the case of a diffuse vibration field a wide band is used (the width of the band is greater than the bending wavelength). One end of the band is deadened, i.e., it is immersed in sand or is faced with a vibration-absorbing coating. The analyzed barrier is placed in the middle of the band and vibrations are excited with band noise. This device can be used for measuring the vibration damping of a barrier by the following methods.

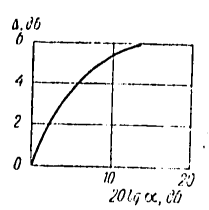

Figure 13.14. Δ as function of α.

Reverberation Method. The rate of decay (loss coefficient) of the amplitude of vibrations of the part of the plate in front of the barrier is measured after the driver is turned off. The vibration damping of the barrier is

[ВИ=VD; и=b]

$$\text{ВИ} = 10\lg\left[\frac{\lambda_{\text{и}}}{b\pi^2(\eta_\Sigma - \eta_1)}\right], \qquad (13.9.7)$$

where η_1 is the natural loss coefficient of the part of the plate in front of the barrier with no energy passing through it; η_Σ is the measured loss coefficient of the part of the plate

APPROVED FOR RELEASE: 2007/02/08: CIA-RDP82-00850R000200100009-9

APPROVED FOR RELEASE: 2007/02/08: CIA-RDP82-00850R000200100009-9

in front of the barrier in consideration of leakage of energy into the other plate. To obtain reliable results it is necessary to satisfy the condition $\eta_\Sigma \geq 2\eta_1$. Therefore this method cannot be used for measuring vibration damping exceeding 10-15 dB.

Vibration Level Gradient Method. The vibration VD, in dB, of a barrier is determined by the difference of the mean square level of the diffuse vibration field of plate 1 and the mean square level of the traveling vibration field of plate 2 by the expression

$$VD = 20 \log \alpha - \Delta,$$

where $\alpha = \left|\frac{\dot{\xi}_{1d}}{\dot{\xi}_{2m}}\right|$; Δ is determined by Figure 13.14.

The values $\dot{\xi}_{1d}$ and $\dot{\xi}_{2m}$ are found by algebraic averaging of the results of measurements of vibration velocity in at least five randomly selected places on the corresponding plate. This method is essentially analogous to the vibration level gradient method for normal incidence (see page 460), but in this case the maximum Δ does not exceed 3 dB (earlier it was 6 dB).

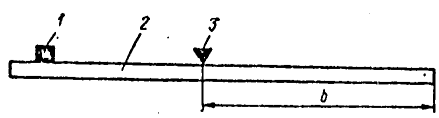

Figure 13.15. Setup for measuring vibration damping by mean square gradient of $\ddot{\xi}$: 1 -- vibrator; 2 -- plate; 3 -- tested barrier.

Mean Square Vibration Level Gradient Method. A setup for measuring vibration damping by this method is illustrated in Figure 13.15. A diffuse vibration field is excited in a plate by a third or half-octave noise signal. No special vibration damping measures are taken in the part of the plate behind the barrier, and a diffuse vibration field is generated in it. The mean square amplitudes of the vibrations in front of and behind the barrier (at at least five points in each case) and the loss coefficient behind the barrier are measured. The vibration damping VD, in dB, of the tested barrier is determined by the expression

$$\text{ВИ} = 10 \lg \frac{1}{\tau_{12}} = 10 \lg (\alpha - 1) + 10 \lg \frac{\lambda_{\text{и}}}{b} - 10 \lg \pi^2 \eta_2. \qquad (13.9.8)$$

where τ_{12} is the transmission coefficient; $\alpha = \left|\frac{\hat{\xi}_1^2}{\hat{\xi}_2^2}\right|$; λ_b is the bending wavelength; b is the distance between the barrier and the ends of the plate; η_2 is the loss coefficient in the plate after the barrier.

APPROVED FOR RELEASE: 2007/02/08: CIA-RDP82-00850R000200100009-9

APPROVED FOR RELEASE: 2007/02/08: CIA-RDP82-00850R000200100009-9

BIBLIOGRAPHY

1. "Antivibration Towers," IZOBRETATEL' I RATSIONALIZATOR [Inventor and Efficiency Analyst], 1964, No 6, pp 38-42.

2. Boroditskiy, L. S. and V. M. Spiridonov, "Snizheniye Strukturnogo Shuma v Sudovykh Pomeshcheniyakh" [Reduction of Structural Noise in Ship Compartments], Leningrad, Sudostroyeniye, 1974.

3. Vozhzhova, A. I. and V. K. Zakharov, "Zashchita ot Shuma i Vibratsii na Sovremennykh Sredstvakh Transporta" [Protection from Noise and Vibration in Modern Transportation], Leningrad, Meditsina, 1968.

4. Lyapunov, V. T. and A. S. Nikiforov, "Vibroizolyatsiya v Sudovykh Konstruktsiyakh" [Vibration Damping in Ship Structures], Leningrad, Sudostroyeniye, 1974.

5. Nikiforov, A. S. and S. V. Budrin, "Rasprostraneniye i Pogloshcheniye Zvukovoy Vibratsii na Sudakh" [Propagation and Absorption of Acoustic Vibration on Ships], Leningrad, Sudostroyeniye, 1968.

6. Yanke, Ye. and F. Emde, "Tablitsy Funktsiy s Formulami i Krivymi" [Tables of Functions with Formulas and Curves], Moscow, Fizmatgiz, 1959.

APPROVED FOR RELEASE: 2007/02/08: CIA-RDP82-00850R000200100009-9

APPROVED FOR RELEASE: 2007/02/08: CIA-RDP82-00850R000200100009-9

CHAPTER 14. VIBRATION ABSORPTION ON SHIPS

14.1. Absorption of Vibration Energy in Deformable Media and Structures

We shall examine the basic laws of absorption of energy of elastic vibrations by way of example of a system with one degree of freedom. The equation of its motion under the influence of a harmonic force with amplitude F_0 may be expressed as

$$m\ddot{x} + \bar{c}x = F_0 \sin\omega t, \tag{14.1.1}$$

where m is mass; $\bar{c}$ is complex elasticity, equal to $\bar{c} = c(1 + j\eta)$*; η is the loss coefficient.

The solution of (14.1.1) for the case of free vibrations ($F_0 = 0$) is

$$x(t) = x_0 e^{j\sqrt{\frac{\bar{c}}{m}}t} \approx x_0 e^{j\omega_0^* t - \delta t} = x_0 e^{j\sqrt{\omega_0^2 - \delta^2}t} e^{-\omega_0 \frac{\eta}{2} t}, \tag{14.1.2}$$

where ω_0^* and ω_0 are the free vibration frequencies of the system with and without losses, respectively; δ is the attenuation constant of the system.

As can be seen, the free vibrations of a system cease faster as the loss coefficient increases.

The loss coefficient η is related to the absorption coefficient ψ ($\psi = V_{ab}/V_{pot}$, where V_{ab} is the energy absorbed in a system in a vibration period; V_{pot} is the maximum potential energy of the system, equal to $V_{pot} = x_0^2 c/2$; x_0 is the amplitude of induced vibrations of the system) by the relation

$$\eta = \frac{\psi}{2\pi} = \frac{2\delta}{\omega_0}. \tag{14.1.3}$$

*See the footnote on page 397.

APPROVED FOR RELEASE: 2007/02/08: CIA-RDP82-00850R000200100009-9

APPROVED FOR RELEASE: 2007/02/08: CIA-RDP82-00850R000200100009-9

Thus, the loss coefficient physically determines the energy absorbed in a system in approximately 1/6 of a period. Sometimes the logarithmic decrement of vibrations is used:

$$d = \pi\eta. \tag{14.1.4}$$

Equations (14.1.3) and (14.1.4) are valid for $\eta^2 \ll 1$. For larger values of η the relation between d and η becomes more complicated [5]:

$$\eta = \frac{2d}{\sqrt{4\pi^2 + d^2}}. \tag{14.1.5}$$

The loss coefficient is related to the Q-factor of a system as

$$\eta = 1/Q. \tag{14.1.6}$$

Consequently, the frequency band $\Delta\omega$, on whose boundaries the amplitude of vibrations in a system is $\sqrt{2}$ times less than the maximum amplitude x_0 (Figure 14.1), may be expressed through the loss coefficient:

$$\Delta\omega = \frac{\omega_0}{Q} = \omega_0\eta. \tag{14.1.7}$$

The vibration velocity of a system on frequency $\omega = \omega_0$ is

$$\dot{x}_0 = \frac{\omega_0 F_0}{\eta c} \tag{14.1.8}$$

and consequently it decreases as the loss coefficient increases.

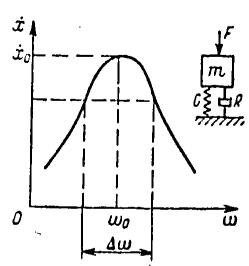

Figure 14.1. Amplitude of vibration velocity as function of driving force (system with one degree of freedom).

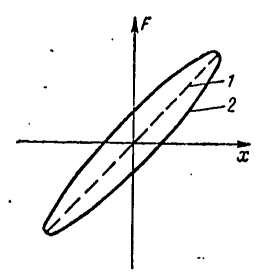

Figure 14.2. Displacement as function of driving force on resonance frequency (system with one degree of freedom). 1 -- $\eta = 0$; 2 -- $\eta \neq 0$.

In the absence of losses the function x(F) in coordinate system x, F is a straight line (Figure 14.2). In the presence of losses this function becomes an ellipse, the area of which is equal to the work done in the system in a given period:

APPROVED FOR RELEASE: 2007/02/08: CIA-RDP82-00850R000200100009-9

APPROVED FOR RELEASE: 2007/02/08: CIA-RDP82-00850R000200100009-9

$$s_{el} = \pi x_0^2 c\eta. \qquad (14.1.9)$$

The absorption of vibration energy in deformable elastic media (plates, rods, etc.) is complicated, but it is still similar to the phenomenon examined above by way of example of a system with one degree of freedom. Let us examine the causes of absorption of energy in deformable elastic media.

1. Viscous (fluid) friction. It is caused by friction between particles of a substance, and it increases with the relative velocity of the particles. Since this velocity increases with frequency the viscous loss coefficient increases accordingly.

2. Mechanical hysteresis (solid friction). When a force acts upon an elastic medium irreversible microchanges of the structure occur in the latter (rotation and breakdown of crystals in metals, separation of fibers in wood, etc.). As a result, when the force is released residual deformation appears, which in a periodic process leads to a phase lag of the deformation in relation to the stress that caused it. A hysteresis relationship exists between them and acquires the form of a loop in the stress-deformation plane. For small deformations this loop is an ellipse. In this case the hysteresis constant (the ratio of residual deformation to the maximum displacement) is equal to the loss coefficient. In ideal hysteresis (residual deformation is not a function of time) the hysteresis constant, and consequently the corresponding loss coefficient, are not functions of frequency.

3. Plastic flow. In a creeping material residual deformation is proportional to the time of application of force. Since the time of application of periodic force is proportional to the period the loss coefficient in plastic flow is inversely proportional to frequency.

4. Relaxation. In a relaxing medium with constant deformation the stress that causes the deformation gradually diminishes. As a result a phase shift appears between the stress and the deformation and, as a consequence, vibration energy is absorbed in the medium. Relaxation occurs as a result of a change of molecular structure, excitation of molecules, equalization of the temperatures between portions of the medium with opposite signs of deformation, etc. The maximum intensity of relaxation processes and the corresponding maximum loss coefficient occur in a frequency range where the vibration period is comparable with the relaxation constant.

The loss coefficients of the above-mentioned types are plotted in Figure 14.3 as functions of frequency.

All the described types of losses of vibration energy occur in any material, and one of them usually dominates, depending on the properties of the material.

APPROVED FOR RELEASE: 2007/02/08: CIA-RDP82-00850R000200100009-9

APPROVED FOR RELEASE: 2007/02/08: CIA-RDP82-00850R000200100009-9

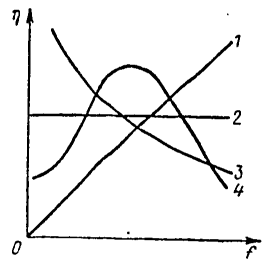

Figure 14.3. Loss coefficients of deformable elastic medium as functions of frequency: 1 -- liquid losses; 2 -- solid losses; 3 -- plastic creep; 4 -- losses due to relaxation.

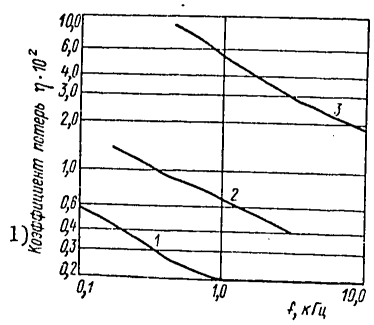

Figure 14.4. Loss coefficients of various structures: 1 -- steel ship; 2 -- duralumin ship; 3 -- electric motor. [кГц=kHz]
Key: 1. Loss coefficient $\eta \cdot 10^2$

The characteristic materials of ship structures (steel, duralumin) have a loss coefficient of the order of 10^{-4}. The values of the same coefficient for ship structures made of the mentioned materials are substantially higher (Figure 14.4) and are of the order of 10^{-2}-10^{-3}. The reason is that the basic losses in such structures occur in places where individual elements are fastened together. As can be seen in Figure 14.4, losses in ship structures on low frequencies are caused by the plasticity of the material in the indicated connections. The loss curve on high frequencies is the hysteresis curve.

The loss coefficients in structures of ship machinery are an order of magnitude greater than the loss coefficient of a ship's hull (see Figure 14.4).

14.2. Hard Vibration-Absorbing Coatings

Hard vibration-absorbing coatings, first developed by G. Oberst, and in our country by B. D. Tartakovskiy, are a layer of stiff plastic, applied on a structure to be damped. The structure of the coating and the character of its deformation when the damped plate bends are shown in Figure 14.5. As can be seen, the deformation of the coating appears as expansion and compression in the direction of its plane.

The loss coefficient of a plate faced with a hard vibration-damping coating is approximated by the formula [17]:

$$\eta = \frac{\eta_2 \alpha_2 \beta_2 (\alpha_2^2 + 12\alpha_{21}^2)}{1 + \alpha_2 f_2 (\alpha_2^2 + 12\alpha_{21}^2)}, \qquad (14.2.1)$$

APPROVED FOR RELEASE: 2007/02/08: CIA-RDP82-00850R000200100009-9

APPROVED FOR RELEASE: 2007/02/08: CIA-RDP82-00850R000200100009-9

where η_2 is the loss coefficient of the material of the coating; $\alpha_2 = t_2/t_1$; $\beta_2 = E_2/E_1$; $\alpha_{21} = t_{21}/t_1 = 1 + \alpha_2/2$; t_1, t_2 are the thicknesses of the deformed plate and of the coating; E_1, E_2 are the Young's moduli of the deformed plate and coating; t_{21} is the distance between the neutral planes of the plate and coating.

Formula (14.2.1) is valid for the practical condition $\beta_2 << 1$. As can be seen by this formula, the loss coefficient of a plate with a hard coating increases with the product $\eta_2 E_2$, which is called the loss modulus.

The loss coefficient of a plate with a hard coating is plotted in Figure 14.6 as a function of the ratio of the thickness of the coating to the thickness of the plate α_2. As this ratio increases, clearly, loss coefficient η also increases asymptotically to the loss coefficient η_2 of the coating material. As α_2 continues to increase η ceases to increase. The reason is that the neutral plane of the compound plate shifts toward the coating, and strain deformation of the coating and the absorption of energy in it decrease correspondingly. In practice the values of α_2 are limited to the order of $\alpha_2 = 1.5$-2.

If a liner of lightweight and hard material is inserted between the layer of rigid plastic and damped plate strain deformation of the plastic will increase and the loss coefficient in the plate will increase accordingly. To effectively transmit strain deformation to the plastic layer the liner material must have sufficient shear modulus, corresponding to the condition

[и=b]

$$G_2 \geqslant 10 E_3 t_3 t_1 k_{\text{н}}^2, \qquad (14.2.2)$$

where E_3, t_3 are the Young's modulus and thickness of the plastic layer; k_b is the bending wave number of the vibrations of the damped plate.

It follows from formula (14.2.2) that when the frequency increases this condition is violated. This is the result of an increase of shear deformation of the liner and corresponding reduction of strain deformation of the plastic layer.

Special materials based on polyvinyl chloride and other polymers have been developed for hard vibration-absorbing coatings. Plasticizers are added to the polymers to impart the necessary properties in the required temperature range, and fillers are added (graphite, mica, etc.) for improving absorption properties. Heat insulation and finishing materials may also be used as hard vibration-absorbing coatings. They are substantially inferior, of course, to the special materials in terms of vibration-absorbing capacity.

APPROVED FOR RELEASE: 2007/02/08: CIA-RDP82-00850R000200100009-9

APPROVED FOR RELEASE: 2007/02/08: CIA-RDP82-00850R000200100009-9

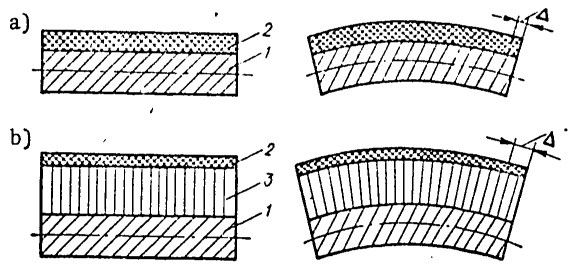

Figure 14.5. Structure of hard vibration-absorbing coating (left) and nature of its deformation (right): a -- hard coating; b -- hard coating with liner. 1 -- damped plate; 2 -- vibration-absorbing material (plastic); 3 -- liner; Δ -- deformation of vibration-absorbing material.

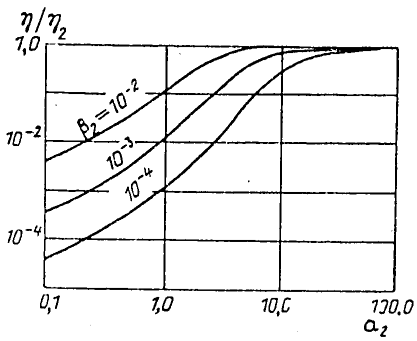

Figure 14.6. Reduced loss coefficient η/η_2 of plate faced with hard vibration-absorbing coating as function of thickness ratio of coating and plate $\alpha_2 = t_2/t_1$ for different ratios $\beta_2 = E_2/E_1$.

Loss modulus ηE of materials for hard coatings usually depends to a great extent on temperature. This relationship is plotted in Figure 14.7 for Antivibrit-2 material [16]. As can be seen, its acoustic effectiveness is high in the temperature range to approximately 30°C and is maximum near +20°C.

The physicochemical properties of special and other materials that can be used in shipbuilding for hard vibration-absorbing coatings are listed in Table 14.1. Special materials obviously produce the best results. Antivibrit-2 vibration-absorbing mastic, as calculation by formula (14.2.1) shows, gives a lined plate a loss coefficient of about 0.1 for the ratio $\alpha_2 = 1.5$. When linoleum is used as a hard vibration-absorbing coating the loss coefficient in the plate will be more than an order of magnitude lower.

PKhV-1 foam plastic is used as a liner for a hard coating. The data are: $G = 4 \cdot 10^6$ N/m^2, $\rho = 10^{-4}$ kg/m^3, $\eta = 0.04$.

APPROVED FOR RELEASE: 2007/02/08: CIA-RDP82-00850R000200100009-9

APPROVED FOR RELEASE: 2007/02/08: CIA-RDP82-00850R000200100009-9

Table 14.1. Characteristics of Materials for Hard Vibration-Absorbing Materials

1) Материал	2) Вид материала	3) Температура максимальной эффективности, °С	4) Коэффициент потерь η	5) Модуль Юнга $E \cdot 10^8$, Н/м²	6) Модуль потерь $E\eta \cdot 10^8$, Н/м²	7) Плотность, ρ, г/см³
8) Линолеум ПХВ	9) Листовой	—	0,03	1,18	0,054	—
10) «Нева»	11) Мастика	—	0,016	4	0,064	—
12) «Агат»	9) Листовой	20	0,25	20	5	1,35
13) «Антивибрит-2»	11) Мастика	20	0,6	50	30	—
«Антивибрит-1»	11) Мастика	20	0,5	30	15	—

Key: 1. Material
2. Kind of material
3. Temperature of maximum effectiveness, °C
4. Loss coefficient η
5. Young's modulus $E \cdot 10^8$, N/m²
6. Loss modulus $E\eta \cdot 10^8$, N/m²
7. Density ρ, g/cm³
8. PKhV linoleum
9. Sheet
10. "Neva"
11. Mastic
12. "Agat"
13. "Antivibrit- "

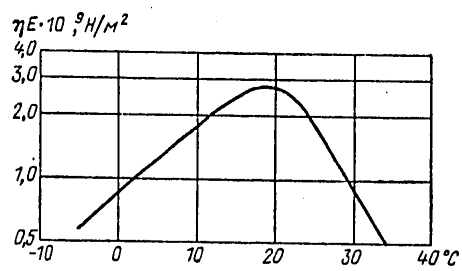

Figure 14.7. Loss modulus ηE of Antivibrit-2 vibration-absorbing mastic as function of temperature.

The technology used for applying a hard coating depends on the properties of the coating. Sheet materials are applied with cement (of the PN-E type in particular), and mastics are sprayed or plastered, which in many cases is technologically more convenient. Coatings are applied on a grounded surface.

Hard vibration-absorbing coatings are discussed in greater detail in the literature [17].

APPROVED FOR RELEASE: 2007/02/08: CIA-RDP82-00850R000200100009-9

APPROVED FOR RELEASE: 2007/02/08: CIA-RDP82-00850R000200100009-9

14.3. Soft Vibration-Absorbing Coatings

A soft vibration-absorbing coating [9] is a layer of viscoelastic material that is easily compressed in thickness. Losses of vibration energy in such a coating are attributed to deformations that occur during the propagation of an elastic wave in the direction of the thickness of the coating. This wave is created by transverse displacements of the bending-vibrating-damped plate.

The loss coefficient in a plate covered with a soft vibration-absorbing coating is described by the expression [17]

$$\eta = \frac{\eta_2 [2 \operatorname{sh}(\nu_2\eta_2) - \eta_2 \sin(2\nu_2)]}{2\chi\eta_2\nu_2 [\cos(2\nu_2) + \operatorname{ch}(\nu_2\eta_2)] + \eta_2 \sin(2\nu_2) + 2 \operatorname{sh}(\nu_2\eta_2)}, \qquad (14.3.1)$$

where η_2 is the loss coefficient of the coating; $\chi = m_1/m_2$; $\nu_2 = k_2t_2$; $k_2 = \omega/c_2$; m_1, m_2 are the masses of the plate and coating, expressed per unit area; c_2 is the velocity of an elastic wave through the thickness of the coating.

The typical dependence of the loss coefficient, calculated by formula (14.3.1), is shown in Figure 14.8. This figure, and an analysis of expression (14.3.1), show that on frequencies

[p=r]

$$f_{p\,n} = \frac{2n-1}{4t_2} c_2 \quad (n = 1, 2, 3, \ldots) \qquad (14.3.2)$$

the loss coefficient has maximums. These frequencies correspond to resonance longitudinal vibrations of a rod with length t_2 made of a material for which $c_{r.lo} = c_2$. The value of η_2 on frequencies $f = f_{r\,n}$ is

$$\eta_{p\,n} = \frac{\eta_2}{1 + \chi\eta_2\nu_{p\,n} \operatorname{th}\left(\frac{\nu_{p\,n}\eta_2}{2}\right)}. \qquad (14.3.3)$$

The maximum value of η_{rn} corresponds to n = 1:

$$\eta_{max} = \eta_{p1} = \frac{\eta_2}{1 + 1{,}23\chi\eta_2^2}. \qquad (14.3.4)$$

On antiresonance frequencies

[ap=ar]

$$f_{ap\,n} = \frac{nc_2}{2t_2} \quad (n = 1, 2, 3, \ldots) \qquad (14.3.5)$$

we have

$$\eta_{ap\,n} = \frac{\eta_2}{1 + \chi\eta_2\nu_{ap.\,n} \operatorname{cth}\left(\frac{\nu_{ap\,n}\eta_2}{2}\right)}. \qquad (14.3.6)$$

APPROVED FOR RELEASE: 2007/02/08: CIA-RDP82-00850R000200100009-9

APPROVED FOR RELEASE: 2007/02/08: CIA-RDP82-00850R000200100009-9

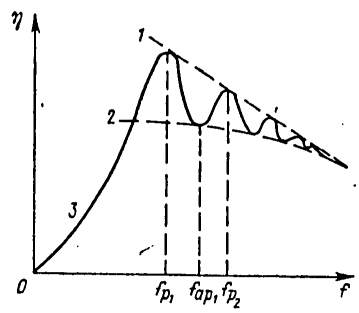

Figure 14.8. Loss coefficient of soft vibration-absorbing coating as function of frequency. 1 -- according to formula (14.3.3); 2 -- according to formula (14.3.6); 3 -- according to formula (14.1.3). [p=r; ap=ar]

On low frequencies ($\nu_2 << 1$)

$$\eta \approx \frac{\eta_2 \nu_2^2}{3(1+\chi)}, \tag{14.3.7}$$

and on high frequencies

$$\eta \approx \frac{\rho_2 c_2}{\omega m_1}, \tag{14.3.8}$$

where ρ_2 is the density of the material of the coating.

In the latter case all the energy radiated by the damped plate into the coating is entirely absorbed in it. The optimum value of η_2, for which η is maximum, is

$$\eta_{2\,opt} = \frac{0{,}9}{\sqrt{\chi}}. \tag{14.3.9}$$

Frequency f_{r1} can be reduced by increasing the thickness of the coating t_2 and by decreasing the value of c_2. The latter is done either by forming in the material of the coating air cavities [9], or by adding to it heavy metal particles [22]. The dimensions of the cavities and particles should be much smaller than wavelength $\lambda_2 = c_2/f$ on the highest frequency, where the coating is required to be effective.

A soft vibration-absorbing coating, in contrast to other types of coatings, effectively damps longitudinal and shear vibrations of plates, since shear waves are excited in the coating. Therefore the loss coefficient of a coating in the case at hand can be calculated by the formulas derived above, in which is substituted $c_2 = c_{s2}$, where c_{s2} is the velocity of shear waves in the material of the coating.

APPROVED FOR RELEASE: 2007/02/08: CIA-RDP82-00850R000200100009-9

APPROVED FOR RELEASE: 2007/02/08: CIA-RDP82-00850R000200100009-9

14.4. Reinforced Vibration-Absorbing Coatings

Reinforced vibration-absorbing coatings are layers of viscoelastic material, over which is applied a thin reinforcing layer. The structure of a reinforced coating and the nature of its deformations on a damped plate in bending vibrations are illustrated in Figure 14.9.

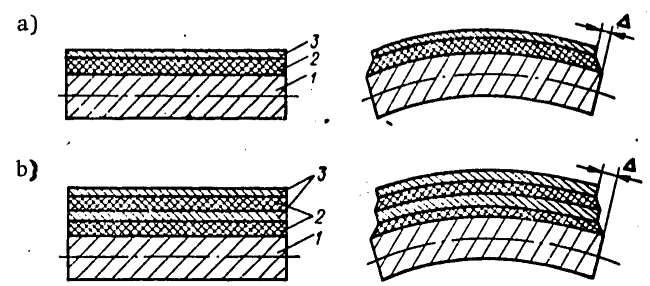

Figure 14.9. Structure of reinforced vibration-absorbing coating (left) and nature of deformations (right): a -- single reinforced coating; b -- laminated reinforced coating. 1 -- damped plate; 2 -- viscoelastic layer; 3 -- reinforcing layer; Δ -- deformation of vibration-absorbing material.

The absorption of vibration energy in a reinforced coating is attributed to the shear deformation of the reinforcing layer. Rubber or rubbery plastic are usually used as such a layer.

The loss coefficient η of a plate lined with reinforced vibration-absorbing coating is determined by the formula [16]

$$\eta = \frac{\eta_2 \gamma g_2}{(1+g_2)^2 + \eta_2^2 g_2^2 + \gamma g_2 [1 + g_2 (1+\eta_2^2)]}, \qquad (14.4.1)$$

where η_2 is the loss coefficient of the viscoelastic material;

$$\gamma \approx 12\alpha_{31}^2 \alpha_3 \beta_3; \qquad (14.4.2)$$

[и=b]

$$g_2 = \frac{G_2}{E_3 t_2 t_3 k_{н1}^2}; \qquad (14.4.3)$$

$\alpha_3 = t_3/t_1$; $\alpha_{31} = \alpha_2 + \alpha_3/2 + 1/2$; $\alpha_2 = t_2/t_1$; $\beta_3 = E_3/E_1$; t_1, t_2, t_3 are the thicknesses of the plate, viscoelastic and reinforcing layers; E_1, E_2, E_3 are the Young's moduli of the plate, viscoelastic and reinforcing layers; G_2 is the shear modulus of the viscoelastic layer.

APPROVED FOR RELEASE: 2007/02/08: CIA-RDP82-00850R000200100009-9

APPROVED FOR RELEASE: 2007/02/08: CIA-RDP82-00850R000200100009-9

The dependence of the loss coefficient η on the thickness of the layers of the coating and damped plate is determined by the value of γ, sometimes called the geometric parameter of the coating. The frequency dependence of η is determined by the shear parameter g_2, which, as can be seen by formula (14.4.3), is inversely proportional to frequency.

The loss coefficient of a plate, lined with a reinforced coating, is plotted in Figure 14.10 as a function of the frequency-dependent parameter g_2 for $\eta_2 = 1$. It is important to remember that an increase of g_2 corresponds to a decrease of frequency. There obviously exists a frequency f_{opt}, on which the loss coefficient of a plate is maximum. As frequency deviates from this frequency the value η decreases monotonically. It is also obvious that an increase of parameter γ leads to an increase of the loss coefficient η of a plate.

For

$$g_{2\,opt} = \frac{1}{\sqrt{(1+\gamma)(1+\eta_2^2)}} \tag{14.4.4}$$

the loss coefficient acquires the maximum value

$$\eta_{max} = \frac{\eta_2\gamma}{\gamma + 2\left(1 + g_{2opt}^{-1}\right)}. \tag{14.4.5}$$

The frequency corresponding to g_{2opt} is

$$f_{opt} = \frac{G_2 t_1}{2\pi E_3 t_2 t_3}\sqrt{\frac{E_1(1+\gamma)(1+\eta_2^2)}{12\rho_1}}, \tag{14.4.6}$$

where ρ_1 is the density of the material of the plate.

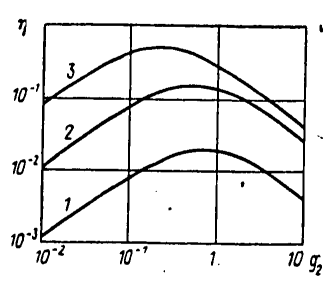

Figure 14.10. Loss coefficient of plate faced with reinforced vibration-absorbing coating as function of parameter g_2 for $\eta_2 = 1$. 1 -- $\gamma = 0.1$; 2 -- $\gamma = 1$; 3 -- $\gamma = 10$.

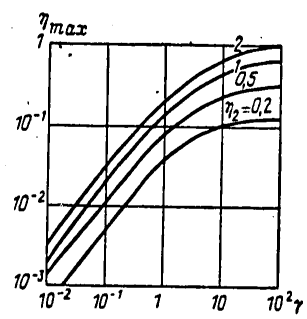

Figure 14.11. Maximum loss coefficient of plate η_{max}, lined with reinforced coating, as function of parameter γ.

APPROVED FOR RELEASE: 2007/02/08: CIA-RDP82-00850R000200100009-9

APPROVED FOR RELEASE: 2007/02/08: CIA-RDP82-00850R000200100009-9

The dependence of η_{max} on the parameter γ is plotted in Figure 14.11 for different values of η_2. As can be seen η_{max} ceases to increase when parameter γ reaches the value $\gamma \approx 10$. The figure also shows that it is not desirable to increase the loss coefficient of the viscoelastic material η_2 above $\eta_2 = 1$.

Rubbers with oil-resistant and other necessary operational properties are used as viscoelastic layers. A sticky viscoelastic material, which also functions as a bond between the damped plate and reinforcing layer, is also used occasionally for this purpose. Reinforcing coatings of this kind, called "damping tape," are used abroad.

Several layers of reinforced coating are applied on a damped plate to increase the loss coefficient. A coating of this kind, called Poliakril-V [4], is used on ships. It represents alternating layers of viscoelastic material made of acrylic polymer with a thickness of 0.12-0.2 mm, reinforced with 0.06 mm thick aluminum foil. The loss coefficient of a coating with a relative mass of 0.4-0.5, applied on a lightweight alloy plate, is about 0.1 in the 50-10,000 Hz frequency range.

Reinforced vibration-absorbing coatings are discussed at greater length in the literature [17].

14.5. Vibration-Absorbing Construction Materials

Vibration-absorbing construction materials have built-in losses. Therefore there is no need to apply vibration-absorbing coatings on structures made of these materials. Vibration-absorbing construction materials include so-called laminated materials, consisting of two metal plates (usually of the identical thickness), bonded with viscoelastic cement. They are called "sandwiches" in the foreign technical literature. Sound-insulating hoods, lightweight partitions, pylons and other elements of hull structures with a small static load can be manufactured in shipbuilding from this type of construction material.

The structure and nature of the deformation of a viscoelastic layer on materials in bending vibrations are illustrated in Figure 14.12. As can be seen, the viscoelastic material here, just as in reinforced vibration-absorbing coatings, experiences shear deformation.

The loss coefficient of a symmetric laminated construction material ($t_1 = t_3$) can be determined by the formula [6]

$$\eta = \frac{2\eta_2 g\gamma}{1 + 2g(2+\gamma) + 4g^2(1+\gamma)}, \qquad (14.5.1)$$

where $g = G_2(E_1 t_1 t_2 k_b^2)^{-1}$ is the shear parameter; η_2, G_2 are the loss coefficient and shear modulus of the viscoelastic material; $\gamma = 3(\frac{t_2}{t_1} + 1)^2$

APPROVED FOR RELEASE: 2007/02/08: CIA-RDP82-00850R000200100009-9

APPROVED FOR RELEASE: 2007/02/08: CIA-RDP82-00850R000200100009-9

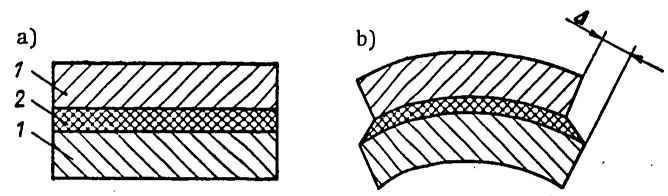

Figure 14.12. Structure of laminated vibration-absorbing material without (a) and with (b) deformation: 1 -- metal plates; 2 -- viscoelastic material; Δ -- deformation of viscoelastic material.

is a geometric parameter; t_1, t_2 are the thicknesses of the metal and viscoelastic layers; E_1 is the Young's modulus of the material of the metal plates; k_b is the bending wave number of vibrations in a structure, which is approximately $k_{b\,1}$.

Formula (14.5.1) is valid for $E_1 t_1 \gg E_2 t_2$.

An analysis of formula (14.5.1) shows that the dependence of the loss coefficient η on frequency peaks at

$$g_{opt} = \frac{1}{2\sqrt{1+\gamma}}, \tag{14.5.2}$$

and the peak value is

$$\eta_{max} = \frac{\eta_2 \gamma}{2\sqrt{1+\gamma}+2+\gamma}. \tag{14.5.3}$$

To the value of the shear parameter described by formula (14.5.2) corresponds the frequency

$$f_{opt} \approx \frac{G_2\sqrt{1+\gamma}}{\pi t_2 \sqrt{12 E_1 \rho_1}}. \tag{14.5.4}$$

Formulas (14.5.3) and (14.5.4) can be used to select the parameters of a construction material such that it will produce the maximum effect on a given frequency, usually 1 kHz.

The dependence of η_{max} on γ is plotted in Figure 14.13 for different η_2. As can be seen, when $\gamma \approx 3$ $\eta_{max} = \eta_2/3$. We note that γ = 3 corresponds to the practical structures in which $t_2 \ll t_1$.

The metal of which a laminated material is made may be steel or duralumin. The frequency dependence of the loss coefficient of laminated material made of 1.5 mm thick duralumin and a viscoelastic layer of ML-25 mastic

APPROVED FOR RELEASE: 2007/02/08: CIA-RDP82-00850R000200100009-9

APPROVED FOR RELEASE: 2007/02/08: CIA-RDP82-00850R000200100009-9

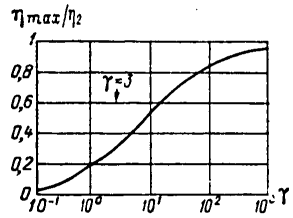

Figure 14.13. Reduced maximum loss coefficient of laminated vibration-absorbing material as function of geometric parameter γ.

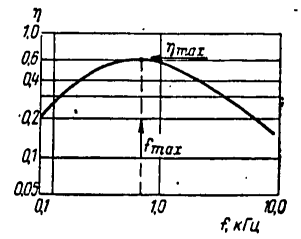

Figure 14.14. Loss coefficient of laminated vibration-absorbing material made of duralumin and ML-25 mastic.

($C_2 = 2 \cdot 10^7$ N/m^2, $\eta_2 = 1.13$) [6] is given in Figure 14.14. As can be seen, the loss coefficient of this laminated material is extremely high ($\eta_{max} = 0.6$) and peaks at $f_{opt} = 800$ Hz.

14.6. Bulk Vibration Absorbers and Bituminous Damping Materials

Bulk Vibration Absorbers. The high internal friction of bulk materials, their cheapness and ease of application (with a binder), as fillers for various kinds of tubular and box-beam bearing structures makes these materials extremely promising for use on ships as vibration absorbers [18]. Their application in bearing structures of ship machinery has proved to be effective [13, 19].

Curves of the loss coefficients of a steel plate with a layer of sand of varying thickness, plotted by I. I. Klyukin and A. I. Kurbatov, are shown in Figure 14.15. The thickness of the plate is 6 mm and the dimensions in plan are 100 × 50 cm. The measurement method was reverberation. The measurement apparatus differed from setups of this kind [8] in that it incorporated digital computer technology, which automated the measurement process.

The figure shows that the loss coefficient of sand in the high acoustic frequency range is greater than in the medium frequency range. When the ratio of the thickness of the sand layer to the plate thickness $h_p/h_{lay} > 2$-3 increases one can no longer count on a considerable increase of vibration absorption.

Analogous studies of sandblasted iron shot, 0.5-0.6 mm in diameter, disclosed that the effectiveness of vibration absorption provided by it was an average of 10% less than the effectiveness of sand. When shot is used there is less possibility of foreign particles getting into running parts of machinery when accidental damage occurs to the protective coating of

APPROVED FOR RELEASE: 2007/02/08: CIA-RDP82-00850R000200100009-9

APPROVED FOR RELEASE: 2007/02/08: CIA-RDP82-00850R000200100009-9

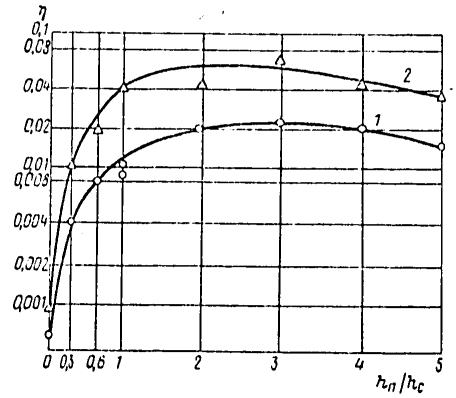

Figure 14.15. Loss coefficients of steel plate with layer of sand, averaged in two frequency ranges, as functions of ratio of thickness h_{lay} of the layer to plate thickness h_p. 1 -- 200-1,600 Hz; 2 -- 1,600-12,800 Hz. [п=p; c=lay]

bulk vibration absorbers. The mass of the shot fill is 2-3 times greater, depending on the packing tightness, than the mass of sand fill, which in some cases may be useful for increasing the vibration insulation of shock absorbers that rest on a damped structure.

The structure of a welded tube frame, damped with sand or shot, is illustrated in Figure 14.16. The use of sand produced 3-4 dB vibration attenuation of the base of the frame on 300 Hz and 5-6 dB on 3 Hz, in comparison with an undamped frame.

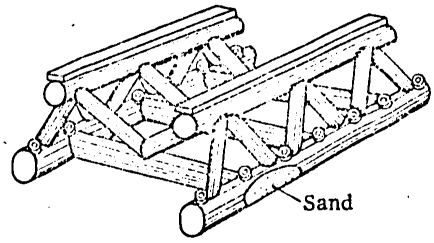

Figure 14.16. Tubular truss frame for auxiliary ship machine, damped with bulk filler.

Damping Compositions Containing Bulk Materials. The loss coefficient of a steel plate, damped with a layer consisting of a mixture (50% by volume) of sand and crushed foam plastic, is plotted in Figure 14.17 as a function

APPROVED FOR RELEASE: 2007/02/08: CIA-RDP82-00850R000200100009-9

APPROVED FOR RELEASE: 2007/02/08: CIA-RDP82-00850R000200100009-9

of vibration frequency. Curve 2 corresponds to the case when the surface of the bulk vibration absorber is exposed, and curve 3 to the case when the surface is covered with an extra metal plate (a sand-metal sandwich). A comparison of these curves with curve 1, corresponding to the case of the damping of a plate with a layer of pure sand, shows that when composite vibration absorbers are used the peak of vibration absorption is shifted toward lower frequencies. An increase of absorption on low frequencies presumably may be attributed to resonance vibration absorption, related to the interaction in the layer of the elastic elements (crushed foam plastic) and inertial elements (sand and metal).

The influence of a layer of sand over a coating of semihard rubber, applied on a metal sheet, on the loss coefficient of the sheet is illustrated in Figure 14.18. As the thickness of the sand layer increases, i.e., as its mass increases, the resonance frequencies of the resulting antivibration system decrease and the absorption on low frequencies increases, which agrees perfectly with the theory of resonant antivibration systems [10, 14]. We note that the loss coefficient of a damped plate on high frequencies remains quite high and reaches 0.1-0.2.

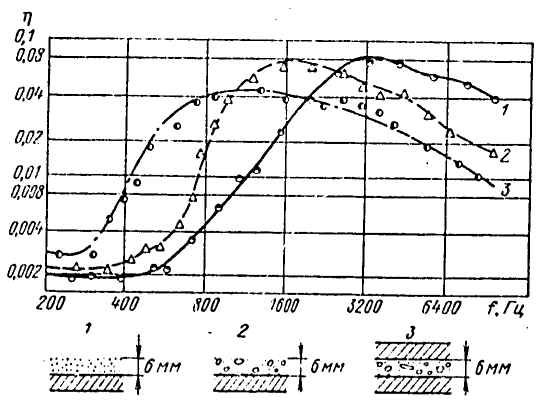

Figure 14.17. Loss coefficient of steel plate with different vibration-absorbing layers as function of vibration frequency: 1 -- steel plate with 6 mm thick sand layer, equal to the thickness of the plate; 2 -- plate with sand layer mixed with crushed hard foam plastic (50% by volume), layer and plate of equal thickness; 3 -- second steel plate placed over sand layer on plate (sand-metal "sandwich"). [Гц=Hz]

From the structural point of view rubber-sand compositions can be used both on flat metal structures (in "sandwich" form), and in tubular and box-beam profiles, where a rubber (or plastic) coating is applied on the inner wall

APPROVED FOR RELEASE: 2007/02/08: CIA-RDP82-00850R000200100009-9

APPROVED FOR RELEASE: 2007/02/08: CIA-RDP82-00850R000200100009-9

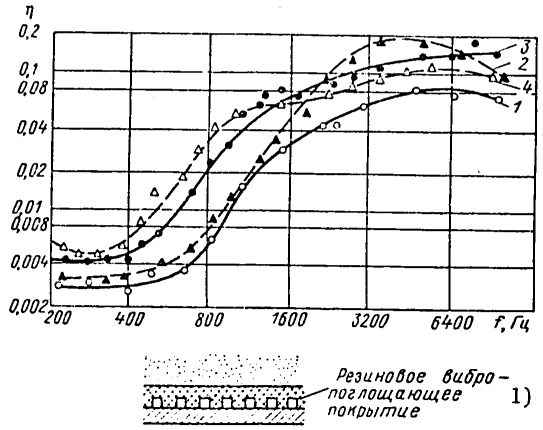

Figure 14.18. Loss coefficient of steel plate with rubber-sand compositions as function of vibration frequency: 1 -- plate with 8 mm thick rubber vibration-absorbing coating; 2 -- 76 mm thick sand layer over coating; 3 -- 12 mm thick sand layer over coating; 4 -- 18 mm thick sand layer over coating.
Key: 1. Rubber vibration-absorbing coating

of the profile. The coaxial elements of bearing structures can be made of telescoping tubes (with a hole through which sand can be poured) or of box-beams, on which a rubber or plastic coating is applied. The coating should not extend to the ends of the elements in order to prevent burning of the coating near the ends, where they are welded together in the bearing structure (as illustrated in Figure 14.16, for example). The bulk filler should be packed and covered with an asbestos plug at the lined (welded) ends of hollow elements.

Bituminous Vibration-Absorbing Materials. Bitumens have long been used for vibration-absorbing purposes [11, 21]. Ordinary construction bitumen is most often used. VNIIPKneftekhimii [not further identified] of the UkrSSR developed in recent years for the automobile industry bituminous compositions with high vibration-absorbing characteristics. One such material is Vibroplastbit, the raw material for which is straight-run tar from Eastern Ukrainian crudes. Another bitumen-base vibration-absorbing material -- VPM, includes bitumen-impregnated cardboard.

The frequency dependences of the loss coefficient of a metal plate with certain bituminous materials are compared in Figure 14.19 with the analogous dependence for a sheet metal reinforced rubber coating, also applied on a damping metal sheet. The thickness of the damped sheet is 6 mm, the thickness of the bituminous layers is 15 mm, and the thickness of

APPROVED FOR RELEASE: 2007/02/08: CIA-RDP82-00850R000200100009-9

APPROVED FOR RELEASE: 2007/02/08: CIA-RDP82-00850R000200100009-9

ON

BY

3 JULY 1980 I. I. KLYUKIN AND I. I. BOGOLEPOV 6 OF 6

APPROVED FOR RELEASE: 2007/02/08: CIA-RDP82-00850R000200100009-9

APPROVED FOR RELEASE: 2007/02/08: CIA-RDP82-00850R000200100009-9

the rubber layer of the reinforced coating is 8 mm; this coating, along with the reinforcing metal backing, was somewhat heavier in the described test than each of the investigated bituminous damping materials.

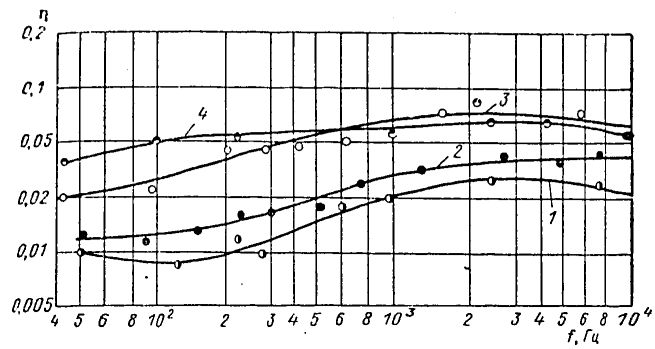

Figure 14.19. Loss coefficient of metal plate, damped with bituminous-base coatings and reinforced rubber coating: 1 -- construction bitumen; 2 -- Vibroplastbit; 3 -- VPM; 4 -- reinforced rubber coating.

An examination of the curves in Figure 14.19 shows that ordinary construction bitumen has the least damping effect, and VPM material has the greatest. The loss coefficient of sheet steel, lined with it, is the same as the loss coefficient of sheet with a reinforced rubber coating, beginning at frequencies of 200-300 Hz. A comparison with the curves in Figure 14.15 leads to the conclusion that the damping properties of bituminous materials are better on frequencies below 500-600 Hz than those of sand (this assumption is also valid in relation to a bulk vibration absorber such as small-diameter iron shot).

14.7. Local Vibration Absorbers

Antivibrators with One Degree of Freedom. The classic works of S. P. Timoshenko, D. Den-Hartog, et al, demonstrated the feasibility of using vibration absorbers for quieting down low-frequency vibrations of machines and their individual parts. Vibration dampers and antivibrators with an elastic rubber element for deadening the vibrations of plates, rods and ship hull structures in a wide frequency range have also been proposed [1, 10]. The theory of their action on the mentioned simplest elements -- plates and rods, is examined in the literature [2, 10, 14, 19]. Their effectiveness when installed on the frames or flanges of vibration-damped machinery at places where a shock absorber transmits vibrations (Figure 14.20) is examined below.

APPROVED FOR RELEASE: 2007/02/08: CIA-RDP82-00850R000200100009-9

APPROVED FOR RELEASE: 2007/02/08: CIA-RDP82-00850R000200100009-9

In the absence of an antivibrator (Figure 14.20a) the pattern of the vibrations of the frame or flange of a vibration-damped machine under the influence of vertical force F_0 can be expressed by the matrix equation

[ф=f]
$$\begin{bmatrix} F_0 \\ \dot{y} \end{bmatrix} = \begin{bmatrix} A_1 B_1 \\ C_1 D_1 \end{bmatrix} \begin{bmatrix} A_2 B_2 \\ C_2 D_2 \end{bmatrix} \begin{bmatrix} F_\phi - \dot{y}_\phi Z_\phi \\ \dot{y}_\phi \end{bmatrix}, \qquad (14.7.1)$$

where $\dot{y}$ is the vibration velocity of the frame; $\dot{y}_f$ is the vibration velocity of the foundation; Z_f is its impedance; F_f is the vibration force on it; A_1, B_1, C_1, D_1 are coefficients of the mechanical quadrupole corresponding to a frame (the same terms with the subscript 2 refer to shock absorbers).

It may be assumed on the basis of published data [19] that up to certain frequencies a frame is a concentrated mass m_{fr} (including the part of the mass of a machine that rests on one mount). Equation (14.7.1) is written in the form

[p=fr; am=sa]
$$\begin{bmatrix} F_0 \\ \dot{y} \end{bmatrix} = \begin{bmatrix} 1 & j\omega m_p \\ 0 & 1 \end{bmatrix} \begin{bmatrix} 1 & 0 \\ j\dfrac{\omega}{c_{aм}} & 1 \end{bmatrix} \begin{bmatrix} \dot{y}_\phi Z_\phi \\ \dot{y}_\phi \end{bmatrix}, \qquad (14.7.2)$$

where c_{sa} is the stiffness of the shock absorber; ω is the circular frequency of vibrations.

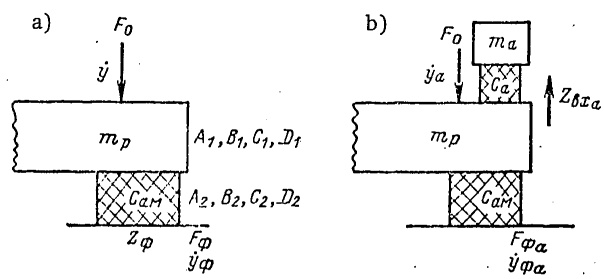

Figure 14.20. Determination of vibration-damping effect of local antivibrator with one degree of freedom on frame (flange) of machine: a -- system without antivibrator; b -- system with antivibrator. [p=fr; ф=f; вх=in; am=sa]

When a simple shock absorber with input impedance $Z_{in.a}$ is installed on a frame the equation

APPROVED FOR RELEASE: 2007/02/08: CIA-RDP82-00850R000200100009-9

APPROVED FOR RELEASE: 2007/02/08: CIA-RDP82-00850R000200100009-9

[вх=in;
p=fr; ф=f;
am=sa]

$$\begin{bmatrix} F_0 \\ \dot{y}_a \end{bmatrix} = \begin{bmatrix} 1 & Z_{\text{вх.а}} \\ 0 & 1 \end{bmatrix} \begin{bmatrix} 1 & j\omega m_p \\ 0 & 1 \end{bmatrix} \begin{bmatrix} 1 & 0 \\ j\dfrac{\omega}{c_{\text{аМ}}} & 1 \end{bmatrix} \begin{bmatrix} \dot{y}_{\text{фа}} Z_{\text{ф}} \\ \dot{y}_{\text{фа}} \end{bmatrix} \tag{14.7.3}$$

is valid, where the subscript "a" indicates the existence of a shock absorber in the system (see Figure 14.20a, b).

The input impedance of a shock absorber with mass m_a, natural frequency ω_{0a} and loss coefficient η_a in its elastic element is [10]

$$Z_{\text{вх.а}} = j\omega m_a \frac{\eta_a - j}{\eta_a + j\left[\left(\dfrac{\omega}{\omega_{0a}}\right)^2 - 1\right]}; \tag{14.7.4}$$

From equations (14.7.1)-(14.7.3) in consideration of expression (14.7.4) it is possible to find the effectiveness of the vibration absorption of a shock absorber with one degree of freedom on a frame (flange) of a damped machine ΔL, in dB, as

$$\Delta L = 20\lg\left|\frac{\dot{y}}{\dot{y}_a}\right| - 20\lg\left|\frac{\dot{y}_{\text{ф}}}{\dot{y}_{\text{фа}}}\right| = 20\lg\frac{\sqrt{M^2 + N^2}}{\left|m_p + m_{\text{ф}} - \left(\dfrac{f}{f_0}\right) m_{\text{ф}}\right| \left\{\eta_a^2 + \left[\left(\dfrac{f}{f_a}\right)^2 - 1\right]\right\}} \tag{14.7.5}$$

where $\dot{y}_{f.a}$, $F_{f.a}$ are the vibration velocity and force on the foundation with a shock absorber with mass m_a:

$$M = m_a\left(\frac{f}{f_{0a}}\right)\left[1 - \frac{\omega^2 m_{\text{ф}}}{c_{\text{аМ}}}\right];$$

$$N = \left\{m_{\text{ф}}\left[1 - \left(\frac{f}{f_0}\right)^2\right] + m_p\right\}\left\{\eta_a^2 + \left[\left(\frac{f}{f_{0a}}\right)^2 - 1\right]^2\right\} + m_a\left[\left(\frac{f}{f_{0a}}\right)^2 - 1 - \eta_a\right]\left(\frac{\omega^2 m_{\text{ф}}}{c_{\text{аМ}}} - 1\right);$$

$f_0 = \frac{1}{2\pi}\sqrt{\frac{C_{\text{аМ}}}{m_0}}$ is the natural frequency of mass m_{fr} on a shock absorber with elasticity c_{sa}; f_{0a} is the natural frequency of the shock absorber.

The results of calculation of the effectiveness of the vibration damping of a foundation (and frame) with a rubberized metal shock absorber are presented in Figure 14.21. The raw data for the calculation are: mass of the frame (and part of the machine) per shock absorber and antivibrator 50 kg; mass of foundation m_f = 100 kg; natural frequency of shock-absorbing mount f_0 = 13 Hz; stifness of each shock absorber C_{sa} = 350,000 N/m; loss

APPROVED FOR RELEASE: 2007/02/08: CIA-RDP82-00850R000200100009-9

APPROVED FOR RELEASE: 2007/02/08: CIA-RDP82-00850R000200100009-9

coefficient of antivibrator $\eta_a = 0.1$; the other data on the antivibrator are given in the key.

As can be seen in Figure 14.21, the antivibrator exerts much of its effect primarily on its own natural frequency. But in addition to this maximum there is an additional maximum on lower frequencies. An effect can also be observed between them, i.e., the antivibrator behaves as a more or less wide-band device. The effect of vibration damping increases with the mass of the antivibrator.

Such sharp peaks should not be expected in the curves of the acoustic effectiveness of a real antivibrator, as in the theoretical curves. The flattening of the curves of vibration damping of a real antivibrator is attributed both to the existence of losses in the shock absorbers and foundation that are not taken into account in the given calculation, and to the fact that a real antivibrator is a system with six degrees of freedom, the effects in which will be superimposed one on the other.

Experimental Data. To determine the acoustic characteristics of antivibrators one may use a test stand, such as the one schematically depicted in Figure 14.22. It is a plate (12 mm thick), installed on shock absorbers. The shock absorbers are fastened through a welded intermediate foundation to rails in the concrete bed of the test stand. The antivibrator is installed on a plate over the shock absorbers; the plate is driven by a vibrator, which develops a force with constant frequency (using a compression circuit). Additional weights, simulating machines of different weights, may be placed on the plate if needed.

A sample of the spectrograms that were recorded is presented in Figure 14.23. As can be seen by the figure, the effect of the vibration damping of an antivibrator (the difference of the ordinates of the curves) is manifested not only on the natural vertical frequency of the antivibrator (85 Hz), but also on frequencies above and below that frequency due, in particular, to the absorption of vibration in other degrees of freedom of the antivibrator.

The characteristics of antivibrators, in which the elastic elements are the familiar AKSS shock absorbers, are presented in Table 14.2. Data on the impedance and weight of the antivibrators may be used for selecting the necessary degree of vibration damping in bearing structures with different mechanical impedances.

Multielement Antivibrator. An antivibrator with three independent absorbing elements, the frequencies of which are separated relative to each other, is illustrated in Figure 14.24. The input impedance of this kind of antivibrator, consisting of n elements, is

APPROVED FOR RELEASE: 2007/02/08: CIA-RDP82-00850R000200100009-9

APPROVED FOR RELEASE: 2007/02/08: CIA-RDP82-00850R000200100009-9

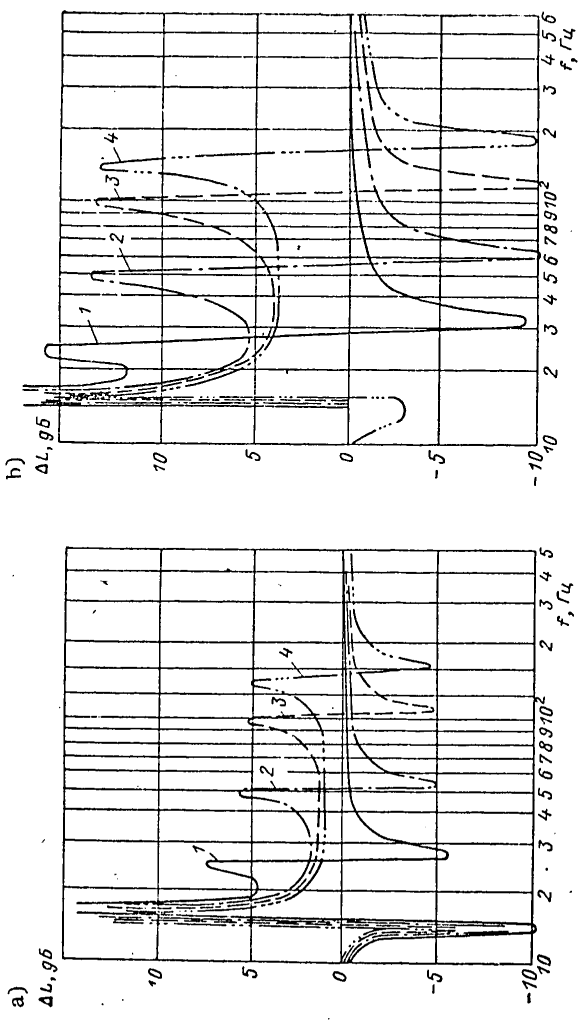

Figure 14.21. Calculated vibration damping of frame (flange) of damped machine by antivibrators with one degree of freedom. Mass of antivibrator 5 kg (a) and 20 kg (b), natural frequencies of antivibrators: 1 -- f_{0a} = 25 Hz; 2 -- f_{0a} = 50 Hz; 3 -- f_{0a} = 100 Hz; 4 -- f_{0a} = 150 Hz; other data presented in text. [gб=dB; Гц=Hz]

APPROVED FOR RELEASE: 2007/02/08: CIA-RDP82-00850R000200100009-9

APPROVED FOR RELEASE: 2007/02/08: CIA-RDP82-00850R000200100009-9

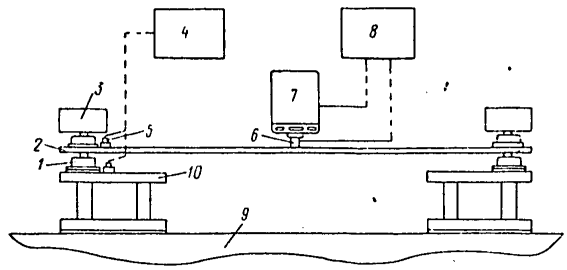

Figure 14.22. Experimental setup for studying vibration-damping effect of antivibrators: 1 -- shock absorber; 2 -- steel plate simulating frame of machine; 3 -- test antivibrator; 4 -- electronic circuit for measuring and analyzing vibrations; 5 -- vibration meter; 6 -- force transmitter; 7 -- vibrator; 8 -- excitation circuit; 9 -- foundation of stand; 10 -- intermediate (mounting) foundation.

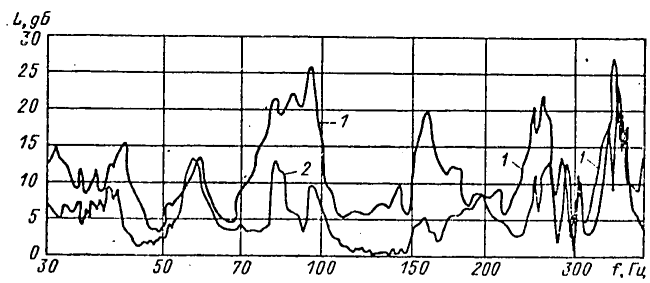

Figure 14.23. Vibration spectra of test foundation under vibration-damped plate: 1 -- plate without antivibrator; 2 -- antivibrators installed on plate under shock absorbers (f_{0a} = 86 Hz). [дБ=dB; Гц=Hz]

[вх=in]

$$Z_{\text{вх.а}} = \sum_{i=1}^{n} Z_{\text{вх.а}\,i}, \qquad (14.7.6)$$

where $Z_{in.ai}$ is the input impedance of each of the elements on a given frequency in a given direction.

Experimental studies of a test specimen of an antivibrator disclosed that the vibration of a 2 mm thick plate is attenuated by (4-5)-(15-18) dB in the 100-3,000 Hz range. The attenuation in the bottom of that frequency range is attributed basically to the inertial reaction of the rather

APPROVED FOR RELEASE: 2007/02/08: CIA-RDP82-00850R000200100009-9

APPROVED FOR RELEASE: 2007/02/08: CIA-RDP82-00850R000200100009-9

Table 14.2. Characteristics of Antivibrators with AKSS Shock Absorbers

1) Марка амортизатора	2) Собственная частота вертикальных колебаний, Гц	3) Количество амортизаторов на один антивибратор	4) Общая динамическая жесткость, (Н/м)·10⁻⁶	5) Масса антивибратора, кг	6) Импеданс антивибратора на резонансе, (Н·с/м)·10⁻¹
АКСС-25И	25	1	0,6	31	3,2
АКСС-60И		1	1,0	89	9,2
АКСС-60И	50	1	1,0	10	14,0
АКСС-25М		1	1,1	11	15,4
АКСС-60И		2	2,0	20	28,0
АКСС-60М		1	2,2	22	30,8
АКСС-400И		1	5,7	53	74,3
АКСС-220М		1	9,8	100	140,0
АКСС-220И	100	1	3,9	10	28,0
АКСС-220И		2	7,9	20	55,9
АКСС-220М		2	19,6	50	140,0
АКСС-220М		4	39,2	100	280,0
АКСС-400М		3	42,7	107,5	301,0
АКСС-220М	150	1	9,8	11	45,9
АКСС-220М		2	19,6	22	91,8
АКСС-400М		3	56,9	64,5	270
АКСС-400М		4	42,7	48,3	198
АКСС-400М		6	86,3	97,6	409

Key: 1. Brand of shock absorber
2. Natural frequency of vertical vibrations, Hz
3. Number of shock absorbers per antivibrator
4. Total dynamic rigidity $(N/m)\cdot 10^{-6}$
5. Weight of antivibrator, kg
6. Impedance of antivibrator on resonance, $(N\cdot s/m)\cdot 10^{-1}$

[АКСС=AKSS; И=I]

massive hardware (bracket) of the antivibrator (the vibration-damping effect of masses is discussed below).

Multistage Antivibrator. Shock-absorbing elements in an antivibrator may, in principle, be installed not in parallel (in the mechanical sense) but in series (Figure 14.25). The input impedance of such an antivibrator, consisting of two identical stages, is

$$Z_{\text{вх.а}} \approx \frac{2-\left(\frac{\omega}{\omega_{0a}}\right)^2 - 2j\eta_a}{(1+j\eta_a) - 3\left(\frac{\omega}{\omega_{0a}}\right)^2 + 1 - 2j}, \qquad (14.7.7)$$

APPROVED FOR RELEASE: 2007/02/08: CIA-RDP82-00850R000200100009-9

APPROVED FOR RELEASE: 2007/02/08: CIA-RDP82-00850R000200100009-9

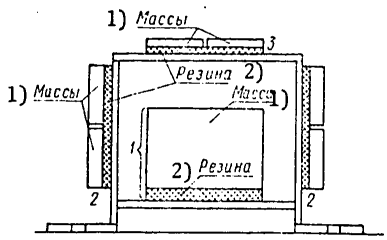

Figure 14.24. Multielement rubberized metal antivibrator: 1 -- low-frequency element; 2 -- elements tuned to intermediate frequencies; 3 -- high-frequency elements.
Key: 1. Weights
2. Rubber

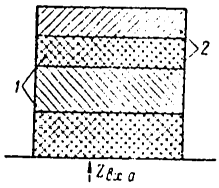

Figure 14.25. Two-stage antivibrator: 1 -- viscoelastic pads; 2 -- metal plates. [вх=in]

where, as before, ω_{0a} is the natural circular frequency of one stage (antivibrator element) of the antivibrator, and η_a is its loss coefficient.

The results of calculation of ΔL for such an antivibrator show that although the frequency band of vibration damping is expanded in comparison with a single-element antivibrator, the expressions for the frequencies of maximum vibration damping are connected to each other, which greatly hampers their selection in comparison with the case when the antivibration elements have independent effects (see Figure 14.24.

Equifrequency Single-Element Antivibrator with Six Degrees of Freedom. According to the results of tests of rubberized metal antivibrators on frames and platforms of machines, when antivibrators are tuned to the frequency of the strong vertical component of vibration the required vibration-damping effect sometimes is not achieved, and strong vibrations are transmitted to the foundation through the shock absorbers. This may be the result of rotation vibrations on a given frequency.

A design of rubberized metal antivibrator, in which all six frequencies of free vibrations (three rotation and three reciprocating) are close to each other (equal at the limit), is illustrated in Figure 14.26. This antivibrator should absorb all forms of vibrations on a given frequency where it is installed on the frame or flange of a machine. The mass of the antivibrator is mounted on two rows of elastic pads, so designed as to separate connected vibrations in different degrees of freedom and approximately equalize the natural frequencies in these degrees of freedom. A device (coupling nut) with which the rotary stiffnesses of the elastic mount can be changed by changing the distance between the rubber elements and the center of inertia of the antivibrator mass, is used for fine-tuning

APPROVED FOR RELEASE: 2007/02/08: CIA-RDP82-00850R000200100009-9

APPROVED FOR RELEASE: 2007/02/08: CIA-RDP82-00850R000200100009-9

the frequencies of rotation vibrations. Another solution may be to install the antivibrator mass on inclined shock absorbers to equalize the natural frequencies in the six degrees of freedom [7, 12].

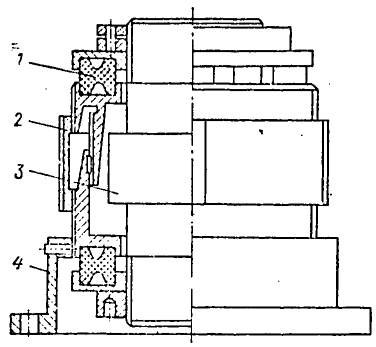

Figure 14.26. Rubberized metal equifrequency antivibrator: 1 -- rubber element; 2 -- double thread coupling nut for changing vertical arms of rubber elements relative to center of gravity of mass; 3 -- antivibrator mass; 4 -- antivibrator frame with mounting plate.

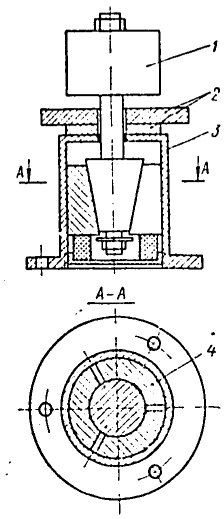

Figure 14.27. Surface friction antivibrator for damping reciprocating and rotating vibrations simultaneously: 1 -- weight applying uniform pressure on parts of piston against cylinder wall; 2 -- friction disks; 3 -- antivibrator case; 4 -- sectional piston.

A local antivibrator with surface (dry) friction is depicted schematically in Figure 14.27. Like the preceding antivibrator, it is used for absorbing all kinds of vibrations of the surface on which it is installed, and on different frequencies (because dry friction, as is known, occurs due to wide frequency range).

This antivibrator has sectional piston 4 for absorbing vertical vibrations. The piston, along with the inner surface of block 3, comprises a friction pair. A thrust cone with weight 1 installed on it exerts uniform pressure on the parts of the piston, holding them against the block. Horizontal reciprocating vibrations and rotary vibrations are absorbed by friction disks 2.

APPROVED FOR RELEASE: 2007/02/08: CIA-RDP82-00850R000200100009-9

APPROVED FOR RELEASE: 2007/02/08: CIA-RDP82-00850R000200100009-9

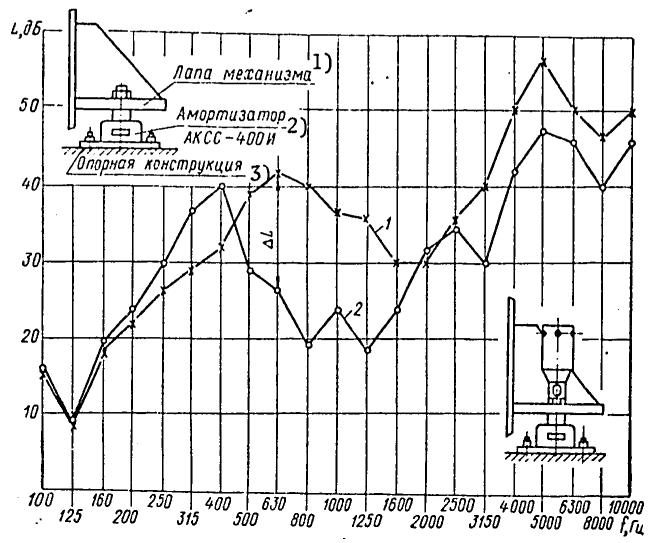

Figure 14.28. Effect of utilization of vibration-absorbing masses on flanges of damped marine refrigerator: 1 -- vibration levels in absence of masses; 2 -- vibration levels with masses in place (lower right).
Key: 1. Lug of machine
2. AKSS-400I shock absorber
3. Bearing structure
[ЭБ=dB; Гц=Hz]

For a machine with high-frequency vibrations concentrated masses may be an effective means of local vibration damping [11]. The spectrum of the vibration acceleration of a large ship refrigerator, installed on AKSS-400 shock absorbers (curve 1), is given in Figure 14.28. After a 15 kg weight was placed on each shock absorber the vibration decreased appreciably on high and middle frequencies (curve 2). The vibration damping ΔL of the foundation reaches 20 dB on some frequencies. The vibration through the spectrum was reduced by 10 dB on the average. The placement of the weight is shown in Figure 14.28 on the right. The hole in the bottom of the weight is used for inserting a vibration sensor, and the holes in the top are used for screwing the weight onto the mounting bolt.

14.8. Where to Install Vibration Absorbers in Ship Structures

General recommendations on the application of vibration-damping coatings on ships amount to the following.

Areas on which vibration-absorbing coatings are to be applied should be selected on the basis of an analysis of the distribution of acoustic

APPROVED FOR RELEASE: 2007/02/08: CIA-RDP82-00850R000200100009-9

APPROVED FOR RELEASE: 2007/02/08: CIA-RDP82-00850R000200100009-9

vibration levels through the hull of a ship and of propagation paths of vibration energy from sources (machines) to the rooms to be quieted.

To produce the desired effect the coating must be placed as close as possible to the acoustic vibration source. This reduces the noise in most of the rooms in which acoustic vibrations from a given source produce noise. For example, applying a coating on the foundations of machinery and second floor decking of the engine room, where the machinery is installed, is effective. At the same time, applying coatings on stringers and floors in the vicinity of the engine room does not produce much additional effect. If the noise in a particular room must be reduced the coating should be applied on the walls of the room, especially those that have the highest vibration levels. To reduce airborne noise in rooms over the engine department it is advisable to apply a coating on the deckhead, sides and bulkheads of the engine room. This has little effect, however, in rooms fore and aft of the engine room.

A general requirement on the choice of installation of a vibration-absorbing coating is the need to apply it on all vibration-conducting connections between machinery and rooms in which the noise level must be reduced. For example, it is useless to apply coating on individual hull structures between machinery and a noisy room without damping other structures near those that have been damped.

It is advisable to apply vibration-absorbing coatings on pipes that connect an acoustic vibration source (machine) and the walls of the engine room. Leaving these pipes uncoated can substantially reduce the effectiveness of the damping of foundation structures and of hull structures next to machinery.

Applying a vibration-damping coating on bulkheads of the engine room may produce a beneficial effect in relation to noise in adjacent rooms. This is because the acoustic insulation of the bulkheads is increased in the vicinity of the resonance frequency due to an increase of losses. Applying a vibration-absorbing coating on a vibrating machine may be effective, but the effect is manifested primarily on high frequencies.

For a comparative analysis of the effectiveness of the described techniques we will produce results obtained by means of electrical modeling of the hull of a ship [17]. It was assumed during measurements on the model that the machine (diesel engine) operates in the engine room. The effect of applying a vibration coating on various parts of the ship hull was determined in relation to the reduction of vibrations at two points on 10 kHz. The first point was in a room forward of the engine room, and the second was in a room directly over the engine room.

Applying a vibration-absorbing coating on the second floor of the engine room, on which the engine operates, reduces the vibration levels through

APPROVED FOR RELEASE: 2007/02/08: CIA-RDP82-00850R000200100009-9

APPROVED FOR RELEASE: 2007/02/08: CIA-RDP82-00850R000200100009-9

the entire hull of a ship by an average of 6 dB; applying coatings on stringers and floors in the engine room as well adds to that dampening effect only 2 dB.

The application of a coating on the bulkheads, sides and deckheads of the engine room reduces acoustic vibrations at the first point by an average of 3 dB, and at the second point by 10 dB. Lining the described parts of the hull with a coating reduces acoustic vibrations principally in rooms above the engine room. The coating applied on the deckhead of the engine room accounts for most of the effect (8 dB). In rooms distant from the engine room, fore and aft, the effectiveness of coating applied on the sides, bulkheads and ceiling of the engine room is not as appreciable (7 dB). The application of a coating directly on a bulkhead, the acoustic vibrations of which must be reduced, provides a local effect, equal to an average of 4 dB.

This example graphically illustrates the advantage of using an electrical model of a hull to determine the optimum places in a ship to install vibration damping. The results of measurement of the electrical modeling agree satisfactorily with measurements on ships.

14.9. Analysis of Effectiveness of Vibration Absorption Techniques in Ship Structures

The use of vibration-absorbing devices, as was pointed out in §14.1, increases the loss coefficient in a damped structure and reduces the amplitude of vibrations. Since the loss coefficient characterizes the absorption of energy in a vibrating system, it is convenient to determine the effectiveness of a vibration-absorbing device E, in dB, as the ratio of the mean square vibration velocities at a given point of the system, before and after application:

[Э=E]

$$Э = 10 \lg \frac{\langle \dot{\xi}_0^2 \rangle}{\langle \dot{\xi}^2 \rangle}. \qquad (14.9.1)$$

Since vibration-absorbing coatings are most often used in ship structures for damping, an analysis of the effectiveness of this vibration-absorbing technique is presented below. The effectiveness of a coating E, in dB, used for damping the vibrations of an individual plate, is

$$Э = 10 \lg \frac{\eta}{\eta_0}, \qquad (14.9.2)$$

where η and η_0 are the loss coefficients in the plate after the application of coating and before application. Here $\eta = \eta_p + \eta_0$, where η_p is the loss coefficient, contributed to the plate by the vibration-absorbing coating.

If a vibration-absorbing coating is applied on an isotropic (without obstacles or bending waves) plate between a source of vibration and a point of observation, the effectiveness of the coating at the point E, in dB, [17], is

APPROVED FOR RELEASE: 2007/02/08: CIA-RDP82-00850R000200100009-9

APPROVED FOR RELEASE: 2007/02/08: CIA-RDP82-00850R000200100009-9

[и=b]

$$Э = 13{,}5\,(\eta - \eta_0)\,\frac{l}{\lambda_и}, \qquad (14.9.3)$$

where l is the length of the lined part of the plate along a straight line, connecting the source and the observation point; λ_b is the bending wavelength in the plate.

The effect of applying a vibration-absorbing coating on a rod can also be determined by formula (14.9.3) if λ_b is assumed to be the bending wavelength in the rod.

When a vibration-absorbing coating is applied on ribbed structures (plates with stiffening ribs) the effectiveness at the point of observation E, in dB, [4] is

$$Э \approx 10{,}7\,\sqrt{\frac{l_0}{\alpha\lambda_и}}\,(\sqrt{\eta} - \sqrt{\eta_0})\,n, \qquad (14.9.4)$$

where l_0 is the frame spacing distance; n is the number of frame spaces between the vibration source and the point of observation, lined with the coating; α is the transmission coefficient of bending wave energy through a stiffening rib, equal for a diffuse wave field to $\alpha = 0.25$. The other symbols are the same as in the preceding formulas.

Formula (14.9.4) is valid for $2\eta l_0 \leqslant \alpha\lambda_b$. For estimations the effect of the vibration-absorbing coating of a ribbed plate may be assumed to be 1 dB per frame spacing. This corresponds to a frequency of 1 kHz, a plate thickness of 1 cm, a frame spacing distance of 50 cm and loss coefficient of 0.2.

Formula (14.9.4) shows that a change of these values in intervals that are experienced in practice has little effect on the indicated effect of a coating.

In real ship hull structures the vibration energy from the source reaches an observation point through several paths. Under these conditions formulas (14.9.3) and (14.9.4) are applicable if the vibration-absorbing coating is applied on the structures that form the shortest distance for vibrations between the source and point of observation, and if the attenuation of the amplitude of vibrations on the next longer path is greater than the next shorter path in consideration of the coating applied on it. Otherwise the effectiveness of vibration-absorbing coatings, as of other vibration-damping techniques, should be evaluated with the aid of an electrical model of the ship's hull, as is suggested in [17], or with an electronic digital computer [4].

APPROVED FOR RELEASE: 2007/02/08: CIA-RDP82-00850R000200100009-9

APPROVED FOR RELEASE: 2007/02/08: CIA-RDP82-00850R000200100009-9

14.10. Measurement of Vibration Absorption[1]

Vibration absorption measurement techniques are based on the determination of the loss coefficients in plates or rods, made of vibration-absorbing materials, or with vibration-absorbing coatings applied on them [8, 17].

Measurement of Width of Resonance Characteristic of Vibrating System. The loss coefficient in which we are interested is equal to the relative width of the resonance characteristic $\Delta f/f_0$ at the 0.707 level (-3 dB) of the maximum vibration velocity. This method is also applicable to the frequency characteristic of a mechanical structure.

This method gives high precision on several first resonance frequencies, where the density of resonances is low. To measure small loss coefficients it is necessary to prevent leakage of the vibration energy of the measured system through suspensions. To do this the mounts of the system being measured should be placed in the locations of the minimum vibration velocities (nodes) and be made as small as possible.

Pulse Method. In this method Fourier transforms are taken of the autocorrelation function of the reaction of a vibrating system to a pulse force. Vector diagrams (impedance hodograph) are constructed on the basis of the results. The loss coefficient is determined by the vector diagram. The method is convenient on frequencies up to 500-1,000 Hz using a computer.

Space Attenuation Method. The loss coefficient is determined by the expression

[и=b]

$$\eta = \frac{\Lambda_и \lambda_и}{13{,}5} \qquad (14.10.1)$$

on the basis of the attenuation of the vibration level per unit length (Λ_b) of a rod, on which a vibration coating is applied, and on the basis of bending wavelength λ_b. When waves are reflected from one end of the rod the pattern of the amplitude distribution along the rod appears similar to the one shown in Figure 14.29. The loss coefficient here is determined by subsequent processing of the amplitude distribution recording:

1) the envelope of the standing wave peaks is drawn (curve 1);

2) the envelope of the standing wave minima is drawn (curve 2);

3) the difference between curves 1 and 2 (h_1) is determined at several points;

4) the values of h_2, marked off from curve 1, are found on the graph in Figure 14.30.

[1]This section was written by S. V. Budrin.

APPROVED FOR RELEASE: 2007/02/08: CIA-RDP82-00850R000200100009-9

APPROVED FOR RELEASE: 2007/02/08: CIA-RDP82-00850R000200100009-9

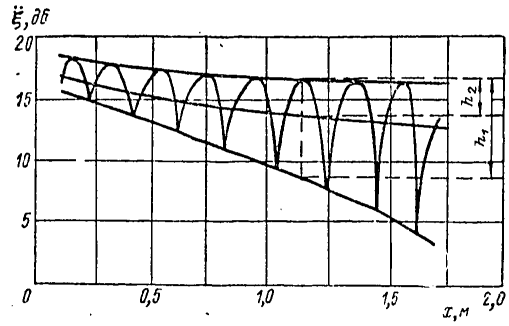

Figure 14.29. Determination of loss coefficient from space attenuation of vibrations of rod. [ЭБ=dB]

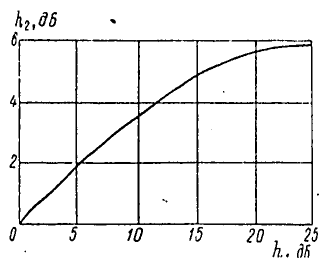

Figure 14.30. h_2 as function of h_1.

The points thus marked off should lie on a straight line (plotted in logarithmic scale). The slope of the line corresponds to the rate of attenuation in the absence of reflection from the end of the rod.

The space attenuation method should be used for measuring the loss coefficients of substantial magnitude on high frequencies.

Resonance Amplitude Method. In cases when the loss coefficients of a specimen must be measured on comparatively low acoustic frequencies and the specimen is small, the amplitude in resonance may be measured. To do this the specimen is rigidly fastened to the vibration source in order to prevent rotation at the fastening point. The other end of the specimen is free. The amplitude ratio of the vibrations of the free and driven ends in resonance (γ) will express the loss coefficient in accordance with the formula

$$\eta = 1{,}569\,|\gamma|^{-1} + 0{,}9615\,|\gamma|^{-3} + 0{,}8306\,|\gamma|^{-5}. \qquad (14.10.2)$$

Reverberation Method and Modifications. The reverberation method is more convenient for practical application. The advantages of this method are the wide range of measurable frequencies and loss coefficients, comparative simplicity, and its capability of best simulating the actual operating conditions of vibration-absorbing devices. In the reverberation method resonance vibrations are excited in the analyzed specimen or structure. Then excitation is terminated, after which the amplitude of vibrations of a specimen gradually decreases due to vibration absorption.

APPROVED FOR RELEASE: 2007/02/08: CIA-RDP82-00850R000200100009-9

APPROVED FOR RELEASE: 2007/02/08: CIA-RDP82-00850R000200100009-9

If the amplitude ratio is taken at moments of time t_1 and t_2, then

$$\eta = \frac{\lg \gamma}{1{,}35 f_0 \Delta t}, \qquad (14.10.3)$$

where $\gamma = \xi_1/\xi_2$; $\Delta t = t_2 - t_1$; f_0 is the frequency of vibrations.

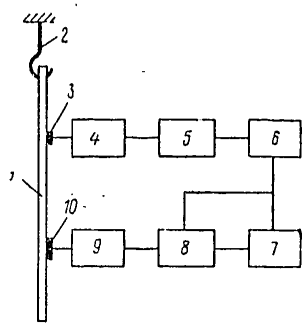

Figure 14.31. Measurement of loss coefficient by reverberation method: 1 -- test specimen; 2 -- suspension; 3 -- vibration receiver; 4 -- amplifier; 5 -- filter; 6 -- control unit; 7 -- oscillograph; 8 -- acoustic generator; 9 -- power amplifier; 10 -- vibrator.

A recording of attenuating vibrations, obtained from the level recorder or loop oscillograph, is used for measuring the loss coefficient by the reverberation method on low frequencies and when losses are small. If the loss coefficient is large the time constant of the mentioned recording instruments will not be sufficient for measurements. In these cases the pulse reverberation method is used and an electronic oscillograph is used as the recording instrument. A still picture of the attenuation of vibrations in the analyzed specimen appears on the screen of the oscillograph as a result of repetition of the excitation and attenuation process many times. A schematic diagram of the experimental setup is shown in Figure 14.31. The pulse reverberation method can offer several ways of determining the loss coefficient:

by the time of ten-fold attenuation of amplitude

$$\eta = \frac{0.735}{\Delta t f}; \qquad (14.10.4)$$

by the number of periods of attenuation of the amplitude of vibrations by a certain amount. If the number of periods n in which the amplitude increases by a factor of 22.4 is known, then

$$\eta = \frac{1}{n}; \qquad (14.10.5)$$

by comparing on the oscillograph screen the process of attenuation of the vibrations in a measured specimen with the DC voltage drop in an RC-circuit. Here the loss coefficient can be measured directly with the instrument that sets the RC value;

APPROVED FOR RELEASE: 2007/02/08: CIA-RDP82-00850R000200100009-9

APPROVED FOR RELEASE: 2007/02/08: CIA-RDP82-00850R000200100009-9

by the slope of the logarithm of the envelope of the attenuation process, which is proportional to the loss coefficient.

The last method is especially convenient for determining losses in connected vibration systems; a broken line appears on the oscillograph screen in this case. The loss coefficients of each individual system can be determined on the basis of the loss coefficients on the straight line parts of the curve.

BIBLIOGRAPHY

1. Alekseyev, A. M., I. I. Klyukin and A. K. Sborovskiy, "Vibration Damper for Attenuating Vibrations of Ship Hull," SUDOSTROYENIYE [Shipbuilding], 1961, No 12, pp 127-130.

2. Alekseyev, A. M. and A. K. Sborovskiy, "Sudovyye Vibrogasiteli" [Ship Vibration Dampers], Leningrad, Sudpromgiz, 1962.

3. Belyakovskiy, N. G., "Konstruktivnaya Amortizatsiya Mekhanizmov, Priborov i Apparatury na Sudakh" [Structural Vibration Damping of Machinery, Instruments and Hardware on Ships], Leningrad, Sudostroyeniye, 1965.

4. Boroditskiy, L. S. and V. M. Spiridonov, "Snizheniye Strukturnogo Shuma v Sudovykh Pomeshcheniyakh" [Reduction of Structural Noise in Ship Rooms], Leningrad, Sudostroyeniye, 1974.

5. Vyalyshev, A. I. and B. D. Tartakovskiy, "Vibrations of Systems with Large Losses," "Kolebaniya, Izlucheniye i Dempfirovaniye Uprugikh Struktur" [Vibrations, Emission and Damping of Elastic Structures], Moscow, Nauka, 1973, pp 27-29.

6. Gulyayev, V. A., "Laminated Construction Materials with High Losses," "Kolebaniya, Izlucheniye i Dempfirovaniye Uprugikh Struktur," Moscow, Nauka, 1973, pp 212-215.

7. Klyukin, I. I., "Shock-Absorbing Mount with Extremely Narrow Natural Frequency Range," "Trudy 7-y Vsesoyuznoy Akusticheskoy Konferentsii" [Proceedings of 7th All-Union Acoustics Conference], Izd-vo LKI, 1973.

8. Klyukin, I. I. and A. Ye. Kolesnikov, "Akusticheskiye Izmereniya v Sudostroyenii" [Acoustic Measurements in Shipbuilding], Leningrad, Sudostroyeniye, 1968.

9. Klyukin, I. I., "Method of Damping Vibration of Decking or Bulkheads in Ship Rooms," Patent No. 119084, priority 2 August 1947, published in BYULLETEN IZOBRETENIY [Bulletin of Inventions], 1969, No 7, p 61.

APPROVED FOR RELEASE: 2007/02/08: CIA-RDP82-00850R000200100009-9

APPROVED FOR RELEASE: 2007/02/08: CIA-RDP82-00850R000200100009-9

10. Klyukin, I. I., "On Attenuation of Bending Waves in Rods and Plates Using Resonance Vibration Systems," AKUSTICHESKIY ZHURNAL AN SSSR [Acoustics Journal of the USSR Academy of Sciences], 1960, No 2, pp 213-219.

11. Klyukin, I. I., "Vibration Absorption and Vibration Damping," "Bor'ba s Shumom" [Noise Control], edited by Ye. Ya. Yudin, Moscow, Stroyizdat, 1964.

12. Klyukin, I. I., "On One Kind of Shock-Absorbing Mount for Ship Machinery," SUDOSTROYENIYE, 1956, No 10, pp 48-50.

13. Kurnatov, V. D., "Mounting Frame with High Vibration Attenuation," SUDOSTROYENIYE, 1972, No 5, pp 40-41.

14. Lyapunov, V. T. and A. S. Nikiforov, "Vibroizolyatsiya v Sudovykh Konstruktsiyakh" [Vibration Damping in Ship Structures], Leningrad, Sudostroyeniye, 1974.

15. Naumkina, N. I., B. D. Tartakovskiy and M. M. Efrussi, "Two-Layer Vibration-Absorbing Structure," AKUSTICHESKIY ZHURNAL [Acoustics Journal], 1959, Vol 5, No 4, pp 498-499.

16. Naumkina, N. I., M. I. Paley and B. D. Tartakovskiy, "Polymer-Base Vibration-Absorbing Materials," "Vibratsii i Shumy" [Vibrations and Noises], Moscow, Nauka, 1969.

17. Nikiforov, A. S. and S. V. Budrin, "Rasprostraneniye i Pogloshcheniye Zvukovoy Vibratsii na Sudakh" [Propagation and Absorption of Acoustic Vibration on Ships], Leningrad, Sudostroyeniye, 1968.

18. Panenko, S. M., "Features of Noise Safety on Dredges 'Chernoye More' and 'Baltiyskoye More'," SUDOSTROYENIYE, 1967, No 2, p 28.

19. Popkov, V. I., "Vibrodiagnostika i Umen'sheniye Vibroaktivnosti Sudovykh Mekhanizmov" [Vibration Diagnosis and Reduction of Vibration Activity of Ship Machinery], Leningrad, Sudostroyeniye, 1974.

20. Skuchik, Ye., "Prostyye i Slozhnyye Kolebatel'nyye Sistemy" [Simple and Complicated Vibration Systems], Moscow, Mir, 1971.

21. Slavin, I. I., "Proizvodstvennyy Shum i Bor'ba s Nim" [Industrial Noise and How to Control It], Moscow, Profizdat, 1955.

22. Ungar, E. and E. Kerwin, "Plate Damping due to Thickness of Visco-elastic Layers," JASA, 1964, Vol 36, No 2, pp 386-394.

APPROVED FOR RELEASE: 2007/02/08: CIA-RDP82-00850R000200100009-9

APPROVED FOR RELEASE: 2007/02/08: CIA-RDP82-00850R000200100009-9

CHAPTER 15. FORECASTING OF ACOUSTIC SITUATION AND COMBINED APPLICATION OF NOISE CONTROL TECHNIQUES ON SHIPS

15.1. General Description of Problem

Measures to reduce noise on ships may be divided into three groups:

reduction of noise and acoustic vibration levels of sources;

design of efficient general layout plans;

application of ship structural noise control techniques (SNCT).

The first group includes, in particular, a variety of design and technological measures, aimed at weakening noisy processes and vibrations or their transmission for each specific type of source. Questions related to this subject are discussed in Chapters 5-9.

When selecting the types of ship machinery, units and systems the designer must consider their acoustical characteristics. It is entirely possible that a case may arise, when it is better to use a heavier or more expensive machine because it produces lower noise and vibration levels.

Meeting the acoustic requirements that are imposed on marine machinery and mechanisms is the objective of the initial stages of ship design.

The second group of measures also directly involves the early stages of the design of a ship. The acoustic requirements on the general layout amount to the fact that rooms with noise levels that must be brought within standards should be as far away as possible from the noise sources. Of course, rooms with the most rigid noise requirements must be the farthest. Uninhabited "buffer" rooms (storerooms, auxiliary social and service rooms) should be placed between noisy and quiet rooms. Also, an effort should be made to concentrate basic noise sources in one or a few zones. This not only helps to place quiet rooms farther from noise sources, but it also makes more economical utilization of ship structures for reducing noise.

APPROVED FOR RELEASE: 2007/02/08: CIA-RDP82-00850R000200100009-9

APPROVED FOR RELEASE: 2007/02/08: CIA-RDP82-00850R000200100009-9

During an examination of the problem of combatting noise on ships the basic content of the problem usually pertains to the third group of measures -- structural means of reducing noise. The basic ways of reducing airborne noise and vibration and the structural types and methods of calculating the systems that can be used are discussed in Chapters 10-14.

The required reduction of noise levels on ships usually cannot be achieved by using separate systems. Even the entire arsenal of existing techniques sometimes does not give the desired result. Since noise control measures add to construction costs and have some negative effect on the performance and technical characteristics of a ship, the planning process of a noise control complex always involves a search for the best compromise between the combinations of requirements on a ship and the practical possibilities for meeting them.

In principle there are two variations of the optimum complex:

one that provides a given amount of noise reduction in rooms at the optimum values of all other characteristics (for instance, minimum weight or cost);

one that provides the maximum acoustic effectiveness for prescribed values of other characteristics (for instance, for a given total additional weight of all other structural noise control systems).

The basic characteristics of a complex for technical-economic analysis of efficiency are: the acoustic effectiveness; additional structural weight for reducing noise; cost of measures for reducing noise during both construction and operation.

In addition to these basic characteristics it is also necessary to consider others: sacrifice of useful space; compliance with technical and health requirements and standards; technological suitability and performance reliability of structural noise control systems; requirements of technical esthetics, etc.

The development of an antinoise complex is based on an analysis of the acoustic situation on a ship, which is characterized by the following factors:

1) noise levels in all ship rooms in the inhabited zone;

2) health-hygiene requirements and standards for all ship rooms in accordance with their functional purpose and ship operating conditions;

3) contribution of individual sources of noise and acoustic vibrations to the noise level on a ship;

APPROVED FOR RELEASE: 2007/02/08: CIA-RDP82-00850R000200100009-9

APPROVED FOR RELEASE: 2007/02/08: CIA-RDP82-00850R000200100009-9

4) causes of high noise levels in different rooms for each noise and acoustic vibration source, i.e., the relation of individual components of the total acoustic field in different rooms from each noise source (see §15.2);

5) acoustic effectiveness (reduction of noise levels) of special noise control systems, used on a ship;

6) acoustic characteristics and effectiveness of individual structural general purpose systems (covers, liners, etc.), used on a ship.

15.2. Forecasting of Noise Level on Ship in Design Stage

The acoustic situation must be forecast during the design stage in order to develop a sound structural noise control technique complex. This can be done in two ways:

on the basis of test data on a prototype ship;

by analytical calculation on the basis of general relations, which permit various parameters to change in a wide range: acoustic characteristics of sources, general layout of ship rooms, design features of hull structures, liners, covers, etc.

The advantage of the first method is its comparative ease, but its capabilities are extremely limited, since it does not disclose the causes of high noise levels, and furthermore it is applicable only when the conditions of acoustic and structural similarity between the prototype and the planned ship are observed.

The best method of forecasting the acoustic situation is to calculate the noise levels. Its advantages are the following: the anticipated noise level can be estimated with or without an appropriate prototype; the influence of various factors on noise levels can be estimated; different versions of a planned ship and different versions of the noise control complex on it can be compared, and all the data needed for analyzing the causes of high noise level from each source are available.

The noise in a room can be caused by several phenomena: direct emission from sources near a room; penetration of noise from adjacent rooms through partitioning hull structures; radiation of sound by enclosing hull structures as a result of their vibration.

The levels of the first two components of noise are denoted by the subscript "a" -- L_a (airborne noise). The third component is the result of the radiation of sound by enclosing structures. The levels of this noise are denoted by the subscript "s" -- L_s.

APPROVED FOR RELEASE: 2007/02/08: CIA-RDP82-00850R000200100009-9

APPROVED FOR RELEASE: 2007/02/08: CIA-RDP82-00850R000200100009-9

There are primary L_{sp} and secondary L_{ss} noises, produced by vibrations of partitions. The first is caused by the propagation of primary acoustic vibration through hull structures directly from the source to the hull through main bearing and rigid nonbearing connections (for instance, through the foundation and plumbing of ship machinery). The second is related to secondary acoustic vibration, which occurs in the hull of a ship under the influence of noise on structures that surround the room containing the source (or exterior hull structures, if the noise source is external).

The relationship between the indicated noise levels depends on the type of noise source and on how far away a given room is from the noise source.

Screws may be assumed to be a source of only primary noise, i.e., in this case $L_{sp} >> L_a$ and $L_{sp} >> L_{ss}$ for all rooms. For the ventilation system, if standard shock absorbers are installed under the blowers and vibration-damping sections are installed in ventilation ducts, $L_a >> L_{sp}$. Ventilation shafts are also usually a source of just airborne noise ($L_a >> L_{sp}$), but in contrast to the ventilation system, it is necessary to consider here secondary noise as well, since the noise levels in shafts are high and shaft walls are usually rigidly connected to hull structures.

The exhaust system for most rooms is a source of airborne noise. However, it is important to remember that for rooms located near the duct work of the system noise produced by acoustic vibration, transmitted from the engine through the ducts, can also play an important part. Both the air intake and the exhaust are sources of external noise, which penetrates through exterior decking into rooms of the superstructure.

In spite of the variety of conditions that must be considered, general qualitative principles can be uncovered, which characterize the dependence of the influence of acoustic vibration on the distance between rooms and machinery [1].

From this standpoint all rooms are divided into three groups:

noisy rooms, in which noise sources are located; for these rooms usually $L_a >> L_{sp}$ and always $L_a >> L_{ss}$;

adjacent rooms, i.e., rooms that directly border on noisy rooms and are partitioned from them by hull structures;

distant rooms, separated from noisy rooms by one or several intermediate rooms ($L_a << L_{ss}$).

This classification is valid only in relation to one source or to a group of sources in the same room. Any given room can be in different groups for

APPROVED FOR RELEASE: 2007/02/08: CIA-RDP82-00850R000200100009-9

APPROVED FOR RELEASE: 2007/02/08: CIA-RDP82-00850R000200100009-9

different noise sources. In particular, an important external noise source for most ship rooms is the air distribution hardware of the ventilation system, while in relation to other basic sources most rooms are in the second or third group.

15.3. Basic Relations and General Calculation Procedure

Calculation of the anticipated noise level in the general case consists of the separate calculation of the components L_a, L_{sp} and L_{ss}. The calculation procedures should be examined in consideration of the specific features of the various groups of rooms, mentioned in §15.2.

Levels L_a in Source Room. For these rooms calculation amounts to the calculation of just this component, which can be done on the basis of simple relations:

[в=a; и=i; п=r]

$$L_в = L_и - \Delta L_п, \quad (15.3.1)$$

[дБ=dB]

$$\Delta L_п = 10 \lg \left[\frac{1}{4\pi r^2} + \frac{4}{Q} \right] + 5 \text{ дБ}, \quad (15.3.2)$$

where L_i are the initial noise levels near the source, dB; r is the distance betwee the source and calculation point, m; $Q = \frac{A}{1 - \alpha_{av}}$ is the constant of a room, m^2; A is the total sound absorption in a room; α_{av} is the average sound absorption coefficient for reflecting surfaces in a room.

Formula (15.3.2) is based on the assumption that initial levels L_i are measured at a distance of 0.5 m from the source, the source is small and the room is of sufficiently simple shape (without separate spaces). Formula (15.3.2) can be modified for three cases, when the described conditions are not satisfied.

Determination of Total Sound Absorption in Room. It is extremely difficult in practice to calculate the values of A as the sum of the sound absorptions of the reflecting surfaces in a room in consideration of all the machinery in it. Therefore it is recommended that this value be determined on the basis of empirical data in accordance with the type of room as follows:

$$A = \alpha_{red} S_r, \quad (15.3.3)$$

where α_{red} is the reduced average sound absorption coefficient, which can be found in Table 15.1 (based on G. S. Beregova's data); S_r is the total area of structures surrounding the room (decks, bulkheads, deckheads), m^2.

APPROVED FOR RELEASE: 2007/02/08: CIA-RDP82-00850R000200100009-9

APPROVED FOR RELEASE: 2007/02/08: CIA-RDP82-00850R000200100009-9

If a room is equipped with special sound-absorbing structures, characterized by acoustic absorption coefficient α_{st} and area S_{st}, the value of A should be calculated by the formula

[k=st; пр=red]

$$A = \alpha_к S_к + \alpha_{пр}(S_п - S_к) = \alpha_{пр} S_п + (\alpha_к - \alpha_{пр}) S_к. \quad (15.3.4)$$

The values of α are determined on the basis of data in Chapter 11.

The average acoustic absorption coefficient of a room in this case is determined by the formula

[cp=av]

$$\alpha_{ср} = \alpha_{пр} + (\alpha_к - \alpha_{пр}) \frac{S_к}{S_п} \quad (15.3.5)$$

Table 15.1. Reduced Acoustic Absorption Coefficients α_{red} for Different Rooms

1) Тип помещений	2) Частоты октавных полос, Гц							
	63	125	250	500	1000	2000	4000	8000
3) Румпельные и рефрижераторные отделения	0,04	0,06	0,08	0,10	0,13	0,15	0,18	0,20
4) Машинные, котельные и дизель-генераторные отделения	0,04	0,08	0,11	0,14	0,17	0,20	0,24	0,27
5) Кают-компании, столовые, салоны, посты и рубки	0,12	0,17	0,19	0,20	0,21	0,21	0,22	0,22
6) Кубрики и каюты	0,12	0,21	0,25	0,27	0,28	0,29	0,29	0,29

Key: 1. Type of room
2. Frequencies of octave bands, Hz
3. Tiller and refrigerator compartments
4. Engine, boiler and diesel-generator rooms
5. Mess rooms, dining rooms, salons, work stations and wheelhouses
6. Crew quarters and state rooms

Calculation of Levels L_{a2} for Contiguous Rooms. The calculations are done by the formula

[отв=hol]

$$L_{в2} = L_{в1} - R + \Delta R_{отв} + 10 \lg \frac{S}{A_2}, \quad (15.3.6)$$

where L_{a1} is the noise level near a partition on the noisy room side, in dB; R and S are the sound-absorbing capacity and area of the partition between the rooms, in dB and m^2; ΔR_{hol} is a correction factor for acoustic insulation, which takes into account the existence of slots and holes in the partition; A_2 is the total acoustic absorption in the contiguous room, in m^2.

APPROVED FOR RELEASE: 2007/02/08: CIA-RDP82-00850R000200100009-9

APPROVED FOR RELEASE: 2007/02/08: CIA-RDP82-00850R000200100009-9

R is determined by methods explained in Chapter 10.

If the partition is inhomogeneous in terms of area R should be reduced to some value for a conditionally homogeneous partition:

[пр=red]

$$R_{\text{пр}} = 10 \lg \sum_{i=1}^{i=n} \frac{S_i}{S \cdot 10^{0,1R_i}}, \qquad (15.3.7)$$

where n is the number of inhomogeneities (sections); S_i and R_i are the area and acoustic insulation capacity of the i-th section.

ΔR_{hol} can be found on the basis of experimental data [2].

Calculation of Acoustic Vibration Levels of Hull Structures. The practical methods of calculation are based on the energy interpretation of the process whereby acoustic vibrations propagate in the hull. Methods of calculating vibration levels in consideration of vibration damping and vibration absorption in hull structures, and also of the vibration damping of shock absorbers, are examined in Chapters 12-14.

On the assumption of a diffuse bending wave field [1, 3] within an individual enclosure[1], the energy density distribution is characterized by the following basic equation system:

[п=e]

$$\sum_{i=1}^{j=n_{\text{п}}} \alpha_{ij} w_i + \beta_i w_i - \sum_{j=1}^{j=n_{\text{п}}} \alpha_{ji} w_j = \sum_{k=0}^{k=K_i} W_{ik} \quad (i = 1, 2, 3, \ldots, n_{\text{п}}), \qquad (15.3.8)$$

where $w_i = \dot{y}_0 \cdot 10^{0,1N_i} \frac{\rho_i s_i}{2}$ is the vibration energy density on the i-th enclosure; $w_j = \dot{y}_0 \cdot 10^{0,1N_j} \frac{\rho_j s_j}{2}$ is the same on the j-th enclosure;

[и=b]

$$\alpha_{ij} = \frac{2\tau_{ij} l_{ij} c_{\text{и}i}}{\pi} = \frac{1\tau_{ij} l_{ij} c \sqrt{\varphi_i}}{\pi};$$

$$\alpha_{ji} = \frac{2\tau_{ji} l_{ji} c \sqrt{\varphi_j}}{\pi};$$

$$\beta_i = 2\pi S_i \eta_i f;$$

[1]An enclosure is defined as a section of the basic hull structure (second floor, deck, side, bulkheads) or a lightweight partition, bounded by a contour described by the intersection of this structure with adjacent structures, located in different planes. Examples of the partitioning of regions of a ship into enclosures are given in Figure 15.7.

APPROVED FOR RELEASE: 2007/02/08: CIA-RDP82-00850R000200100009-9

APPROVED FOR RELEASE: 2007/02/08: CIA-RDP82-00850R000200100009-9

$\dot{y}_0 = 5 \cdot 10^{-8}$ m/s; s_i, s_j are the thicknesses of the i-th and j-th enclosures; c_b is the phase velocity of bending waves; c is the speed of sound in air; $\phi_i = f/f_{i\ cr}$; $\phi_j = f/f_{j\ cr}$; $f_{i\ cr}$, $f_{j\ cr}$ are the critical frequencies of the i-th and j-th enclosures; l_{ij} - l_{ji} is the length of the total contour of the i-th and j-th enclosures; τ_{ij}, τ_{ji} are the coefficients of direct transmission and retransmission of the energy of bending waves from the i-th enclosure to the j-th through the corner connection between them; η_i is the loss coefficient of the i-th enclosure; W_{ik} is the power transmitted by the k-th vibration source to the i-th enclosure; K_i is the number of vibration sources installed on the i-th enclosure; n_e is the total number of enclosures.

Transmission coefficients τ_{ij} are determined for enclosures of homogeneous thickness by the following formula

$$\tau_{ij} = \tau_{0ij}\psi(b_{ij}). \qquad (15.3.9)$$

Here $\psi(b_{ij})$ is a function described by the curve in Figure 15.1 as a function of $b_{ij} = f_{i\ cr}/f_{j\ cr}$; τ_{0ij} is the transmission coefficient for normal incidence, calculated by the formula

$$\tau_{0ij} = \frac{2\beta_{ij}}{\left[1 + \sum_{q=1}^{q=M} (\beta_{ij})_q\right]^2}, \qquad (15.3.10)$$

where

[kp=cr] $$\beta_{ij} = \frac{\rho_j s_j}{\rho_i s_i}\left(\frac{f_{i\,\text{кр}}}{f_{j\,\text{кр}}}\right)^{3/2}.$$

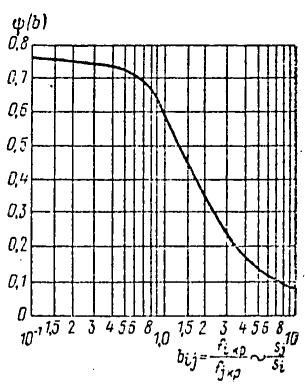

Figure 15.1. Curve of function $\psi(b)$. [kp=cr]

The value of β_{ij} for an examined enclosure, into which energy is transferred, must be substituted into the numerator of formula (15.3.10). In the denominator is the sum of values of β_{ij} for all the enclosures contiguous with the i-th enclosure in an examined corner. The number of terms in this sum depends on the type of corner connection: for a cross connection M = 3, for a T-connection M = 2, and for an L-connection M = 1.

APPROVED FOR RELEASE: 2007/02/08: CIA-RDP82-00850R000200100009-9

APPROVED FOR RELEASE: 2007/02/08: CIA-RDP82-00850R000200100009-9

For corners with vibration damping coamings τ_{ij} can be calculated by special formulas.

Loss coefficient η_i depends on losses in the main plating of the enclosure (η_{i0}) and on the effective (reduced to the main plating) additives due to covers ($\Delta\eta_{ic}$), liners ($\Delta\eta_{ilin}$) and radiation ($\Delta\eta_{rad}$), i.e.,

$$\eta_i = \eta_{i0} + \Delta\eta_{ic} + \Delta\eta_{ilin} + \Delta\eta_{irad}. \qquad (15.3.11)$$

The value of η_{i0}, and also of $\Delta\eta_{ic}$ for general purpose covers can be determined on the basis of experimental data, which are presented in Chapter 14. When special vibration-damping coatings are applied special calculation methods, presented in Chapter 14, must be used. The value $\Delta\eta_{ilin}$ is calculated by the formula

[э=lin]

$$\Delta\eta_{i\text{э}} = \eta_2 \frac{m_2}{m_1} \Omega(f), \qquad (15.3.12)$$

where m_1 is the mass per unit area of the main plating; m_2, η_2 are the mass and loss coefficient of a lining.

The function $\Omega(f)$ expresses the ratio of the squared amplitudes of the main plating and lining. It is most easily determined on the basis of empirical data.

In order to solve system (15.3.8) it is necessary to have data on the acoustic power of the vibration source. However, these data usually are not available. Therefore it is necessary to use another method to solve the problem, on the basis of the initial levels on individual enclosures. The enclosures are those that surround the source room. The set of enclosures must be taken into consideration when calculating secondary acoustic vibration. However, when calculating primary vibration the initial levels need be known only for one enclosure -- the mounting enclosure, on which a ship machine or other source of vibration is directly mounted. The mounting enclosure for a screw is a section of the outer bottom plating above the screw, bounded by transverse bulkheads and longitudinal bulkheads or sides.

To solve the problem the equations that correspond to enclosures with given initial levels are excluded from basic equation system (15.3.8). The corresponding columns in the remaining equations make up the right hand sides.

Vibration Levels of Mounting Enclosure. The initial vibration and acoustic characteristics of ship machinery are usually the vibration levels on flanges. To determine the vibration levels of a mounting enclosure it is necessary to consider the vibration damping of the foundation and shock

APPROVED FOR RELEASE: 2007/02/08: CIA-RDP82-00850R000200100009-9

APPROVED FOR RELEASE: 2007/02/08: CIA-RDP82-00850R000200100009-9

absorbers. The calculation procedures for them are examined in Chapter 12. For an ordinary bed plate vibration levels N_{r0} on the mounting enclosure at distance r_0 from the foundation in the middle of the plates separated from the foundation by one framing element, can be calculated on the basis of empirical relations (based on data of K. I. Mal'tsev and V. V. Chernoberevskiy):

[и=i; ф=f]

$$N_{r_0} = N_и - \Delta N_ф + \Delta, \qquad (15.3.13)$$

where N_i is the vibration level on the flanges; Δ is some variable, determined graphically (Figure 15.2) as a function of the frequency parameter $2f/(f_b + f_t)$, where f_b and f_t are the first components of the frequency of the smallest (plate B in Figure 15.3) and the largest (plate A) plates of the mounting enclosure.

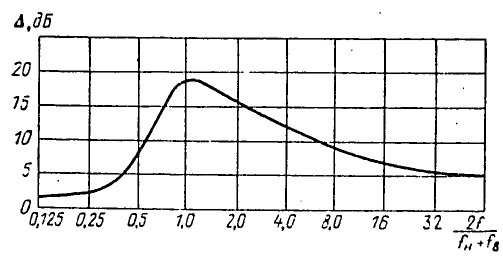

Figure 15.2. Δ as function of frequency.
[дБ=dB; н=b; в=t]

ΔN_f is equal to the vibration level gradient on the shock absorbers, and when there are no shock absorbers (i.e., in the case of rigid mounting) it is calculated by the formula

$$\Delta N_ф = 20 \lg \frac{m_1 + m_2}{m_2}, \qquad (15.3.14)$$

where m_1 is the reduced mass of the enclosure in consideration of the framing, machinery and conjugate water mass; m_2 is the mass of the machine.

The vibration levels fall off appreciably within a mounting enclosure as the distance from the foundation increases. Therefore it is reasonable to assign different energy densities w_{1i} for different parts of the contour of a mounting enclosure to solve equation system (15.3.8). The magnitude of the decrement can be estimated by the following empirical relation:

[kp=cr]

$$\Delta N_0 = N_{r_0} - N_{1i} = 10 \lg \frac{r_1 + r_2}{a + 2r_0} \frac{1 - 0{,}35\varepsilon_r}{1 - 0{,}35\varepsilon_0} + 0{,}7\eta_1 \frac{\sqrt{f_{1\,кр} f}}{c}, \qquad (15.3.15)$$

APPROVED FOR RELEASE: 2007/02/08: CIA-RDP82-00850R000200100009-9

APPROVED FOR RELEASE: 2007/02/08: CIA-RDP82-00850R000200100009-9

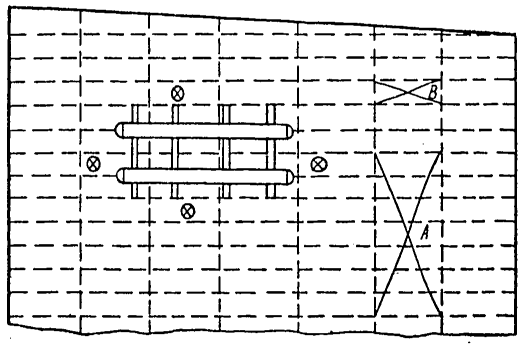

Figure 15.3. Layout of plates and points with vibration level N_{r0} on mounting enclosure.

where r_1 and r_2 are the distances between the ends of the foundation and the middle of the examined segment of the contour of the mounting enclosure (Figure 15.4); r is the shortest distance between the foundation and the same point;

$$\varepsilon_0 = \frac{(a-b)(a+b+4r_0)}{(a+2r_0)^2};$$

$$\varepsilon_r = \frac{(a-b)(a+b+4r_0)}{(r_1+r_2)^2};$$

a and b are the length and width of the foundation; η_1 and f_{1cr} are the loss coefficient and critical frequency of the mounting enclosure.

For screws the vibration levels of the mounting enclosure are calculated by relations presented in Chapter 9.

Radiation of Noise by Vibrating Hull Structures. When bending vibrations propagate through plates reinforced with ribs the noise levels radiated into a room can be calculated by the familiar relation [1, 3]:

$$L_{ci} = N_{vi} + 10\lg\frac{S_i}{A} + 10\lg\gamma_i - \Delta_1 L_{ci} - \Delta_2 L_{ci}, \qquad (15.3.16)$$

where N_{vi} is the vibration level in terms of velocity relative to $\dot{y}_0 = 5\cdot10^{-8}$ m/s; S_i is the area of the structure; A is the total acoustic absorption of the room; γ_i is the radiation coefficient; $\Delta_1 L_{ci}$ and $\Delta_2 L_{ci}$ are correction factors for the influence of the sound absorber and lining on the radiating surface.

APPROVED FOR RELEASE: 2007/02/08: CIA-RDP82-00850R000200100009-9

APPROVED FOR RELEASE: 2007/02/08: CIA-RDP82-00850R000200100009-9

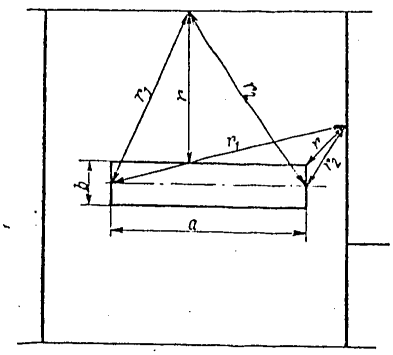

Figure 15.4. How to determine distances r_1, r_2, r.

The calculation of γ_i poses the greatest difficulty, since it is determined by different formulas for different frequency ranges. These ranges are determined by the values of the dimensionless parameter $\phi_i = f/f_{i\ cr}$.

When $\phi_i < 0.8$ the radiation coefficient is determined by the formula

$$\gamma_i = \psi_1 g_1(\varphi_i) + \psi_2 g_2(\varphi_i) + \psi_3 g_3(\varphi_i)\zeta(\varphi_i), \tag{15.3.17}$$

where

$$\psi_1 = \frac{cP_i}{f_{i\,\text{кр}} S_i}; \quad \psi_2 = \frac{c^2}{f_{i\,\text{кр}}^2 S_i};$$

$$\psi_3 = \frac{c}{f_{i\,\text{кр}}}\left(\frac{1}{\lambda_{1i}} + \frac{1}{\lambda_{2i}} + \frac{P_i}{2S_i}\right),$$

$$g_1(\varphi_i) = \frac{1}{2\pi^2}\frac{1}{(1-\varphi_i)^{3/2}}\left[2\sqrt{\varphi_i} + (1-\varphi_i)\ln\frac{1+\sqrt{\varphi_i}}{1-\sqrt{\varphi_i}}\right];$$

$$g_2(\varphi_i) = \begin{cases} \dfrac{16}{\pi^4}\dfrac{1}{\sqrt{\varphi_i}}\dfrac{1-2\varphi_i}{\sqrt{1-\varphi_i}} & \text{for } \varphi_i < 0{,}5; \\ 0 & \text{for } \varphi_i \geqslant 0{,}5; \end{cases}$$

$g_3(\phi_i)$ is a function determined graphically (Figure 15.5)

$$\zeta(\varphi_i) = \begin{cases} 0 & \text{for } \varphi_i \leqslant \varphi_1 = \dfrac{c^2}{4f_{i\,\text{кр}}^2}\left(\dfrac{1}{\lambda_{1i}^2} + \dfrac{1}{\lambda_{2i}^2}\right); \\ \dfrac{\varphi_i - \varphi_1}{\varphi_2 - \varphi_1} & \text{for } \varphi_1 < \varphi_i < \varphi_2 = \dfrac{4{,}55c^2}{f_{i\,\text{кр}}^2 \lambda_{1i}\lambda_{2i}}; \\ 1 & \text{for } \varphi_i \geqslant \varphi_2. \end{cases}$$

APPROVED FOR RELEASE: 2007/02/08: CIA-RDP82-00850R000200100009-9

APPROVED FOR RELEASE: 2007/02/08: CIA-RDP82-00850R000200100009-9

For $0.8 \leq \phi_i < 1$ the value of γ_i should be calculated by the formula

$$\gamma_i = \gamma_3 + (1 - \gamma_3)(5\varphi_i - 4), \qquad (15.3.18)$$

where $\gamma_3 = 1.3\psi_1 + \psi_3$.

When $\phi \geq 1$ one should use $\gamma_i = 1$.

The values $\Delta_1 L_{ci}$ and $\Delta_2 L_{ci}$ can be calculated by the methods used for analyzing the influence of various factors on acoustic insulation (see Chapter 10).

The effect of linings that do not have acoustic bridges is determined by the following formulas:

[гр=gr; кр=cr]

$$\Delta_2 L_{ci} = \begin{cases} 0 \text{ for } f \leqslant f_{гр}; \\ \dfrac{\lg f/f_{гр}}{\lg 1{,}5 f_{1кр}/f_{гр}} \left\{ 10 \lg \dfrac{3\pi f_{1кр} m_2}{\rho c} + 5 \lg \dfrac{\eta_2 m_2 \sigma}{\eta_1 m_1} [(1-\sigma)^2 + \eta_2^2 \sigma^2] \right\} \\ \qquad \text{for } f_{гр} < f < 1{,}5 f_{1кр}; \\ 10 \lg \dfrac{2\pi f m_2}{\rho c} + 5 \lg \dfrac{\eta_2 m_2 \sigma}{\eta_1 m_1} [(1-\sigma)^2 + \eta_2^2 \sigma^2] \text{ for } f > 1{,}5 f_{1кр}, \end{cases} \qquad (15.3.19)$$

where $\sigma = f_{1кр}^2 / f_{2кр}^2$; $f_{гр} = 266 \sqrt{\dfrac{m_1 + m_2}{l m_1 m_2}}$; l is the length of the air space between the lining and main plating, in cm; m is mass per unit area, in g/cm^2; η is the loss coefficient.

The subscript 1 in formulas (15.3.19) indicates that a given value refers to the main plating, and the subscript 2 refers to the lining.

Initial Secondary Acoustic Vibration Levels. These levels, necessary for solving (15.3.8) and for subsequent calculation of noise levels L_{ss}, can be found from the following formula [5]:

$$N_{vi} = L_i - 10 \lg \frac{2\pi m_i f_{i\,кр}}{\rho c} - 10 \lg \frac{1}{\mu_i} - 20 \lg \varphi_i - \Delta_1 L_{ci} - \Delta_2 L_{ci}, \qquad (15.3.20)$$

where $\dfrac{1}{\mu_i} = 1 + \dfrac{2\pi \eta_i m_i f_{i\,кр}}{\gamma_i \rho c} \varphi_i$; L_i is the acoustic pressure level at the center of the enclosure.

The other values entering in formula (15.3.20) are the same as in formulas (1513.16) and (15.3.19).

General Calculation Procedure. The calculation relations presented above are basic. In addition to them there are certain other formulas that can

APPROVED FOR RELEASE: 2007/02/08: CIA-RDP82-00850R000200100009-9

APPROVED FOR RELEASE: 2007/02/08: CIA-RDP82-00850R000200100009-9

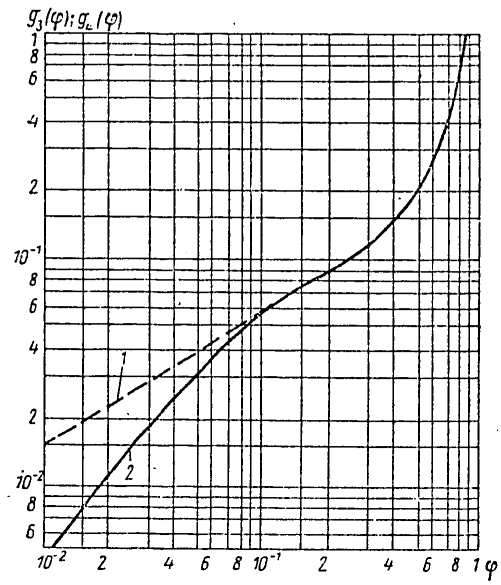

Figure 15.5. Curves of functions $g_3(\phi)$ (curve 1) and $g_4(\phi)$ (curve 2).

be used (for instance, for considering the influence of a sound-insulating hood, for calculating the acoustic absorption coefficients and loss coefficients, etc.). The order of the calculations can vary, since components L_a, L_{ss} and L_{sp} can be calculated largely independently of each other and separately for different rooms. However, there are some constraints imposed on the order of individual operations. In addition, some of the formulas are based on the utilization of the identical intermediate calculation parameters (for instance f_{cr}, η), which should be separated into individual substeps of the calculation. With this in mind it is possible to construct a logical procedure for solving the problem as a whole.

15.4. Requirements on Programming of Calculation of Anticipated Noise Level with Computer

The main advantages of mechanized calculation are: great precision and reliability (can be used in a wide range of design parameters of hull structures), elimination of calculation errors, less labor involved and shorter calculation time.

The algorithm of the program is assigned by a group of relations, most of which are presented in §15.3, and by the logical procedure described above.

APPROVED FOR RELEASE: 2007/02/08: CIA-RDP82-00850R000200100009-9

APPROVED FOR RELEASE: 2007/02/08: CIA-RDP82-00850R000200100009-9

For computer programming it is preferable to have analytical representations of the relations, and not graphic and tabular, and also general relations, and not specific relations for individual special cases.

Calculation programming is a difficult and time-consuming operation. Therefore computer calculations can be done during the ship design stage only if a ready-made program is available. It is preferable to use a general purpose program, which can be used in different computer centers with different types of computers. Such a program should meet certain requirements in relation to the algorithmic language utilized, program notation, operator convenience, etc.

[б=b;
в=c;
г=d]

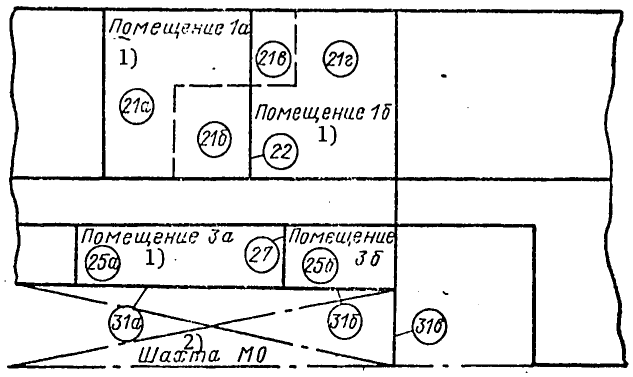

Figure 15.6. Layout of rooms and partitions.
Key: 1. Room 2. Engine room shaft

The laying out of calculation blocks, i.e., the partitioning of regions of a ship, for which the noise levels can be calculated individually, is the basis on which the raw data are compared. The size of the calculation blocks depends on the maximum number of partitions in them, i.e., on the limiting order of system (15.3.8), prescribed by the program. For a complete description of the anticipated noise level it is necessary to determine it for all the rooms to be brought within standards. However, computer capabilities are limited; moreover, if there are too many partitions in a calculation block it is difficult to compare the raw data. At the same time, if there are too few partitions in a block the number of blocks for a ship becomes too large and it becomes difficult to lay out blocks for rooms that are distant from a source. Experience shows that the optimum number of partitions in a block is 70-80.

The number of calculation blocks for partitioning the hull of a ship depends on the number of rooms designated for calculation, on their relative location and distance from the source. For small ships one or two blocks are sufficient, and for medium-displacement ships with an aft superstructure three or four blocks are usually necessary.

APPROVED FOR RELEASE: 2007/02/08: CIA-RDP82-00850R000200100009-9

APPROVED FOR RELEASE: 2007/02/08: CIA-RDP82-00850R000200100009-9

Each block should contain a mounting enclosure and enclosures that bound source rooms in the zone of quiet rooms, which comprise the basis of a block (in particular, engine room shaft walls). If the calculation rooms in a source room are separated by intermediate rooms that do not need to be brought within noise standards, certain secondary structures (for example, lightweight partitions) can be excluded from the block without sacrificing the basic shortest paths of acoustic vibration propagation.

Each block should contain distant rooms in addition to contiguous rooms.

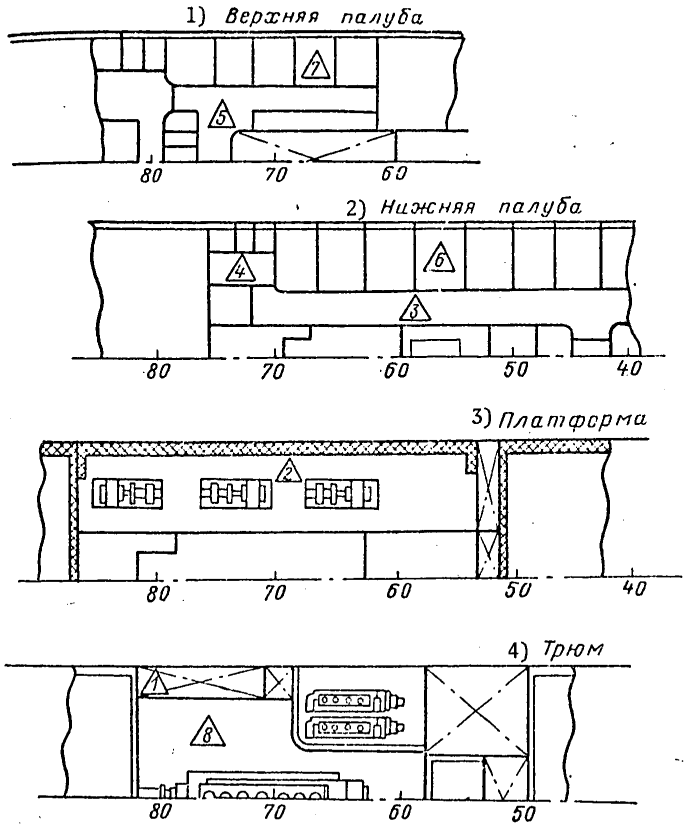

Figure 15.7. Layout of rooms.
Key: 1. Top deck 3. Platform
2. Bottom deck 4. Hold

APPROVED FOR RELEASE: 2007/02/08: CIA-RDP82-00850R000200100009-9

APPROVED FOR RELEASE: 2007/02/08: CIA-RDP82-00850R000200100009-9

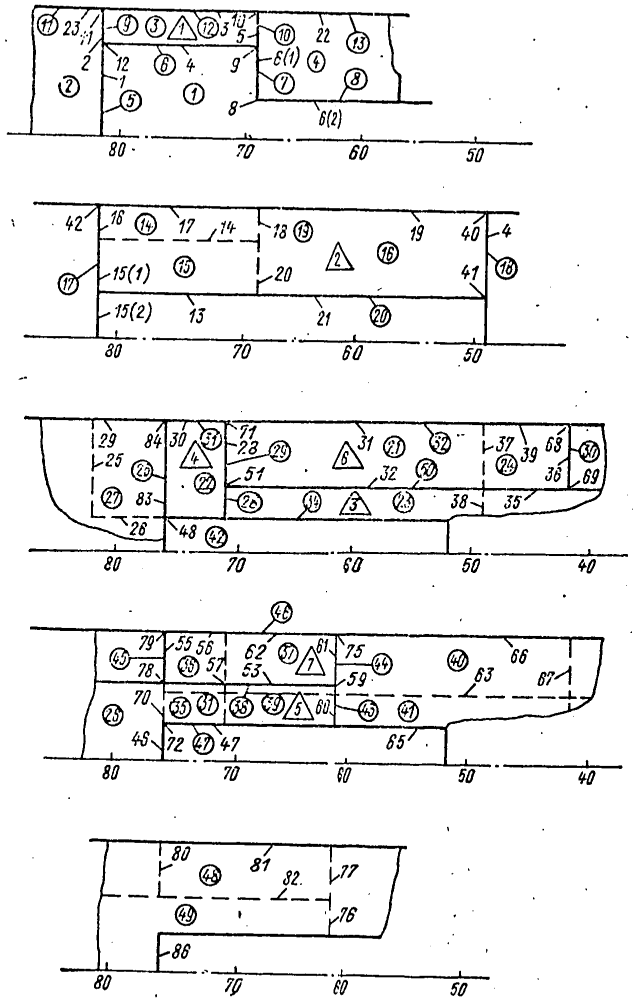

Figure 15.8. Plan of calculation block.

APPROVED FOR RELEASE: 2007/02/08: CIA-RDP82-00850R000200100009-9

APPROVED FOR RELEASE: 2007/02/08: CIA-RDP82-00850R000200100009-9

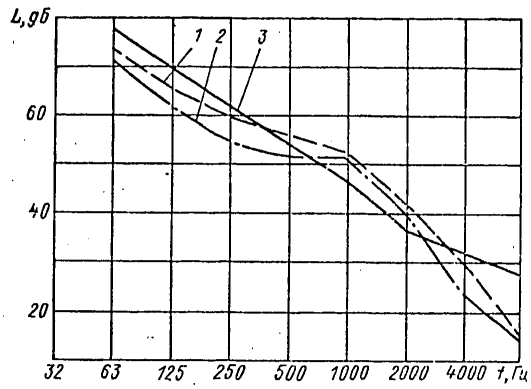

Figure 15.9. Noise levels in main deck cabins: 1 -- computer calculation; 2 -- graphoanalytical calculation; 3 -- measurements. [дБ=dB; Гц=Hz]

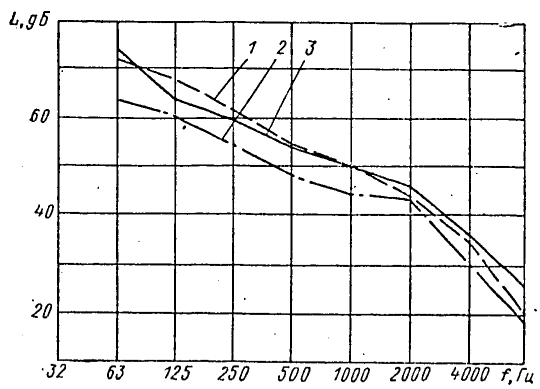

Figure 15.10. Noise levels in top deck cabins: 1 -- computer calculation; 2 -- graphoanalytical calculation; 3 -- measurements.

Homogeneous rooms and enclosures in a block with the approximately identical acoustical conditions (for example, several cabins in a row on one deck) should be combined in order to reduce the number of partitions and thus increase the length of the block.

An example of how rooms and partitions are combined is given in Figure 15.6, where the individual partitions and rooms that are conditionally combined under one number are designated by different letters. The numbers of

APPROVED FOR RELEASE: 2007/02/08: CIA-RDP82-00850R000200100009-9

APPROVED FOR RELEASE: 2007/02/08: CIA-RDP82-00850R000200100009-9

partitions are given in circles. Rooms 1a and 1b are combined into a single calculation room. The bulkhead (partition 22) between can be eliminated altogether if need be, from the calculation block. The same can be done for rooms 3a and 3b, which in this case, like room 5, are presumed not to be covered by noise standards (otherwise an independent number would have to be assigned to partition 31c).

To calculate the noise levels that penetrate into rooms of superstructures and into the wheelhouses on the outer decks it is necessary to mark off separate blocks of these rooms and of other adjacent rooms below them. The noise levels near exterior enclosing structures should be calculated by the formulas used for open space.

An example of how to mark off a calculation block for a fishing trawler is given in Figure 15.8. The layout of the rooms and noise sources in the examined part of the ship is illustrated in Figure 15.7. In Figure 15.8 the numbers in circles denote the numbers of partitions in a block, the numbers in triangles denote the numbers of rooms, the uncircled numbers with lines denote the conditional numbers of corner connections. The results of the calculation are presented in Figures 15.9 and 15.10. The results of measurements are also given in those figures for comparison with the results of graphoanalytical calculation.

15.5. Graphoanalytical Calculation of Anticipated Noise Level

General Description of Procedure. The calculation relations used for graphoanalytical calculation, based on general relations, are presented in §15.3. All alterations are made for the sake of simplification so that the calculation procedure can be used without a computer without too much calculation time and labor.

Most of the simplifications are made in the parts of the calculation procedure that involve the most laborious computations of L_{sp} and L_{ss}. The essence of these simplifications consists in the simplification of the relations themselves, or in the introduction of generalized characteristics, structural and physical parameters of individual partitions, rooms, etc. This is either reflected on individual elements of the calculation procedure (for instance, during the calculation of the acoustic vibration levels of partitions), or is related to changes in the general calculation procedure (for instance, during estimation of the anticipated noise level in distant rooms).

The calculations can be carried out to the accuracy of the third significant digit. All intermediate values in decibels (L_a, L_s, R, ΔR, N, ΔN, etc.) should be rounded off to the nearest tenth, and all totals (i.e., summary noise levels for each room) to the nearest whole number.

APPROVED FOR RELEASE: 2007/02/08: CIA-RDP82-00850R000200100009-9

APPROVED FOR RELEASE: 2007/02/08: CIA-RDP82-00850R000200100009-9

The anticipated noise level should be calculated graphoanalytically in the following order:

calculation for noisy rooms; in this step must be found the levels that will be the raw data for future calculation of contiguous rooms (the noise levels at the center points of partitioning bulkheads);

calculation for quiet rooms contiguous with noisy rooms;

calculation for quiet rooms distant from noisy rooms;

calculation of noise from external sources;

calculation of noise in aft rooms.

Calculation Relations, Specific for Graphoanalytical Procedure. One of the important differences between these relations and the ones presented in §15.3 is the fact that the acoustic vibration levels of hull structures are computed. The solution of equation system (15.3.8) is replaced with the calculation of the vibration levels on individual enclosures one at a time, with increasing distance from the source. This method is applicable under certain assumptions concerning the character of energy exchange between individual enclosures [1].

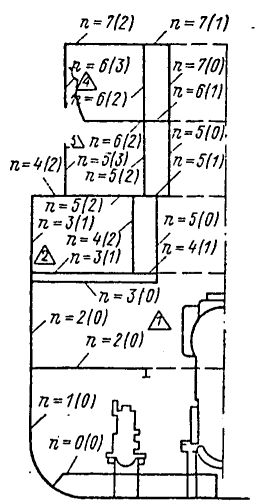

Figure 15.11. Numbering of enclosures.

To do the calculation all hull bulkheads in an examined region of the ship must be numbered in accordance with their distance from the mounting enclosure.

The number system is selected such that to each enclosure is assigned a number n, which corresponds to the number of corner connections on the shortest distance between the machine and each examined enclosure (in other words, between the n-th enclosure and mounting enclosure there are on that path n intermediate enclosures). In this system the zero number (n = 0) corresponds to the mounting enclosure, and to all enclosures directly bordering on the mounting enclosure corresponds the number 1 (n = 1), etc. An example of how the enclosures are enumerated is shown in Figure 15.11.

The calculation of average vibration levels is done for each enclosure one at a time, from small to large numbers by the formula

APPROVED FOR RELEASE: 2007/02/08: CIA-RDP82-00850R000200100009-9

APPROVED FOR RELEASE: 2007/02/08: CIA-RDP82-00850R000200100009-9

$$N_n = N_{n-1} - \Delta N_n, \tag{15.5.1}$$

where N_n is the vibration level on an examined enclosure, in dB (the subscript n corresponds to the number of the enclosure in accordance with the above-described number system); N_{n-1} is the vibration level on the enclosure that abuts the examined enclosure, located closer to the source, in dB (its number is n - 1, which is expressed by the corresponding subscript); this enclosure henceforth will be called the starting enclosure.

The value ΔN_n, which determines the vibration level gradient between enclosures, is calculated by the formula

[kp=cr]

$$\Delta N_n = 10\lg\frac{s_n}{s_{n-1}} + 10\lg\frac{1}{\tau_{n-1,n}} + 10\lg G_n + 5\lg\frac{\rho_n f_{(n-1)\,\text{кр}}}{\rho_{n-1} f_{n\,\text{кр}}}, \tag{15.5.2}$$

where

$$G_n = A_n + B_n\frac{D_n}{D_n + B_n} + D_n;$$

$$A_n = \frac{\sum_{j=1}^{j=M_{nj}} (l_{n-1})_j (\tau_{n,n-1})_j}{l_{n-1,n}};$$

$$B_n = \frac{\sum_{i=0}^{i=M_{ni}} (l_{n+1})_i (\tau_{n,n+1})_i}{l_{n-1,n}};$$

$$D_n = \frac{\pi^2}{c}\frac{S_n\eta_n\sqrt{ff_{n\,\text{кр}}}}{l_{n-1,n}},$$

where $l_{n-1,n}$ is the total length of the contour between the examined and starting enclosures, in m; $\tau_{n-1,n}$ is the coefficient of transmission of energy from the starting enclosure to the examined one through the corner connection between them; $(l_{n-1})_j$ is the total contour length between the examined enclosure and one contiguous enclosure with the smaller number, i.e., n - 1, in m; $(\tau_{n,n-1})_j$ is the coefficient of transmission of energy into the enclosure with the number n - 1, through the corner connection between them, and the examined enclosure; M_{nj} is the number of enclosures with the number n - 1, contiguous with the examined enclosure, i.e., the number of starting enclosures for a given examined enclosure; $(l_{n+1})_i$ is the total length of the part of the contour between the examined enclosure and the one contiguous with it with the larger number (i.e., the number n + 1, in m; $(\tau_{n,n+1})_i$ is the coefficient of transmission into that

APPROVED FOR RELEASE: 2007/02/08: CIA-RDP82-00850R000200100009-9

APPROVED FOR RELEASE: 2007/02/08: CIA-RDP82-00850R000200100009-9

enclosure; M_{ni} is the number of contiguous enclosures with the number n + 1 (i.e., the number of enclosures for which the given enclosure is the starting enclosure).

The coefficients $\tau_{n-1,n}$, $\tau_{n,n-1}$ and $\tau_{n,n+1}$ are determined on the basis of formulas (15.3.9) and (15.3.10). The other values are indicated in the explanation to formula (15.3.8) in the list of basic conventional symbols, and all subscripts correspond to the numbers of enclosures, indicating whether a given value refers to an examined (the subscript n) or to the starting (the subscript n - 1) enclosure.

If the material of the examined and starting enclosures is identical, which is usually the case, formula (15.5.2) acquires the form

$$\Delta N_n = \Delta_s + \Delta_\tau + \Delta_G, \qquad (15.5.3)$$

where

$$\Delta_s = 15 \lg \frac{s_n}{s_{n-1}}; \quad \Delta_\tau = 10 \lg \frac{1}{\tau_{n-1,n}}; \quad \Delta_G = 10 \lg G_n.$$

Calculation by formula (15.5.2) for separate enclosures sometimes can be done in several versions, corresponding to different vibration propagation paths. Such is the case when an examined enclosure with the number n borders on several enclosures with the number n - 1. Some of the latter may not be among the structures that bound an examined room. In this case it is essential, in principle, to do the calculation for each version (the number of such versions cannot exceed four) and to combine the resulting levels by the level addition rule.

The influence of adjacent enclosures with the identical number as the examined must be taken into consideration if the thickness of the examined enclosure is greater than that of the others and the calculated vibration level on it is 8 dB and more lower than on the mentioned enclosures. The calculation should be done in such cases by formula (15.5.2), and one of the indicated enclosures must be taken as the starting enclosure (the subscript n - 1 in this case will be one smaller than the number corresponding to the starting enclosure).

Vibration levels can be calculated by this procedure for all enclosures that bound any room, but it is best to use the formulas presented above only for rooms contiguous with a source room.

In most cases the calculation can be limited to enclosures with the smallest number for a given room. Of enclosures with a larger number it is desirable to consider only those that have greater thickness than any enclosure with the minimum number for an examined room. If enclosures with the smallest numbers have linings (decorative, etc.) on the side of an examined room it is necessary to do the calculation for the enclosures with larger numbers which have no linings.

APPROVED FOR RELEASE: 2007/02/08: CIA-RDP82-00850R000200100009-9

APPROVED FOR RELEASE: 2007/02/08: CIA-RDP82-00850R000200100009-9

Another important feature of the graphoanalytical calculation procedure is related to distant rooms. In this group of rooms the noise level is determined by the acoustic vibration of surrounding structures (see §15.2). The calculation of the anticipated noise level can, in principle, be done on the basis of the relations presented in §15.3 and formula (15.5.2).

The noise levels for distant rooms are calculated one at a time, from the least distant to the most distant rooms from the source.

If two adjacent rooms are separated by a wall with the number n, then the room must have walls contiguous with the partitioning enclosure and with the number n - 1, so that one of these rooms can be considered to be closer to the source (these rooms are called starting rooms). For example, room 2 in the layout illustrated in Figure 15.11 should be considered the starting room for room 3, which, in turn, is the starting room for room 4.

The distance of individual hull structures in relation to secondary acoustic vibration can be characterized by a number, which is determined on the same principle as for the primary acoustic vibration, but starting with the nearest enclosure that bounds the source room. Thus, all enclosures that bound the source room have the number n = 0, all enclosures of adjacent rooms contiguous with them have the number n = 1, etc. Numbers pertaining to secondary acoustic vibration are enclosed in parentheses in Figure 15.11 to illustrate this numbering principle.

The noise levels in distant rooms are calculated by the formula [1]

[ср=av; ВИ=VD; з=lin]

$$L_2 = L_1 + 10\lg\frac{\alpha_{1ср}}{\alpha_{2ср}} - \Delta L_{ВИ} - \Delta L_з, \qquad (15.5.4)$$

where ΔL_{VD} is the change of noise levels due to the attenuation of vibration and difference in the effectiveness of radiation between the starting and examined rooms; ΔL_{lin} is a correction factor that takes into account the influence of liners in the starting and examined rooms.

The subscripts of L and α_{av} indicate the ratio of these values to a particular room: the subscript 1 is used for the starting room and the subscript 2 for an examined room.

The value ΔL_{VD} should be determined by the formula

$$\Delta L_{ВИ} = 10\lg\varkappa\frac{\varepsilon_1' + \varepsilon_1''}{\varepsilon_2' + \varepsilon_2''}, \qquad (15.5.5)$$

where $\varkappa$ is a coefficient that characterizes the reduction of vibration levels between an examined and starting rooms; ε_1', ε_1'', ε_2', ε_2'' are radiation coefficients for thicknesses s_1', s_1'', s_2', s_2''; s_1' is the least of the

APPROVED FOR RELEASE: 2007/02/08: CIA-RDP82-00850R000200100009-9

APPROVED FOR RELEASE: 2007/02/08: CIA-RDP82-00850R000200100009-9

thicknesses of the enclosures surrounding a starting room (excluding the enclosure that separates the starting and examined rooms), in mm; s_1'' is the greatest of the thicknesses of the indicated enclosures, in mm; s_2'' is the greatest of the thicknesses of the enclosures bounding an examined room, in mm; s_2' is the least of the thicknesses of the same enclosures, in mm.

The value κ is determined by the formula

$$\varkappa = \left(\frac{s_{2cp}}{s_{1cp}}\right)^{3/2}\left[1 + D_2\frac{D_2+2}{D_2+1}\right], \qquad (15.5.6)$$

where $D_2 = \frac{\pi^2 l_2 \bar{\eta}_2 \sqrt{f f_{2кр}}}{c\tau_{cp}}$; $s_{1cp} = \frac{s_2' + s_1''}{2}$ -- see the explanations to formula (15.5.5); $s_{2cp} = \frac{s_2' + s_2''}{2}$ -- see the explanations to formula (15.5.5); τ_{av} is the transmission coefficient, determined graphically in Figure 15.12 as a function of the ratio $s_0/s_{1\ av}$ (s_0 is the thickness of the partitioning enclosure); $\bar{\eta}_2 = \frac{\sum_{(i)} \eta_i S_i}{\sum_{(i)} S_i}$ is the average loss coefficient for the enclosures in examined rooms; l_2 is the average length of an examined room in the direction perpendicular to the partitioning enclosure, in m; F_{2cr} is the average critical frequency, which is determined for thickness s_{2av}.

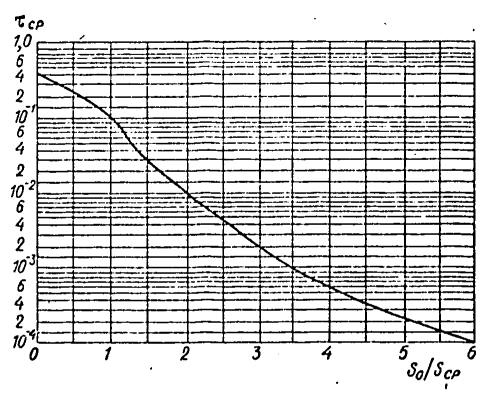

Figure 15.12. τ_{av} as function of thickness ratio. [cp=av]

APPROVED FOR RELEASE: 2007/02/08: CIA-RDP82-00850R000200100009-9

APPROVED FOR RELEASE: 2007/02/08: CIA-RDP82-00850R000200100009-9

In some cases the radiation coefficient should be approximated as a function of just the critical frequency. The approximate radiation coefficient ε_i is calculated by the formulas

[kp=cr]

$$\varepsilon_i = \begin{cases} \frac{850}{f_{i\,\text{кр}}} g_4(\varphi i) & \text{for } \varphi_i < 0{,}8; \\ \frac{850}{f_{i\,\text{кр}}} + \left(1 - \frac{850}{f_{i\,\text{кр}}}\right)(5\varphi_i - 4) & \text{for } 0{,}8 \leqslant \varphi_i < 1; \\ 1 & \text{for } \varphi_i \geqslant 1, \end{cases} \qquad (15.5.7)$$

where $g_4(\phi_i)$ is determined graphically (see Figure 15.5).

The value ΔL_{lin} is calculated by the formula

[з=lin; п=r; c=s]

$$\Delta L_з = 10\lg \frac{1 - \frac{S_1'}{S_{1п}}\left(1 - 10^{-0{,}1\overline{\Delta_2 L_{c1}}}\right)}{1 - \frac{S_2'}{S_{2п}}\left(1 - 10^{-0{,}1\overline{\Delta_2 L_{c2}}}\right)}, \qquad (15.5.8)$$

where S_{1r} is the total area of the enclosing surfaces in the starting room; S_{2r} is the same in the examined room; S_1' is the total area of the enclosure, covered with liners, in the starting room; S_2' is the same in the examined room; $\overline{\Delta_2 L_{s1}}$ is the average effectiveness of the liners in the starting room, determined on the basis of the average parameters of all the liners; $\overline{\Delta_2 L_{s2}}$ is the same for the liners in the examined room.

Nomograms and Auxiliary Graphs. To facilitate the calculations it is advisable to use special nomograms, constructed on the basis of the corresponding relations. The use of these nomograms is especially effective in the case when there is a complex function of a few parameters. Examples of these nomograms are given in Figures 15.13-15.16. The dash lines with arrows in the working field of the nomograms indicate the procedure for using the nomograms. The input values are denoted by the symbol ▼ on the corresponding scales. The intermediate points in the field of the nomograms are numbered with Roman numerals, corresponding to the order in which they are plotted. In cases when there are different possible variations of the utilization of a nomogram the procedure for each nomogram is indicated. The literal designations of the input and output values correspond to the symbols used in the formulas in §15.3 and §15.5. The measurement units are indicated in the corresponding scales next to the literal designation. Additional graphics -- keys that explain the utilization of the nomograms, are also given.

APPROVED FOR RELEASE: 2007/02/08: CIA-RDP82-00850R000200100009-9

APPROVED FOR RELEASE: 2007/02/08: CIA-RDP82-00850R000200100009-9

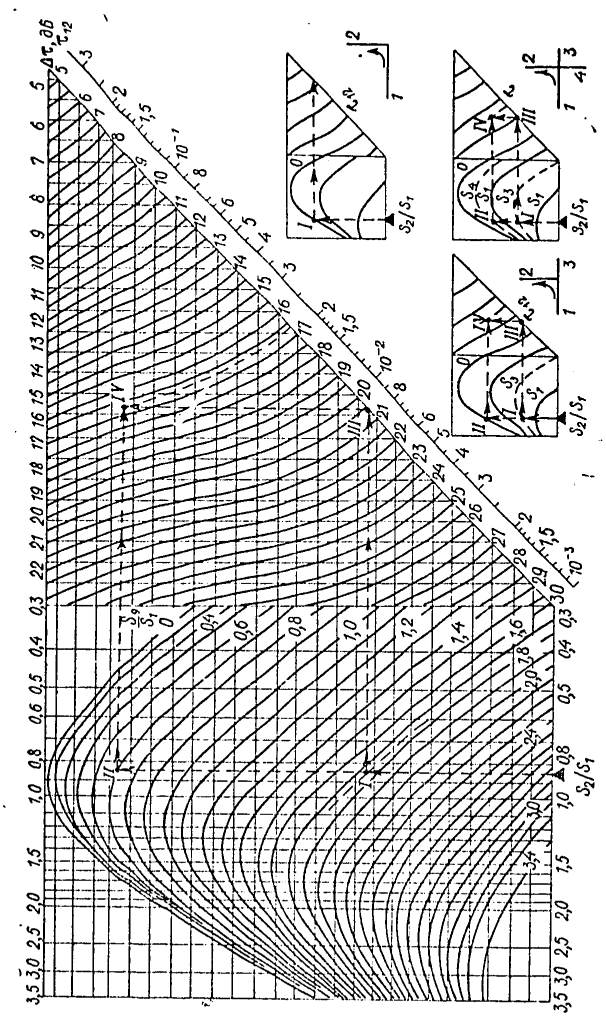

Figure 15.13. Nomogram for determining $\Delta\tau$ and τ. [дБ=dB]

APPROVED FOR RELEASE: 2007/02/08: CIA-RDP82-00850R000200100009-9

APPROVED FOR RELEASE: 2007/02/08: CIA-RDP82-00850R000200100009-9

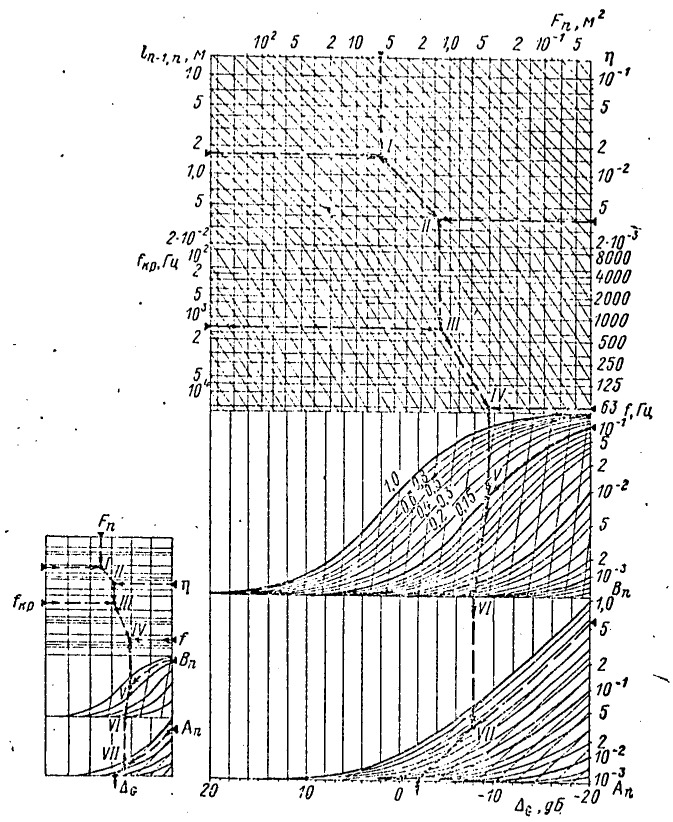

Figure 15.14. Nomogram for determining Δ_c.
[kp=cr; Гц=Hz; gБ=dB]

Calculation of the values ΔN_n on the basis of formulas (15.5.2) and (15.5.3) is a difficult operation which, incidentally, is repeated many times. Therefore it is particularly important to simplify this stage of the calculations. One variation of simplification is to use the nomograms presented in Figures 15.13 and 15.14. Each of them can be used for determining one of the terms in formula (15.5.3).

The nomogram in Figure 15.13 should be used for determining the values $\tau_{(n-1,n)}$ and Δ_τ for an arbitrary corner connection (with not more than four branches, which is characteristic of a ship hull) of plates of identical

APPROVED FOR RELEASE: 2007/02/08: CIA-RDP82-00850R000200100009-9

APPROVED FOR RELEASE: 2007/02/08: CIA-RDP82-00850R000200100009-9

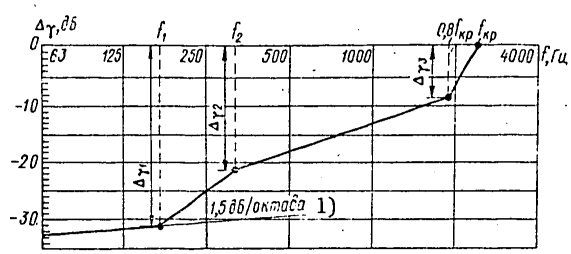

Figure 15.15. Typical curve of $\Delta\gamma$ as function of frequency. [дБ=dB; кр=cr; Гц=Hz]

$$\Delta\gamma_1 = 10\lg[\psi_1 g_1(\varphi_1) + \psi_2 g_2(\varphi_1)];\quad \Delta\gamma_2 = 10\lg[\psi_1 g_1(\varphi_2) + \psi_2 g_2(\varphi_2) + \psi_3 g_3(\varphi_2)];\quad \Delta\gamma_3 = 10\lg[1{,}3\psi_1 + \psi_3];\quad \varphi_1 = f_1/f_{кр};\quad \varphi_2 = f_2/f_{кр};\quad f_1 = \frac{c^2}{4f_{кр}}\left(\frac{1}{\lambda_1^2} + \frac{1}{\lambda_2^2}\right);\quad f_2 = \frac{4{,}55c^2}{f_{кр}\lambda_1\lambda_2};\quad \psi_1 = \frac{cP}{f_{кр}F};\quad \psi_2 = \frac{c^2}{f_{кр}F};\quad \psi_3 = \frac{c}{f_{кр}}\left(\frac{1}{\lambda_1} + \frac{1}{\lambda_2} + \frac{p}{2F}\right).$$

Key: 1. 1.5 dB per octave

materials. In this case formulas (15.3.9) and (15.3.10) retain their general form, but the values of β_{ij} are functions only of the thickness ratio: $\beta_{ij} = (s_j/s_i)^{5/2}$.

The nomogram is used for determining the transmission coefficient from branch 1 into branch 2. The nomogram is plotted as a function of two parameters: s_2/s_1 and s_g/s_1. Here s_1 is the thickness of the enclosure, from which the transmission of energy is examined (branch 1); s_2 is the thickness of the enclosure, into which this energy goes (branch 2); s_g is the thickness of any of the other enclosures, involved in the corner connection. In the general case s_g corresponds to thicknesses s_3 and s_4. In the special case, for an L-connection, $s_3 = s_4 = 0$, for a T-connection $s_4 = 0$, and only for a cross connection are s_3 and s_4 not equal to zero. The ratios s_3/s_1 and s_4/s_1 are symmetric variables in formula (15.3.10), and the influence of these parameters is taken into account by one family of curves, the general index of which is denoted in the nomogram by the ratio s_g/s_1 and $s_g = s_3$ for one reflection and $s_g = s_4$ for another reflection in the first part of the nomogram.

A nomogram for determining Δ_G, in which ΔN_n is plotted as a function of frequency, is given in Figure 15.14. The values of A_n and B_n necessary for finding Δ_G should be determined in accordance with the explanations to

APPROVED FOR RELEASE: 2007/02/08: CIA-RDP82-00850R000200100009-9

APPROVED FOR RELEASE: 2007/02/08: CIA-RDP82-00850R000200100009-9

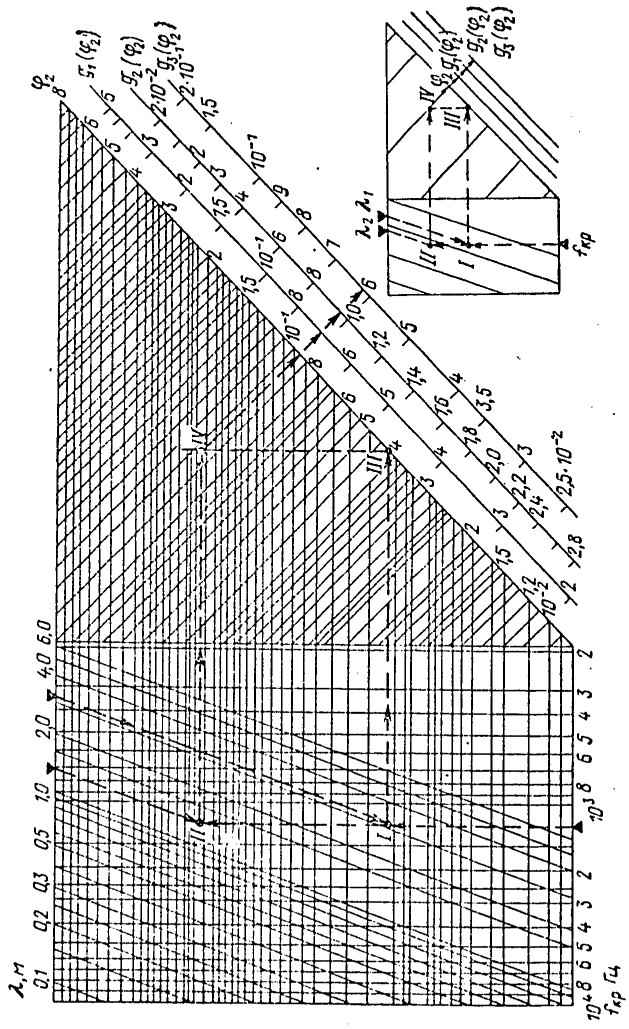

Figure 15.16. Nomogram for determining Φ_2; $g_1(\Phi_2)$; $g_2(\Phi_2)$; $g_3(\Phi_2)$. [kp=cr]

APPROVED FOR RELEASE: 2007/02/08: CIA-RDP82-00850R000200100009-9

APPROVED FOR RELEASE: 2007/02/08: CIA-RDP82-00850R000200100009-9

formula (15.5.2). Instead of calculating Δ_G and ΔN_n on all frequencies it is recommended that the graphical procedure be used, which consists in the plotting of a smooth line, connecting three points, found by calculations using formulas and nomograms for frequencies of 63, 500 and 8,000 Hz. All other values of ΔN_n can be found on this curve.

Another example of how to plot auxiliary curves instead of computing them is the procedure recommended for determining the values of $\Delta_{\gamma_i} = 10 \log \gamma_i$, which is the most laborious step of calculation of levels L_{si} by formula (15.3.16). This procedure is based on the typical curve of Δ_γ as a function of frequency. As can be seen in Figure 15.15, the typical curve is a broken line with four characteristic inflection points, corresponding to the following values of frequency parameter ϕ: ϕ_1, ϕ_2, 0.8, 1.0.

For $\phi = 1$ and $\gamma = 1$, and for other values of ϕ the value of Δ_γ should be computed. The values ϕ_1 and ϕ_2 and the corresponding values of γ are determined by formulas (15.3.17). For $\phi = 0.8$ γ is equal to $\gamma_3 = 1.3\psi_1 + \psi_3$. To facilitate the calculations of ψ_1, ψ_2, ψ_3, ϕ_1, ϕ_2 and of $g_1(\phi_1)$, $g_2(\phi_1)$, $g_1(\phi_2)$, $g_2(\phi_2)$ and $g_3(\phi_2)$ it is recommended that nomograms, one of which is given in Figure 15.16, be used.

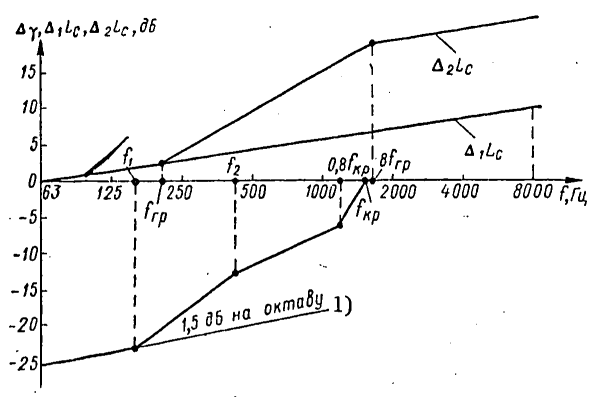

Figure 15.17. Combined graph of Δ_γ, $\Delta_1 L_s$, $\Delta_2 L_s$.
Key: 1. 1.5 dB per octave [c=s; дБ=dB; kp=cr]

The values of Δ_γ for all calculated frequencies are taken from the graph, constructed by the described method. In addition to Δ_γ, it is also

APPROVED FOR RELEASE: 2007/02/08: CIA-RDP82-00850R000200100009-9

APPROVED FOR RELEASE: 2007/02/08: CIA-RDP82-00850R000200100009-9

advisable to plot on the graph the graphic functions for $\Delta_1 L_s$ and $\Delta_2 L_s$. Here it is possible to use for $\Delta_1 L_s$ the readily simplified linear dependence ($\Delta_1 L_s = 0$ for f = 63 Hz), and $\Delta_2 L_s$ can be marked off at the top from the line $\Delta_1 L_s$. Then the summary value ($\Delta_\gamma - \Delta_1 L_s - \Delta_2 L_s$) will be equal to the length of the vertical segments between the top and bottom lines of the combined graph. An example of such a graph is shown in Figure 15.17.

Example of Calculation of Anticipated Noise Level in Rooms. The calculation is done for cabins on the main and top decks of a large refrigerator trawler. The room layout is illustrated in Figure 15.7. The noise source is a compressor in the refrigerator room. The calculation is done in tabular forms (Tables 15.2-15.10), in which all the necessary structural characteristics are indicated. The results of the calculation are presented graphically in Figure 15.18.

Table 15.2. Calculation of Noise Levels in Refrigerator Room (S_r = 247 m^2, r_A = 1.5 m, r_B = 5 m)

1) Расчетные величины	2) Значения расчетных величин							
1. f, Гц	63	125	250	500	1000	2000	4000	8000
2. $\alpha_{пр}$	0,04	0,06	0,08	0,10	0,13	0,15	0,18	0,20
3. Q	10,3	15,9	22,4	27,5	36,8	43,6	53,0	62,0
4. $L_и$, дБ	84	92,5	89	90	92,5	95	81	73
5. $\Delta L_п^{(А)}$, дБ	+1,0	—0,8	—2,0	—2,5	—3,5	—4,2	—4,7	—4,9
6. $L^{(А)}$, дБ	85,0	91,7	87,0	87,5	89,0	90,8	76,3	68,1
7. $\Delta L_п^{(Б)}$, дБ	+1,0	—1,0	—2,5	—3,3	—4,4	—5,4	—6,2	6,9
8. $L^{(Б)}$, дБ	85,0	91,5	86,5	86,7	88,1	89,6	74,8	66,1

Key: 1. Calculated values 2. Calculation results
[Гц=Hz; пр=red; и=b; п=r; дБ=dB; Б=B]

15.6. Features of Combined Application of Noise Control Techniques

Noise reduction techniques were examined independently in the preceding chapters, and the acoustic effectiveness of each technique was determined for their basic purpose. In practice, however, the situation is substantially more complicated. First, it is necessary to consider how the application of a particular device is reflected in a particular place of installation, i.e., the relationship between the overall and local effects. Second, many techniques, in addition to a main effect, have secondary

APPROVED FOR RELEASE: 2007/02/08: CIA-RDP82-00850R000200100009-9

APPROVED FOR RELEASE: 2007/02/08: CIA-RDP82-00850R000200100009-9

Table 15.3. Calculation of L_B Levels in Main Deck Cabins (with Refrigerator Operating in Refrigerator Room) ($S = 8.9\ m^2$, $S_r = 52\ m^2$, $I = 10 \log S/S_r = -7.7$ dB)

1) Расчетные величины	2) Значения расчетных величин							
1. f, Гц	63	125	250	500	1000	2000	4000	8000
2. $10 \lg 1/\alpha_{пр}$, дБ	9,2	6,8	6,0	5,7	5,5	5,4	5,4	5,4
3. $\Delta_1 = I + (2)$	1,5	—0,9	—1,7	—2,0	—2,2	—2,3	—2,3	—2,3
4. $\Delta R_{отв}$, дБ	—	—	—	—	—	—	—	—
5. Δ_2, дБ	—	—	—	—	—	—	—	—
6. (3) + (4) + (5)	1,5	—0,9	—1,7	—2,0	—2,2	—2,3	—2,3	—2,3
7. $R_{пр}$, дБ	22	26	31	35	36	31	37	43
8. (7)—(6)	20,5	26,9	32,7	37,0	38,2	33,3	39,3	45,3
9. L_1, дБ	85,0	91,7	87,0	87,5	89,0	90,8	76,3	68,1
10. L_2 = (9)—(8)	64,5	64,8	54,3	50,5	50,8	57,5	37,0	22,8

Key: 1. Calculated values 2. Calculation results
[отв=hol]

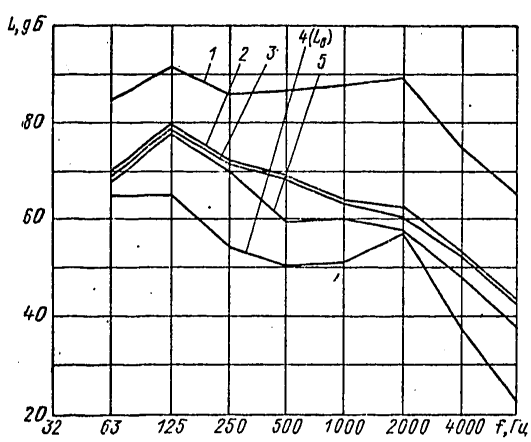

Figure 15.18. Calculated noise spectra in rooms:
1 -- refrigerator room;
2, 3, 4 -- main deck cabins;
(2 -- L_Σ, 3 -- L_s, 4 -- L_a);
5 -- top deck cabins.
[дБ=dB; Гц=Hz; в=a]

APPROVED FOR RELEASE: 2007/02/08: CIA-RDP82-00850R000200100009-9

APPROVED FOR RELEASE: 2007/02/08: CIA-RDP82-00850R000200100009-9

Table 15.4. Calculation of Side Vibration Levels in Refrigerator Room at Initial Vibration Levels on Platform

1) Расчетные величины	2) Значения расчетных величин							
1. f, Гц	63	125	250	500	1000	2000	4000	8000
2. η_1	0,005	0,0041	0,0036	0,0031	0,003	0,0028	0,0027	0,0026
3. Δ_G, дБ	−4,0	−3,4	−2,7	−1,9	−1,0	0	+1,0	+2,0
4. $\Delta N_1 = \Delta_s + \Delta_\tau + \Delta_G$	9,6	10,2	10,9	11,7	12,6	13,6	14,6	15,6
5. $N_0 = N_{r0} - \Delta N_0$	85,9	95,9	87,9	83,9	76,9	70,9	63,9	57,9
6. $N_1 = (5)-(4)$	76,3	85,7	77,0	72,2	64,3	57,3	49,3	42,3

3) Примечание. Исходные характеристики и вспомогательные параметры: $a = 3$ м; $b = 1,1$ м; $r_0 = 0,2$ м; $r = 2,1$ м; $r_1 = 3,0$ м; $r_2 = 4,0$ м; $\Delta N_0 = 4,1$ дБ; $l_0 = 9,5$ м; $\tau_{1,0} = 0,105$; $A_1 = 0,105$

$(l_2)_i$, м	18,2	18,2	2,5	2,5	2,5
$(\tau_{1,2})_i$	0,21	0,105	0,21	0,29	0,057

$B_1 = 0,75$; $l_{0,1} = 9,5$ м; $s_1 = 11$ мм; $s_0 = 8$ мм; $S_1 = 46,2$ м²; $f_{1\,кр} = 1090$ Гц; $\Delta_s = 2,1$ дБ; $\Delta_\tau = 11,5$ дБ.

Table 15.5. Calculation of Forward Bulkhead Vibration Levels in Refrigerator Room at Initial Vibration Levels on Platform

1) Расчетные величины	2) Значения расчетных величин							
1. f, Гц	63	125	250	500	1000	2000	4000	8000
2. η_1	0,003	0,0026	0,0024	0,0021	0,002	0,0018	0,0017	0,0016
3. Δ_G, дБ	−5,5	−5,0	−4,4	−3,7	−3,0	−2,0	−1,0	0
4. $\Delta N_1 = \Delta_s + \Delta_\tau + \Delta_G$	2,7	3,2	3,8	4,5	5,2	6,2	7,2	8,2
5. $N_0 = N_{r0} - \Delta N_0$	83,4	93,4	85,4	81,4	74,4	68,4	61,4	55,4
6. $N_1 = (5)-(4)$	80,7	90,2	81,6	76,9	69,2	62,2	55,2	47,2

3) Примечание. Исходные характеристики и вспомогательные параметры: $a = 3,0$ м; $b = 1,1$ м; $r_0 = 0,2$ м; $r = 6,0$ м; $r_1 = 6,0$ м; $r_2 = 6,0$ м; $\Delta N_0 = 6,6$ дБ; $l_0 = 3,7$ м; $\tau_{1,0} = 0,15$; $A_1 = 0,15$; $(l_2)_1 = 2,8$ м; $(l_2)_2 = 3,7$ м; $(l_2)_3 = 3,7$ м; $(l_2)_4 = 2,8$ м; $(\tau_{1,2})_1 = 0,07$; $(\tau_{1,2})_2 = 0,17$; $(\tau_{1,2})_3 = 0,17$; $(\tau_{1,2})_4 = 0,29$; $B_1 = 0,69$; $l_{0,1} = 3,7$ м; $s_1 = 8,0$ мм; $s_0 = 8,0$ мм; $S_1 = 10,4$ м², $f_{1\,кр} = 1500$ Гц; $\Delta_s = 0$; $\Delta_\tau = 8,2$ дБ.

Key: 1. Calculated values
2. Calculation results
3. Comment. The initial characteristics and auxiliary parameters are:
[Гц=Hz; дБ=dB; kp=cr]

APPROVED FOR RELEASE: 2007/02/08: CIA-RDP82-00850R000200100009-9

APPROVED FOR RELEASE: 2007/02/08: CIA-RDP82-00850R000200100009-9

Table 15.6. Calculation of Side Vibration Levels in Main Deck Cabins at Initial Side Vibration Levels in Room

1) Расчетные величины	2) Значения расчетных величин							
1. f, Гц	63	125	250	500	1000	2000	4000	8000
2. η_s	0,005	0,0041	0,0036	0,0031	0,003	0,0028	0,0027	0,0026
3. Δ_G, дБ	−4,0	−3,5	−2,9	−2,2	−1,5	−0,7	+0,1	+1,0
4. $\Delta N_2 = \Delta_s + \Delta_\tau + \Delta_G$	2,8	3,3	3,9	4,6	5,3	6,1	6,9	7,8
5. N_1, дБ	76,3	85,7	77,0	72,2	64,3	57,3	49,3	43,3
6. $N_2 = (5) - (4)$	73,5	82,4	73,1	67,6	59,0	51,2	42,4	35,5

3) Примечание. Исходные характеристики и вспомогательные параметры: $(l_1)_1 = 11,5$ м; $(\tau_{2,1}) = 0,21$; $A_2 = 0,21$; $(l_3)_1 = 15,8$ м; $(l_3)_2 = 15,8$ м; $(l_3)_3 = 2,8$ м; $(l_3)_4 = 2,8$ м; $(\tau_{2,3})_1 = 0,2$; $(\tau_{2,3})_2 = 0,12$; $(\tau_{2,3})_3 = 0,015$; $(\tau_{2,3})_4 = 0,3$; $B_2 = 0,52$; $s_2 = 11$ мм; $f_{2\,кр} = 1090$ Гц; $S_2 = 44,2$ м²; $l_{1,2} = 11,5$ м; $s_1 = 11$ мм; $\Delta s = 0$; $\Delta_\tau = 6,8$ дБ.

Table 15.7. Calculation of Deck Vibration Levels in Cabins on Main Deck at Initial Side (j = 1) and Forward Bulkhead (j = 2) Vibration Levels

1) Расчетные величины	2) Значения расчетных величин							
1. f, Гц	63	125	250	500	1000	2000	4000	8000
2. η_s	0,01	0,0096	0,0071	0,0071	0,006	0,0058	0,0047	0,0046
3. $(\Delta_G)_1$, дБ	−3,0	−2,3	−1,6	−0,8	0	0,8	1,7	2,5
4. $(\Delta N_2)_1$, дБ	2,7	3,4	4,1	4,9	5,7	6,5	7,4	8,2
5. $(N_1)_1$, дБ	76,3	85,7	77,0	72,2	64,3	57,3	49,3	42,3
6. $(N_2)_1 = (5) - (4)$	73,6	82,3	72,9	67,3	58,6	50,8	41,9	34,1
7. $(\Delta_G)_2$, дБ	−2,2	−1,6	−0,8	+0,1	1,0	1,8	2,6	3,5
8. $(\Delta N_2)_2 = \Delta_s + \Delta_\tau + (7)$	3,5	4,1	4,9	5,8	6,7	7,5	8,3	9,2
9. $(N_1)_2$, дБ	80,7	90,2	81,6	76,9	69,2	62,2	55,2	47,2
10. $(N_2)_2 = (9) - (8)$	77,2	86,1	76,7	71,1	62,5	54,7	46,9	38,0
11. $N_{2\Sigma}$, дБ	78,8	87,7	78,3	72,7	64,0	56,2	48,4	39,5

3) Примечание. Исходные характеристики и вспомогательные параметры: $(l_1)_1 = 11,5$ мм; $(l_1)_2 = 3,7$ м; $(A_2)_1 = 0,1$; $(A_2)_2 = 0,3$; $(\tau_{2,1})_1 = 0,057$; $(\tau_{2,1})_2 = 0,13$; $(l_3)_1 = 3,7$ м; $(l_3)_2 = 11,5$ м; $(\tau_{2,3})_1 = 0,05$; $(\tau_{2,3})_2 = 0,021$; $(B_2)_1 = 0,04$; $(B_2)_2 = 0,115$; $s_2 = 6$ мм; $f_{2\,кр} = 2000$ Гц; $S_2 = 41,6$ м²; $(s_1)_1 = 11$ мм; $(s_1)_2 = 8$ мм; $(l_{1,2})_1 = 11,5$ м; $(l_{1,2})_2 = 3,7$ м; $(\Delta_s)_1 = -4,0$ дБ; $(\Delta_s)_2 = -1,9$ дБ; $(\Delta_\tau)_1 = 9,7$ дБ; $(\Delta_\tau)_2 = 7,6$ дБ.

Key: See key at bottom of page 532.

APPROVED FOR RELEASE: 2007/02/08: CIA-RDP82-00850R000200100009-9

APPROVED FOR RELEASE: 2007/02/08: CIA-RDP82-00850R000200100009-9

Table 15.8. Calculation of L_c Levels of Noise Radiated by Side in Main Deck Cabins (with Refrigerator Running)

1) Расчетные величины	2) Значения расчетных величин							
1. f, Гц	63	125	250	500	1000	2000	4000	8000
2. Δ_γ, дБ	−15,5	−12,2	−9,5	−4,3	0	0	0	
3. $10 \lg 1/\alpha_{пр}$, дБ	9,2	6,8	6,0	5,7	5,5	5,4	5,4	5,4
4. (3) + I, дБ	0,3	−2,1	−2,9	−3,2	−3,4	−3,5	−3,5	−3,5
5. (2)+(4) + 6 дБ	−9,2	−8,3	−6,4	−1,5	+2,6	2,5	2,5	2,5
6 $\Delta_1 L_{ci}$, дБ	—	—	—	—	—	—	—	—
7. $\Delta_2 L_c$, дБ	0	3,0	7,0	11,0	12,0	12,0	12,0	12,0
8. (5)−(6)−(7)	−9,2	−11,3	−13,4	−12,5	−9,4	−9,5	−9,5	−9,5
9. N_{vl}, дБ	73,5	82,4	73,1	67,6	59,0	51,2	42,4	35,5
10. L_{ci} = (9)+(8)	64,3	71,1	59,7	55,1	49,6	41,7	32,9	26,0

3) Примечание. Исходные характеристики и вспомогательные параметры: $f_{l\,кр} = 1090$ Гц; $S_l = 6{,}7$ м²; $P_l = 10{,}4$ м; $\lambda_1 = 2{,}8$ м; $\lambda_2 = 0{,}6$ м; $a_п = 2{,}8$ м; $b_п = 2{,}4$ м; $S_п = 52$ м²; $\psi_1 = 0{,}45$; $\psi_2 = 0{,}011$; $\psi_3 = 0{,}41$; $\varphi_1 = 0{,}073$; $\varphi_2 = 0{,}24$; $g_1(\varphi_1) = 0{,}06$; $g_2(\varphi_1) = 0{,}57$; $g_1(\varphi_2) = 0{,}155$; $g_2(\varphi_2) = 0{,}19$; $g_3(\varphi_2) = 0{,}1$; $I = 18{,}3$ см; $f_{гр} = 80$ Гц; $\Delta_{\gamma_1} = -14{,}8$ дБ; $\Delta_{\gamma_2} = -9{,}5$ дБ; $\Delta_{\gamma_3} = 0$; $I = 10 \lg \frac{S_l}{S_п} = -8{,}9$ дБ.

Table 15.9. Calculation of L_c Levels of Noise Radiated by Deck in Main Deck Cabins (with Refrigerator Running)

1) Расчетные величины	2) Значения расчетных величин							
1. f, Гц	63	125	250	500	1000	2000	4000	8000
2. $\Delta\gamma$, дБ	−18,8	−14,7	−11,3	−7,8	−4,4	0	0	0
3. $10 \lg 1/\alpha_{пр}$, дБ	9,2	6,8	6,0	5,7	5,5	5,4	5,4	5,4
4. (3) + I	1,5	−0,9	−1,7	−2,0	−2,2	−2,3	−2,3	−2,3
5. (2) + (4) + 6 дБ	−11,3	−9,6	−7,0	−3,8	−0,6	3,7	3,7	3,7
6. $\Delta_1 L_{cl}$, дБ	—	—	—	—	—	—	—	—
7. $\Delta_2 L_{ci}$, дБ	—	—	—	—	—	—	—	—
8. (5)−(6)−(7)	−11,3	−9,6	−7,0	−3,8	−0,6	3,7	3,7	3,7
9. N_{vl}, дБ	78,8	87,7	78,3	72,7	64,0	56,2	48,4	39,5
10 L_{ci} = (9) + (8)	67,5	78,1	71,3	68,9	63,4	59,9	52,1	43,2

3) Примечание. Исходные характеристики и вспомогательные параметры: $f_{l\,кр} = 2000$ Гц; $S_l = 8{,}9$ м²; $P_l = 12{,}2$ м²; $\lambda_1 = 3{,}7$ м; $\lambda_2 = 0{,}6$; $a_п = 3{,}7$; $b_п = 2{,}4$ м; $S_п = 52$ м²; $\psi_1 = 0{,}22$; $\psi_2 = 0{,}0035$; $\psi_3 = 0{,}22$; $\varphi_1 = 0{,}02$; $\varphi_2 = 0{,}058$; $g_1(\varphi_1) = 0{,}032$; $g_2(\varphi_1) = 1{,}1$; $g_1(\varphi_2) = 0{,}05$; $g_2(\varphi_2) = 0{,}64$; $g_3(\varphi_2) = 0{,}049$; $\Delta_{\gamma_1} = -19{,}7$ дБ; $\Delta_{\gamma_2} = -16$ дБ; $\Delta_{\gamma_3} = -3{,}0$ дБ; $I = 10 \lg s_l/s_п = -7{,}7$ дБ.

Key: See key at bottom of page 532.

APPROVED FOR RELEASE: 2007/02/08: CIA-RDP82-00850R000200100009-9

APPROVED FOR RELEASE: 2007/02/08: CIA-RDP82-00850R000200100009-9

Table 15.10. Calculation of ΔL_{VD} for Top Deck Cabins at Initial Levels in Main Deck Cabins (with Refrigerator Running)

1) Расчетные величины	2) Значения расчетных величин							
1. f, Гц	63	125	250	500	1000	2000	4000	8000
2. $\sqrt{f}$	7,93	11,2	15,8	22,2	31,7	44,8	61,3	89,5
3. $\bar{\eta}_2$	0,004	0,0033	0,003	0,0026	0,0024	0,0023	0,0022	0,0021
4 $D_2 = l_2 \cdot (2) \cdot (3)$	1,2	1,41	1,8	2,2	2,88	3,91	5,12	7,15
5. $\frac{[(4)+2]}{[(4)+1]}$	1,45	1,42	1,36	1,31	1,26	1,205	1,17	1,12
6. (4)·(5)	1,74	2,0	2,45	2,88	3,63	4,71	6,0	8,0
7. (1) + (6)	2,74	3,0	3,45	3,88	4,63	5,71	7,0	9,0
8. $\varkappa = l_1 \cdot (7)$	0,96	1,05	1,21	1,36	1,62	2,00	2,45	3,15
9. ε_1'	$7,1 \cdot 10^{-4}$	$1,4 \cdot 10^{-3}$	$3,5 \cdot 10^{-3}$	$7,1 \cdot 10^{-3}$	0,011	0,020	0,057	1,0
10. ε_1''	$2,8 \cdot 10^{-2}$	0,05	0,08	0,90	1,0	1,0	1,0	1,0
11. (9) + (10)	$2,8 \cdot 10^{-2}$	0,0514	0,0835	0,907	1,011	1,02	1,057	2,0
12. ε_2'	$7,1 \cdot 10^{-4}$	$1,4 \cdot 10^{-3}$	$3,5 \cdot 10^{-3}$	$7,1 \cdot 10^{-3}$	0,011	0,020	0,057	1,0
13. ε_2''	$2,3 \cdot 10^{-2}$	0,042	0,078	0,12	0,76	1,00	1,00	1,00
14. (12) + (13)	$2,37 \cdot 10^{-2}$	0,0434	0,0815	0,1277	0,771	1,02	1,057	2,0
15. (11)/(14)	1,21	1,18	1,15	7,05	1,44	1,0	1,0	1,0
16. (8)·(15)	1,16	1,24	1,4	9,7	2,36	2,0	2,45	3,15
17. $\Delta L_{ВИ} = 10 \lg (16)$	0,6	0,9	1,5	9,9	3,7	3,0	3,9	5,0

3) Примечание. Исходные характеристики и вспомогательные параметры: $l_2 = 2,5$ м; $s_1' = 2$ мм; $s_1'' = 11$ мм; $s_{1\,ср} = 6,5$ мм; $s_0 = 7,0$ мм; $\tau_{ср} = 0,085$; $f_{2\,кр} = 2000$ Гц; $s_2' = 2$ мм; $s_2'' = 10$ мм; $s_{2\,ср} = 6$ мм; $l_1 = (s_{2\,ср}/s_{1\,ср})^{3/2} = 0,35$; $l_2 = \pi^2 \frac{l_1 \sqrt{f_{2\,кр}}}{c\tau_{ср}} = 38$.

Key: 1. Calculated values
2. Calculation results
3. Comment. The initial characteristics and auxiliary parameters are: [Гц=Hz; ВИ=VD; ср=av; кр=cr]

effects. Finally, the question arises of the mutual influence of separate techniques when used in combination.

Local and General Effects. General effect is defined as the reduction of the corresponding components of noise (L_{sp} or L_a and L_{ss}) from a given source in the entire combination of ship rooms by the identical amount. Near vibration-damping and acoustic insulation of sources has a general effect. Local effect is defined as a reduction of the corresponding

APPROVED FOR RELEASE: 2007/02/08: CIA-RDP82-00850R000200100009-9

APPROVED FOR RELEASE: 2007/02/08: CIA-RDP82-00850R000200100009-9

Table 15.11. Calculation of ΔL_{1in} and Noise Levels in Top Deck Cabins at Initial Levels in Main Cabins with Refrigerator Running (S_{1r} = 52 m^2; S_{2r} = 36.8 m^2; S_1' = = 43 m^2; S_2' = 30.2 m^2)

1) Расчетные величины	2) Значения расчетных величин							
1. f, Гц	63	125	250	500	1000	2000	4000	8000
2. $\alpha_{1\,пр}$	0,12	0,21	0,25	0,27	0,28	0,29	0,29	0,29
3. $\alpha_{2\,пр}$	0,12	0,21	0,25	0,27	0,28	0,29	0,29	0,29
4. (3)/(2)	1,0	1,0	1,0	1,0	1,0	1,0	1,0	1,0
5. 10 lg (4), дБ	0	0	0	0	0	0	0	0
6. $\overline{\Delta_2 L_{c_1}}$, дБ	0	0	3	6	8	10	10	10
7. $10^{-0,1}$ (6)	1,0	1,0	0,5	0,25	0,158	0,1	0,1	0,1
8. 1 − (7)	0	0	0,5	0,75	0,842	0,9	0,9	0,9
9. $1-\frac{s_1'}{s_{1п}}\cdot$ (8)	1,0	1,0	0,584	0,38	0,315	0,255	0,255	0,255
10. $\overline{\Delta_2 L_{c2}}$, дБ	0	0	3	6	8	10	10	10
11. $10^{-0,1}\cdot$(10)	0	0	0,5	0,25	0,158	0,1	0,1	0,1
12. 1 − (11)	1	1	0,5	0,75	0,842	0,9	0,9	0,9
13. $1-\frac{s_2'}{s_{2п}}\cdot$(12)	1,0	1,0	0,584	0,38	0,315	0,255	0,255	0,255
14. (9)/(13)	1,0	1,0	1,0	1,0	1,0	1,0	1,0	1,0
15. $\Delta L3$ = 10 lg (14)	0	0	0	0	0	0	0	0
16. $\Delta L_{ВИ}$, дБ	0,6	0,9	1,5	9,9	3,7	3,0	3,9	5,0
17. (16) + (15) + (5)	0,6	0,9	1,5	9,9	3,7	3,0	3,9	5,0
18. L_1, дБ	70	79	72	69	64	60	52	43
19. L_2 = (18)−(17)	69	78	70	59	60	57	48	38

Key: 1. Calculated values [Гц=Hz; пр=red; дБ=dB; п=r; ВИ=VD]
2. Calculation results

components of noise in just one particular room (or the reduction of the acoustic vibration levels of a particular hull structure).

Acoustic-insulating and floating structures have a virtually local effect. The former reduce the penetrating noise levels for one of the contiguous rooms, and the latter, by weakening the radiation of individual structures surrounding a room, reduce the noise levels in just that room.

Systems with a general effect include air intake shaft and ventilation duct mufflers, if they are installed in the immediate vicinity of noise sources -- motors or blowers. In individual cases, however, a different arrangement is used. This is not important in terms of the total reduction

APPROVED FOR RELEASE: 2007/02/08: CIA-RDP82-00850R000200100009-9

APPROVED FOR RELEASE: 2007/02/08: CIA-RDP82-00850R000200100009-9

of the exhaust noise of a shaft or duct, but for rooms through which (or next to which) they pass it can be of considerable importance. In practice it is necessary in all cases to find a structural solution, whereby mufflers are installed most efficiently right next to the noise source, and therefore these systems may be assumed to be devices with a general effect.

The situation is substantially more complicated in terms of the other noise control techniques. They have an effect, the amount of which differs from room to room and depends on the area of application. Such an effect can be called locally general. Devices with this effect include vibration-absorbing coatings and vibration-damping coamings and weights.

Vibration-absorbing structures exert a perceptible effect only when they are installed either directly on the structures that surround an examined room, or in the space between it and a source room. However, damping of partitions farther from the source has virtually no effect on the vibration levels of partitions that are closer to the source. Vibration-damping coamings, which basically reduce vibration levels in partitions located beyond the corresponding corner connections, have this kind of effect. It is also important to remember that when coamings are installed in just the direct path from the source to the corresponding partitions, secondary (i.e., longer, detour) acoustic vibration propagation paths begin to exert a stronger influence. Therefore it is necessary to increase the vibration damping of these paths as well. This is done in practice by installing coamings around the entire perimeter of the hull structures in individual regions of a ship. A similar phenomenon occurs, though to a lesser extent, when vibration-absorbing coatings are used. Therefore they should also be applied on contiguous main hull structures between the noise source and examined room, and not just on the shortest path.

Associated Effects. During the design of structural noise control complexes it is important to consider, in addition to the basic effect, which is determined by the main purpose of each system, secondary and associated effects of these systems as well. These effects are characteristic of the following measures: acoustic-insulating structures (AIS), sound-absorbing structures (SAS), floating structures (FS) and vibration-absorbing coatings (VAC).

An associated effect of the use of double-wall AIS may be double-edged in nature. If the second wall (liner) is installed on the quiet side the associated effect will be manifested as the attenuation of the acoustic radiation of the main hull structure as acoustic vibration propagates from the source, i.e., as a reduction of levels L_{sp} in the contiguous room. But if the lining is installed on the source side it should attenuate the excitation of the main hull side by airborne noise and reduce to some extent the L_{ss} levels in all the rooms located in that region.

APPROVED FOR RELEASE: 2007/02/08: CIA-RDP82-00850R000200100009-9

APPROVED FOR RELEASE: 2007/02/08: CIA-RDP82-00850R000200100009-9

The acoustic insulation of hull structures (both single-wall and double-wall) can be increased also by increasing the thickness of the plating of the main bulkhead. In this case an associated effect will be a change of the vibration insulation of corner connections on the contour of the bulkhead. These changes can vary: they can both increase and decrease for different contiguous enclosures, but in most cases the effect as a whole is the attenuation of acoustic vibration propagation around the contour and, accordingly, some reduction of levels L_{sp} and L_{ss}.

An associated effect of VAC is manifested in cases when they are installed on enclosures that surround the source room. It is expressed in the attenuation of the excitation of these enclosures by airborne noise, i.e., in a reduction of levels L_{ss}. If, in addition, some enclosure is a partition for one of the contiguous rooms, the existence of VAC on it leads to some increase of acoustic insulation (due to an increase of mass and of internal energy losses), i.e., a reduction of the L_a levels in that room.

SAS also have various associated effects. Their application for the basic purpose in a source room produces the following secondary results:

reduction of penetrating noise in adjacent rooms L_a due to a reduction of the initial noise levels in the source room and some increase of the acoustic insulation of the partitions that separate it and contiguous rooms;

reduction of L_{ss} levels due to a reduction of noise in the source room and attenuation of the excitation of the partitioning structures on which SAS are installed.

The application of SAS in quiet rooms, in addition to a reduction of the levels of all components of noise (L_a, L_{ss}, L_{sp}) due to an increase of acoustic absorption in the room, is accompanied by the following effects:

additional reduction of the levels of penetrating noise L_a due to an increase of the acoustic insulation of the partitioning enclosures, if SAS are installed on them;

attenuation of the radiation of noise, i.e., reduction of the L_{sp} and L_{ss} levels from the surrounding enclosures, on which SAS are installed.

The combined application of different noise control techniques can be expected to exert a mutual influence. This influence may, in principle, be positive (i.e., the summary effectiveness of combined application may be greater than the sum of the effectivenesses of separate application), and negative.

APPROVED FOR RELEASE: 2007/02/08: CIA-RDP82-00850R000200100009-9

APPROVED FOR RELEASE: 2007/02/08: CIA-RDP82-00850R000200100009-9

For example, a positive effect can be expected from the combined application of vibration-damping and vibration-absorbing techniques. A negative effect can be expected to some extent from the combined application of elastic foundations and shock absorbers.

The features of the acoustic effectiveness of different noise control techniques, characterizing their basic purpose and associated effects, determine the feasibility of using these techniques for reducing noise in ship rooms at different distances from a noise source.

BIBLIOGRAPHY

1. Boroditskiy, L. S. and V. M. Spiridonov, "Snizheniye Strukturnogo Shuma v Sudovykh Pomeshcheniyakh" [Reduction of Structural Noise in Ship Rooms], Leningrad, Sudostroyeniye, 1974.

2. Klyukin, I. I., "Bor'ba s Shumom i Zvukovoy Vibratsiyey na Sudakh" [Control of Noise and Acoustic Vibrations on Ships], Leningrad, Sudostroyeniye, 1971.

3. Nikiforov, A. S. and S. V. Budrin, "Rasprostraneniye i Pogloshcheniye Zvukovoy Vibratsii na Sudakh" [Propagation and Absorption of Acoustic Vibration on Ships], Leningrad, Sudostroyeniye, 1968.

4. Maidanik, G., "Response of Ribbed Panels to Reverberant Acoustic Fields," J. OF THE ACOUST. SOC. OF AMERICA, 1962, Vol 34, No 6, pp 809-826.

5. Smith, P., "Response and Radiation of Structural Modes Excited by Sound," J. OF ACOUST. SOC. OF AMERICA, 1962, Vol 34, No 5, pp 640-646.

COPYRIGHT: Izdatel'stvo "Sudostroyeniye", 1978
[8144/0921-7872]

7872
CSO: 8144/0921

-END-

APPROVED FOR RELEASE: 2007/02/08: CIA-RDP82-00850R000200100009-9